THE SPIRODIEPOXIDE: A PLATFORM FOR DIVERSITY AND TARGET ORIENTED SYNTHESIS

by

ROJITA SHARMA

A dissertation submitted to the

Graduate School-New Brunswick

Rutgers, The State University of New Jersey

In partial fulfillment of the requirements

For the degree of

Doctor of Philosophy

Graduate Program in Chemistry and Chemical Biology

Written under the direction of

Professor Lawrence J. Williams

And approved by

New Brunswick, New Jersey

OCTOBER, 2013

ABSTRACT OF THE DISSERTATION

THE SPIRODIEPOXIDE: A PLATFORM FOR DIVERSITY AND TARGET ORIENTED SYNTHESIS

By ROJITA SHARMA

Dissertation Director:

Professor Lawrence J. Williams

Revealed are studies on the reactivity and mechanism of spirodiepoxides and their utilization in the synthesis of highly functionalized diverse motifs. New spirodiepoxide based methodologies have been discussed including the method for synthesis of *syn* substituted hydroxyketone, diendiol, diyndiol, α′-hydroxy-γ-enone, dihydrofuranone, butenolide, and δ-lactone. Two complementary and stereochemically divergent methods for the synthesis of oxetan-3-ones starting from allenes via spirodiepoxides are also presented. Spirodiepoxide based cascades have also been used in the studies towards the synthesis of pectenotoxin 4 (PTX4). An unprecedented hydrogen bond directed allene epoxidation and spontaneous opening of the spirodiepoxide by the free hydroxyl group was employed in the synthesis of the F ring of PTX4. Improved protocol for the synthesis of allene and a new method for the synthesis of bromohydroxyketone have also been disclosed.

ACKNOWLEDGEMENTS

I would like to express my gratitude to Professor Lawrence Williams for the opportunity to do my graduate research in his group. I highly value his insightful advice, inspiration and encouragement.

I would like to thank Dr. Bruce Ellsworth, Professor Kai Hultzsch and Professor Roger Jones for being on my thesis defense committee and for all their help and useful insights. I would also like to thank all my coworkers in the Williams group.

I would like to express my gratefulness to my parents (Ram Nath Sharma and Puspa Baral), my sisters (Rejina Sharma and Reena Baral), and my beloved husband (Subash Regmi) for their love and support. Their love and support kept me moving forward and helped me in my journey.

DEDICATION

This dissertation is dedicated to my father, Ram Nath Sharma Baral, and my mother, Puspa Baral.

Table of Contents

List of Tables

List of Figures

List of Schemes

Chapter 1

List of Abbreviations

°C	degrees Celsius
Å	Angstrom
acac	acetylacetonate
ac	acetate
aq	aqueous
ATP	adenosine triphosphate
BDP	1,2-bis(diphenylphosphine)benzene
Bn	benzyl
Boc	*t*-butyloxycarbonyl
Bu	butyl
*i*Bu	isobutyl
br	broad
calcd	calculated
cm	centimeter
CSA	camphorsulfonic acid
δ	chemical shift (parts per million)
d	doublet
dba	dibenzylideneacetone
DCM	dichloromethane
DDQ	2,3-dichloro-5,6-dicyano-1,4-bezoquinone
DEDO	diethyl dioxirane
DEK	diethyl ketone

DFT	density functional theory
DIAD	diisopropyl azodicarboxylate
DIBAL-H	diisobutylaluminum hydride
DIPT	diisopropyl tartrate
DMAP	4-(*N*,*N*-dimethylamino)pyridine
DMDO	dimethyldioxirane
DMF	dimethylformamide
DMP	Dess-Martin periodinane
DMPU	1,3-dimethyltetrahydropyrimidin-2(1H)-one
DMSO	dimethylsulfoxide
dr	diastereomeric ratio
E	entgegen
ee	enantiomeric excess
equiv	equivalent
FCC	flash column chromatography
FT	Fourier transform
g	gram
h	hour(s)
HOAc	Acetic acid
HOMO	highest occupied molecular orbital
HMDS	hexamethyldisilazide
HMPA	hexamethylphosphorus triamide
HPLC	high performance liquid chromatography

Hz	hertz
i	iso
IBCF	isobutyl chloroformate
imid.	imidazole
IR	infrared
LDA	lithium diisopropylamide
LiDBB	lithium di-*tert*-butyldiphenylide
m	multiplet
M	molar (moles/liter)
m-CBA	meta-chlorobenzoic acid
m-CPBA	meta-chloroperoxybenzoic acid
Me	methyl
MEDO	methylethyl dioxirane
MEK	methylethyl ketone
m-FBn	3-fluorobenzyl
mg	milligram
min	minutes
ml	milliliters
mol	moles
MS	molecular sieves
Ms	methanesulfonyl
MW	microwave
m/*z*	mass to charge ratio

n-BuLi	n-butyllithium
NBS	*N*-bromosuccinimide
NBSH	2-nitrobenzenesulfonylhydrazide
nM	nanomolar
NMO	*N*-Methylmorpholine-*N*-oxide
NMP	*N*-Methylpyrrolidone
NMR	nuclear magnetic resonance
NOE	nuclear Overhauser effect
NOESY	nuclear Overhauser effect spectroscopy
Nu	nucleophile
[O]	oxidant
OTf	trifluoromethanesulfonyl
P	protecting group (generic)
p	para
Pd/C	palladium on carbon
pg	page
Ph	phenyl
Piv	pivaloyl
PMB	(4-methoxy)benzyl
PMHS	polymethylhydrosiloxane
PMP	4-methoxyphenyl
ppm	parts per million
pr	propyl

PPTS	pyridinium *p*-toluenesulfonate
PPTS	*p*-toluene sulfonic acid
PTX	pectenotoxin
q	quartet
R	rectus (Cahn-Inglod-Prelog system)
R	alkyl group (generic)
Ref	reference
rt	room temperature
s	singlet
S	sinister (Cahn-Inglod-Prelog system)
SAA	Sharpless asymmetric aminohydroxylation
SDE	spirodiepoxide
SEM	2-trimethylsilylethoxymethoxy
S_N2	bimolecular nucleophilic substitution
t	tertiary
t	triplet
TAS-F	tris(dimethylamino)sulfur(trimethylsilyl)difluoride
TBAB	tetra(*n*-butyl)ammonium bromide
TBAF	tetra(*n*-butyl)ammonium fluoride
TBAI	tetra(n-butyl)ammonium iodide
TBDPS	*tert*-butyldiphenylsilyl
TBHP	*tert*-butyl hydroperoxide
TBODPS	*tert*-butoxydiphenylsilyl

TBS	*tert*-butyldimethylsilyl
t-BuLi	*tert*-butyllithium
t-BuOH	*tert*-butylalcohol
TEA	Triethyl amine
TEMPO	2,2,6,6-tetramethylpiperidine-1-oxyl
TES	triethylsilyl
TFA	trifluoroacetic acid
THF	tetrahydrofuran
TIPS	triisopropylsilyl
TLC	thin layer chromatography
TMS	trimethylsilyl
TPAP	tetra-n-propylammonium perruthenate
Ts	tosyl
TS	transition state
TsDPEN	N-(4-toluenesulfonyl)-1,2-diphenylethylenediamine
UV	ultraviolet
Z	zusammen

Chapter 1

The Spirodiepoxide: A New Functional Group for Organic Synthesis

1.1 Introduction

Allene oxidation chemistry expands the paradigm of C-C π-bond functionalization. Whereas alkene epoxidation/epoxide opening engages two and sometimes three or more contiguous carbons, allene epoxidation/epoxide opening engages three and sometimes four or more contiguous carbons (**S1.1→S1.2→S1.3-S1.7**, Scheme 1). For example, spirodiepoxides can be opened by external or internal nucleophiles (→**S1.3-S1.5**), undergo elimination (→**S1.6**) or rearrangement (→**S1.7**), or more complex cascade reactions. These processes may be facilitated by external or internal activation (e.g. **S1.8-S1.10**).

This chapter focuses on our work with the spirodiepoxide functional group. In contrast to the epoxide, a functionality whose origins are traceable to the very roots of modern chemistry, the spirodiepoxide is new to target-oriented synthesis. We begin here with a brief historical overview of the spirodiepoxide and in subsequent sections discuss the selective preparation of this group via allene epoxidation, and then discuss trends in spirodiepoxide reactivity. To date, the spirodiepoxide has been shown to participate in many reactions and cascade sequences that are applicable to the preparation of highly functionalized motifs. We have had particular success with the preparation of vicinal stereotriads, heterocycles, and highly enantioenriched ketones. This chemistry is discussed in increasingly complex contexts of motif-building and target-oriented synthesis. The final section describes mechanistic insight gained from experimental and computational studies.

Scheme 1. Spirodiepoxide and its Reactivity

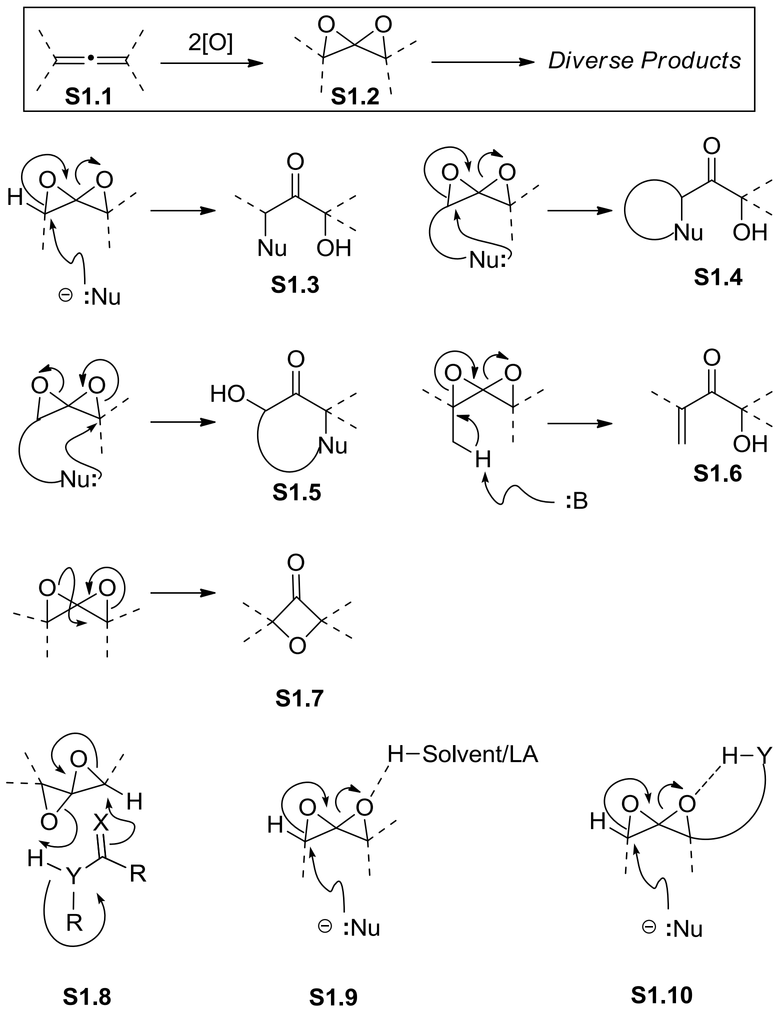

The history of the spirodiepoxide follows the sometimes disjointed path of the allene. An excellent series of monographs describes the history of the allene in detail.[1] A brief overview of the interplay between the allene chemistry and allene spirodiepoxidation is provided here and summarized in Figure 1.

Jacobus H. van't Hoff published his argument for the tetrahedral carbon in 1875, including his famous rationale that allenes may exist and that if asymmetrically substituted they would exist as optical isomers not geometrical isomers.[2] Experimental validation of this speculation lagged. Although von Pechmann and Burton advanced an allene synthesis in 1887,[3] that this procedure produced allenes was not proven until Jones, Mansfield and Whiting used infrared spectroscopy to characterize the products in 1954.[4] The allene had come to be accepted as a reality along with the three dimensional nature of these molecules long before this point had been addressed, of course. For example, chiral allenes were resolved by Kohler and Tishler[5] and independently by Maitland and Mills in 1935.[6]

Figure 1. Milestones in the Early History of Allenes and Spirodiepoxides

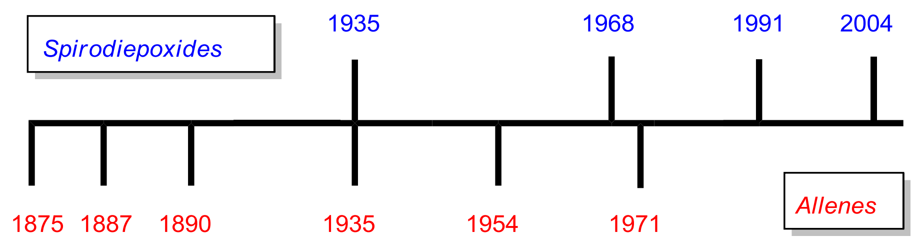

1875 Allene structure and chirality proposed by van't Hoff*
1887 Allene synthesized*
1890 Peridinin, an allene-containing natural product, isolated*
1935 Spirodiepoxide proposed as allene oxidation product*
1935 Chiral allene resolved
1954 Allene synthesis of 1887 proven correct
1968 Spirodiepoxide isolated
1971 Peridinin structure determined
1991 Spirodiepoxide characterization and general synthesis reported
2004 Spirodiepoxide used in total synthesis

* structural claims not proven

Spirodiepoxides first appeared in the literature in the same timeframe. Boeseken suggested in 1935 that spirodiepoxides might have been intermediates in his studies on allene oxidation with peracids, which were new reagents at the time.[7] More than three decades passed before additional insight was gained into allene epoxidation.

In the 1960's there was much interest in understanding the relationship between cyclopropanone (**S1.11**), the oxyallyl zwitterion (**S1.12**) and allene oxide (**S1.13**, Figure 2). In an effort to prepare an allene oxide, Crandall initiated a study on allene epoxidation. These studies led to the first isolable spirodiepoxide in 1968[8,9] and describe a fascinating investigative tale that rationalizes a mesmerizing range of transformations in terms of allene oxides, cyclopropanones, and spirodiepoxides. The upshot of these investigations was that allene oxides and spirodiepoxides appear particularly unstable to acid.[10–12] The peracid oxidants used for the epoxidation generate carboxylic acids, which induce the decomposition process. Without the availability of an alternative oxidant an impasse seemed to have been reached that lasted another two decades.

Figure 2. Cyclopropanone, Oxyallyl Zwitterion, Allene Oxide and Dimethyldioxirane

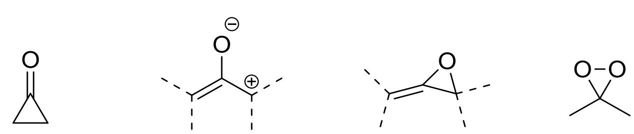

S1.11 **S1.12** **S1.13** **S1.14**

Interest in spirodiepoxides was reinvigorated with Murray's method for generating dimethyldioxirane (DMDO, **S1.14**, Figure 2).[13] This oxygen atom transfer reagent produces acetone as the by-product. Importantly, Crandall showed that otherwise simple spirodiepoxides are readily prepared and isolated, and key data were gathered from a series of primarily achiral and minimally functionalized allenes. Together, they provided strong evidence that allene epoxidation could well be used in organic synthesis:

the oxidation appeared driven by steric factors and, under neutral or slightly basic conditions, spirodiepoxide opening with nucleophiles seemed not to involve cationic intermediates.[14,15]

Our interest in spirodiepoxides developed from the desire to introduce α– and α′–functionality to a carbonyl simultaneously and to achieve their introduction with complete stereocontrol. No methods were known to achieve this transformation. However, consideration of the role the carbonyl might play – disguised as a strained bicyclic acetal – led us to consider the spirodiepoxide as a precursor. At the time our notions were highly speculative. Spirodiepoxides were laced with high reactivity and their uncharted chemistry raised many questions. Still, it occurred to us that highly enantioenriched spirodiepoxides may be prepared and leveraged to realize concise chemical syntheses. As depicted in Scheme 1, oxidation/nucleophilic opening would install three functional groups – nucleophile, ketone, and alcohol – with *syn* selectivity. Importantly, these transformations would be achieved in the absence of other stereodirecting functionality and would convert the chiral axis of an allene into two centres of chirality.

1.2 Spirodiepoxide Synthesis

Many allenes undergo diastereoselective epoxidation to form spirodiepoxides, which can then be opened by various reagents to form, for example, α-substituted-α′-hydroxy ketones. Throughout our synthetic work, the *syn* stereochemistry of the nucleophilic addition has been proven to be the major product. We have used spirodiepoxide-based cascade reactions in the syntheses of epoxomicin (**S1.15**),[16,17] psymberin (**S1.16**),[18,19] epi-citreodiol (**S1.17**)[20] and jaspine (**S1.18**, Figure 3).[21] We have also applied our spirodiepoxide-based chemistry in the synthesis of analogs of erythromycin (**S1.19**)[22,23] and fragments of pectenotoxin 4 (PTX4, **S1.20**).[24–27] In the course of these studies we accumulated extensive crystallographic, chemical correlation, and spectral data that support the product assignments, and based on these the stereochemistry of spirodiepoxides can be reliably predicted.

Figure 3. 1,3- syn Relationship of Nucleophilic Addition Product

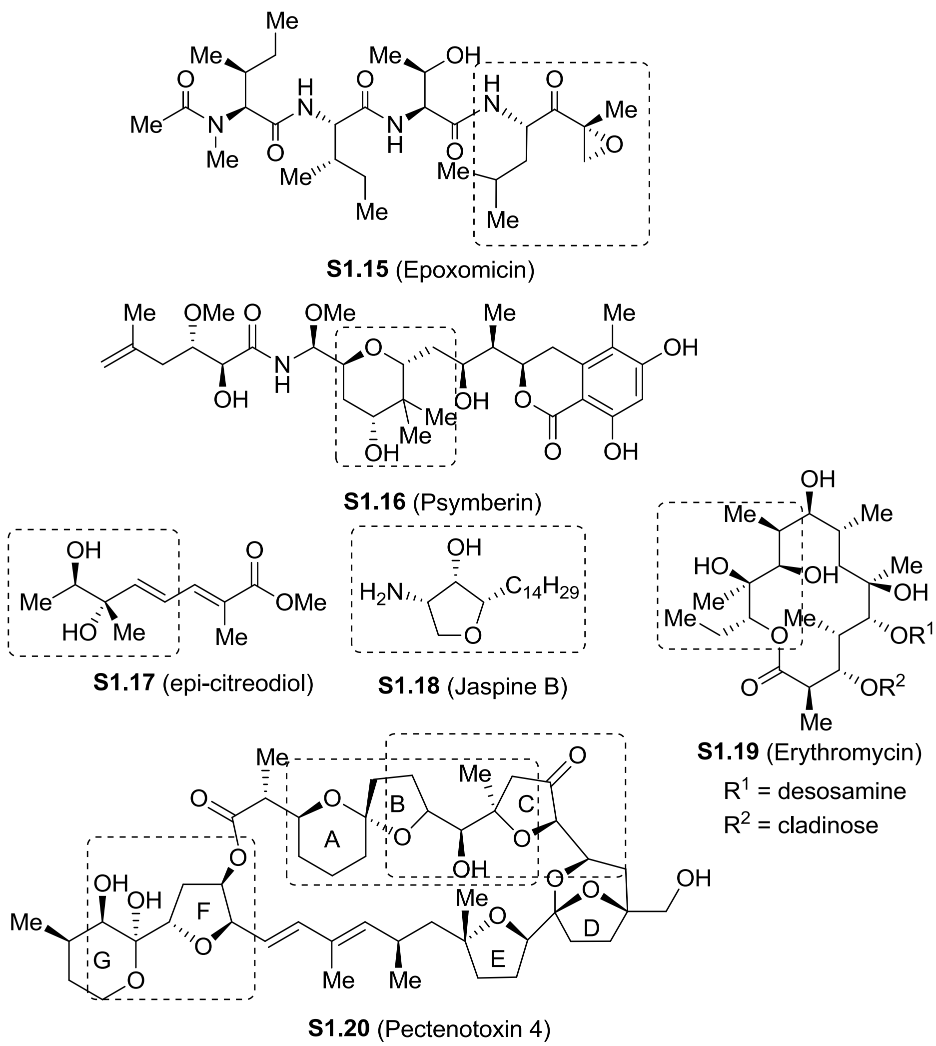

At the outset of our studies, there was one instance in which the stereochemistry of the nucleophilic addition product had been proven. The addition of water to 9-membered spirodiepoxide **S1.21** was deduced to be *syn* based on the products derived from ketone **S1.22** (Scheme 2).[14] These findings were consistent with the rationale that (a) π-bond nucleophilicity dictates the site of the first epoxidation, (b) sterics govern the face selectivity of the first and second epoxidation, and (c) accessibility dictates which terminus of the spirodiepoxide undergoes nucleophilic addition (Scheme 3). Hence, trisubstituted allene **S1.23** (L^1, L^2 = large substituents and S = small substituent) would be epoxidized in a regioselective and stereoselective manner to form allene oxide **S1.24**. The allene oxide would be epoxidized to form spirodiepoxide **S1.25**. The oxygen atoms of spirodiepoxide **S1.25** are *anti*, and this functional group would open in an S_N2 fashion to give *syn* product **S1.26**.

Scheme 2. 1,3- syn Relationship Proven in Cyclic System

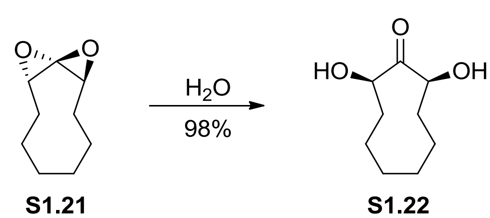

Scheme 3. Steric Model for Steroselective Allene Epoxidation

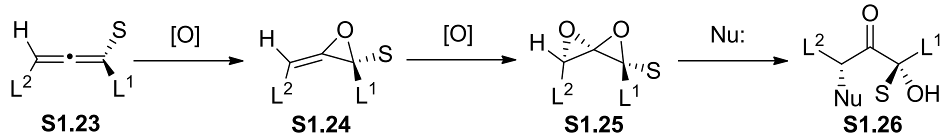

However, this picture is somewhat oversimplified, and Scheme 4 illustrates this point. Although the first oxidation of an allene can be stereoselective, the degree of face selectivity is critical.[14] Oxygen atom transfer to the allene to the most accessible face is governed by the relative size of the substituents on the non-reacting terminus (i.e. *anti* to the large substituent, L^2, Scheme 4). Thus, **S1.23** would be expected to give allene oxide **S1.24**. The diastereomeric allene oxide **S1.27** may also form, and this product has the opposite absolute arrangement at the new stereocenter. The second oxidation may also be stereoselective. Again, face selectivity of the oxygen atom transfer process is governed by the relative size of the substituents on the non-reacting terminus. Accordingly, epoxidation of **S1.24** may give two spirodiepoxides, the major **S1.25** (*anti*/*anti*) and the minor **S1.28** (*anti*/*syn*). Allene oxide **S1.27** would lead to the formation of **S1.29** (*syn*/*anti*) and **S1.30** (*syn*/*syn*). Nucleophilic addition to these spirodiepoxides at the most accessible terminus would give **S1.26** and **S1.27**, along with their antipodal isomers **S1.32** and **S1.33**. The antipodes are traceable to the selectivity of the first epoxidation (**S1.22→S1.23 + S1.27**). Hence, enantiomerically pure allenes will give rise to spirodiepoxide-derived products of low enantiopurity in cases where the selectivity of the first oxidation is low. One of our early goals, therefore, was to address the face selectivity of the critical first epoxidation.

We evaluated several parameters of allene epoxidation in an effort to understand epoxidation face selectivity, including solvent, temperature, oxidant (Figure 4), and allene structure. The diastereoselectivity was shown to depend primarily on the steric and electronic properties of the allene and was relatively insensitive to dioxirane structure and to solvent. When one substituent is hydrogen and the other is carbon, the first oxidation is highly regioselective and favors the most substituted allene double bond regardless of oxidant or solvent (**S1.40**, arrow, Figure 4). Although increasing the steric bulk of the

Scheme 4. Allene Oxidation Framework

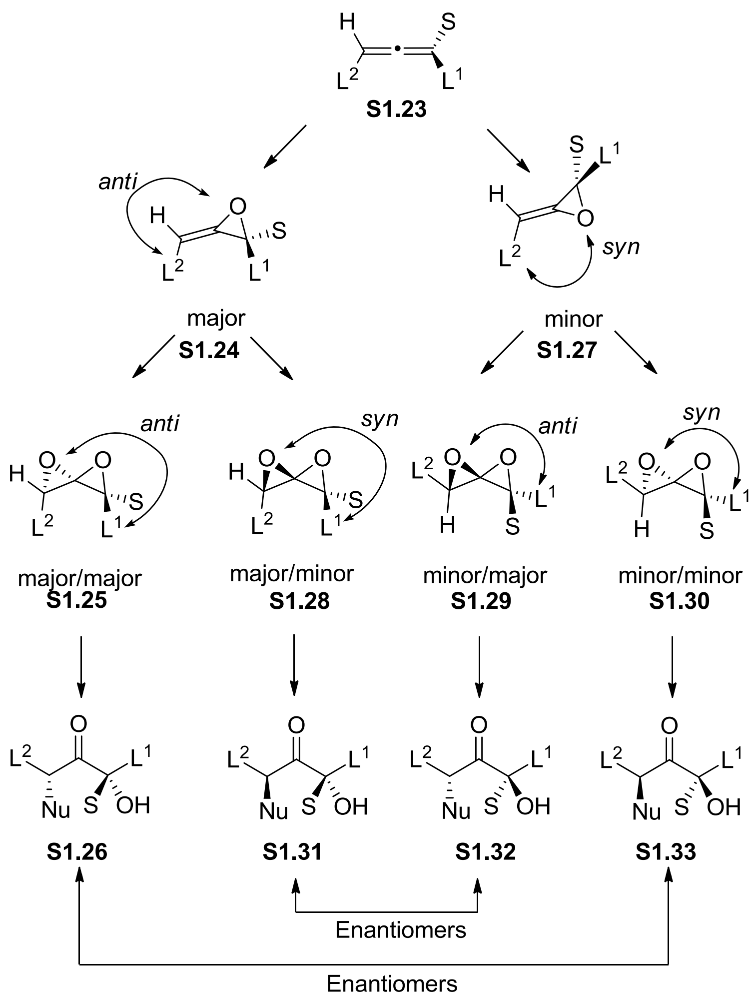

Figure 4. Oxidants

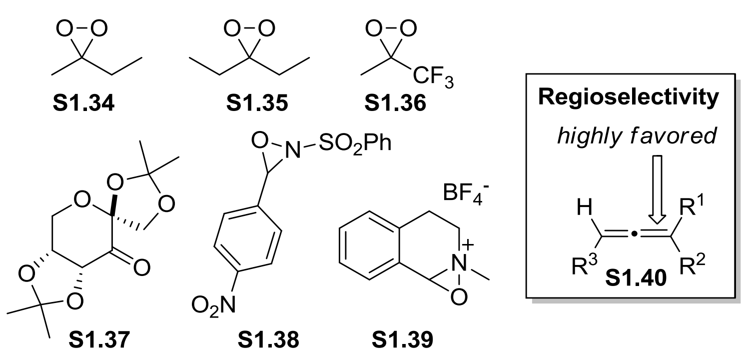

dioxirane improved the selectivity for the first oxidation, there was little substantive difference between DMDO in acetone (Table 1, entry 1), methyl ethyl dioxirane (MEDO,**S1.34**) in methyl ethyl ketone (entry 2), and diethyl dioxirane (DEDO, **S1.35**) in diethyl ketone (entry 3). Other oxidants, such as the Shi (**S1.37**) and Davis (**S1.38**) reagents were largely ineffective. The oxaziridinium reagent (**S1.39**) was promising and the use of a chiral oxaziridinium reagent is described in the following section. Remarkably, DMDO in chloroform gave selective allene oxidation that surpassed other dioxiranes and gave only a single isomer (entry 4). In more elaborate allenic substrates only two products were observed, which further indicates very high selectivity in the first oxidation and a lower degree of selectivity in the second oxidation. Nevertheless, DMDO in chloroform gave superior results for the oxidation of both double bonds of the allene (entries 5-8). Although the mechanism is not well-understood, such solvent effects for DMDO oxidation are well-documented.[17,28]

The model of sterics-based face selectivity outlined in Scheme 3 was sufficient to explain our observations in simple systems. For all substrate, reagent, and solvent combinations, the face selectivity of the first oxidation appears to depend primarily on the relative size of the substituents on the non-reacting terminus. In the case of a smaller substituent (linear alkyl, H), the diastereoselectivity is low (dr = 2:1, for L^1 = *n*-Bu, *i*-Bu). In allenes with larger substituent (α branched alkyl) the diastereoselectivity is higher (dr = 3.3:1 and 5:1 for L^1 = *i*-Pr).[17] Importantly, the face selectivity in the first oxidation of biased allenic substrates is excellent (dr >20:1), which guarantees the enantiopurity of the derived products (>95%) and greatly enabled the development of new methods and strategies for the synthesis of complex targets.

Silyl substituted allenes are also conveniently and reliably epoxidized in DMDO/chloroform solutions. The silyl group represents a shift from the simple systems discussed above and the more complex systems described in the next section. In cases where the silyl group is directly attached to the allene, the site and face selectivity of the epoxidations are high. The first oxidation occurs on the double bond proximal to the silyl group, and in trisubstituted silyl allenes of type **S1.44**, the most accessible face was favored for both the first (dr >20:1) and second oxidation (dr > 10:1, Scheme 5). The face selectivity of the second epoxidation is slightly and reproducibly higher than the all-carbon analogs (*cf*. Table 1, entry 8), probably because of the length of C-Si bonds and the corresponding increased steric crowding of the reacting π-bond.[20] The site selectivity is predicted by the HOMO, which is proximal to silyl group in trisubstituted allenes (see **S1.43**, Scheme 5).

Table 1. Effect of Oxidants and Solvents on Diastereoselectivity

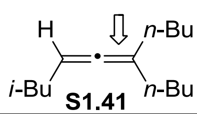

S1.41

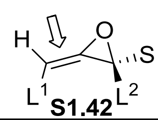

S1.42

Entry	Oxidant	Solvent	dr	Entry	L^1	L^2	S	dr
1	**S1.14**	acetone	10:1	5	*n*-Bu	*n*-Bu	H	2:1
2	**S1.34**	MEK	14:1	6	*i*-Bu	CH_2OTBS	Me	2:1
3	**S1.35**	DEK	16:1	7	*i*-Pr	*i*-Pr	Me	3.3:1
4	**S1.14**	$CHCl_3$	>20:1	8	*i*-Pr	*i*-Pr	H	5:1

Scheme 5. Formation of Silyl Spirodiepoxide

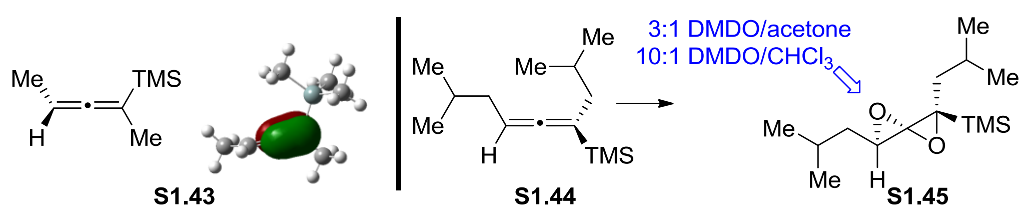

1.3 Stereoselective Formation of Spirodiepoxides

Although the model of face selectivity outlined in Scheme 3 is adequate for simple dioxiranes and allenes, it does not adequately explain other observations. For example, it does describe diastereoselective processes that are either substrate or reagent controlled; we have noted both. Scheme 6 illustrates a diastereoselectivity phenomenon we encountered in the process of preparing analogues of the proteasome inhibitor epoxomicin (**S1.15**). The relative configuration in allene **S1.46** significantly influences the face selectivity of the second epoxidation, and thereby gives rise to matched and mismatched arrangements that lead to enhanced (dr = 5:1) or compromised (dr = ~1:1) selectivities relative to simple analogs. Macrocyclic allenes also show greatly enhanced face selectivity in comparison to their acyclic analogues (not shown).[29] A better model includes the topography of the relevant allene and allene oxide conformers. In the case of **S1.46**, the major spirodiepoxide is favored by the conformational properties of the side chain in the allene oxide intermediate.[17] Thus the mismatched isomer favors the conformation approximated by structure **I**, which is facially unbiased, whereas the matched isomer is biased (*cf*. **II**). Structure **III** represents the favored conformer of the most common type of disubstituted allene encountered thus far (X = H or heteroatom), and structure **IV** represents the most common type of trisubstituted allene.[30] These conformers are compatible with a favorable stereoelectronic arrangement, wherein a good σ-donor is antiperiplanar to the highly polarized C-O bond of the strained allene oxide. Hence, for complex allenes, this conformational model is qualitatively predictive and anticipates the observed face selective oxidation.

Scheme 6. Diasteroselective Model for Spirodiepoxide Synthesis

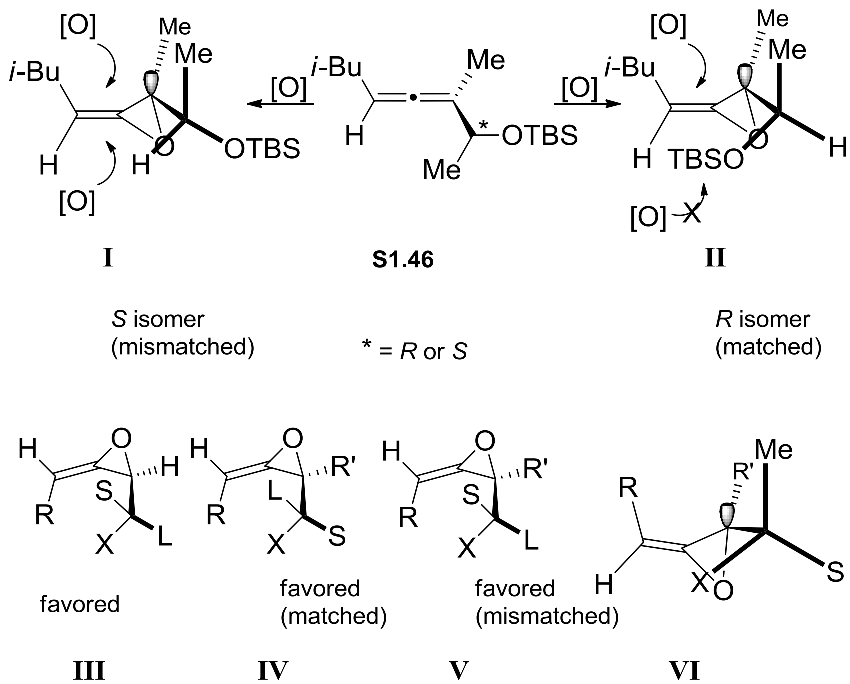

Scheme 7. Catalytic and Stereoselective Allene Oxidation

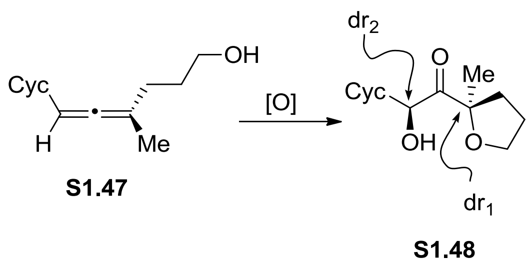

Oxidant	dr_1	dr_2
3 equiv. DMDO	>20:1	2:1
0.1 equiv. **S1.49**, $NaHCO_3$, Oxone	>20:1	29:2

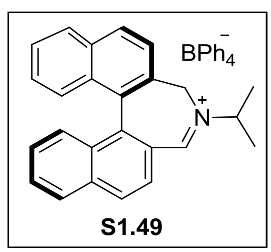

The chiral oxaziridinium catalyst (**S1.49**) appears to operate in a fundamentally different manner. The catalyst differentiates the two faces of the allene oxide through interactions involving the reacting terminus, which varies as a function of R. In our transition structure model, the catalyst (**S1.49**) is syn to the methyl group of the distal terminus and there is minimal interaction between the substrate and the catalyst (see for example, **VIII**, Scheme 8).[31]

The study and design of stereocontrolled allene epoxidation reactions has provided a much-improved understanding of allene reactivity towards these and related electrophiles.[22,23] This insight has been compiled through sustained investigations that also aimed to appraise and harness the reactivity of spirodiepoxides. The following section provides a sketch of this reactivity beginning with simple mildly basic nucleophilic addition reactions and culminating in a series of acid-induced cascade sequences.

Scheme 8. Catalytic Allene Oxidation Framework

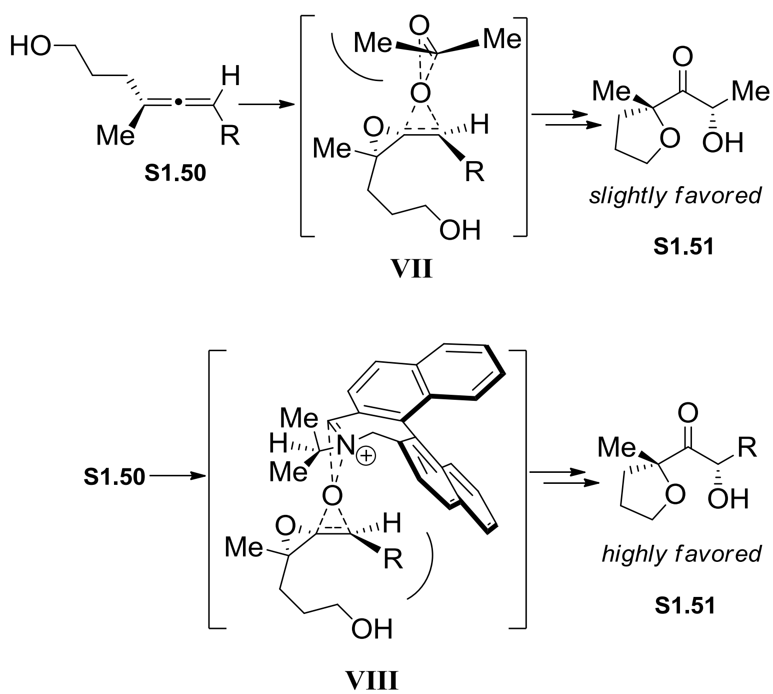

1.4 Reactions of Spirodiepoxide

Crandall Group was the first to report on the addition of heteronucleophiles – including water, ammonia, benzylamine, *n*-propylamine, imidazole, diethylamine, thiophenol, fluoride, and others – to simple spirodiepoxides. His Group demonstrated that an external nucleophile strongly favors addition to the most accessible terminus of the spirodiepoxide.[14] This was by no means obvious. Acid-promoted reaction pathways for this functionality are known; they favor reaction at the terminus most readily able to support positive charge; and they can compromise the fidelity of stereochemical information transfer from spirodiepoxide to ring-opened product. Although reactions done by Crandall Group were not optimized, the results suggested that nucleophilic addition to spirodiepoxides could well lead to useful products. Indeed, spirodiepoxides have proven synthetically useful and undergo many remarkable reactions.

High ring strain and low energy pathways that relieve this strain impart high reactivity to spirodiepoxide. Investigating the scope and limitations of this reactivity captured our imagination and led us to consider an array of possible transformations beyond simple nucleophilic addition. Still, we felt that several important nucleophile types should be evaluated and others reevaluated. Thus, heteronucleophiles, carbon nucleophiles, and ambiphilic nucleophiles, along with bases and Lewis acids and organometallics were investigated and determined to efficiently engage the spirodiepoxide functional group. Depending on the structural details and the reaction conditions, initial products may undergo further reaction to form heterocycles, oxygenated stereotriads, rearranged products, and other highly functionalized motifs.

Scheme 9 summarizes several heteronucleophile findings.[33,34] Examples of products derived from oxygen nucleophiles (**S1.55 - S1.57**),[33,34] halide (**S1.58 - S1.61**),[34] azide (**S1.62**),[33] and sulfonamide (**S1.63**)[33] are given. For many nucleophiles, the use of lithium as the gegenion leads to distinct improvements in yield. This seems to reflect a Lewis acid role for the counter ion that thereby promotes the reaction with weak nucleophiles.[34] The alternative approach of enhancing nucleophilicity, for example the use of potassium and 18-crown-6, is also effective at promoting reaction.[34] Some nucleophiles, e.g. water, methanol, and phenol, do not require use of base to promote addition. In these cases, excess nucleophile is necessary to achieve reaction with a sufficiently rapid rate to be synthetically useful. Tertiary butanol and trifluoroethanol, however, do not add efficiently to the spirodiepoxides that have been studied to date. And although sodium trifluoroethoxide adds under mildly basic conditions (**S1.56**),[34] *tert*-butanol does not add under basic conditions. Hence, pKa, solvation, and steric considerations govern these pathways in accord with other S_N2 reactions.

In many ways, nucleophilic addition to spirodiepoxides mirrors addition to epoxides. However, there are certain nucleophiles that diverge somewhat from epoxide chemistry and others that are altogether different.[34] In principle, phenoxide may react at either carbon or oxygen; only the phenyl ether is obtained (**S1.57**). Similarly, indole is alkylated by spirodiepoxides at nitrogen (**S1.64**). These indicate that the spirodiepoxide is somewhat hard. However, benzenesulfinate adds at the sulfur atom to give sulfone **S1.65** instead of adding at the oxygen atom to form a sulfinate ester.[34] Formation of the sulfone indicates that the spirodiepoxide functionality is relatively soft. *N,N*-dialkyl amides do not appear to react with spirodiepoxides, but dimethylformamide does, perhaps because

Scheme 9. Reaction of Spirodiepoxide with Heteronucleophile

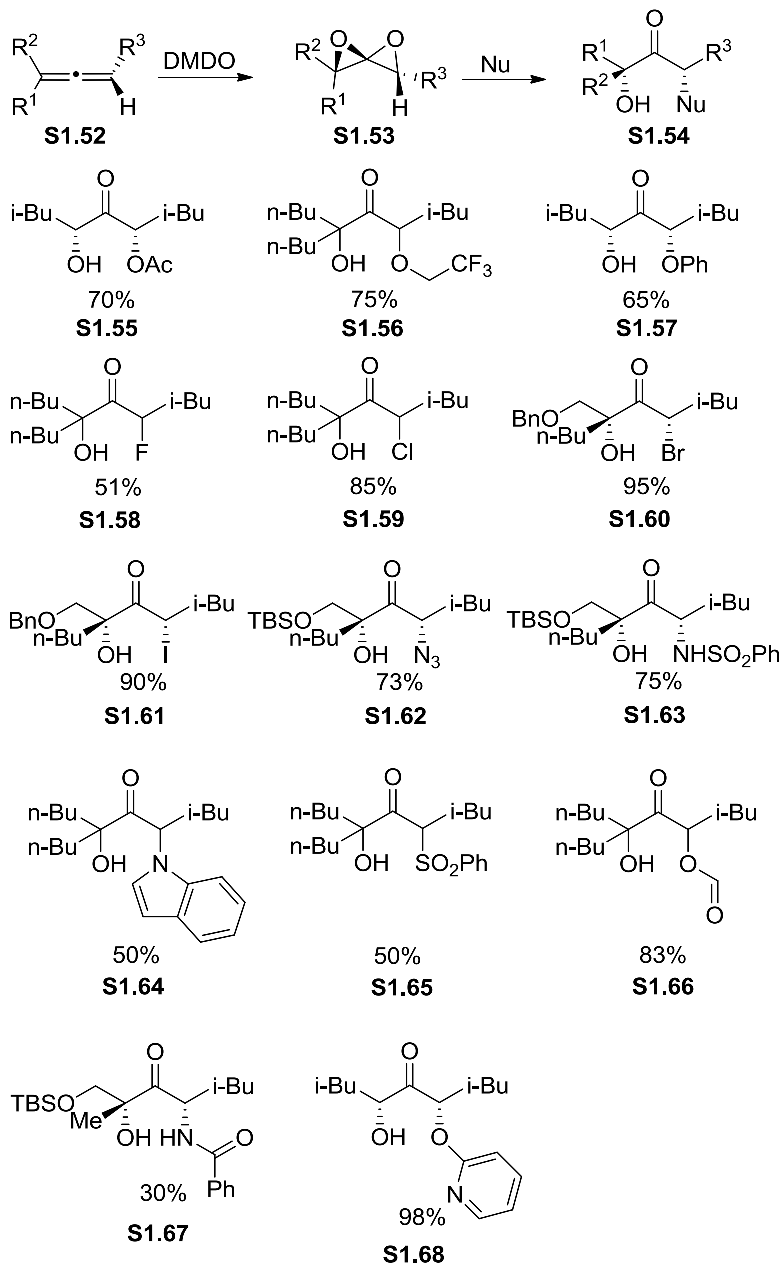

DMF can be used as solvent.[34] The formate product (**S1.66**) is obtained in very good yield. Under basic conditions, primary amides add to give the corresponding alkyl amide, but many other side reactions are evident and the yield of the resultant alkyl amide is modest. Remarkably, one equivalent of the cis amide 2-pyridinone reacts rapidly with spirodiepoxide – in the absence of base – to give the ether in excellent yield (**S1.68**).[33] Primary amides add under neutral conditions as well in stoichiometric ratios (5 equivalents of amide), but the products are heterocycles (see Scheme 18). These data indicate reactivity that is dependent upon the structures of the nucleophile and the spirodiepoxide functional group and do not mirror simple epoxides.

Silyl substituted spirodiepoxides are much less reactive than their non-silyl counterparts. Silyl spirodiepoxides are stable in the presence of water and even neat alcohol. Unlike a nonsilyl spirodiepoxide, the silyl spirodiepoxide does not undergo uncontrolled decomposition in the presence of carboxylic acid. For example, the silyl spirodiepoxide derived from allene **S1.69** reacts smoothly with benzoic acid to give substituted hydroxyketone **S1.70** in 79% yield as a single diastereomeric (Scheme 10). Similarly, this spirodiepoxide reacts with acetic acid to give substituted hydroxyketone **S1.71** in 81% yield.[20] For these substrates, the nucleophile adds to the epoxide proximal to the silyl group, much like silyl substituted epoxides.[35] Thus, the silyl substituent controls much of the behavior of the allene: it directs the initial allene epoxidation regiochemistry, the face selectivity of the second oxidation (vide supra, Section 2), and the site-selective opening of the spirodiepoxide. However, to date, mild acid is required. Although these substrates readily undergo elimination reactions (see below), they do not readily undergo anionic addition reactions.

We have developed organometallic mediated openings of spirodiepoxides, including C-C bond forming reactions. This method is based on cuprate technology and the products are α-alkyl-α′-hydroxyketones. Many organocuprates were evaluated. Most cuprate reagents, except for lower order lithium cyanocuprates, give two products:

substituted hydroxyketone **S1.73** and hydroxyketone **S1.74** (Scheme 11).[36] A mechanistic framework provides a simple rationale for these observations (Scheme 12). Although several reagent combinations are effective, lower order cyanocuprates, generated from alkyl lithium species, gave the most reliable and highest yields of the desired substituted products (**S1.79**, Scheme 13).

Scheme 10. Addition of Nucleophile to Silyl Spirodiepoxide

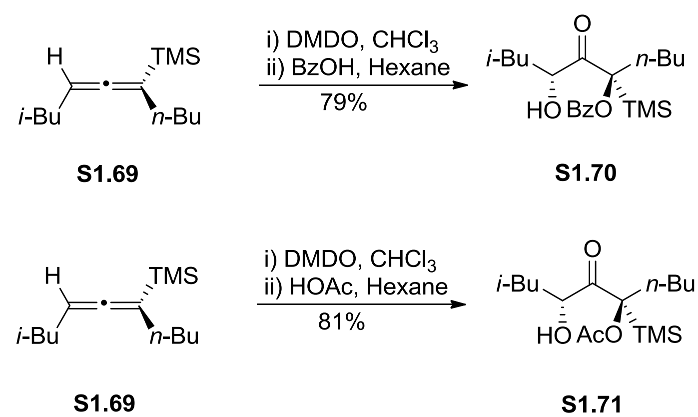

Scheme 11. Addition of Cuprate to Spirodiepoxide and Mechanistic Framework

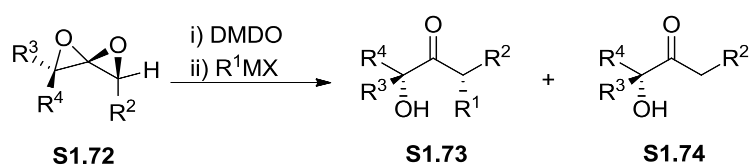

As shown in Scheme 12, the desired α-alkyl-α′-hydroxyketone (**S1.73**) appears to form via nucleophilic opening of the spirodiepoxide by the cuprate to give a Cu (III) intermediate of type **S1.75** followed by reductive elimination to form the desired product. Alternatively, Cu (III) intermediate **S1.75** may isomerize to form enolate **S1.77**, and then α-hydroxyketone **S1.74**.[36] Although not unexpected, it is noteworthy that the cuprate does not add to the resultant ketone. The favored pathway depends primarily upon the cuprate salt and secondarily upon the organic ligand and spirodiepoxide. For example, the standard method was used to prepare **S1.80** - **S1.85** efficiently. In the synthesis of **S1.86** the cyanocuprate founder on the bulk of the organic ligand. In this case, the more reactive Gilman reagent proved to be superior and gave addition products **S1.86** in good yield.[36] In the case of very complex spirodiepoxides such as **S1.87**, the cuprate method has not delivered the desired products, instead rearranged products have been noted (described in Section 5).[22]

Scheme 12. Mechanistic Framework for Cuprate Addition

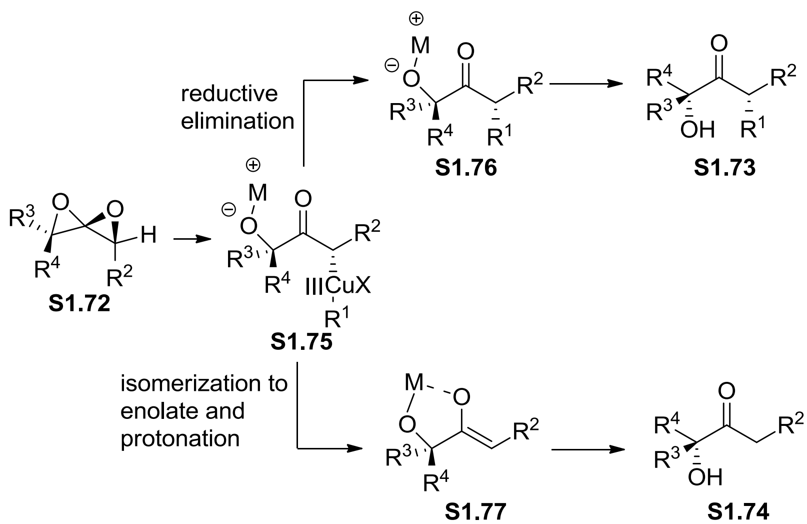

Cuprates were required to realize efficient addition of highly basic sp^3-type carbanion nucleophiles to spirodiepoxides; however, in case of more stable carbanions the use of cuprates has been unnecessary (Scheme 14). Thus, cyanide adds to spirodiepoxides to form the corresponding nitrile derivatives (e.g. **S1.89**→ **S1.90**, Scheme 14).[33,34] The acetonitrile anion added smoothly, as well (**S1.91**→ **S1.92**). Interestingly, addition of the nucleophile to the ketone product was not observed under these basic conditions. Additionally, alkynyl and vinyl lithium reagents add to spirodiepoxides without the aid of copper-based organometallic reagents. The products obtained from these reactions, however, were diols (**S1.93** and **S1.94**, Scheme 14).[34] For these more basic nucleophiles, a second nucleophilic addition was observed and was highly stereoselective. A mechanistic framework for the formation of **S1.93** and **S1.94** is discussed in Chapter 3.

Scheme 13. Spirodiepoxide Reaction with Cuprates

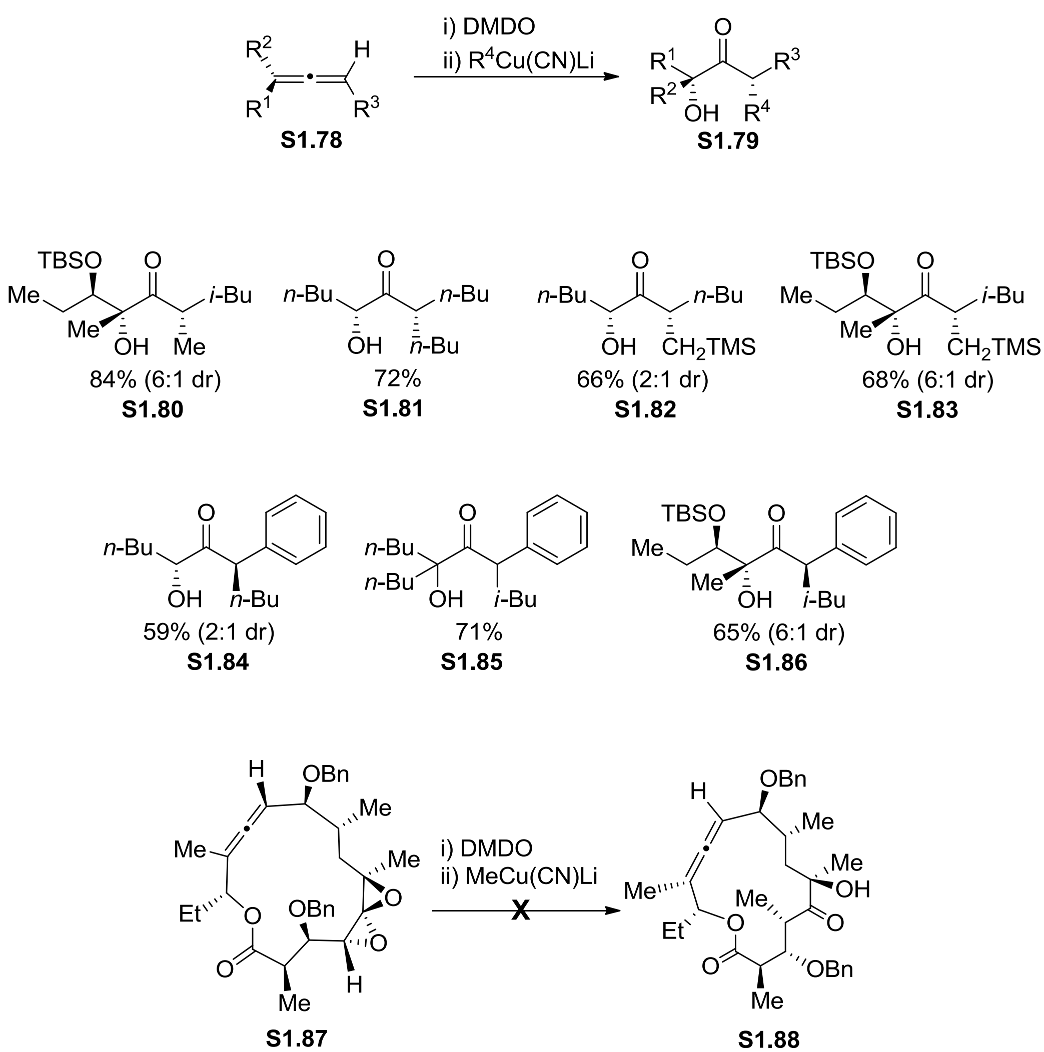

Annulations reactions are also readily achieved with spirodiepoxides by careful choice of reagents. The synthesis of furanones points up the high reactivity of these electrophiles in a remarkable way.[34] Isonitriles are weakly nucleophilic and upon alkylation become electrophilic. We reported that the simple combination of spirodiepoxides with this ambiphilic nucleophile gave the corresponding furanone (**S1.96**, Scheme 15).[34] A mechanistic framework for the formation of **S1.96** is discussed in Chapter 3.

Scheme 14. Addition of Carbon Nucleophile

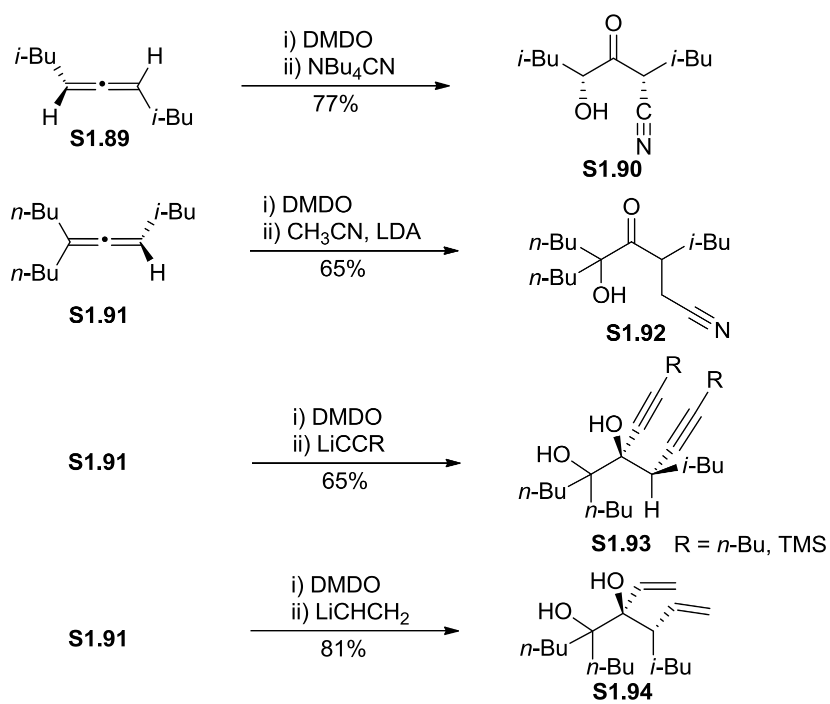

Scheme 15. Synthesis of Furanones from Spirodiepoxide

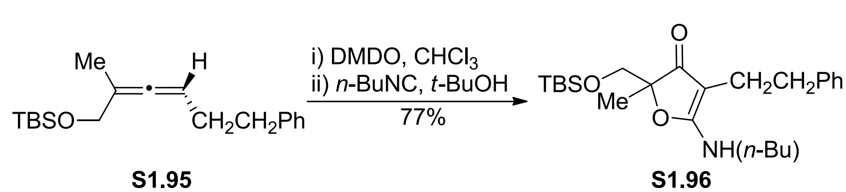

Malonate addition to spirodiepoxides is accompanied by ring formation by way of spontaneous lactonization (**S1.91→ S1.97**, Scheme 16).[34] This useful transformation creates a new C-C bond, a new C-O bond, and a new stereocenter.

Scheme 16. Synthesis of Lactones from Spirodiepoxide

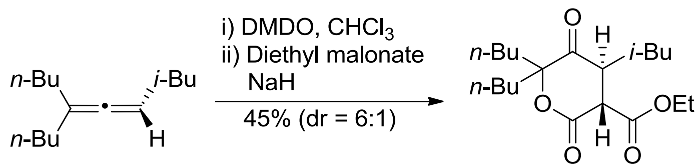

S1.91 **S1.97**

The previous annulation reactions create rings by engaging the hydroxyl group that results from nucleophilic addition to the spirodiepoxide. We also reported a cascade annulation – formation of butenolides – that engages the nascent carbonyl formed from spirodiepoxide opening (Scheme 17).[34] For example, allene **S1.98** was epoxidized and then exposed to 2-(diepoxyphosphoryl)acetic acid in the presence of potassium carbonate and crown ether. Butenolide **S1.99** was isolated in good yield.

Scheme 17. Synthesis of Butenolide from Spirodiepoxide

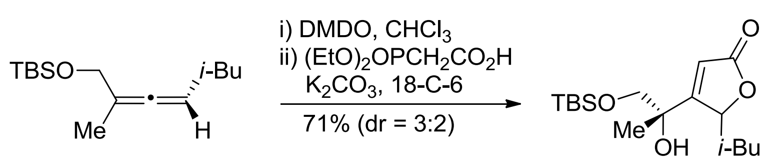

S1.98 **S1.99**

In additional to saturated and partially saturated heterocycles of various classes, aromatic heterocycles can be prepared from spirodiepoxide.[34] The addition of amides to spirodiepoxides in the context of simple nucleophilic additions was described in Scheme 9. This initial insight was further developed into a method for preparing azolines (**S1.100**) and the corresponding aromatized azoles (**S1.105**, Scheme 18). The transformation is effective for preparing highly enantioenriched heterocycles that bear a tertiary alcohol in the pseudo-benzylic position from trisubstituted allenes. A simpler single-flask procedure was developed using silyl substituted allenes. This substrate class allows for aromatic heterocycle synthesis under milder conditions and the preparation of highly enantioenriched products that bear a secondary alcohol in the pseudo-benzylic position. Hence, amides, amidines, and thioamides add efficiently to spirodiepoxides. Amides give oxazolines, thioamides give thiazolines, and amidines give imidazolines. The imidazolines are difficult to isolate in pure form since they readily aromatize to imidazoles. The oxazoline and thiazolines can be converted to oxazoles and thiazoles, respectively, by dehydration. For example, the synthesis of azoles **S1.105** involves spirodiepoxidation of allene **S1.103**, addition of amide **S1.105**, and then reflux in *p*TsOH. As expected, thiobenzamides and benzamidines add faster to spirodiepoxides compared to benzamides. The silyl substituted spirodiepoxides behave similarly, and are conveniently converted to the unsaturated heterocycles in a single reaction vessel. Silyl allenes can also be used to synthesize the aromatic heterocycles (Scheme 18). As expected, the silyl substituted spirodiepoxides react slower than non-silyl spirodiepoxides. The reaction proceeds with migration of the silyl group to the adjacent oxygen followed by methanol-promoted loss of the silyl group to form the azoles **S1.107**.[20]

The chemistry of silyl substituted spirodiepoxides has not been extensively studied. However, another interesting and highly useful transformation has been identified: the site-selective and stereoselective synthesis of α′-hydroxyenones (**S1.109→**

S1.110→ S1.111 or **S1.112**, Scheme 19). The silyl group appears to govern the formation of the hydroxyenone and the stereochemical outcome, depending on the conditions used.[20]

Scheme 18. Synthesis of Azolines and Azoles from Spirodiepoxide

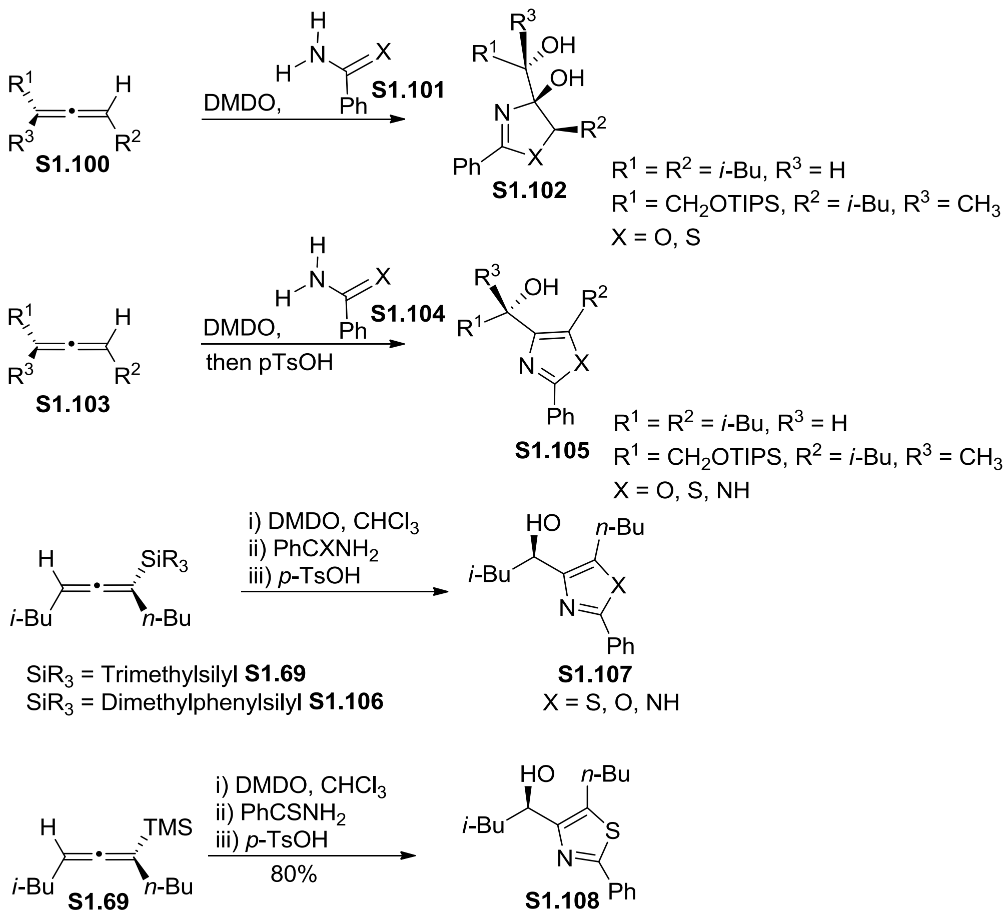

Scheme 19. Mechanistic Framework for the Eliminative Opening of Silyl Spirodiepoxide

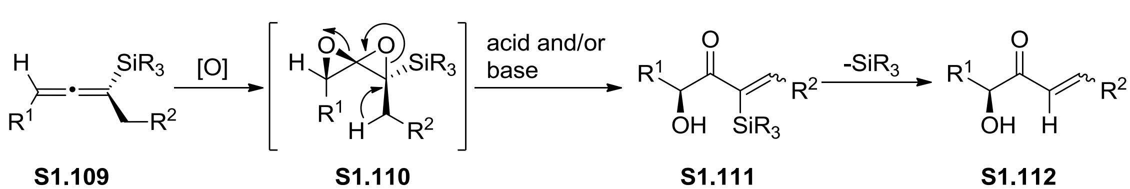

Alkyl lithium and alkyl magnesium reagents, as well as cyclopentadienyltitanium (IV) chloride in presence of zinc dust convert spirodiepoxides to α′-hydroxyenones (Scheme 20). The *E*/*Z* selectivity depends on the reagent used and the substrate structure. Reagent mixtures containing cyclopentadienyltitanium (IV) chloride and zinc dust favor α′-hydroxy-*Z*-enone product **S1.113**. Organolithium and alkyl magnesium bromide favor α,β-dihydroxy olefins **S1.114** and **S1.115**, where methyllithium gives the *E* enone (**S1.114**), and methyl magnesium bromide favor *Z* enone (**S1.115**). The mechanisms by which these reactions take place have not been investigated, even though the transformations and the mechanistic possibilities are intriguing.

The above Lewis acid- and organometallic-promoted reactions are remarkable in part because acids normally promote the uncontrolled decomposition of spirodiepoxides. For example, early on, it was shown that Brønsted acid exposure results in the formation of multiple products from a single spirodiepoxide (**S1.116**). The product includes mixtures of stereo- and regio-isomers from nucleophilic addition of the carboxylate (**S1.117**), rearrangement products, such as oxetanones (**S1.118**) and skeletal rearrangements (not shown), as well as various α′-hydroxyenone isomers (**S1.119**) among others (Scheme 21).[8-10]

Spirodiepoxides are clearly reactive. Still, they are much less problematic than might have been expected. For example the controlled rearrangement of a spirodiepoxide was achieved using the Brønsted acid derived as a byproduct from *m*-CPBA.[37] The elimination design is shown in Scheme 22 (**S1.120→ S1.122**). A substrate (**S1.121**) was designed to undergo site selective Brønsted acid promoted heterolytic bond cleavage. Additionaly, a disposable group was placed proximal to the anticipated site of carbocation formation. In this way, the transformation converged on a single enone product (**S1.122**). Thus epoxide was designed to give **S1.121** and then the byproduct of the epoxidation, a Brønsted acid, would promote the heterolysis and thence product formation.

Scheme 20. Eliminative Opening of Silyl Spirodiepoxide

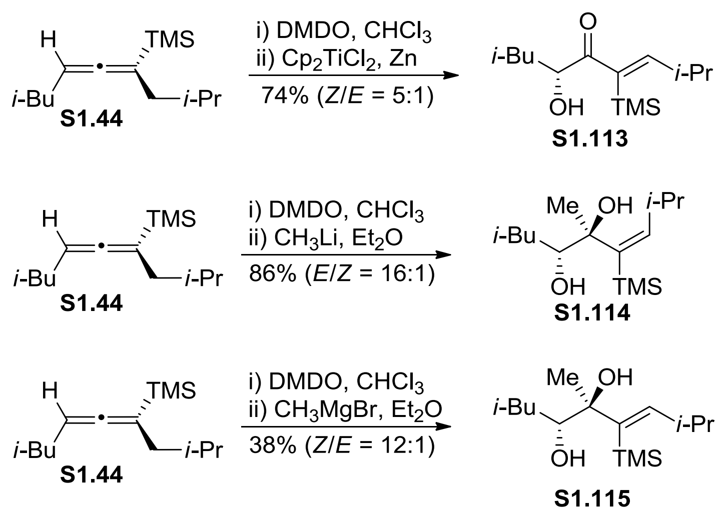

Scheme 21. Instability of Spirodiepoxide in Acid

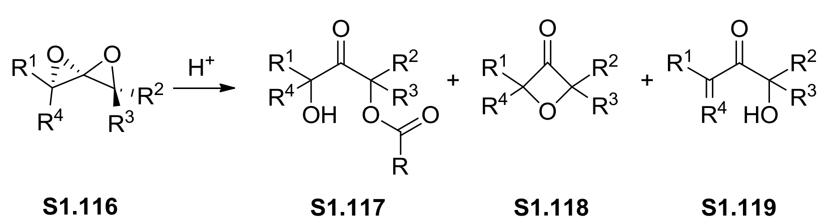

Scheme 22. Controlled Acid Induced Spirodiepoxide Rearrangement

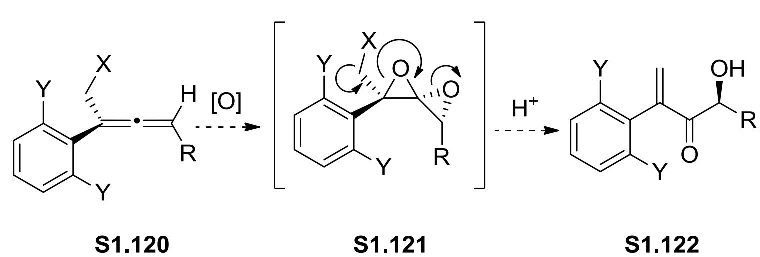

We used highly functionalized aryl allene **S1.123**. Upon subjection to *m*-CPBA two enones were isolated, **S1.124** and **S1.125** (dr = 5:2, Scheme 23). The diastereomeric ratio suggests that the oxidation of the allene oxide is selective, and the product yield indicates a highly efficient process. Thus, at least for properly designed substrates, controlled Brønsted acid-induced rearrangements are feasible with the spirodiepoxide functional group.

The oxidation of allene **S1.123** probably occurs at the disubstituted site first to form allene oxide **S1.126** (Scheme 24). An alternative conformation is shown as **S1.127**. Allene oxide **S1.126** suffers from destabilizing interaction between the silyl substituent and the aryl group, whereas **S1.127** does not. The second epoxidation should favor approach to **S1.127** from the top face to give spirodiepoxide **S1.128**, which undergoes rearrangement to give the observed enones.

Scheme 23. Formation of Enones

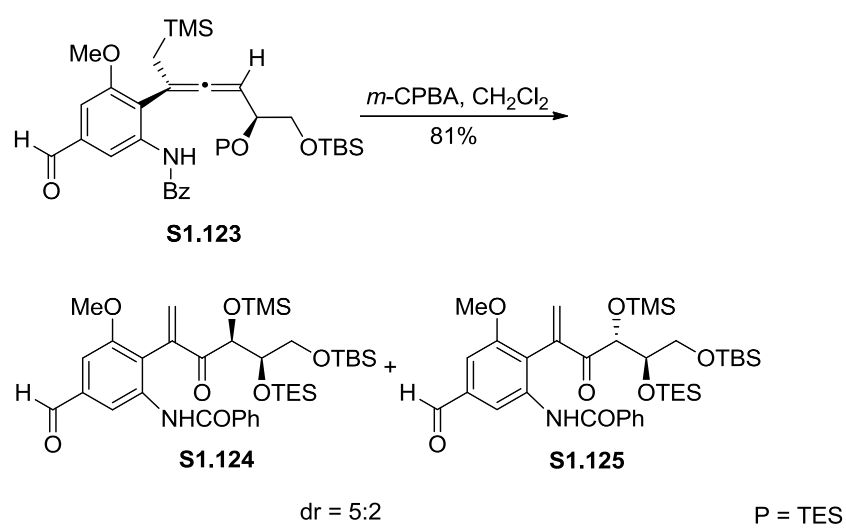

Scheme 24. Synthesis of the Spirodiepoxide

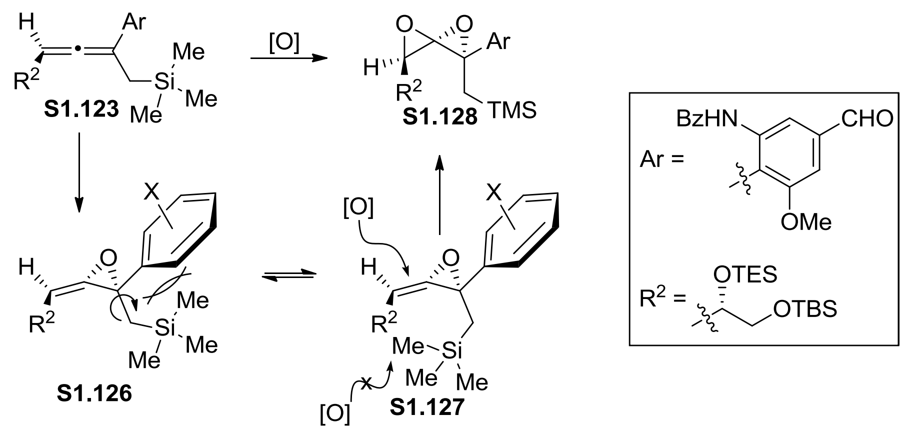

1.5 Spirodiepoxide in Complex Molecule Synthesis

Spirodiepoxide based transformation are cascade reactions. As with other cascade reactions, the spirodiepoxide functionality allows direct entry into densely functionalized cyclic and acyclic motifs. We have used spirodiepoxide based cascade in the synthesis of various natural products (see Figure 3, page 6).

The first application of a spirodiepoxide in the synthesis of complex molecules was reported in 1996 by Andrews and co-workers.[38] They used spirodiepoxide **S1.130** in the synthesis of betamethasone **S1.132** (Scheme 25). The allene (**S1.129**) was subjected to DMDO epoxidation and the corresponding spirodiepoxide (**S1.130**) was treated with tetrabutylammonium acetate to generate α-acetate-α′-hydroxy ketone **S1.131**, which was eventually converted to betamethasone **S1.132**.

We have utilized spirodiepoxide base cascade in the total synthesis of epoxomicin **S1.15** (Scheme 26).[16,17] The epoximicin (**S1.15**), a potent proteasome inhibitor, was prepared enantioselectively using a highly efficient route (20% overall yield). The enantioenriched propargyl alcohol (**S1.133**) was converted to chiral allene **S1.134**. The allene (**S1.134**) was subjected to DMDO spirodiepoxidation followed by addition of an azide to give the *syn* α-azido-α′-hydroxy ketone (**S1.135**) in 73% yield (dr = 3:1). The α-azido-α′-hydroxy ketone (**S1.135**) was then exposed to *in situ* reduction and protection sequence to give amine salt **S1.135** in 91% yield. The coupling partner was prepared from **S1.136**. Coupling of **S1.136** with methyl isoleucinate, Boc removal and acetylation, saponification, coupling to threonine and then hydrogenolysis gave the peptide coupling partner. The amine salt (**S1.135**) was coupled efficiently with its peptide coupling partner to give epoxmicin **S1.15**.

Scheme 25. Spirodiepoxide in the Synthesis of Betamethasone

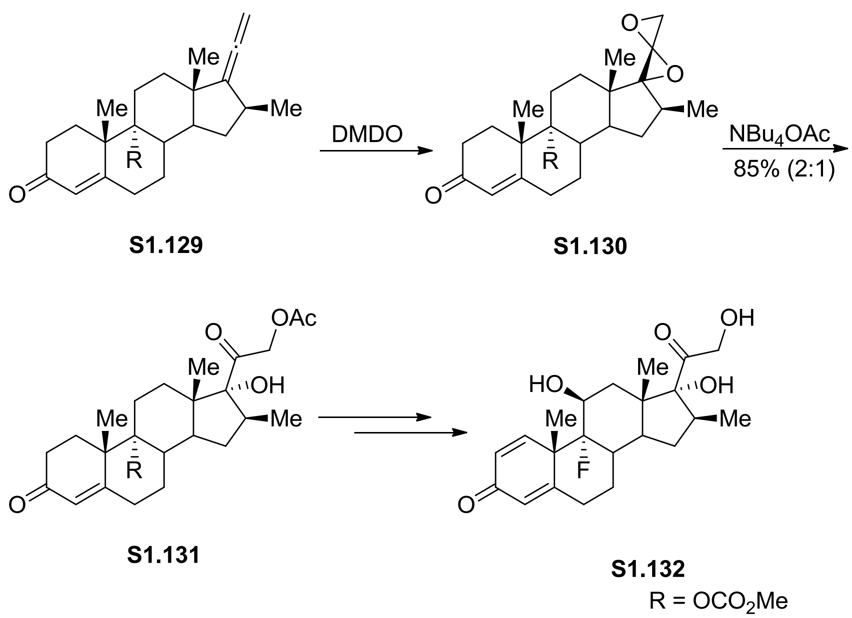

We have applied spirodiepoxide functionality in our study towards the synthesis of erythromycin **S1.19**. We utilized macrocyclic bisallene **S1.139** and **S1.140** as a platform to access various functionalized motifs.[22] The bisallenes (**S1.139** and **S1.140**) were prepared from propargyl alcohol **S1.137** (Scheme 27). The propargyl alcohol

(**S1.137**) was converted to corresponding bisallene **S1.138** in one step. Macrolactonization of bisallaene **S1.138** gave 1:1 separable mixture of allenes **S1.139** and **S1.140**, in good yield.

Scheme 26. Spirodiepoxide in the Synthesis of Epoxomicin

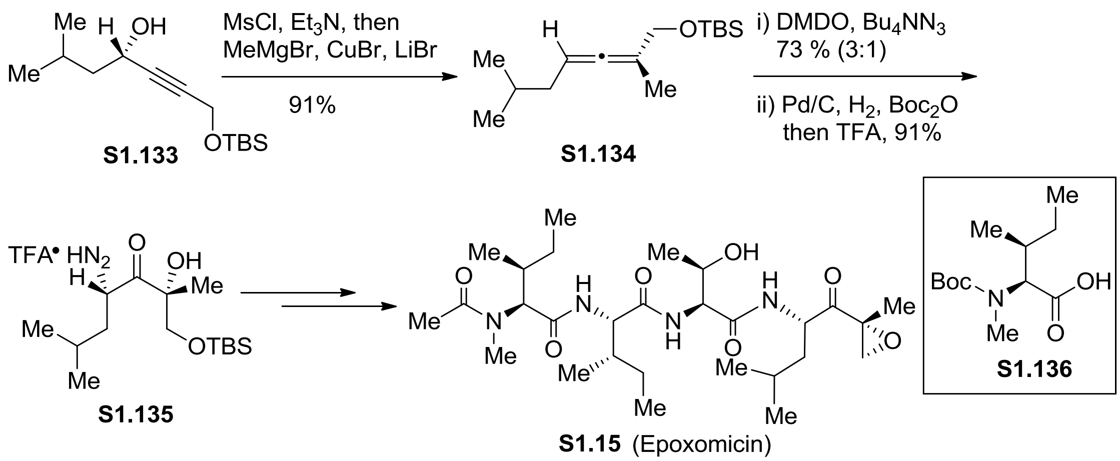

The macrocyclic bisallene (**S1.139**) was selectively spirodiepoxidized to generate mono[spirodiepoxide]. Addition of water to the mono[spirodiepoxide] resulted in the formation of diol. Protection of the secondary alcohol in the presence of tertiary alcohol gave hydroxyl ketone **S1.141** (Scheme 27). In cyclic system, bias for the approach of an oxidant is reinforced, so oxidation of allene **S1.139** followed by addition of water gave single diastereomer of the diol.

We have used the cuprate mediate opening of a spirodiepoxide in the synthesis of the stereotetrad of erythromycin (Scheme 28).[36] The oxygenated polypropionate stereotetrad (**S1.145**) was prepared in short, efficient and selective route via oxidation/organocuprate addition of allene **S1.143**. The allene (**S1.143**) was subjected to DMDO in $CHCl_3$ to form spirodiepoxide. The spirodiepoxide was then exposed to methylcyanocuprate to form the α-methyl-α′-hydroxy ketone (**S1.144**) in 80% yield (dr = 8:1). The ketone (**S1.144**) was then converted to **S1.145** in four additional steps.

Scheme 27. Spirodiepoxide Based Cascade in Macrocyclic Bisallene

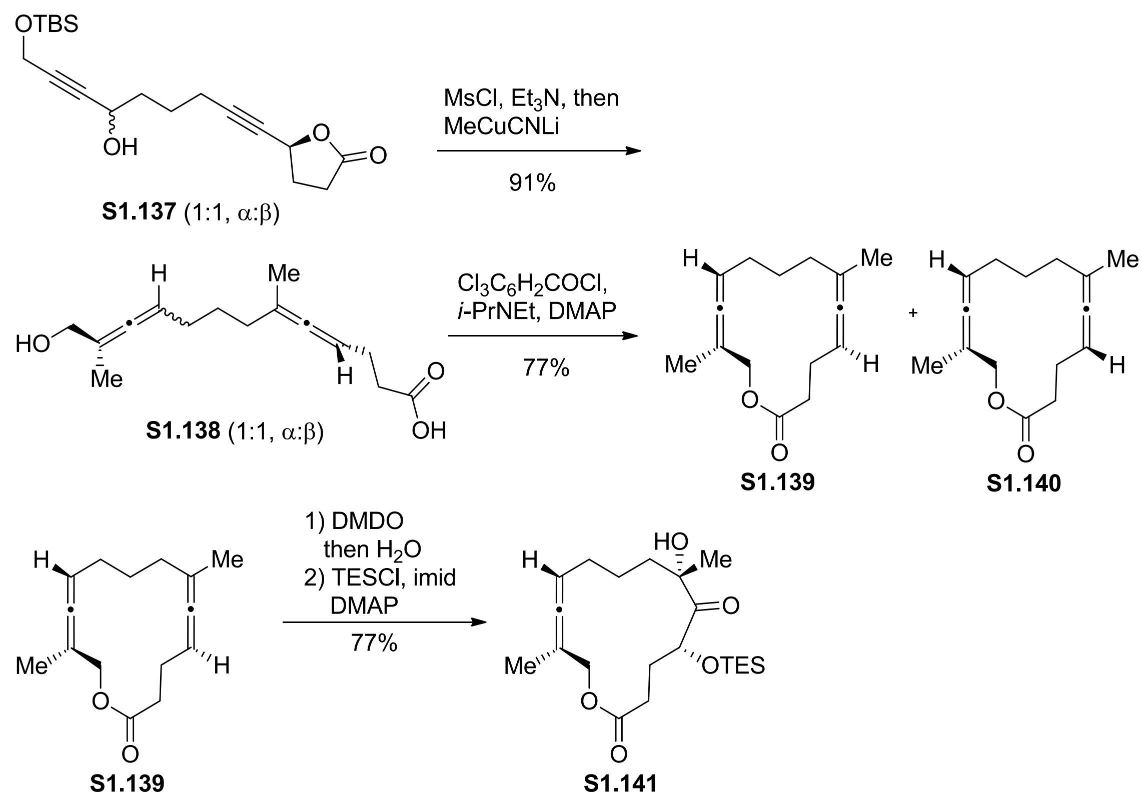

Scheme 28. Spirodiepoxide in the Synthesis of Stereotetrad of Erythromycin

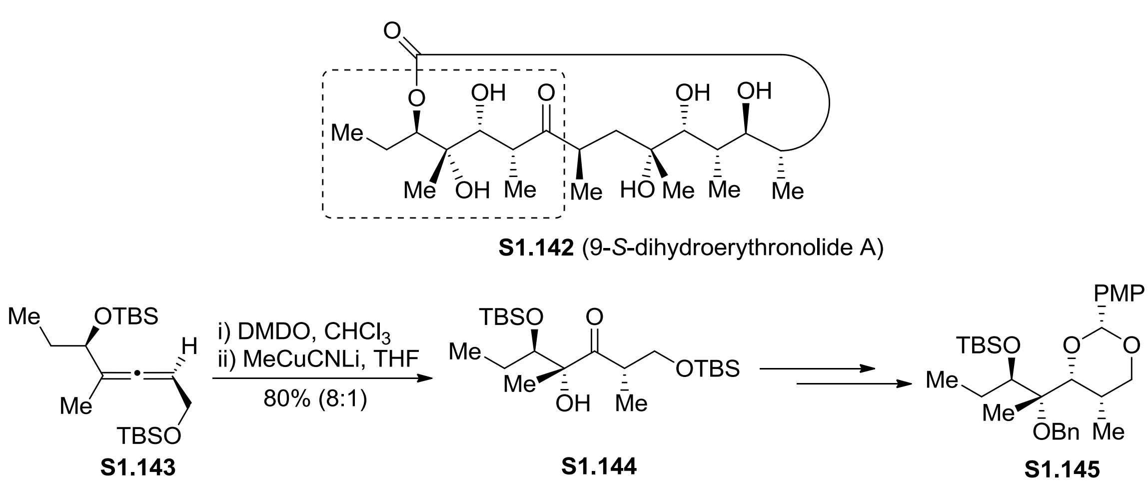

We have utilized cuprate method, outlined in Scheme 13, in complex allene **S1.140** (Scheme 29).[22] Use of super stoichiometric amount of DMDO resulted in the epoxidization of both allenes of macrocyclic bisallene **S1.140**. The bis[spirodiepoxide] was then opened by methylcyanocuprate to form the addition product (**S1.146**) and the rearranged product (**S1.147**). The addition product (**S1.146**) was obtained in 22% yield and single diastereomer. The 22% yield is very impressive because in one step we were able to introduce four oxygens as bis[spirodiepoxide] and then convert the bis[spirodiepoxide] to two ketones, two tertiary alcohols and two methyl groups. In this transformation, we established six stereogenic centers and added new functionalities in just one step. The rearranged product (**S1.147**) was obtained in 17% yield. We reasoned that the Lewis acid mediated rearrangement of one of the spirodiepoxide of the bis[spirodiepoxide] facilitated the formation of oxetan-3-one **S1.147**.

Scheme 29. Cuprate Mediated Opening of Macrocyclic bis[spirodiepoxide]

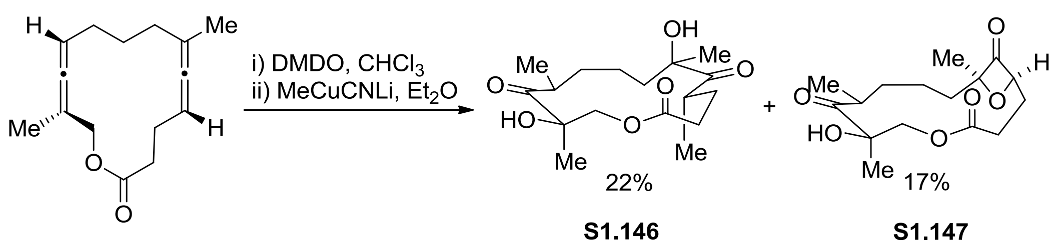

S1.140 **S1.146** **S1.147**

After our success in the addition of methylcyanocuprate to the bisallene **S1.140**, we wanted to add methylcyanocuprate to the bisallene **S1.148** (Scheme 30).[23] The cyclic bisallene **S1.148** was subjected to DMDO mediated spirodiepoxidation followed by the addition of methylcyanocuprate. Instead of forming the desired product **S1.88** (see Scheme 13), the reaction resulted in the formation of furanone **S1.149**.

Scheme 30. Cuprate Mediated Rearrangement of Spirodiepoxide

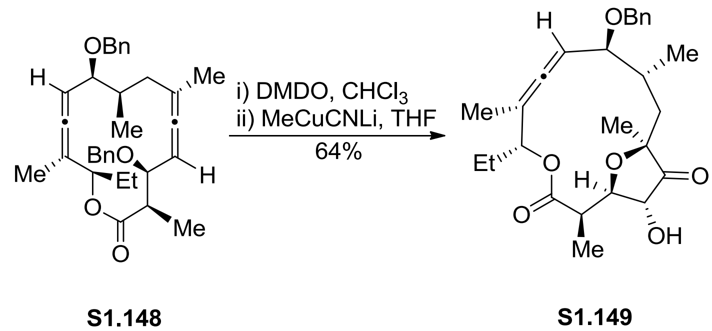

We rationalized that the formation of furanone **S1.149** involves Lewis acid mediated rearrangement of spirodiepoxide **S1.87** (Scheme 31). Selective oxidation of one allene of bisallene **S1.148** resulted in the formation of spirodiepoxide **S1.87**. The spirodiepoxide (**S1.87**) is unstable in the reaction condition and the C3 benzyloxy group is in the close proximity. So, the spirodiepoxide (**S1.87**) captures the C3 benzyloxy group to form **S1.150**. The benzyloxy group is then lost to form the furanone **S1.149**.

Scheme 31. Mechanistic Framework for the Synthesis of Furanone

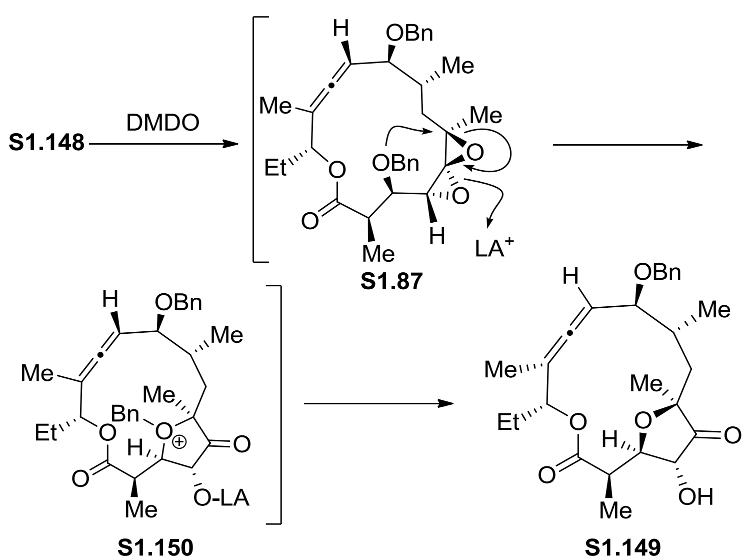

We also used the macrocyclic bisallene to synthesize **S1.151** (Scheme 32).[23] Selective epoxidation of one allene of cyclic bisallene **S1.148** resulted in the formation of mono[spirodiepoxide]. In the presence of methanol, the mono[spirodiepoxide] rearranged to form **S1.151**.

We reasoned that the formation of **S1.151** involves allene oxide **S1.152** rather than spirodiepoxide (Scheme 33). We believe that the bisallene forms allene oxide **S1.152**. The allene oxide (**S1.152**) opens to form oxyallyl zwitterion **S1.153**. The zwitterion (**S1.153**) captures the C3 benzyloxy group to form **S1.154**. The intermediate **S1.154** undergoes 3,4-elimination to form **S1.151**.

Scheme 32. Spirodiepoxide Based Rearrangement in the Synthesis of Erythronolide

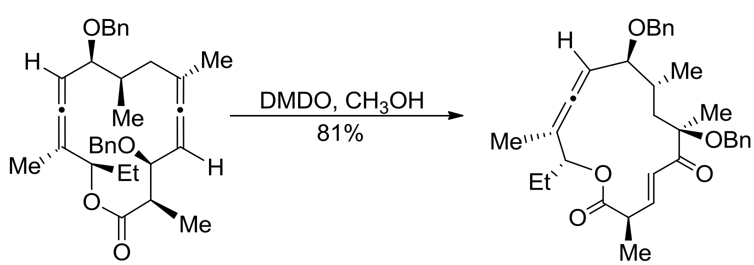

S1.148 **S1.151**

We have developed an efficient method for the synthesis of azolines and azoles (see Scheme 21).[33] We utilized the method outlined in Scheme 21 in the synthesis of **S1.155** and **S1.156** (Scheme 34).[22] Oxidation of bisallenes **S1.139** and **S1.140** followed by addition of thiobenzamide resulted in the formation of functionalized bis[thiazolines] **S1.155** and **S1.156**, respectively. In this transformation we were able to introduce four oxygen atoms and two rings to the cyclic bisallene in just one step.

Scheme 33. Mechanistic Rationale

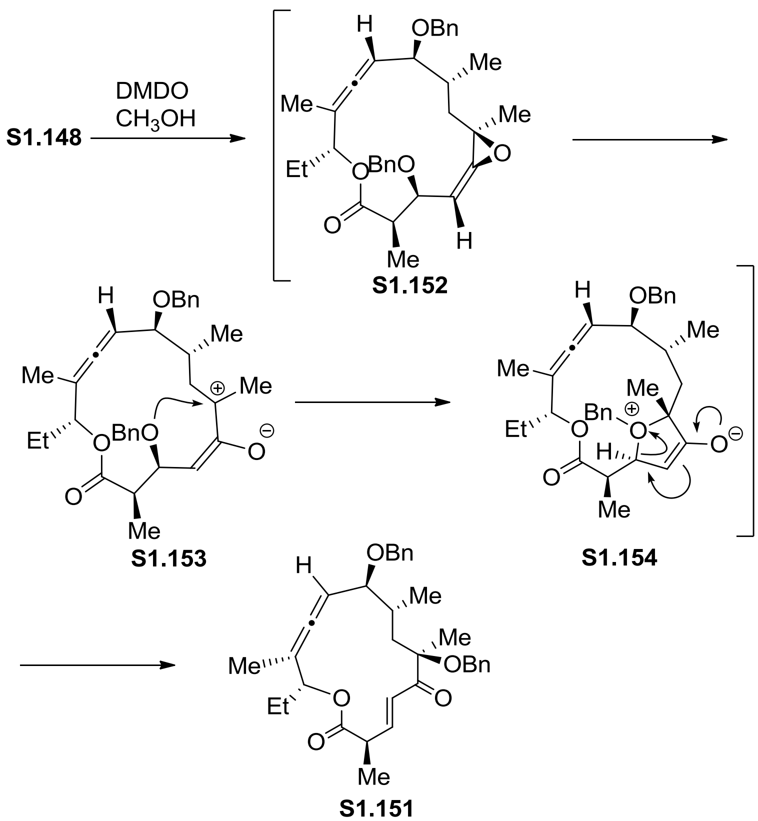

Scheme 34. Spirodiepoxide in the Synthesis of bis[thiazoline]

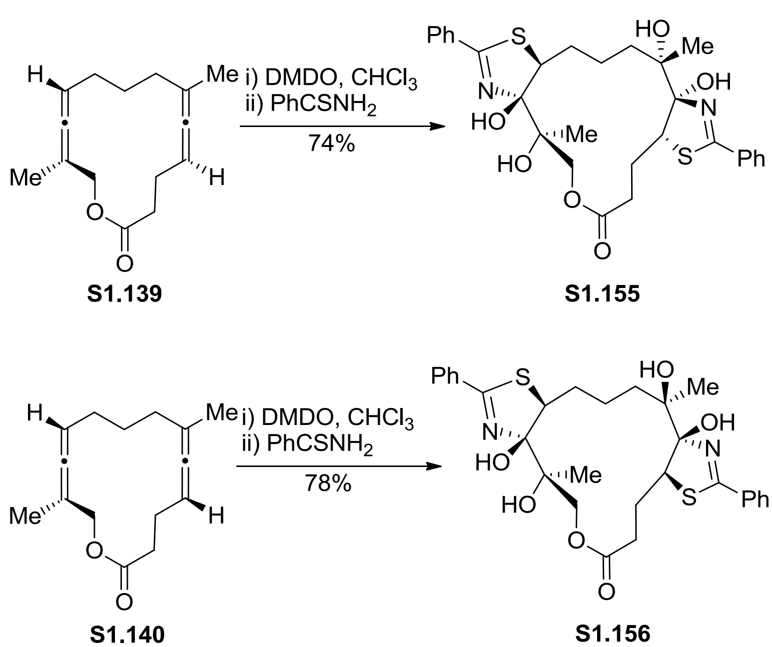

We have used spirodiepoxide based cascade in the formal synthesis of psymberin **S1.16**, a selective and potent *anti*-tumor agent, and have prepared key intermediate **S1.159** (Scheme 35).[18,19] We have used our spirodiepoxide based cascade in the synthesis of the pyran (**S1.158**) of psymberin **S1.16**. The functionalized trans-2,6-disubstituted pyran **S1.158** was synthesized by oxidation of the 1,3-disubstituted allene (**S1.157**) in the presence of methanol, followed by *endo* cyclization.

Scheme 35. Spirodiepoxide in the Synthesis of Psymberin

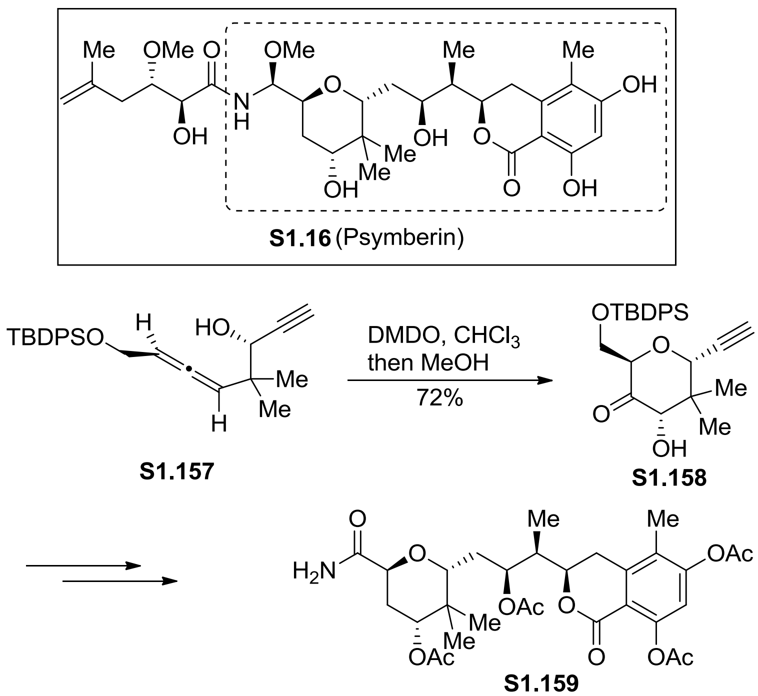

The allene **S1.157** did not convert smoothly to the corresponding pyran. The synthesis of pyran **S1.158** required addition of methanol. We rationalized that the spirodiepoxide can attain two confirmations **S1.160** and **S1.161** (Scheme 36). Both spirodiepoxides **S1.160** and **S1.161** resists cyclization. Spirodiepoxide **S1.160** is stabilized by the hydrogen bond interaction and thus does not undergo smooth conversion. Spirodiepoxide **S1.161** is reactive. However, spirodiepoxide **S1.161** is destabilized by unfavorable steric interaction between the spirodiepoxide and the alkyne. The use of methanol facilitates the cyclization. Methanol disrupts hydrogen bond present in spirodiepoxide **S1.160** and induces cyclization to give desired pyran **S1.158**.

During our formal synthesis of Psymberin, we discovered that the spirodiepoxide opening is configuration dependent. The synthesis of *trans*-pyran **S1.158** from allene **S1.157** required methanol (Scheme 35). Unlike the synthesis of pyran **S1.158**, the synthesis of *cis*-pyran **S1.163** did not require methanol. The allene **S1.162** smoothly converted to *cis*-pyran **S1.163** (Scheme 37). We rationalized that the oxidation of allene **S1.162** results in the formation of spirodiepoxide, which can attain two confirmations **S1.164** and **S1.165** (Scheme 37, bottom). The hydrogen bonded spirodiepoxide (**S1.164**) is destabilized by severe steric interaction and is thus not favored. However, spirodiepoxide **S1.165** is favored and leads to the synthesis of pyran **S1.163**.

Scheme 36. Spirodiepoxide Cyclization Model

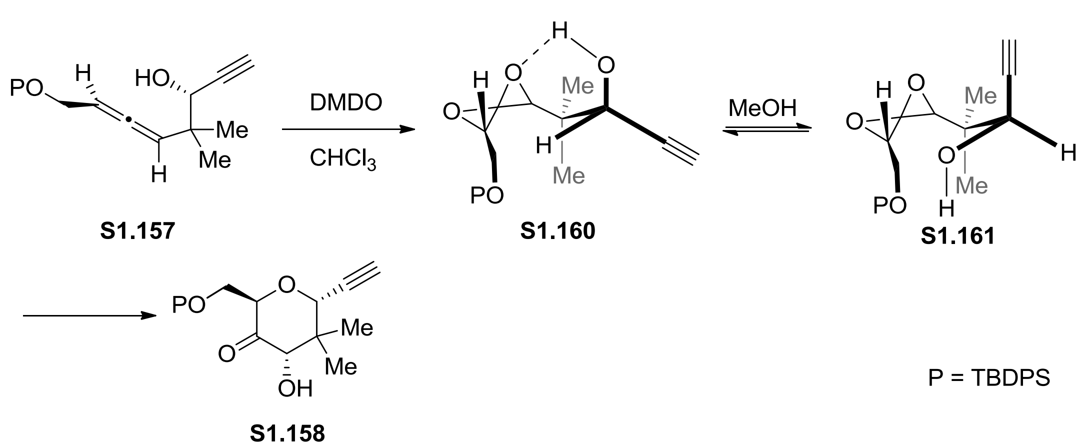

Scheme 37. Synthesis of cis-pyran

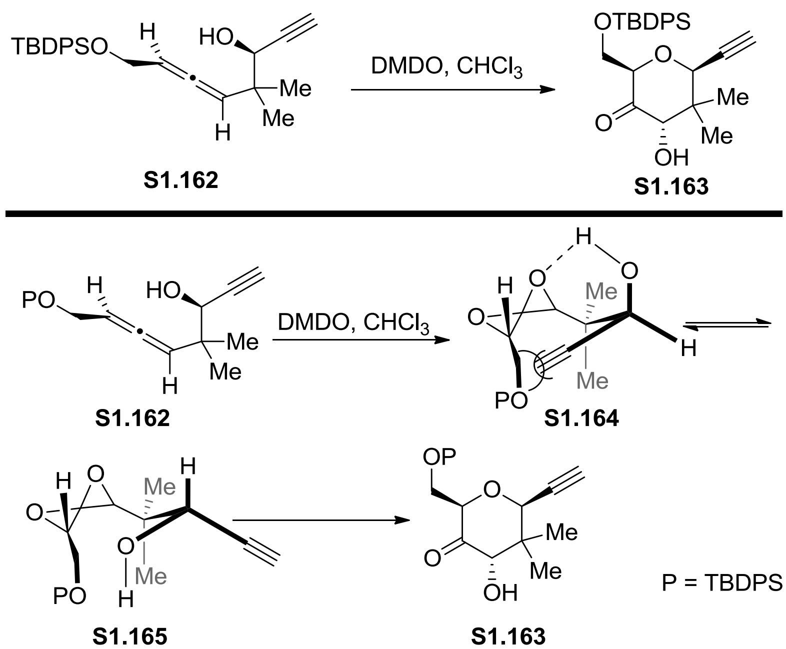

We have utilized silyl spirodiepoxide derived from silyl allene **S1.43** in the first total synthesis of epi-citreodiol **S1.17** (Scheme 38).[20] We used spirodiepoxide based transformation in the synthesis of diol **S1.166**. Oxidation of silyl allene **S1.43**, reaction with methyllithium in ether, followed by proteodesilation in acetonitrile gave diol **S1.166** as single isomer in 69% yield, which was converted to epi-citreodiol **S1.17** in an additional step.

Scheme 38. Two Flask Synthesis of epi-citreodiol

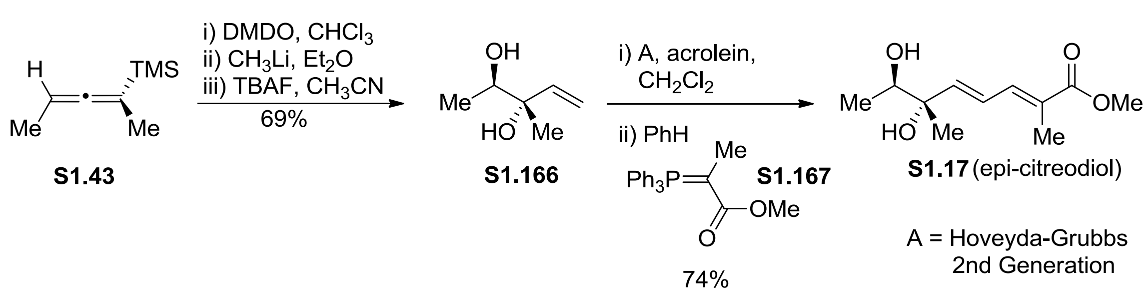

We have utilized spirodiepoxide based cascade in the synthesis of Jaspine B **S1.18** (Scheme 39).[21] Allenol **S1.168** was subjected to DMDO mediated oxidation in the presence of lithium perchlorate, a mild Lewis acid, to obtain cyclized α-hydroxy ketone **S1.169** in 79% yield and 1:1 mixture of diastereomers, which was converted to Jaspine B **S1.18**.

Scheme 39. Synthesis of Jaspine B

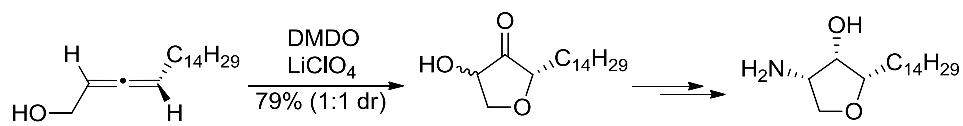

S1.168 **S1.169** **S1.18** (Jaspine B)

The PTX4 (**S1.20**) is a highly functionalized polyoxacyclic macrolide that consists of nineteen stereocenters, two acetals, one hemi-acetal, and three tetrahydrofurans. We have used spirodiepoxide based cascades in the synthesis of furans of PTX4 (Scheme 40-44).

Spirodiepoxide based transformation was used in the synthesis of the F ring of PTX4 (Scheme 40).[26] The disubstituted allene (**S1.170**) was used to synthesize fragment **S1.171**. The synthesis of the F ring involved oxidative cleavage of the PMB group to form the free hydroxyl, formation of spirodiepoxide and the opening of spirodiepoxide by the addition of the newly revealed hydroxyl.

Unlike trisubstituted allenes, the first oxidation of disubstituted allene is not regioselective. So in principal the oxidation of disubstituted allene should result in the formation of three spirodiepoxide. However, in the case of allene **S1.170** only two spirodiepoxides were formed. Experimental and computational analysis concluded that the first oxidation is directed by the hydrogen bond and occurs selectively at one double bond of the allene. Computational analysis showed that the hydrogen bonded transition state **S1.172** is more stable and thus more favorable. The result from our computational analysis further supported our hypothesis that the first oxidation is hydrogen bond directed (Figure 5).

Scheme 40. Spirodiepoxide Based Cascade in the Synthesis of F-ring of PTX4.

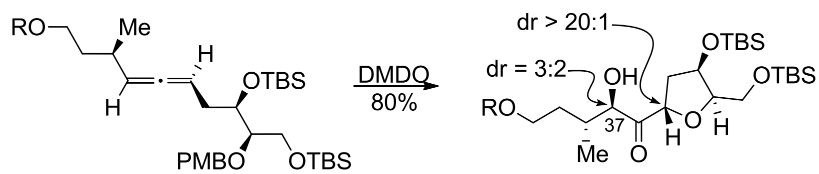

S1.170 **S1.171**

R = TBDPS

Figure 5. Hydrogen Bond Directed Oxidation of Allene

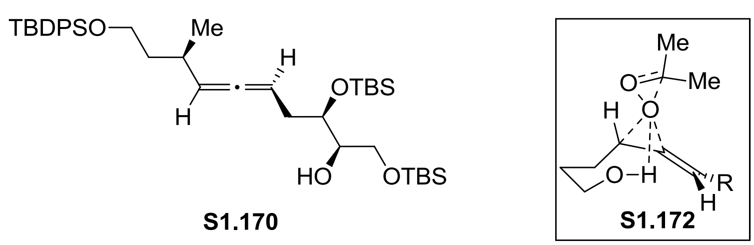

S1.170 **S1.172**

In 2007, we reported the synthesis of C1-C15 fragment **S1.175** of PTX4 (**S1.20**, Scheme 41).[24] The keto allene (**S1.174**) was used to synthesize the AB spiroketal of PTX4. Cleavage of the PMB group of allene **S1.173** by DDQ formed allene **S1.174**. DMDO mediated epoxidation of allene **S1.174** in the presence of methanol followed by the addition of acid lead to the formation of the AB spiroketal of the C1-C15 fragment

(**S1.174**) in 89% yield and 7:1 diastereomeric ratio. We have rationalized two possible pathways for the formation of the AB spiroketal and they are discussed in Chapter 5.

Scheme 41. Spirodiepoxide Based Cascade in the Synthesis of Spiroketal of PTX4.

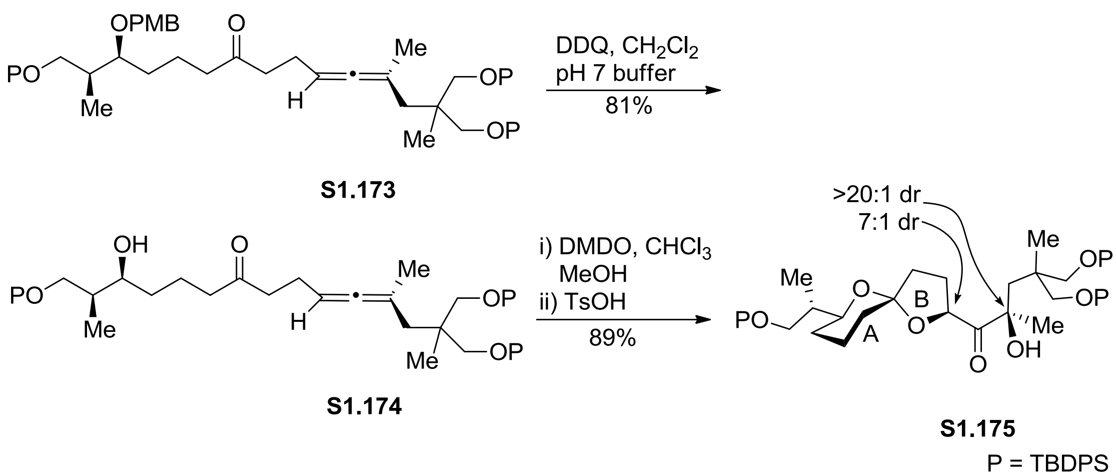

In 2010 we reported the synthesis of a C1-C19 fragment (**S1.179**) of PTX4 (Scheme 42).[25] In this synthesis sequence we constructed the C ring by the oxidation of allene **S1.177** followed by *exo* cyclization. Reaction of allene **S1.176** with DDQ resulted in the cleavage of the PMB group followed by spontaneous opening of epoxide to form **S1.177**. The epoxidation of allene **S1.177** resulted in the formation of spirodiepoxide **S1.178**. The free hydroxyl group of spirodiepoxide **S1.178** added at the proximal C-O bond of the proximal epoxide to form the C ring of **S1.179** in 54% (dr >10:1).

The major byproduct in the synthesis of **S1.179** was oxepanone **S1.180** (Figure 6). The oxepanone (**S1.180**) was formed in 20% yield and >10:1 diastereomeric ratio. Close examination of the oxepanone (**S1.180**) suggested that it is formed from the diastereomer of **S1.178** via 7-*endo*-tet cyclization.

Scheme 42. Spirodiepoxide Based Cascade in the Synthesis of C Ring of PTX4.

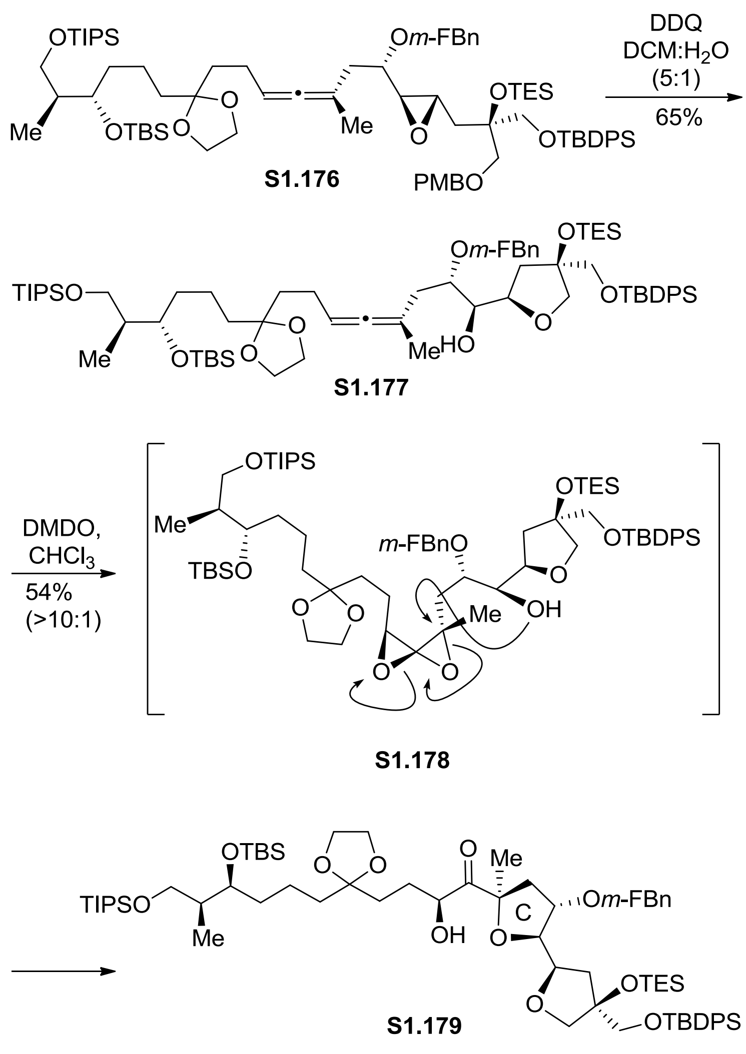

Figure 6. Oxepanone

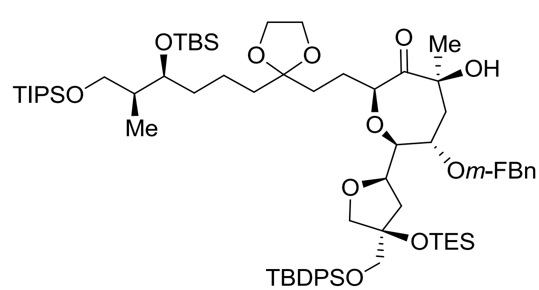

S1.180

Our spirodiepoxide based cascade was used in the synthesis of the A, B and C ring of PTX4 in just one step from allene **S1.181** (Scheme 43).[27] The epoxidation of allene **S1.181** in the presence of methanol resulted in the formation of **S1.182**.

Scheme 43. Synthesis of A, B and C Rings of PTX4

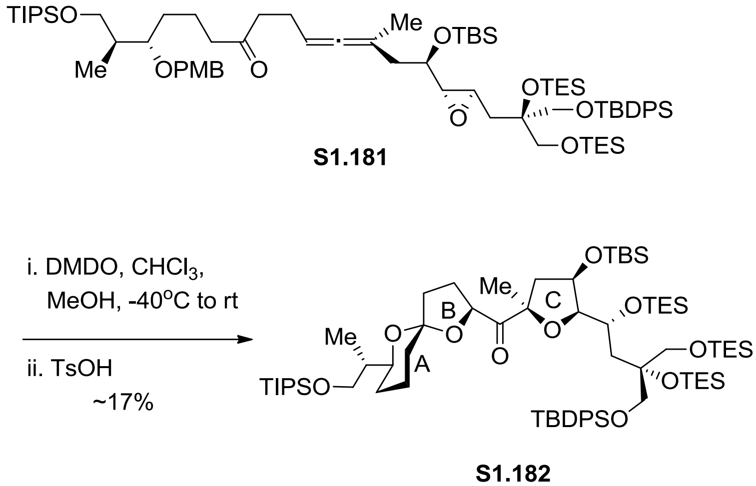

We reasoned that the A, B and C rings of fragment **S1.182** were formed by an extended cascade sequence that involved cleavage of the PMB group to the reveal hydroxyl group, spirodiepoxide formation, opening of spirodiepoxide by ketone to form oxocarbenium ion by the revealed hydroxyl group, and then opening of epoxide by the hydroxyl group obtained after opening of spirodiepoxide (Figure 7).

Figure 7. Extended Spirodiepoxide Based Cascade

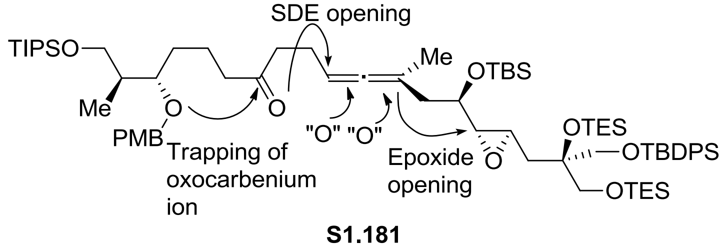

1.6 Structure and Mechanism

The use of neutral oxidizing agent, DMDO, allowed convenient isolation of spirodiepoxides. Isolation of spirodiepoxides allowed spectral studies to be performed. Spirodiepoxides possess a distinct IR band around 1620 cm^{-1}. In the NMR spectrum, the central carbon of a spirodiepoxide is found around 85 ppm and the ring hydrogen appears around 3.5 ppm. It has been reasoned that the effect of the adjacent oxide ring causes the ring hydrogen of spirodiepoxide to be downfield compared to the ring hydrogen of a simple epoxide. Even though, spirodiepoxide was isolated in 1968, the crystal structure of a spirodiepoxide was not published until 2007.[33] In 2007, we reported the first crystal structure of spirodiepoxide **S1.184** (Figure 8).[33] The crystal structure of **S1.184** showed that C2-C1/C3 and C2-O1/O2 bonds are shorter than the C1-C2 and C1-O1 bonds of tetramethyl epoxide **S1.185**. The C1-O1 and C3-O2 bonds of spirodiepoxide **S1.184** are longer than the average C-O bond of epoxide.

Figure 8. Spectral Data and Crystal Structure of Spirodiepoxide

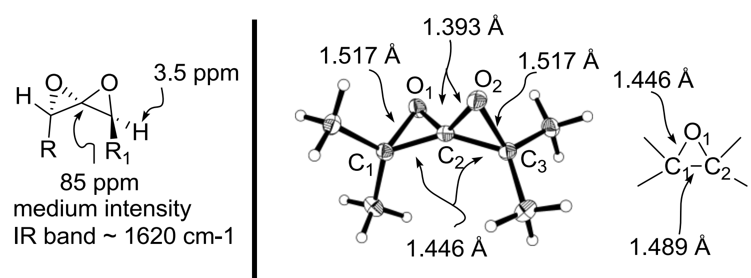

S1.183 **S1.184** **S1.185**

Supported by the computational and experimental analysis, we have generated a new mechanistic model for the nucleophilic spirodiepoxide opening and it is outlined in Scheme 44.[33] Depending upon the type of the acid promoters and nucleophiles used, the reaction pathway varies. When a strong acid is used, the spirodiepoxide undergoes stepwise opening and forms carbocationic intermediate, which lead into formation of different types of products. In case of a weak acid and a good nucleophile, the spirodiepoxide opens in a concerted asynchronous fashion. The nucleophile adds at the least substituted site with inversion at that position. Computational analysis revealed that the spirodiepoxide opening is highly exothermic and involves concerted opening of both epoxides. The C1-O1 bond elongates, the O1-C2 bond shortens and the C2-O2 bond elongates during the nucleophilic attack of spirodiepoxide **S1.186**. Computational analysis also revealed that hydrogen bond activation and Lewis or Brønsted acid activation can accelerate spirodiepoxide opening. In case of spirodiepoxide **S1.189**, the solvent hydrogen bonds with the distal oxygen (O2) and lowers the energy barrier for the attack of nucleophile to carbon atom of the proximal epoxide of spirodiepoxide **S1.189** (see **S1.190**). Based on the intrinsic reaction coordinate calculation we determine that singly opened spirodiepoxides do not represent stable intermediates.[33]

A reagent that is a combination of a weak acid and weak nucleophile also adds in a concerted fashion to a spirodiepoxide, provided a proper geometry is attained. For example, carboxamide and *cis*-N-alkyl amine reacts with spirodiepoxide in absence of a promoter. The hydrogen of the NH hydrogen bonds with the oxygen of the distal epoxide and activates the spirodiepoxide. The oxygen of the amide carbonyl then adds to the proximal epoxide (see **IX** and **S1.193**, Scheme 44). The 2-pyrrolidinone reacted with spirodiepoxide **S1.192** to give addition product **S1.194**.

Carboxamide and *cis*-N-alkyl amine reacts with spirodiepoxide in absence of a promoter. However, *trans*-N-alkyl amides or related nucleophiles with similar or lower

Scheme 44. Mechanistic Framework

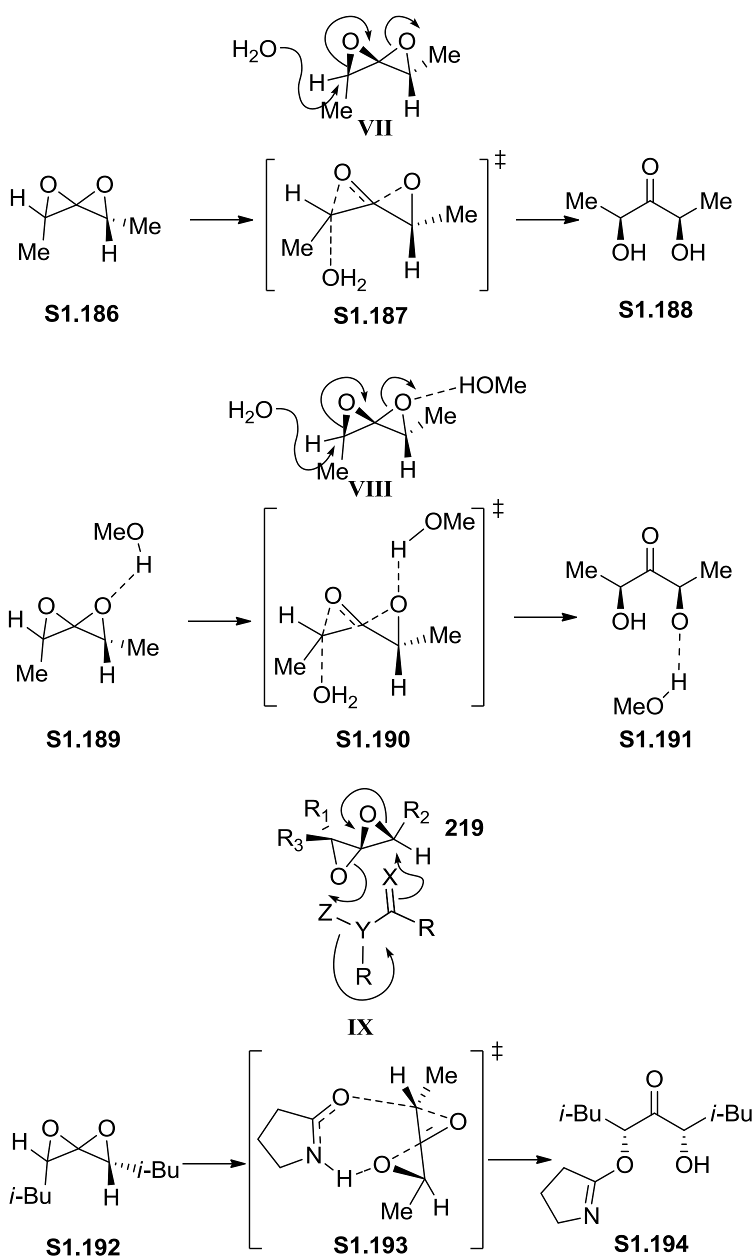

Figure 9. Amides

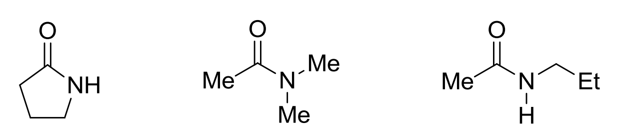

S1.195 S1.196 S1.197

pKa do not add to spirodiepoxide. We reasoned that for an amide to induce spirodiepoxide opening the amide has to be in the *cis* conformation and that it has to have a proton *syn* to the amide carbonyl. The *cis* amide 2-pyrrolidinone **S1.195** reacts with spirodiepoxide because it has hydrogen *syn* to the amide carbonyl. N,N-dimethyl acetamide **S1.196** does not react with spirodiepoxide because the amide does not have an amide hydrogen. N-ethyl acetamide **S1.197** does not react with spirodiepoxide because the amide attains *trans* conformation (Figure 9).

1.7 Conclusion

This functional group, spirodiepoxide, is new to the synthesis of complex molecules and undergoes many interesting and useful transformations, including cascade sequences that generate densely functionalized motifs rich in functionality and stereochemistry. This chapter provided a brief history of spirodiepoxide research and summarized the chemistry of spirodiepoxide: its reactivity, its uses in complex molecule synthesis, and mechanistic insight into these reaction processes.

1.8 References

1. a) Krause, N., Hashmi, A. S. K., Eds. *Modern Allene Chemistry, Volume 1*; Wiley-VCH Verlag GmbH & Co. KGaA: Weinheim, Germany, 2004; b) Krause, N., Hashmi, A. S. K., Eds. *Modern Allene Chemistry, Volume 2*; Wiley-VCH Verlag GmbH & Co. KGaA: Weinheim, Germany, 2004; c) Brummond, K. M.; DeForrest, J. E. *Synthesis* **2007**, *6*, 795.
2. van't Hoff, J. H. *La Chimie dans L'Espace*, Bazendijk, P. M., Rotterdam, **1875**.
3. Burton, B. S.; Pechman, H. V. *Ber. Dtsch. Chem. Ges.* **1887**, *20*, 145.

4. Jones, E. R. H.; Mansfield, G. H.; Whiting, M. L. H. *J. Chem. Soc.* **1954**, 3208.

5. Kohler, E. P.; Walker, J. T.; Tishler, M. *J. Am. Chem. Soc.* **1935**, *57*, 1743.

6. Maitland, P.; Mills, W. H. *Nature* **1935**, *135*, 994.

7. Boeseken, J. *Rec. Trav. Chim. Pays-Bas.* **1935**, *54*, 657.

8. Despite earlier claims of spirodiepoxide isolation, which Crandall dismissed as unlikely.

9. Crandall, J. K.; Machleder, W. H.; Thomas, M. J. *J. Am. Chem. Soc.* **1968**, *90*, 7346.

10. Crandall, J. K.; Machleder, W. H. *J. Am. Chem. Soc.* **1968**, *90*, 7292.

11. Crandall, J. K.; Conover, W. W.; Komin, J. B.; Machleder, W. H. *J. Org. Chem.* **1974**, *39*, 1723.

12. Crandall, J. K.; Batal, D. J. *J. Org. Chem.* **1988**, *53*, 1338.

13. Murray, R. W.; Jeyaraman, R. *J. Org. Chem.* **1985**, *50*, 2847.

14. Crandall, J. K.; Batal, D. J.; Sebesta, D.P.; Lin, F. *J. Org. Chem.* **1991**, *56*, 1153.

15. Hess Jr., B. A.; Cha, J. K.; Schaad, L. J.; Polavarapu, P. L. *J. Org. Chem.* **1992**, *57*, 6367.

16. Katukojvala, S.; Barlett, K. N.; Lotesta,S. D.; Williams, L. J. *J. Am. Chem. Soc.* **2004**, *126*, 15348.

17. Zhang, Y.; Cusick, J. R.; Ghosh, P.; Shangguan, N.; Katukojvala, S.; Inghrim, J.; Emge, T. J.; Williams, L. J. *J. Org. Chem.* **2009**, *74*, 7707.

18. Kiren, S.; Williams, L. J. *Org. Lett.* **2005**, *7*, 2905.

19. Shangguan, N.; Kiren, S.; Williams, L. J. *Org. Lett.* **2007**, *9*, 1093.

20. Ghosh, P.; Cusick, J. R.; Inghrim, J.; Williams, L. J. *Org. Lett.* **2009**, *11*, 4672.

21. Cusick, J. R.; Williams, L. J. Manuscript in preparation.

22. Ghosh, P.; Zhang, Y.; Emge, T. J.; Williams, L. J. *Org. Lett.* **2009**, *11*, 4402.

23. Liu, K.; Kim, H.; Ghosh, P.; Akhmedov, N. G.; Williams, L. J. *J. Am. Chem. Soc.* **2011**, *133*, 14968.

24. Lotesta, S. D.; Hou, Y.; Williams, L. J. *Org. Lett.* **2007**, *9*, 869.

25. Joyasawal, S.; Lotesta, S. D.; Akhmedov, N. G.; Williams, L. J. *Org. Lett.* **2010**, *12*, 988.

26. Sharma R.; Williams, L. J. Manuscript in preparation.

27. Xu, D.; Williams, L. J. Manuscript in preparation.

28. a) Murray, R. W.; Gu, D. *J. Chem. Soc., Perkin Trans. 2* **1993**, 2203; b) Murray, R. W.; Gu, H. *J. Phys. Org. Chem.* **1996**, *9*, 751; c) Murray, R. W.; Singh, M.; Williams, B. L.; Moncrieff, H. M. *J. Org. Chem.* **1996**, *61*, 1830.

29. Illustrative examples can be found in references 14, 22, and 23.

30. The selectivity for these epoxidations should be governed by $A^{1,3}$ strain, however the observed face selectivity is lower than non-allene oxide systems. This is attributable, at least in part, to a reduced facial bias in allene oxides because of the distorted bond angles relative to other facially biased alkenes.

31. Hu, G.; Drahl, M. A.; Williams, L. J. Manuscript in preparation.

32. a) Baumstark, A. L.; McClosky, C. J. *Tetrahedron Lett.* **1987**, *28*, 3311; b) Baumstark, A. L.; Vasquez, P. C. *J. Org. Chem.* **1988**, *53*, 3437; c) Bach, R. D.; Andres, J. L.; Owensby, A. L.; Schlegel, H. B.; McDouall, J. J. W. *J. Am. Chem. Soc.* **1992**, *114*, 7207; d) Houk, K. N.; Liu, J.; DeMello, N. C.; Condroski, K. R. *J. Am. Chem. Soc.* **1997**, *119*, 10147; e) Jenson, C.; Liu, J.; Houk, K. N.; Jorgensen, W. L. *J. Am. Chem. Soc.* **1997**, *119*, 12982.

33. Lotesta, S. D.; Kiren, S.; Sauers, R. R.; Williams, L. J. *Angew*. *Chem*. *Int*. *Ed*. **2007**, *46*, 7108.

34. Sharma, R.; Manpadi, M.; Zhang, Y.; Kim, H.; Ahkmedov, N. G.; Williams, L. J. *Org*. *Lett*. **2011**, *13*, 3352.

35. Hudrlik, P. F.; Tafesse, L.; Hudrlik, A. M. *J*. *Am*. *Chem*. *Soc*. **1997**, *119*, 11689.

36. Ghosh, P.; Lotesta, S. D.; Williams, L. J. *J*. *Am*. *Chem*. *Soc*. **2007**, *129*, 2438.

37. Wang, Z.; Shangguan, N.; Cusick, J. R.; Williams, L. J. *Synlett* **2008**, *2*, 213.

38. Andrews, D. R.; Giusto, R. A.; Sudhakar, A. R. *Tetrahedron Lett*. **1996**, *37*, 3417.

39. Sharma, R.; Williams, L. J. *Org*. *Lett*. **2013**, *15*, 2202.

Chapter 2

Allene Synthesis

2.1 Introduction

Chapter 1 provided a brief history of allenes. This chapter presents a multicomponent single flask allene synthesis method developed by our group. There are many methods for making allenes.[1] The most generally useful and stereoselective method available is the cuprate mediated S_N2' displacement method.[2] In 1968 Rona and Crabbé reported the first cuprate mediated synthesis of allene.[3] In their synthesis, a lithium dialkylcopper reagent was added to propargylic acetate **S2.1** to generate alkyl allene **S2.2** (Scheme 1).

Scheme 1. Allene Synthesis by Rona and Crabbé

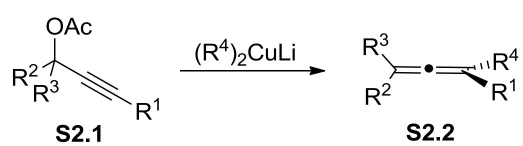

After Rona and Crabbé's report there have been many reports on the use of activated propargyl alcohol in the synthesis of allenes. The activated propargyl alcohols used include propargylic benzoate, carbonate, sulfonate, ethers, halides, oxiranes, aziridines and trifluoromethanesulfonyl.[2,4]

The allenes obtained by copper mediated S_N2' displacement of activated propargylic electrophiles have *anti* stereochemistry. The *anti* stereochemistry in an organocuprate promoted S_N2' displacement was explained by Corey and Boaz in 1984.[5]

Corey and Boaz explained that the d orbital of copper interacts with the σ* and π* orbitals of the substrate which leads to an anti S_N2' displacement (**S2.3**, Scheme 2).[2c,3]

In 1989, Elsevier and Vermeer reported the synthesis of chiral alkylallenes by the organocopper mediated S_N2' displacement of chiral propargyl mesylates or sulfinates.[6] They also outlined the mechanistic framework for the synthesis of chiral alkylallenes. They suggested that organocopper reacted with propargyl sulfinate **S2.4** to form a π complex **S2.5**, which led to the formation of allenylcopper(III) intermediate **S2.7**. Reductive elimination of **S2.7** resulted in the formation of allene **S2.8**, stereospecifically (Scheme 2).

Scheme 2. Anti S_N2' Displacement

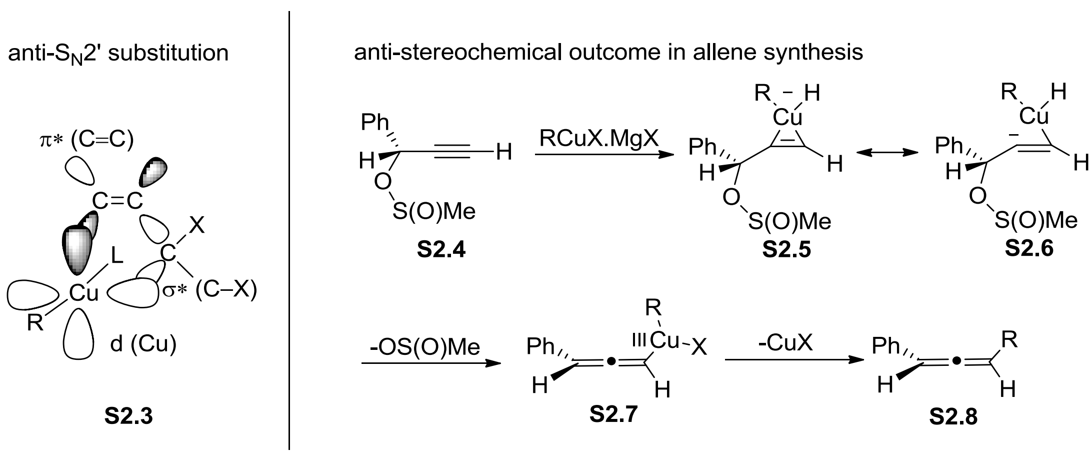

2.2 Synthesis of Allene

We work on the spirodiepoxide functionality. We strive to develop a framework for spirodiepoxide reactivity, to demonstrate the strategic advantages that allene oxidation offers in complex molecule synthesis, and to identify reactions that give access to diverse structural motifs. Utilization of spirodiepoxides to access highly functionalized oxygenated motifs has been demonstrated extensively by our group, including in total syntheses.[7] Since spirodiepoxides use allene precursors, it is essential to formulate an effective and convenient method to generate allenes. For us, the ideal synthesis would be the one that makes allenes from simple precursors in a single step without any purifications or isolation of the intermediates. We have developed a multicomponent single flask allene synthesis method. More precisely, it is a simplified procedure and an improved protocol for making allenes. The method involves sequential addition of alkyne, aldehyde or ketone, and cuprate (Table 1 and Table 2).[8]

Table 1 presents the method to synthesize trisubstituted allenes. In the method discussed in Table 1, a propargyl alcohol is assembled by deprotonation of an alkyne (**S2.9**) followed by the addition of an aldehyde (**S2.10**). The resultant propargyl alcohol is converted to a suitable leaving group by the addition of methanesulfonyl chloride and triethylamine. It is then subjected to a cuprate mediated SN2′ substitution to give the allene (**S2.11→ S2.12**). The use of triethylamine, though not strictly necessary, improved the yield and reproducibility of the synthesis. The propargyl mesylate mixture has to be added to the cuprate reagent at low temperature in order to suppress the S_N2 pathway and to favor S_N2' product formation. The method outlined in Table 1 is efficient for a range of substituents, including aryl (entries 1, 2 and 10), silyl (entries 7, 9 and 11), and α-branched alkyl (entries 4 and 6).

We have also developed an efficient method to synthesize haloallene (Table 2). Our method to generate haloallene **S2.27** involves coupling of alkyne **S2.24** and aldehyde or ketone **S2.25**, *in-situ* activation of propargyl alcohol (→**S2.26**), introduction of the

Table 1. Synthesis of Trisubstituted Allenes

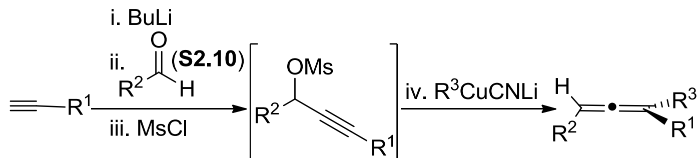

S2.9 **S2.11** **S2.12**

Entry	R^1	R^2	R^3	Allene	Yield %
1	*n*-Bu	$PhCH_2CH_3$	Me	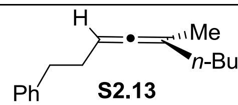 **S2.13**	93
2	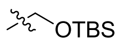	$PhCH_2CH_3$	Me	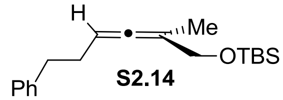 **S2.14**	82
3	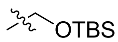	*i*-Bu	Me	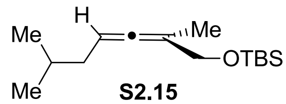 **S2.15**	93
4	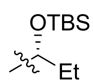	*i*-Pr	Me	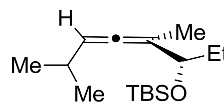 **S2.16**	79
5	*n*-Bu	*i*-Bu	*n*-Bu	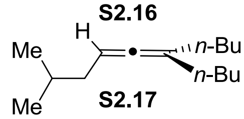 **S2.17**	91
6	*t*-Bu	*i*-Bu	*n*-Bu	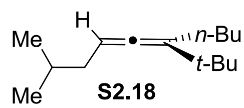 **S2.18**	84
7	TMS	*i*-Bu	*n*-Bu	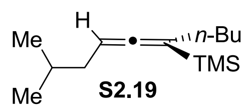 **S2.19**	78
8	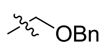	*i*-Bu	*n*-Bu	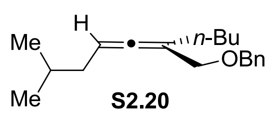 **S2.20**	92
9	TMS	*n*-Bu	*n*-Bu	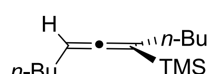 **S2.21**	80
10	*n*-Bu	CH_2CH_2Ph	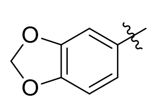	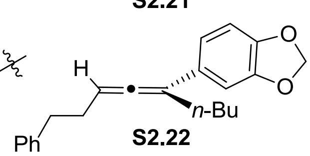 **S2.22**	81
11	*n*-Bu	*i*-Bu	$PhMe_2Si$	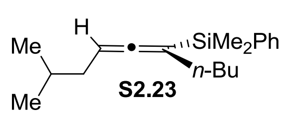 **S2.23**	74

Conditions: (i) 1.05 equiv of *n*-BuLi, THF, −78°C to 0°C, 35 min; (ii) 1.0 equiv of aldehyde, −78°C to 0°C, 0.5-2 h; (iii) 1.05 equiv of MsCl, 1.05 equiv Et_3N, 0°C, 1-2 h; (iv) $Cu(R^4)CNLi$, THF, −78°C to rt, 1-3 h.

Table 2. Synthesis of Trisubstituted Haloallenes

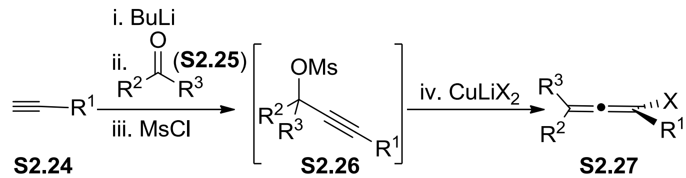

Entry	R^1	R^2	R^3	X	Allene	Yield %
1	*n*-Bu	i-Bu	H	Cl	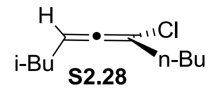 **S2.28**	68
2	*n*-Bu	n-Bu	H	Cl	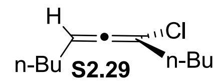 **S2.29**	62
3	*n*-Bu	CH_2CH_2Ph	H	Cl	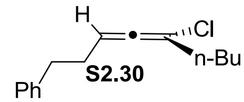 **S2.30**	65
4	*n*-Bu	Ph	H	Cl	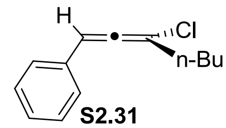 **S2.31**	61
5	TMS	CH_2CH_2Ph	H	Cl	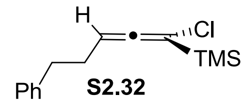 **S2.32**	60
6	CH_2OTBS	*t*-Bu	H	Cl	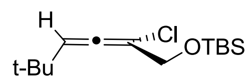 **S2.33**	64
7[a]	CH_2OTBS	Et	Et	Cl	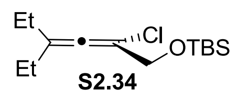 **S2.34**	58
8[a]	*t*-Bu	t-Bu	H	Br	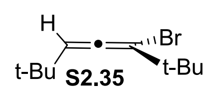 **S2.35**	50
9[a]	*n*-Bu	CH_2CH_2Ph	H	I	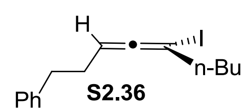 **S2.36**	63

Conditions: (i) 1.05 equiv of *n*-BuLi, THF, −78°C to 0°C, 35 min; (ii) 1.0 equiv of carbonyl (aldehyde/ketone), −78°C to 0°C, 0.5-2 h; (iii) 1.05 equiv of MsCl, 1.05 equiv Et_3N, 0°C, 1-2 h; (iv) $Cu(R^4)_2Li$, THF, −78°C to rt, 1-3 h. [a]Ms_2O was used instead of MsCl, THF.

reaction mixture to freshly prepared $LiCuX_2$, and then aging at room temperature for a couple of hours. The method outlined in Table 2 is efficient for a range of substituents, including aryl (entry 4) and silyl (entry 5) groups. This method also allows for the synthesis of tetrasubstituted allenes that bear halide (entry 7).

In the course of developing method for the synthesis of chloroallenes, we realized that addition of $LiCuCl_2$ is not essential to generate chloroallene. Reaction of alkyne with aldehyde to form propargyl alcohol, addition of methanesulfonyl chloride to form propargyl mesylate, and then introduction of $Cu(OAc)_2.H_2O$ resulted in the formation of chloroallene. However, the above described procedure was inferior to the method outlined in Table 2. The $LiCuCl_2$ system reduced the reaction time and increased the efficiency of the chloroallene formation.

2.3 Conclusion

We have developed an effective single flask protocol for the synthesis of allene. The allene synthesis method is less time consuming, produces minimal waste and is efficient for a range of substituents. It is simple to perform and reliably gives allenic products. The ready availability of allenes facilitates all allene-based chemistry, including our work on allene oxidation – the subject of the following chapters.

2.4 References

1. a) Krause, N., Hashmi, A. S. K., Eds. *Modern Allene Chemistry, Volume 1*; Wiley-VCH Verlag GmbH & Co. KGaA: Weinheim, Germany, 2004; b) Brummond, K. M.; DeForrest, J. E. *Synthesis* **2007**, *6*, 795.
2. a) Hoffmann-Röder, A.; Krause, N. Metal-Mediated Synthesis of Allenes. In *Modern Allene Chemistry* Krause, N., Hashmi, A. S. K., Eds.; Wiley-VCH Verlag GmbH &

Co. KGaA: Weinheim, 2004; Vol. 1, pp 52-70, and references therein; b) Ogasawara, M.; Hayashi, T. Transition Metal-Catalyzed Synthesis of Allenes. In *Modern Allene Chemistry* Krause, N., Hashmi, A. S. K., Eds.; Wiley-VCH Verlag GmbH & Co. KGaA: Weinheim, 2004; Vol. 1, pp 107-110, and references therein; c) Ohno, H.; Nagaoka, Y.; Tomioka, K. Enantioselective Synthesis of Allenes. In *Modern Allene Chemistry* Krause, N., Hashmi, A. S. K., Eds.; Wiley-VCH Verlag GmbH & Co. KGaA: Weinheim, 2004; Vol. 1, pp 141-151, and references therein

3. a) Rona, P.; Crabbé, P. *J. Am. Chem. Soc.* **1968**, *90*, 4733; b) Rona, P.; Crabbé, P. *J. Am. Chem. Soc.* **1969**, *91*, 3289.
4. a) Tadema, G.; Vermeer, P.; Meijer, J.; Brandsma, L. *Recl. Trav. Chim. Pays-Bas* **1976**, *95*, 66; b) Alexakis, A.; Commerçon, A.; Villiéras, J.; Normant, J. F. *Tetrahedron Lett.* **1976**, *17*, 2313; c) Moreau, J. –L.; Gaudemar, M. J. *Organomet. Chem.* **1976**, *108*, 159; d) Marek, I.; Mangeney, P.; Alexakis, A.; Normant, J. F. *Tetrahedron Lett.* **1986**, 2*7*, 5499; e) Alexakis, A.; Marek, I.; Mangeney, P.; Normant, J. F. *J. Am. Chem. Soc.* **1990**, *112*, 8042; f) Daeuble, J. F.; McGettigan, C.; Stryker, J. M. *Tetrahedron Lett.* **1990**, *31*, 2397; g) Ansorge, K.; Polborn, K.; Müller, T. J. J. *Organomet. Chem.* **2001**, *630*, 198; h) Nantz, M. H.; bender, D. M.; Janaki, S. *Synthesis* **1993**, *6*, 577; i) Elsevier, C. J.; Vermeer, P. *J. Org. Chem.* **1989**, *54*, 3726; j) Gooding, O. W.; Beard, C. C.; Jackson, D. Y.; Wren, D. L.; Cooper, G. F. *J. Org. Chem.* **1991**, *56*, 1083.
5. Corey, E. J.; Boaz, N. W. *Tetrahedron Lett.* **1984**, *25*, 3063.
6. Elsevier, C. J.; Vermeer, P. *J. Org. Chem.* **1989**, *54*, 3726.

7. a) Sharma, R.; Williams, L. J. *Org*. *Lett*. **2013**, *15*, 2202; b) Joyasawal, S.; Lotesta, S. D.; Akhmedov, N. G.; Williams, L. J. *Org*. *Lett*. **2010**, *12*, 988; c) Zhang, Y.; Cusick, J. R.; Shangguan, N.; Katukojvala, S.; Inghrim, J.; Emge, T. J.; Williams, L. J. *J*. *Org*. *Chem*. **2009**, *74*, 7707; d) Ghosh, P.; Zhang, Y.; Emge, T. J.; Williams, L. J. *Org*. *Lett*. **2009**, *11*, 4402; e) Ghosh, P.; Cusick, J. R.; Inghrim, J.; Williams, L. J. *Org*. *Lett*. **2009**, *11*, 4672; f) Wang, Z. H.; Shangguan, N.; Cusick, J. R.; Williams, L. J. *Synlett* **2008**, *2*, 213; g) Ghosh, P.; Lotesta, S. D.; Williams, L. J. *J*. *Am*. *Chem*. *Soc*. **2007**, *129*, 2438; h) Shangguan, N.; Kiren, S.; Williams, L. J. *Org*. *Lett*. **2007**, *9*, 1093; i) Lotesta, S. D.; Kiren, S. K.; Sauers, R. R.; Williams, L. J. *Angew*. *Chem*. *Int*. *Ed*. **2007**, *46*, 7108; j) D.; Hou, Y.; Williams, L. J. *Org*. *Lett*. **2007**, *9*, 869; k) Katukojvala, S.; Barlett, K. N.; Lotesta, S. D.; Williams, L. J. *J*. *Am*. *Chem*. *Soc*. **2004**, *126*, 15348.

8. Results discussed in this chapter have been published. See: Sharma, R.; Manpadi, M.; Zhang, Y.; Kim, H.; Ahkmedov, N. G.; Williams, L. J. *Org*. *Lett*. **2011**, *13*, 3352.

Chapter 3

Spirodiepoxide Based Cascades: Direct Access to Diverse Motifs

3.1 Introduction

The spirodiepoxide is a reactive and useful functionality that is obtained by double epoxidation of an allene.[1] Dimethyldioxirane (DMDO) readily transfers oxygen to allenes and to allene oxides to form spirodiepoxides (**S3.1**→**S3.2**→**S3.3**, Scheme 1). The first epoxidation of an allene leads to the formation of an allene oxide (**S3.2**) and sets the absolute configuration of the spirodiepoxide that eventually forms. In case of a trisubstituted allene, the first epoxidation is highly selective (dr >20:1). The epoxidation of an allene oxide (**S3.2**) determines the diastereomeric ratio within the enantiomeric series and yields spirodiepoxide (**S3.3**). The selectivity of the second epoxidation depends on the substrate and it can vary from 1:1 to >20:1.

Scheme 1. Spirodiepoxide Formation

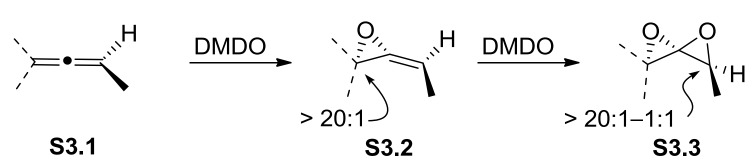

The spirodiepoxide functionality can be used as a platform to access highly functionalized motifs of great value in complex molecule synthesis and in the search of bioactive compounds. A suitable nucleophile adds to the spirodiepoxide and then sets the stage for subsequent transformations. A spirodiepoxide can be opened by hetero, ambiphilic and carbon nucleophile in concerted fashion to give α-substituted-α′-hydroxyketone, which can undergo further rearrangement to form heterocycles, oxygenated stereotriads, and other highly functionalized motifs (Scheme 2).[2]

Scheme 2. Spirodiepoxide: A Platform for Constructing Functionalized Motifs

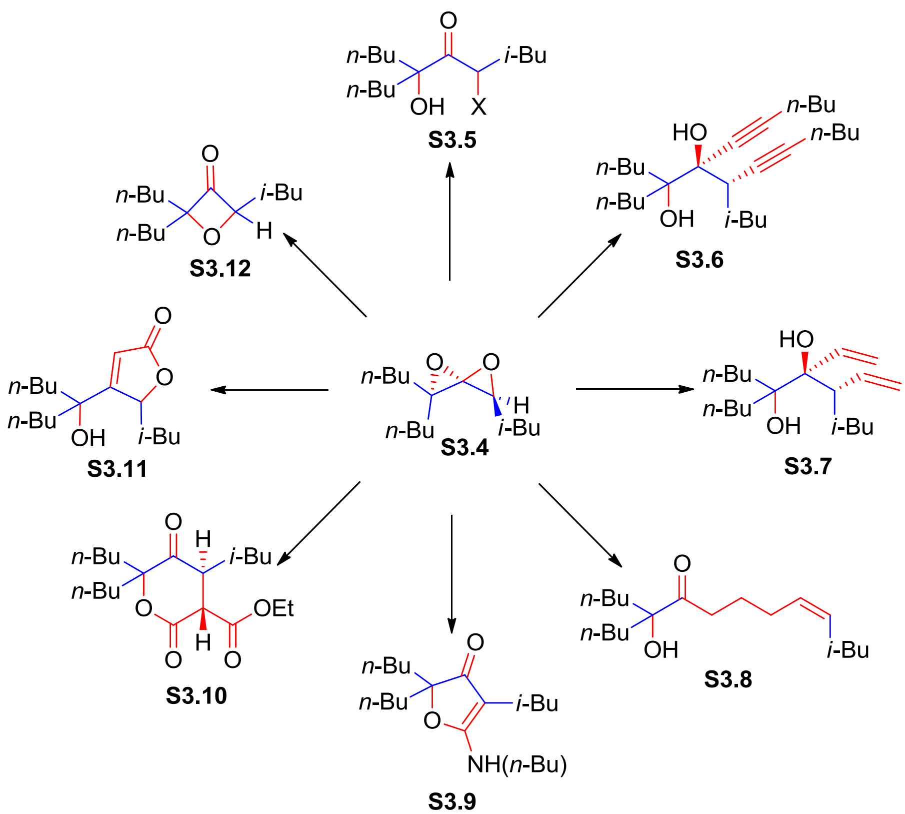

Chapter 1 provides detail information on the formation, reactivity and application of spirodiepoxide. This chapter discusses our motivations for and presents greater insights into certain spirodiepoxide based reactions. In particular, this chapter demonstrates the utilization of the spirodiepoxide functionality in a diversity oriented synthesis. This chapter shows the conversion of a single spirodiepoxide (**S3.4**) to a diverse range of products via oxidation/derivatization reactions (**S3.5**–**S3.11**, Scheme 2). To further demonstrate a diversity-focused methodology, this chapter presents the bromide addition, the iodide addition, the dihydrofuranone cascade, and butenolide cascade reactions performed on other spirodiepoxides. The yields for these substrates were excellent and paralleled the yields of the simpler spirodiepoxide (**S3.4**).

3.2 Reaction with Simple Heteronucleophile

Simple heteronucleophiles like benzenesulfinate, trifluoroethoxide, indole and halides add efficiently to spirodiepoxides to give *syn* substituted hydroxyketones (Table 1). The reaction of sodium benzenesulfinate with spirodiepoxide **S3.4** in the presence of 15-crown-5 ether resulted in the formation of sulfone **S3.15**. The addition of 15-crown-5 ether was essential for the success of this reaction; no reaction took place in the absence of 15-crown-5 ether. The synthesis of sulfone **S3.15** instead of sulfinate ester, an *O*-alkylation product, suggested that the spirodiepoxide functionality is a relatively soft electrophile.[3]

Approximately stoichiometric sodium trifluoroethoxide added efficiently to spirodiepoxide **S3.4** to give addition product **S3.16** (Table 1, entry 2). We discovered that an excess of nucleophilic reagent is required in the case of weakly acidic nucleophiles like water, methanol, and phenol.[4,5] However, trifluoroethanol did not add to the spriodiepoxide under neutral conditions even in large excess.

Epoxides react with indole in the presence of Lewis acid to generate a C-3 addition products.[6] Reaction of indole with spirodiepoxide diverges from epoxide chemistry. The addition of indole with spirodiepoxide **S3.4** did not require added Lewis acid and the addition took place exclusively on the indole nitrogen to give **S3.17** (Table 1). Spirodiepoxides react with halides to give highly versatile haloketone functionality.

Table 1. Simple Heteronucleophile Addition

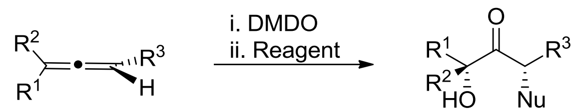

S3.13 S3.14

Entry	Reagent	Product	Yield %	Entry	Reagent	Product	Yield %
1[a]	$PhSO_2Na$	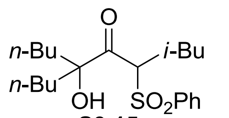 **S3.15**	50	7[g]	LiBr	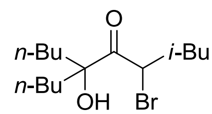 **S3.20**	88
2[b]	CF_3CH_2ONa	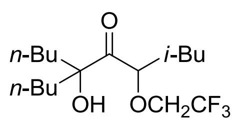 **S3.16**	75	8[g]	LiBr	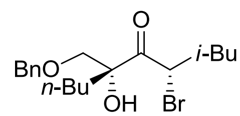 **S3.21**	95 (dr=1.4:1)
3[c]	Indole/LDA	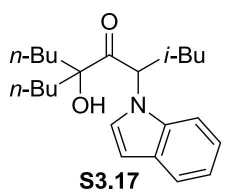 **S3.17**	50	9[g]	LiCl	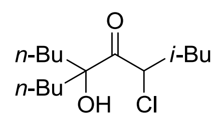 **S3.19**	85
4[d]	$(n\text{-Bu})_4NF$	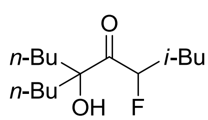 **S3.18**	51	10[h]	LiI	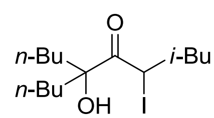 **S3.22**	85
5[e]	$PhCH_2(CH_3)_3NCl$	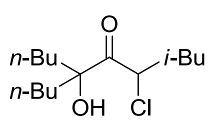 **S3.19**	60	11[h]	LiI	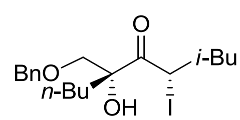 **S3.23**	90 (dr=1.3:1)
6[f]	$(n\text{-Bu})_4NBr$	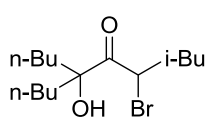 **S3.20**	50				

Conditions: i. DMDO, $CHCl_3$, −40°C, 30 min. ii. [a]1.5 equiv of $PhSO_2Na$, 1.5 equiv of 15-crown-5, THF 0°C to rt, 5 h. [b]1.5 equiv of NaH, CF_3CH_2OH, 0°C to rt, 1 h. [c]3.0 equiv of *n*-BuLi, 3.0 equiv of indole, THF, −78°C to 0°C, 4 h. [d]2.0 equiv of TBAF, THF, 0°C to rt, 4 h. [e]2.0 equiv of Benzyltrimethylammonium chloride, THF, 0°C to rt, 4 h. [f]2.0 equiv of TBAB, THF, 0°C to rt, 4 h. [g]3.0 equiv of LiX (X= Cl, Br, I), THF, 0°C to rt, 4 h, [h]10.0 equiv of LiX (X= Br, I), $CHCl_3$, 0°C to rt, 4 h.

Halides added to spirodiepoxides to give α-halo-α′-hydroxyketones (**S3.18**−**S3.23**). We discovered that compared to tetraalkylammonium salt, lithium halide salt is the superior source of halide. These reactions proceed in workable but capricious yield when tetraalkylammonium salts were used (e.g., Table 1, entries 4−6).[7] In contrast, lithium halide salts reacted rapidly and reliably to give the haloketones in excellent yields (Table 1, entries 7−11). The benefit of the lithium gegenion is especially noteworthy, since there are no reported examples of Lewis acid promoted spirodiepoxide opening.

3.3 Reaction with Complex Nucleophile

Spirodiepoxides participate in many C-C bond forming reactions (see Table 2). Similar to heteronucleophiles, carbon nucleophiles add to spirodiepoxides, efficiently. As mentioned in Chapter 1, cyanide adds smoothly to spirodiepoxides to give the corresponding nitrile derivative.[4] The anion derived from acetonitrile and LDA added to spirodiepoxide **S3.4** to generate the homologous ketonitrile (**S3.25**, Table 2, entry 1). Usually nitriles add to ketones. However, only the mono-addition product (**S3.25**) was obtained in the reaction of acetonitrile with spirodiepoxide. Another interesting factor about this reaction is that no organocopper reagent was required to facilitate the addition of nitrile anion to spirodiepoxide. We determined that organocopper reagent is required for the addition of unstable sp^3 type carbanion.[8] However in case of stable carbanions, like cyanide, no organocopper reagent was needed.

We have used isonitriles to add to spirodiepoxide and to form dihydrofuranones (Table 3, entry 2 and 3). The addition of *n*-butylisonitrile in *t*-BuOH to spirodiepoxides led to the slow but efficient formation of dihydrofuranones (**S3.9** and **S3.26**). Isonitriles are known to add to epoxide only in the presence of a Lewis acid.[9] However, no Lewis acid is required to promote the reaction of spirodiepoxides with isonitriles. Actually,

Table 2. Complex Nucleophile Addition

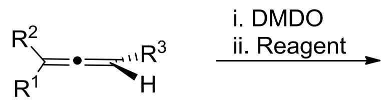

Product

S3.24

Entry	Reagent	Product	Yield %	Entry	Reagent	Product	Yield %
1[a]	CH_3CN, LDA	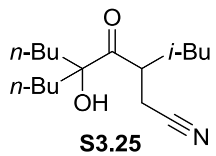 **S3.25**	66	6[d]	$(EtO)_2OPCH_2CO_2H$ K_2CO_3, 18-C-6	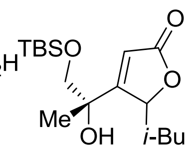 **S3.27**	71 (dr=1.6:1)
2[b]	*n*-BuNC, *t*-BuOH	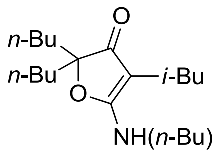 **S3.9**	81	7[e]	Li-vinyl	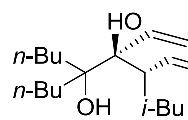 **S3.7**	81
3[b]	*n*-BuNC, *t*-BuOH	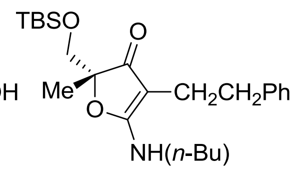 **S3.26**	77	8[f]	LiCC(*n*-Bu)	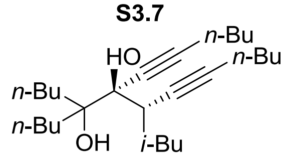 **S3.6**	65
4[c]	Diethyl malonate NaH	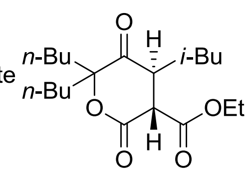 **S3.10**	45 (dr=6:1)	9[f]	LiCC(TMS)	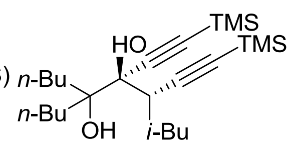 **S3.28**	65
5[d]	$(EtO)_2OPCH_2CO_2H$ K_2CO_3, 18-C-6	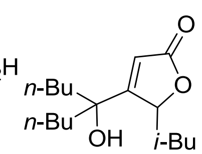 **S3.11**	71	10[g]	Li-vinyl HMPA	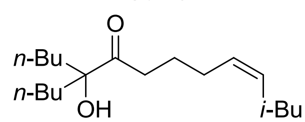 **S3.8**	61

Conditions: i. DMDO, $CHCl_3$, −40°C, 30 min. ii. [a]3.0 equiv of LDA, 3.0 equiv of CH_3CN, −78°C to 0°C, 4 h. [b]10 equiv of *n*-BuNC, *t*-BuOH, rt, 2 d. [c]1.5 equiv of diethyl malonate, 1.5 equiv of NaH, 0°C to rt, 4 h. [d]2.0 equiv of $(EtO)_2OPCH_2CO_2H$, 6.0 equiv of K_2CO_3, 2 equiv of 18-C-6, rt, 4 h. [e]4.0 equiv of $LiCHCH_2$, 0°C to rt, 2 h. [f]4.0 equiv of *n*-BuLi, 4.0 equiv of HCCR (R= Bu, TMS), −78°C to 0°C, 2 h. [g]4.0 equiv of $LiCHCH_2$, 0°C to rt, 1 h; 20 equiv of HMPA, 0°C to rt, 1 h.

introduction of Lewis acid, $LiClO_4$, to the above reaction led to the formation of side products and decreased the yield of desired products **S3.9** and **S3.26**. The formation of dihydrofuranones is consistent with formation of nitrilium ion intermediate **S3.30,** spontaneous cyclization to **S3.31**, and then isomerization of the olefin to furnish furanone **S3.9** (Scheme 3).

Scheme 3. Mechanistic Outline for the Synthesis of Furanone

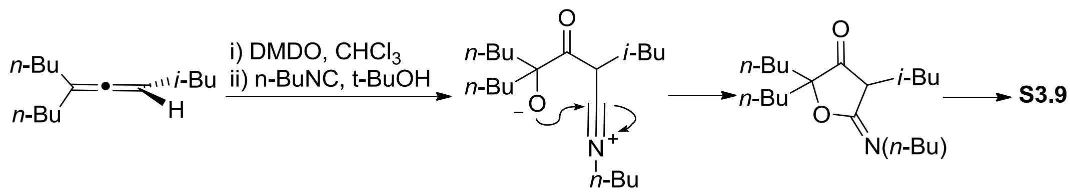

S3.29 **S3.30** **S3.31**

The mixture of diethyl malonate and sodium hydride in THF was reacted with spirodiepoxide **S3.4** to furnish lactone **S3.10** (Table 2, entry 4). Diethyl malonate added to spirodiepoxide **S3.4** and cyclized spontaneously to form lactone **S3.10**. We examined various bases and realized that sodium hydride to be most productive. This transformation not only established new C-C, C-O and new ring connectivity but also set a new stereocenter (dr = 6:1).[10]

We have developed a method to synthesize butenolides, a class of unsaturated five membered lactones and biologically important molecules. Butenolides can be synthesized from allene via a spirodiepoxide-based cascade. Addition of 2-(diepoxyphosphoryl)acetic acid, in the presence of potassium carbonate and crown ether, to spirodiepoxide yields butenolide (**S3.11** and **S3.27**, Table 2, entry 5 and 6).[11]

The formation of butenolide **S3.11** is rationalized in Scheme 4. We reasoned that the phosphonate **S3.32** adds to spirodiepoxide **S3.4** to form alkoxide **S3.33**, a basic species.[12] The alkoxide **S3.33** acts as a base and pulls the hydrogen from the carbon atom adjacent to the phosphorous to form ylide. The ylide adds to carbonyl and then undergo intramolecular Horner-Wadsworth-Emmons reaction to form butenolide **S3.11.**

In the reaction of spirodiepoxide with carbon nucleophile, addition of organocopper is essential to promote nucleophilic opening and suppress eliminative opening.[8] However, no organocopper was required for the opening of spirodiepoxide with vinyl lithium reagent. A vinyl lithium reagent adds efficiently to a spirodiepoxide and unlike other less reactive nucleophiles it adds twice to form diol (**S3.7**, Table 2, entry 7). Two equivalents of the vinyl lithium reagent are taken up by the spirodiepoxide, and a single diol **S3.7** is obtained. An alkynyl lithium reagent reacts similar to vinyl lithium reagent. An alkynyl lithium reagent adds to spirodiepoxides to generate a single diastereomer of diols (**S3.6** and **S3.28**, entry 8 and 9). The formation of single diastereomer can be readily understood in terms of steric congestion. It is likely that upon spirodiepoxide opening, the lithium alkoxide is involved in chelation with the carbonyl (**S3.34**, Scheme 5). The combination of steric congestion and the comparatively small alkynyl and alkenyl substituents favor π-facial addition, as drawn, to give **S3.6**.[13]

Scheme 4. Mechanistic Outline for the Synthesis of Butenolide

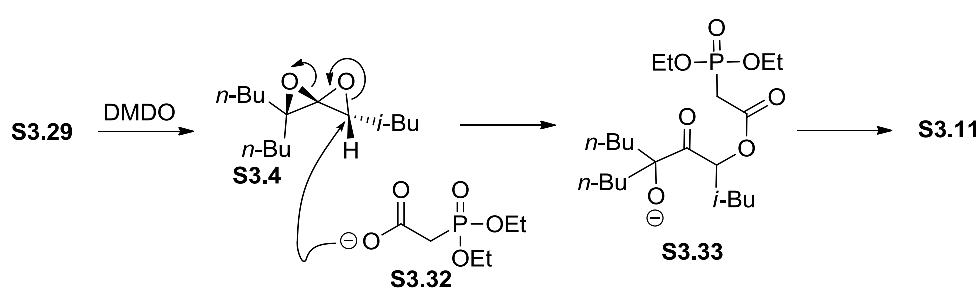

We realized that the dianion intermediate, obtained after the addition of two equivalents of vinyl lithium, is an ideal candidate for anion accelerated oxy cope rearrangement. Exposure of the divinyl addition product (**S3.7**) to potassium hydride and 18-crown-6 ether resulted in the formation of *cis* olefin **S3.8**. Exposure of the divinyl addition reaction mixture of Table 2, entry 7 to HMPA allowed for the dianion intermediate to undergo rearrangement to form *cis* olefin **S3.8** (entry 10).

Scheme 5. Mechanistic Outline for the Synthesis of S3.6

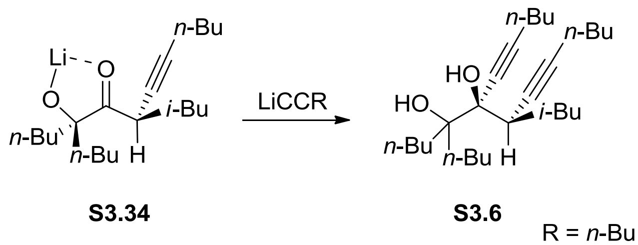

The oxy cope rearrangement favours the formation of *trans* olefins.[14] However, allene **S3.29** resulted in the formation of *cis* olefin **S3.8**. We reasoned that the cis olefin is favoured because the dianion intermediate attains the conformation (**S3.35**) that avoids *syn*-pentane interaction (Scheme 6). In **S3.35**, the *i*-Bu group is pseudo equatorial in order to avoid *syn* pentane interaction. The dianion intermediate **S3.35** forms **S3.36**, which eventually results in the formation of *cis* olefin **S3.8**.

Scheme 6. Mechanistic Outline for the Anion Accelerated Oxy Cope Rearrangement

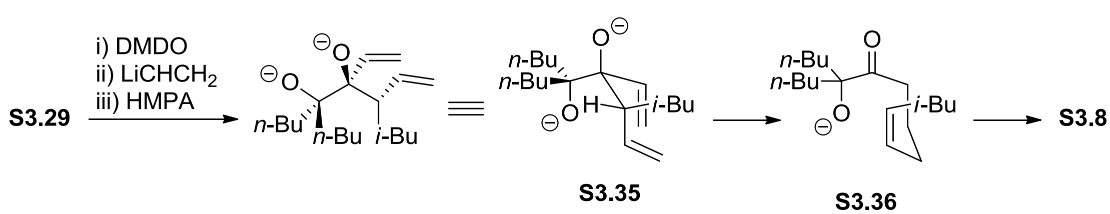

We used spirodiepoxide to synthesize oxetan-3-ones. Spirodiepoxidation of allene **S3.29** to form spirodiepoxide **S3.4** and then heating in microwave at 200°C for 30 min resulted in the formation of oxetan-3-one **S3.12** (Scheme 7). Oxetan-3-one **S3.12** was synthesized by employing a three-step sequence: spirodiepoxidation of allene **S3.29**, opening of spirodiepoxide **S3.4** by bromide, and intramolecular displacement of bromide by alkoxide.

Scheme 7. Synthesis of Oxetan-3-one S3.12

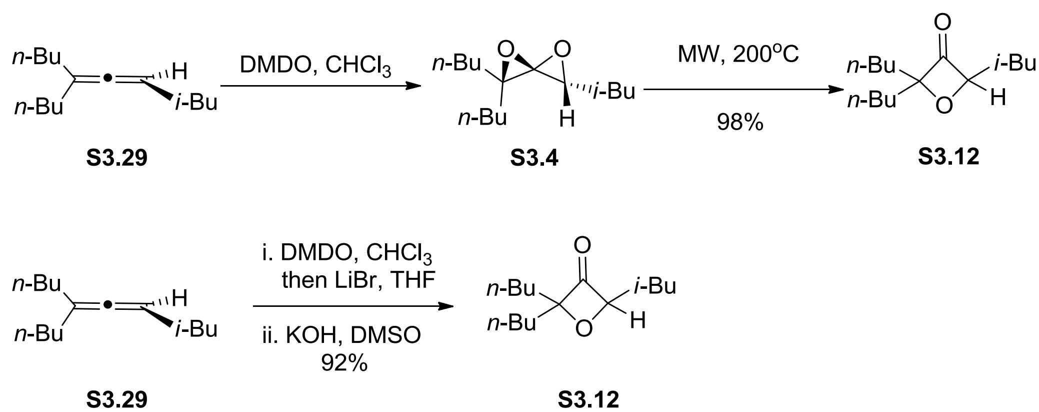

3.4 Conclusion

This chapter emphasizes the utilization of the spirodiepoxide functionality as a platform to access highly functionalized motifs of great value in complex molecule synthesis and in the search of bioactive compounds. This chapter summarizes allene epoxide formation/opening reaction sequences that enable direct access to diverse products like *syn* substituted hydroxy ketones, diendiols, diyndiols, α′-hydroxy-γ-enones, dihydrofuranones, butenolides and δ-lactones from a single allene.

3.5 References

1. For detail information on the structure, formation and reactivity of spirodiepoxide see Chapter 1.

2. Results discussed in this chapter have been published. See: Sharma, R.; Manpadi, M.; Zhang, Y.; Kim, H.; Ahkmedov, N. G.; Williams, L. J. *Org. Lett.* **2011**, *13*, 3352.
3. Meek, J. S.; Fowler, J. S. *J. Org. Chem.* **1968**, *33*, 3422.
4. Lotesta, S. D.; Kiren, S.;Sauers, R. R.; Williams, L. J. *Angew. Chem. Int. Ed.* **2007**, *46*, 7108.
5. Exceptions are known, see: a) Zhang, Y.; Cusick, J. R.; Shangguan, N.; Katukojvala, S.; Inghrim, J.; Emge, T. J.; Williams, L. J. *J. Org. Chem.* **2009**, *74*, 7707; b) Ghosh, P.; Cusick, J. R.; Inghrim, J.; Williams, L. J. *Org. Lett.* **2009**, *11*, 4672; c) Shangguan, N.; Kiren, S.; Williams, L. J. *Org. Lett.* **2007**, *9*, 1093; d) Lotesta, S. D.; Kiren, S. K.; Sauers, R. R.; Williams, L. J. *Angew. Chem. Int. Ed.* **2007**, *46*, 15.
6. *C.f.* Westermaier, M.; Mayr, H. *Chem. Eur. J.* **2008**, *14*, 1638.
7. Crandall, J. K.; Batal, D. J.; Sebesta, D. P.; Ling, F. *J. Org. Chem.* **1991**, *56*, 1153. The history of the tetraalkyl ammonium reagent appears to strongly influence reproducibility.
8. Ghosh, P.; Lotesta, S. D.; Williams,L.J. *J. Am. Chem. Soc.* **2007**, *129*, 2438.
9. a) Imi, K.; Yanagihara, N.; Utimoto, K. *J. Org. Chem.* **1987**, *52*, 1013; b) Kern, O. T.; Motherwell, W. B. *Chem. Commun.* **2003**, *24*, 2988.
10. *C.f.* the reaction of malonates with epoxides: Van Zyl, G.; Van Tamelen, E. E. *J. Am. Chem. Soc.* **1950**, *72*, 1357.
11. For general review discussing synthesis of butenolides see: a) Rao, Y. S. *Chemical Reviews* **1976**, *76*, 625; b) Knight, D. W. *Contemp. Org. Synth.* **1994**, *1*, 287.

12. The formation of a highly basic species by release of ring strain is well known. See for example a recent review on applications of the Favorskii rearrangement: Guijarro, D.; Yus, M. *Curr. Org. Chem.* **2005**, *9*, 1713.

13. a) Cram, D. J.; Elhafez, F. A. A. *J. Am. Chem. Soc.* **1952**, *74*, 5828; b) Cram, D. J.; Greene, F. D. *J. Am. Chem. Soc.* **1953**, *75*, 6004; c) Cram, D. J.; Wilson, D. R. *J. Am. Chem. Soc.* **1963**, *85*, 1245; d) Fleming, I.; Hill, J. H. M.; Parker, D.; Waterson, D. *J. Chem. Soc., Chem. Commun.* **1985**, 318; e) Mengel, A.; Reiser, O. *Chem Rev.* **1999**, *99*, 1191; f) The pi-facial selectivity of ketones of this type have not been evaluated previously.

14. a) Evans, D. A.; Golob, A. M. *J. Am. Chem. Soc.*, **1975**, *97*, 4765; b) Evans, D. A.; Baillargeon, D. J.; Nelson, J. V. *J. Am. Chem. Soc.*, 1978, **100**, 2242; c) Paquette, L. A. *Tetrahedron* **1997**, *53*, 13971.

Chapter 4

Facile Synthesis of Oxetan-3-ones from Allenes via Spirodiepoxides

4.1 Introduction

Oxetan-3-ones have many uses in synthetic chemistry, medicinal chemistry and drug discovery.[1] Steroids containing oxetan-3-ones have demonstrated antiflammatory and antiglucocorticoid activities.[2,3] Oxetan-3-ones have been utilized as precursors in the preparation of oxetanes (**S4.1**), as well as 3-aminooxetanes (**S4.2**), oxetanocins (**S4.3**), and other oxetane derivatives (Figure 1).[4a–c] The oxetane moiety, which can be made from oxetan-3-ones, can be used as a gem-dimethyl variant and to influence solubility, lipophilicity, metabolic stability, and molecular conformation.[5,6]

Figure 1. Oxetanes, 3-aminooxetane Derivative and Oextanocin A

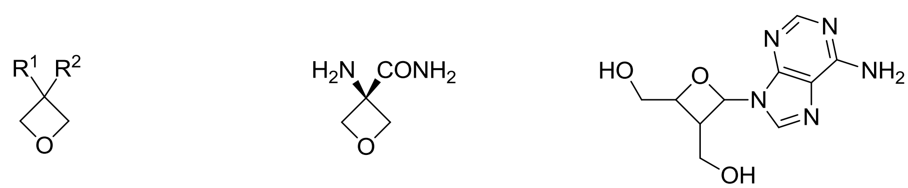

Oxetane (**S4.1**) 3-aminooxetane-3-carboxylic acid (**S4.2**) Oxetanocin A (**S4.3**)

Oxetan-3-ones are useful molecules. However, there are only a limited number of known methods for the synthesis of oxetanones.[1,7] There is a need for the development of concise and efficient methods for the synthesis of oxetanones. Recently, Zhang reported a method for the synthesis of oxetanones and the method involves a gold catalyzed oxidative cyclization of propargyl alcohols.[7n] The method developed by Zhang is advantageous to other multistep routes. However, the method developed by Zhang does not give access to tetra- and tri-substituted oxetan-3-ones that do not bear electron-withdrawing groups adjacent to the heterocycle. We recognized that we can use spirodiepoxide based cascade to synthesize oxetan-3-ones.

Oxetan-3-ones are commonly observed as byproducts in the peroxy acid oxidation of allenes.[8] In the presence of acid, even on TLC plate, spirodiepoxide decomposes to give various products, including oxetan-3-ones. We obtained oxetan-3-one **S4.6** as a byproduct in the epoxidation of bis[allene] **S4.4** followed by exposure to lithium methylcyanocuprate (Scheme 1).[9] Though oxetan-3-ones are frequently obtained as side-products in the acid promoted decomposition of spirodiepoxide, there has been only one report on the flash vacuum pyrolysis mediated thermal rearrangement of a spirodiepoxide to a oxetan-3-one. Crandall reported a synthesis of the 4-butyl-2,2-dimethyloxetan-3-one. Oxidation of 2-methylocta-2,3-diene followed by flash vacuum pyrolysis furnished the 4-butyl-2,2-dimethyloxetan-3-one.[8d]

Scheme 1. Oxetan-3-one Formation from Spirodiepoxide

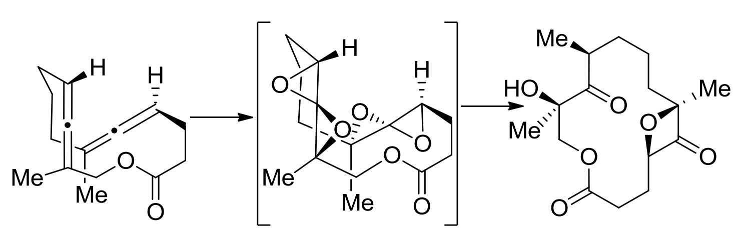

S4.4 **S4.5** **S4.6**

We have developed two methods for oxetan-3-ones synthesis.[10] The first method employs a three-step sequence: (1) double oxidation of allene to obtain spirodiepoxide,

(2) opening of the spirodiepoxide by bromide, and (3) the intramolecular displacement of the bromide by the alkoxide. This simple procedure requires only two work-ups and a final purification. The second method is even simpler and it is a single flask procedure that involves formation of oxetan-3-one by thermal rearrangement of the corresponding spirodiepoxide. These two methods are complementary and stereochemically divergent.

4.2 Oxetan-3-one Synthesis: Nucleophilic Addition/Intramolecular Displacement

We envisioned a two-step process for the generation of oxetan-3-ones: nucleophile induced opening of spirodiepoxide followed by treatment with base. Since the nucleophile also needs to be a good leaving group, we identified halide as the nucleophile. Consequently, we started our study with iodide. Addition of sodium iodide to a solution of acetonitrile and spirodiepoxide gave three products: the desired oxetan-3-one **S4.8**, the α–hydroxy–α′–iodoketone **S4.9**, and the α–hydroxylketone **S4.10** (Scheme 2). In contrast, lithium iodide gave iodohydroxylketone **S4.9** as the sole product in good yield. Alternatively, subsequent addition of HMPA to the lithium iodide reaction mixture gave the oxetan-3-one **S4.8** (Scheme 2, condition A), as desired. However, these conditions were not general for other substrates and often favored the hydroxyketone product. The ready loss of iodide from α-iodoketones is well known.[11] So, we studied the use of bromide instead of iodide. After extensive experimentations we determined a simple, efficient, and reliable procedure for oxetan-3-one synthesis under mild condition. Addition of lithium bromide to the spirodieoxide in tetrahydrofuran, followed by replacement of the solvent by methyl sulfoxide and then exposure to potassium hydroxide gave oxetan-3-one **S4.8** in excellent yield (92%, Scheme 2, Condition B).

We used this method to convert several allenes to oxetan-3-ones as shown in Table 1. For achiral trisubstituted allenes the yields were excellent (entries 1–4). However, for chiral trisubstituted allenes the yields were modest (entries 5–7). The major by-product was the simple hydroxyketone. Evidently, debromination competes with cyclization for some substrates. The above approach is effective in generating trisubstituted oxetan-3-ones. We recognized this method is not adaptable to all substitution patterns. For example, nucleophilic addition is highly regioselective in trisubstituted allenes but not in unsymmetrical disubstituted allenes. In case of trisubstituted allene, nucleophile adds exclusively to the most accessible site. However, in case of disubstituted allene, nucleophile can add to either site.

Scheme 2. Iodide Induced Oxetan-3-one Synthesis

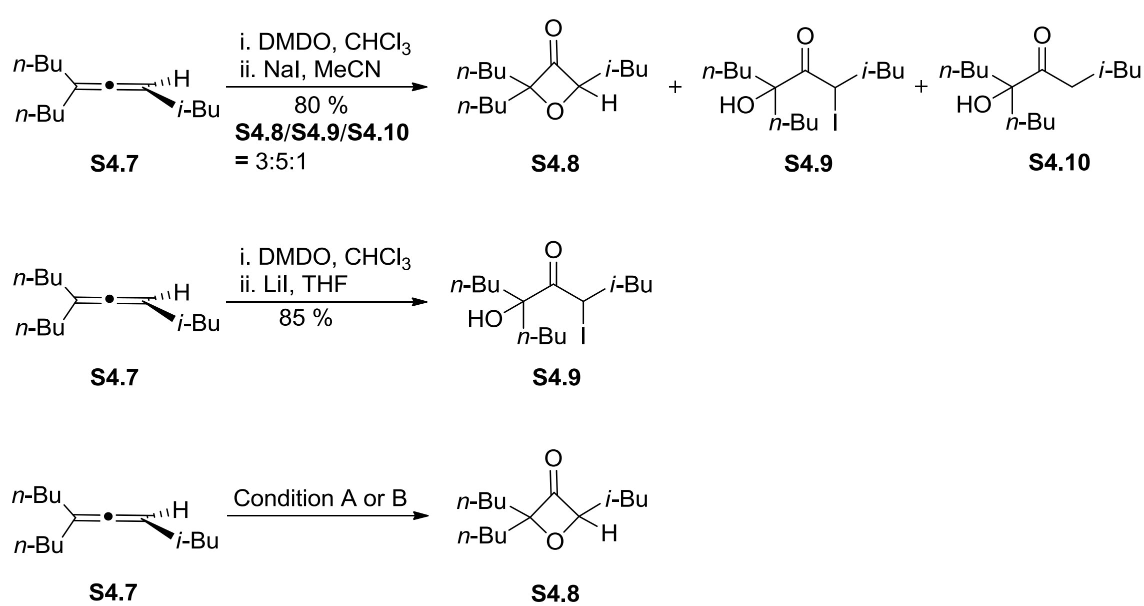

Condition A: DMDO, $CHCl_3$; LiI, THF then HMPA (76 %)
Condition B: DMDO, $CHCl_3$; LiBr, THF; KOH, DMSO (92 %)

Table 1. Bromide Induced Oxetan-3-one Synthesis

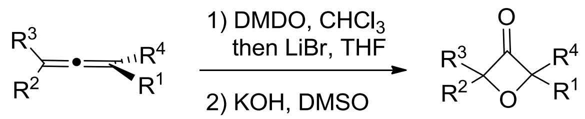

S4.11 → **S4.12**

Entry	Product	Yield (%)	Entry	Product	Yield (%), (dr)
1	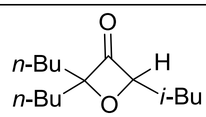 **S4.8**	92	5	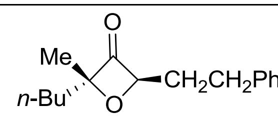 **S4.16**	45 (1.4:1)
2	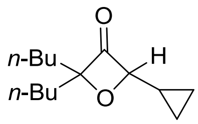 **S4.13**	93	6	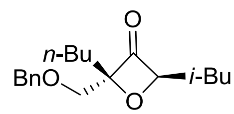 **S4.17**	41 (1.1:1)
3	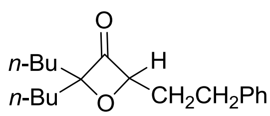 **S4.14**	90	7	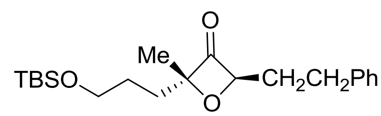 **S4.18**	41 (1.4:1)
4	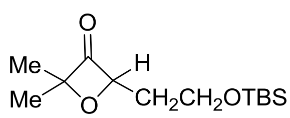 **S4.15**	86			

Conditions: DMDO (2.5 equiv), $CHCl_3$, −20°C, 1–2 h; LiBr (1.1 equiv), THF, 0°C to rt, 1–3 h; KOH (1.10 equiv), DMSO, 5–10 min.

4.3 Oxetan-3-one Synthesis: Thermal Rearrangement

We wondered whether a thermal rearrangement of a spirodiepoxide could be a simple and general method to synthesize oxetan-3-ones. We have shown that spirodiepoxides have good kinetic stability in non-acidic conditions and that they can also be prepared on multi-gram scale, manipulated, and used without purification.[12] The data in Tables 2 and 3 demonstrate that spirodiepoxides also have good thermal stability. In our earlier optimization efforts in this area, we found refluxing toluene to be suitable for some substrates and *p*-xylene to be suitable for other substrates. Similar to the report by Crandall, many spirodiepoxides failed to rearrange and only slow decomposition was noted after extended reaction times when refluxing toluene was used.[8f] However, our aim was to find a general method that would be suitable for most substrates. We determined that microwave heating of spirodiepoxides at 200 °C effected the smooth and efficient rearrangement of spirodiepoxide to the corresponding oxetan-3-ones. It should be noted that high quality DMDO is especially important in the thermal rearrangement reaction.

Table 2. Oxetan-3-one Synthesis by Thermal Rearrangement

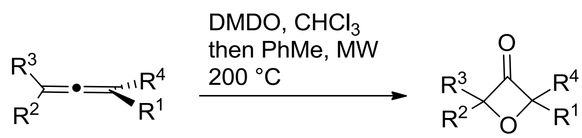

S4.19 → **S4.20**

Entry	Product	Yield (%)	Entry	Product	Yield (%), (dr)
1	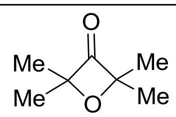 **S4.21**	51	5	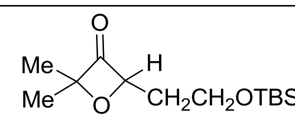 **S4.15**	83
2	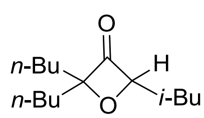 **S4.8**	98	6	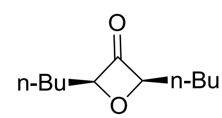 **S4.22**	88 (2:1)
3	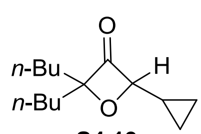 **S4.13**	95	7	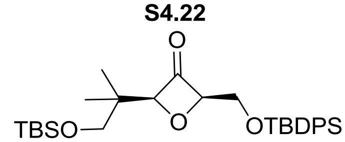 **S4.23**	73 (8:1)
4	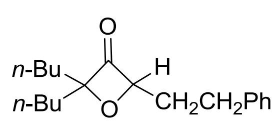 **S4.14**	95	8	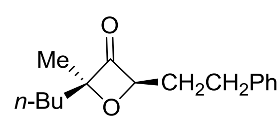 **S4.24**	82 (1.4:1)

Conditions: 2.50 equiv DMDO, $CHCl_3$, −20°C, 1–2 h; conc., PhMe, MW 200°C, 1–1.5 h.

The microwave promoted thermal rearrangement method was effective for a range of allenes including tetrasubstituted (entry 1), trisubstituted (entries 2–5, and 8) and disubstituted (entry 6 and 7) substrates. We suspected the yield for oxetan-3-one **S4.21** is low because the intermediate tetramethyl spirodiepoxide and the oxetan-3-one product **S4.21** are volatile.

The diastereomeric ratios of the spirodiepoxide precursors and the oxetan-3-one products were identical (entries 6 and 7). We suggested that the rearrangement is concerted based on the stereochemical fidelity of the transformation. We reduced the ketone of the oxetan-3-one **S4.22** to determine the stereochemical assignment of oxetan-2-one **S4.22**.[13] The major oxetan-3-one must be the *cis* isomer, as shown, because the sodium borohydride reduction of the major oxetan-3-one (**S4.22**) gave two diastereomeric alcohols (**S4.25** and **S4.26**). The minor oxetan-3-one must be the *trans* isomer because the minor oxetan-3-one (**S4.27**) gave a single diastereomer (**S4.28**) (Scheme 3). Reduction of **S4.27** compound can give only one alcohol, since the hydroxyl-bearing carbon is not stereogenic.

Scheme 3. Proof of Stereochemical Assignment

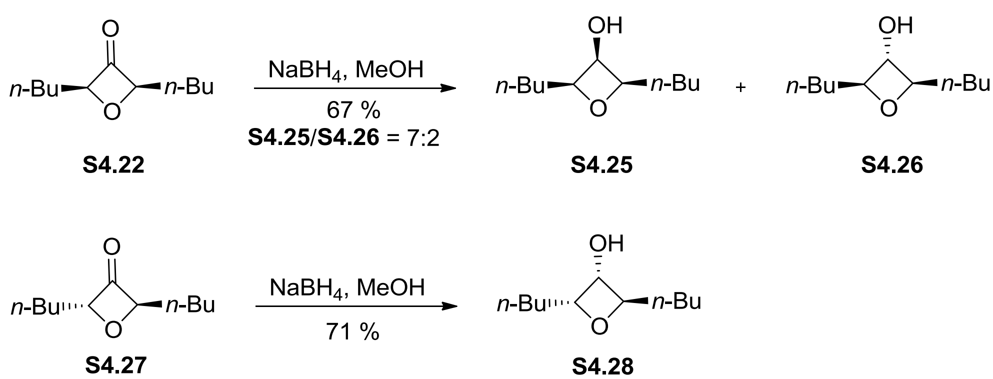

Table 3 lists data for the thermal rearrangement of terminal allenes. Both acyclic and cyclic 1, 1-disubstituted allene substrates were converted to the corresponding oxetan-3-ones in good yield (**S4.31** and **S4.32**, entry 1 and 2). Monosubstituted allenes were also efficiently transformed to corresponding oxetan-3-ones (**S4.33** and **S4.34**, entry 3 and 4).

Table 3. Terminal Oxetan-3-one Synthesis by Thermal Rearrangement

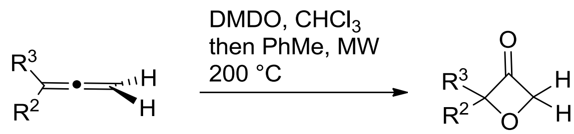

S4.29 → **S4.30**

Entry	Product	Yield (%)	Entry	Product	Yield (%)
1	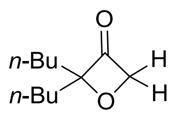 **S4.31**	70	3	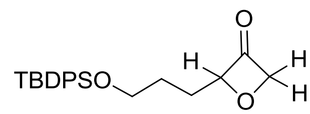 **S4.33**	86
2	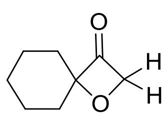 **S4.32**	68	4	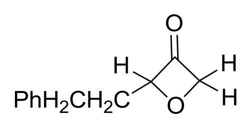 **S4.34**	65

Conditions: 2.50 equiv DMDO, $CHCl_3$, −20°C, 1–2 h; conc., PhMe, MW 200°C, 1–1.5 h.

Spirodiepoxides derived from terminal allenes are particularly sensitive to manipulation. It may be that the lack of steric interference makes the terminal carbon highly reactive. However, the synthesis of oxetan-3-one by thermal rearrangement of terminal spirodiepoxide worked well.

4.4 Oxetan-3-one Synthesis: Mechanistic Outline

Experimental and computational analysis of oxetan-3-ones formed by the nucleophilic addition/intramolecular displacement and thermal rearrangement method revealed that these two methods are stereochemically divergent and highly complementary.

The stereochemistry of the oxetan-3-one formed by the halide-induced method is inverted twice at the least substituted site. We reasoned that in the halide-induced method the bromide opens the spirodiepoxide at the least substituted site (Scheme 4, top, **S4.35→S4.36**). Addition of bromide results in the inversion at that carbon. The alkoxide then displaces the bromide and this carbon center is inverted again with overall retention (**S4.36→S4.37**). We reasoned that the thermal rearrangement method is a concerted one-step process and that the pathway is asynchronous with inversion of configuration and build up of positive charge on the terminal carbon during migration of the oxygen. The reaction should take place at the more substituted terminus: the terminus which is most able to stabilize positive charge. This pathway should lead to inversion at only one center. The first method should engage the less substituted terminus of the epoxide and the second method should engage the more substituted terminus, and these oxetan-3-one syntheses should lead to divergent stereochemical outcomes.

We experimentally evaluated our prediction (Scheme 4, bottom). Spirodiepoxides derived from enantioenriched allene **S4.40** gave oxetan-3-one **S4.16** as the major product. The major product of thermal rearrangement was **S4.24**. The minor product of the bromide induced method is the antipode of **S4.24**. The minor product of the thermal rearrangement method is the antipode of **S4.16**.

The two methods are highly complementary, as either diastereomeric oxetan-3-one can be prepared as the major product. The first epoxidation of an allene effectively sets the absolute configuration of the spirodiepoxide, as it converts the chiral axis to center chirality. The second epoxidation determines the diastereomeric ratio within that enantiomeric series. In the halide-induced method, both configurations are retained. In the thermal rearrangement, the center that sets the absolute configuration is inverted – reversing the enantiomeric series. This is the only center that is inverted; consequently, the diastereotopicity is also reversed relative to the halide-based method.

Scheme 4. Mechanistic Framework

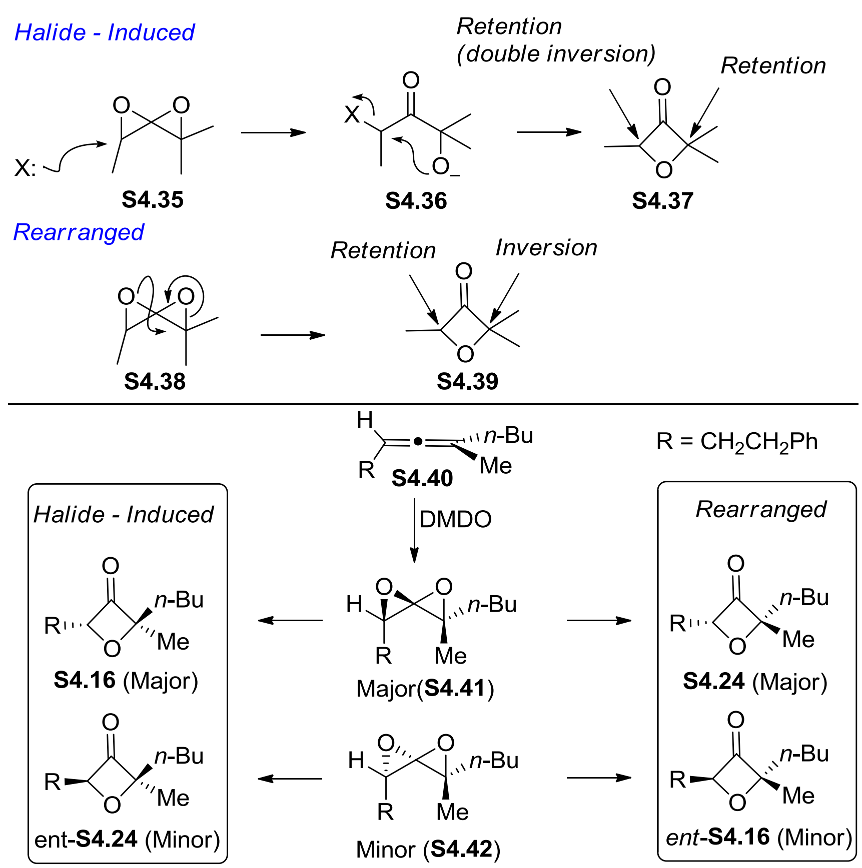

We evaluated the thermal rearrangement computationally (Figure 2). As expected and consistent with the above experimental findings we found the thermal rearrangement to be concerted and asynchronous. A single barrier separates the starting material from product. The barrier is large, consistent with high reaction temperature. Not surprisingly, the reaction is highly exothermic. Key bond lengths of the computed transition structure (**S4.44**) are indicated. As the transition structure is approached, C^1–O^1 elongates, O^1–C^2 contracts, C^2–O^2 elongates, and O^2–C^1 contracts. Importantly, the C^1–O^1 bond distance increases by 0.627 Å without compensating contraction between O^2 and C^1, consistent with significant charge build-up on carbon.[14] This insight supports the above rationale and is consistent with the stereochemical data and mechanistic framework outlined in Scheme 4.

Figure 2.Computational Analysis of Thermal Rearrangement (kcal/mol)[15]

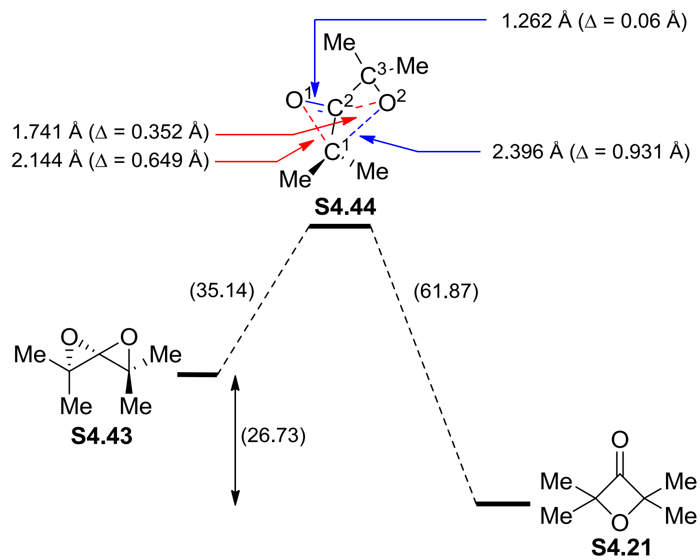

4.5 Conclusion

In summary, we have reported two complementary methods of preparing oxetan-3-ones from allenes. We have shown that the oxetan-3-one motifs can be readily accessed in one (Table 2 and 3) or two steps (Table 1) starting from allenes via spirodiepoxides. We have also described key stereochemical and mechanistic features of the synthesis of oxetan-3-ones via allene. Mechanistic studies provided a framework for understanding the thermal rearrangement of a spirodiepoxide to form an oxetan-3-one.

4.6 References

1. Dejaegher, Y.; Kuz'menok, N. M.; Zvonok, A. M.; De Kimpe, N. *Chem. Rev.* **2002,** *102,* 29.

2. Hirschmann, R.; Bailey, G. A.; Poos, G. I.; Walker, R.; Chemerda, J. M. *J. Am. Chem. Soc.* **1956,** *78,* 4814.

3. Rowland, A. T.; Bennett, P. J.; Shoupe, T. S. *J.Org.Chem.* **1968**, *33,* 2426.

4. a) Kozikowski, A. P.; Fauq, A. H. *Synlett* **1991,** *1991,* 783; b) Hamzik, P. J.; Brubaker, J. D. *Org. Lett.* **2010,** *12,* 1116; c) Kitagawa, M.; Hasegawa, S.; Saito, S.; Shimada, N.; Takita, T. *Tetrahedron Lett.* **1991,** *32,* 3531.

5. Wuitschik, G.; Rogers-Evans, M.; Müller, K.; Fischer, H.; Wagner, B.; Schuler, F.; Polonchuk, L.; Carreira, E. M. *Angew. Chem., Int. Ed.* **2006,** *45,* 7736.

6. Wuitschik, G.; Carreira, E. M.; Wagner, B.; Fischer, H.; Parrilla, I.; Schuler, F.; Rogers-Evans, M.; Müller, K. *J. Med. Chem.* **2010**, *53*, 3227.

7. (a) Matsuda, I.; Ogiso, A.; Sato, S. *J. Am. Chem. Soc.* **1990**, *112*, 6120; b) Campi, E. M.; Dyall, K.; Fallon, G.; Jackson, W. R.; Perlmutter, P.; Smallridge, A. J. *Synthesis* **1990**, 855; c) Adam, W.; Albert, R.; Dachs Grau, N.; Hasemann, L.; Nestler, B.; Peters, E. M.; Peters, K.; Prechtl, F.; Von Schnering, H. G. *J. Org. Chem.* **1991**, *56*, 5778; d) Roso-Levi, G.; Amer, I. *J. Mol. Catal. A: Chem.* **1996**, *106*, 51; e) Zhang, C.; Lu, X. *Synthesis* **1996**, 586–589. (f) Gabriele, B.; Salerno, G.; DePascali, F.; Costa, M.; Chiusoli, G. P. *J. Chem. Soc., Perkin Trans. 1* **1997**, 147; g) Bartels, A.; Jones, P. G.; Liebscher, J. *Synthesis* **1998**, 1645; h) Dollinger, L. M.; Ndakala, A. J.;

Hashemzadeh, M.; Wang, G.; Wang, Y.; Martinez, I.; Arcari, J. T.; Galluzzo, D. J.; Howell, A. R.; Rheingold, A. L.; Figuero, J. S. *J. Org. Chem.* **1999**, *64*, 7074; i) Martinez, I.; Andrews, A. E.; Emch, J. D.; Ndakala, A. J.; Wang, J.; Howell, A. R. *Org. Lett.* **2003**, *5*, 399; j) Ma, S.; Wu, B.; Jiang, X.; Zhao, S. *J. Org. Chem.* **2005**, *70*, 2568; k) For a review, see: Tidwell, T. T. *Eur. J. Org. Chem.* **2006**, 563; l) Raju, R.; Howell, A. R. *Org.Lett.* **2006**, *8*, 2139; m) Bejot, R.; Anjaiah, S.; Falck, J. R.; Mioskowski, C. *Eur. J. Org. Chem.* **2007**, 101; n) Ye, L.; He, W.; Zhang, L. *J. Am. Chem. Soc.* **2010**, *132*, 8550; o) Maegawa, T.; Otake, K.; Hirosawa, K.; Goto, A.; Fujioka, H. *Org. Lett.* **2012**, *14*, 4798.

8. a) Crandall, J. K.; Machleder, W. H. *Tetrahedron Lett.* **1966**, *7*, 6037; b) Crandall, J. K.; Machleder, W. H.; Thomas, M. J. *J. Am. Chem. Soc.* **1968**, *90*, 7292; c) Crandall, J. K.; Conover, W. W.; Komin, J. B.; Machleder, W. H. *J. Org. Chem.* **1974**, *39*, 1723; d) 2-methylocta-2,3-diene was converted to the oxetan-3-one after epoxidation and then flash vacuum pyrolysis. See: Crandall,J. K.; Batal, D. J. *J.Org.Chem.* **1988**, *53*, 1338; e) Crandall, J. K.; Batal, D. J.; Sebesta, D. P.; Lin, F. *J. Org. Chem.* **1991**, *56*, 1153; f) Crandall, J. K.; Batal, D. J.; Lin, F.; Reix, T.; Nadol, G. S.; Ng, R. A. *Tetrahedron* **1992**, *48*, 1427.
9. Ghosh, P.; Zhang, Y.; Emge, T. J.; Williams, L. J. *Org. Lett.* **2009**, *11*, 4402.
10. Results discussed in this chapter have been published. See: Sharma, R.; Williams, L. J. *Org. Lett.* **2013**, *15*, 2202.
11. a) Zimmerman, H.; Mais, A. *J. Am. Chem. Soc.* **1959**, *81*, 3644; b) Townsend, J. M.; Spencer, T. A. *Tetrahedron Lett.* **1971**, *2*, 137; c) Olah, G. A.; Arvanaghi, M.; Vankar, Y. D. *J. Org. Chem.* **1980**, *45*, 3531; d) Gemal, A. L.; Luche, J. L.

Tetrahedron Lett. **1980**, *21*, 3195; e) Ono, A.; Fujimoto, E.; Ueno, M. *Synthesis* 1986, 570; f) Ono, A.; Kamimura, J.; Suzuki, N. *Synthesis* **1987**, 406.

12. a) Sharma, R.; Manpadi, M.; Zhang, Y.; Kim, H.; Ahkmedov, N. G.; Williams, L. J. *Org*. *Lett*. **2011**, *13*, 3352; b) Joyasawal, S.; Lotesta, S. D.; Akhmedov, N. G.; Williams, L. J. *Org*. *Lett*. **2010**, *12*, 988; c) Zhang, Y.; Cusick, J. R.; Shangguan, N.; Katukojvala, S.; Inghrim, J.; Emge, T. J.; Williams, L. J. *J*. *Org*. *Chem*. **2009**, *74*, 7707; d) Ghosh, P.; Zhang, Y.; Emge, T. J.; Williams, L. J. *Org*. *Lett*. **2009**, *11*, 4402; e) Ghosh, P.; Cusick, J. R.; Inghrim, J.; Williams, L. J. *Org*. *Lett*. **2009**, *11*, 4672; f) Wang, Z. H.; Shangguan, N.; Cusick, J. R.; Williams, L. J. *Synlett* **2008**, *2*, 213; g) Ghosh, P.; Lotesta, S. D.; Williams, L. J. *J*. *Am*. *Chem*. *Soc*. **2007**, *129*, 2438; h) Shangguan, N.; Kiren, S.; Williams, L. J. *Org*. *Lett*. **2007**, *9*, 1093; i) Lotesta, S. D.; Kiren, S. K.; Sauers, R. R.; Williams, L. J. *Angew*. *Chem*. *Int*. *Ed*. **2007**, *46*, 7108; j) D.; Hou, Y.; Williams, L. J. *Org*. *Lett*. **2007**, *9*, 869; k) Katukojvala, S.; Barlett, K. N.; Lotesta, S. D.; Williams, L. J. *J*. *Am*. *Chem*. *Soc*. **2004**, *126*, 15348.
13. The stereochemical assignment for Table 2, entries 7 and 8 was based on entry 6.
14. a) The frequency calculation of the transition structure revealed a vibrational mode similar to a vibrational mode in the spirodiepoxide starting material. This relationship suggests a vibrational pathway that enables the concerted process; see: b) Ess, D. H. & Houk, K. N. *J*. *Am*. *Chem*. *Soc*. 2007, 129, 10646; c) Ess, D. H.; Houk, K. N. *J*. *Am*. *Chem*. *Soc*. 2008, *130*, 10187; d) Kolakowski, R. V.; Williams, L. J. *Nat*. *Chemistry* 2010, *2*, 303 and references cited therein.
15. a) Electronic structure calculation were performed and optimized using DFT (B3LYP) and the G631* basis Gaussian 03 (Revision B.02): Frisch, M. J.; Trucks, G.

W.; Schlegel, H. B.; Scuseria, G. E.; Robb, M. A.; Cheeseman, J.R.; Montgomery, J. A. Jr.; Vreven, T.; Kudin, K. N.; Burant, J. C.; Millam, J. M.; Iyengar, S.S.; Tomasi, J.; Barone, V.; Mennucci, B.; Cossi, M.; Scalmani, G.; Rega, N.; Petersson, G.A.; Nakatsuji, H.; Hada, M.; Ehara, M.; Toyota, K.; Fukuda, R.; Hasegawa, J.; Ishida, M.; Nakajima, T.; Honda, Y.; Kitao, O.; Nakai, H.; Klene, M.; Li, X.; Knox, J. E.; Hratchian,H. P.; Cross, J. B.; Adamo, C.; Jaramillo, J.; Gomperts, R.; Stratmann, R. E.; Yazyev, O.; Austin, A. J.; Cammi, R.; Pomelli, C.; Ochterski, J. W.; Ayala, P. Y.; Morokuma, K.; Voth, G. A.; Salvador, P.; Dannenberg, J. J.; Zakrzewski, V. G.; Dapprich, S.; Daniels, A. D.; Strain, M. C.; Farkas, O.; Malick, D. K.; Rabuck, A. D.; Raghavachari, K.; Foresman, J. B.; Ortiz, J. V.; Cui, Q.; Baboul, A. G.; Clifford, S.; Cioslowski, J.; Stefanov, B. B.; Liu, G.; Liashenko, A.; Piskorz, P.; Komaromi, I.; Martin, R. L.; Fox, D. J.; Keith, T.; Al-Laham, M. A.; Peng, C. Y.; Nanayakkara, A.; Challacombe, M.; Gill, P. M. W.; Johnson B.; Chen,W.; Wong, M. W.; Gonzalez, C.; Pople, J. A.: Gaussian, Inc.: Pittsburgh, 2003; B3LYP functional: b) Becke, A. D. *J. Chem. Phys.* 1993, *98*, 5648; c) Lee, C.; Yang, W.; Parr, R. G. *Phys. Rev.B.* 1988, *37*, 785; 6-31g(d,p) basis sets: d) Clark, T.; Chandrasekhar, J.; Spitznagel, G. W.; Schleyer, P.v.R. *J. Comp. Chem.* 1983, *4*, 294; e) McLean, A. D.; Chandler, G. S. *J. Chem. Phys.* 1980, *72*, 5639; f) Krishnan, R.; Binkley, J. S.; Seeger, R.; Pople, J. A. *J. Chem. Phys.* 1980, *72*, 650; g) Hariharan, P. C.; Pople, J. A. *Mol. Phys.* 1974, *27*, 209; h) Ditchfield, R.; Hehre, W. J.; Pople, J. A. *J. Chem. Phys.* 1971, *54*, 721; CPCM: i) Cossi, M.; Barone, V. *J. Phys. Chem. A* 1998, *102*, 1995.

Chapter 5

Spirodiepoxide Based Cascades in the Studies towards the Synthesis of Pectenotoxin 4 (PTX4)

5.1 Introduction

The pectenotoxins (PTXs) (Figure 1) are a group of marine natural products linked to diarrhetic shellfish poisoning. Since the first isolation of PTX1-5 (**S5.1**-**S5.4**) from *Patinopecten yessoenis* by Yasumoto *et al*. in 1985[1], nine new PTXs have been isolated.[2] It is now believed that the dinoflagellate, *Dinophysis fortii*, living within the shellfish is the progenitor of the PTXs. Out of these fourteen, PTX2 (**S5.2**) is the only one thought to be produced by the dinoflagellate and is thus considered to be the parent compound of the entire family.[3,4] Once produced, PTX2 (**S5.2**) is amassed and modified in the hepatopancrease of the shellfish. In the digestive gland various analogues of the PTX family are produced.[4,5]

The full structures of all the PTXs have been determined except for PTX5 and PTX10. Structural determination was performed by extensive spectroscopic analysis.[6] The PTXs are polyoxocyclic macrolides that house 19 or 20 stereogenic carbons, a spiroketal, a bicyclic ketal, a hemiketal and three tetrahydrofuran rings. The configuration of the anomeric spiroketal at C7, substitution at C18, and structural variation in the F and G ring systems differentiate the PTXs (Figure 1). The 36*S*-PTX12 (**S5.8**) and 36*R*-PTX12 (**S5.9**) are present in seco acid form also.

Figure 1. Structure of the Pectenotoxins

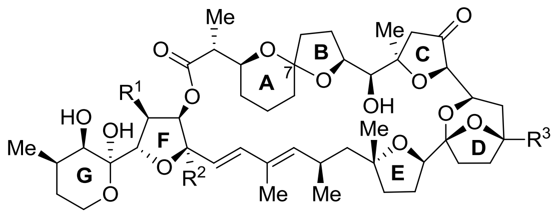

	C7	R^1	R^2	R^3
PTX-1 (**S5.1**)	R	H	H	CH_2OH
PTX-2 (**S5.2**)	R	H	H	Me
PTX-3 (**S5.3**)	R	H	H	CHO
PTX-4 (**S5.4**)	S	H	H	CH_2OH
PTX-6 (**S5.5**)	R	H	H	CO_2H
PTX-7 (**S5.6**)	S	H	H	CO_2H
PTX-11 (**S5.7**)	R	OH	H	Me

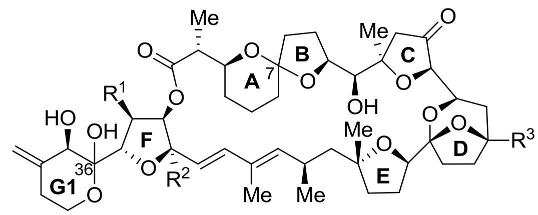

	C7	R^1	R^2	R^3
36S-PTX-12 (**S5.8**)	R	H	H	Me
36R-PTX-12 (**S5.9**)	R	H	H	Me
PTX-13 (**S5.10**)	R	H	OH	Me

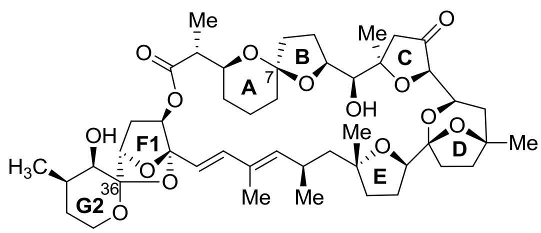

PTX-14 (**S5.11**)

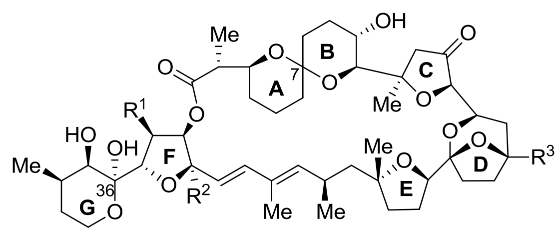

	C7	R^1	R^2	R^3
PTX-8 (**S5.12**)	S	H	H	CH_2OH
PTX-9 (**S5.13**)	S	H	H	COOH

The PTXs have been classified as diarrhetic shellfish poisons.[1] However, results obtained from recent studies have contradicted the original classification. It has been determined that PTXs have minimal to no diarrhetic effect.[2] Nevertheless, PTXs are biologically interesting molecules. The PTXs depolymerize actin, induce apoptosis, and are hepatotoxic and cytotoxic.[7a] The mechanism of action of the PTXs appears to be unique. Unlike other actin targeting cytotoxins, the PTXs work solely by preventing polymerization of actin monomers and do not cause severing of actin polymers.[7b] The mode of action of the PTXs was unknown until 2007 when the x-ray structure of a PTX2-

actin complex was published [PTX2 (**S5.2**) depicted in gold, water as green and ATP as green and red ball-and-stick, Figure 2)].[7c] The crystal structure of the PTX2-actin complex suggests that PTX2 (**S5.2**) binds to the barbed end of the actin filament and blocks another actin monomer from interacting with the filament (Figure 3[8]).

Figure 2. X-ray Structure of a PTX2-Actin Complex[7c]

There is considerable variability in the potency of the PTXs. It has been determined that PTX2 (**S5.2**) is the most biologically active member of the PTX family. PTX2 (**S5.2**) appears to make several important contacts with actin, especially near C5, C6, C9, C22, C23, C28, C29, C30, C39, C40, C45, C47, O6, O11, O12, O13 and O14 (Red line represent hydrogen bonding of water molecule with the amino acid residue and black line shows Van derWaals interaction, Figure 4).[7c] The presence of macrolactone ring, configuration at C-7 and substitution at C-18 also appear to play an important role in rendering biological activities to PTXs.[9] Studies have shown that 200nM of PTX1 (**S5.1**), PTX2 (**S5.2**), and PTX11 (**S5.7**) causes 25%±4%, 50%±6%, and 46%±4% depolymerization of actin in neuroblastoma cells, respectively.

Figure 3. Mechanism of Action of PTX[8]

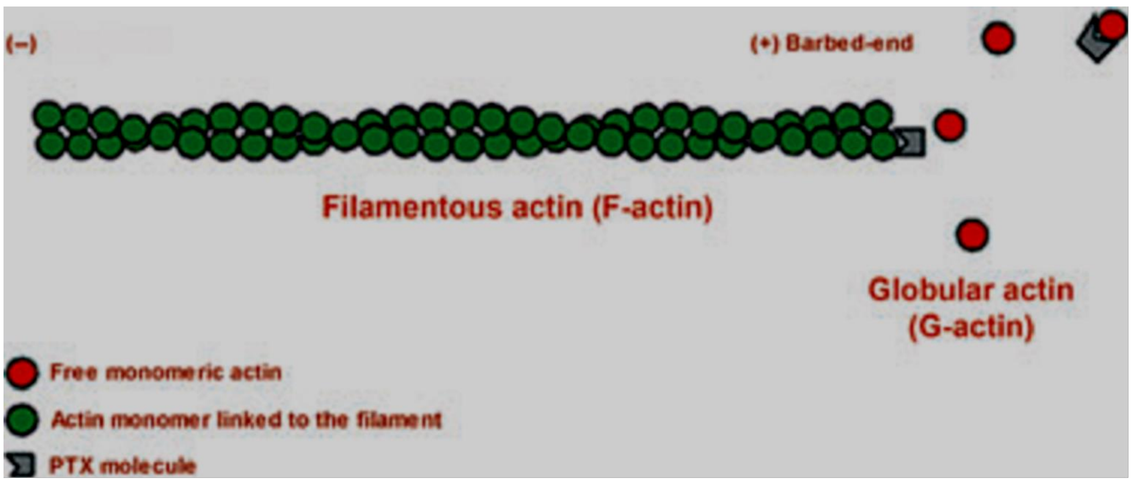

Figure 4. LIGPLOT Analysis of the Interaction of PTX2 with Actin[7c]

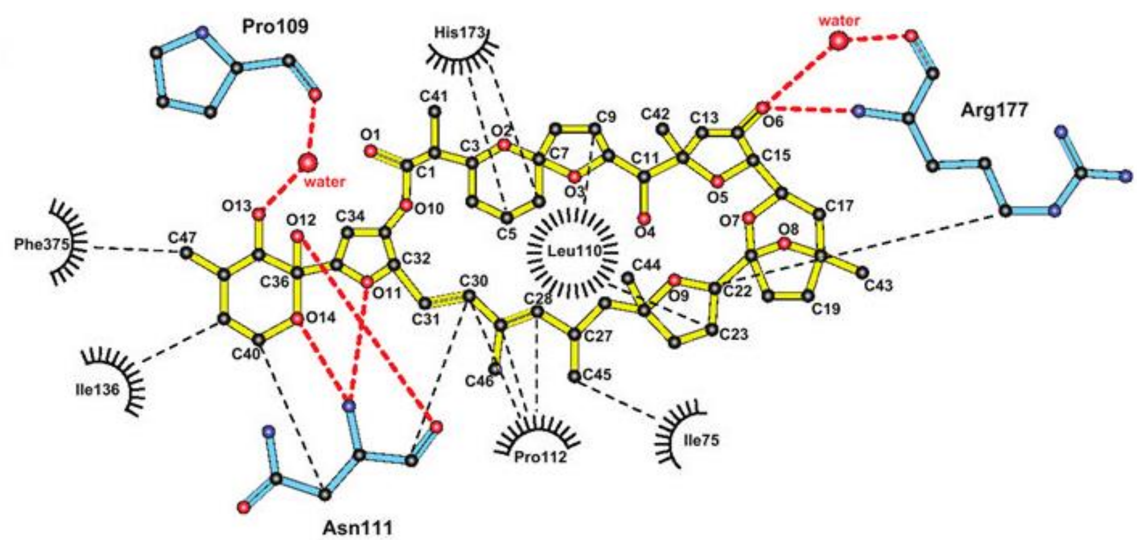

5.2 Previous Partial Syntheses of PTX

The promising biological activities as well as the complex architecture of the PTXs have inspired many scientists to study the synthesis of the molecules. In addition to our work in this area, several fragment syntheses have appeared. In 1997, Murai and Fujiwara Group reported synthesis of the incorrect enantiomer of the PTX2 FG ring (**S5.14**) and in 2005 the correct enantiomer (**S5.15**, Figure 5).[10a,10b] Murai and Fujiwara Group also published routes to a C8-C20 fragment (**S5.16**) and a C21-C30 fragment (**S5.17**) of PTX2 (**S5.2**).[10c]

Figure 5. Fragments of PTX Synthesized by Murai and Fujiwara Group

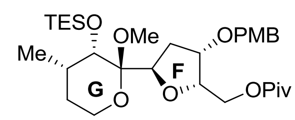

Incorrect FG enantiomer fragment (**S5.14**)

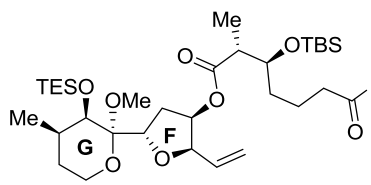

Correct FG enantiomer fragment (**S5.15**)

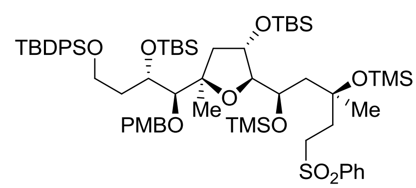

C8-C20 fragment of PTX2 (**S5.16**)

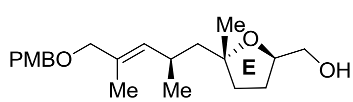

C21-C30 fragment of PTX2 (**S5.17**)

In 2001, Roush Group published a synthesis of a C11-C26 fragment (**S5.18**, Figure 6).[11] Paquette Group published the synthesis of a C29-C40 fragment (**S5.19**) and a C1-C26 fragment (**S5.20**).[12] Brimble Group contributed the synthesis of a C1-C16 fragment (**S5.21**), the FG ring (**S5.22**) and a C12-C28 fragment (**S5.23**).[13] Pihko Group synthesized both anomers of the PTX spiroketal (**S5.24**), a C10-C26 fragment (**S5.25**), and a C10-C22 fragment (**S5.26**) of PTX2.[14] Similarly, in 2007 Rychnovsky Group reported a stereoselective synthesis of the AB spiroketal (**S5.27**).[15]

Figure 6. Synthesized fragments of PTX

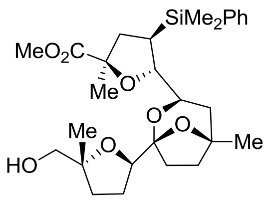

C11-C26 fragment of PTX2 Roush Group (**S5.18**)

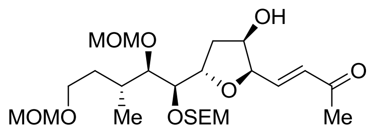

C29-C40 fragment by Paquette Group (**S5.19**)

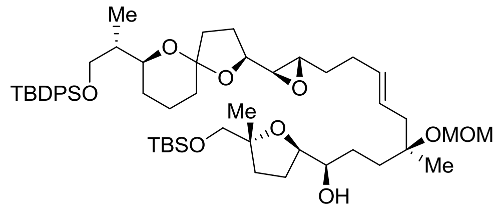

C1-C26 fragment by Paquette Group (**S5.20**)

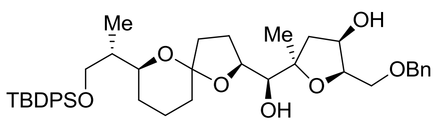

C1-C16 fragment by Brimble Group (**S5.21**)

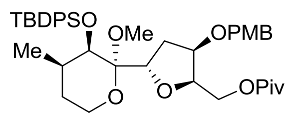

FG ring by Brimble Group (**S5.22**)

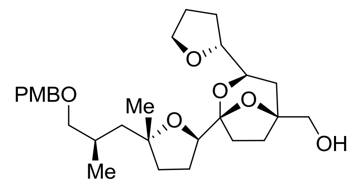

C12-C28 by Brimble Group (**S5.23**)

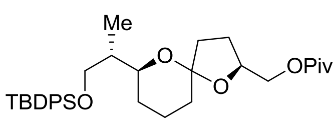

Anomers of spiroketal by Pihko Group (**S5.24**)

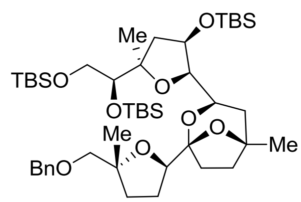

C10-C26 by Pihko Group (**S5.25**)

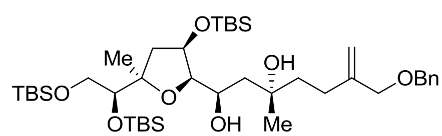

C10-C22 fragment by Pihko Group (**S5.26**)

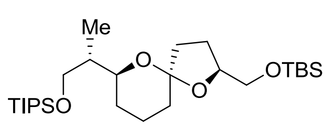

AB spiroketal ring by Rychnovsky Group (**S5.27**)

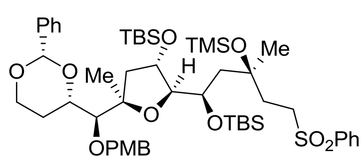

C8-C20 fragment by Suzuki Group (**S5.28**)

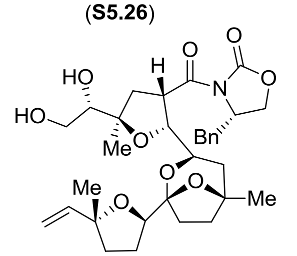

CDE ring by Micalizio Group (**S5.29**)

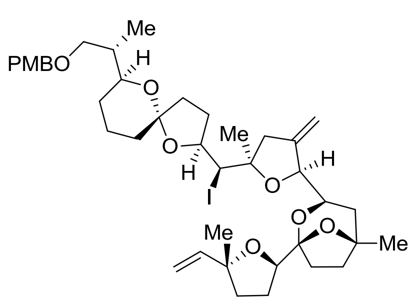

C1-C26 fragment by Micalizio Group (**S5.30**)

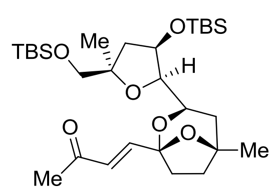

CD ring by Vassilikogiannakis Group (**S5.31**)

Suzuki Group reported the synthesis of a C8-C20 fragment (**S5.28**, Figure 6).[16] Micalizio Group published the synthesis of a CDE ring (**S5.29**) and a C1-C26 fragment (**S5.30**) of PTX2.[17] In 2013, Vassikikogiannakis Group reported the synthesis of a CD ring (**S5.31**) of PTX.[18]

5.3 Previous Total Synthesis of PTX4

Although many groups have reported syntheses of PTXs fragments, to date only one group has achieved a total synthesis of a PTX. In 2002, Evans Group published the total synthesis of PTX4 along with the synthesis of PTX8 from PTX4.[19] The synthesis of PTX4 was accomplished by the coupling of three fragments: a C1-C19 fragment (**S5.32**, Scheme 1), a C31-C40 fragment (**S5.33**) and a C20-C30 fragment (**S5.34**).

Scheme 1. Evans' Total Synthesis of PTX4: Retrosynthetic Analysis

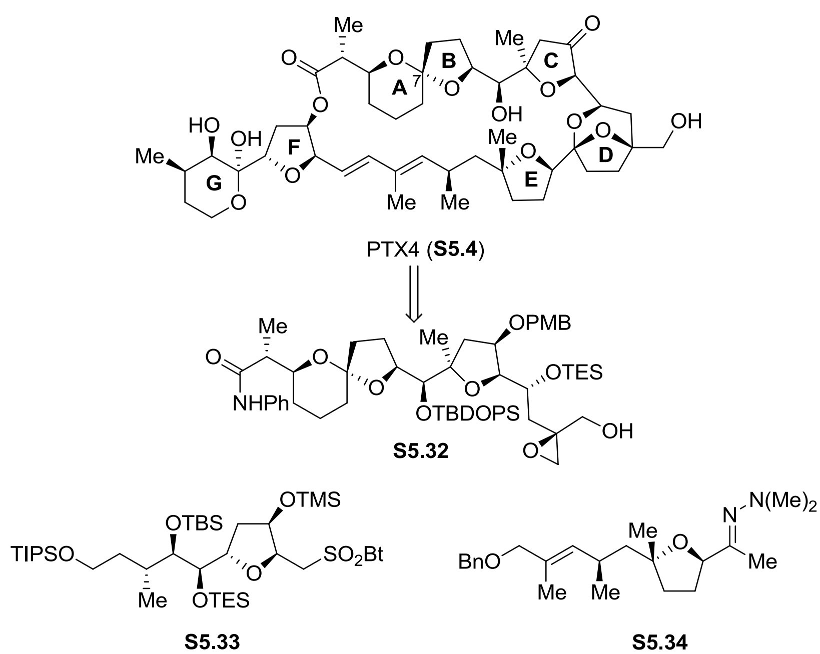

The C1-C19 fragment (**S5.32**) was synthesized in a 19 step longest linear sequence (Scheme 2). An anomeric spiroketal **S5.37** was obtained by performing a Wittig reaction between phosphonium salt **S5.35** (4 steps from 5-hexenol) and **S5.36** (3 steps from ethyl glyoxylate) followed by treatment with acid. The epoxy diol **S5.38** was furnished in 5 additional steps by the virtue of functional group manipulation along with chain elongation. The 5-*exo*-trig cyclization of **S5.38** established the C ring. Acid mediated cyclization of **S5.38**, followed by Barton deoxygenation, subsequent protection/deprotection, and then Felkin controlled asymmetric allylation yielded **S5.39**. The **S5.32** was formed from **S5.39** by protection followed by deprotection, and then Sharpless epoxidation.

Scheme 2. Synthesis of S5.32

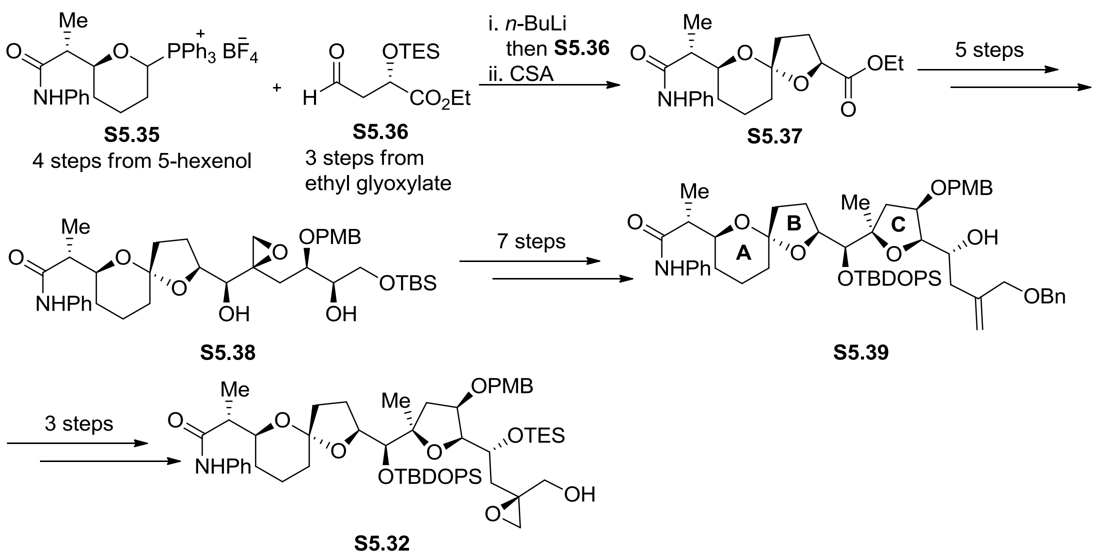

The C31-C40 fragment (**S5.33**) was furnished in 18 step longet linear sequence from commercially available 1,3:4,5-di-*O*-benzylidenemannitol (Scheme 3). The **S5.40** (5 steps from 1,3:4,5-di-*O*-benzylidenemannitol) was converted to phosphonium salt **S5.41** in 4 steps. The **S5.42** (1 steps from ethyl glyoxylate) was converted to aldehyde **S5.43** in 6 steps. Coupling of **S5.42** and **S5.43** yielded the *Z*-olefin (**S5.44**). The F ring was obtained in 5 steps from **S5.44**. Hydroxyl directed epoxidation, followed by protection, deprotection, and the acid mediated 5-*exo*-tet cyclization formed **S5.45**. The benzthiazole was synthesized in 5 steps from **S5.45**.

Scheme 3. Synthesis of S5.33

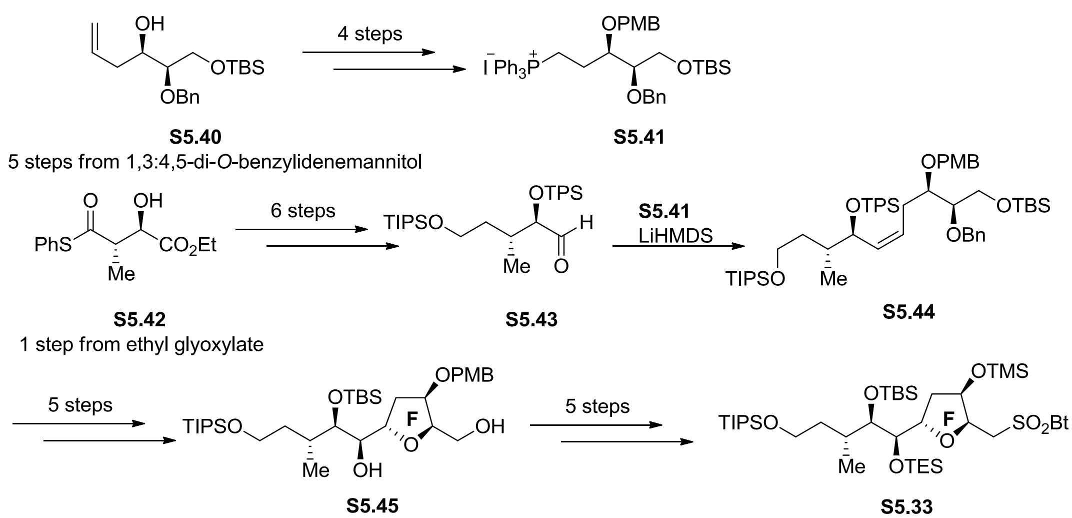

The C20-C30 fragment (**S5.34**) was synthesized in 17 steps from **S5.46** (Scheme 4). The diene **S5.47** was formed in 5 steps from **S5.46**. Claisen rearrangement and then chelation controlled reduction of the resultant ketone yielded **S5.48**. The E ring was formed by the iodoetherification of **S5.48**. The *N*, *N*-dimethylhydrazone adduct (**S5.34**) was obtained in 10 steps from **S5.48**.

The synthesis of PTX4 was accomplished in 37 steps (overall longest linear sequence) and 0.30% overall yield. The C1-C19 fragment (**S5.32**) was converted to $MgBr_2$-activated epoxide (**S5.50**). The C20-C30 fragment (**S5.34**) was converted to metalloenamine (**S5.51**) and coupled with **S5.50** to form **S5.52** (Scheme 5). The alcohol at C30 of the **S5.52** was converted to aldehyde and then coupled with **S5.33** via Julia olefination. Yamaguchi macrolactonization of the intermediate yielded **S5.53**. Deprotection and oxidation followed by global deprotection furnished PTX4 (**S5.4**). Exposure of PTX4 to TFA induced partial isomerization of the AB spiroketal ring. This product corresponds to PTX8.

Scheme 4. Synthesis of S5.34

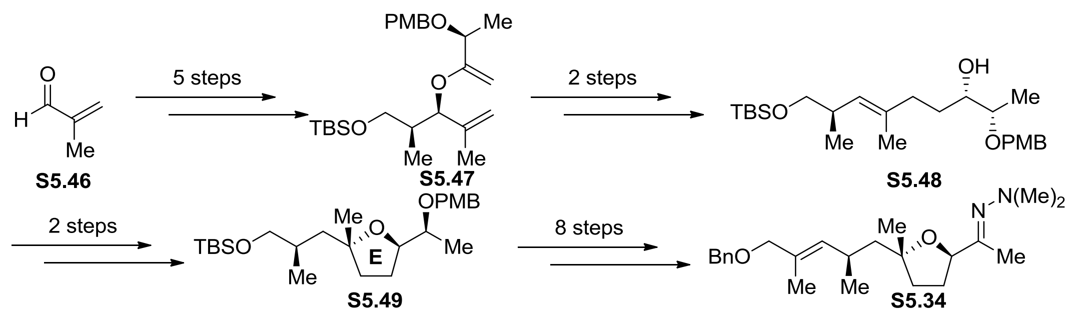

Scheme 5. Completion of Total Synthesis of PTX4

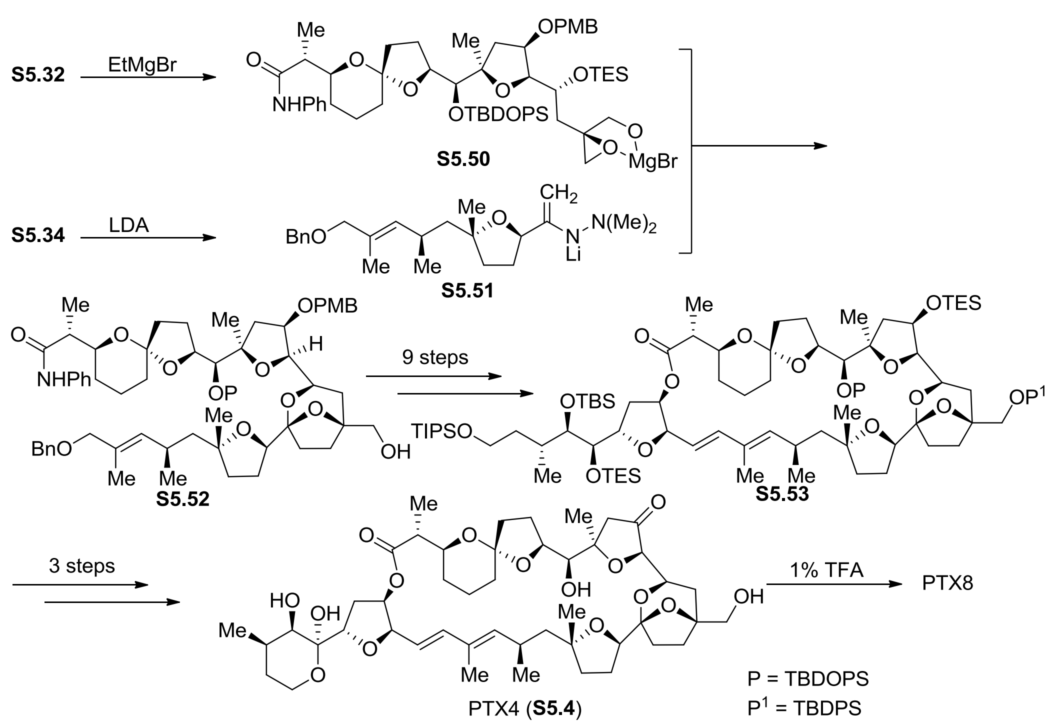

5.4 Our Strategy for the Synthesis of PTX4

The total synthesis of PTX4 (**S5.4**) by Evans Group was accomplished in 37 steps longest linear sequence and 89 total steps. Evans used a flurry of diverse and creative chemistry and masterfully orchestrated these transformations to prepare PTX4 (**S5.4**) and set many of the stereocenters with good control. We wanted to use a unified strategy to control the stereochemistry and to make the cyclic ethers of PTX4 (**S5.4**). The stereocomplexity of the PTXs was the primary motive of our effort. The presence of the highly functionalized cyclic ethers in PTX4 (**S5.4**) served as a particularly enticing feature.

The presence of the three highly functionalized tetrahydrofurans in PTX4 (**S5.4**) made it an obvious, though challenging, target to further demonstrate, evaluate, and develop the spirodiepoxide based method (Scheme 6). In addition to the utilization and evaluation of our spirodiepoxide based chemistry, the goal of our endeavor was to realize a concise, efficient, and highly stereoselective route.

Scheme 6. Spirodiepoxide Based Cascade in the Synthesis of Furas of PTX4

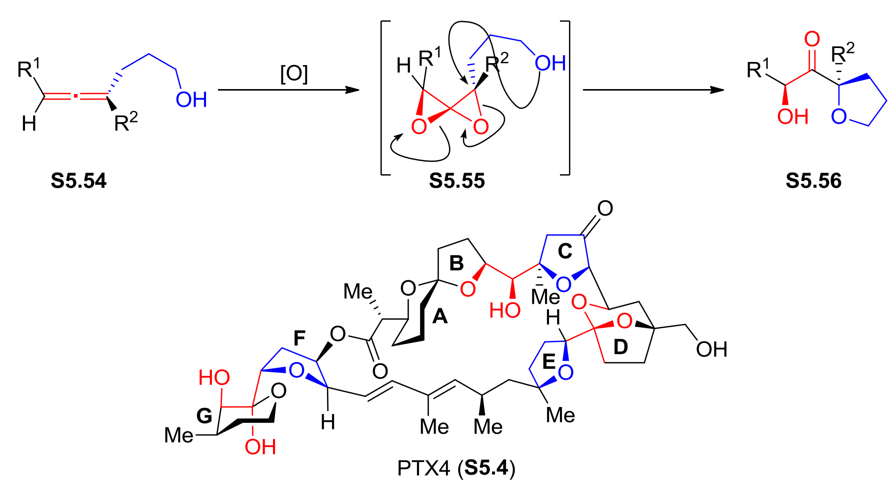

We envisioned constructing PTX4 (**S5.4**) by coupling the upper hemisphere (C1-C20 fragment, **S5.58**, Scheme 7) and the lower hemisphere (C21-C40 fragment, **S5.61**). Both hemispheres would be made by manipulation of modular allenes: **S5.57**, **S5.59** and **S5.60**. We recognized the opportunity to implement spirodiepoxide-cascade sequence to prepare key portion of these fragments. My colleague Da Xu, used spirodiepoxide based cascade reaction to construct A, B and C ring of the PTX4. The treatment of allene (**S5.57**) with dimethyldioxirane (DMDO) gave the product of an extended cascade sequence (**S5.58**).

Scheme 7. Key Disconnection

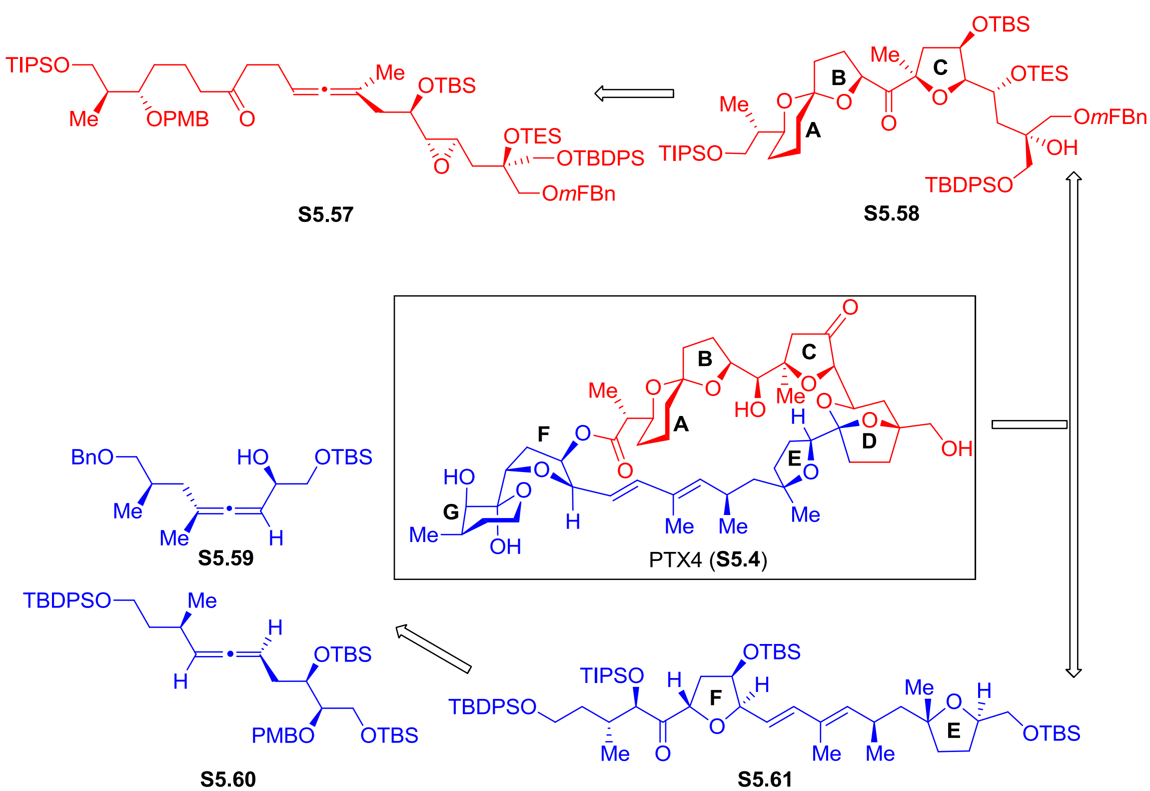

My route to the lower hemisphere (C21-C40) focused on the use of sp^2 – sp^2 coupling, viz. Stille, of a C21-C29 and a C30-C40 fragment. The planned assembly of the

E ring was to use the silver mediated cyclization of allene **S5.59** and subsequent reduction. The plan for the F ring was to use reagent controlled epoxidation and spontaneous opening of the spirodiepoxide by the free hydroxyl group. Thus, the key transformation in the synthesis of the C30-C40 fragment was to involve a cascade reaction sequence as well.

5.5 Synthesis of the AB Spiroketal Ring System of PTX4

In 2007, we reported the synthesis of the PTX4 AB spiroketal (**S5.71**, Scheme 8).[20b] The key step of this synthesis was the formation of the cyclic ether via a spirodiepoxide based cascade. The synthesis was achieved by coupling of aldehyde **S5.64** with allene **S5.68**. The aldehyde **S5.64** was synthesized from the *syn*-aldol product **S5.62**. Reduction of **S5.62**, followed by *p*-methoxybenzyl (PMP) acetal formation, semi-reduction of PMP acetal, formation of *t*-butyldiphenylsilyl (TBDPS) ether (→**S5.63**), and then Lemieux-Johnson oxidation formed aldehyde **S5.64**.

The synthesis of allene **S5.68** was achieved in three steps from amide **S5.65** (Scheme 8). Alkynylation of amide **S5.65** with alkyne **S5.66** gave ynone **S5.67**. The ynone **S5.67** was converted to enantiopure propargyl alcohol under Noyori reduction conditions. The enantiopure propargyl alcohol was mesylated and then subjected to organocuprate mediated S_N2' displacement to yield allene **S5.68**. Deprotection of the primary alcohol, conversion to the corresponding iodide, and the coupling with aldehyde **S5.64** gave allene **S5.69**. Dess-Martin oxidation of the secondary alcohol of **S5.69** and the removal of the PMB group formed allene **S5.70**. Exposure of the allene **S5.70** to

DMDO in the presence of methanol, followed by treatment with acid gave the spiroketal **S5.71** in 89% as a mixture of two isomers (dr = 7:1).

Scheme 8. Synthesis of the AB Spiroketal Ring of PTX4

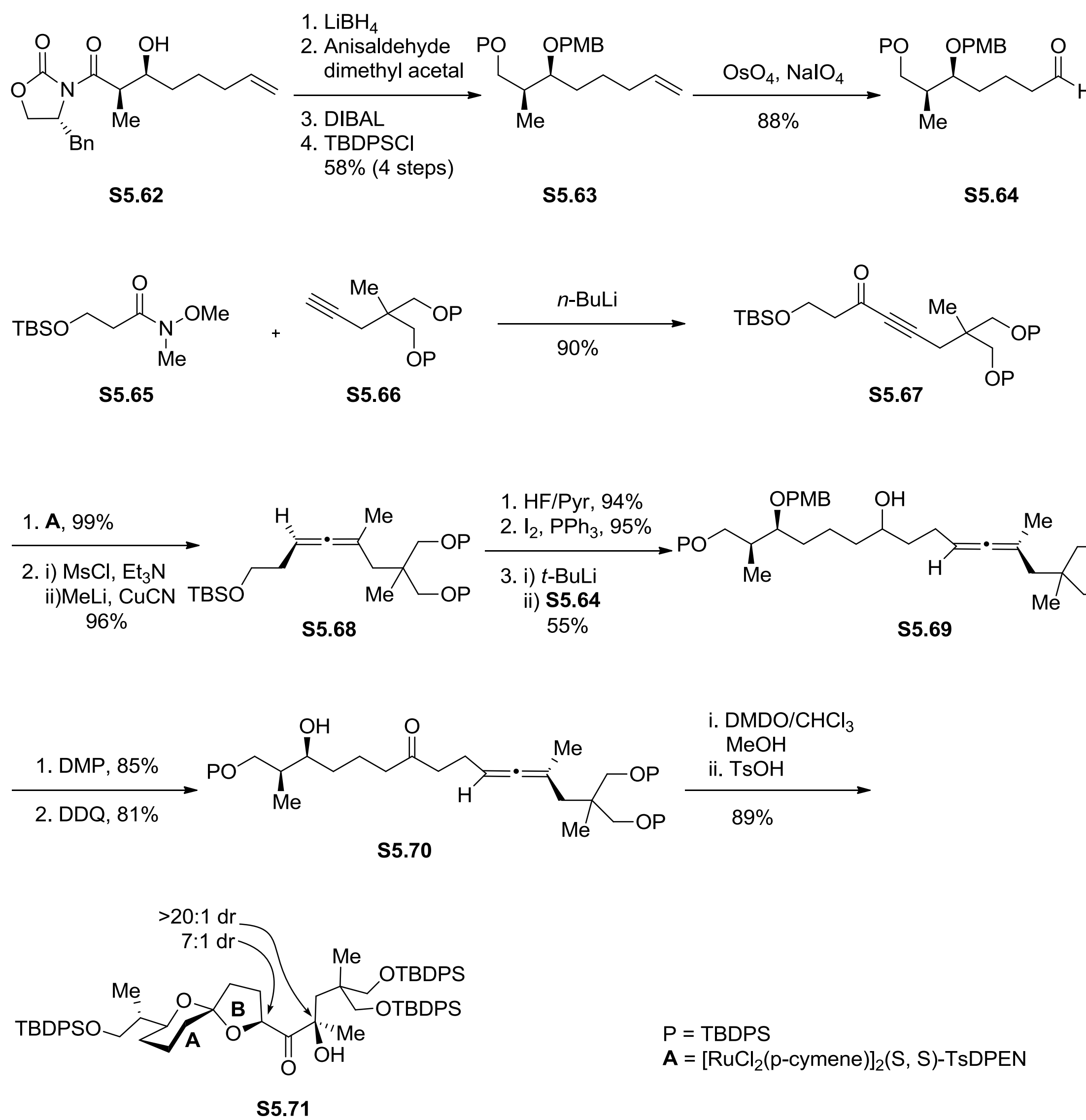

We demonstrated that it was not essential to remove the PMB group prior to spirodiepoxide formation. The allene obtained after Dess-Martin oxidation of **S5.69** was exposed to the solution of DMDO in $CHCl_3$ followed by treatment with acid to give the spiroketal **S5.71** in 72% as mixture of two isomers (dr = 7:1).

We outlined two possible pathways for the formation of the spiroketal (Scheme 9). The first pathway involves opening of spirodiepoxide **S5.72** by ketone (Scheme 9A). The ketone of spirodiepoxide **S5.72** could attack the proximal C-O bond of the epoxide to form **S5.73**. The alcohol of **S5.73** could then trap the oxocarbenium ion to form spiroketal **S5.71**. The second pathway involved lactol initiated opening of spirodiepoxide (Scheme 9B). The allene **S5.70** form lactol **S5.74**. Epoxidation of this allene **S5.74** could form spirodiepoxide **S5.75**, and the free hydroxyl of the lactol **S5.75** could then open the spirodiepoxide to form the observed spiroketal product.

Scheme 9. Mechanistic Outline

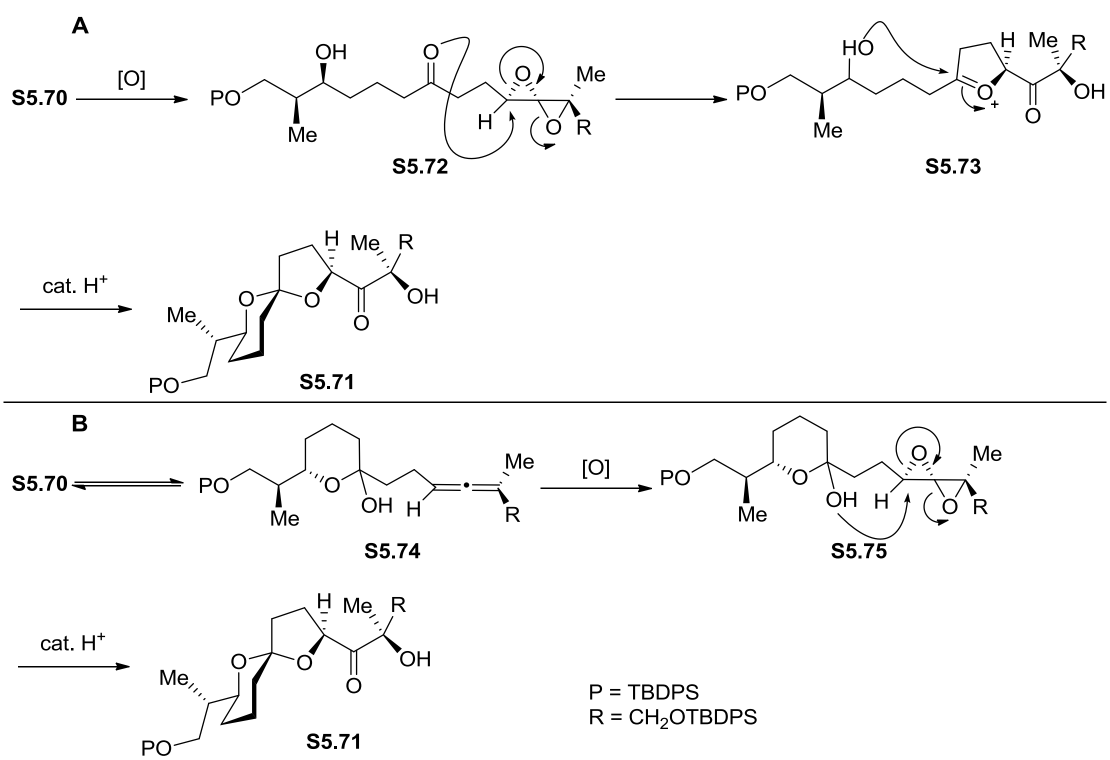

5.6 Synthesis of the C1-C19 Fragment of PTX4

Two years after our report on the synthesis of the AB spiroketal (**S5.71**), we described the synthesis of a C ring-containing fragment (**S5.93**) of PTX4.[20c] As in the case of the synthesis of the AB spiroketal (**S5.71**, Scheme 8), this synthesis illustrates the power of our spirodiepoxide based chemistry to construct highly functionalized oxygenated motifs. The synthesis involved coupling alkyne **S5.82** (Scheme 10) and amide **S5.89** (Scheme 11).

Alkyne **S5.82** was synthesized in 11 steps from commercially available diol **S5.76** (Scheme 10). Selective mono protection of alcohol by PMB, followed by Sharpless epoxidation, and then protection of the primary alcohol by TBDPS yielded **S5.77**. Opening of the epoxide by **S5.78** and protection of alcohol by TES gave differentially protected triol **S5.79** in 92% yield. Conversion of the olefin to the aldehyde, followed by homolygation, and then reduction generated alcohol **S5.80**. Shi epoxidation and Dess-Martin oxidation gave the aldehyde **S5.81**. Propargylation and formation of *m*-fluorobenzyl ether (*m*-FBn) gave the alkyne **S5.82**.

Amide **S5.89** was synthesized by alkene metathesis between **S5.86** and **S5.88** followed by hydrogenation (Scheme 11). The alkene precursors, **S5.86** and **S5.88**, were synthesized as outlined in Scheme 11 following standard procedures. The **S5.86** and **S5.88** was synthesized from known *syn* aldol and silyl enol ether, respectively.

The secondary alcohol of known *syn* aldol **S5.85** was converted to the TBS ether followed by reduction with $LiBH_4$, and then protection of primary alcohol by TIPS yielded olefin **S5.86** (Scheme 11). The amide **S5.88** was synthesized from silyl enol ether **S5.87** by ozonolysis, followed by methylation, and then amide formation.

The alkyne **S5.82** was coupled with the amide **S5.89** to form ynone (Scheme 11). The ynone was converted to enantiopure propargyl alcohol under Noyori reduction condition. The enantiopure propargyl alcohol was mesylated and then subjected to organocuprate mediated S_N2' displacement to yield allene **S5.90**. Cleavage of the PMB group by DDQ followed by spontaneous epoxide opening gave **S5.91**. Exposure of the allene **S5.91** to DMDO yielded **S5.93** in 54% yield.

Scheme 10. Synthesis of Alkyne S5.82

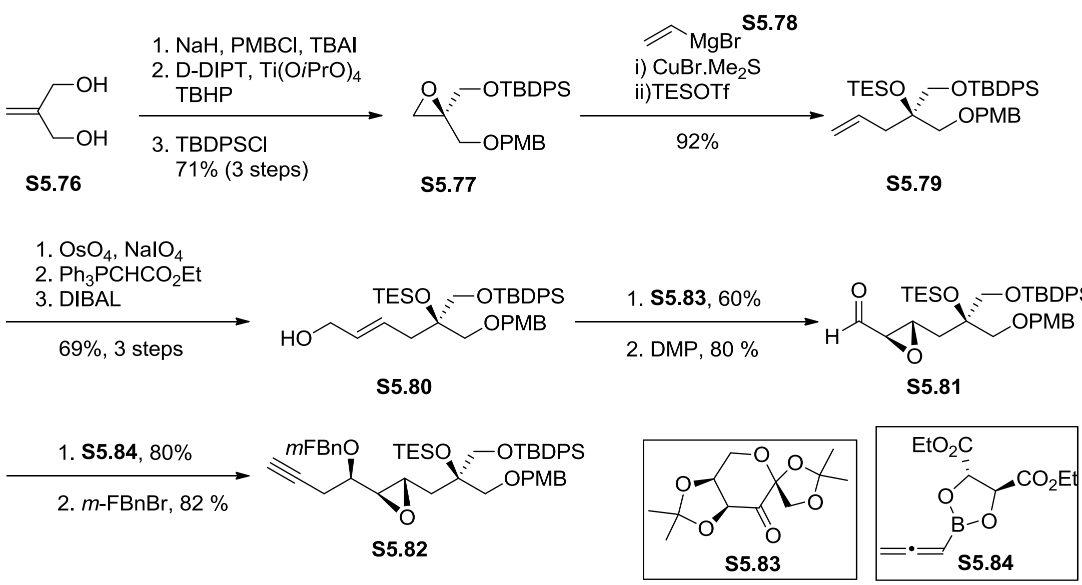

Scheme 11. Synthesis of Weinreb Amide S5.89 and the C1-C19 Fragment

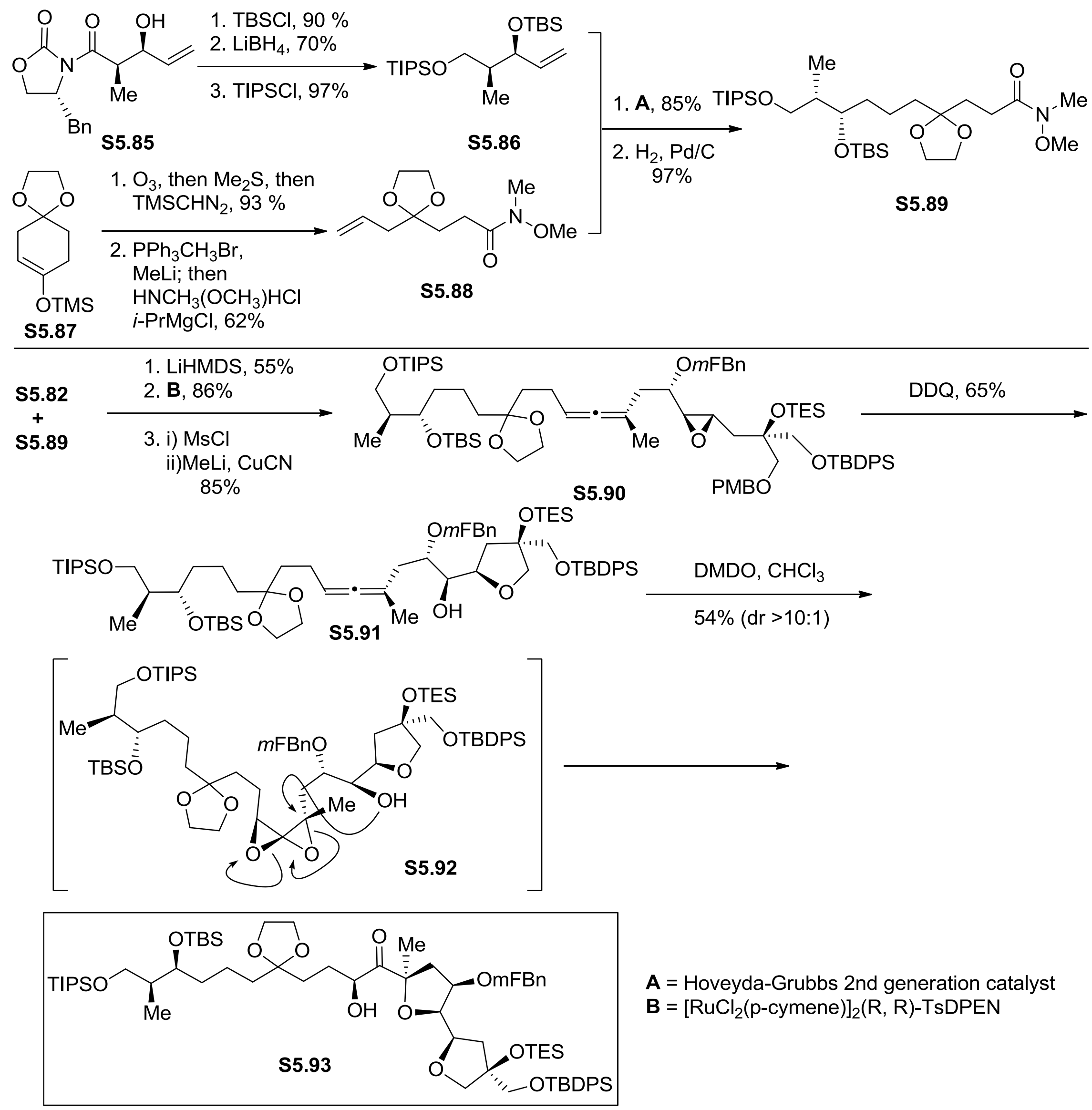

5.7 Synthesis of the C21-C28 Fragment of PTX4

Actually, our first disclosure in the area of PTX4 synthesis appeared in 2007, in which we described the synthesis of a C21-C28 segment of PTX4.[20a] The longest linear sequence in this synthesis required fourteen steps (Scheme 12). The E ring of the PTX4 was generated by silver meditated cyclization of allene **S5.59** followed by reduction. The allene **S5.59** was obtained by a organocuprate mediated S_N2' displacement of propargyl alcohol (**S5.101**), which is obtained by coupling of alkyne (**S5.100**) with aldehyde (**S5.96**).

Scheme 12. Synthesis of a C21-C28 Fragment of PTX4

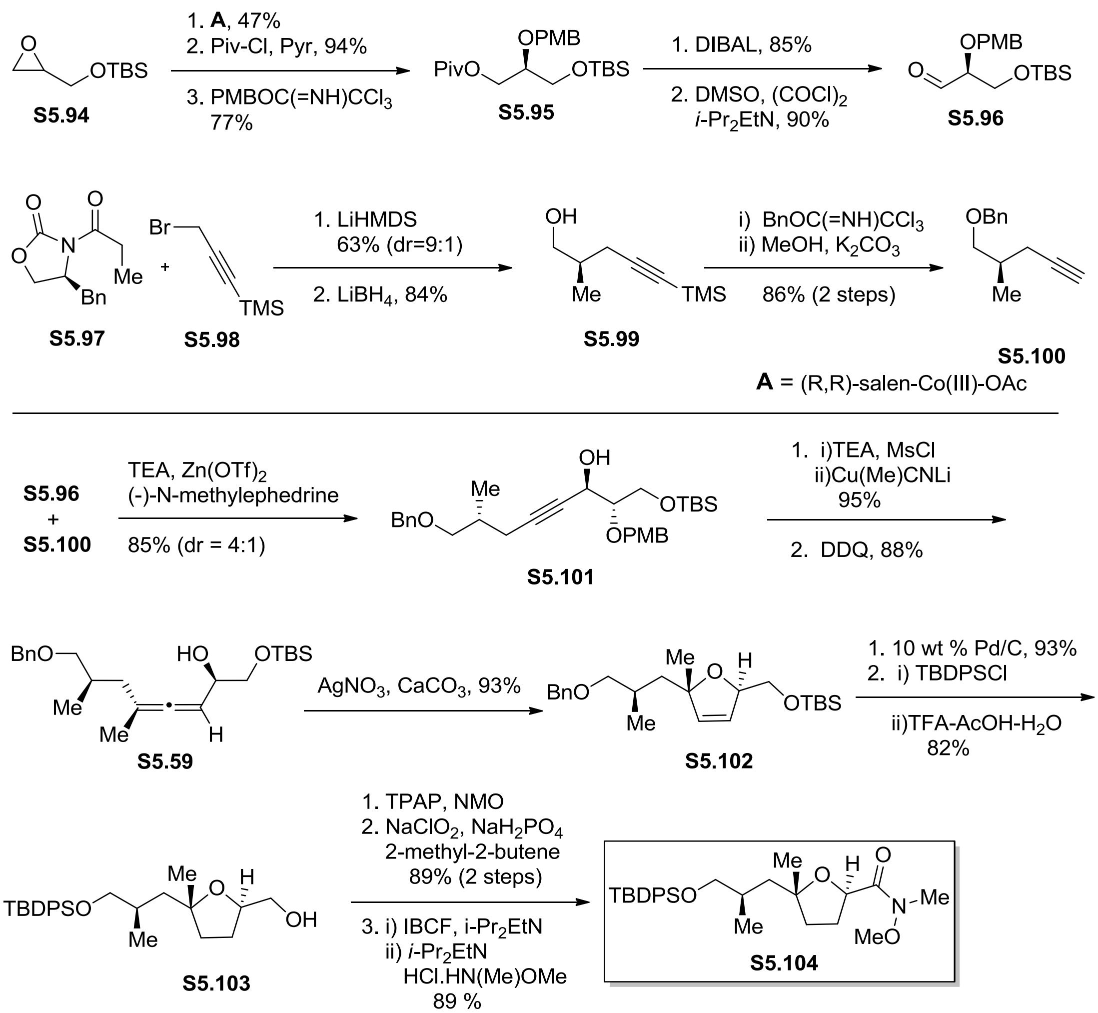

Synthesis of the aldehyde **S5.96** commenced with glycidol **S5.94** (Scheme 12). Kinetic hydrolytic resolution of glycidol **S5.94** gave enantiopure triol. Selective protection of the primary alcohol with pivaloyl chloride and then the protection of the secondary alcohol with PMB gave the differentially protected triol **S5.95**. The alkyne

S5.100 was constructed in three steps. Alkylation of oxazolidinone **S5.97** with propargyl bromide **S5.98** and then reduction with LiHMDS gave **S5.99**. Protection of primary alcohol of **S5.99** with benzyl imidate and then cleavage of trimethylsilyl (TMS) group gave alkyne **S5.100**.

Carreira alkynylation of **S5.96** and **S5.100** gave propargyl alcohol **S5.101** (Scheme 12). The propargyl alcohol **S5.101** was subjected to our single flask allene synthesis conditions, which after removal of the *p*-methoxybenzyl (PMB) group gave allenol **S5.59**. The allenol was subjected to Marshall cyclization conditions to furnish dihydrofuran **S5.102**. Hydrogenation with simultaneous hydrogenolysis of **S5.102**, followed by protection of the primary alcohol with TBDPSCl and then cleavage of TBS group generated furan **S5.103**. Oxidation of the alcohol first to aldehyde, then to the acid and final conversion to amide afforded the C21-C28 fragment (**S5.104**) of PTX4.

5.8 Synthesis of the C30-C40 Fragment of PTX4

The F ring of the PTX4 was synthesized via a spirodiepoxide-based cascade. The hydrogen bond directed epoxidation of allene **S5.60** followed by spontaneous opening of the spirodiepoxide by the free hydroxyl group generated the F ring of the PTX4. The allene **S5.60** was prepared from the propargyl alcohol furnished from the union of alkyne **S5.105** and aldehyde **S5.106** (Scheme 13). Aldehyde **S5.106** was prepared by stereoselective alkylation and alkyne **S5.105** was generated by an epoxide rearrangement. A cascade sequence effected oxidation and cyclization, and a final homologation gave the vinyl stannane **S5.107**.

Scheme 13. Synthesis of C30-C40 Fragment

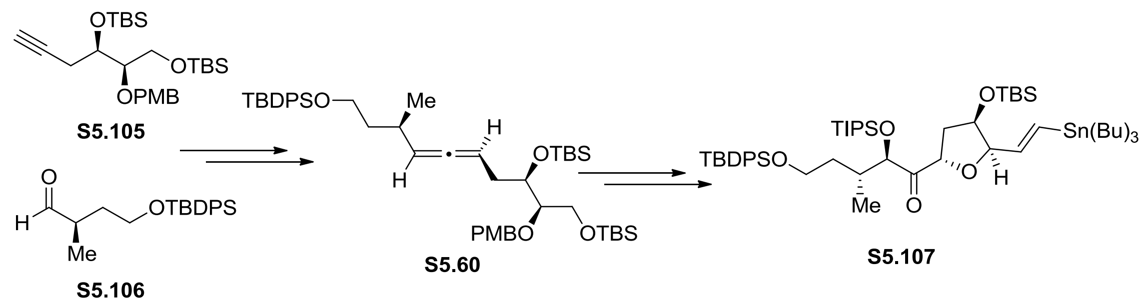

The synthesis of the F-ring of PTX4 represented new challenges for spirodiepoxide-based synthetic methods. In particular, it posed the substantial issue of site selectivity in an apparently unbiased system. The formation of spirodiepoxide in a disubstituted allene faces the problem of regioselectivity. Although there is ample evidence that the first oxidation of this functionality will be highly stereoselective independent of which double bond reacts first. However, low selectivity is expected for the second oxidation and thus renders the issue of site-selectivity. The combination of low site selectivity with low stereoselectivity in the second oxidation will give a gross mixture of isomers. This problem was successfully addressed, as discussed below.

The disubstituted allene **S5.60** was obtained from propargyl alcohol formed by the coupling of alkyne **S5.105** and aldehyde **S5.106**. We examined many routes for the construction of alkyne **S5.105**. Three are described below (Scheme 14, 15 and 16).

In order to obtain direct entry to the masked vicinal triol sector of **S5.60**, we examined the kinetic resolution of **S5.108** (**S5.108**→**S5.109**, Scheme 14).[21,22] Kinetic resolution of diol **S5.108**, followed by epoxidation yielded **S5.110** (dr = 3:1). Subsequent PMB protection, epoxide opening (→**S5.111**), TMS cleavage, and then silyl ether formation gave alkyne **S5.105**. The major diastereomer **S5.110** was prepared from **S5.109**. Although **S5.110** appeared suitable for subsequent transformations, the initial steps were unsatisfactory. Optical resolution is intrinsically wasteful and the epoxidation proved slow and only modestly selective. The Sharpless kinetic resolution is slow and takes about 12 days to give excellent enantiomeric excess (ee) of the desired alcohol **S5.109**. Doubling the amount of peroxide reduced the reaction time in half. However, a further increase in the equivalents of peroxide did not influence the reaction time or ee. Since this step is a kinetic resolution, the maximum theoretical yield is 50%. Furthermore, the diasteromeric ratio (dr) obtained in the subsequent epoxidation step is disappointing, as expected for a mismatched epoxidation of this sort. The route outlined in Scheme 14 was thus abandoned.

Scheme 14. Sharpless Kinetic Resolution Route

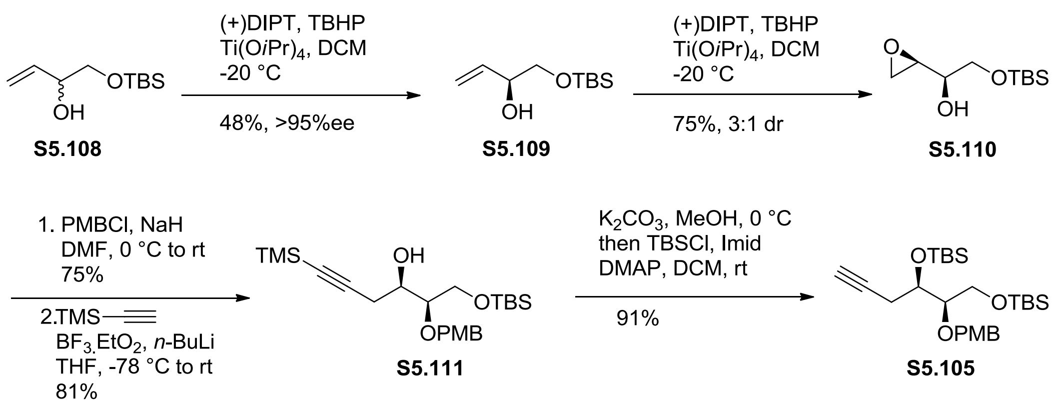

Alternatively, enantioenriched epoxide **S5.112**[23] gave **S5.113** directly when exposed to lithium trimethylsilylacetylide and the action of Lewis acid (Scheme 15). Under these conditions Payne rearrangement (**S5.112→S5.113**) and terminal epoxide opening was fast and selective (→**S5.114**). Protection of the resultant diol as a PMP acetal and then cleavage of TMS group gave **S5.115**. However, after preliminary study and analysis it was determined that the route outlined in Scheme 15 had some shortcomings. Payne rearrangement gave only 68% of the desired product and the resultant secondary alcohol (**S5.113**) was difficult to differentiate from its isomer. Moreover, semi-reduction of the PMP was not regioselective (data not shown).

Scheme 15. Payne Rearrangement Route

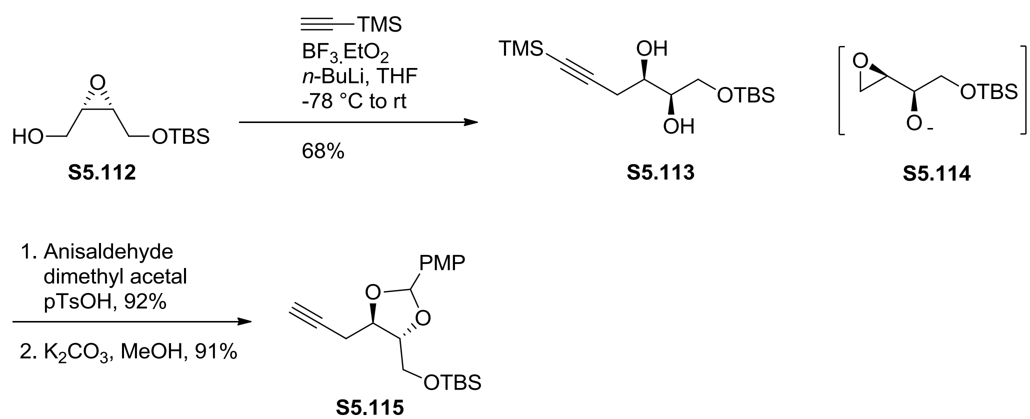

The promising features of the approaches outline in Scheme 14 and Scheme 15 were combined to realize a five step route to **S5.105** (Scheme 16). Commercial alkene **S5.116** was converted to epoxide **S5.117**. Hydrolytic resolution/asymmetric Payne rearrangement of meso epoxide **S5.117** generated the terminal epoxide, which was silylated in situ to give **S5.118** in highly enantioenriched form.[24] Conversion to the PMB ether was followed by alkynylation (→**S5.111**), and then single flask silylation/desilylation completed the sequence to give alkyne **S5.105**.

Scheme 16. Asymmetric Payne Rearrangement Route

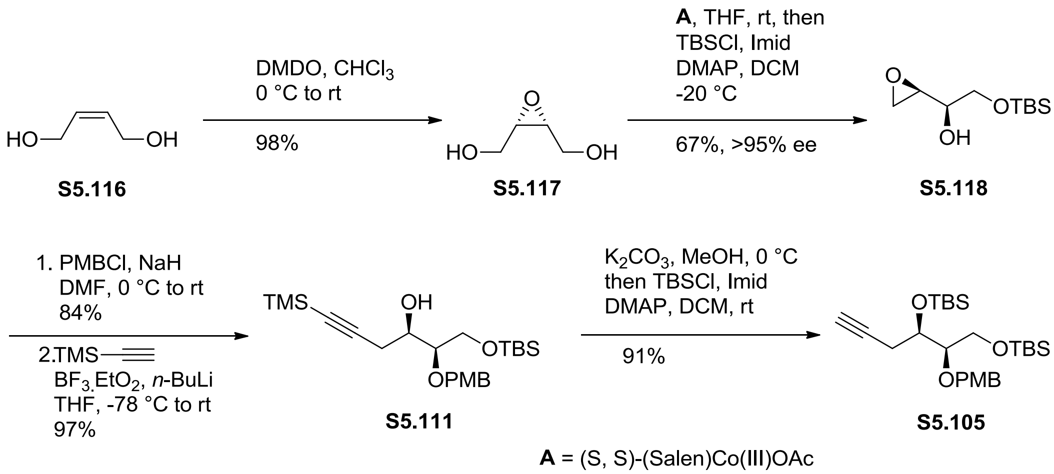

The above route provides ready access to alkyne **S5.105**. A suitable coupling partner (**S5.106**) for the alkyne **S5.105** was prepared as shown in Scheme 17. Aldehyde **S5.106**[25] was obtained in two steps starting from (*1S,2S*)-pseudoephedrinepropionamide (**S5.119**).[26] Alkylation with TBDPS protected 2-iodoethanol (**S5.120**) gave the amide **S5.121**. Subsequent reduction of the amide **S5.121** with DIBALH furnished the known aldehyde **S5.106** in good selectivity and yield.

Scheme 17. Synthesis of a C37-C40 Fragment of the PTX4

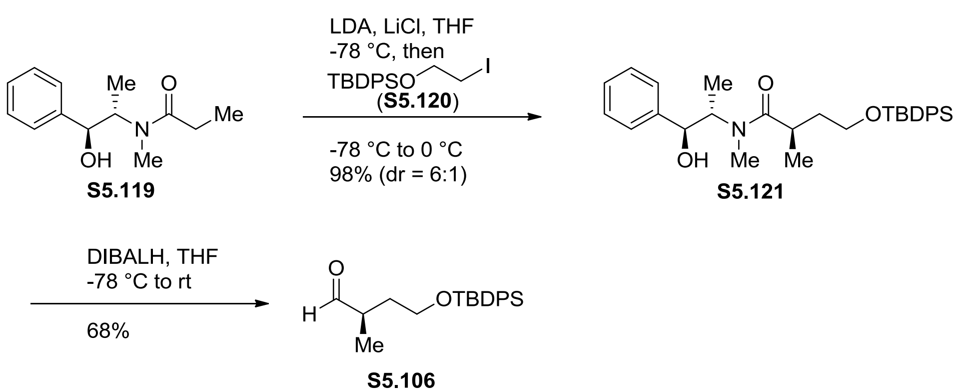

With both coupling partners in hand, alkynylation was performed to give propargyl alcohol (Scheme 18). The direct stereoselective union of **S5.105** with **S5.106** via Carriera asymmetric alknylation was examined in detail. We have had considerable success with this reaction. However, for this substrate, the yield and selectivity were low and the reaction was slow. Direct addition of the lithium or magnesium chloride alkynylide derived from **S5.105** to the Weinreb amide derived from **S5.106** was also low yielding (~40%, data not shown). Consequently, we implemented the sequence shown in Scheme 18 for the construction of the propargyl alcohol. Deprotonation of **S5.105** followed by addition of **S5.106** gave a 1:1 mixture of propargyl alcohols that included **S5.122**. A simple oxidation/reduction protocol converted the mixture to **S5.122** as a single isomer. This two-step maneuver conveniently avoided the tedious separation of isomeric propargyl alcohols and provided significant quantities of material (>60% yield from **S5.105**). Application of the original conditions for the Myers allene synthesis proved superior to more recent modifications and thereby smoothly fashioned **S5.60**.[27]

Scheme 18. Assembly of C31-C40 Fragment

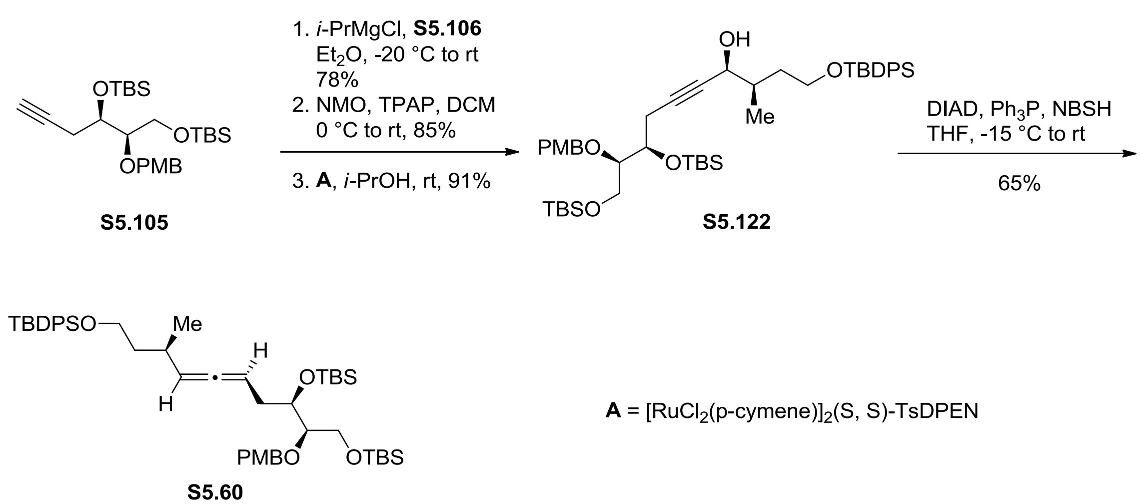

With the allene **S5.60** in hand, which was obtained in a longest linear sequence of 9 steps, we tested the key spirodiepoxide reaction sequence. Exposure of **S5.60** to DMDO in chloroform gave the desired oxolane and a stereoisomer (**S5.123**, Scheme 19). Examination of the crude ^{1}H-NMR showed the presence of anisaldehyde and these products (the desired oxolane and a stereoisomer, **S5.123**). Thus, surprisingly, only two spirodiepoxides appear to have formed – not three – and both underwent spontaneous and rapid cyclization. And further examination, via H/D exchange, showed that the two isomers of **S5.123** differ in the stereochemistry at C37 (pectenotoxin numbering). These results are in contrast to the behavior of allene with silyl ether (**S5.124**), which was obtained from **S5.60** by selective PMB removal and subsequent protection of the free alcohol with TES. Exposure of this compound to DMDO under the same conditions gave three spirodiepoxides in approximately equal ratios. We conclude that the conversion of **S5.60** to **S5.123** represents a substrate-directed epoxidation that is not operative for **S5.124**.

Scheme 19. Oxidation of Allenes S5.60 and S5.124

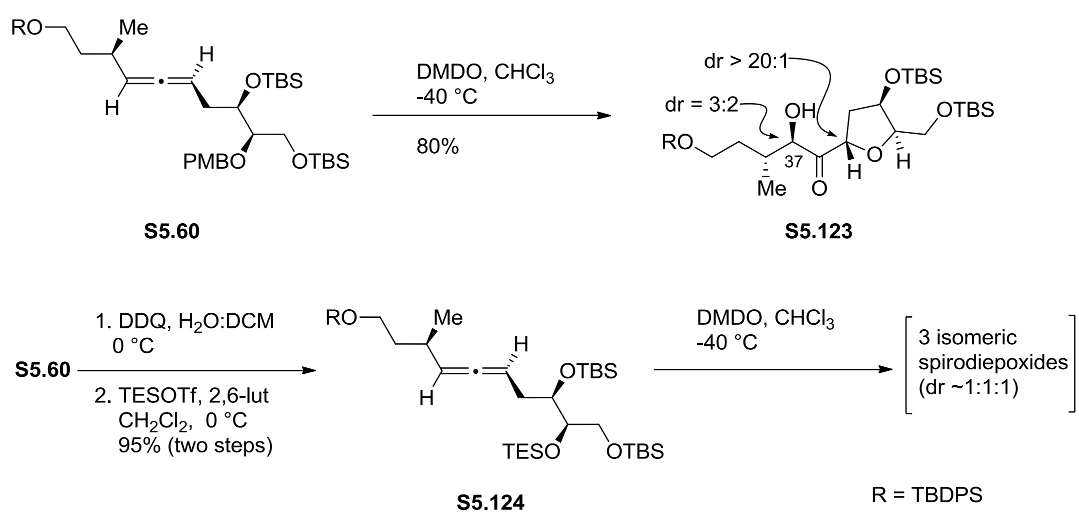

Scheme 20 presents a rationale for these observations. The first oxidation of allenes of type **I** should proceed to give allene oxides of type **II** and **III**. Thus oxidation occurs with excellent face selectivity but with no regiochemical preference for 1,3-disubstituted allenes. The intrinsic face selectivity for epoxidation of simple allene oxides is low. Two spirodiepoxide products should form from each allene oxide, and one of the two spirodiepoxides derived from each allene oxide will be identical. Hence, **IV** and **V** should be derived from **II** whereas **V** and **VI** from **III**. Therefore, in the absence of other governing effects, three diastereomeric spirodiepoxides should form. This rationale is consistent with the behavior of **S5.124** and is inconsistent with the behavior of **S5.60**. The epoxidation of **S5.60** could be substrate directed by way of a hydrogen bond between the allenol and the dioxirane. The hydroxyl group could steer the first oxidation to the proximal double bond, as in **VII→VIII**. The second oxidation would then give two spirodiepoxides (**IX** and **X**) and thence two oxolanes that differ only in their stereoarrangement at C37 (**S5.123**), as observed.

The allene epoxidation reaction was modelled computationally. Figure 7 provides the key features of the calculated energy surface and transition structures. With model allene **XI** and dioxirane **XII**, a stable hydrogen bonded complex, **XIII** ($\Delta H_{calc} = -1.06$ kcal/mol), was found in a conformation suitable for epoxidation from the most accessible face of the allene. Complex **XIII** was then used to identify a transition structure for epoxidation of the proximal π-bond of the allene (**TSI**, $\Delta H^{\ddagger}_{calc} = 15.0$ kcal/mol). IRC analysis demonstrates that **TSI** connects complex **XIII** to the allene oxide product (**XIV**). Epoxidation of the most accessible face of the distal π-bond of the allene was also evaluated for this conformer (**XI**) and the regioisomeric transition structure (**TSII**) was determined. This non-directed pathway is significantly higher in energy than the directed pathway ($\Delta\Delta H^{\ddagger}_{calc}$ = 2.64 kcal). As before, IRC analysis demonstrates energy surface connectivity between **XI** and **XV**. No stable hydrogen bond complex was identified in ground or transition structures for oxidation of the π-bond that is distal to the hydroxyl group.

Scheme 20. Framework for Allene Epoxidation

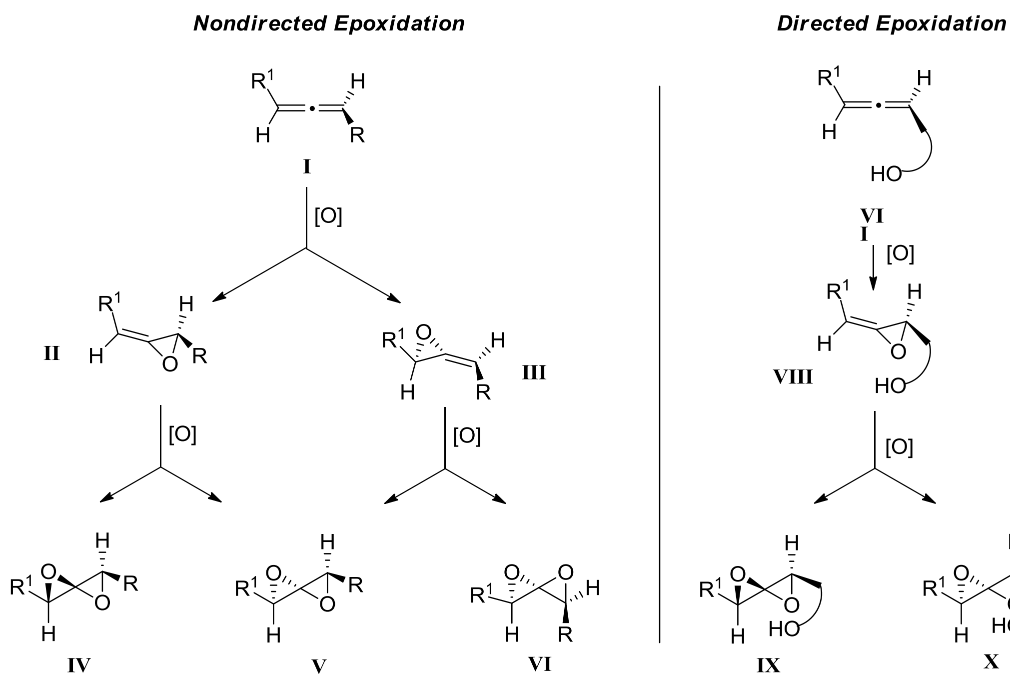

Computational analysis of allene epoxidation processes has not been described previously.[28] Not surprisingly, both directed and non-directed allene epoxidation structures closely parallel computed structures for alkene epoxidation with DMDO. The barriers are higher and the transition states are later for the allenic substrate. The differences are best understood in terms of the distortional framework recently described.[29] As shown in Table 1, hydrogen bonding to DMDO activates the oxidant and facilitates epoxidation relative to the non-directed pathway (cf. bond lengths O1-O2, C2-

O1, C4-O2). The substantial difference in energy between the directed and non-directed pathways is traceable to the presence of the directing hydrogen bond and is consistent with the experimental data and the rationale in Scheme 20: the hydroxyl group efficiently directs the first epoxidation to the proximal double bond of the allene.

Table 1. Selected bond lengths for computed structures TSI and TSII in Å

	O_1-O_2	C_2-O_1	C_4-O_2
TSI	1.877	2.055	1.336
TSII	1.854	1.940	1.347

Figure 7. Computed Epoxidation Pathways (values given in kcal/mol)[30]

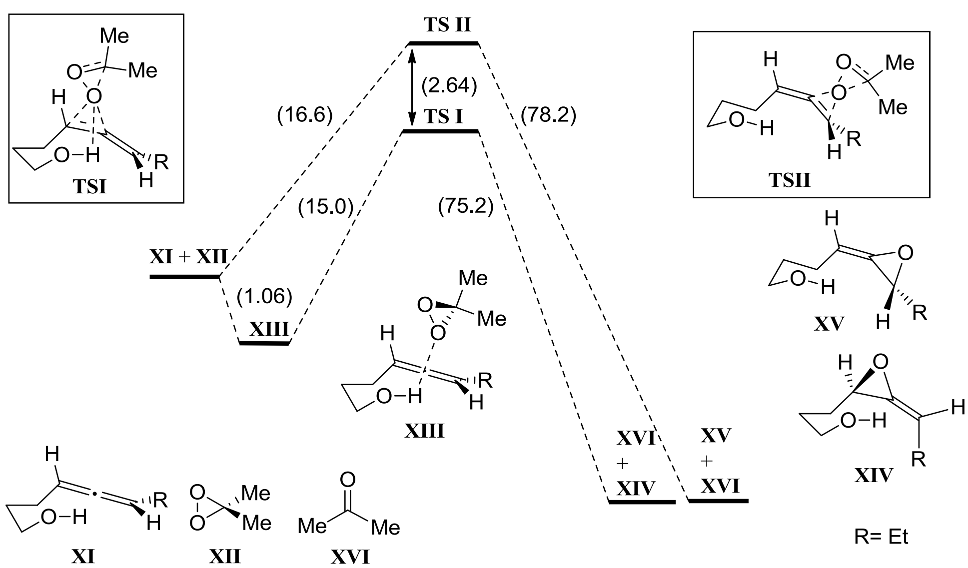

The final step of this ten step route to the fragment of PTX (**S5.123**) is remarkable. We suggest that the sequence of this cascade proceeds as (a) oxidative cleavage of the PMB group to reveal a transient hydroxyl at C32, (b) selective allene epoxidation directed by way of hydrogen bonding between the hydroxyl and dimethyldioxirane to give a single allene oxide, (c) a second epoxidation to form two spirodiepoxides, and (d) spirodiepoxide opening via addition of the newly revealed hydroxyl to give the highly functionalized oxolane target (**S5.123**).

With the desired oxolane in hand, the precursor for Stille coupling (**S5.107**) was obtained in five additional steps (Scheme 21). The secondary alcohol of **S5.123** was converted to the triisopropylsilyl ether. However, conversion of the secondary alcohol of **S5.123** to the triisopropylsilyl ether was problematic. Various conditions failed to give the desired product. When TIPSOTf was used, the **S5.123** decomposed. Even huge excess of TIPSCl in the presence of imidazole and DMAP/triethylamine did not give the triisopropylsilyl ether. Pleasing, TIPSCl in the presence of $AgNO_3$ and pyridine proved to efficiently give the silyl ether.[31]

In the optimized sequence, formation of triisopropylsilyl ether and then removal of the primary TBS group gave **S5.125** (Scheme 21). The primary alcohol of **S5.125** was then converted to the corresponding aldehyde (**S5.126**). Homologation of **S5.126** gave alkyne **S5.127**. And finally, reaction of **S5.127** with tributyltin hydride gave the vinylstannane **S5.107**.

Scheme 21. Synthesis of the C30-C40 Fragment of PTX4

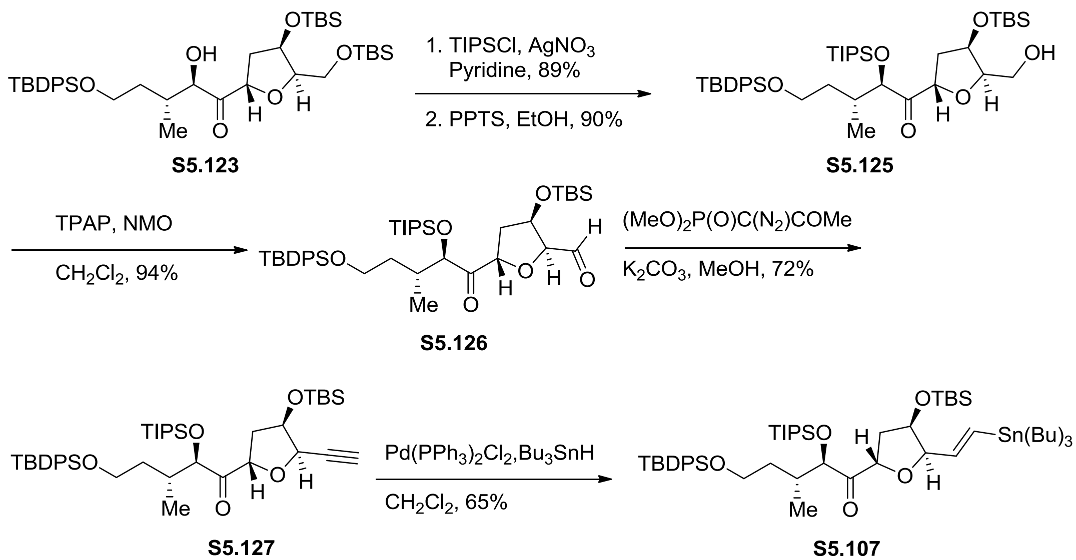

5.9 Synthesis of the C21-C29 Fragment of PTX4

Stille coupling partner, **S5.130**, was obtained in 14 steps (longest linear sequence, Scheme 22). As described in Scheme 12, we had completed the synthesis of a PTX4 C21-C28 fragment (**S5.104**). The product obtained from the silver mediated cyclization (**S5.102**, see Scheme 12) was used to obtain **S5.130**, the C21-C29 fragment.

Scheme 22. Synthesis of the C21-C29 Fragment of PTX4

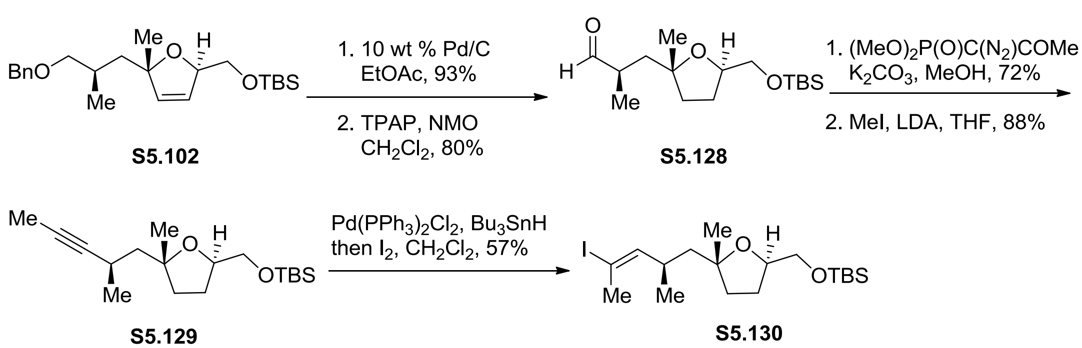

Thus dihydrofuran **S5.102** was subjected to hydrogenation/hydrogenolysis conditions, and then oxidation of the primary alcohol gave the aldehyde (**S5.128**, Scheme 22). Homologation of **S5.128** and then methylation furnished internal alkyne **S5.129**. Vinylstannation/iodination of **S5.129** yielded the vinyliodide **S5.130**.[32]

5.10 Synthesis of the C21-C40 Fragment of PTX4

The C21-C40 fragment (**S5.61**) of PTX4 was obtained by Stille coupling of the C21-C29 fragment (**S5.130**) with the C30-C40 fragment (**S5.107**, Scheme 23 and 24). The use of 10 mol% $Pd(PPh_3)_4$ in DMF did not give the desired coupling product (**S5.61,** Scheme 23).[33] No desired coupling product (**S5.61**) was obtained when either Ph_3As or PPh_3 was used with $Pd_2(dba)_3$.[34,35]

All three conditions outlined in the Scheme 23 resulted in proteodestannylation, desilyation and homodimerization. The problems associated with protocols shown in Scheme 23 were overcome by using the procedure shown in Scheme 24.[36] Use of $Pd_2(dba)_3.CHCl_3$ in the presence of $CdCl_2$ and *i*-Pr_2NEt. The use of *i*-Pr_2NEt and $CdCl_2$ reduced the amount of protodestannylation and homodimerization products, respectively.

Scheme 23. Coupling Attempts

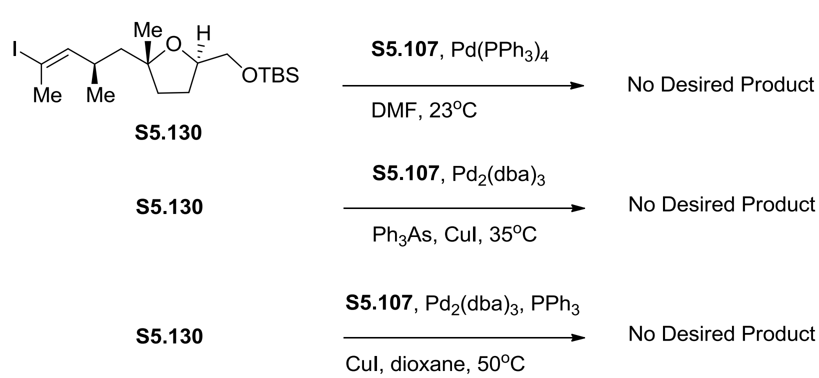

Scheme 24. Coupling of the C21-C29 Fragment with the C30-C40 Fragment

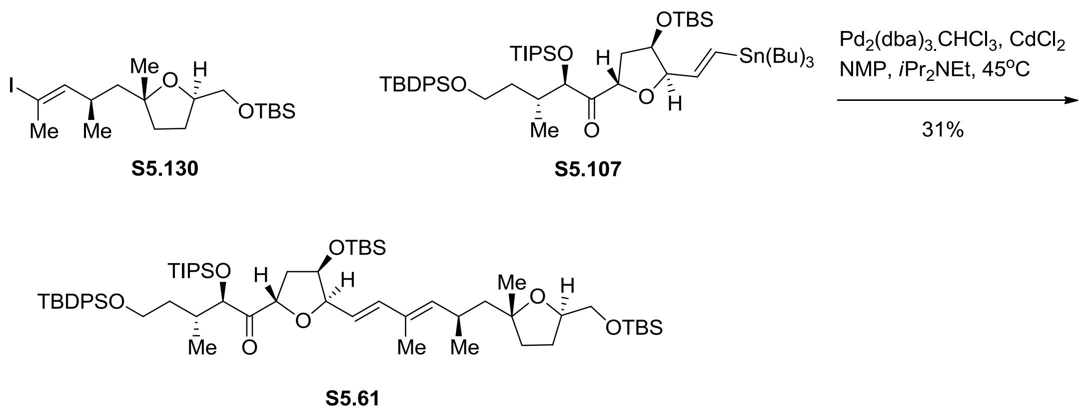

5.11 Future Studies Towards PTX4

Our planned route for the completion of the synthesis of PTX4 is briefly outlined in the Scheme 25. From the outset we planned to couple the lower hemisphere (**S5.131**) with upper hemisphere (**S5.132**). Deprotonation of an alkyne of type **S5.132** and its addition to an amide of type **S5.131** should afford an ynone (**S5.133**). We have shown that ynones of type **S5.133** can be reduced to ketones of type **S5.134** by employing the condition developed by Lipshutz.[37] We expected that mild acidic conditions should cleave the TIPS at C1, both TES and both TBS groups and promote formation of the acetal will be formed (**S5.135,** see arrow).[19] The plan continues toward selective oxidation of the primary alcohol in a two- step process to give acid **S5.135**. Yamaguchi macrolactonization,[38] followed by oxidation of C14 and C33 will give **S5.136**, the fully protected natural product. In the final step, the remaining silyl ethers will be removed to furnish Pectenotoxin 4.

Scheme 25. Proposed Synthetic Route to the Total Synthesis of PTX4

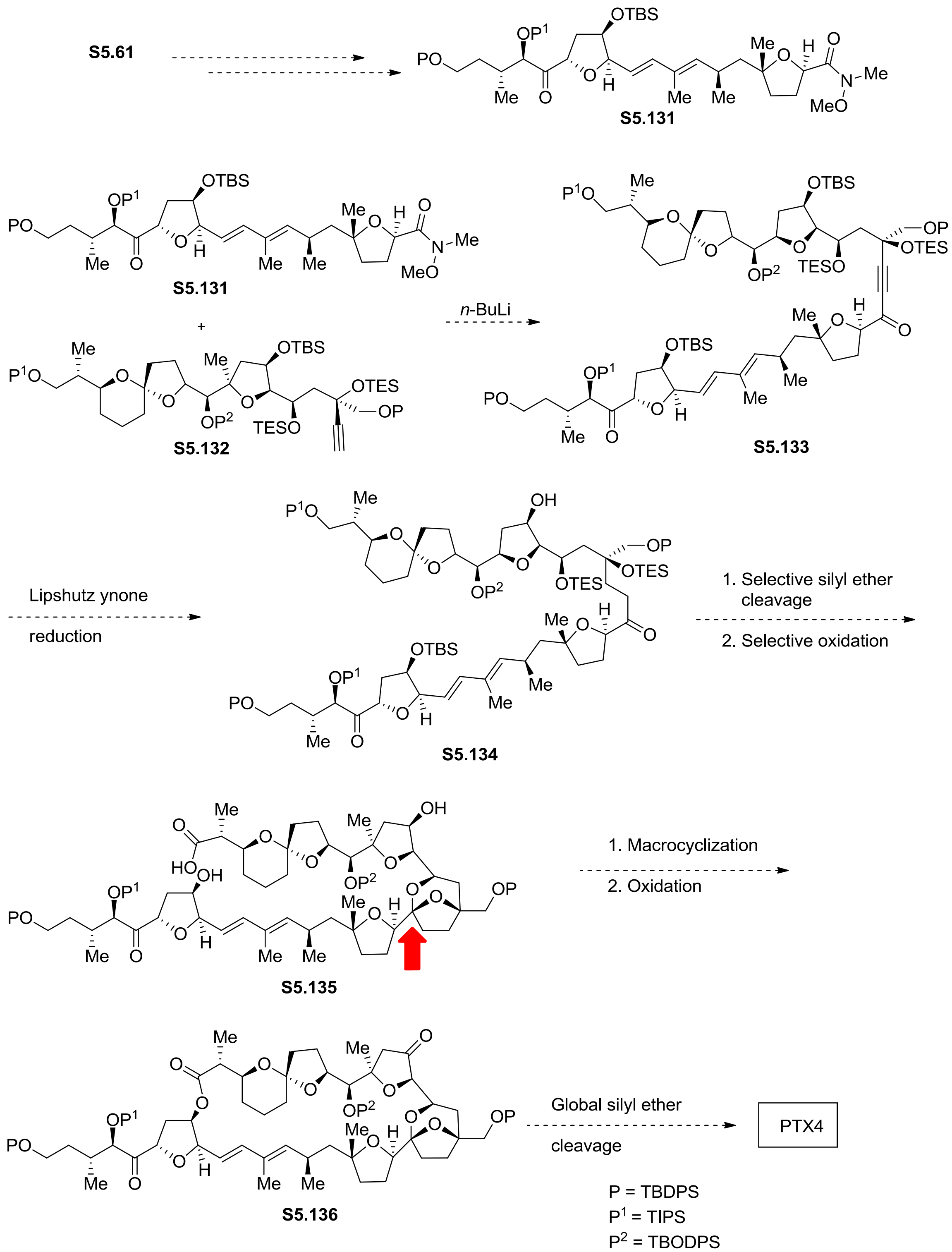

5.12 Conclusion

Here we showcased improved methods and strategies for the efficient and seteroselective synthesis of PTX4. We have used spirodiepoxide-based cascades not just to synthesize the cyclic ethers (AB spiroketal and the F ring), but also to directly access the proper oxygenated adjacent functionalities those are attached to these rings. Although we have not completed the synthesis, our route controls the stereochemistry at all sites (C3, C7, C10, C11, C12, C15, C32, C35 and C37) and all stereocenters are installed, except for the thermodynamic acetal at C21. At present, the spirodiepoxide chemistry used to invoke the functionality at C37 is low (2:1), but all other centers are set with excellent selectivity. This route compares very favorably with routes reported by Evans Group (17 steps to C20-C30 and 18 steps to C31-C40), Paquette Group (16 steps to C29-C40), Fujiwara Group (13 steps to C20-C30) and Brimble Group (19 steps to C31-C40).

5.13 References

1. Yasumoto, T.; Murata , M.; Oshima, Y.; Sano, M.; Matsumoto, G. K.; Clardy, J. *Tetrahedron* **1985**, *41*, 1019.
2. Halim, R.; Brimble, M.A. *Org. Biomol. Chem.* **2006**, *4*, 4048.
3. Lee, J.-S.; Igarashi, T.; Fraga, S.; Dahl, E.; Hovgaard, P.; Yasumoto, T. *J. Appl. Phycol.* **1989**, *1*, 147.
4. Draisci, R.; Lucentini, L.; Gianetti, L.; Boria, P.; Poletti, R. *Toxicon* **1996**, *34*, 923.
5. Yasumoto, T.; Murata, M.; Lee, J.-S.; Torigoe, K. in *Bioactive Molecules: Mycotoxins and Phycotoxins '88*; Natori, S., Hashimoto, K., Ueno, Y., Eds.; Elsevier: New York, 1989; Vol 10, p 375.

6. a) Draisci, R.; Lucentini, L.; Mascioni, A. in *Seafood and Freshwater Toxins: Pharmacology, Physiology and Detection*, ed. Botana, L.M. Marcel Dekker, Inc, New York, 2000, pp. 289; b) V. Burgess and G. Shaw, *Environ. Int.* **2001**, *27*, 275.
7. a) Zhou, Z.H.; Komiyama, M.; Terao, K.; Shimada, Y. *Nat. Toxins* **1994**, *2*,132; b) Leira, F.; Cadado, A.G.; Vieytes, M.R.; Roman, Y.; Alfonso, A.; Botana, L.M.; Yasumoto, T.; Malaguti, C.; Rossini, G.P. *Biochem. Pharmacol.* **2002**, *63*, 1979; c) Allingham, J.S.; Klenchin, V.A.; Rayment, I. *J. Mol. Biol.* **2007**, *371*, 959.
8. Espina, B.; Rubiolo, J.A. *FEBS Journals* **2008**, *275*, 6082.
9. Ares, I.R.; Louzao, M.C.; Espina, B.; Vieytes, M.R.; Miles, C.O. Yasumoto, T.; Botana, L.M. *Cell Physiol. Biochem* **2007**, 19, 283.
10. a) Amano, S.; Fujiwara, K.; Murai, A. *Synlett* **1997**, 1300; b) Fujiwara, K.; Kobayashi, M.; Yamamoto, F.; Aki, Y.; Kawamura, M.; Awakura, D.; Amano, S.; Okano, A.; Murai, A.; Kawai, H.; Suzuki, T. *Tetrahedron Lett.* **2005**, *46*, 5067; c) Fujiwara, K.; Aki, Y.; Yamamoto, F.; Kawamura, M.; Kobayashi, M.; Okano, A.; Awakura, D.; Shiga, S.; Murai, A.; Kawai, H.; Suzuki, T. *Tetrahedron Lett.* **2007**, *48*, 4523.
11. Micalizio, G.C.; Roush, W.R. *Org. Lett.* **2001**, *3*, 1949.
12. a) Paquette, L.A.; Peng, X.; Bondar, D. *Org. Lett.* **2002**, *4*, 937; b) Bondar, D.; Liu, J.; Muller, T.; Paquette, L.A. *Org. Lett.* **2005**, *7*, 1813.
13. a) Halim, R.; Brimble, M.A.; Merten, J. *Org. Lett.* **2005**, *7*, 2659; b) Heapy, A.M.; Wagner, T.W.; Brimble, M.A. *Synlett* **2007**, *15*, 2359; c) Carley, S.; Brimble, M.A. *Org. Lett.* **2009**, *11*, 563.

14. a) Pihko, P.M.; Aho, J.E. *Org*. *Lett*. **2004**, *6*, 3849; b) Helmboldt, H.; Aho, J.E.; Pihko, P.M. *Org*. *Lett*. **2008**, *10*, 4183; c) Aho, J.E.; Salomäki, S.; Rissanen K.; Pihko, P.M. *Org*. *Lett*. **2008**, *10*, 4179.

15. Vellucci, D.; Rychnovsky, S.D. *Org*. *Lett*. **2007**, *9*, 711.

16. Fujiwara, K.; Suzuki, Y.; Koseki, N.; Murata, S.; Murai, A.; Kawai, H.; Suzuki, T. *Tetrahedron Lett*. **2011**, *52*, 5589.

17. a) Canterbury, D. P.; Micalizio, G. C. *Org*. *Lett*. **2011**, *13*, 2384; b) Kubo, O.; Canterbury, D. P.; Micalizio, G. C. *Org*. *Lett*. **2012**, *14*, 5748.

18. Kouridaki, A.; Montagnon, T.; Kalaitzakis, D.; Vassilikogiannakis, G. *Org*. *Biomol*. *Chem*. **2013**, *11*, 537.

19. a) Evans, D.A.; Rajapakse, H.A.; Stenkamp, D. *Angew*. *Chem*., *Int*. *Ed*. **2002**, *41*, 4569; b) Evans, D.A.; Rajapakse, H.A.; Chiu, A.; Stenkamp, D. *Angew*. *Chem*., *Int*. *Ed*. **2002**, *41*, 4573.

20. a) Kolakowski, R.V.; Williams, L.J. *Tetrahedron Lett*. **2007**, *48*, 4761; b) Lotesta, S.D.; Hou, Y.; Williams, L.J. *Org*. *Lett*. **2007**, *9*, 869; c) Joyasawal, S.; Lotesta, S.D.; Akhmedov, N.G.; Williams, L.J. *Org*. *Lett*. **2010**, *12*, 988.

21. Gravestock, M. B.; Knight, D. W.; Lovell, J. S.; Thornton, S. R. *J*. *Chem*. *Soc*., *Perkin Trans*. *1* **1999**, *21*, 3143.

22. Martin, V.; Woodard, S.; Katsuki, T.; Yamada, Y.; Ikeda, M.; Sharpless, K. B. *J*. *Am*. *Chem*. *Soc*., **1981**, *103*, 6237.

23. Nakanishi, A.; Mori, K. *Biosci*. *Biotechnol*. *Biochem*. **2005**, *69*, 1007.

24. Wu, M. H.; Hansen, K. B.; Jacobsen, E, N. *Angew*. *Chem*. *Int*. *Ed*. **1999**, *38*, 2012.

25. Fürstner, A.; Bouchez, L. C.; Morency, L.; Funel, J.; Liepins, V.; Porée, F.; Gilmour, R.; Laurich, D.; Beaufils, F.; Tamiya, M *Chem. Eur. J.* **2009**, *15*, 3983.

26. Myers, A. G.; Yang, B. H.; Chen, H.; McKinstry, L.; Kopecky, D. J.; Gleason, J. L. *J. Am. Chem. Soc.* **1997**, *119*, 6496.

27. Myers, A. G.; Zheng B. *J. Am. Chem. Soc.* **1996**, *118*, 4492.

28. a) Cho, Kyung-Bin; Lai, W.; Hamberg, M.; Raman, C. S.; Shaik, S. *Archives of Biochemistry and Biophysics* **2011**, *507*, 14; b) Gao, B.; Boeglin, W. E.; Zheng, Y.; Schneider, C.; Brash, A. R. *Journal of Biological Chemistry* **2009**, *284*, 22087; c) Brash, A. R. *Phytochemistry* **2009,** *70*, 1522.

29. a) Ess, D. H.; Houk, K. N. *J. Am. Chem. Soc.* **2007**, 129, 10646; b) Ess, D. H.; Houk, K. N. *J. Am. Chem. Soc.* **2008**, *130*, 10187; c) Kolakowski, R. V.; Williams, L. J. *Nat. Chemistry* **2010**, *2*, 303.

30. a) Electronic structure calculation were performed and optimized using DFT (B3LYP) and the G631* basis Gaussian 03 (Revision B.02): Frisch, M. J.; Trucks, G. W.; Schlegel, H. B.; Scuseria, G. E.; Robb, M. A.; Cheeseman, J.R.; Montgomery, J. A. Jr.; Vreven, T.; Kudin, K. N.; Burant, J. C.; Millam, J. M.; Iyengar, S.S.; Tomasi, J.; Barone, V.; Mennucci, B.; Cossi, M.; Scalmani, G.; Rega, N.; Petersson, G.A.; Nakatsuji, H.; Hada, M.; Ehara, M.; Toyota, K.; Fukuda, R.; Hasegawa, J.; Ishida, M.; Nakajima, T.; Honda, Y.; Kitao, O.; Nakai, H.; Klene, M.; Li, X.; Knox, J. E.; Hratchian,H. P.; Cross, J. B.; Adamo, C.; Jaramillo, J.; Gomperts, R.; Stratmann, R. E.; Yazyev, O.; Austin, A. J.; Cammi, R.; Pomelli, C.; Ochterski, J. W.; Ayala, P. Y.; Morokuma, K.; Voth, G. A.; Salvador, P.; Dannenberg, J. J.; Zakrzewski, V. G.; Dapprich, S.; Daniels, A. D.; Strain, M. C.; Farkas, O.; Malick, D. K.; Rabuck, A. D.;

Raghavachari, K.; Foresman, J. B.; Ortiz, J. V.; Cui, Q.; Baboul, A. G.; Clifford, S.; Cioslowski, J.; Stefanov, B. B.; Liu, G.; Liashenko, A.; Piskorz, P.; Komaromi, I.; Martin, R. L.; Fox, D. J.; Keith, T.; Al-Laham, M. A.; Peng, C. Y.; Nanayakkara, A.; Challacombe, M.; Gill, P. M. W.; Johnson B.; Chen,W.; Wong, M. W.; Gonzalez, C.; Pople, J. A.: Gaussian, Inc.: Pittsburgh, 2003; B3LYP functional: b) Becke, A. D. *J. Chem. Phys.* 1993, *98*, 5648; c) Lee, C.; Yang, W.; Parr, R. G. *Phys. Rev.B.* 1988, *37*, 785; 6-31g(d,p) basis sets: d) Clark, T.; Chandrasekhar, J.; Spitznagel, G. W.; Schleyer, P.v.R. *J. Comp. Chem.* 1983, *4*, 294; e) McLean, A. D.; Chandler, G. S. *J. Chem. Phys.* 1980, *72*, 5639; f) Krishnan, R.; Binkley, J. S.; Seeger, R.; Pople, J. A. *J. Chem. Phys.* 1980, *72*, 650; g) Hariharan, P. C.; Pople, J. A. *Mol. Phys.* 1974, *27*, 209; h) Ditchfield, R.; Hehre, W. J.; Pople, J. A. *J. Chem. Phys.* 1971, *54*, 721; CPCM: i) Cossi, M.; Barone, V. *J. Phys. Chem. A* 1998, *102*, 1995.

31. Li, D. R.; Sun, C. Y.; Su, C.; Lin, G-Q; Zhou, W-S *Org. Lett.* **2004**, *6*, 4261.
32. Smith, A. B.; Ott, G. R. *J. Am. Chem. Soc.* **1998**, *120*, 3935.
33. Stille, J. K. *Angew. Chem. Int. Ed. Engl.* **1986**, *25*, 508.
34. Farina, V.; Krishnan, B. J. *J. Am. Chem. Soc.* **1991**, *113*, 9585.
35. Farina, V.; Kapadia, S.; Krishnan, B. J.; Wang, C.; Liebeskind, L. S. *J. Org. Chem.* **1994**, *59*, 5905.
36. Evans, D. A.; Black, W. D. *J. Am. Chem. Soc.* **1993**, *115*, 4497.
37. Baker, B.A.; Boskovic, Z.V.; Lipshutz, B.H. *Org. Lett.* **2008**, *10*, 289.
38. Inanaga, J.; Hirata, K.; Saeki, H.; Katsuki, T.; Yamaguchi, M. *Bull. Chem. Soc. Jpn.* **1979**, *52*, 1989.

Chapter 6

Synthesis of Bromohydroxyketones by Catalytic Aminohydroxylation of Allenes

6.1 Introduction

Secondary and tertiary alcohols are versatile building blocks in the synthesis of biologically active molecules and are also present in many pharmaceuticals and natural products. In earlier chapters we have described allene epoxidation/derivatization methods for introducing tertiary as well as secondary alcohols in complex settings.[1−4] These methods involve epoxidation of an allene followed by addition of a nucleophile, or the use of another reagent-type, to provide α-substituted-α′-hydroxy ketones (**S6.1**→**S6.2**→**S6.3**, Scheme 1).

We have also developed a method that is complementary to the spirodiepoxide based method. It relies upon allene osmylation to form an osmium enol ester **S6.4** followed by addition of an electrophile (**S6.1**→**S6.4**→**S6.5**). Similar to the spirodiepoxide based method, the allene osmylation/electrophile addition method generates α-substituted-α′-hydroxy ketone. In contrast to the spirodiepoxide based method, the product obtained from allene osmylation/electrophile addition method is *anti*-substituted. We reasoned that the spirodiepoxide based method gives the *syn* addition product (**S6.3**) because the nucleophile adds from the back side of the epoxide. In case of the allene osmylation/electrophile addition method, the electrophile approaches the osmate enol ester (**S6.4**) from the less hindered side to give the *anti*-addition product (**S6.5**).

Scheme 1. Allene Epoxidation vs. Allene Osmylation

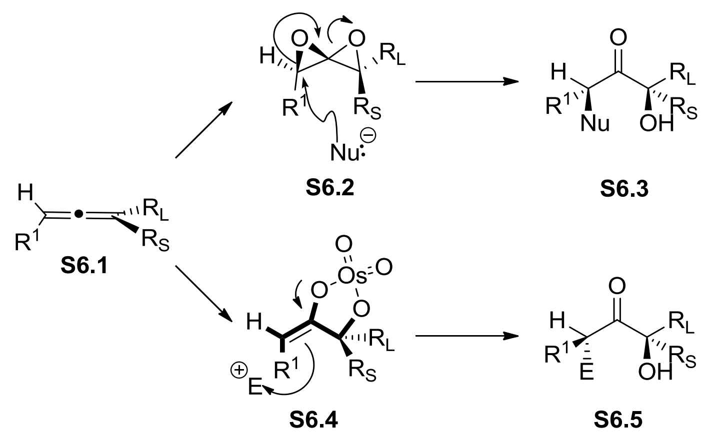

Prior to our work, no studies have been reported on catalytic allene osmylation/electrophile addition. Previous studies were restricted to osmium mediated allene dihydroxylation.[5] Most of the previous studies used achiral allenes and stoichiometric amount of osmium. There have been limited reports on asymmetric osmylation.[6,7] The reports indicated that the reactions were slow and low yielding.

Gratifyingly, we successfully developed a catalytic allene osmylation/electrophile addition method. This method calls for 10 mol% of OsO_4 as oxidant, 4-Methylmorpholine *N*-oxide (NMO) as co-oxidant, and a suitable electrophile (Scheme 2).

Catalytic allene osmylation/electrophile addition method is efficient; however, it suffers from some limitations. The catalytic allene osmylation/electrophile addition method does not work well in the case of bromine addition. In the case of bromination, we use *N*-Bromosuccinimide (NBS) as the source of bromine, but NBS reacts rapidly with many allenes faster than osmium tetroxide to give bromohydrin as a major side product. Additionally allene osmylation can be slow and has limited substrate scope. For example, aryl substituted allenes suffer from low yield, overoxidation, and inefficient electrophile capture. Nevertheless, the catalytic allene osmylation/electrophile addition method can be efficient, and we have used this method even in highly complex molecule.[8]

Scheme 2. Catalytic Allene Osmylation/Electrophile Addition

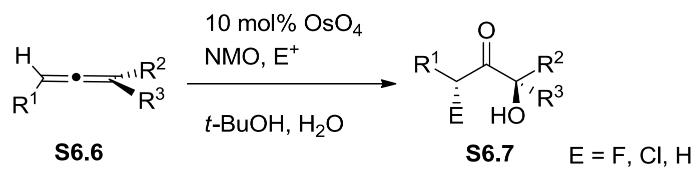

6.2 Brief Overview of Alkene Aminohydroxylation

After our success in the development of allene osmylation/electrophile addition method, we wondered about the potential of allene aminohydroxylation. Allene aminohydroxylation is unexplored. Unlike allene aminohydroxylation, alkene aminohydroxylation is well studied. Sharpless has developed asymmetric aminohydroxylation method known as Sharpless Asymmetric Aminohydroxylation (SAA).[9,10] SAA uses dihydroquinine ligand to induce enantioselectivity and a nitrogen containing co-oxidant (Scheme 3).

The accepted mechanism of SAA involves [3+2] cycloaddition of alkene **S6.8** with imidotriooxoosmium (VIII) intermediate **S6.12** followed by hydrolysis (Scheme 4). The SAA works well with aryl alkenes. However, in the case of non-aryl alkenes, *regio* control is poor.[11, 12]

Scheme 3. The Sharpless Asymmetric Aminohydroxylation

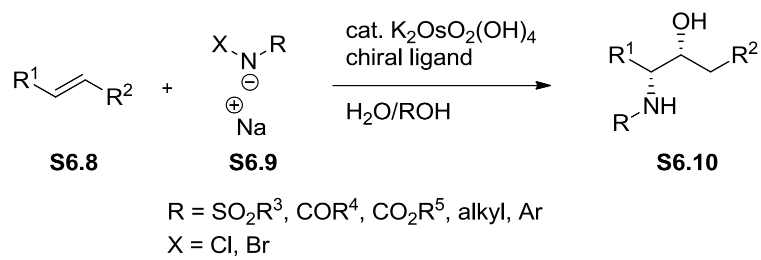

Scheme 4. Mechanism of Sharpless Asymmetric Aminohydroxylation

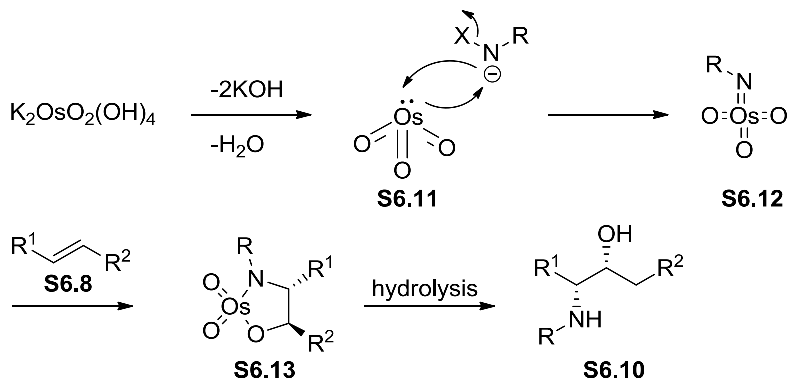

6.3 Catalytic Allene Aminohydroxylation: Synthesis of α-bromo-α′-hydroxy ketone

In contrast to alkene aminohydroxylation, nothing is known about allene aminohydroxylation as no reports in the literature describe efforts in this area. Still, e wanted to study the reactivity of allenes under aminohydroxylation condition. At the outset, we were not sure if the nitrogen would be delivered to the central carbon or the terminal carbon of an allene **S6.14** (Scheme 5). If the nitrogen were to add to the central carbon of the allene (**S6.14→S6.15**) the immediate product would be a hydroxyl *N*-acylenamide. If the nitrogen were to add to the terminal carbon of the allene then an amine (and osmium enolate) would be formed. Regardless of where the nitrogen adds, the corresponding product would be of great interest in the synthesis of biologically active molecules.

Scheme 5. Proposed Allene Aminohydroxylation

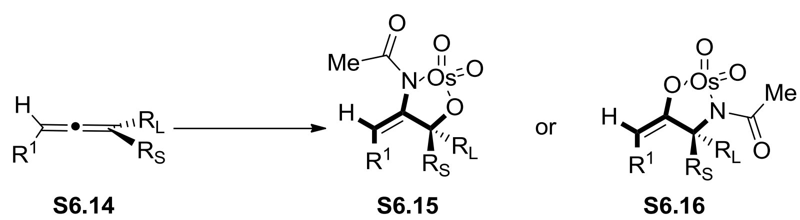

Our initial attempts to perform the aminohydroxylation were not successful. Many attempts resulted in the formation of complex inseparable mixtures. After screening various reaction parameters, we identified a favorable reaction condition. The reaction of the allene **S6.17** with the 5 equivalents of *N*-bromoacetamide in the presence of catalytic $K_2OsO_2(OH)_4$ and 5 equivalents of LiOH gave a single product. This reaction was completed within 15 min giving bromohydroxyketone **S6.18** as the product (Scheme 6).

Scheme 6. Catalytic Allene Aminohydroxylation of Allene S6.17

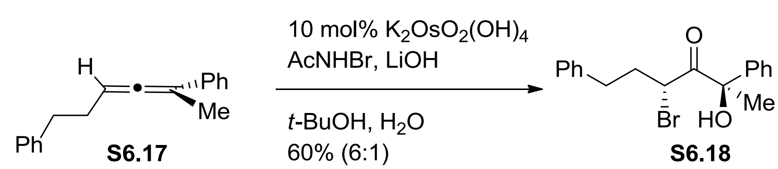

The formation of this product was unexpected but not unreasonable. One possible mechanistic framework is outlined below (Scheme 7). The imidotriooxoosmium (VIII) intermediate **S6.19** adds to the allene **S6.20** at the most electron rich double bond to form osmium aza enolate **S6.21** with the larger acylimido group, apparently, approaching the less sterically congested central allenic carbon. The addition of the imidotriooxoosmium (VIII) intermediate **S6.19** is face selective as well, and it adds *anti* to the larger substituent at the non-reacting terminus of the allene **S6.20** to form *trans* osmium aza enolate **S6.21**. The resulting aza enolate **S6.21** is nucleophilic, which attacks the unreacted *N*-bromoacetamide **S6.22** to form the bromo acylimine. The resulting bromo imine is hydrolyzed to generate the α-bromo-α′-hydroxy ketone **S6.23**. This mechanistic pathway is reasonable; however, the pathway that involves internal delivery of the bromine may also be relevant. Hence, the deprotonated *N*-bromoacetamide can add to **S6.21** to give **S6.24**. The bromine can then be delivered internally to give, as the final product, the α-bromo-α′-hydroxy ketone (**S6.23**).

Scheme 7. Mechanistic Framework for Catalytic Allene Aminohydroxylation

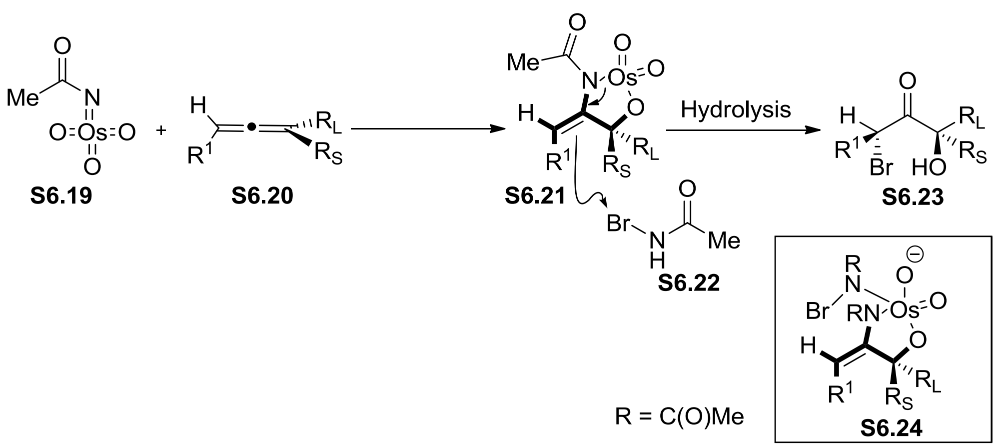

This catalytic allene aminohydroxylation method is superior to the previous allene osmylation/bromination sequence. For example, the allene osmylation/bromination sequence fails to synthesize α-bromo-α′-hydroxy ketone from aryl allene. The osmylation/bromination sequence yielded monohydroxylation as well as dihydroxylation products when aryl allenes were used, and this could be due to high reaction rate of OsO_4

towards aryl allene.[7] Unlike osmylation/bromination sequence, the use of catalytic $K_2OsO_2(OH)_4$, and excess of LiOH and *N*-bromoacetamide successfully generated α-bromo-α′-hydroxy ketone from the aryl allene.

We determined that to ensure the success and reproducibility of this reaction, we need to use 10 mol% of $K_2OsO_2(OH)_4$ and 5 equivalents each of N-bromoacetamide and LiOH (Table 1). The best solvent system was *tert*-butanol and water (2:1). The reaction when conducted at room temperature gave better result than when conducted at 0°C or 50°C. We also realized that it is important to add exactly 1:1 ratio of *N*-bromoacetamide and LiOH to guarantee the efficiency of this reaction.

Table 1. Optimization of Catalytic Allene Aminohydroxylation

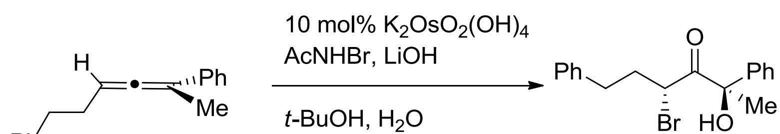

S6.17 S6.18

Reagent Ratio AcNHBr:LiOH	Solvent Ratio *t*BuOH:H_2O	Temperature	Time (min)	Yield (%)	dr
1:1	1:1	rt	10	57	5:1
1:1	1:2	rt	14	61	5:1
1:1	2:1	rt	14	60	6:1
2:1	2:1	rt	12	16	4:1
1:2	2:1	rt	12	trace	
1:1	2:1	0°C to rt	30	53	6:1
1:1	2:1	50°C	8	48	5:1

We evaluated the optimized reaction conditions on many substrates (Table 2). The reaction worked well for achiral trisubstituted allenes (**S6.27** and **S6.28**). We were pleased to see that the catalytic allene aminohydroxylation gave superior diastereomeric ratio. The catalytic allene aminohydroxylation reaction can differentiate even between aryl and *n*-butyl substituents of the allene (d.r. = 5:2 for **S6.29**). The diastereomeric ratio is even higher when the *n*-butyl group is replaced with methyl group (see **S6.30** to **S6.34**; d.r. = 4:1 to 8:1). The electron donating aryl group resulted in higher yield compared to electron withdrawing group (**S6.31** and **S6.32**). Also surprisingly, this method can differentiate between *n*-butyl and methyl substituent of an allene to give α-bromo-α′-hydroxy ketone product with diastereomeric ratio of 3:1 (see **S6.35**).

The catalytic allene aminohydroxylation method is significantly faster than allene osmylation/bromination. The allene osmylation/bromination method takes about 6 hours for the reaction to go to completion, whereas the catalytic allene aminohydroxylation method often requires less than 15 minutes to reach completion. The yield as well as the diastereomeric ratio of the α-bromo-α′-hydroxy ketone product obtained from catalytic allene aminohydroxylation method is higher than that obtained from allene osmylation/bromination method. For example, the α-bromo-α′-hydroxy ketone product **S6.35** is obtained only in 64% yield and in a diastereomeric ratio of 2:1 when allene osmylation/bromination method is used (Scheme 8). The ability of allene aminohydroxylation method to differentiate between *n*-butyl and methyl group is very impressive. The face selectivity of bromination in the catalytic allene aminohydroxylation method is excellent and we believe it is governed by $A^{1,3}$-strain.

Scheme 8. Catalytic Allene Osmylation/Bromination of Allene S6.41

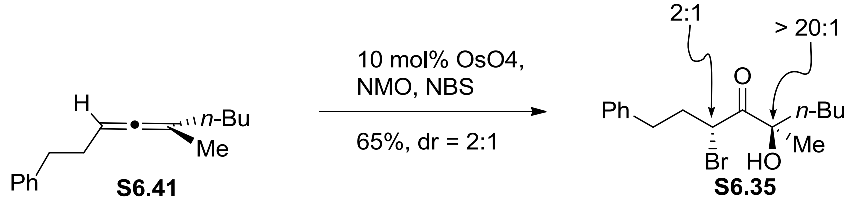

Table 2.Catalytic Allene Aminohydroxylation: Synthesis of α-bromo-α'-hydroxy ketone

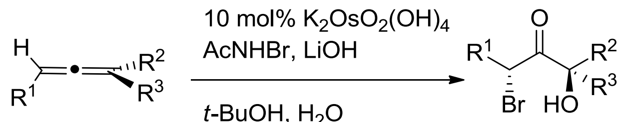

S6.25 **S6.26**

Entry	**Allene**	**Product**	***d.r.*** [a] ***r*** [1]	***r*** [2]	***Yield (%)***
1	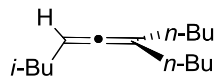	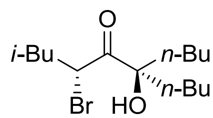 **S6.27**	>20:1	—	97
2	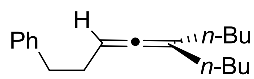	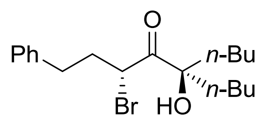 **S6.28**	>20:1	—	84
3	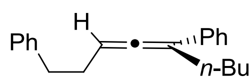	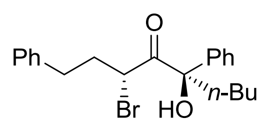 **S6.29**	>20:1	5:2	59
4	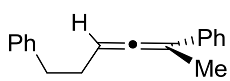	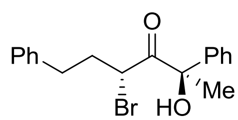 **S6.30**	>20:1	6:1	60
5	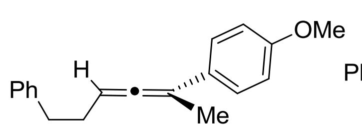	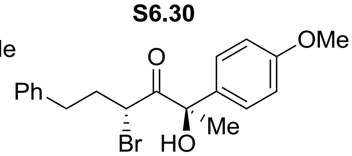 **S6.31**	>20:1	6:1	67
6	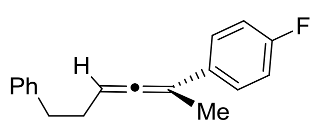	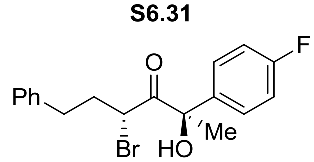 **S6.32**	>20:1	5:1	32
7	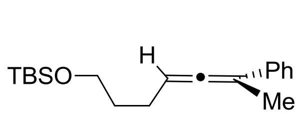	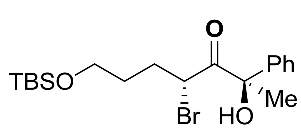 **S6.33**	>20:1	4.2:1	42

Table 2, contd.

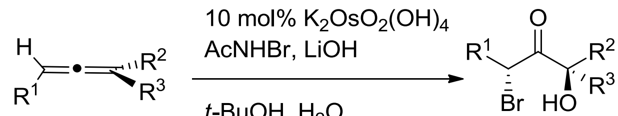

S6.25 → **S6.26**

Entry	Allene	Product	d.r.[a] r[1]	d.r.[a] r[2]	Yield (%)
8	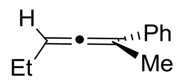	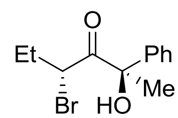 **S6.34**	>20:1	8:1	54
9	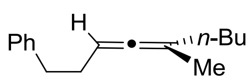	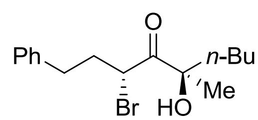 **S6.35**	>20:1	3.2:1	77
10	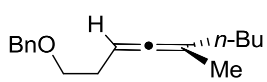	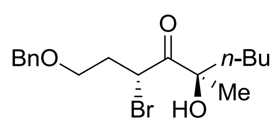 **S6.36**	>20:1	2:1	50
11	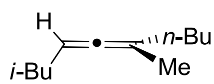	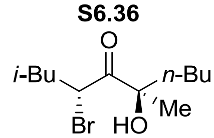 **S6.37**	>20:1	3:1	58
12	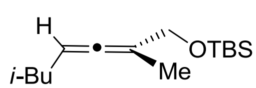	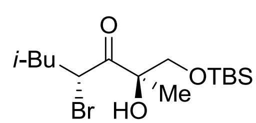 **S6.38**	>20:1	1.8:1	73
13	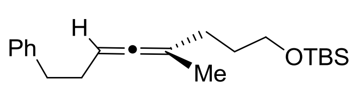	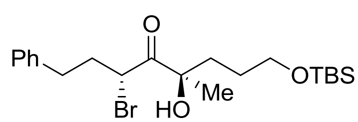 **S6.39**	>20:1	3.5:1	74
14	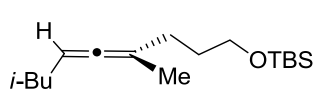	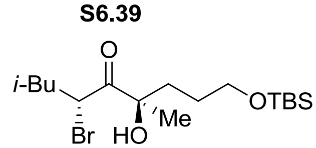 **S6.40**	>20:1	3.2:1	78

The α-bromo-α′-hydroxy ketone products are synthetically useful, and can be further derivatized to access diverse product motifs of significant use in complex molecule synthesis of biological interest. The ketone of the α-bromo-α′-hydroxy ketone **S6.27** and **S6.28** can be reduced to form alcohol, and in doing so, we can efficiently synthesize diols **S6.42** and **S6.43** (Table 3). The bromine of α-bromo-α′-hydroxy ketone can be eliminated to synthesize olefin. We can also displace the bromine of α-bromo-α′-hydroxy ketone with azide to form α-azido-α′-hydroxy ketone. The azido product can be further utilized in peptide synthesis.[13] The α-bromo-α′-hydroxy ketone can also be used to synthesize motifs like epoxide, oxetan-3-ones[14] and others. Other related studies are ongoing as well. For example, we have performed the reaction of allene **S6.44** with *N*-chlorotosylamide sodium salt. The use of Chloramine-T resulted in the synthesis of α-chloro-α′-hydroxy ketone **S6.45** and – remarkably – α-tosylamine-α′-hydroxy ketone **S6.46** (Scheme 9). Future studies will focus on further optimizing the products of this reaction.

Table 3. Derivatization of α-bromo-α'-hydroxy ketone

Entry	*Ketone*	*Product*	*Yield(%)*
1	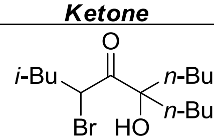 **S6.27**	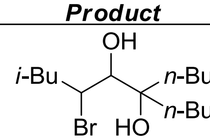 **S6.42**	83
2	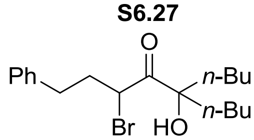 **S6.28**	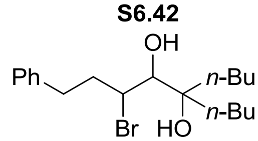 **S6.43**	72

Scheme 9. Reaction of Allene S6.44 with N-chlorotosylamide Sodium Salt

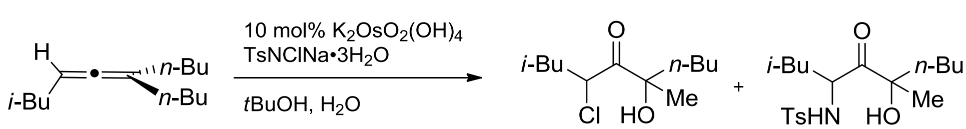

S6.44 **S6.45** 24% **S6.46** 11%

6.4 Conclusion

We have developed a catalytic allene aminohydroxylation method to synthesize α-bromo-α′-hydroxy ketone with high diastereoselectivity. The catalytic allene aminohydroxylation method proved to be very advantageous in the synthesis of α-bromo-α′-hydroxy ketone over other methods.

6.5 References

1. Sharma, R.; Manpadi, M.; Zhang, Y.; Kim, H.; Ahkmedov, N. G.; Williams, L. J. *Org. Lett.* **2011**, *13*, 3352.
2. Ghosh, P.; Cusick, J. R.; Inghrim, J.; Williams, L. J. *Org. Lett.* **2009**, *11*, 4672.
3. Lotesta, S. D.; Kiren, S. K.; Sauers, R. R.; Williams, L. J. *Angew. Chem. Int. Ed.* **2007**, *46*, 7108.
4. Ghosh, P.; Lotesta, S. D.; Williams, L. J. *J. Am. Chem. Soc.* **2007**, *129*, 2438.
5. Biollaz, M.; Haefliger, W.; Velarde, E.; Crabbe, P.; Fried, J. H. *J. Chem. Soc. D:Chem. Comm.* **1971**, *21*, 1322.
6. Fleming, S. A.; Carroll, S. M.; Hirschi, J.; Liu, R.; Lee Pace, J.; Ty Redd, J. *Tetrahedron Lett.* **2004,** *45*, 3341.
7. Fleming, S. A.; Liu, R.; Redd, J. T. *Tetrahedron Lett.* **2005,** *46*, 8095.
8. Liu, K.; Kim, H.; Ghosh, P.; Akhmedov, N. G.; Williams, L. J. *J. Am. Chem. Soc.* **2011,** *133*, 14968.
9. Li, G.; Chang, H-T.; Sharpless, K. B. *Angew. Chem. Int. Ed. Engl.* **1996**, *35*, 451.
10. Bodkin, J. A.; McLeod, M. D. *J. Chem. Soc., Perkin Trans. 1* **2002**, 2733 and references therein.

11. Tao, B.; Schlingloff, G.; Sharpless, K. B. *Tetrahedron Lett*. **1998**, *39*, 2507.

12. Han, H.; Cho, C-W.; Janda, K. D. *Chem. Eur. J*. **1999**, *5*, 1565.

13. Shangguan, N.; Katukojvala, S.; Greenberg, R.; Williams, L. J. *J. Am. Chem. Soc*. **2003,** *125*, 7754.

14. Sharma, R.; Williams, L. J. *Org. Lett*. **2013**, *15*, 2202.

Chapter 7

Experimental Section

7.1 General Experimental

Reagents and solvents were purchased from commercial suppliers (Aldrich and Fischer) and used without further purification. Anhydrous tetrahydrofuran (THF), diethyl ether, chloroform, toluene, and dichloromethane were obtained from a solvent purification system consisting of alumina based columns. All reactions were conducted in oven-dried (135 ºC) glassware under an inert atmosphere of dry nitrogen. The progress of reactions was monitored by silica gel thin layer chromatography (TLC) plates (mesh size 60Å with fluorescent indicator, Sigma-Aldrich), visualized under UV and charred using vanillin, cerium or *p*-anisaldehyde stain. Products were purified by flash column chromatography (FCC) on 120–400 mesh silica gel (Fisher). Infrared (FTIR) spectra were recorded on an ATI Mattson Genesis Series FT-Infrared spectrophotometer. HPLC analysis was carried out on an Agilent 1100 series instrument with auto sampler and multiple wavelength detectors. Proton nuclear magnetic resonance spectra (^{1}H NMR) were recorded on a Varian-300 instrument (300 MHz), Varian-400 instrument (400 MHz), or Varian-500 instrument (500 MHz). Chemical shifts are reported in ppm relative to tetramethylsilane (TMS) as the internal standard. Data are reported as follows: chemical shift, integration, multiplicity (s=singlet, d=doublet, t=triplet, q=quartet, br=broad, m=multiplet), and coupling constants (Hz). Carbon nuclear magnetic resonance spectra (^{13}C NMR) were recorded on a Varian-300 instrument (75 MHz), Varian-400 instrument (100 MHz) or Varian-500 instrument (125 MHz). Chemical shifts are reported in ppm relative to TMS as the internal standard. Mass spectra were recorded on a Finnigan LCQ-DUO mass spectrometer.

7.2 Chapter 2: Allene Synthesis

General procedure for allene synthesis (Table 1, entry 1-11):

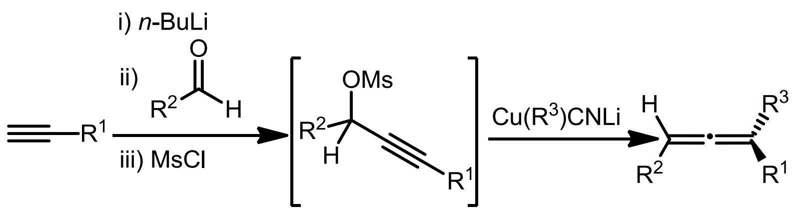

To a solution of alkyne (1.05 equiv) in dry THF (0.10 M) was added *n*-BuLi (1.05 equiv) dropwise at −78 ºC. The reaction mixture was stirred at −78 ºC for 15 min, 0 ºC for 20 min and then cooled back to −78 ºC. Aldehyde (1.00 equiv) was added dropwise to the reaction mixture at −78 ºC. The reaction mixture was stirred at −78 ºC for 15 min and at 0 ºC until complete consumption of aldehyde based on TLC (0.5-2 h). To the reaction at 0 ºC was added methanesulfonyl chloride (MsCl) (1.05 equiv) followed by Et_3N (1.05 equiv). The reaction was stirred at 0 ºC until TLC indicated complete consumption of the propargyl alcohol (1-2 h).

In a separate round-bottom flask, a suspension of CuCN (2.00 equiv, activated by a gentle flame under high vacuum) in anhydrous THF (2.00 M) was degassed for 2 min with argon. The suspension was cooled to −78 ºC and a solution of the corresponding R^4Li (2.00 equiv) in THF (1.60 M) was added dropwise. The reaction mixture was warmed to 0 ºC and stirred for 10 min. The organocuprate solution was cooled back to −78 ºC and the mesylate mixture (above) was added via cannula. The reaction mixture was allowed to warm to rt over 1 h and was monitored by TLC. Upon completion of reaction as judged by TLC (1-3h), a solution of NH_4Cl: NH_4OH (9:1) was added. The organic layer was separated, and the aqueous layer was extracted with Et_2O. The organic layers were combined, dried over Na_2SO_4, filtered, evaporated and then purified by FCC.

All the spectroscopic data for entries 3, 5, 7 and 9 match the published results for these known compounds.[1-3]

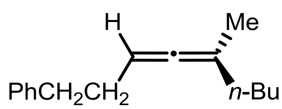

5-methylnona-3,4-dien-1-yl)benzene (**S2.13**, Table 1, entry 1): 93% (743 mg); IR ν_{max}(neat)/cm^{-1}: 3012, 2929, 2856, 1966, 1598, 1471, 1364, 1254; δ_H (500 MHz, $CDCl_3$) 7.30-7.24 (2H, m), 7.22 – 7.14 (3H, m), 5.04 (1H, td, J = 5.8, 2.8 Hz), 2.70 (2H, t, J = 7.6 Hz), 2.32 – 2.25 (2H, m), 1.89 (2H, m), 1.62 (3H, s), 1.33 (4H, ddd, J = 10.5, 9.1, 5.5 Hz), 0.89 (3H, m); δ_C (125 MHz, $CDCl_3$) 201.57, 142.36, 128.72, 128.41, 125.89, 100.09, 89.61, 35.83, 33.98, 31.30, 29.94, 22.58, 19.44, 14.21; (ESI/MS) Calcd for m/z $C_{16}H_{23}^+$: 215.2 $[M+H]^+$; found 215.2.

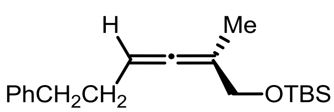

tert-butyldimethyl((2-methyl-6-phenylhexa-2,3-dien-1-yl)oxy)silane (**S2.14**, Table 1, entry 2): 82% (2.75 g); IR ν_{max}(neat)/cm^{-1}: 3012, 2928, 2856, 1964, 1471, 1462, 1254, 1103; δ_H (500 MHz, $CDCl_3$) 7.30 – 7.24 (2H, m), 7.20 – 7.15 (3H, m), 5.16 – 5.09 (1H, m), 4.06 – 3.99 (2H, s), 2.71 (2H, t, J = 7.7 Hz), 2.33 – 2.26 (2H, m), 1.66 – 1.61 (3H, s), 0.90 (9H, s), 0.06 (6H, s); δ_C (125 MHz, $CDCl_3$) 201.37, 142.12, 128.73, 128.44, 125.97, 100.17, 90.60, 65.68, 35.81, 30.94, 26.14, 18.61, 15.87, -4.98, -5.00; (ESI/MS) Calcd for m/z $C_{19}H_{31}OSi^+$: 303.2 $[M+H]^+$; found 303.2.

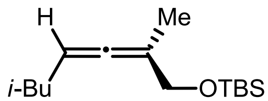

tert-butyl((2,6-dimethylhepta-2,3-dien-1-yl)oxy)dimethylsilane (**S2.15**, Table 1, entry 3): 93% (648mg). The spectroscopic data match the published results.[1]

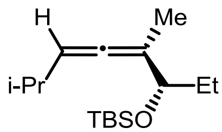

tert-butyl(((3S,5R)-4,7-dimethylocta-4,5-dien-3-yl)oxy)dimethylsilane (**S2.16**, Table 1, entry 4): 79% (453 mg, as a 1:1 mixture of diastereomers); IR ν_{max}(neat)/cm^{-1} 3018, 2856, 1945, 1496, 1261; δ_H (400 MHz, $CDCl_3$) 5.01 – 4.91 (1H, m), 4.00 (1H, t, J = 6.5 Hz), 1.90 – 1.81 (2H, m), 1.60 (4H, dt, J = 5.9, 3.3 Hz), 0.91 – 0.86 (18H, m), 0.04 – 0.01 (6H, m); δ_C (100 MHz, $CDCl_3$) (Carbon count for the 1:1 mixture of diastereomers) 202.19, 201.90, 100.96, 100.58, 89.11, 88.58, 76.92, 76.42, 38.96, 38.71, 29.45, 29.18, 28.84, 28.69, 26.11, 25.93, 22.41, 22.39, 18.50, 18.47, 13.32, 12.79, 10.55, 10.49, -4.41, -4.45, -4.80, -4.84; (ESI/MS) m/z Calcd for $C_{16}H_{33}OSi^+$: 269.5 $[M+H]^+$; found: 270.0.

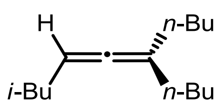

6-butyl-2-methyldeca-4,5-diene (**S2.17**, Table 1, entry 5): 91% (8.67 g). The spectroscopic data match the published results.[2]

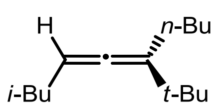

6-(tert-butyl)-2-methyldeca-4,5-diene (**S2.18**, Table 1, entry 6): 84% (530 mg); IR ν_{max}(neat)/cm^{-1}: 2958, 2869, 1955, 1464, 1361; δ_H (500 MHz, $CDCl_3$) 5.05 (1H, ddd, J = 10.5, 7.0, 3.3 Hz), 1.89 (4H, ddd, J = 13.7, 8.0, 6.4 Hz), 1.66 (1H, tq, J = 13.2, 6.6 Hz), 1.39 – 1.28 (4H, m), 1.02 (9H, s), 0.91 (9H, dd, J = 14.9, 6.7 Hz); δ_C (125

MHz, $CDCl_3$) 200.25, 112.95, 92.06, 39.63, 33.72, 30.92, 29.67, 29.10, 27.05, 22.83, 22.71, 14.33; (ESI/MS) Calcd for *m/z* $C_{15}H_{29}^+$: 209.2 $[M+H]^+$; found 209.5.

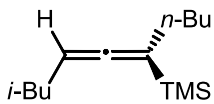
trimethyl(9-methyldeca-5,6-dien-5-yl)silane (**S2.19**, Table 1, entry 7): 78% (750 mg). The spectroscopic data match the published results.[3]

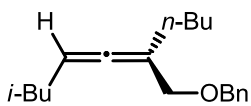
(((2-butyl-6-methylhepta-2,3-dien-1-yl)oxy)methyl)benzene (**S2.20**, Table 1, entry 8): 92% (817 mg); IR ν_{max}(neat)/cm^{-1}: 2955, 2826, 2868, 1962, 1465, 1382, 1071, 733; δ_H (400 MHz, $CDCl_3$) 7.40 – 7.22 (5H, m), 5.18 – 5.05 (1H, m), 4.49 (2H, s), 4.01 (2H,s), 2.05 (2H, td, *J* = 7.5, 3.0 Hz), 1.91 (2H, q, *J* = 6.5 Hz), 1.67 (1H, tt, *J* = 13.3, 6.6 Hz), 1.49 – 1.30 (4H, m), 0.96 – 0.86 (9H, m); δ_C (125 MHz, $CDCl_3$) 203.09, 138.75, 128.54, 128.05, 127.71, 100.56, 90.60, 72.00, 71.50, 38.97, 30.03, 29.46, 28.81, 22.68, 22.51, 22.50, 14.22; (ESI/MS) Calcd for *m/z* $C_{19}H_{29}O^+$: 273.2 $[M+H]^+$; found 273.2.

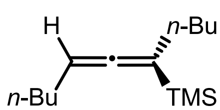
trimethyl(undeca-5,6-dien-5-yl)silane (**S2.21**, Table 1, entry 9): 80% (250 mg). All the spectroscopic data matches with that of the published result.[3]

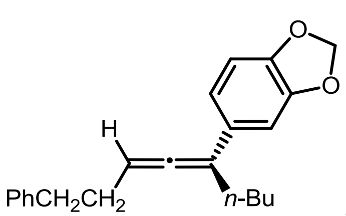
5-(1-phenylnona-3,4-dien-5-yl)benzo[d][1,3]dioxole (**S2.22**, Table 1, entry 10): 81% (450 mg); IR ν_{max}(neat)/cm^{-1}: 3440, 2955, 2077, 1639, 1486, 1440; δ_H (500 MHz, $CDCl_3$) 7.29 – 7.24 (2H, m), 7.21 – 7.16 (3H, m), 6.86–6.67 (3H,

m), 5.92 (2H, s), 5.54 – 5.43 (1H, m), 2.77 (2H, t, J = 7.6 Hz), 2.42 (2H, dq, J = 8.1, 6.7 Hz), 2.30 (2H, td, J = 7.3, 2.9 Hz), 1.46 – 1.35 (4H, m), 0.90 (3H, t, J = 7.80 Hz); δ_C (125 MHz, $CDCl_3$) 203.69, 147.95, 145.41, 141.96, 131.77, 128.75, 128.54, 126.11, 119.14, 108.21, 106.96, 106.07, 101.12, 93.91, 35.78, 31.22, 30.37, 30.21, 22.74, 14.24; (ESI/MS) Calcd for m/z $C_{22}H_{25}O_2^+$: 321.2 $[M+H]^+$; found 321.2.

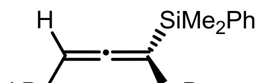

dimethyl(9-methyldeca-5,6-dien-5-yl)(phenyl)silane (**S2.23**, Table 1, entry 11): 74% (250 mg); IR ν_{max}(neat)/cm^{-1}: 3084, 2928, 2855, 1832, 1264, 1170; δ_H (500 MHz, $CDCl_3$) 7.18 – 6.90 (5H, m), 4.49 – 4.43 (1H, m), 1.57 – 1.51 (4H, m), 1.02 (1H, d, J = 7.5 Hz), 0.94 – 0.90 (4H, m), 0.55 (9H, dd, J = 15.1, 6.8 Hz), 0.00 (6H, s); δ_C (125 MHz, $CDCl_3$) 207.25, 138.91, 134.05, 129.07, 127.85, 94.34, 84.97, 38.53, 31.48, 29.51, 29.24, 22.69, 22.47, 14.34, 14.15, -2.51, -2.61; (ESI/MS) Calcd for m/z $C_{19}H_{30}Si+H_2O$: 304.2 $[M+H_2O]^+$; found 304.2.

General procedure for allene synthesis (Table 2, entry 1-9):

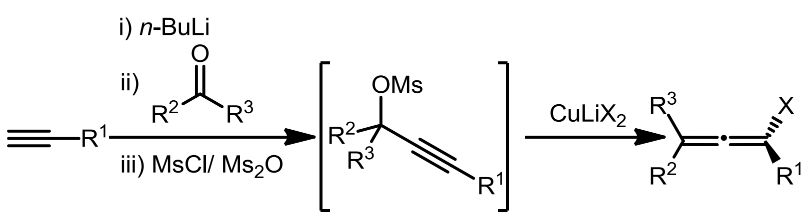

To a solution of alkyne (1.05 equiv) in dry THF (0.10 M) was added n-BuLi (1.05 equiv) dropwise at −78 ºC. The reaction was stirred at −78 °C for 15 min, 0 ºC for 20 min and cooled back to −78 ºC. Aldehyde/ketone (1.00 equiv) was added dropwise to the reaction at −78 ºC. The reaction was stirred at −78 ºC for 15 min and at 0 ºC until the complete consumption of aldehyde/ketone as judged by TLC (0.5-2 h). To the reaction at

0 ºC was added MsCl (when X = Cl) or Ms_2O (when X = Br or I) (1.05 equiv) followed by Et_3N (1.05 equiv). The reaction was stirred at 0 ºC until TLC indicated complete consumption of the propargyl alcohol (1-2 h).

In a separate round-bottom flask, a suspension of CuX (4.00 equiv when X= Cl; 2 equiv when X= Br or I) and LiX (4.00 equiv when X= Cl; 2.00 equiv when X= Br or I, activated by a gentle flame under high vacuum) in anhydrous THF (2.00 M) was degassed for 2 min with argon. The suspension was cooled to 0 ºC and the mesylate (above) was added via cannula. The reaction was allowed to warm to rt over 1 h and monitored by TLC. Upon completion of reaction as judged by TLC (1-5 h), a solution of NH_4Cl: NH_4OH (9:1) was added. The organic layer was separated, and the aqueous layer was extracted with Et_2O. The organic layers were combined, dried over Na_2SO_4, filtered, evaporated and purified by FCC.

The spectroscopic data for entry 19 match the published data for this known compound.[4]

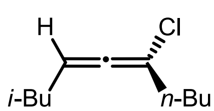

6-chloro-2-methyldeca-4,5-diene (**S2.28**, Table 2, entry 1): 68% (275 mg), IR ν_{max}(neat)/cm^{-1}: 2956, 2931, 2871, 1968, 1465, 908, 735; δ_H (500 MHz, $CDCl_3$) 5.44 (1H, tdd, J = 7.3, 3.7, 2.0 Hz), 2.35-2.28 (2H, m), 2.04 – 1.91 (2H, m), 1.72 (1H, qq, J = 13.2, 6.6 Hz), 1.54 – 1.46 (2H, m), 1.40 – 1.31 (2H, m), 0.95 – 0.89 (9H, m); δ_C (125 MHz, $CDCl_3$) 199.77, 105.38, 98.77, 38.91, 36.41, 29.50, 28.31, 22.49, 22.42, 21.95, 14.00; (ESI/MS) Calcd for m/z $C_{11}H_{19}Cl^+$: 186.2 $[M]^{+\cdot}$; found 186.2.

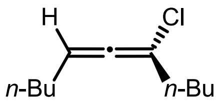 **5-chloroundeca-5,6-diene** (**S2.29**, Table 2, entry 2): 62% (173 mg), IR v_{max}(neat)/cm^{-1}: 2957, 2929, 2872, 1967, 1463, 908; δ_H (500 MHz, $CDCl_3$) 5.49 (1H, ddd, *J* = 9.4, 6.3, 2.8 Hz), 2.33 (2H, td, *J* = 7.4, 2.8 Hz), 2.10 (2H, dd, *J* = 14.1, 7.0 Hz), 1.54 – 1.49 (2H, m), 1.46 – 1.34 (6H, m), 0.92 (6H, t, *J* = 7.3 Hz); δ_C (125 MHz, $CDCl_3$) 199.19, 105.84, 100.10, 36.44, 30.82, 29.53, 29.26, 22.33, 21.97, 14.03, 13.98; (ESI/MS) *m/z* Calcd for $C_{11}H_{19}Cl^{+}$: 186.2 $[M]^{+\cdot}$; found 186.1.

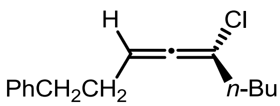 **(5-chlorononа-3,4-dien-1-yl)benzene** (**S2.30**, Table 2, entry 3): 65% (157 mg), IR v_{max}(neat)/cm^{-1}: 3060, 3027, 2957, 2929, 2871, 1969, 1603, 1456, 1453, 745, 698; δ_H (500 MHz, $CDCl_3$) 7.28 (2H, dd, *J* = 9.7, 5.4 Hz), 7.21 – 7.16 (3H, m), 5.54 – 5.50 (1H, m), 2.75 (2H, td, *J* = 7.8, 3.2 Hz), 2.48 – 2.35 (2H, m), 2.26 (2H, td, *J* = 7.3, 2.9 Hz), 1.47 – 1.38 (2H, m), 1.37 – 1.28 (2H, m), 0.89 (3H, t, *J* = 7.3 Hz); δ_C (125 MHz, $CDCl_3$) 199.45, 141.44, 128.68, 128.60, 126.24, 106.45, 99.34, 36.40, 34.93, 31.18, 29.44, 22.00, 14.04; (ESI/MS) *m/z* Calcd for $C_{15}H_{20}Cl^{+}$: 235.1 $[M+H]^{+}$; found 235.1

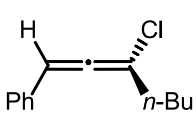 **(3-chlorohepta-1,2-dien-1-yl)benzene** (**S2.31**, Table 2, entry 4): 61% (133 mg), IR v_{max}(neat)/cm^{-1}: 3030, 3027, 2950, 1969, 1607, 772; δ_H (500 MHz, $CDCl_3$) 7.24 – 7.18 (4H, d, *J* = 4.4 Hz), 7.13 (1H, dt, *J* = 4.8, 4.1 Hz), 6.29 (1H, t, *J* = 2.9 Hz), 2.37 – 2.31 (2H, m), 1.48 – 1.41 (2H, m), 1.30 – 1.23 (2H, m), 0.78 (3H, t, *J* = 7.4 Hz); δ_C (125 MHz, $CDCl_3$) 200.62, 133.56, 128.98, 128.41, 127.97, 109.07, 101.95, 36.56, 29.51, 22.11, 14.02; (ESI/MS) *m/z* Calcd for $C_{13}H_{16}Cl^{+}$: 207.1 $[M+H]^{+}$; found 207.1.

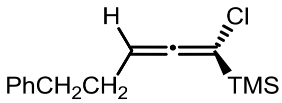
(1-chloro-5-phenylpenta-1,2-dien-1-yl)trimethylsilane (**S2.32**, Table 2, entry 5): 60% (427 mg), IR ν_{max}(neat)/cm^{-1}: 3028, 2959, 1968, 1496, 1454, 1250, 843, 760; δ_H (500 MHz, $CDCl_3$) 7.13 (2H, dt, J = 8.5, 3.4 Hz), 7.03 (3H, dd, J = 9.5, 3.8 Hz), 5.27 (1H, t, J = 6.6 Hz), 2.59 (2H, t, J = 7.7 Hz), 2.27 (2H, dt, J = 8.0, 6.4 Hz), 0.01 (9H, s); δ_C (125 MHz, $CDCl_3$) 204.99, 141.37, 128.65, 128.64, 126.29, 100.65, 96.45, 35.24, 30.45, -1.94; (ESI/MS) m/z Calcd for $C_{14}H_{20}ClSi^+$: 251.1 $[M+H]^+$; found 251.0.

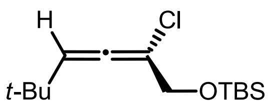
tert-butyl((2-chloro-5,5-dimethylhexa-2,3-dien-1-yl)oxy)dimethylsilane (**S2.33**, Table 2, entry 6): 64% (130 mg), IR ν_{max}(neat)/cm^{-1}: 2959, 1968, 1472, 1363, 1256, 1105, 838, 777; δ_H (500 MHz, $CDCl_3$) 5.51 (1H, td, J = 2.7, 1.0 Hz), 4.16 (2H, td, J = 2.8, 1.0 Hz), 0.99 (9H, d, J = 1.0 Hz), 0.81 (9H, d, J = 1.0 Hz), 0.00 (6H, s); δ_C (125 MHz, $CDCl_3$) 196.28, 113.39, 105.89, 65.23, 33.48, 29.84, 26.05, 18.60, -5.01, -5.05; (ESI/MS) m/z Calcd for $C_{14}H_{28}ClOSi^+$: 275.2 $[M+H]^+$; found 275.2.

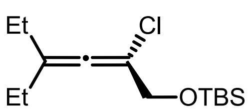
tert-butyl((2-chloro-4-ethylhexa-2,3-dien-1-yl)oxy)dimethylsilane (**S2.34**, Table 2, entry 7): 58% (650 mg), IR ν_{max}(neat)/cm^{-1}: 2963, 2930, 2857, 1965, 1461, 1257, 1114, 838, 777; δ_H (500 MHz, $CDCl_3$) 4.24 (2H, d, J = 1.2 Hz), 2.09 (4H, q, J = 7.4 Hz); 1.04 (6H, td, J = 7.3, 1.0 Hz); 0.90 (9H, d, J = 1.2 Hz), 0.10 – 0.07 (6H, d, J = 1.2 Hz); δ_C (100 MHz, $CDCl_3$) 194.78, 120.74, 106.19, 65.40, 29.92, 26.64, 25.97, 18.50, 12.19, -5.07; (ESI/MS) m/z Calcd for $C_{14}H_{27}OSi^+$: 239.2 $[M-Cl]^+$; found 239.2.

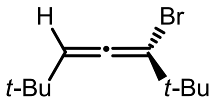 **3-bromo-2,2,6,6-tetramethylhepta-3,4-diene** (**S2.35**, Table 2, entry 8): 50% (150 mg). The spectroscopic data match the published results.[4]

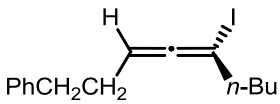 **(5-iodonona-3,4-dien-1-yl)benzene** (**S2.36**, Table 2, entry 9): 63% (780 mg), IR ν_{max}(neat)/cm^{-1}: 3026, 2956, 2926, 1957, 1603, 1496, 1453, 743, 697; δ_H (500 MHz, $CDCl_3$) 7.33 – 7.27 (2H, m), 7.22 – 7.16 (3H, m), 5.07 – 5.01 (1H, m), 2.76 (2H, td, J = 7.7, 3.2 Hz), 2.47 – 2.31 (2H, m), 2.30 – 2.25 (2H, m), 1.39 – 1.29 (4H, m), 0.89 (3H, td, J = 7.2, 1.3 Hz); δ_C (125 MHz, $CDCl_3$) 202.48, 141.47, 128.67, 128.61, 126.22, 93.69, 64.21, 40.85, 34.81, 31.45, 30.19, 21.69, 14.04; (ESI/MS) m/z Calcd for $C_{15}H_{20}I^+$: 327.2 $[M+H]^+$; found 327.1.

7.3 Chapter 3: Spirodiepoxide Based Cascades: Direct Access to Diverse Motifs

General Procedure for Spirodiepoxide Formation

Dimethyldioxirane (DMDO) was prepared following a modified Murray procedure.[5] For photo of the set up for this procedure see Ref 6. The DMDO was extracted out of acetone and into $CHCl_3$ by known procedure.[7, 8]

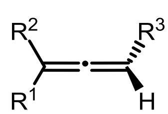

The allene was taken upon $CHCl_3$ (0.10 M) and cooled to −40 ºC. To this was added solution of freshly prepared DMDO in $CHCl_3$ (~0.20 M, 2.00 equiv) dropwise. The reaction was stirred under nitrogen. Upon the complete consumption of allene as judged by TLC (30-120 min), the volatiles were removed under vacuum and the spirodiepoxide was taken on as described below.

Simple Heteronucleophile Addition (Table 1):

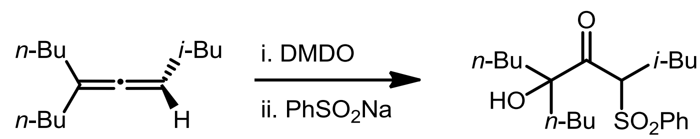

6**-butyl-6-hydroxy-2-methyl-4-(phenylsulfonyl)decan-5-one** (**S3.15**, Table 1, entry 1): To the suspension of sodium benzenesulfinate (20.5 mg, 0.125 mmol) in THF (0.50 ml) was added the freshly prepared spirodiepoxide (see General Procedure for Spirodiepoxide Formation on pg 148), obtained from the oxidation of 17.3 mg of the allene (0.0830 mmol), in THF (0.5 ml) at 0 ºC followed by 15-crown-5 (0.025 ml, 0.125 mmol). The reaction was slowly warmed to rt over 1 h. Upon completion of reaction as judged by TLC (4 h), the reaction mixture was concentrated and purified by FCC (4 % EtOAc/Hexanes) to obtain the product (15.9 mg, 50 % yield). IR ν_{max}(neat)/cm^{-1} 3505, 2957, 2932, 2871, 1716, 1143; δ_H (500 MHz, $CDCl_3$) 7.78 (2H, dd, J = 7.5, 1.0 Hz), 7.74 – 7.68 (1H, m), 7.62 – 7.55 (2H, m), 5.7 (1H, dd, J = 10.2, 3.6 Hz), 3.99 (1H, bs), 1.81 (2H, td, J = 9.2, 4.5 Hz), 1.63 – 1.55 (1H, m), 1.44 – 1.33 (6H, m), 1.33 – 1.09 (6H, m), 1.00 – 0.90 (3H, m), 0.89 – 0.81 (6H, m), 0.79 (3H, d, J = 6.5 Hz); δ_C (125 MHz, $CDCl_3$) 206.71, 136.44, 134.61, 129.66, 129.27, 82.84, 66.66, 36.81, 36.32, 36.11, 25.52, 25.31, 25.28, 23.50, 23.33, 23.14, 21.52, 14.27, 14.04; (ESI/MS) Calcd for m/z $C_{21}H_{35}O_4S^+$: 383.2 $[M+H]^+$; found 383.2.

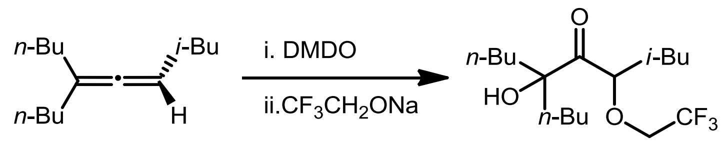

6-butyl-6-hydroxy-2-methyl-4-(2,2,2-trifluoroethoxy)decan-5-one (S3.16, Table 1, entry 2): To 0.50 mL of 2,2,2-trifluoroethanol was added sodium hydride (5.0 mg, 60% in mineral oil, 0.125 mmol) at 0 ºC. The freshly prepared spirodiepoxide (see General Procedure for Spirodiepoxide Formation on pg 148), obtained from the oxidation of 17.3 mg of the allene (0.0830 mmol), was dissolved in 0.20 ml of 2,2,2-trifluoroethanol and added to the reaction mixture at 0 ºC. The reaction was slowly warmed to rt over 30 min. Upon completion of reaction as judged by TLC (30 min), the reaction was quenched with saturated aq. NH_4Cl (2.0 ml), extracted with Et_2O (3 x 5.0 ml), dried over anhydrous Na_2SO_4, filtered, concentrated and purified by FCC (4 % EtOAc/Hexanes) to obtain product (21.2 mg, 75 % yield) as a colorless oil. IR ν_{max}(neat)/cm^{-1} 3497, 2960, 2874, 1713, 1468, 1283, 1161, 670; δ_H (500 MHz, $CDCl_3$) 4.55 (1 H, dd, *J* = 8.9, 3.8 Hz), 3.98 – 3.91 (1H, m), 3.68 – 3.61 (1H, m), 2.58 (1H, d, *J* = 3.0 Hz), 1.92 – 1.50 (7H, m), 1.45 – 1.23 (6H, m), 1.15 – 1.01 (2H, m), 0.96 (6H, t, *J* = 6.8 Hz), 0.89 (6H, td, *J* = 7.3, 1.9 Hz); δ_C (125 MHz, $CDCl_3$) 212.90, 123.81 (q, *J* = 279 Hz), 82.47 (d, *J* = 1.8 Hz), 81.14, 66.76 (m), 39.74, 39.63, 38.74, 38.71, 38.34, 38.32, 25.48, 25.39, 24.49, 23.21, 22.93, 22.92, 21.32, 13.85, 13.84; (ESI/MS) Calcd for *m/z* $C_{17}H_{32}F_3O_3^+$: 341.2 $[M+H]^+$; found 341.2.

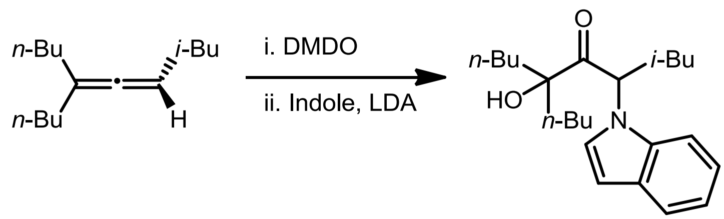

6-butyl-6-hydroxy-4-(1H-indol-1-yl)-2-methyldecan-5-one (**S3.17**, Table 1, entry 3): To the solution of indole (29.3 mg, 0.250 mmol) in THF (0.50 ml) was added 2.5 M *n*-BuLi (0.10 mL, 0.250 mmol) dropwise at -78 ºC. The reaction was stirred at -78 ºC for 45 min. The freshly prepared spirodiepoxide (see General Procedure for Spirodiepoxide Formation on pg 148), obtained from the oxidation of 17.3 mg of the allene (0.0830 mmol), was dissolved in THF (0.20 ml) and added to the reaction mixture at -78 ºC. The reaction was allowed to warm to 0 ºC over 2 h. Upon completion of reaction as judged by TLC (2 h), the reaction was quenched with saturated aq. NH_4Cl (2 ml), extracted with Et_2O (3 x 5.0 ml), dried over anhydrous Na_2SO_4, filtered, concentrated and purified by FCC (4 % EtOAc/Hexanes) to obtain product (14.8 mg, 50 % yield) as a colorless oil. IR ν_{max}(neat)/cm^{-1} 3504, 2958, 2871, 1811, 1714, 1459, 738; δ_H (500 MHz, $CDCl_3$) 7.60 (1H, d, *J* = 7.90 Hz), 7.42 (1H, d, *J* = 8.30 Hz), 7.22 (1H, td, *J* = 7.70, 1.10 Hz), 7.10 (1H, td, *J* = 7.50, 0.80 Hz), 6.56 (1H, d, *J* = 3.20 Hz), 5.62 (1H, dd, *J* = 11.0, 3.80 Hz), 2.99 (1H, bs), 2.19 (1H, td, *J* = 12.5, 3.80 Hz), 1.79-1.47 (6H, m), 1.45-1.19 (6H, m), 1.19-1.05 (1H, m), 1.03-0.79 (12H, m), 0.51 (2H, t, *J* = 3.20 Hz); δ_C (125 MHz, $CDCl_3$) 210.99, 136.21, 128.49, 125.23, 121.84, 121.21, 119.83, 108.94, 103.07, 82.53, 40.83, 38.71, 38.25, 25.49, 25.12, 24.20, 23.24, 22.88, 22.52, 21.79, 13.82, 13.52; (ESI/MS) Calcd for *m/z* $C_{23}H_{36}NO_2^+$: 358.6 $[M+H]^+$; found 358.6.

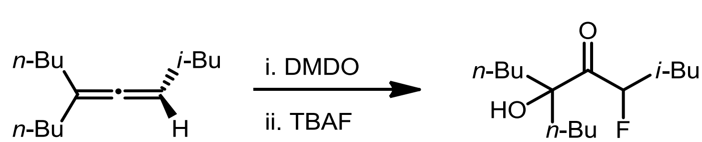

6-butyl-4-fluoro-6-hydroxy-2-methyldecan-5-one (**S3.18**, Table 1, entry 4): The freshly prepared spirodiepoxide (see General Procedure for Spirodiepoxide Formation on pg 148), obtained from the oxidation of 17.3 mg of the allene (0.0830 mmol), was dissolved in THF (0.50 ml) and cooled to 0 ºC. Dry 1 M TBAF (0.17 mL, 0.170 mmol) was added to the reaction at 0 ºC. The reaction was allowed to warm to rt over 2 h. Upon the completion of reaction as judged by TLC (2 h), the reaction was quenched with saturated aq. NH_4Cl (2.0 ml), extracted with Et_2O (3 x 5.0 ml), dried over anhydrous Na_2SO_4, filtered, concentrated and purified by FCC (4 % EtOAc/Hexanes) to obtain product (11.0 mg, 51 % yield) as a colorless oil. IR ν_{max} (neat) /cm^{-1} 3488, 2957, 2932, 2871, 1707, 1467, 1380, 1260; δ_H (500 MHz, $CDCl_3$) 5.10 (1H, ddd, *J* = 50.1, 10.0, 3.1 Hz), 3.44 (1H, bs), 1.94 – 1.60 (8H, m), 1.46 – 1.24 (7H, m), 1.00 – 0.98 (6H, m), 0.89 (6H, td, *J* = 7.3, 1.3 Hz); δ_C (125 MHz, $CDCl_3$) 212.94, 94.68, 93.22, 82.66, 82.63, 40.93, 40.77, 37.90 (d), 37.79 (d), 25.78 (d), 24.64 (d), 23.12, 22.95 (d), 21.28, 13.90 (d); (ESI/MS) Calcd for *m/z* $C_{15}H_{30}FO_2^+$: 261.2 $[M+H]^+$; found 261.2.

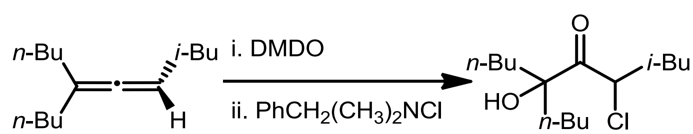

6-butyl-4-chloro-6-hydroxy-2-methyldecan-5-one (**S3.19**, Table 1, entry 5): The freshly prepared spirodiepoxide (see General Procedure for Spirodiepoxide Formation on pg 148), obtained from the oxidation of 17.3 mg of the allene (0.0830 mmol), was dissolved in THF (0.50 ml) and cooled to 0 ºC. Benzyltrimethylammonium chloride (32. mg, 0.170 mmol) was added to the reaction at 0 ºC. The reaction was allowed to warm to rt over 2 h. Upon completion of reaction as judged by TLC (2 h), the reaction was quenched with saturated aq. NH_4Cl (2.0 ml), extracted with Et_2O (3 x 5.0 ml), dried over anhydrous Na_2SO_4, filtered, concentrated and purified by FCC (4 % EtOAc/Hexanes) to obtain product (13.8 mg, 60 % yield) as a colorless oil.). IR ν_{max} (neat) /cm^{-1} 3513, 2958, 2932, 2872, 1720, 1467; δ_H (500 MHz, $CHCl_3$) 4.79 (1H, dd, *J*=

10.3, 3.9 Hz), 3.02 (1H, bs), 1.92-1.03 (15H, m), 0.99-0.98 (3H, d, *J*=6.6 Hz), 0.95-0.91 (3H, d, *J*= 6.6 Hz), 0.91-0.87 (6H, m); δc (125 MHz, $CHCl_3$) 209.03, 82.96, 54.49, 42.12, 38.83, 38.69, 25.80, 25.69, 24.96, 23.30, 23.13, 23.11, 21.30, 14.08, 14.07; (ESI/MS) Calcd for m/z $C_{15}H_{30}ClO_2^+$: 277.2 $[M+H]^+$; found 277.2.

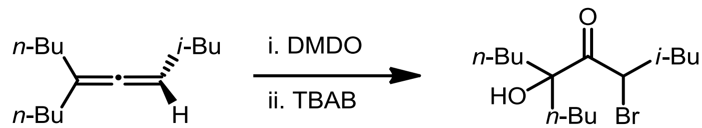

4-bromo-6-butyl-6-hydroxy-2-methyldecan-5-one (**S3.20**, Table 1, entry 6): The freshly prepared spirodiepoxide (see General Procedure for Spirodiepoxide Formation on pg 148), obtained from the oxidation of 17.3 mg of the allene (0.0830 mmol), was dissolved in THF (0.50 ml) and cooled to 0 ºC. Dry 1 M TBAB (0.17 mL, 0.170 mmol) was added to the reaction at 0 ºC. The reaction was allowed to warm to rt over 2 h. Upon completion of reaction as judged by TLC (2 h), the reaction was quenched with saturated aq. NH_4Cl (2.0 ml), extracted with Et_2O (3 x 5.0 ml), dried over anhydrous Na_2SO_4, filtered, concentrated and purified by FCC (4 % EtOAc/Hexane) to obtain product (13.3 mg, 50 % yield) as a colorless oil. IR ν_{max} (neat) /cm^{-1} 3506, 2957, 2932, 2872, 1712, 1467; δ_H (500 MHz, $CHCl_3$) 4.82 (1H, dd, *J*= 10.1, 4.5 Hz), 2.90 (1H, s), 1.98 (1H, ddd, *J* = 14.7, 10.1, 4.8 Hz), 1.88 – 1.26 (13H, m), 1.20 – 1.07 (1H, m), 0.99 – 0.98 (3H, d, *J*=6.6 Hz), 0.94 – 0.92 (3H, d, *J*= 6.61 Hz), 0.91 – 0.87 (6H, m); δc (125 MHz, $CHCl_3$) 208.77, 82.96, 44.85, 42.16, 39.07, 38.68, 25.88, 25.75, 23.15, 23.25, 23.12, 21.50, 14.11; (ESI/MS) Calcd for m/z $C_{15}H_{30}BrO_2^+$: 321.1 $[M+H]^+$; found 321.1.

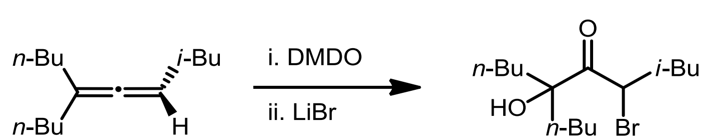

4-bromo-6-butyl-6-hydroxy-2-methyldecan-5-one (**S3.20**, Table 1, entry 7): The freshly prepared spirodiepoxide (see General Procedure for Spirodiepoxide Formation on pg 148), obtained from the oxidation of 1.30 g of the allene (6.24 mmol), was dissolved in THF (30. ml) and cooled to 0 ºC. To the spirodiepoxide in THF was added LiBr (1.63 g, 18.73 mmol). The reaction was allowed to warm to rt and stirred at rt for 4 h. Upon the completion of reaction as judged by TLC (4 h), the reaction mixture was diluted in water and the organic layer was extracted in Et_2O. The crude was purified by FCC (3 % EtOAc/Hexane) to obtain product (1.77 g, 88 % yield) as colorless oil.

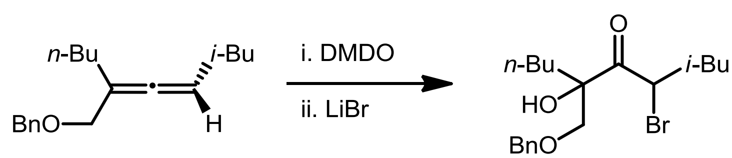

6-((benzyloxy)methyl)-4-bromo-6-hydroxy-2-methyldecan-5-one (**S3.21**, Table 1, entry 8): The solution of freshly prepared DMDO (see General Procedure for Spirodiepoxide Formation on pg 148) in $CHCl_3$ (0.20 M, 3.7 ml) was added to the allene (100.0 mg, 0.367 mmol) dropwise at −40 ºC. Upon the consumption of allene as judged by TLC (2 h), LiBr (318 mg, 3.67 mmol) was added to the reaction mixture. The reaction was allowed to warm to rt and stirred at rt for 2 h. Upon completion of the reaction as judged by TLC (2 h), the reaction mixture was diluted in water and the organic layer was extracted in CH_2Cl_2. The crude was purified by FCC (3 % EtOAc/Hexane) to obtain two diastereomers (1.4: 1) in a combined yield of 95 % (134 mg) as colorless oil. IR ν_{max} (neat) /cm^{-1} 3500, 2958, 2932, 2871, 1718, 1467, 1454, 1386, 1369; δ_H of major diastereomer (500 MHz, $CHCl_3$) 7.36 – 7.26 (5H, m), 5.04 (1H, dd, *J* = 9.4, 5.1 Hz), 4.56 – 4.46 (2H, m), 3.74 (1H, d, *J* = 9.0 Hz), 3.48 (1H, d, *J* = 9.0 Hz), 3.13 (1H, s), 1.87 –

1.76 (2H, m), 1.70 – 1.62 (2H, m), 1.38 – 1.25 (5H, m), 0.90 (3H, d, *J* = 6.6 Hz), 0.88 (3H, d, *J* = 7.1 Hz), 0.84 (3H, d, *J* = 6.5 Hz); δ_H of minor diastereomer (500 MHz, $CHCl_3$) 7.39 – 7.24 (5H, m), 4.87 (1H, dd, *J*= 9.9, 4.7 Hz), 4.53 (2H, s), 3.86 (1H, d, *J* = 9.4 Hz), 3.57 (1H, s), 3.44 (1H, d, *J* = 9.5 Hz), 1.95 (1H, ddd, *J* = 14.7, 9.9, 4.9 Hz), 1.80 (1H, dt, *J* = 19.9, 6.5 Hz), 1.71 – 1.56 (3H, m), 1.38 (1H, ddd, *J* = 19.3, 11.8, 4.8 Hz), 1.28 (2H, dd, *J* = 14.6, 7.3 Hz), 1.17 (1H, ddd, *J* = 14.4, 9.5, 4.1 Hz), 0.95 (3H, d, *J* = 6.6 Hz), 0.87 (6H, m); δ_C (125 MHz, $CHCl_3$) of major diastereomer 208.34, 137.45, 128.67, 128.17, 128.04, 82.59, 75.58, 73.99, 46.23, 41.93, 36.11, 26.13, 25.45, 23.16, 23.03, 21.55, 14.08; δ_C (125 MHz, $CHCl_3$) of minor diastereomer 207.69, 137.59, 128.63, 128.04, 127.89, 82.41, 74.43, 73.95, 45.13, 41.77, 35.99, 25.98, 25.29, 23.13, 21.47, 14.04; (ESI/MS) Calcd for *m/z* $C_{19}H_{30}BrO_3^+$: 385.1 $[M+Na]^+$; found 407.2, 409.1.

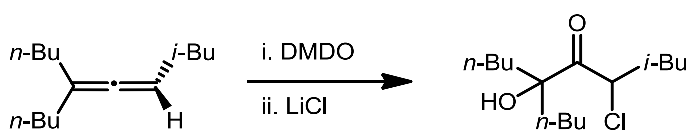

6-butyl-4-chloro-6-hydroxy-2-methyldecan-5-one (**S3.19**, Table 1, entry 9): The freshly prepared spirodiepoxide (see General Procedure for Spirodiepoxide Formation on pg 148), obtained from the oxidation of 100. mg of the allene (0.480 mmol), was dissolved in THF (10. ml) and cooled to 0 ºC. To the spirodiepoxide in THF was added LiCl (61.0 mg, 1.44 mmol). The reaction was allowed to warm to rt and stirred at rt for 4 h. Upon the completion of reaction as judged by TLC (4 h), the reaction mixture was diluted in water and the organic layer was extracted in Et_2O. The crude was purified by FCC (3 % EtOAc/Hexane) to obtain product (113 mg, 85 % yield) as colorless oil.

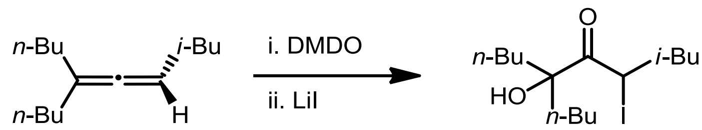

6-butyl-6-hydroxy-4-iodo-2-methyldecan-5-one (**S3.22**, Table 1, entry 10): The solution of freshly prepared DMDO (see General Procedure for Spirodiepoxide Formation on pg 148) in $CHCl_3$ (0.16 M, 3.0 ml) was added to the allene (50.0 mg, 0.240 mmol) dropwise at −40 ºC. The reaction was stirred under nitrogen for 30 min. Upon the consumption of allene as judged by TLC, LiI (321 mg, 2.40 mmol) was added to the reaction mixture. The reaction was allowed to warm to rt and stirred at rt for 2 h. Upon completion of the reaction as judged by TLC (2 h), the reaction mixture was diluted in water and the organic layer was extracted in CH_2Cl_2. The crude was purified by FCC (4 % EtOAc/Hexane) to obtain product (75.1 mg, 85 % yield) as colorless oil. IR ν_{max}(neat)/cm^{-1} 3507, 2956, 2871, 1699, 1466; δ_H (500 MHz, $CDCl_3$) 4.97 (1H, dd, J = 9.8, 5.1 Hz), 2.69 (1H, s), 2.01 (1H, ddd, J = 14.8, 9.9, 5.0 Hz), 1.86 – 1.59 (5H, m), 1.45 – 1.25 (7H, m), 1.18 (2H, qdd, J = 11.9, 7.1, 4.5 Hz), 1.00 (3H, d, J = 6.6 Hz), 0.93 – 0.86 (9H, m); δ_C (125 MHz, $CDCl_3$) 209.83, 82.97, 43.38, 39.46, 38.86, 27.99, 26.07, 25.91, 24.35, 23.15, 22.98, 21.60, 14.16, 14.15; (ESI/MS) Calcd for m/z $C_{15}H_{30}IO_2^+$: 369.1 $[M+H]^+$; found 369.1.

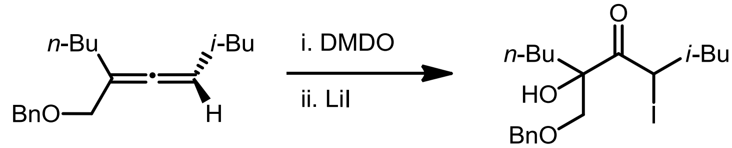

6-((benzyloxy)methyl)-6-hydroxy-4-iodo-2-methyldecan-5-one (**S3.23**, Table 1, entry 11): The solution of freshly prepared DMDO (see General Procedure for Spirodiepoxide Formation on pg 148) in $CHCl_3$ (0.20 M, 3.2 ml) was added to the allene

(86.0 mg, 0.316 mmol) dropwise at −40 ºC. Upon the consumption of allene as judged by TLC (2 h), LiI (423 mg, 3.16 mmol) was added to the reaction mixture. The reaction was allowed to warm to rt and stirred at rt for 2 h. Upon completion of the reaction as judged by TLC (2 h), the reaction mixture was diluted in water and the organic layer was extracted in CH_2Cl_2. The crude was purified by FCC (3 % EtOAc/Hexane) to obtain two diastereomers (1.3: 1) in a combined yield of 90 % (123 mg) as colorless oil. IR ν_{max} (neat) /cm^{-1} 3500, 3031, 2956, 2930, 2869, 1705, 1497, 1454, 1101; δ_H of major diastereomer (500 MHz, $CHCl_3$) 7.39-7.27 (5H, m), 5.15 (1H, dd, *J* = 9.1, 5.9 Hz), 4.51 (2H, d, *J* = 4.1 Hz), 3.71 (1H, d, *J* = 8.9 Hz), 3.50 (1H, d, *J* = 8.9 Hz), 3.10 (1H, s), 1.99 – 1.28 (9H, m), 0.98 – 0.87 (6H, m), 0.82 (3H, d, *J* = 6.5 Hz); δ_H of minor diastereomer (500 MHz, CDCl3) 7.40 – 7.30 (5H), 5.06 (1H, dd, *J*= 9.6, 5.5 Hz), 4.59 (2H, d, *J* = 1.8 Hz), 3.92 (1H, d, *J* = 9.3 Hz), 3.45 (1H, d, *J* = 2.3 Hz), 3.42 (1H, s), 2.00 (1H, ddd, *J* = 14.7, 9.6, 5.2 Hz), 1.77 – 1.13 (8H, m), 0.99 (3H, d, *J* = 6.6 Hz), 0.89 (6H, m); δ_C of major diastereomer (125 MHz, $CHCl_3$) 209.45, 137.43, 128.57, 128.18, 128.10, 82.39, 75.88, 74.02, 43.17, 36.58, 28.02, 25.74, 25.27, 23.15, 22.78, 21.66, 14.12; δ_C of minor diastereomer (125 MHz, $CHCl_3$) 208.80, 137.71, 128.61, 128.02, 127.95, 82.30, 74.11, 73.88, 43.06, 36.43, 27.97, 25.41, 24.59, 23.17, 22.91, 21.63, 14.07; (ESI/MS) Calcd for m/z $C_{19}H_{30}IO_3^+$: 433.1 [M+Na]$^+$; found 455.0.

Complex Nucleophile Addition (Table 2):

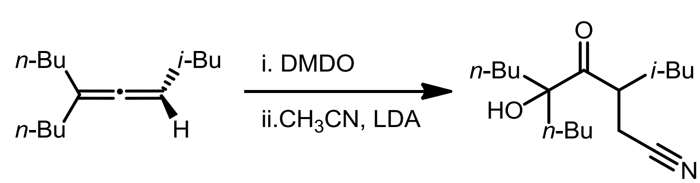

5-butyl-5-hydroxy-3-isobutyl-4-oxononanenitrile (**S3.25**, Table 2, entry 1): To a solution of diisopropylamine (35 µL, 0.250 mmol) in THF (0.50 ml) at −78 ºC was added 2.5 M *n*-BuLi (0.10 mL, 0.250 mmol) dropwise. The reaction mixture was stirred at −78 ºC for 45 min. Acetonitrile (13 µL, 0.250 mmol) was added to the above LDA solution at −78 ºC. The freshly prepared spirodiepoxide (see General Procedure for Spirodiepoxide Formation on pg 148), obtained from the oxidation of 17.3 mg of the allene (0.0830 mmol), was dissolved in THF (0.20 ml) and added to the above solution. The reaction was allowed to warm up to 0 ºC over 2 h. Upon the completion of reaction as judged by TLC (2 h), the reaction was quenched with saturated aq. NH_4Cl (2.0 ml), extracted with Et_2O (3 x 5.0 ml), dried over anhydrous Na_2SO_4, evaporated and purified by FCC (5 % EtOAc/Hexane) to obtain product (15.2 mg, 65 % yield) as colorless oil. IR ν_{max}(neat)/cm^{-1} 3488, 2958, 2932, 2872, 2252, 1709, 1467; δ_H (500 MHz, $CDCl_3$) 3.43 (1H, ddt, *J* = 9.3, 7.7, 4.7 Hz), 2.61 (1H, dd, *J* = 16.9, 7.5 Hz), 2.50 (1H, bs), 2.42 (1H, dd, *J* = 16.9, 5.1 Hz), 1.72 – 1.55 (6H, m), 1.41 – 1.27 (7H, m), 1.15 – 1.04 (2H, m), 0.96 (6H, dd, *J* = 6.5, 3.2 Hz), 0.90 (6H, t, *J* = 7.3 Hz); δ_C (125 MHz, $CDCl_3$) 214.4, 118.3, 82.7, 40.2, 40.0, 38.3, 38.0, 25.6, 25.5, 23.3, 22.9 (2), 18.6, 13.9; (ESI/MS) Calcd for *m/z* $C_{17}H_{32}NO_2^+$: 282.2 [M+H]$^+$; found 282.2.

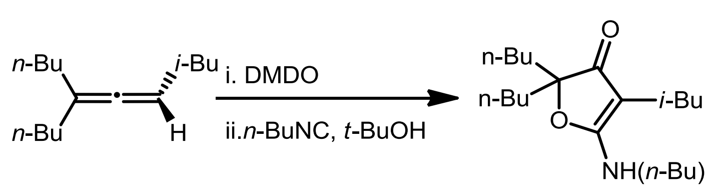

2,2-dibutyl-5-(butylamino)-4-isobutylfuran-3(2H)-one (**S3.9**, Table 2, entry 2): To the freshly prepared spirodiepoxide (see General Procedure for Spirodiepoxide Formation on pg 148), obtained from the oxidation of 128 mg of the allene (0.614 mmol), was added n-butyl isocyanide (0.64 ml, 6.14 mmol) followed by t-BuOH (2.5 ml) at rt. The reaction was stirred at rt for 48 h. Upon the completion of reaction as judged by TLC (48 h), the reaction mixture was diluted in water and the organic layer was extracted in CH_2Cl_2. The crude was purified by FCC (20 % EtOAc/Hexane) to obtain product (161 mg, 81 % yield) as colorless oil. IR ν_{max} (neat) /cm^{-1} 3211, 2956, 2932, 2871, 1561, 1467; δ_H (500 MHz, $CHCl_3$) 4.70 (1H, s), 3.37 (2H, dd, J = 13.2, 7.0 Hz), 1.91(3H, d, J=7.1 Hz), 1.84 – 1.65 (5H, m), 1.59 (3H, ddd, J = 14.7, 12.1, 5.8 Hz), 1.44 – 1.34 (2H, m), 1.34 – 1.10 (9H, m), 0.96 (3H, t, J=7.4 Hz), 0.90 – 0.83 (9H, m); δ_C (125 MHz, $CHCl_3$) 197.09, 176.24, 93.60, 91.34, 41.33, 36.22, 32.71, 30.18, 28.40, 25.32, 23.06, 22.74, 19.98, 14.21, 13.90; (ESI/MS) Calcd for m/z $C_{20}H_{38}NO_2^+$: 324.3 $[M+H]^+$; found 324.5.

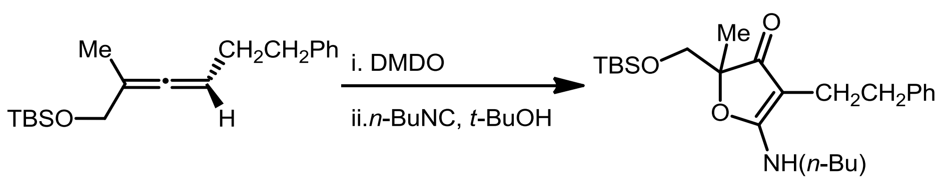

2,2-dibutyl-5-(butylamino)-4-isobutylfuran-3(2H)-one (**S3.26**, Table 2, entry 3): To the freshly prepared spirodiepoxide (see General Procedure for Spirodiepoxide Formation on pg 148), obtained from the oxidation of 143 mg of the allene (0.473 mmol), was added n-butyl isocyanide (1.5 ml, 14.2 mmol) followed by t-BuOH (1.9 ml) at rt. The reaction was stirred at rt for 5 d. Upon the completion of reaction as judged by TLC (5 d), the reaction mixture was diluted in water and the organic layer was extracted in CH_2Cl_2. The crude was purified by FCC (30 % EtOAc/Hexane) to obtain product (152 mg, 77 % yield) as colorless oil. IR ν_{max} (neat) /cm^{-1} 3215, 2930, 2857, 1741, 1713, 1556, 1454, 1365, 1255, 1095, 838; δ_H (500 MHz, $CHCl_3$) 7.30 – 7.25 (2H, m), 7.20 (3H, dd, J = 10.5, 4.5 Hz), 4.01 (1H, t, J = 5.7 Hz), 3.73 – 3.67 (2H, s), 3.09 – 2.96 (2H, m), 2.78 –

2.69 (2H, m), 2.44 – 2.29 (2H, m), 1.35 (3H, s), 1.29 – 1.15 (4H, m), 0.96 – 0.77 (12H, m), 0.04 (6H, d, J = 1.6 Hz); δ_C (125 MHz, $CHCl_3$) 195.30, 176.26, 143.09, 128.97, 128.73, 126.28, 91.21, 89.95, 66.58, 41.21, 35.47, 32.19, 25.99, 23.51, 19.88, 18.49, 13.82, -5.17, -5.22; (ESI/MS) Calcd for m/z $C_{24}H_{40}NO_3Si^+$: 418.3 $[M+H]^+$; found 418.3.

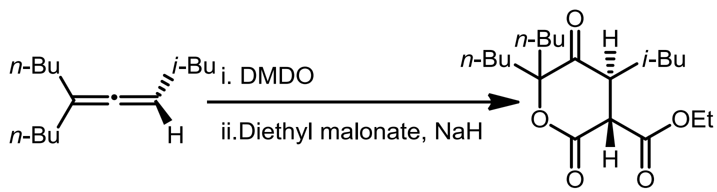

(3R,4S)-ethyl-6,6-dibutyl-4-isobutyl-2,5-dioxotetrahydro-2H-pyran-3-carboxylate (**S3.10**, Table 2, entry 4): To a solution of diethylmalonate (19 µL, 0.125 mmol) in THF (0.50 ml) at 0 ºC was added sodium hydride (5.0 mg, 60 % in mineral oil, 0.125 mol). The suspension was allowed to warm to rt over 30 min at which point it was cooled to 0 ºC. The freshly prepared spirodiepoxide (see General Procedure for Spirodiepoxide Formation on pg 148), obtained from the oxidation of 17.3 mg of the allene (0.0830 mmol), was dissolved in THF (0.20 ml) and added to the above solution. The reaction was allowed to warm to rt over 2 h. Upon the completion of reaction as judged by TLC (2 h), the reaction was quenched with ice cold H_2O (2.0 ml), extracted with Et_2O (3 x 5.0 ml), dried over anhydrous Na_2SO_4, evaporated and purified by FCC (4 % EtOAc/Hexane) to obtain two diastereomers (6:1) as an inseparable mixture in 45 % yield (13.2 mg) as colorless oil. IR ν_{max}(neat)/cm^{-1} 2959, 2930, 2872, 1735, 1467, 1370; δ_H (500 MHz, $CDCl_3$) 4.34 – 4.24 (2H, qd, J = 7.1, 2.2 Hz), 3.52 – 3.47 (1H, d, J = 12.9 Hz), 3.07 (1H, ddd, J = 11.7, 6.8, 2.9 Hz), 1.90 – 1.69 (6H, m), 1.48 – 1.38 (1H, m), 1.37 – 1.32 (3H, m), 1.32 – 1.23 (6H, m), 1.23 – 1.11 (2H, m), 0.93 – 0.86 (12H, m); δ_C (125 MHz, $CDCl_3$) 208.25, 206.88, 166.91, 166.62, 165.54, 165.12, 93.32, 93.04, 62.79, 62.64, 52.08, 51.93, 44.59, 44.19, 38.75, 38.53, 37.81, 37.43, 36.88, 34.07, 26.49, 25.87, 25.61, 25.44, 24.98, 23.28, 23.07, 22.94, 22.92, 22.91, 22.87, 22.23, 21.91, 14.26, 14.23, 14.09, 13.97; (ESI/MS) Calcd for *m/z* $C_{20}H_{35}O_5^+$: 355.2 $[M+H]^+$; found 355.2.

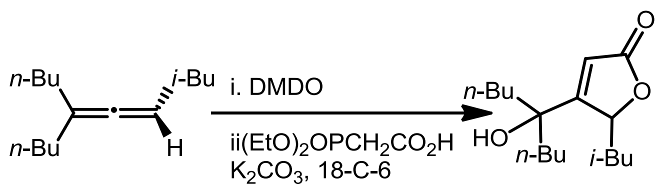

4-(5-hydroxynonan-5-yl)-5-isobutylfuran-2(5H)-one (**S3.11**, Table 2, entry 5): To a solution of diethylphosphonoacetic acid (27 µL, 0.166 mmol) in THF (1.0 ml) was added potassium carbonate (69.0 mg, 0.500 mmol) and 18-crown-6 (35 µL, 0.166 mmol). The reaction mixture was stirred for 1 h at rt. The freshly prepared spirodiepoxide (see General Procedure for Spirodiepoxide Formation on pg 148), obtained from the oxidation of 17.3 mg of the allene (0.0830 mmol), was dissolved in THF (0.20 ml) and added to above solution at rt. The reaction was stirred for 4 h at rt. Upon the completion of reaction as judged by TLC (4 h), the reaction was quenched with saturated aq. NH_4Cl (2.0 ml), extracted with Et_2O (3 x 5.0 ml), dried over anhydrous Na_2SO_4, evaporated and purified by FCC (4 % EtOAc/Hexane) to obtain product (16.6 mg, 71 % yield) as colorless oil. IR ν_{max} (neat) /cm^{-1} 3448, 2957, 2933, 2871, 1735, 1467; δ_H (400 MHz, $CDCl_3$) 5.77 (1H, d, *J* = 1.6 Hz), 5.05 (1H, dt, *J* = 10.9, 1.9 Hz), 2.05 – 1.89 (2H, m), 1.71 – 1.64 (4H, m), 1.41 – 1.12 (10H, m), 1.01 (3H, d, *J* = 6.3 Hz), 0.97 (3H, d, *J* = 6.3 Hz), 0.91 (6H, q, *J* = 7.1 Hz); δ_C (100 MHz, $CDCl_3$) 177.79, 172.77, 115.89, 82.62, 76.04, 42.47, 41.66, 41.23, 25.59, 25.35, 23.67, 22.86, 22.83, 21.04, 13.92, 13.91; (ESI/MS) *m/z* Calcd for $C_{17}H_{31}O_3^+$: 283.2 $[M+H]^+$; found 283.2.

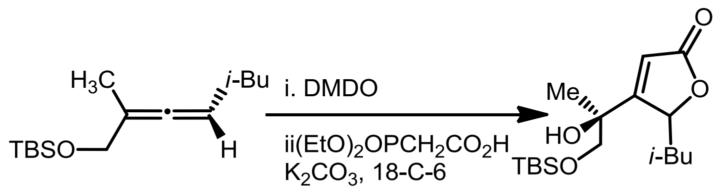

4-((S)-1-((tert-butyldimethylsilyl)oxy)-2-hydroxypropan-2-yl)-5-isobutylfuran-2(5H)-one (**S3.27**, Table 2, entry 6): Procedure same as Table3, entry 4 (48 mg of the allene used). Upon purification by FCC (15 % EtOAc/Hexanes) gave compound in 71 % (44.0 mg) yield as mixture of cis:trans isomers (1.6:1). The products were further separated by another column.

Major: IR ν_{max}(neat)/cm^{-1}: 3351, 3084, 3026, 1654, 1263, 1247; δ_H (500 MHz, $CDCl_3$) 5.68 (1H, d, J = 1.4 Hz), 5.03 (1H, dt, J = 10.9, 1.7 Hz), 3.59 (1H, d, J = 9.3 Hz), 3.45 (1H, d, J = 9.3 Hz), 2.85 (1H, s), 1.94 (2H, m), 1.34 (3H, s), 0.95 (3H, d, J = 6.4 Hz), 0.90 (3H, d, J = 6.4 Hz), 0.82 (9H, s), 0.03 (3H, s), 0.01 (3H, s); δ_C (125 MHz, $CDCl_3$) 177.30, 172.89, 115.08, 83.00, 73.12, 70.78, 42.85, 25.98, 25.81, 25.55, 23.88, 21.39, 18.43, -5.25, -5.27 ; (ESI/MS) Calcd for m/z $C_{17}H_{33}O_4Si^+$: 329.2 $[M+H]^+$; found 329.1.

Minor: IR ν_{max}(neat)/cm^{-1}: 3351, 3084, 3026, 1654, 1263, 1247; δ_H (500 MHz, $CDCl_3$) 5.89 (1H, s), 5.17 (1H, d, J = 7.4 Hz), 3.59 (1H, d, J = 9.7 Hz), 3.51 (1H, d, J = 9.7 Hz), 2.75 (1H, s), 2.04 – 1.95 (1H, m), 1.85 (1H, ddd, J = 12.6, 10.2, 2.2 Hz), 1.40 (3H, s), 1.02 (3H, d, J = 6.5 Hz), 0.95 (3H, d, J = 6.5 Hz), 0.90 (9H, s), 0.10 (6H, d, J = 2.6 Hz); δ_C (125 MHz, $CDCl_3$) 177.00, 172.81, 116.55, 82.10, 73.21, 69.67, 42.99, 26.01, 25.74, 23.90, 21.32, 18.45, -5.26, -5.28; (ESI/MS) Calcd for m/z $C_{17}H_{33}O_4Si^+$: 329.2 $[M+H]^+$; found 329.1.

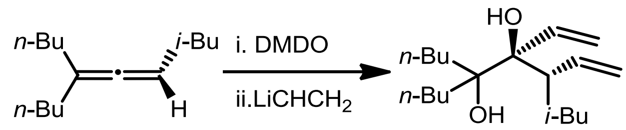

(4S,5S)-6-butyl-2-methyl-4,5-divinyldecane-5,6-diol (**S3.7**, Table 2, entry 7): The freshly prepared spirodiepoxide (see General Procedure for Spirodiepoxide Formation on pg 148), obtained from the oxidation of 17.3 mg of the allene (0.0830 mmol), was dissolved in THF (0.5 ml) and cooled to 0 ºC. To the above solution 2.8 M vinyllithium (0.12 mL, 0.333 mmol) was added dropwise at 0 ºC. The reaction mixture was allowed to warm to rt over 1 h. Upon the completion of reaction as judged by TLC (1 h), the reaction was quenched with saturated aq. NH_4Cl (2.0 ml), extracted with Et_2O (3 x 5.0 ml), dried over anhydrous Na_2SO_4, evaporated and purified by FCC (2 % EtOAc/Hexanes) to obtain product as a single isomer (20.0 mg, 81 % yield) as colorless oil. IR ν_{max}(neat)/cm^{-1} 3501, 3073, 2957, 2871, 1467, 922; δ_H (500 MHz, $CDCl_3$) 5.84 – 5.70 (2H, m), 5.38 (1H, dd, J = 17.1, 2.1 Hz), 5.24 – 5.17 (2H, m), 5.13 (1H, dd, J = 17.5, 1.9 Hz), 2.82 (1H, bs), 2.42 (1H, td, J = 10.6, 2.6 Hz), 2.01 (1H, bs), 1.69 (2H, m), 1.47 (3H, m), 1.39 – 1.18 (10 H, m), 0.98 – 0.76 (12 H, m); δ_C (100 MHz, $CDCl_3$) 141.10, 139.27, 117.62, 115.00, 81.42, 79.55, 47.56, 38.18, 35.69, 34.81, 26.60, 26.15, 24.79, 24.17, 23.65, 23.54, 20.78, 14.12, 14.05; (ESI/MS) Calcd for m/z $C_{19}H_{37}O_2^+$: 297.3 $[M+H]^+$; found 297.3.

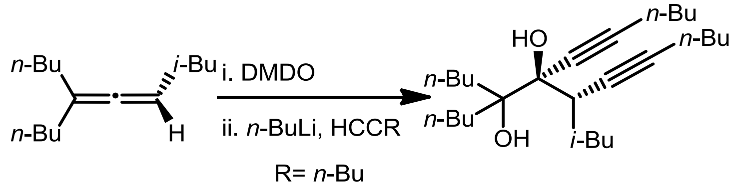

(6R,7S)-5-butyl-6-(hex-1-yn-1-yl)-7-isobutyltridec-8-yne-5,6-diol (**S3.6**, Table 2, entry 8): To a solution of 1-hexyne (38 µL, 0.330 mmol) in THF (0.50 ml) at −78 ºC was added 2.5 M *n*-BuLi (0.13 mL, 0.330 mmol) dropwise. The freshly prepared spirodiepoxide (see General Procedure for Spirodiepoxide Formation on pg 148), obtained from the oxidation of 17.3 mg of the allene (0.0830 mmol), was dissolved in THF (0.20 ml) and added to the above solution at −78 ºC. The mixture was allowed to warm to 0 ºC over 1 h. Upon the completion of the reaction as judged by TLC (1 h), the reaction was quenched with saturated aq. NH_4Cl (2.0 ml), extracted with Et_2O (3 x 5.0 ml), dried over anhydrous Na_2SO_4, evaporated and purified by FCC (2 % EtOAc/Hexanes) to obtain product as a single isomer (22.0 mg, 65 % yield) as colorless oil. IR ν_{max}(neat)/cm^{-1} 3501, 2957, 2871, 2234, 1685, 1467; δ_H (400 MHz, $CDCl_3$) 3.42 (1H, bs), 3.22 (1H, bs), 2.68 – 2.60 (1H, m), 2.23 – 2.16 (4H, m), 1.84 – 1.71 (7H, m), 1.50 – 1.30 (16H, m), 0.99 – 0.87 (18H, m); δ_C (100 MHz, $CDCl_3$) 87.78, 87.04, 80.84, 80.51, 79.91, 76.32, 39.97, 38.02, 36.27, 34.54, 30.84, 30.43, 27.13, 25.88, 25.71, 23.96, 23.56, 21.96, 21.93, 21.06, 18.43, 18.40, 14.14, 14.02, 13.51; (ESI/MS) *m/z* Calcd for $C_{27}H_{49}O_2^+$: 405.4 [M+H]$^+$; found 405.4.

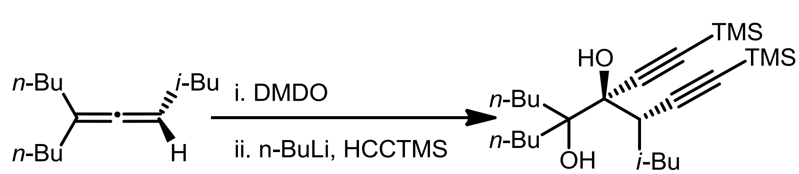

(4S,5R)-6-butyl-2-methyl-4,5-bis((trimethylsilyl)ethynyl)decane-5,6-diol (**S3.28**, Table 2, entry 9): To a solution of trimethylsilylacetylene (47 µL, 0.330 mmol) in THF (0.50 ml) at −78 ºC was added 2.5 M *n*-BuLi (0.13 mL, 0.330 mmol) dropwise. The freshly prepared spirodiepoxide (see General Procedure for Spirodiepoxide Formation on pg 148), obtained from the oxidation of 17.3 mg of the allene (0.0830 mmol), was dissolved in THF (0.20 ml) and added to above solution at −78 ºC. The mixture was allowed to warm to 0 ºC over 1 h until the completion of reaction as judged by TLC (1 h). The reaction was then quenched with saturated aq. NH_4Cl (2.0 ml), extracted with Et_2O (3 x 5.0 ml), dried over anhydrous Na_2SO_4, evaporated and purified by FCC (2 % EtOAc/Hexanes) to obtain product as a single isomer (23.6 mg, 65 % yield) as colorless oil. IR ν_{max}(neat)/cm^{-1} 3500, 2958, 2869, 2233, 1685, 1466; δ_H (400 MHz, $CDCl_3$) 3.55 (1H, s), 3.25 (1H, d, J = 0.7 Hz), 2.67 (1H, dd, J = 10.3, 3.5 Hz), 1.90 – 1.70 (6H, m), 1.55 – 1.25 (9H, m), 1.00 – 0.88 (12H, m), 0.16 (9H, s), 0.15 (9H, s); δ_C (100 MHz, $CDCl_3$) 108.09, 106.05, 92.22, 91.48, 79.96, 76.57, 39.66, 38.87, 36.27, 34.61, 27.42, 25.79, 25.74, 23.85, 23.60, 23.50, 21.22 14.12, 14.08, -0.11, -0.41; (ESI/MS) *m/z* Calcd for $C_{25}H_{49}O_2Si_2^+$: 437.3 [M+H]$^+$; found 437.3.

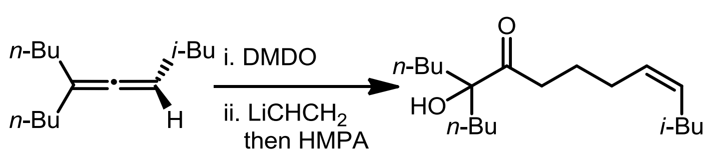

(Z)-5-butyl-5-hydroxy-13-methyltetradec-10-en-6-one (**S3.8**, Table 2, entry 10): The freshly prepared spirodiepoxide (see General Procedure for Spirodiepoxide Formation on pg 148), obtained from the oxidation of 17.3 mg of the allene (0.083 mmol), was dissolved in THF (0.50 ml) and cooled to 0 ºC. To above solution was added 2.8 M vinyllithium (0.12 mL, 0.333 mmol) dropwise at 0 ºC. The reaction mixture was allowed to warm to rt over 1 h. HMPA (0.29 mL, 1.66 mmol) was then added to the reaction mixture. The reaction was stirred at 0 ºC for another hour. Upon the completion of reaction as judged by TLC (1 h), the reaction was quenched with saturated aq. NH_4Cl

(2.0 ml), extracted with Et_2O (3 x 5.0 ml), dried over anhydrous Na_2SO_4, evaporated and purified by FCC (2 % EtOAc/Hexanes) to obtain product as a single isomer (15.0 mg, 61 % yield) as colorless oil. IR ν_{max}(neat)/cm^{-1} 3482, 3007, 2956, 2871, 1704, 1455, 1086; δ_H (500 MHz, $CDCl_3$) 5.47 – 5.34 (2H, m), 3.88 (1H, bs), 2.47 – 2.43 (2H, t, J = 7.5 Hz), 2.07 (2H, q, J = 7.3 Hz), 1.93 – 1.90 (2H, t, J = 6.9 Hz), 1.70 – 1.59 (8H, m), 1.42 – 1.23 (7H, m), 0.90 – 0.85 (12H, m); δ_C (125 MHz, $CDCl_3$) 214.45, 129.88, 129.12, 81.53, 38.73, 36.40, 35.36, 28.62, 26.67, 25.39, 23.43, 22.94, 22.34, 13.89; (ESI/MS) m/z Calcd for $C_{19}H_{37}O_2^+$: 297.3 $[M+H]^+$; found 297.3.

The cis configuration was confirmed by 1D NOESY.

7.4 Chapter 4: Facile Synthesis of Oxetan-3-ones from Allenes via Spirodiepoxides

Method A: General procedure for oxetan-3-one synthesis by nucleophilic addition/ intramolecular displacement (Table 1):

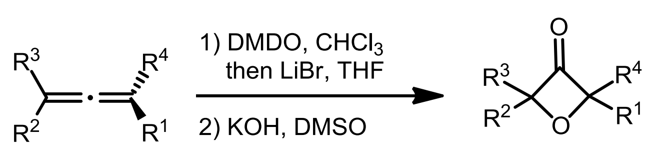

Dimethyldioxirane (DMDO) was prepared following a modified Murray procedure.[5] For photo of the set up for this procedure see Ref 6. The DMDO was extracted out of acetone and into $CHCl_3$ by known procedure.[7, 8]

To the allene was added $CHCl_3$ (0.10 M) and cooled to −20 ºC. To this was added solution of freshly prepared DMDO in $CHCl_3$ (~0.20 M, 2.50 equiv) dropwise. The reaction was stirred under nitrogen. Upon the complete consumption of allene as judged by TLC (1–2 h), the volatiles were removed under vacuum and the spirodiepoxide (SDE) was dissolved in THF (0.20 M) and cooled to 0 ºC. To the SDE in THF was added LiBr (1.10 equiv). The reaction was then allowed to warm to room temperature (rt). Upon the completion of reaction as judged by TLC (1–3 h), the reaction mixture was diluted in water and the organic layer was extracted in diethyl ether, dried over anhydrous Na_2SO_4, filtered and evaporated. The crude was dissolved in dimethyl sulfoxide (DMSO) (0.05 M). To the reaction mixture was added KOH (1.21 N, 1.10 equiv) at rt. Upon the completion of reaction as judged by TLC (5–10 min), the reaction was diluted with water and the organic layer was extracted in 1:1 solution of Hexane:diethyl ether, dried over anhydrous Na_2SO_4, filtered, evaporated and purified by FCC.

All the spectroscopic data for entry 4 match the published results for this known compound.[9]

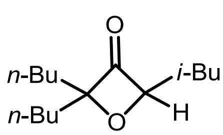

2,2-dibutyl-4-isobutyloxetan-3-one (**S4.8**, Table 1, entry 1 and Table 2, entry 2): Method A: 92 % (78.3 mg); Method B: 98 % (346.2 mg); IR ν_{max}(neat)/cm^{-1} 2957, 2933, 2871, 1811, 1467, 953; δ_H (500 MHz, $CDCl_3$) 5.21 (1H, dd, J = 8.8, 5.5 Hz), 1.87 – 1.58 (7H, m), 1.57 – 1.44 (2H, m), 1.39 – 1.24 (6H, m), 0.99 – 0.87 (12H, m); δ_C (125 MHz, $CDCl_3$) 210.22, 108.39, 96.07, 40.15, 35.49, 35.30, 26.10, 26.01, 25.28, 23.19, 23.15, 22.39, 14.11, 14.06; (ESI/MS) Calcd for m/z $[C_{15}H_{28}NaO_2]^+$: 263.2 $[M+Na]^+$; found 263.2.

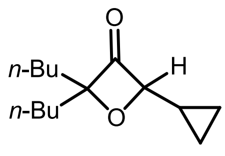 **2,2-dibutyl-4-cyclopropyloxetan-3-one** (**S4.13**, Table 1, entry 2 and Table 2, entry 3): Method A: 93 % (19.0 mg); Method B: 95 % (57.0 mg); IR ν_{max}(neat)/cm^{-1} 2957, 2932, 2871, 1812, 1466, 1024, 955; δ_H (400 MHz, CDCl3) 4.53 (1H, d, J = 8.8 Hz), 1.77 – 1.66 (4H, m), 1.56 – 1.42 (2H, m), 1.38 – 1.14 (6H, m), 0.96 – 0.84 (7H, m), 0.68 – 0.59 (2H, m), 0.46 – 0.35 (2H, m); δ_C (100 MHz, $CDCl_3$) 208.38, 107.76, 101.18, 34.84, 34.81, 25.72, 23.00, 22.94, 13.87, 13.84, 11.22, 2.57, 2.11; (ESI/MS) Calcd for *m/z* $[C_{14}H_{24}NaO_2]^+$: 247.2 $[M+Na]^+$; found 247.2.

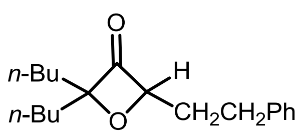 **2,2-dibutyl-4-phenethyloxetan-3-one** (**S4.14**, Table 1, entry 3 and Table 2, entry 4): Method A: 90 % (332.5 mg); Method B: 95 % (468.3 mg); IR ν_{max}(neat)/cm^{-1} 2956, 2934, 2863, 1808, 1455, 962; δ_H (500 MHz, $CDCl_3$) 7.30 (2H, ddd, *J* = 16.5, 7.5, 2.5 Hz), 7.22 (3H, tt, *J* = 16.5, 8.1 Hz), 5.16 (1H, dd, *J* = 8.5, 6.1 Hz), 2.87 – 2.71 (2H, m), 2.21 – 2.05 (2H, m), 1.82 – 1.70 (4H, m), 1.60 – 1.47 (2H, m), 1.41 – 1.23 (6H, m), 0.97 – 0.84 (6H, m); δ_C (125 MHz, $CDCl_3$) 209.56, 140.86, 128.73, 128.66, 126.41, 108.61, 95.91, 35.32, 35.19, 32.96, 31.09, 26.06, 26.00, 23.21, 23.18, 14.09, 14.07; (ESI/MS) Calcd for *m/z* $[C_{19}H_{29}O_2]^+$: 289.2 $[M+H]^+$; found 289.2.

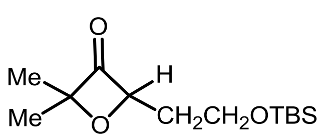 **4-(2-((*tert*-butyldimethylsilyl)oxy)ethyl)-2,2-dimethyloxetan-3-one** (**S4.15**, Table 1, entry 4 and Table 2, entry 5): Method A: 86 % (145.2 mg); Method B: 83 % (111.8 mg). The spectroscopic data match the published results.[9]

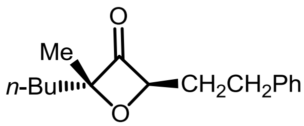

2-butyl-2-methyl-4-phenethyloxetan-3-one (**S4.16**, Table 1, entry 5): 45 % (134.5 mg as a 1.4:1 mixture of diastereomers); IR ν_{max}(neat)/cm^{-1} 2957, 2933, 2863, 1812, 1454, 1012, 975; (* indicates diastereomer signals) δ_H (500 MHz, $CDCl_3$) 7.34 – 7.30 (2H, m), 7.25 – 7.21 (3H, m), 5.32 – 5.25 (1H, m)*, 5.22 (1H, t, *J* = 6.9 Hz), 2.86 – 2.74 (2H, m), 2.22 – 2.07 (2H, m), 1.83 – 1.71 (2H, m), 1.60 – 1.52 (1H, m), 1.48 (3H, s), 1.43 – 1.32 (3H, m), 0.99 – 0.88 (3H, m); δ_C (125 MHz, $CDCl_3$) (Carbon count for the 1.4:1 mixture of diastereomers) 209.32, 209.12, 140.82, 140.78, 128.74, 128.68, 128.65, 126.43, 105.71, 105.38, 96.16, 95.29, 36.91, 36.74, 34.01, 32.89, 31.02, 26.09, 26.02, 23.13, 23.10, 22.09, 21.70, 14.09, 14.07; (ESI/MS) Calcd for *m/z* $[C_{16}H_{23}O_2]^+$: 247.1 $[M+H]^+$; found 247.1.

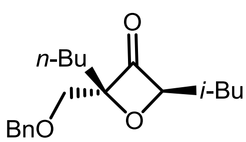

2-((benzyloxy)methyl)-2-butyl-4-isobutyloxetan-3-one (**S4.17**, Table 1, entry 6): 41 % (18.5 mg as a 1.1:1 mixture of diastereomers); IR ν_{max}(neat)/cm^{-1} 2956, 2930, 2870, 1815, 1466, 1454, 1112; δ_H (500 MHz, $CDCl_3$) (* indicates diastereomer signals) 7.37 – 7.25 (5H, m), 5.41 (1H, dd, *J* = 9.0, 5.4 Hz), 5.24 (1H, dd, *J* = 9.0, 5.5 Hz)*, 4.69 – 4.53 (2H, m), 3.70 – 3.55 (2H, m), 1.96 – 1.42 (6H, m), 1.37 – 1.27 (3H, m), 1.00 – 0.83 (9H, m); (Carbon count for the 1.1:1 mixture of diastereomers) δ_C (125 MHz, $CDCl_3$) 208.05, 207.85, 138.02, 138.00, 128.63, 128.55, 127.88, 127.83, 127.76, 127.67, 108.00, 107.61, 97.94, 97.76, 73.85, 73.79, 72.43, 71.71, 39.80, 38.91, 32.69, 32.58, 25.91, 25.68, 25.28, 25.00, 23.19, 23.17, 22.45, 22.35, 14.06, 14.00; (ESI/MS) Calcd for *m/z* $[C_{19}H_{29}O_3]^+$: 305.2 $[M+H]^+$; found 305.2.

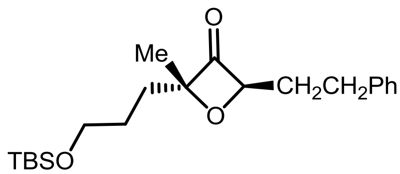

2-(3-((tert-butyldimethylsilyl)oxy)propyl)-2-methyl-4-phenethyloxetan-3-one (**S4.18**, Table 1, entry 7): 41 % (23.7 mg as a 1.4:1 mixture of diastereomers); IR ν_{max}(neat)/cm^{-1} 2954, 2928, 2857, 1813, 1471, 1255, 1101, 836; δ_H (500 MHz, $CDCl_3$) (* indicates diastereomer signals) 7.33 – 7.24 (2H, m), 7.21 (3H, t, *J* = 6.8 Hz), 5.26 (1H, dd, *J* = 7.8, 6.2 Hz)*, 5.20 (1H, dd, *J* = 7.8, 6.2 Hz), 3.68 – 3.56 (2H, m), 2.78 (2H, t, *J* = 7.9 Hz), 2.18 – 2.06 (2H, m), 1.87 – 1.70 (3H, m), 1.62 – 1.53 (1H, m), 1.48 (3H, s), 0.90 (9H, d, *J* = 5.0 Hz), 0.05 (6H, s); (Carbon count for the 1.4:1 mixture of diastereomers) δ_C (125 MHz, $CDCl_3$) 209.11, 208.91, 140.76, 140.73, 128.74, 128.73, 128.68, 128.66, 126.43, 105.42, 105.09, 96.16, 95.36, 63.00, 62.98, 33.99, 33.57, 33.45, 32.96, 30.99, 29.93, 27.29, 27.23, 26.16, 26.15, 22.05, 21.65, 18.53, 18.52, –5.07, –5.09; (ESI/MS) Calcd for *m/z* $[C_{21}H_{35}O_3Si]^+$: 363.2 $[M+H]^+$; found 363.2.

Method B: General procedure for oxetan-3-one synthesis by thermal rearrangement (Table 2 and Table 3):

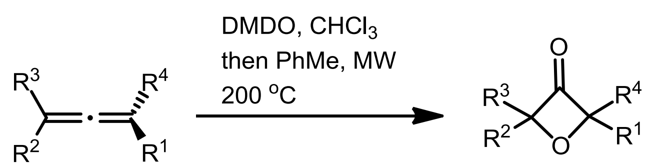

To the allene was added $CHCl_3$ (0.10 M) and cooled to −20 ºC. To this was added solution of freshly prepared DMDO in $CHCl_3$ (~0.20 M, 2.50 equiv) dropwise. The reaction was stirred under nitrogen. Upon the complete consumption of allene as judged by TLC (1–2 h), the volatiles were removed under vacuum. The spirodiepoxide (SDE) was dissolved in toluene and heated in microwave at 200 ºC for 1–1.5 h. The reaction was allowed to cool to room temperature and the crude was purified by FCC.

All the spectroscopic data for Table 2, entry 5 and Table 3, entry 4 match the published results for these known compounds.[9,10]

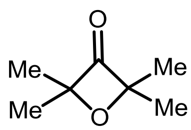

2,2,4,4-tetramethyloxetan-3-one (**S4.21**, Table 2, entry 1): 51 % (47.5 mg); IR ν_{max}(neat)/cm^{-1} 2977, 1819, 1459, 1366, 1111, 914; δ_H (500 MHz, $CDCl_3$) 1.38 (12H, s); δ_C (125 MHz, $CDCl_3$) 211.36, 99.18, 24.23; (ESI/MS) Calcd for *m/z* $[C_7H_{12}NaO_2]^+$: 151.1 $[M+Na]^+$; found 151.1.

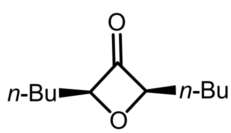

2,4-dibutyloxetan-3-one (**S4.22**, Table 2, entry 6): 88 % (267.6 mg as a 2:1 mixture of diastereomers); IR ν_{max}(neat)/cm^{-1} 2958, 2932, 2873, 1816, 1466, 954; δ_H of major diastereomer (500 MHz, $CHCl_3$) 5.29 (2H, t, J = 6.8 Hz), 1.85 – 1.73 (4H, m), 1.50 – 1.28 (8H, m), 0.96 – 0.85 (6H, m); δ_H of minor diastereomer (500 MHz, $CHCl_3$) 5.32 (2H, t, J = 6.8 Hz), 1.88 – 1.75 (4H, m), 1.53 – 1.17 (8H, m), 0.96 – 0.84 (6H, m); δ_C of major diastereomer (125 MHz, $CHCl_3$) 206.80, 99.75, 31.39, 26.89, 22.62, 14.01; δ_C of minor diastereomer (125 MHz, $CHCl_3$) 207.06, 100.29, 31.28, 26.68, 22.67, 14.05; (ESI/MS) Calcd for *m/z* $[C_{11}H_{21}O_2]^+$: 185.1 $[M+H]^+$; found 185.1.

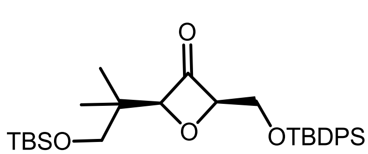

2-(1-((*tert*-butyldimethylsilyl)oxy)-2-methylpropan-2-yl)-4-(((*tert*-butyldiphenylsilyl)oxy)methyl)oxetan-3-one (**S4.23**, Table 2, entry 7): 73 %

(61.6 mg as a 8:1 mixture of diastereomers); IR ν_{max}(neat)/cm^{-1} 2956, 2929, 2857, 1816, 1472, 1112, 837; δ_H (400 MHz, $CHCl_3$) 7.78 – 7.65 (4H, m), 7.47 – 7.36 (6H, m), 5.40 (1H, ddd, *J* = 6.7, 3.8, 1.3 Hz), 5.18 (1H, d, *J* = 1.3 Hz), 3.99 (1H, dd, *J* = 11.9, 6.8 Hz), 3.90 (1H, dd, *J* = 12.0, 6.8 Hz), 3.40 (1H, d, *J* = 9.8 Hz), 3.30 (1H, d, *J* = 9.8 Hz), 1.04 (9H, s), 0.91 (3H, s), 0.90 (3H, s), 0.83 (9H, s), , –0.01 (3H, s), , –0.06 (3H, s); δ_C (125 MHz, $CHCl_3$) 203.36, 135.95, 135.82, 133.31, 133.19, 129.99, 129.97, 127.98, 127.94, 104.28, 99.90, 67.87, 62.82, 40.27, 26.96, 26.05, 20.60, 20.01, 19.38, 18.48, –5.35, –5.38; (ESI/MS) Calcd for *m/z* $[C_{30}H_{47}O_4Si_2]^+$: 527.2 $[M+H]^+$; found 527.2.

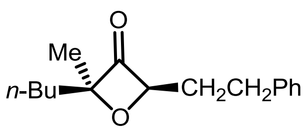

2-butyl-2-methyl-4-phenethyloxetan-3-one (**S4.24**, Table 2, entry 8): 82 % (358.8 mg as a 1.4:1 mixture of diastereomers); IR ν_{max}(neat)/cm^{-1} 2957, 2933, 2863, 1812, 1454, 1012, 975; (* indicates diastereomer signals) δ_H (500 MHz, $CDCl_3$) 7.33 – 7.27 (2H, m), 7.21 (3H, dd, *J* = 9.8, 3.4 Hz), 5.27 (1H, dd, *J* = 8.4, 6.0 Hz), 5.21 (1H, dd, *J* = 7.6, 6.3 Hz)*, 2.85 – 2.74 (2H, m), 2.12 – 2.06 (2H, m), 1.81 – 1.73 (2H, m), 1.56 – 1.51 (1H, m), 1.48 (3H, s), 1.42 – 1.31 (3H, m), 0.97 – 0.90 (3H, m); δ_C (125 MHz, $CDCl_3$) (Carbon count for the 1.4:1 mixture of diastereomers) 209.38, 209.18, 140.82, 140.78, 128.84, 128.75, 128.69, 128.67, 126.45, 105.72, 105.38, 96.15, 95.28, 36.91, 36.74, 34.02, 32.89, 31.03, 26.11, 26.03, 23.15, 23.12, 22.18, 21.72, 14.12, 14.11; (ESI/MS) Calcd for *m/z* $[C_{16}H_{23}O_2]^+$: 247.1 $[M+H]^+$; found 247.1.

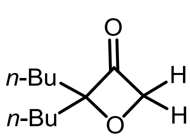

2,2-dibutyloxetan-3-one (**S4.31**, Table 3, entry 1): 70 % (423.1 mg); IR ν_{max}(neat)/cm^{-1} 2958, 2934, 2872, 1815, 1467, 956; ^{1}HNMR for the entry matches the published result;[11] δ_C (125 MHz, $CDCl_3$) 207.42, 112.93, 86.19, 35.23, 25.77, 23.15, 14.07; (ESI/MS) Calcd for *m/z* $[C_{11}H_{20}NaO_2]^+$: 207.1 $[M+Na]^+$; found 207.1.

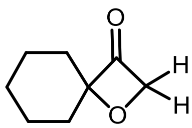
1-oxaspiro[3.5]nonan-3-one (**S4.32**, Table 3, entry 2): 68 % (181.3 mg); IR ν_{max}(neat)/cm^{-1} 2934, 2858, 1812, 1447, 968; δ_H (500 MHz, $CDCl_3$) 5.09 (2H, s), 1.92 – 1.85 (2H, m), 1.75 – 1.67 (2H, m), 1.66 – 1.59 (2H, m), 1.58 – 1.50 (2H, m), 1.44 – 1.36 (1H, m), 1.35 – 1.27 (1H, m); δ_C (125 MHz, $CDCl_3$) 206.38, 108.52, 84.52, 32.49, 24.87, 22.21; (ESI/MS) Calcd for *m/z* $[C_8H_{13}O_2]^+$: 141.1 $[M+H]^+$; found 141.1.

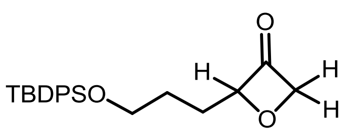
2-(3-((*tert*-butyldiphenylsilyl)oxy)propyl)oxetan-3-one (**S4.33**, Table 3, entry 3): 86 % (306.7 mg); IR ν_{max}(neat)/cm^{-1} 2930, 2857, 1819, 1427, 1111, 962; δ_H (500 MHz, $CDCl_3$) 7.68 (4H, d, *J* = 6.5 Hz), 7.47 – 7.36 (6H, m), 5.49 (1H, dd, *J* = 10.9, 6.6 Hz), 5.29 (1H, d, *J* = 14.6 Hz), 5.21 (1H, dd, *J* = 15.0, 4.3 Hz), 3.71 (2H, t, *J* = 6.1 Hz), 1.97 (2H, dd, *J* = 14.8, 7.5 Hz), 1.80 – 1.66 (2H, m), 1.06 (9H, s); δ_C (125 MHz, $CDCl_3$) 203.48, 135.78, 133.98, 129.86, 127.89, 103.88, 88.92, 63.37, 28.19, 27.29, 27.08, 19.45; (ESI/MS) Calcd for *m/z* $[C_{22}H_{29}O_3Si]^+$: 369.2 $[M+H]^+$; found 369.2.

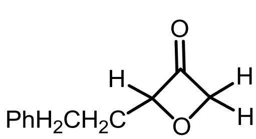
2-phenethyloxetan-3-one (**S4.34**, Table 3, entry 4): 65 % (60.0 mg). The spectroscopic data match the published results.[10]

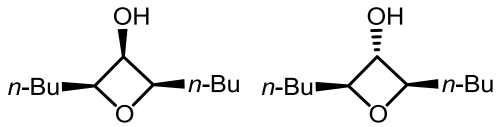

2,4-dibutyloxetan-3-ol (**S4.25** and **S4.26**): 67 % (33.2 mg as a 3.5:1 mixture of diastereomers); IR ν_{max}(neat)/cm^{-1} 3353, 2955, 2929, 2858, 1464, 1377, 1311, 1139, 1096, 953, 872, 734; δ_H (400 MHz, $CDCl_3$) (* indicates diastereomer signals) 4.69 (3H, dq, J = 10.7, 5.4 Hz), 4.35 (2H, dd, J = 12.5, 6.5 Hz)*, 3.87 (1H, t, J = 5.7 Hz)*, 2.09 (1H, bs), 1.75 – 1.57 (4H, m), 1.39 – 1.16 (8H, m), 0.95 – 0.84 (6H, m); (Carbon count for the 3.5:1 mixture of diastereomers) δ_C (100 MHz, $CDCl_3$) 87.41, 84.36, 75.87, 69.32, 35.20, 30.45, 26.94, 26.59, 22.89, 22.81, 14.20; (ESI/MS) Calcd for m/z $[C_{11}H_{22}O_2Na]^+$: 209.2 $[M+Na]^+$; found 209.2.

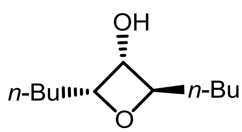

2,4-dibutyloxetan-3-ol (**S4.28**): 71 % (32.5 mg); IR ν_{max}(neat)/cm^{-1} 3353, 2955, 2929, 2858, 1464, 1377, 1311, 1139, 1096, 953, 872, 734; δ_H (500 MHz, $CDCl_3$) 4.61 (1H, dt, J = 8.2, 6.0 Hz), 4.45 (1H, dd, J = 11.8, 6.7 Hz), 4.41 – 4.36 (1H, m), 2.24 (1H, bs), 1.86 – 1.64 (4H, m), 1.45 – 1.23 (8H, m), 0.94 – 0.89 (6H, m); δ_C (125 MHz, $CDCl_3$) 89.58, 83.96, 71.77, 34.85, 29.77, 27.18, 26.77, 22.97, 22.84, 14.24, 14.21; (ESI/MS) Calcd for m/z $[C_{11}H_{22}O_2Na]^+$: 209.2 $[M+Na]^+$; found 209.2.

General Computational Details: Electronic structure calculations, based on density functional theory (DFT), were carried out with the Gaussian 03 suite[12] of programs. We utilized the B3LYP functional[13] with 6-31g(d,p) basis sets.[14] The transition state was verified by observing the nature of the negative imaginary frequency.

2,2,5,5-tetramethyl-1,4-dioxaspiro[2.2]pentane (S4.43)

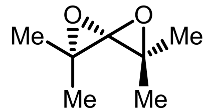

Standard orientation:

Center Number	Atomic Number	Atomic Type	Coordinates (Angstroms) X	Y	Z
1	6	0	1.399167	−0.077275	0.091819
2	8	0	0.757917	0.943205	0.976280
3	6	0	0.000016	0.310110	0.000038
4	6	0	−1.399138	−0.077111	−0.091892
5	8	0	−0.757928	0.944015	−0.975685
6	6	0	−2.387567	0.505573	0.891122
7	1	0	−3.322681	0.765986	0.383858
8	1	0	−2.619726	−0.224677	1.674015
9	1	0	−1.980983	1.402073	1.362784
10	6	0	−1.812088	−1.337063	−0.816927
11	1	0	−2.006063	−2.145984	−0.104207
12	1	0	−2.731912	−1.163195	−1.386006
13	1	0	−1.034101	−1.661938	−1.511472
14	6	0	2.387573	0.506259	−0.890779
15	1	0	3.322870	0.765890	−0.383447
16	1	0	2.619381	−0.223086	−1.674611
17	1	0	1.980989	1.403401	−1.361214
18	6	0	1.812073	−1.337665	0.816080
19	1	0	2.007704	−2.145780	0.102901
20	1	0	2.730950	−1.163507	1.386604
21	1	0	1.033437	−1.663910	1.509267

Zero-point correction= 0.178202 (Hartree/Particle)
Thermal correction to Energy= 0.188740
Thermal correction to Enthalpy= 0.189685
Thermal correction to Gibbs Free Energy= 0.143397
Sum of electronic and zero-point Energies= −424.192772
Sum of electronic and thermal Energies= −424.182234
Sum of electronic and thermal Enthalpies= −424.181289
Sum of electronic and thermal Free Energies= −424.227577

Low frequencies --- −7.0924 −6.7738 −0.0003 0.0003 0.0008 9.3697
E(RB+HF−LYP) = −424.370974020

Transition State (S4.44)

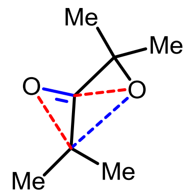

Standard orientation:

Center Number	Atomic Number	Atomic Type	Coordinates (Angstroms) X	Y	Z
1	6	0	1.349021	0.139906	−0.020684
2	8	0	0.314248	−1.432203	−1.046924
3	6	0	0.040591	−0.416846	−0.349507
4	6	0	−1.254585	0.128428	0.128228
5	8	0	−0.597806	−0.392944	1.270275
6	6	0	−2.466014	−0.684122	−0.316797
7	1	0	−3.260919	−0.592683	0.430702
8	1	0	−2.851151	−0.323407	−1.277117
9	1	0	−2.198229	−1.736475	−0.418537
10	6	0	−1.533090	1.625317	0.200867
11	1	0	−1.820009	2.041295	−0.771440
12	1	0	−2.357939	1.799178	0.900758
13	1	0	−0.666982	2.169441	0.586445
14	6	0	2.298499	−0.701420	0.751326
15	1	0	3.227605	−0.874864	0.193831
16	1	0	2.579005	−0.130926	1.648542
17	1	0	1.845342	−1.644689	1.045439
18	6	0	1.859812	1.384586	−0.652913
19	1	0	2.720996	1.800348	−0.123173
20	1	0	2.204003	1.101080	−1.659819
21	1	0	1.081335	2.137786	−0.785546

Zero-point correction= 0.174848 (Hartree/Particle)
Thermal correction to Energy= 0.185673
Thermal correction to Enthalpy= 0.186618
Thermal correction to Gibbs Free Energy= 0.139517
Sum of electronic and zero-point Energies= −424.137067
Sum of electronic and thermal Energies= −424.126242
Sum of electronic and thermal Enthalpies= −424.125297
Sum of electronic and thermal Free Energies= −424.172398

Imaginary frequency = −390.2285
E(RB+HF-LYP) = −424.311915029

2,2,4,4-tetramethyloxetan-3-one (S4.21)

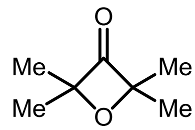

Standard orientation:

Center Number	Atomic Number	Atomic Type	Coordinates (Angstroms) X	Y	Z
1	6	0	1.076698	0.000753	−0.198935
2	8	0	−0.000113	−0.006886	2.101628
3	6	0	−0.000049	−0.002252	0.899180
4	6	0	−1.076545	0.000765	−0.199094
5	8	0	−0.000089	0.003861	−1.192549
6	6	0	−1.921426	1.270038	−0.274269
7	1	0	−2.475406	1.290363	−1.218328
8	1	0	−2.638615	1.299894	0.551718
9	1	0	−1.297577	2.166067	−0.225343
10	6	0	−1.920798	−1.268470	−0.280931
11	1	0	−2.638289	−1.302724	0.544638
12	1	0	−2.474422	−1.284343	−1.225278
13	1	0	−1.296674	−2.164526	−0.236119
14	6	0	1.921454	1.270061	−0.274009
15	1	0	2.639132	1.299630	0.551570
16	1	0	2.474903	1.290803	−1.218374
17	1	0	1.297659	2.166087	−0.224314
18	6	0	1.920880	−1.268473	−0.281125
19	1	0	2.474369	−1.284097	−1.225559
20	1	0	2.638474	−1.302932	0.544342
21	1	0	1.296778	−2.164549	−0.236487

Zero-point correction= 0.178735 (Hartree/Particle)
Thermal correction to Energy= 0.189320
Thermal correction to Enthalpy= 0.190264
Thermal correction to Gibbs Free Energy= 0.143811
Sum of electronic and zero-point Energies= −424.235426
Sum of electronic and thermal Energies= −424.224841
Sum of electronic and thermal Enthalpies= −424.223897
Sum of electronic and thermal Free Energies= −424.270350

Low frequencies--- −12.4322 −5.7461 −4.3006 −0.0002 0.0006 0.0009
E(RB+HF-LYP) = −424.414160631

Key bond lengths [Å] for the proposed transition state and calculated SDE

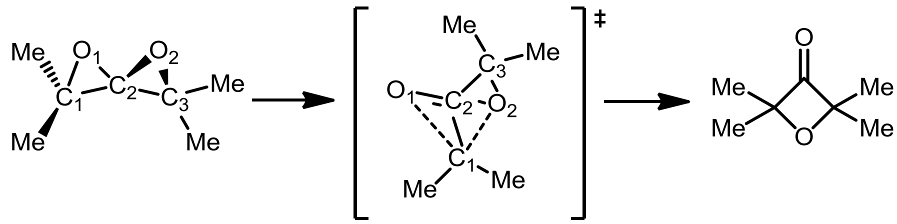

	C1-O1	C1-C2	C2-O1	C2-O2	C2-C3	C3-O2
SDE	1.495	1.455	1.389	1.389	1.455	1.495
TS	2.144	1.459	1.262	1.741	1.484	1.417

7.5 Chapter 5: Spirodiepoxide Based Cascade in the Studies towards the Synthesis of Pectenotoxin 4 (PTX4)

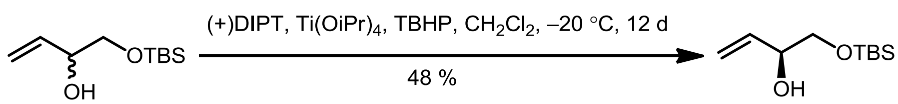

S5.108 **S5.109**

A suspension of 4 Å MS (4.50 g, activated by a gentle flame under vacuum) in CH_2Cl_2 (175 ml) was cooled to −20 °C. L-diisopropyl tartrate (4.97 ml, 23.7 mmol) and Ti(O-*i*Pr)$_4$ (5.86 ml, 19.8 mmol) were added and the reaction mixture was stirred at −20 °C for 30 min. A solution of allylic alcohol **S5.108**[15] (4.00 g, 19.8 mmol) in CH_2Cl_2 (25.0 ml) was added at −20 °C and the reaction mixture was stirred at −20 °C for 30 min. To the reaction mixture at −20 °C was added a 5.5 M solution of *tert*-Butyl hydroperoxide (TBHP) in decane (7.20 ml, 39.6 mmol) and the reaction mixture was aged at −20 °C. After 12 d at −20 °C, H_2O (35.0 ml) was added and the reaction was allowed to warm to rt. A solution of 30% aq. NaOH/NaCl (35.0 ml) was added to the reaction mixture at rt. After 1 h at rt, the reaction mixture was filtered through a pad of Celite and washed with CH_2Cl_2 (4 x 50.0 ml). The CH_2Cl_2 layer was separated and the aqueous layer was extracted with CH_2Cl_2 (2 x 85.0 ml). The CH_2Cl_2 layers were combined, dried over Na_2SO_4, filtered, concentrated and purified by FCC (10% EtOAc/Hexane) to obtain

S5.109 (1.92 g, 48 % yield) as clear colorless oil. Mosher ester analysis of 5 revealed a >95% ee. $[\alpha]_D$ − 4.5 (c = 0.01 g/ml, $CHCl_3$); IR ν_{max}(neat)/cm^{-1}: 3445, 2860, 1645, 1455, 1104, 927, 738, 698; δ_H (500 MHz, $CDCl_3$) 5.81 (1H, ddd, *J* = 17.2, 10.6, 5.7 Hz), 5.34 (1H, dt, *J* = 17.3, 1.5 Hz), 5.19 (1H, dt, *J* = 10.6, 1.4 Hz), 4.20 – 4.14 (1H, m), 3.66 (1H, dd, *J* = 10.0, 3.7 Hz), 3.45 (1H, dd, *J* = 10.0, 7.7 Hz), 2.54 (1H, d, *J* = 3.5 Hz), 0.91 (9H, s), 0.08 (6H, s); δ_C (125 MHz, $CDCl_3$) 136.87, 116.68, 73.23, 67.18, 26.09, 18.53, −5.12, −5.15; (ESI/MS) Calcd for *m/z* $[C_{10}H_{22}O_2Si+Na]^+$: 225.1 $[M+Na]^+$; found 225.1.

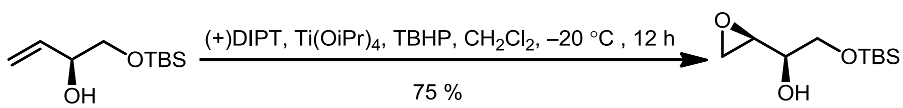

S5.109 **S5.110**

A suspension of 4 Å MS (1.68 g, activated by a gentle flame under vacuum) in CH_2Cl_2 (65.0 ml) was cooled to −20 °C. L-diisopropyl tartrate (1.85 ml, 8.83 mmol) and $Ti(O\text{-}i\text{Pr})_4$ (2.16 ml, 7.36 mmol) were added and the reaction mixture was stirred at −20 °C for 30 min. A solution of allylic alcohol **S5.109** (1.49 g, 7.36 mmol) in CH_2Cl_2 (10.0 ml) was added at −20 °C and the reaction mixture was stirred at that temperature for 30 min. To the reaction mixture at −20 °C was added a 5.5 M solution of TBHP in decane (4.00 ml, 22.1 mmol) and the reaction mixture was aged at −20 °C for 12 h. After 12 h at −20 °C, H_2O (13.0 ml) was added and the reaction mixture was allowed to warm to rt. A solution of 30% aq. NaOH/NaCl (13.0 ml) was added to the reaction mixture at rt and stirred for 1 h. The reaction mixture was then filtered through a pad of Celite and washed with CH_2Cl_2 (4 x 25.0 ml). The CH_2Cl_2 layer was separated and the aqueous layer was extracted with CH_2Cl_2 (2 x 50.0 ml). The CH_2Cl_2 layers were combined, dried over Na_2SO_4, filtered, concentrated and purified by FCC (7% EtOAc/Hexane) to obtain **S5.110**

(1.21 g, 75 % yield) as clear colorless oil. Mosher ester analysis of **S5.110** revealed a diastereomeric ratio of 3:1.

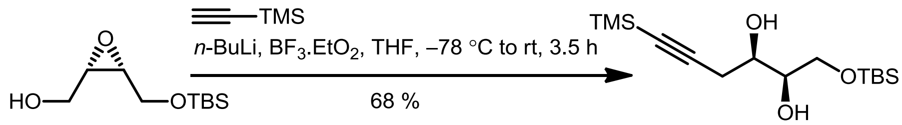

S5.112 **S5.113**

To a solution of trimethylsilylacetylene (3.69 ml, 26.1 mmol) in dry THF (50.0 ml) was added a 1.6 M solution of *n*-BuLi in THF (16.3 ml, 26.1 mmol) dropwise at −78 °C. After stirring the reaction mixture at −78 °C for 1 h, **S5.112**[16] (1.42 g, 6.51 mmol) in THF (2.00 ml) was added followed by $BF_3.EtO_2$ (3.86 ml, 31.3 mmol). The reaction mixture was stirred at −78 °C for 20 min and at rt for 3 h. Upon completion of the reaction, as judged by TLC, saturated solution of NH_4Cl (5.00 ml) and H_2O (10.0 ml) were added. The organic layer was separated and the aqueous layer was extracted with EtOAc (2 x 20.0 ml). The organic layers were combined, dried over Na_2SO_4, filtered, concentrated and purified by FCC (5% EtOAc/Hexane) to obtain **S5.113** (1.40 g, 68 % yield) as clear colorless oil. IR *v*max (neat)/cm-^{1} 3417, 2956, 2928, 2857, 2176, 1471, 1408, 1361, 1250, 1117, 840, 777; δ_H (500 MHz, $CDCl_3$) 3.87 – 3.78 (2H, m), 3.77 – 3.69 (2H, m), 2.88 (1H, d, J = 4.1 Hz), 2.60 (1H, dd, J = 10.5, 6.3 Hz), 2.54 (2H, dd, J = 8.6, 6.6 Hz), 0.91 (9H, s), 0.15 (9H, s), 0.09 (6H, s); δ_C (125 MHz, $CDCl_3$) 103.15, 87.41, 71.78, 71.03, 65.99, 26.07, 25.30, 18.44, 0.28, 0.26, −5.21, −5.24; (ESI/MS) Calcd for *m*/*z* $[C_{15}H_{32}O_3Si_2+Na]^+$: 339.2 $[M+Na]^+$; found 339.2.

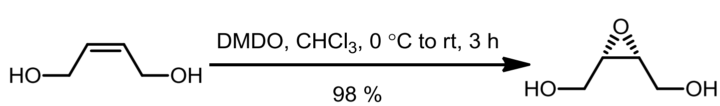

S5.116 **S5.117**

To a solution of DMDO[5-8] in $CHCl_3$ (0.20 M, 300 ml) was added **S5.116** (4.49 ml, 54.6 mmol) at 0 °C. The reaction was slowly warmed to rt over 30 min. Upon completion of reaction as judged by TLC (2.5 h), the reaction mixture was concentrated and purified by FCC (10 % MeOH/CH_2Cl_2) to obtain **S5.117** (5.57 g, 98 % yield) as white solid. The spectroscopic data for **S5.117** match the published data.[17]

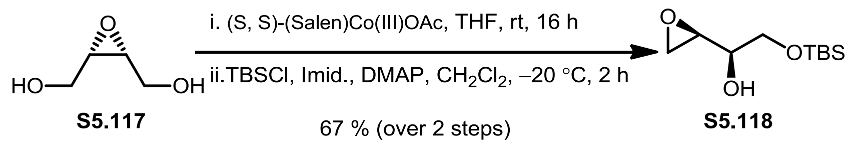

S5.117 **S5.118**

To **S5.117** (3.17 g, 30.5 mmol) was added (S, S)-(Salen)Co(III)OAc[18] (810 mg, 1.22 mmol) and THF (15.0 ml) at rt. The reaction was stirred vigorously under air at rt until ~ 75 % conversion of starting material was observed by ^{1}H NMR (16 h). The solvent was then removed via rotary evaporation and dry CH_2Cl_2 (30.0 ml) was added. To the reaction was added imidazole (2.59 g, 38.1 mmol), DMAP (465 mg, 3.81 mmol) and TBSCl (5.74 g, 38.1 mmol) at −20 °C. Upon completion of the reaction, as judged by TLC (2 h), MeOH (2.00 ml) was added followed by H_2O (10.0 ml). The CH_2Cl_2 layer was separated and the aqueous layer was extracted with CH_2Cl_2 (2 x 50.0 ml). The CH_2Cl_2 layers were combined, dried over Na_2SO_4, filtered, evaporated and purified by FCC (30 % EtOAc/Hexane) to obtain **S5.118** (4.46 g, 67 % yield) as colorless oil. Mosher ester analysis of **S5.118** revealed a >95% ee. $[\alpha]_D$ −9.62 (c = 0.01, $CHCl_3$); IR ν_{max}(neat)/cm^{-1}: 3434, 2929, 2857, 1472, 1254, 1111, 837, 777; δ_H (500 MHz, $CDCl_3$) 3.72 (2H, d, J = 5.7 Hz), 3.63 (1H, qd, J = 5.9, 4.1 Hz), 3.11 (1H, td, J = 4.0, 2.8 Hz), 2.79 (1H, dd, J = 6.3, 2.9 Hz), 2.76 (1H, dd, J = 5.1, 2.8 Hz), 2.25 (1H, d, J = 6.4 Hz, 1H), 0.91 (s, 9H), 0.09 (s, 6H); δ_C (125 MHz, $CDCl_3$) 70.99, 64.86, 52.72, 44.12, 26.05, 18.48, −5.21, −5.23; (ESI/MS) Calcd for m/z $[C_{10}H_{22}O_3Si+Na]^+$: 241.2 $[M+Na]^+$; found 241.1.

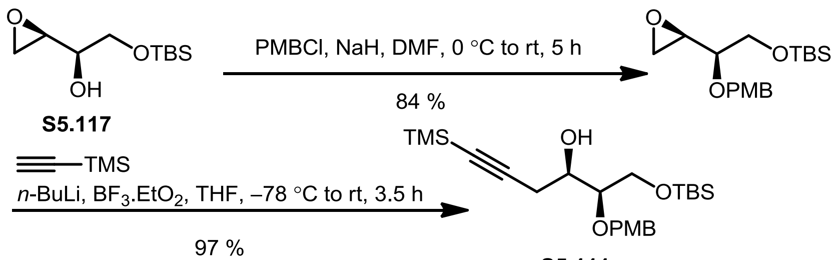

S5.117

S5.111

To a solution of **S5.117** (4.00 g, 18.3 mmol) in dry DMF (75.0 ml) at 0 °C was added sodium hydride (2.93 g, 60 %, 73.2 mmol) portion-wise. The reaction mixture was allowed to warm to rt over 30 min and then cooled back to 0 °C. To the reaction mixture at 0 °C was added *p*-methoxybenzyl chloride (2.73 ml, 20.1 mmol). The reaction mixture was slowly warmed to room temperature and stirred at rt for 4.5 h. Upon completion of the reaction, as judged by TLC, the reaction was quenched with ice cold H_2O (10.0 ml), extracted with Et_2O (5 x 50.0 ml), dried over anhydrous Na_2SO_4, filtered, evaporated and purified by FCC (5 % EtOAc/Hexane) to obtain the fully protected diol (5.20 g, 84 % yield) as colorless oil. $[\alpha]_D$ +3.26 (c = 0.01, $CHCl_3$); IR ν_{max}(neat)/cm^{-1}: 2928, 2856, 1612, 1513, 1463, 1249, 1097, 836, 777; δ_H (500 MHz, $CDCl_3$) 7.30 (2H, dd, J = 8.6, 1.9 Hz), 6.88 (2H, dd, J = 8.6, 2.2 Hz), 4.75 (1H, d, J = 11.5 Hz), 4.59 (1H, d, J = 11.5 Hz), 3.81 (3H, s), 3.76 (1H, ddd, J = 10.4, 5.4, 2.3 Hz), 3.70 (1H, ddd, J = 10.4, 6.9, 2.4 Hz), 3.21 – 3.16 (1H, m), 3.07 (1H, ddd, J = 6.7, 4.6, 2.5 Hz), 2.80 (1H, td, J = 5.0, 2.4 Hz), 2.64 (1H, dt, J = 5.1, 2.5 Hz), 0.89 (9H, s), 0.05 (6H, s); δ_C (125 MHz, $CDCl_3$) 159.41, 130.72, 129.65, 113.97, 80.57, 71.97, 63.65, 55.51, 53.61, 43.72, 26.06, 18.45, −5.22, −5.27; (ESI/MS) Calcd for m/z $C_{18}H_{31}O_4Si^+$: 339.2 $[M+H]^+$; found 339.2.

To a solution of trimethylsilylacetylene (2.97 ml, 21.0 mmol) in dry THF (50.0 ml) was added a 2.5 M solution of *n*-BuLi in THF (8.80 ml, 22.0mmol) dropwise at −78 °C. After stirring the reaction mixture at −78 °C for 30 min, a solution of differentially protected diol (3.55 g, 10.5 mmol) in THF (5.00 ml) was added dropwise followed by $BF_3.EtO_2$ (2.59 ml, 21.0 mmol). Stirring was continued at −78 °C for 30 min and slowly warmed to rt. The reaction was stirred at rt for 2.5 h. Upon completion of the reaction, as judged by TLC, saturated solution of NH_4Cl (5.00 ml) and H_2O (5.00 ml) were added. The organic layer was separated and the aqueous layer was extracted with EtOAc (2 x 20.0 ml). The organic layers were combined, dried over Na_2SO_4, filtered, evaporated and purified by FCC (5% EtOAc/Hexane) to obtain **S5.111** (4.45 g, 97 % yield) as clear colorless oil. $[\alpha]_D$ −47.24 (c = 0.01, $CHCl_3$); IR *v*max (neat)/cm^{-1} 3453, 2955, 2928, 2856, 2175, 1613, 1514, 1463, 1249, 1091, 1038, 842, 776; δ_H (500 MHz, $CDCl_3$) 7.30 – 7.25 (2H, m), 6.90 – 6.86 (2H, m), 4.70 (1H, d, *J* = 11.2 Hz), 4.55 (1H, d, *J* = 11.2 Hz), 3.86 (1H, qd, *J* = 6.9, 2.7 Hz), 3.83 – 3.78 (4H, m), 3.74 (1H, dd, *J* = 10.6, 5.1 Hz), 3.62 (1H, td, *J* = 5.7, 2.7 Hz), 2.59 (1H, d, *J* = 6.8 Hz), 2.52 (2H, d, *J* = 6.5 Hz), 0.90 (9H, s), 0.15 (9H, s), 0.07 (6H, s); δ_C (125 MHz, $CDCl_3$) 159.58, 130.58, 129.89, 114.06, 103.69, 86.95, 78.99, 73.20, 70.53, 63.12, 55.49, 26.10, 25.43, 18.44, 0.30, −5.19, −5.22; (ESI/MS) Calcd for *m/z* $[C_{23}H_{40}O_4Si_2+Na]^+$: 459.2 $[M+Na]^+$; found 459.5.

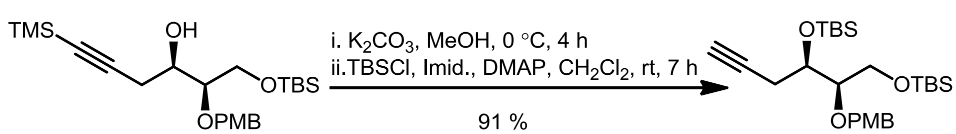

S5.111 **S5.105**

To the solution of **S5.111** (2.50 g, 5.72 mmol) in MeOH (10.0 ml) at 0 °C was added K_2CO_3 (3.95 g, 28.6 mmol). The reaction mixture was allowed to warm to rt over

30 min. The reaction was stirred at rt for 3.5 h. Upon complete consumption of **S5.111**, as judged by TLC, solvents were removed and the crude was dissolved in CH_2Cl_2 (20.0 ml). To the reaction was added imidazole (1.17 g, 17.2 mmol), DMAP (69.8 mg, 0.572 mmol) and TBSCl (2.59 g, 17.2 mmol) at rt. The reaction mixture was stirred at rt for 7 h. Upon completion of the reaction, as judged by TLC, MeOH (2.00 ml) was added followed by H_2O (10.0 ml). The CH_2Cl_2 layer was separated and the aqueous layer was extracted with CH_2Cl_2 (2 x 50.0 ml). The CH_2Cl_2 layers were combined, dried over Na_2SO_4, filtered, evaporated and purified by FCC (2% EtOAc/Hexane) to obtain **S5.105** (2.49 g, 91% yield) as colorless oil. $[\alpha]_D$ −3.75 (c = 0.01, $CHCl_3$); IR *v*max (neat)/cm-[1] 3312, 2953, 2929, 2856, 2100, 1612, 1513, 1471, 1463, 1250, 1101, 1038, 837, 777; δ_H (500 MHz, $CDCl_3$) 7.29 (2H, d, *J* = 8.4 Hz), 6.87 (2H, dd, *J* = 6.7, 1.9 Hz), 4.68 (1H, d, *J* = 11.6 Hz), 4.58 (1H, d, *J* = 11.6 Hz), 3.93 (1H, ddd, *J* = 6.8, 5.8, 3.9 Hz), 3.80 (3H, s), 3.78 (1H, d, *J* = 4.5 Hz), 3.65 (1H, dd, *J* = 10.6, 6.5 Hz), 3.53 (1H, dt, *J* = 6.5, 4.3 Hz), 2.60 (1H, ddd, *J* = 16.7, 5.8, 2.7 Hz), 2.26 (1H, ddd, *J* = 16.7, 6.9, 2.6 Hz) 1.92 (1H, dd, *J* = 3.5, 1.8 Hz), 0.88 (18H, dd, *J* = 4.5, 2.9 Hz), 0.07 (3H, s), 0.03 (9H, s); δ_C (125 MHz, $CDCl_3$) 159.40, 131.38, 129.73, 113.96, 82.63, 81.01, 73.09, 71.45, 69.91, 62.71, 55.58, 26.19, 26.16, 23.26, 18.51, 18.40, −4.22, −4.48, −5.05, −5.12; (ESI/MS) Calcd for *m/z* $C_{26}H_{47}O_4Si_2^+$: 479.2 $[M+H]^+$; found 479.2

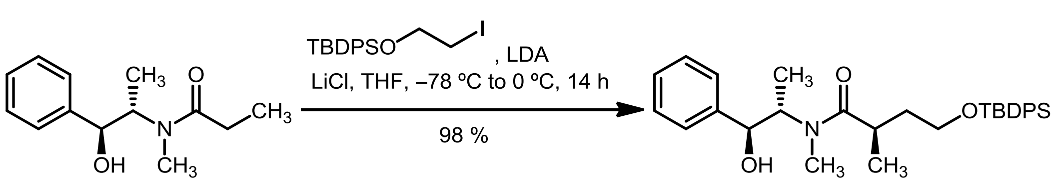

S5.119 **S5.121**

A suspension of LiCl (2.83 g, 66.7 mmol, activated by a gentle flame under vacuum) and *i*-Pr_2NH (3.57 ml, 25.3 mmol) in THF (14.0 ml) was cooled to −78 °C. To the above suspension was added a 1.6 M solution of *n*-BuLi in THF (14.8 ml, 23.7 mmol) dropwise at −78 °C. The reaction mixture was warmed to 0 °C and stirred for 30 min and then cooled back to −78 °C. To the reaction mixture at −78 °C was added cooled solution of **S5.119** (2.50 g, 11.3 mmol) in THF (35.0 ml). The reaction mixture was stirred at −78 °C for 1 h, at 0 °C for 15 min, at rt for 5 min and then cooled back to 0 °C. To the reaction mixture at 0 °C was added *t*-butyl(2-iodoethoxy)diphenylsilane)[19] (6.94 g, 16.9 mmol). The reaction mixture was stirred at 0 °C for 12 h. The reaction was quenched with sat. aq. NH_4Cl (10.0 ml) and the aqueous phase extracted with EtOAc (2 x 30.0 ml). The combined organic layers were dried over Na_2SO_4, filtered, evaporated and purified by FCC (40 % EtOAc/Hexane) to obtain **S5.121** (5.58 g, 98 % yield) as colorless oil. IR *v*max (neat)/cm-^{1} 3371, 2931, 2856, 1618, 1471, 1427, 1101, 1084, 907, 777; δ_H (500 MHz, $CDCl_3$) (* indicates rotamer signals) 7.68* (4H, dd, *J* = 16.1, 8.8 Hz), 7.62 (4H, ddd, *J* = 6.6, 3.8, 1.4 Hz), 7.45 – 7.21 (11H, m), 4.64 – 4.53 (1H, m), 4.43 (1H, s), 3.76 – 3.71 (m, 1H), 3.69 – 3.62 (1H, m), 3.61 – 3.53 (1H, m), 3.17* (1H, dd, *J* = 13.3, 6.6 Hz), 2.99 (1H, dq, *J* = 13.2, 6.6 Hz), 2.87 (3H, s), 2.31* (3H, s), 2.22* (1H, td, *J* = 13.1, 6.5 Hz), 1.83 (1H, dt, *J* = 11.7, 6.5 Hz), 1.63 – 1.57* (1H, m), 1.56 – 1.47 (1H, m), 1.10 (3H, d, *J* = 6.8 Hz), 1.06 (3H, d, *J* = 7.9 Hz), 1.04 – 0.98 (9H, m); δ_C (125 MHz, $CDCl_3$) 179.15, 177.83*, 142.79, 141.29*, 135.72, 133.95, 129.91, 128.87*, 128.54, 127.90, 127.80*, 126.52, 76.75, 75.66*, 62.17*, 61.64, 58.19, 36.93, 36.63*, 32.84, 27.21, 27.11, 19.50, 17.59*, 17.08, 15.67*, 14.69; (ESI/MS) Calcd for *m/z* $C_{31}H_{42}NO_3Si^+$: 504.3 $[M+H]^+$; found 504.3.

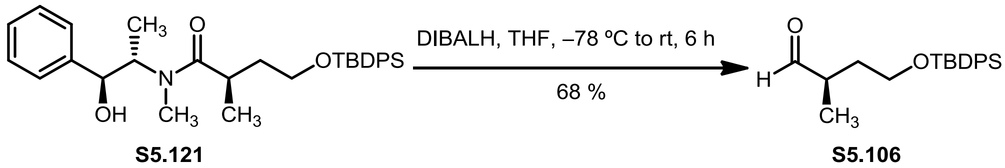

To the solution of **S5.121** (3.52 g, 6.99 mmol) in THF (100 ml) at −78 °C was added a 1.0 M solution of DIBALH in hexane (10.48 ml, 10.48 mmol) dropwise at −78 °C. The reaction mixture was slowly warmed to room temperature and stirred for 6 h. The reaction was quenched by the addition of sat. aq. Rochelle salt (50.0 ml), the CH_2Cl_2 layer was separated, dried over Na_2SO_4, filtered, evaporated and purified by FCC (5% EtOAc/Hexane) to obtain **S5.106** (1.62 g, 68 % yield) as colorless oil. All the spectroscopic data for **S5.106** matched the published data.[20]

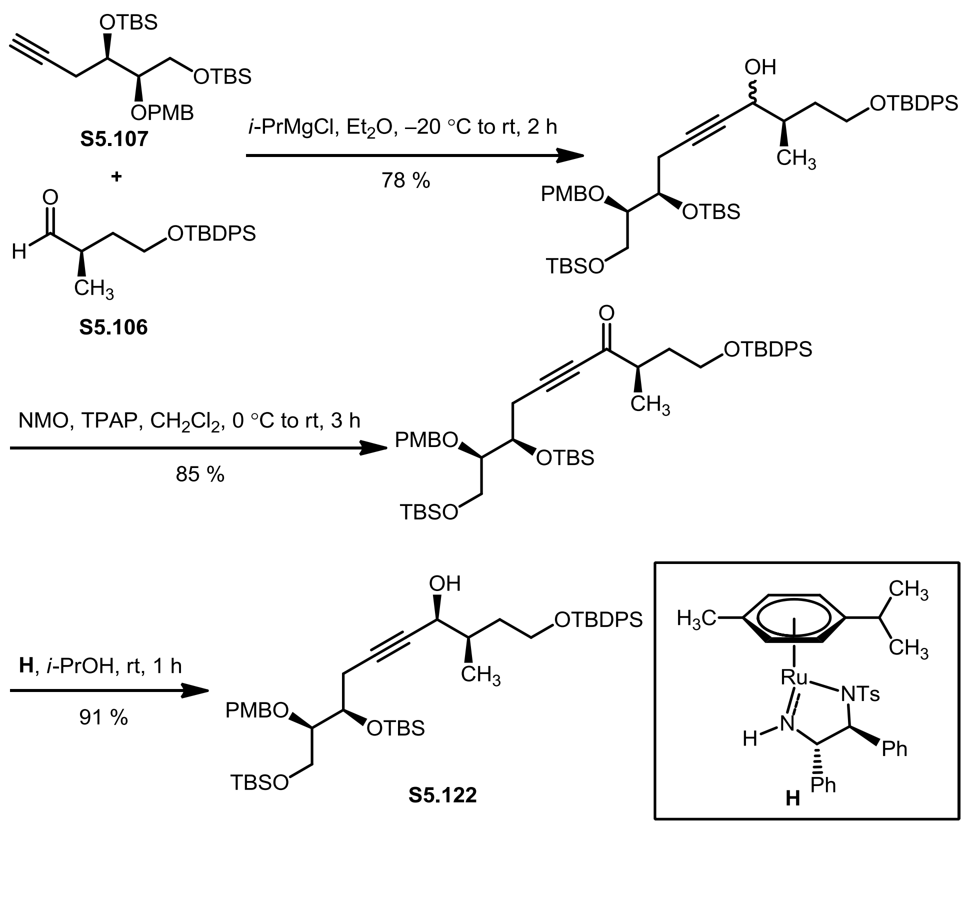

To a solution of **S5.105** (1.47 g, 3.08 mmol) in dry Et_2O (28.0 ml) at −20°C was added 2.0 M solution of *i*-PrMgCl in Et_2O (1.54 ml, 3.08 mmol) dropwise. The reaction mixture was warmed to 0°C. After stirring at 0°C for 30 min, the reaction mixture was cooled to −20°C and to it was added solution of **S5.106** (300 mg, 0.881 mmol) in dry Et_2O (20.0 ml). The reaction was slowly warmed to rt over 30 min and stirred at rt for 1.5 h. The reaction was quenched with sat. aq. NH_4Cl (10.0 ml), organic layer was extracted with Et_2O (5 x 50.0 ml), dried over anhydrous Na_2SO_4, filtered, evaporated and purified by FCC (5 % EtOAc/Hexane) to obtain the propargyl alcohol (562 mg, 78% yield) as colorless oil (refer compound **S5.122** for spectroscopic data).

To the suspension of 4 Å MS (50 mg, activated by a gentle flame under vacuum) in CH_2Cl_2 (25.0 ml) at 0°C was added the propargyl alcohol (500 mg, 0.610 mmol) in CH_2Cl_2 (1.50 ml) followed by NMO (108 mg, 0.921 mmol) and TPAP (11 mg, 0.0310 mmol). The reaction mixture was slowly warmed to rt and stirred for 3 h. Upon completion of reaction, as judged by TLC, the reaction mixture was filtered, concentrated and purified by FCC (4 % EtOAc/Hexane) to obtain the alkynone (424 mg, 85% yield) as colorless oil. $[\alpha]_D$ +6.80 (c = 0.01, $CHCl_3$); IR *v*max (neat)/cm^{-1} 2953, 2929, 2211, 1672, 1612, 1513, 1471, 1428, 1361, 1248, 1105, 834, 700; δ_H (500 MHz, $CDCl_3$) 7.69 – 7.59 (4H, m), 7.44 – 7.31 (6H, m), 7.30 – 7.21 (2H, d, *J* = 8.4 Hz), 6.85 (2H, d, *J* = 8.5 Hz), 4.67 (1H, d, *J* = 11.6 Hz), 4.54 (1H, d, *J* = 11.6 Hz), 3.96 (1H, dt, *J* = 6.9, 5.1 Hz), 3.83 – 3.72 (4H, m), 3.70 – 3.62 (3H, m), 3.47 (1H, dt, *J* = 6.2, 4.1 Hz), 2.77 (2H, ddd, *J* = 13.3, 12.3, 6.0 Hz), 2.46 (1H, dd, *J* = 17.2, 7.0 Hz), 2.16 – 2.06 (1H, m), 1.63 – 1.53 (1H, m), 1.14 (3H, d, *J* = 7.0 Hz), 1.04 (9H, s), 0.87 (18H, dd, *J* = 11.0, 9.8 Hz) 0.03 (12 H, ddd, *J* = 10.3, 9.0, 2.3 Hz); δ_C (125 MHz, $CDCl_3$) 191.58, 159.41, 135.77, 133.96, 130.99, 129.82, 129.66, 127.86, 113.97, 92.84, 81.35, 80.95, 72.92, 70.98, 62.38, 61.62, 55.49, 45.35, 35.23, 27.05, 26.12, 26.03, 23.81, 19.40, 18.44, 18.25, 16.15, −4.40, −4.52, −5.13, −5.17; (ESI/MS) Calcd for *m/z* $[C_{47}H_{72}O_6Si_3+Na]^+$: 839.4 $[M+Na]^+$; found 839.4.

Noyori catalyst (2.5 mol %) was prepared according to the general procedure.[21] To the prepared catalyst was added dry isopropanol (20.0 ml) at rt. Upon complete dissolution of the catalyst, alkynone (420 mg, 0.514 mmol) in dry isopropanol (10.0 ml) was added in 0.50 ml portions over a 30 min period at rt. Upon completion of the reaction, as judged by TLC, the isopropanol was evaporated and purified by FCC (5 % EtOAc/Hexane) to obtain **S5.122** (383 mg, 91%) as colorless oil. $[\alpha]_D$ −24.00 (c = 0.01, $CHCl_3$); IR *v*max (neat)/cm^{-1} 3417, 2953, 2929, 2987, 2197, 1612, 1513, 1471, 1427, 1389, 1361, 1250, 1109, 1037, 1005, 835, 777; δ_H (500 MHz, $CDCl_3$) 7.67 (4H, dtd, *J* = 8.0, 3.2, 1.5 Hz), 7.44 – 7.31 (6H, m), 7.30 – 7.21 (2H, d, *J* = 8.5 Hz), 6.85 (2H, d, *J* = 8.6 Hz), 4.67 (1H, d, *J* = 11.6 Hz), 4.57 (1H, dd, *J* = 11.6, 3.5 Hz), 4.26 (1H, m), 3.92 (1H, ddd, *J* = 15.4, 7.9, 5.0 Hz), 3.81 – 3.72 (5H, m), 3.72 – 3.61 (3H, m), 3.47 (1H, m), 2.65 (1H, m), 2.39 – 2.25 (1H, m), 1.98 – 1.85 (2H, m), 1.75 – 1.43 (1H, m); 1.05 (9H, d, *J* = 1.5 Hz), 0.96 (3H, t, *J* = 6.4 Hz), 0.88 (18H, d, *J* = 2.8 Hz), 0.07 (3H, d, *J* = 4.1 Hz), 0.04 – −0.08 (9H, d, *J* = 2.6 Hz); δ_C (125 MHz, $CDCl_3$) 159.31, 135.79, 133.96, 131.33, 129.92, 129.57, 127.92 113.89, 83.89, 81.58, 80.96, 73.03, 71.48, 67.16, 62.02, 62.67, 55.50, 37.85, 35.57, 27.06, 26.14, 26.11, 23.52, 19.39, 18.45, 18.34, 16.38, −4.24, −4.49, −5.09, −5.15; (ESI/MS) Calcd for *m/z* $[C_{47}H_{74}O_6Si_3+Na]^+$: 841.4 $[M+Na]^+$; found 841.5.

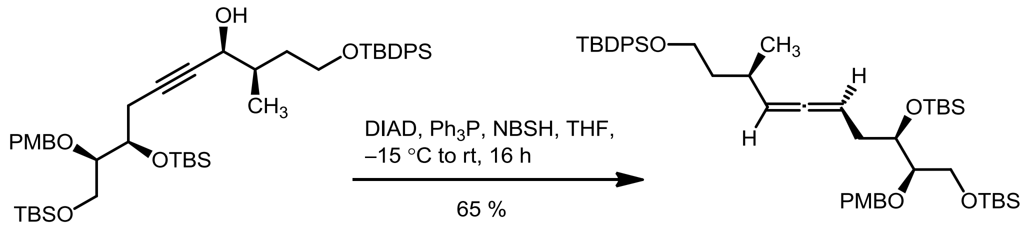

S5.122 **S5.60**

To the solution of Ph_3P (320 mg, 1.22 mmol) in THF (2.0 ml) at −15°C was added DIAD (0.240 ml, 1.22 mmol) and stirred for 15 min. After 15 min at −15°C, **S5.122** (500 mg, 0.610 mmol) in THF (1.5 ml) was added, followed 10 min later by NBSH (265 mg, 1.22 mmol). The reaction mixture was stirred at −15°C for 3 h and then slowly warmed to rt. The reaction mixture was stirred at rt for 13 h. Upon completion of reaction, as judged by TLC, the reaction mixture was concentrated and purified by FCC (2% EtOAc/Hexane) to obtain **S5.60** (319 mg, 65% yield) as colorless oil. $[\alpha]_D$ +23.34 (c = 0.01, $CHCl_3$); IR *v*max (neat)/cm^{-1} 2997, 2928, 1959, 1612, 1513, 1471, 1427, 1388, 1360, 1249, 1109, 1039, 835, 776, 702; δ_H (500 MHz, $CDCl_3$) 7.71 – 7.64 (4H, m), 7.46 – 7.34 (6H, m), 7.30 – 7.21 (2H, m), 6.85 (2H, d, *J* = 8.6 Hz), 5.05 (2H, ddt, *J* = 12.7, 6.2, 4.9 Hz), 4.67 (1H, d, *J* = 11.6 Hz), 4.58 (1H, dd, *J* = 11.6, 2.1 Hz), 3.85 – 3.76 (5H, m), 3.75 – 3.64 (3H, m), 3.47 – 3.40 (1H, m), 2.43 – 2.32 (2H, m), 2.08 – 1.98 (1H, m), 1.60 (2H, dtdd, *J* = 34.0, 26.9, 13.4, 6.6 Hz), 1.04 (9H, s), 0.99 (3H, dd, *J* = 6.8, 4.1 Hz), 0.90 (18H, dd, *J* = 10.7, 3.0 Hz), 0.07 – −0.04 (12H, m); δ_C (125 MHz, $CDCl_3$) 203.81, 159.23, 135.78, 134.28, 131.58, 129.72, 129.54, 127.81, 113.83, 96.70, 89.00, 81.84, 81.77, 72.75, 63.13, 62.25, 55.49, 40.16, 33.07, 30.18, 27.10, 26.15, 20.85, 19.45, 18.46, 18.33, −4.28, −4.36, −5.08, −5.15; (ESI/MS) Calcd for *m/z* $[C_{47}H_{74}O_5Si_3 + Na]^+$: 825.4 $[M+Na]^+$; found 825.5

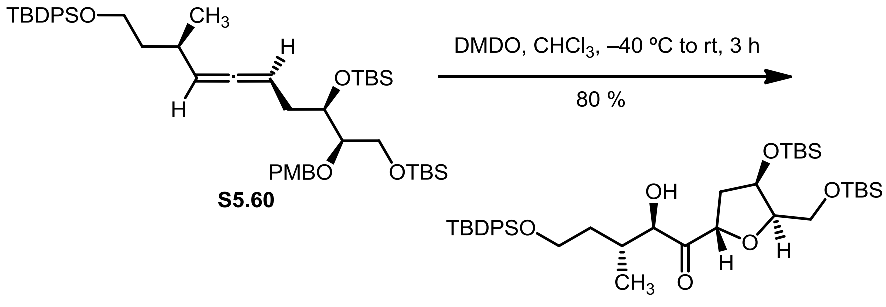

To the solution of allene **S5.60** (50 mg, 0.062 mmol) in $CHCl_3$ (1.0 ml) was added a 0.32 M solution of DMDO in $CHCl_3$ (0.69 ml, 0.22 mmol) dropwise at −40°C. The reaction was slowly allowed to warm to room temperature over the course of 3 h. Upon completion of reaction, as judged by TLC, the solvent was evaporated and the crude was purified by FCC (3% EtOAc/Hexane) to obtain the cyclized product **S5.123** (35.5 mg, 80 % yield, 3:2 dr) as colorless oil. IR *v*max (neat)/cm-[1] 3499, 2929, 2855, 1731, 1471, 1427, 1389, 1361, 1256, 1110, 1037, 1005, 836, 777; δ_H (300 MHz, $CDCl_3$) 7.67 – 7.56 (4H, m), 7.42 – 7.28 (6H, m), 4.71 (1H, t, *J* = 8.1 Hz), 4.50 (1H, s), 4.31 – 4.25 (1H, m), 3.83 – 3.52 (5H, m), 3.24 (1H, s), 2.51 (1H, dd, *J* = 11.9, 5.6 Hz), 2.36 – 2.25 (1H, m), 2.16 – 2.09 (1H, m), 2.03 – 1.94 (1H, m), 1.33 – 1.25 (1H, m), 1.05 – 0.91 (9H, m), 0.90 – 0.81 (18H, m), 0.79 (3H, d, *J* = 6.1 Hz), 0.06 – −0.05 (12H, m); δ_C (100 MHz, $CDCl_3$) 214.83, 135.80, 133.87, 129.81, 127.86, 85.36, 80.65, 79.59, 72.12, 62.00, 61.62, 39.13, 32.63, 32.47, 27.07, 26.19, 25.96, 19.34, 18.53, 18.30, 17.31, −4.47, −4.86, −5.05, −5.08; (ESI/MS) Calcd for *m/z* $C_{39}H_{67}O_6Si_3^+$: 715.4 $[M+H]^+$; found 715.4.

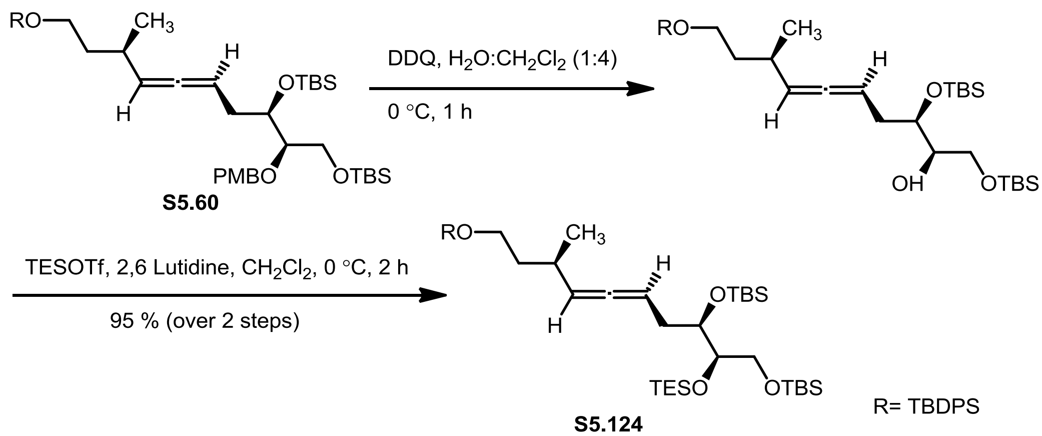

To the solution of allene **S5.60** (50 mg, 0.0622 mmol) in a mixture of CH_2Cl_2 and H_2O (4:1, 5.0 ml) was added DDQ (21 mg, 0.0925 mmol) at 0°C. After 1 h at 0°C, the reaction was quenched with sat. aq. $NaHCO_3$ (1.0 ml), the CH_2Cl_2 layer was separated and the organic layer was extracted with CH_2Cl_2 (2 x 5.0 ml). The CH_2Cl_2 layers were combined, dried over Na_2SO_4, filtered and concentrated. The crude product was used for the next step without further purification.

To the solution of crude unprotected allene in CH_2Cl_2 (2.0 ml) was added 2,6-lutidine (11 μl, 0.0925 mmol) and TESOTf (21 μl, 0.0925 mmol) at 0°C. The reaction was stirred at 0°C for 2 h. Upon completion of reaction, as judged by TLC, H_2O (0.5 ml) was added and the CH_2Cl_2 layer was separated, dried over Na_2SO_4, filtered, concentrated and purified by FCC (3% EtOAc/Hexane) to obtain **S5.124** (47 mg, 95% yield) as colorless oil. $[\alpha]_D$ +37.80 (c = 0.01, $CHCl_3$); IR *v*max (neat)/cm-[1] 2997, 2927, 1959, 1471, 1427, 1388, 1361, 1254, 1100, 1005, 835, 775, 737, 701; δ_H (500 MHz, $CDCl_3$) 7.67 (4H, dd, *J* = 7.9, 1.5 Hz), 7.44 – 7.34 (6H, m), 5.13 – 5.02 (2H, m), 3.79 (1H, dd, *J* = 10.4, 2.1 Hz), 3.74 – 3.69 (4H, m), 3.48 (1H, dd, *J* = 10.1, 6.9 Hz), 2.43 – 2.32 (2H, m), 1.91 (1H, m), 1.58 (2H, m), 1.05 (9H, s), 0.99 – 0.91 (12H, m), 0.92 – 0.80 (18H, m), 0.66 – 0.53 (6H, m), 0.06 – 0.02 (12H, m); δ_C (125 MHz, $CDCl_3$) 203.59, 135.79, 134.33, 129.72, 127.81, 96.73, 89.78, 76.55, 74.75, 64.24, 62.28, 40.12, 32.00, 30.15, 27.10, 26.25, 26.10, 20.86, 19.45, 18.62, 18.28, 7.17, 5.33, −4.15, −4.18, −5.03, −5.15 ; Calcd for m/z $[C_{45}H_{80}O_4Si_4 + Na]^+$: 819.4 $[M+Na]^+$; found 819.5.

General Computational Details: Electronic structure calculations, based on density functional theory (DFT), were carried out with the Gaussian 03 suite[12] of programs. We utilized the B3LYP functional[13] with 6-31g(d,p) basis sets.[14] General solvent effects were incorporated with the polarizable conductor self-consistent reaction field model (CPCM).[22] The **TSI** and **TSII** were verified by observing the nature of the negative imaginary frequency. Atomic coordinates and energies for ground state structures **XI**, **XII**, **XIII**, **XIV**, **XV** and **XVI** are listed.

Transition Structure I

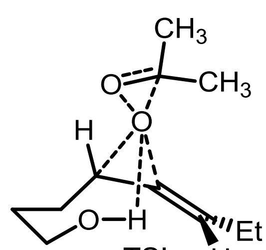

TSI

Standard orientation:

Center Number	Atomic Number	Atomic Type	Coordinates (Angstroms) X	Y	Z
1	6	0	0.798365	−1.845011	0.925594
2	6	0	−2.372602	−0.076436	0.118009
3	6	0	−0.077085	−1.324998	−0.182503
4	6	0	−1.155829	−0.527754	−0.048481
5	6	0	−3.559621	−0.962752	0.438075
6	6	0	2.160266	−2.380208	0.454435
7	6	0	3.125286	−1.335303	−0.117590
8	8	0	2.681205	−0.745140	−1.331890
9	1	0	2.013771	−0.065448	−1.128919

10	1	0	0.243822	−2.674338	1.393435
11	1	0	0.910022	−1.088335	1.710016
12	1	0	−2.570140	0.987348	0.011510
13	1	0	0.157231	−1.672529	−1.191883
14	6	0	−4.654130	−0.873591	−0.636121
15	1	0	−3.973066	−0.645367	1.405010
16	1	0	−3.228992	−1.999593	0.558048
17	1	0	1.996890	−3.156180	−0.304738
18	1	0	2.650613	−2.869963	1.305453
19	1	0	4.076691	−1.830802	−0.344485
20	1	0	3.342104	−0.572188	0.645328
21	1	0	−5.514727	−1.490215	−0.358553
22	1	0	−4.283630	−1.221116	−1.605458
23	1	0	−5.004457	0.156728	−0.759829
24	8	0	0.302712	0.784468	−0.661512
25	6	0	0.578066	2.042004	0.097956
26	8	0	1.242621	2.370440	−1.013563
27	6	0	−0.683950	2.858879	0.352145
28	6	0	1.414888	1.811485	1.348963
29	1	0	−1.285874	2.450378	1.168541
30	1	0	−0.389308	3.876793	0.627949
31	1	0	−1.278906	2.909588	−0.562608
32	1	0	1.706244	2.779486	1.770369
33	1	0	0.854614	1.268034	2.116524
34	1	0	2.322864	1.261689	1.097123

Zero-point correction = 0.292332 (Hartree/Particle)
Thermal correction to Energy = 0.309670
Thermal correction to Enthalpy = 0.310615
Thermal correction to Gibbs Free Energy = 0.246926
Sum of electronic and zero-point Energies = −656.437679
Sum of electronic and thermal Energies = −656.420341
Sum of electronic and thermal Enthalpies = −656.419396
Sum of electronic and thermal Free Energies = −656.483085

Imaginary frequency = −417.89
E(RB+HF−LYP) = −656.73001099

Transition Structure II

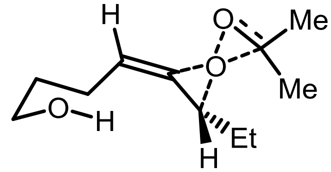

TSII

Standard orientation:

Center Number	Atomic Number	Atomic Type	Coordinates (Angstroms) X	Y	Z
1	6	0	2.435787	1.355929	0.775811
2	1	0	−1.045771	0.959672	−1.673426
3	6	0	−0.872984	1.385826	−0.682454
4	6	0	1.129612	0.592649	0.848182
5	6	0	0.074033	0.836900	0.105334
6	6	0	−1.668908	2.609585	−0.312568
7	6	0	3.689756	0.482557	0.570750
8	6	0	3.783838	−0.196811	−0.797165
9	8	0	2.834884	−1.246677	−0.981361
10	1	0	1.954557	−0.849936	−0.937702
11	1	0	2.544558	1.891243	1.729288
12	1	0	2.380908	2.119482	−0.009199
13	1	0	1.027392	−0.193655	1.598163
14	6	0	−3.187603	2.382832	−0.331872
15	1	0	−1.413569	3.390709	−1.045076
16	1	0	−1.348503	2.973643	0.668417
17	1	0	3.741568	−0.286117	1.352385
18	1	0	4.572192	1.123581	0.694480
19	1	0	4.768244	−0.664562	−0.905682
20	1	0	3.693400	0.557863	−1.595662
21	1	0	−3.714771	3.317419	−0.116975
22	1	0	−3.467888	1.642057	0.419782
23	1	0	−3.523927	2.022735	−1.309924
24	6	0	−1.627149	−1.667394	0.206390
25	8	0	−1.837375	−1.905799	1.515683
26	8	0	−1.364679	−0.315292	0.709364
27	6	0	−0.422229	−2.345705	−0.427556
28	6	0	−2.878467	−1.696761	−0.680636
29	1	0	−0.671342	−3.390900	−0.637109
30	1	0	−0.155590	−1.878239	−1.382025
31	1	0	0.435842	−2.323285	0.245737
32	1	0	−2.960155	−2.648249	−1.215068
33	1	0	−3.761397	−1.563992	−0.051857
34	1	0	−2.852499	−0.894967	−1.423336

Zero-point correction = 0.291658 (Hartree/Particle)
Thermal correction to Energy = 0.309495
Thermal correction to Enthalpy = 0.310440
Thermal correction to Gibbs Free Energy = 0.244922
Sum of electronic and zero-point Energies = −656.433967
Sum of electronic and thermal Energies = −656.416129

Sum of electronic and thermal Enthalpies = −656.415185
Sum of electronic and thermal Free Energies = −656.480702

Imaginary frequency = −489.618
E(RB+HF−LYP) = −656.725624612

Allene (XI)

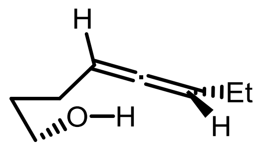

XI

Standard orientation:

Center Number	Atomic Number	Atomic Type	Coordinates (Angstroms) X	Y	Z
1	6	0	−1.398558	−1.364982	−0.096907
2	6	0	1.841180	0.415821	−0.343724
3	6	0	−0.340860	−0.611640	0.688837
4	6	0	0.747876	−0.086796	0.174701
5	6	0	3.154786	−0.325534	−0.486043
6	6	0	−2.822990	−0.793038	0.044107
7	6	0	−2.995685	0.627864	−0.499740
8	8	0	−2.392779	1.630267	0.316993
9	1	0	−1.443632	1.437567	0.351539
10	1	0	−1.409937	−2.406928	0.252690
11	1	0	−1.113903	−1.389853	−1.155452
12	1	0	1.831006	1.453048	−0.692193
13	1	0	−0.506253	−0.527899	1.767695
14	6	0	4.295964	0.347745	0.291596
15	1	0	3.422741	−0.366375	−1.551181
16	1	0	3.029326	−1.360651	−0.150916
17	1	0	−3.128589	−0.800683	1.098571
18	1	0	−3.514689	−1.456296	−0.492077
19	1	0	−4.061477	0.879179	−0.536871
20	1	0	−2.615400	0.678788	−1.533749
21	1	0	5.240639	−0.183525	0.136028
22	1	0	4.084961	0.360190	1.365764
23	1	0	4.437162	1.384662	−0.032757

Zero-point correction = 0.203525 (Hartree/Particle)
Thermal correction to Energy = 0.214608
Thermal correction to Enthalpy = 0.215553
Thermal correction to Gibbs Free Energy = 0.165864

Sum of electronic and zero-point Energies = −388.266821
Sum of electronic and thermal Energies = −388.255737
Sum of electronic and thermal Enthalpies = −388.254793
Sum of electronic and thermal Free Energies = −388.304482

Low frequencies --- −7.6065 −6.1692 −2.5461 7.2861 9.2343 12.4075
E(RB+HF−LYP) = −388.470345837

DMDO (XII)

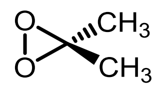

XII

Standard orientation:

Center Number	Atomic Number	Atomic Type	Coordinates (Angstroms) X	Y	Z
1	8	0	1.094709	−0.067423	−0.750678
2	6	0	−0.101039	0.004101	0.001973
3	8	0	1.087385	−0.074769	0.752927
4	6	0	−0.782919	1.347279	−0.000118
5	6	0	−0.958319	−1.233858	−0.002869
6	1	0	−1.407856	1.450990	−0.892680
7	1	0	−1.430842	1.438893	0.877350
8	1	0	−0.037257	2.143757	0.016072
9	1	0	−1.560935	−1.270342	0.910484
10	1	0	−1.643901	−1.212674	−0.856105
11	1	0	−0.322305	−2.118220	−0.067029

Zero-point correction = 0.088230 (Hartree/Particle)
Thermal correction to Energy = 0.093837
Thermal correction to Enthalpy = 0.094781
Thermal correction to Gibbs Free Energy = 0.060015
Sum of electronic and zero-point Energies = −268.193416
Sum of electronic and thermal Energies = −268.187809
Sum of electronic and thermal Enthalpies = −268.186865
Sum of electronic and thermal Free Energies = −268.221631

Low frequencies --- −14.0536 −1.3316 −0.3073 3.8046 19.7295 24.2395
E(RB+HF−LYP) = −268.281646145

Starting Material: Hydrogen Bonded complex

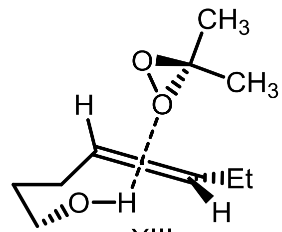

XIII

Standard orientation:

Center Number	Atomic Number	Atomic Type	Coordinates (Angstroms) X	Y	Z
1	6	0	−1.544597	2.674312	−0.473752
2	6	0	−2.171636	−0.969299	−0.241957
3	6	0	−1.766986	1.518115	0.481820
4	6	0	−1.967025	0.272592	0.123216
5	6	0	−3.525871	−1.577382	−0.542782
6	6	0	−0.321055	3.550060	−0.148003
7	6	0	1.041323	2.866924	−0.295354
8	8	0	1.335659	1.938455	0.748110
9	1	0	0.903084	1.095757	0.541083
10	1	0	−2.435834	3.318265	−0.447884
11	1	0	−1.467424	2.291346	−1.498627
12	1	0	−1.307645	−1.631570	−0.324051
13	1	0	−1.784764	1.768217	1.546862
14	6	0	−3.861859	−2.754904	0.385317
15	1	0	−3.532685	−1.931350	−1.583628
16	1	0	−4.299600	−0.805744	−0.466807
17	1	0	−0.401900	3.938379	0.875892
18	1	0	−0.335505	4.421955	−0.816360
19	1	0	1.827435	3.629627	−0.249053
20	1	0	1.117253	2.386093	−1.283238
21	1	0	−4.825609	−3.201251	0.118686
22	1	0	−3.914307	−2.429144	1.429251
23	1	0	−3.099558	−3.539172	0.319412
24	8	0	1.185846	−1.016222	0.014690
25	6	0	2.522522	−1.474630	−0.051965
26	8	0	1.935494	−1.493384	1.227663
27	6	0	2.709299	−2.820004	−0.703369
28	6	0	3.571522	−0.418223	−0.277945
29	1	0	2.755181	−2.708562	−1.791164
30	1	0	3.650475	−3.268976	−0.370621
31	1	0	1.880893	−3.479647	−0.440122
32	1	0	4.528779	−0.752799	0.134853
33	1	0	3.709834	−0.249617	−1.350757
34	1	0	3.262088	0.512046	0.201213

Zero-point correction = 0.293128 (Hartree/Particle)
Thermal correction to Energy = 0.311805
Thermal correction to Enthalpy = 0.312749
Thermal correction to Gibbs Free Energy = 0.242982
Sum of electronic and zero-point Energies = −656.462971
Sum of electronic and thermal Energies = −656.444295
Sum of electronic and thermal Enthalpies = −656.443350
Sum of electronic and thermal Free Energies = −656.513117

Low frequencies --- −5.5598 −1.7394 −0.9907 −0.7208 8.3502 9.4277
E(RB+HF−LYP) = −656.75609928

Allene Oxide (XIV)

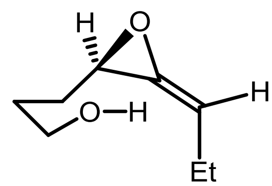

Standard orientation:

Center Number	Atomic Number	Atomic Type	Coordinates (Angstroms) X	Y	Z
1	6	0	1.046191	1.153468	−0.285433
2	6	0	−2.236609	−0.476629	−0.604468
3	6	0	0.260969	0.016091	0.325508
4	6	0	−0.954224	−0.475356	−0.271371
5	6	0	−3.213614	0.588539	−0.175229
6	6	0	2.523960	1.248101	0.126054
7	6	0	3.373790	0.023377	−0.206659
8	8	0	3.088998	−1.023161	0.714785
9	6	0	−4.360270	0.037599	0.687903
10	8	0	0.158250	−1.250498	−0.475491
11	1	0	0.540159	2.084751	0.006340
12	1	0	0.956062	1.081336	−1.376579
13	1	0	−2.609596	−1.305048	−1.208081
14	1	0	0.439195	−0.186023	1.382095
15	1	0	−3.643183	1.071830	−1.064736
16	1	0	−2.682217	1.373938	0.375512
17	1	0	2.600774	1.432066	1.206025
18	1	0	2.959863	2.124839	−0.369876
19	1	0	4.439766	0.301764	−0.154739
20	1	0	3.176760	−0.299448	−1.239460
21	1	0	3.163495	−1.865765	0.228826

22	1	0	−5.069840	0.828831	0.952756
23	1	0	−3.976392	−0.401359	1.614622
24	1	0	−4.913994	−0.743584	0.155101

Zero-point correction = 0.207485 (Hartree/Particle)
Thermal correction to Energy = 0.219609
Thermal correction to Enthalpy = 0.220553
Thermal correction to Gibbs Free Energy = 0.167772
Sum of electronic and zero-point Energies = −463.473738
Sum of electronic and thermal Energies = −463.461614
Sum of electronic and thermal Enthalpies = −463.460670
Sum of electronic and thermal Free Energies = −463.513451

Low frequencies --- −21.8782 −15.1163 −4.2942 −1.0876 7.0124 15.4244
E(RB+HF−LYP) = −463.681222918

Allene oxide (XV)

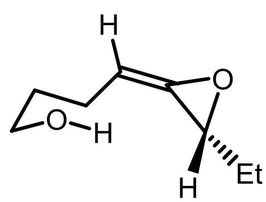

Standard orientation:

Center Number	Atomic Number	Atomic Type	Coordinates (Angstroms) X	Y	Z
1	6	0	1.428307	1.350712	0.221738
2	1	0	−1.558807	−1.056365	−1.086837
3	6	0	−1.661443	−0.328764	−0.277005
4	6	0	0.616408	0.359472	1.023647
5	6	0	−0.543622	−0.139433	0.612524
6	6	0	−2.789984	0.661900	−0.412130
7	6	0	2.884274	0.922536	−0.054287
8	6	0	3.023242	−0.340109	−0.908527
9	8	0	2.663792	−1.535963	−0.217584
10	1	0	1.751913	−1.413203	0.087567
11	1	0	1.452137	2.307494	0.762397
12	1	0	0.922717	1.548045	−0.732256
13	1	0	0.976685	0.071422	2.012214
14	6	0	−4.150490	−0.018544	−0.606584
15	1	0	−2.563711	1.303759	−1.274552
16	1	0	−2.801145	1.309391	0.471611
17	1	0	3.413244	0.760741	0.894023

18	1	0	3.395891	1.747808	−0.567027
19	1	0	4.069006	−0.471682	−1.207278
20	1	0	2.434247	−0.227327	−1.834710
21	1	0	−4.944544	0.727629	−0.704882
22	1	0	−4.395899	−0.665628	0.240987
23	1	0	−4.157074	−0.634879	−1.512394
24	8	0	−1.518143	−0.978265	1.074444

Zero-point correction = 0.208617 (Hartree/Particle)
Thermal correction to Energy = 0.220258
Thermal correction to Enthalpy = 0.221202
Thermal correction to Gibbs Free Energy = 0.170146
Sum of electronic and zero-point Energies = −463.473816
Sum of electronic and thermal Energies = −463.462175
Sum of electronic and thermal Enthalpies = −463.461231
Sum of electronic and thermal Free Energies = −463.512287

Low frequencies --- −18.5804 −7.9522 −3.6366 −0.6617 7.1642 9.9832
E(RB+HF−LYP) = −463.682432918

Acetone (XVI)

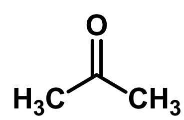

Standard orientation:

Center Number	Atomic Number	Atomic Type	Coordinates (Angstroms) X	Y	Z
1	6	0	0.000652	0.172225	−0.010991
2	8	0	−0.008906	1.399618	0.000581
3	6	0	1.291844	−0.610540	−0.004951
4	6	0	−1.287231	−0.615542	0.001785
5	1	0	1.539217	−0.811710	1.044413
6	1	0	1.196991	−1.565541	−0.528481
7	1	0	2.099364	−0.017606	−0.439393
8	1	0	−1.379719	−1.190850	−0.927238
9	1	0	−1.273792	−1.341290	0.823064
10	1	0	−2.142404	0.053195	0.107924

Zero-point correction = 0.083784 (Hartree/Particle)
Thermal correction to Energy = 0.089082
Thermal correction to Enthalpy = 0.090026
Thermal correction to Gibbs Free Energy = 0.055939
Sum of electronic and zero-point Energies = −193.084827

Sum of electronic and thermal Energies = −193.079528
Sum of electronic and thermal Enthalpies = −193.078584
Sum of electronic and thermal Free Energies = −193.112671

Low frequencies --- −33.0096 −26.0406 −0.5845 −0.3187 3.6087 37.0175
E(RB+HF-LYP) = −193.168610198

Key bond lengths for the proposed transition structures TSI and TSII in Å

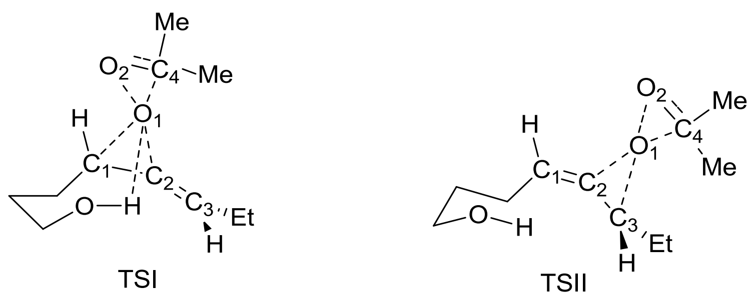

Structure	C_1-C_2	C_2-C_3	C_1-O_1	C_2-O_1	C_4-O_1	C_4-O_2	O_1-O_2	C_3-O_1
TSI	1.348	1.308	2.196	2.055	1.495	1.336	1.877	
TSII	1.314	1.349		1.940	1.466	1.347	1.845	2.252

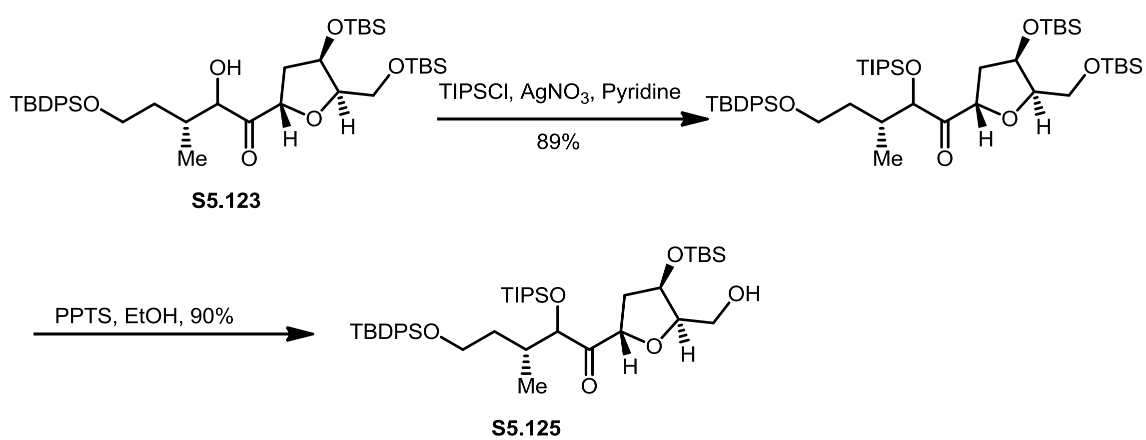

To the solution of **S5.123** (90.0 mg, 0.126 mmol) in dry pyridine (614.0 μl) was added TIPSCl (0.135 ml, 0.629 mmol) followed by $AgNO_3$ (106.9 mg, 0.629 mmol). The reaction was stirred in darkness, at room temperature, for 24 h. Upon completion of reaction, as judged by TLC, Et_2O (6.0 ml) was added and the mixture was washed with

$CuSO_4$. The organic layer was washed with brine, dried over Na_2SO_4, filtered, concentrated and purified by FCC to obtain the triisopropylsilyl ether (97.6 mg, 89% yield) as colorless oil. IR *v*max (neat)/cm-^{1} 2930, 2855, 1731, 1455, 1425, 1381; δ_C (100 MHz, $CDCl_3$) 212.70, 135.78, 134.08, 129.72, 127.81, 85.03, 81.37, 79.75, 72.45, 61.84, 61.71, 39.26, 33.78, 33.60, 27.07, 26.16, 25.98, 18.40, 18.38, 18.35, 17.94, 12.99, 12.53, −4.51, −4.90, −4.99, −5.06; Calcd for *m/z* $[C_{48}H_{86}O_6Si_4\text{+ Na}]^+$: 893.5 $[M\text{+}Na]^+$; found 893.5.

To the solution of the triisopropylsilyl ether (33.8 mg, 0.0376 mmol) in ethanol (1.5 ml) was added pyridinium p-toluenesulfonate (9.5 mg, 0.0378 mmol). The reaction mixture was stirred at room temperature for 18 h. Upon completion of reaction, as judged by TLC, the organic layer was extracted with CH_2Cl_2. The organic layers were combined, dried over Na_2SO_4, filtered, concentrated and purified by FCC to obtain **S2.125** (25.6 mg, 90% yield) as colorless oil. IR *v*max (neat)/cm-^{1} 3499, 2955, 2855, 1734; δ_H (400 MHz, $CDCl_3$) 7.72 – 7.63 (4H, m), 7.46 – 7.35 (6H, m), 4.80 (1H, t, *J* = 7.6 Hz), 4.74 (1H, d, *J* = 2.9 Hz), 4.51 – 4.47 (1H, m), 4.03 – 3.96 (1H, m), 3.83 – 3.67 (4H, m), 2.39 – 2.28 (1H, m), 2.27 – 2.21 (1H, m), 2.16 – 2.10 (1H, m), 1.97 – 1.88 (1H, m), 1.70 – 1.30 (5H, m), 1.38 – 1.30 (27H, m), 0.91 (9H, s), 0.77 (3H, d, *J* = 6.9 Hz), 0.11 (6H, s); δ_C (125 MHz, $CDCl_3$) 211.69, 135.82, 134.13, 129.82, 127.86, 83.01, 80.37, 79.47, 73.55, 62.48, 62.04, 38.85, 36.44, 33.36, 27.11, 25.93, 19.43, 18.40, 18.25, 18.20, 13.38, 13.03, −4.46, −4.98; Calcd for *m/z* $[C_{42}H_{72}O_6Si_3\text{+ Na}]^+$: 779.5 $[M\text{+}Na]^+$; found 779.4.

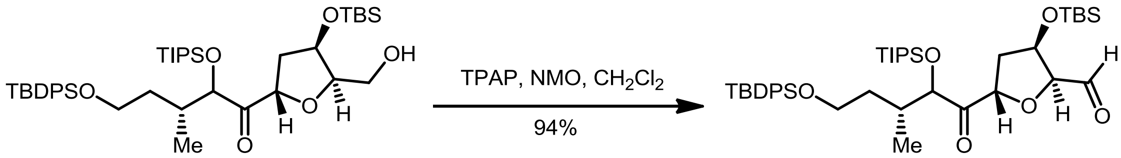

S5.125 **S5.126**

To the suspension of 4 Å MS (10 mg, activated by a gentle flame under vacuum) in CH_2Cl_2 (5.0 ml) at 0°C was added **S5.125** (50 mg, 0.066 mmol) in CH_2Cl_2 (0.50 ml) followed by NMO (11.6 mg, 0.099 mmol) and TPAP (1.16 mg, 0.0033 mmol). The reaction mixture was slowly warmed to rt and stirred for 5 h. Upon completion of reaction, as judged by TLC, the reaction mixture was filtered, concentrated and purified by FCC to obtain **S5.126** (46.8 mg, 94% yield) as colorless oil. IR *v*max (neat)/cm-^{1} 2953, 2929, 1734, 1672; δ_H (400 MHz, $CDCl_3$) 9.58 (1H, d, *J* = 2.1 Hz), 7.67 – 7.60 (4H, m), 7.43 – 7.34 (6H, m), 5.20 – 5.14 (1H, m), 4.76 – 4.70 (1H, m), 4.61 – 4.58 (1H, m), 4.30 – 4.24 (1H, m), 3.78 – 3.67 (2H, m), 2.27 – 2.10 (2H, m), 2.09 – 2.04 (1H, m), 1.70 – 1.30 (5H, m), 1.38 – 1.30 (27H, m), 0.91 (9H, s), 0.77 (3H, d, *J* = 6.9 Hz), 0.11 (6H, s); (ESI/MS) Calcd for *m/z* $[C_{42}H_{70}O_6Si_3+Na]^+$: 777.4 $[M+Na]^+$; found 777.4.

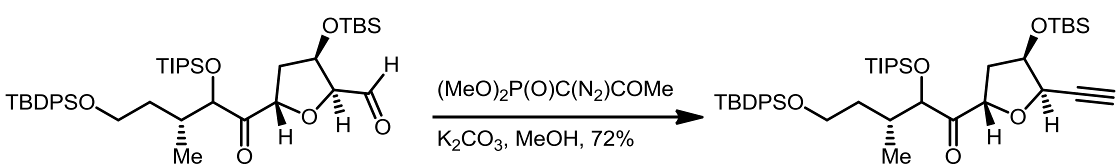

S5.126 **S5.127**

Dimethyl-2-oxopropylphosphate (3.6 µl, 0.0264 mmol) was added to the suspension of K_2CO_3 (9.1 mg, 0.0660 mmol) and 11-15% w/w *p*TsN_3 (47.3 mg) in acetonitrile (0.33 ml). The mixture was stirred for 2 h. The aldehyde **S5.126** (16.6 mg, 0.022 mmol) was dissolved in MeOH (0.066 ml) and then added to the above mixture.

The reaction mixture was stirred for 2 h. Upon completion of reaction, as judged by TLC, the reaction mixture was concentrated and dissolved in Et_2O and water. The organic layer was extracted with Et_2O. The organic layers were combined, dried over Na_2SO_4, filtered, concentrated and purified by FCC to obtain **S5.127** (11.9 mg, 72% yield) as colorless oil. δ_H (400 MHz, $CDCl_3$) 7.69 – 7.62 (4H, m), 7.45 – 7.37 (6H, m), 5.01 (1H, t, J = 7.6 Hz), 4.65 –4.63 (1H, m), 4.62 – 4.60 (1H, m), 4.39 (1H, dd, J = 8.4, 4.2 Hz), 3.75 – 3.68 (1H, m), 3.66 – 3.59 (1H, m), 2.52 – 2.47 (1H, m), 2.23 – 2.13 (2H, m), 1.73 – 1.60 (1H, m), 1.41 – 1.29 (5H, m), 1.38 – 1.30 (27H, m), 0.91 (9H, s), 0.77 (3H, d, J = 6.9 Hz), 0.11 (6H, s); δ_C (125 MHz, $CDCl_3$) 211.55, 135.80, 134.12, 129.75, 127.85, 81.53, 79.63, 79.10, 76.02, 74.60, 73.67, 61.68, 38.19, 34.16, 33.90, 27.11, 26.03, 19.39, 18.39, 18.33, 16.01, 12.98, −4.49, −4.66; (ESI/MS) Calcd for m/z $[C_{43}H_{70}O_5Si_3 + Na]^+$: 773.4 $[M+Na]^+$; found 773.4.

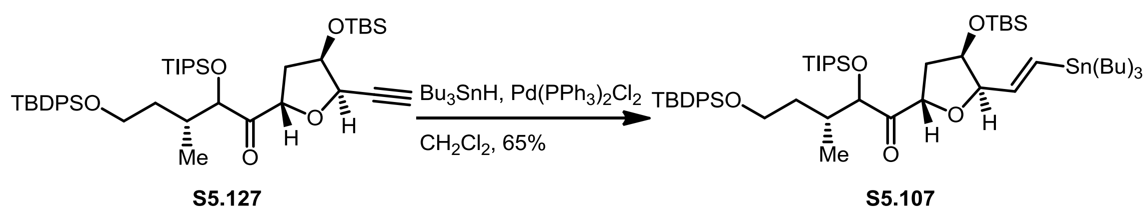

To **S5.127** (8 mg, 0.0106 mmol) in CH_2Cl_2 (100 μl) at 0°C was added $Pd(PPh_3)_2Cl_2$ (800 μg, 0.00114 mmol) and stirred at 0°C for 5 min. To the reaction mixture was then added Bu_3SnH (3.2 μl, 0.0119 mmol) drop wise. Upon complete consumption of **S5.127**, the reaction mixture was concentrated, diluted with a 4:1 solution of EtOAc/Hexane (0.8 ml), filtered through Celite, concentrated, and then purified by FCC to obtain **S5.107** (7.2mg, 65% yield) as oil. (ESI/MS) Calcd for *m/z* $[C_{55}H_{99}O_5Si_3Sn]^+$: 1043.5 $[M+H]^+$; found 1043.5, 1041.5.

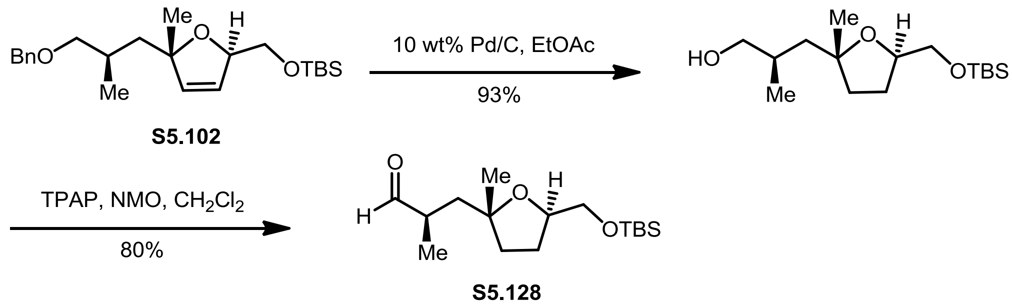

To **S5.102** (180 mg, 0.461 mmol) in EtOAc (9.2 ml) was added 10% Pd on Carbon (37.0 mg). The reaction was evacuated and refilled with argon several times, followed by a final evacuation and the addition of a hydrogen balloon. After stirring the reaction at room temperature for 18 h, the hydrogen balloon was removed. The reaction mixture was filtered through silica gel plug, filtrate concentrated, and then purified by FCC to obtain the tetrahydrofuran (129.4 mg, 93% yield) as oil. δ_H (500 MHz, $CDCl_3$) 4.07 – 4.01 (1H, m), 3.64 – 3.56 (2H, m), 3.53 – 3.48 (1H, m), 3.36 – 3.30 (2H, m), 1.98 – 1.80 (4H, m), 1.73 (1H, dd, J = 14.7, 6.7 Hz), 1.70 – 1.65 (1H, m), 1.49 (1H, dd, J = 14.7, 4.1 Hz), 1.20 (3H, s), 0.93 (3H, d, J = 6.9 Hz), 0.89 (9H, s), 0.05 (6H, s); δ_C (125 MHz, $CDCl_3$) 83.64, 80.56, 69.23, 66.12, 45.57, 36.27, 31.93, 28.77, 28.08, 26.09, 19.54, 18.52, −5.13, −5.17; (ESI/MS) Calcd for *m/z* $[C_{16}H_{34}O_3Si+Na]^+$: 325.2 $[M+Na]^+$; found 325.2.

To the suspension of 4 Å MS (25 mg, activated by a gentle flame under vacuum) in CH_2Cl_2 (5.0 ml) at 0°C was added above tetrahydrofuran (83 mg, 0.274 mmol) in CH_2Cl_2 (1.5 ml) followed by NMO (48.3 mg, 0.412 mmol) and TPAP (4.8 mg, 0.0137 mmol). The reaction mixture was slowly warmed to room temperature and stirred for 3 h.

Upon completion of reaction, as judged by TLC, the reaction mixture was filtered, concentrated and purified by FCC to obtain **S5.128** (65.8 mg, 80% yield) as oil. δ_H (400 MHz, $CDCl_3$) 9.57 (1H, d, *J* = 3.1 Hz), 4.05 – 3.95 (1H, m), 3.59 – 3.49 (2H, m), 2.62 – 2.50 (1H, m), 2.08 – 1.95 (2H, m), 1.78 – 1.65 (3H, m), 1.48 (1H, dd, *J* = 14.3, 4.3 Hz), 1.19 (3H, s), 1.08 (3H, d, *J* = 7.1 Hz), 0.89 (9H, s), 0.04 (6H, s); δ_C (100 MHz, $CDCl_3$) 205.22, 82.73, 79.52, 66.07, 43.44, 42.86, 38.21, 28.37, 26.93, 26.14, 18.55, 15.92, −5.11, −5.14; (ESI/MS) Calcd for *m/z* $[C_{16}H_{32}O_3Si+ Na]^+$: 323.2 $[M+Na]^+$; found 323.2.

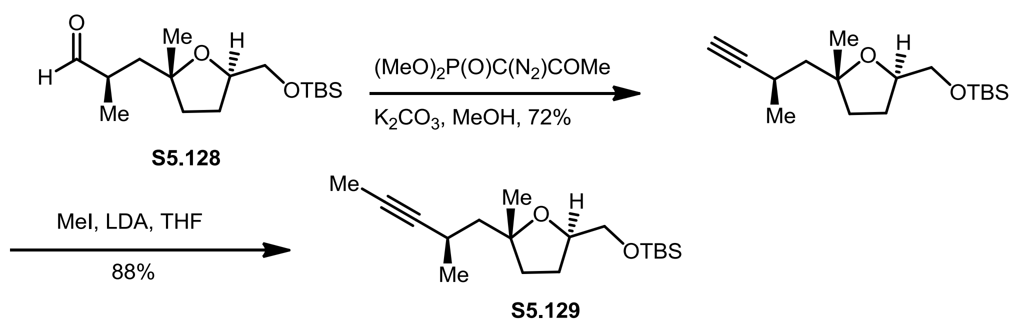

Dimethyl-2-oxopropylphosphate (41 μl, 0.299 mmol) was added to the suspension of K_2CO_3 (103.4 mg, 0.748 mmol) and *p*TsN_3 (454 mg, 0.299 mmol) in acetonitrile (3.75 ml). The mixture was stirred for 2 h. The aldehyde **S5.128** (75 mg, 0.249 mmol) was dissolved in MeOH (0.75 ml) and then added to the above mixture. The reaction mixture was stirred for 3 h. Upon completion of reaction, as judged by TLC, the reaction mixture was concentrated and dissolved in Et_2O and water. The organic layer was extracted with Et_2O. The organic layers were combined, dried over Na_2SO_4, filtered, concentrated and purified by FCC to obtain terminal alkyne (53.3 mg, 72% yield) as colorless oil. δ_C (100 MHz, $CDCl_3$) 90.61, 83.25, 78.74, 68.33, 65.96, 48.18, 35.18, 28.39, 27.52, 26.20, 23.39, 21.57, 18.61, −5.06, −5.10; (ESI/MS) Calcd for *m/z* $[C_{17}H_{32}O_2Si+ Na]^+$: 319.2 $[M+Na]^+$; found 319.2.

n-BuLi (0.323 ml, 0.808 mmol) was added drop wise to the solution of *i*-Pr_2NH (0.12 ml, 0.835 mmol) in THF (2.7 ml) at −10°C. The reaction was stirred at −10°C for 15 min and then cooled to −78°C. To the freshly prepared LDA was added the terminal alkyne (50 mg, 0.169 mmol), DMPU (0.17 ml, 1.42 mmol), and purified MeI (51 µl, 0.813 mmol). The reaction mixture was stirred at 0°C for 5 min and at room temperature for 2.5 h. Upon completion of reaction, as judged by TLC, water was added to the reaction and extracted with Et_2O. The organic layers were combined, dried over Na_2SO_4, filtered, concentrated and purified by FCC to obtain **S5.129** (46.2 mg, 88% yield) as colorless oil. δ_H (400 MHz, $CDCl_3$) 4.06 – 3.99 (1H, m), 3.68 – 3.60 (1H, m), 3.57 – 3.48 (1H, m), 2.58 – 2.48 (1H, m), 2.13 – 1.93 (3H, m), 1.89 – 1.56 (6H, m), 1.25 (3H, s), 1.17 (3H, d, *J* = 6.7 Hz), 0.90 (9H, s), 0.07 (6H, s); δ_C (100 MHz, $CDCl_3$) 85.27, 83.45, 78.61, 75.50, 66.08, 48.70, 35.12, 28.64, 27.48, 26.19, 23.76, 21.91, 18.62, 3.73, −5.08, −5.11; (ESI/MS) Calcd for *m/z* $[C_{18}H_{34}O_2Si+Na]^+$: 333.2 $[M+Na]^+$; found 333.2.

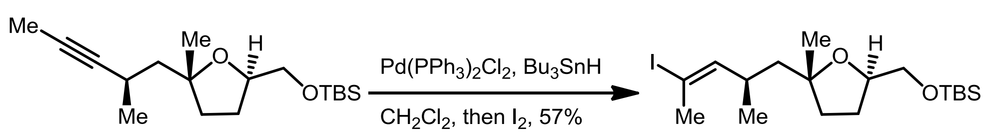

S5.129 S5.130

To **S5.129** (11.3 mg, 0.0363 mmol) in CH_2Cl_2 (0.3 ml) at 0°C was added $Pd(PPh_3)_2Cl_2$ (2.55 mg, 0.0363 mmol) and stirred at 0°C for 5 min. To the reaction was added Bu_3SnH (14.7 µl, 0.0546 mmol) drop wise. Upon complete consumption of **S5.129**, the reaction mixture was concentrated, diluted with a 4:1 solution of EtOAc/Hexane (0.8 ml), filtered through Celite, and then concentrated. The crude was then dissolved in CH_2Cl_2 (0.2 ml), cooled to 0°C, and then to it was added I_2 (9.2 mg, 0.0363 mmol) in CH_2Cl_2 (0.3 ml) drop wise. After addition of I_2 the reaction was stirred for 5min and then to it was added aqueous sodium thiosulfate. The organic was extracted with CH_2Cl_2, dried over Na_2SO_4, filtered, concentrated and purified by FCC to obtain **S5.130** (9 mg, 57% yield) as oil. (ESI/MS) Calcd for *m/z* $[C_{18}H_{36}IO_2Si]^+$: 489.1 $[M+H]^+$; found 489.1.

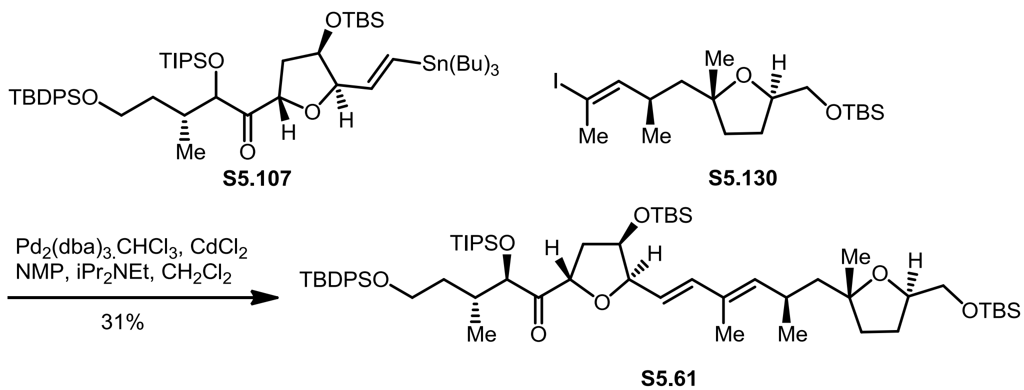

To the solution of **S5.107** (8.6 mg, 0.00825 mmol) in NMP (40 µl) at 45°C were added *i*Pr_2NEt (0.24 µl, 0.00140 mmol) and $CdCl_2$ (0.45 mg, 0.00247 mmol). The reaction was kept in darkness and to it was added solution of **S5.130** (4.3 mg, 0.00990 mmol) in NMP (50 µl) drop wise over 20 min. Meanwhile, $Pd_2(dba)_3.CHCl_3$ (0.3 mg, 0.000247 mmol) in CH_2Cl_2 (30 µl) was added in 10 µl portion over 40 min. After addition of the catalyst was over, additional of $Pd_2(dba)_3.CHCl_3$ (0.3 mg, 0.000247 mmol) was added and the reaction was stirred for 5 h. To it was added brine. The organic was extracted with CH_2Cl_2, dried over Na_2SO_4, filtered, concentrated and purified by FCC to obtain **S5.61** (2.7 mg, 31% yield) as oil. (ESI/MS) Calcd for *m/z* $[C_{61}H_{106}O_7Si_4+Na]^+$: 1085.7 $[M+Na]^+$; found 1085.7, 1086.7.

7.6 Chapter 6: Synthesis of Bromohydroxylketone by Catalytic Aminohydroxylation of Allenes

General procedure for the synthesis of α–bromo-ά-hydroxyl ketone by the catalytic allene aminohydroxylation (Table 2):

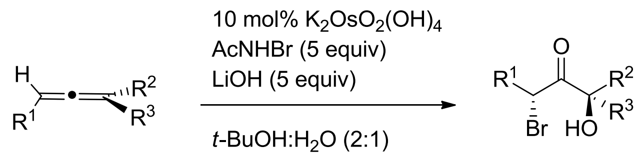

To the flask containing LiOH (5.00 equiv) was added water (0.21 M with respect to allene). $K_2OsO_2(OH)_4$ (10 mol%) followed by *t*-BuOH (0.21 M with respect to allene) was added to the solution of LiOH in water to form dark red solution. N-Bromoacetamide (5.00 equiv) was added to form nearly colorless (light yellow) solution. Solution of allene in *t*-BuOH (0.21 M with respect to allene) was added to the reaction solution. Upon completion of reaction as judged by TLC (10 − 20 min), the reaction was diluted with NH_4Cl and Et_2O. The organic layer was extracted in Et_2O, dried over anhydrous Na_2SO_4, filtered, evaporated and purified by FCC.

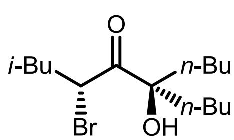 **4-bromo-6-butyl-6-hydroxy-2-methyldecan-5-one** (**S6.27**, Table 2, entry 1): 97% (149.3 mg).

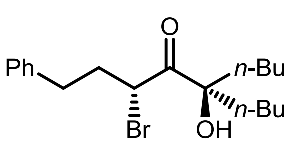 **3-bromo-5-butyl-5-hydroxy-1-phenylnonan-4-one** (**S6.28**, Table 2, entry 2): 84% (163.8 mg); IR ν_{max}(neat)/cm^{-1} 3508, 3027, 2956, 2871, 1712, 1602, 1496, 1454, 1379, 1290, 1250, 1139, 1085, 1030, 745, 699; δ_H (500 MHz, $CDCl_3$) 7.35 – 7.29 (2H, m), 7.27 – 7.19 (3H, m), 4.65 (1H, ddd, *J* = 9.7, 4.2, 2.9 Hz), 2.96 – 2.88 (2H, m), 2.74 (1H, dtd, *J* = 13.9, 8.1, 2.6 Hz), 2.38 – 2.30 (1H, m), 2.18 – 2.09 (1H, m), 1.70 –

1.55 (4H, m), 1.40 – 1.19 (6H, m), 1.16 – 1.07 (1H, m), 1.07 – 0.97 (1H, m), 0.87 (6H, td, J = 7.2, 2.8 Hz); δ_C (125 MHz, $CDCl_3$) 208.74, 140.24, 128.88, 128.65, 126.68, 82.94, 45.37, 39.15, 38.63, 35.01, 33.06, 25.92, 25.73, 23.13, 23.11, 14.15, 14.13; (ESI/MS) Calcd for m/z $[C_{19}H_{30}BrO_2]^+$: 369.1 $[M+H]^+$; found 369.1.

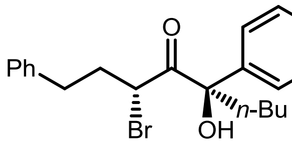

3-bromo-5-hydroxy-1,5-diphenylnonan-4-one (**S6.29**, Table 2, entry 3): 59% (198.3 mg as a 5:2 mixture of diastereomers as indicated by ^{1}H NMR of the crude); IR ν_{max}(neat)/cm^{-1} 3523, 3062, 3027, 2957, 2930, 2864, 1716, 1601, 1494, 1450, 1358, 1162, 1031, 963, 745, 699; δ_H of major diastereomer (400 MHz, $CDCl_3$) 7.55 – 7.42 (2H, m), 7.42 – 7.28 (3H, m), 7.28 – 7.14 (3H, m), 6.93 – 6.86 (2H, m), 4.78 – 4.66 (1H, m), 2.94 (1H, s), 2.42 – 2.27 (2H, m), 2.24 – 2.03 (4H, m), 1.43 – 1.27 (3H, m), 1.26 – 1.08 (1H, m), 0.96 – 0.86 (3H, m); δ_H of minor diastereomer (400 MHz, $CDCl_3$) 7.43 – 7.27 (5H, m), 7.25 – 7.15 (3H, m), 6.94 – 6.82 (2H, m), 4.52 – 4.47 (1H, m), 4.17 (1H, s), 2.46 (1H, ddd, J = 13.3, 8.4, 4.7 Hz), 2.42 – 2.30 (1H, m), 2.23 – 2.11 (2H, m), 2.13 – 2.01 (1H, m), 1.64 (1H, dtd, J = 14.5, 8.2, 4.8 Hz), 1.52 – 1.25 (4H, m), 0.97 – 0.90 (3H, m); δ_C of major diastereomer (100 MHz, $CDCl_3$) 204.97, 140.18, 138.82, 128.87, 128.68, 128.52, 128.27, 126.42, 126.02, 83.95, 44.78, 39.12, 35.29, 32.91, 25.62, 23.01, 14.18; δ_C of minor diastereomer (100 MHz, $CDCl_3$) 206.00, 139.71, 139.53, 129.07, 128.71, 128.52, 128.48, 126.62, 126.44, 83.14, 44.76, 37.20, 35.75, 32.65, 25.68, 23.05, 14.20; (ESI/MS) Calcd for m/z $[C_{21}H_{26}BrO_2]^+$: 389.1 $[M+H]^+$; found 389.1.

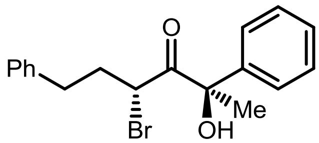 **4-bromo-2-hydroxy-2,6-diphenylhexan-3-one** (**S6.30**, Table 2, entry 4): 60% (262.7 mg as a 6:1 mixture of diastereomers as indicated by ^{1}H NMR of the crude); IR ν_{max}(neat)/cm^{-1} 3516, 3061, 3027, 2932, 2860, 1717, 1601, 1494, 1448, 1370, 1164, 1071, 1028, 996, 913, 698; δ_H (500 MHz, $CDCl_3$) (* indicates diastereomer signals) 7.48 – 7.41 (2H, m), 7.41 – 7.28 (3H, m), 7.28 – 7.15 (3H, m), 6.98 – 6.91 (2H, m), 6.91 – 6.86 (2H, m)*, 4.72 (1H, ddd, *J* = 7.9, 6.4, 5.4 Hz), 4.42 (1H, m)*, 4.33 (1H, s)*, 3.10 (1H, s), 2.49 – 2.34 (2H, m), 2.25 – 2.13 (1H, m), 2.13 – 2.01 (1H, m), 1.88 (3H, d, *J* = 5.3 Hz)*, 1.81 (3H, d, *J* = 5.3 Hz); (Carbon count for the 6:1 mixture of diastereomers) δ_C (125 MHz, $CDCl_3$) 205.90, 205.56, 140.10, 140.03, 139.90, 139.69, 129.15, 128.92, 128.77, 128.72, 128.54, 128.45, 128.43, 126.48, 126.47, 125.87, 80.89, 80.35, 44.61, 44.21, 35.51, 32.98, 32.65, 27.48, 25.46; (ESI/MS) Calcd for *m/z* $[C_{18}H_{19}BrO_2Na]^+$: 369.1, 371.1 $[M+Na]^+$; found 369.1, 371.1.

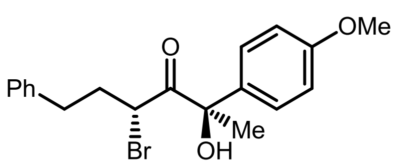 **4-bromo-2-hydroxy-2-(4-methoxyphenyl)-6-phenylhexan-3-one** (**S6.31**, Table 2, entry 5): 67% (141.7 mg as a 6:1 mixture of diastereomers as indicated by ^{1}H NMR of the crude); IR ν_{max}(neat)/cm^{-1} 3479, 3027, 2931, 2837, 1715, 1607, 1510, 1454, 1352, 1303, 1253, 1179, 1096, 1031, 923, 834, 738; δ_H (500 MHz, $CDCl_3$) (* indicates diastereomer signals) 7.37 – 7.30 (2H, m), 7.27 – 7.22 (3H, m), 7.21 – 7.17 (2H, m), 6.99 – 6.96 (1H, m), 6.88 – 6.85 (1H, m), 4.68 (1H, ddd, *J* = 8.0, 6.3, 1.7 Hz), 4.37 (1H, ddd, *J* = 9.0, 4.9, 1.6 Hz)*, 4.28 (1H, s)*, 3.82 (3H, s)*, 3.81 (3H, s), 3.02 (1H, s), 2.51 – 2.36 (2H, m), 2.24 – 2.10 (1H, m), 2.10 – 2.01 (1H, m),

1.85 (3H, s)*, 1.76 (3H, s); (Carbon count for the 6:1 mixture of diastereomers) δ_C (125 MHz, $CDCl_3$) 205.95, 205.56, 159.92, 159.74, 140.13, 131.97, 128.70, 128.68, 128.55, 128.43, 127.81, 127.21, 126.48, 126.44, 114.46, 114.25, 80.49, 79.84, 55.51, 44.57, 44.16, 35.56, 35.50, 33.01, 32.62, 27.26, 25.40; (ESI/MS) Calcd for *m/z* $[C_{19}H_{21}BrO_3Na]^+$: 399.1, 401.1 $[M+Na]^+$; found 399.1, 401.1.

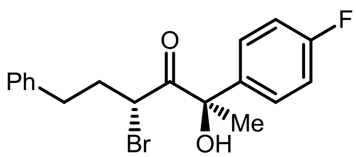

4-bromo-2-(4-fluorophenyl)-2-hydroxy-6-phenylhexan-3-one (**S6.32**, Table 2, entry 6): 32% (75 mg as a 5:1 mixture of diastereomers as indicated by ^1H NMR of the crude); IR ν_{max}(neat)/cm^{-1} 3501, 3027, 2933, 2860, 1716, 1602, 1505, 1455, 1228, 1160, 838, 700; δ_H (500 MHz, $CDCl_3$) (* indicates diastereomer signals, ** indicates the inseparable bromohydrin side product) 7.46 – 7.35 (2H, m), 7.35 – 7.16 (4H, m), 7.07 – 6.89 (3H, m), 6.13 (t, *J* = 6.8 Hz, 1H)**, 4.67 (1H, dd, *J* = 7.2, 7.2 Hz), 4.36 (1H, dd, *J* = 8.8, 4.4 Hz)*, 4.25 (1H, s)*, 3.15 (1H, s), 2.90 – 2.74 (2H, m)**, 2.69 – 2.57 (2H, m)**, 2.56 – 2.37 (2H, m), 2.28 – 2.13 (1H, m), 2.13 – 2.01 (1H, m), 1.84 (3H, s)*, 1.78 (3H, s).; (Carbon count for the 5:1 mixture of diastereomers) δ_C (125 MHz, $CDCl_3$) 205.52, 162.82 (d, *J* = 247.6 Hz), 139.97, 135.90 (d, *J* = 3.1 Hz), 128.77, 128.52, 127.82 (d, *J* = 8.3 Hz), 126.57, 115.77 (d, *J* = 21.5 Hz), 80.46, 44.35, 43.90, 35.48, 35.41, 32.98, 32.59, 27.62, 25.79; (ESI/MS) Calcd for *m/z* $[C_{18}H_{18}BrFO_2Na]^+$: 389.1, 387.1 $[M+Na]^+$; found 389.1, 387.1.

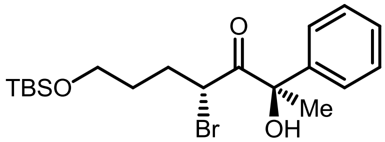

4-bromo-7-((tert-butyldimethylsilyl)oxy)-2-hydroxy-2-phenylheptan-3-one (**S6.33**, Table 2, entry 7): 42% (112 mg as a 4.2:1 mixture of diastereomers as indicated by ^{1}H NMR of the crude); IR ν_{max}(neat)/cm^{-1} 3500, 2929, 2857, 1722, 1472, 1447, 1256, 1108, 836, 776, 699; δ_H (500 MHz, $CDCl_3$) (* indicates diastereomer signals) 7.52 – 7.43 (2H, m), 7.40 – 7.27 (3H, m), 4.80 (1H, dd, J = 7.9, 6.9 Hz), 4.55 (1H, dd, J = 7.9, 6.6 Hz)*, 4.31 (1H, s)*, 3.53 – 3.34 (2H, m), 3.19 (1H, s), 1.97 – 1.86 (2H, m), 1.84 (3H, s), 1.39 – 1.12 (2H, m), 0.89 – 0.79 (9H, m), 0.02 – -0.05 (6H, m); (Carbon count for the 4.2:1 mixture of diastereomers) δ_C (125 MHz, $CDCl_3$) 205.90, 205.78, 140.12, 129.06, 128.85, 128.83, 128.43, 126.51, 125.90, 80.83, 80.38, 62.11, 62.08, 45.37, 44.69, 31.29, 30.65, 30.19, 30.13, 27.32, 26.12, 25.73, 18.46, 18.45, -5.15; (ESI/MS) Calcd for m/z $[C_{19}H_{31}BrO_3SiNa]^+$: 437.1, 439.1 $[M+Na]^+$; found 437.1, 439.1.

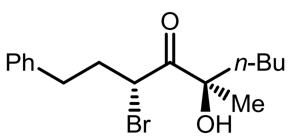

3-bromo-5-hydroxy-5-methyl-1-phenylnonan-4-one (**S6.35**, Table 2, entry 9): 77% (237.5 mg as a 3.2:1 mixture of diastereomers as indicated by ^{1}H NMR of the crude); IR ν_{max}(neat)/cm^{-1} 3505, 3027, 2957, 2932, 2862, 1714, 1603, 1497, 1454, 1371, 1229, 1178, 1091, 1030, 1003; δ_H (500 MHz, $CDCl_3$) (* indicates diastereomer signals) 7.35 – 7.29 (2H, m), 7.26 – 7.19 (3H, m), 4.76 (1H, dt, J = 8.7, 5.3 Hz), 4.69 (1H, dt, J = 8.9, 5.2 Hz)*, 3.01 (1H, s)*, 2.86 (2H, tt, J = 10.0, 5.0 Hz), 2.76 – 2.65 (1H, m), 2.41 – 2.28 (1H, m), 2.28 – 2.17 (1H, m), 1.76 – 1.53 (3H, m), 1.42 (3H, s), 1.36 (3H, s)*, 1.33 – 1.23 (2H, m), 1.20 – 1.08 (1H, m), 0.88 (3H, t, J = 7.3 Hz); (Carbon count for the 3.2:1 mixture of diastereomers) δ_C (125 MHz, $CDCl_3$) 209.08, 208.41, 140.23, 140.19, 128.89, 128.87, 128.64, 126.70, 126.67, 80.01, 79.95, 45.31, 44.69, 40.20, 39.59, 35.15, 33.32, 33.23, 26.87, 26.03, 25.79, 23.08, 23.06, 14.16; (ESI/MS) Calcd for m/z $[C_{16}H_{23}BrO_2Na]^+$: 349.2, 351.2 $[M+Na]^+$; found 349.2, 351.2.

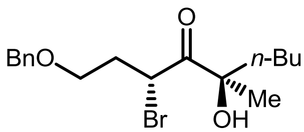 **1-(benzyloxy)-3-bromo-5-hydroxy-5-methylnonan-4-one** (**S6.36**, Table 2, entry 10): 50% (73 mg as a 2:1 mixture of diastereomers as indicated by ^{1}H NMR of the crude); IR ν_{max}(neat)/cm^{-1} 3501, 2957, 2863, 1715, 1455, 1361, 1174, 1104, 736, 698; δ_H (500 MHz, C_6D_6) (* indicates diastereomer signals) 7.16 – 7.07 (4H, m), 7.07 – 7.01 (1H, m), 5.15 – 5.02 (1H, m), 4.16 – 4.04 (2H, m), 3.32 – 3.22 (1H, m), 3.15 – 3.03 (1H, m), 2.74 (1H, s)*, 2.56 (1H, s), 2.30 – 2.16 (1H, m), 2.11 – 1.99 (1H, m), 1.63 – 1.46 (1H, m), 1.45 – 1.36 (1H, m), 1.36 – 1.25 (1H, m), 1.23 (3H, m), 1.16 (3H, s)*, 1.15 – 1.05 (3H, m), 0.84 – 0.69 (3H, m); (Carbon count for the 2:1 mixture of diastereomers) δ_C (125 MHz, C_6D_6) 208.47, 207.74, 138.33, 138.20, 128.47, 128.45, 128.08, 127.88, 127.71, 127.69, 79.63, 79.44, 72.88, 72.84, 67.00, 66.89, 42.94, 42.67, 40.02, 39.37, 34.69, 34.42, 26.34, 25.79, 25.66, 25.26, 23.06, 13.98, 13.95; (ESI/MS) Calcd for m/z $[C_{17}H_{25}BrO_3Na]^+$: 379.1, 381.1 $[M+Na]^+$; found 379.1, 381.1.

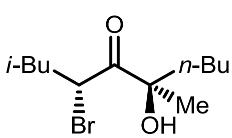 **4-bromo-6-hydroxy-2,6-dimethyldecan-5-one** (**S6.37**, Table 2, entry 11): 58 % (146 mg as a 3:1 mixture of diastereomers as indicated by ^{1}H NMR of the crude); IR ν_{max}(neat)/cm^{-1} 3508, 2958, 2872, 1716, 1467, 1370, 1172, 1060, 874, 774; δ_H (500 MHz, $CDCl_3$) (* indicates diastereomer signals) 4.86 (1H, dd, J = 9.2, 5.6 Hz), 4.83 (1H, dd, J = 9.2, 5.6 Hz)*, 3.03 (1H, s)*, 2.92 (1H, s), 1.96 – 1.85 (1H, m), 1.78 – 1.54 (4H, m), 1.44 (3H, s), 1.38 (3H,s)*, 1.42 – 1.32 (1H, m), 1.32 – 1.21 (2H, m), 1.17 – 1.07 (1H, m), 0.98 – 0.81 (9H, m); (Carbon count for the 3:1 mixture of diastereomers) δ_C (125 MHz, $CDCl_3$) 209.16, 208.44, 80.01, 79.92, 44.56, 44.08, 42.30, 42.24, 40.21,

39.67, 26.95, 26.21, 26.16, 25.94, 25.81, 25.75, 23.05, 23.04, 22.91, 22.88, 21.79, 14.10; (ESI/MS) Calcd for m/z $[C_{12}H_{23}BrO_2Na]^+$: 301.1, 303.1 $[M+Na]^+$; found 301.1, 303.1.

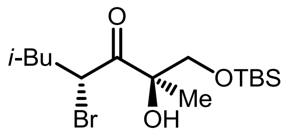

4-bromo-1-((tert-butyldimethylsilyl)oxy)-2-hydroxy-2,6-dimethylheptan-3-one (**S6.38**, Table 2, entry 12): 73% (268.1 mg as a 1.8:1 mixture of diastereomers as indicated by ^{1}H NMR of the crude); IR ν_{max}(neat)/cm^{-1} 3540, 2957, 2931, 2858, 1720, 1467, 1369, 1327, 1256, 1172, 1097, 1008, 941, 837, 779; δ_H (500 MHz, $CDCl_3$) (* indicates diastereomer signals) 5.04 (1H, dd, J = 9.3, 5.4 Hz), 4.94 (1H, dd, J = 8.6, 6.2 Hz)*, 4.03 (1H, d, J = 9.8 Hz)*, 3.91 (1H, d, J = 9.6 Hz), 3.58 (1H, s)*, 3.43 (1H, d, J = 9.6 Hz), 3.42 (1H, d, J = 9.6 Hz)*, 3.31 (1H, s), 1.92 – 1.81 (1H, m), 1.81 – 1.69 (1H, m), 1.69 – 1.61 (1H, m), 1.40 (3H, s), 1.24 (3H, s)*, 0.94 (3H, d, J = 6.6 Hz), 0.91 (3H, d, J = 6.6 Hz)*, 0.89 (3H, d, J = 6.6 Hz), 0.87 (9H, s)*, 0.86 (9H, s), 0.06 (3H, s), 0.05 (3H, s)*, 0.02 (3H, s); (Carbon count for the 1.8:1 mixture of diastereomers) δ_C (125 MHz, $CDCl_3$) 208.91, 207.37, 80.23, 80.05, 69.53, 68.36, 45.30, 44.49, 42.03, 41.78, 26.34,26.16, 26.06, 26.01, 23.74, 23.13, 22.83, 21.97, 21.91, 21.72, 18.49, 18.42, –5.21, –5.32, –5.36, –5.37; (ESI/MS) Calcd for m/z $[C_{15}H_{31}BrO_3SiNa]^+$: 389.1, 391.1 $[M+Na]^+$; found 389.1, 391.1.

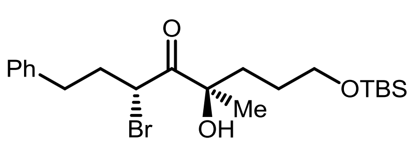

3-bromo-8-((tert-butyldimethylsilyl)oxy)-5-hydroxy-5-methyl-1-phenyloctan-4-one (**S6.39**, Table 2, entry 13): 74% (138.8 mg as a 3.5:1 mixture of diastereomers as indicated by ^{1}H NMR of the crude); IR ν_{max}(neat)/cm^{-1} 3508, 3351, 3027, 2929, 2857, 1715, 1602, 1496, 1455, 1362, 1255, 1097, 1030, 940, 835, 777, 662; δ_H (500 MHz, $CDCl_3$) (* indicates diastereomer signals) 7.32 – 7.26 (2H, m), 7.23 – 7.17 (3H, m), 4.98 (1H, ddd, J = 7.9, 6.5, 1.5 Hz)*, 4.90 (1H, ddd, J = 8.5, 5.6, 1.6 Hz), 4.44 (1H, s)*, 3.96 (1H, s), 3.64 – 3.55 (2H, m), 2.89 – 2.78 (1H, m), 2.72 – 2.62 (1H, m), 2.33 – 2.17 (2H, m), 1.95 – 1.85 (1H, m), 1.75 – 1.52 (3H, m), 1.43 (3H, s), 1.31 (3H, s)*, 0.92 (9H, d, J = 1.7 Hz)*, 0.90 (9H, d, J = 1.7 Hz), 0.09 – 0.05 (6H, m); (Carbon count for the 3.5:1 mixture of diastereomers) δ_C (125 MHz, $CDCl_3$) 209.56, 209.48, 140.51, 140.42, 128.80, 128.78, 128.63, 126.56, 126.52, 79.56, 79.38, 63.96, 63.70, 45.63, 45.57, 37.65, 37.45, 35.41, 35.28, 33.63, 33.50, 27.28, 27.13, 26.21, 26.17, 18.61, 18.56, –5.13, –5.14, –5.15, –5.17; (ESI/MS) Calcd for m/z $[C_{21}H_{35}BrO_3SiNa]^+$: 467.1, 465.1 $[M+Na]^+$; found 467.1, 465.1.

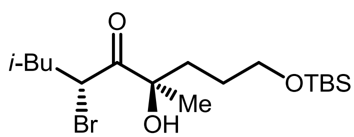

6-bromo-1-((tert-butyldimethylsilyl)oxy)-4-hydroxy-4,8-dimethylnonan-5-one (**S6.40**, Table 2, entry 14): 78% (221 mg as a 3.2:1 mixture of diastereomers as indicated by ^{1}H NMR of the crude); IR ν_{max}(neat)/cm^{-1} 3507, 2957, 2858, 1716, 1471, 1388, 1369, 1256, 1100, 814, 777; δ_H (500 MHz, C_6D_6) (* indicates diastereomer signals) 5.17 (1H, dd, J = 8.3, 6.7 Hz)*, 5.07 (1H, dd, J = 8.7, 6.0 Hz), 4.17 (1H, s)*, 3.43 – 3.23 (3H, m), 1.97 – 1.79 (2H, m), 1.79 – 1.38 (5H, m), 1.31 (3H, s), 1.22 (3H, s)*, 0.93 – 0.87 (9H, m), 0.74 – 0.67 (6H, m), -0.01 – -0.06 (6H, m); (Carbon count for the 3.2:1 mixture of diastereomers) δ_C (125 MHz, C_6D_6) 208.68, 208.64, 79.31, 79.08, 63.77, 63.49, 44.46, 44.43, 42.59, 42.40, 37.71, 37.43, 27.22, 27.11, 27.08, 26.36, 26.21, 26.07, 25.97, 25.94, 22.43, 22.30, 21.70, 21.56, 18.37, 18.32, -5.48, -5.57; (ESI/MS) Calcd for m/z $[C_{17}H_{35}BrO_3SiNa]^+$: 417.2, 419.2 $[M+Na]^+$; found 417.2, 419.2.

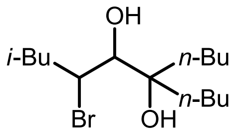 **4-bromo-6-butyl-2-methyldecane-5,6-diol** (**S6.42**, Table 3, entry 1): 83% (57.6 mg); To 4-bromo-6-butyl-6-hydroxy-2-methyldecan-5-one (0.215 mmol, 69.0 mg) in methanol (0.04 M) at 0°C was added $NaBH_4$ (0.238 mmol, 9.0 mg). Upon completion of reaction as judged by TLC (30 min), the reaction was quenched by careful addition of sat. aq. NH_4Cl. The reaction was then warmed to room temperature and to it was added dichloromethane. The organic layer was extracted in dichloromethane, dried over anhydrous Na_2SO_4, filtered, evaporated and purified by FCC to obtain 4-bromo-6-butyl-2-methyldecane-5,6-diol in 83% yield (57.6 mg). IR ν_{max}(neat)/cm^{-1} 3542, 2956, 2871, 1467, 1385, 1368, 1261, 1137, 1076, 1036; δ_H (500 MHz, $CDCl_3$) 4.27 (1H, dd, J = 9.5, 5.1 Hz), 3.32 (1H, d, J = 10.1 Hz), 2.78 (1H, d, J = 10.1 Hz), 2.21 (1H, s), 2.11 – 2.02 (1H, m), 1.91 – 1.81 (1H, m), 1.69 – 1.10 (13H, m), 0.99 – 0.86 (12H, m); δ_C (125 MHz, $CDCl_3$) 77.04, 74.52, 58.03, 46.13, 35.53, 35.16, 25.99, 25.83, 25.69, 23.49, 23.39, 22.91, 21.65, 14.28, 14.22; (ESI/MS) Calcd for m/z $[C_{15}H_{31}BrO_2Na]^+$: 345.1, 347.1 $[M+Na]^+$; found 345.1, 347.1.

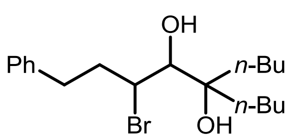 **3-bromo-5-butyl-1-phenylnonane-4,5-diol** (**S6.43**, Table 3, entry 2): 72% (48.2 mg); To 3-bromo-5-butyl-5-hydroxy-1-phenylnonan-4-one (0.180 mmol, 66.5 mg) in methanol (0.04 M) at 0°C was added $NaBH_4$ (0.198 mmol, 7.5 mg). Upon completion of reaction as judged by TLC (30 min), the reaction was quenched by careful addition of sat. aq. NH_4Cl. The reaction was then warmed to room temperature and to it was added dichloromethane. The organic layer was extracted in dichloromethane, dried

over anhydrous Na_2SO_4, filtered, evaporated and purified by FCC to obtain 4-bromo-6-butyl-2-methyldecane-5,6-diol in 72% yield (48.2 mg). IR ν_{max}(neat)/cm^{-1} 3542, 3085, 3062, 3026, 2955, 1603, 1496, 1455, 1379, 1263, 1230, 1134, 1088, 1030, 1002, 910; δ_H (400 MHz, $CDCl_3$) 7.33 – 7.27 (2H, m), 7.21 (3H, dd, *J* = 10.6, 4.1 Hz), 4.12 – 4.06 (1H, m), 3.34 (1H, s), 2.90 (1H, ddd, *J* = 13.6, 7.8, 5.5 Hz), 2.83 (1H, s), 2.82 – 2.73 (1H, m), 2.45 (1H, dddd, *J* = 13.5, 9.4, 8.0, 5.4 Hz), 2.25 – 2.15 (1H, m), 2.08 (1H, s), 1.63 – 1.54 (2H, m), 1.49 (1H, ddd, *J* = 13.8, 11.3, 5.5 Hz), 1.42 – 1.13 (8H, m), 0.99 – 0.93 (1H, m), 0.91 (3H, t, *J* = 7.3 Hz), 0.84 (3H, t, *J* = 7.3 Hz); δ_C (100 MHz, $CDCl_3$) 140.64, 128.77, 128.73, 126.47, 76.92, 74.75, 58.67, 38.77, 35.57, 35.20, 33.46, 25.83, 25.57, 23.42, 23.39, 14.30, 14.15; (ESI/MS) Calcd for *m*/*z* $[C_{19}H_{31}BrO_2Na]^+$: 393.1, 395.1 $[M+Na]^+$; found 393.1, 395.1.

7.7 References

1. Katukojvala, S.; Barlett, K. N.; Lotesta, S. D.; Williams, L. J. *J. Am. Chem. Soc.* **2004**, *126*, 15348.
2. Ghosh, P.; Lotesta, S. D.; Williams, L. J. *J. Am. Chem. Soc.* **2007**, *129*, 2438.
3. Ghosh, P.; Cusick, J. R.; Inghrim, J.; Williams, L. J. *Org. Lett.* **2009**, *11*, 4672.
4. Corey, E. J.; Boaz, N. W. *Tetrahedron Lett.* **1984**, *25*, 3055.
5. Murray, R. W.; Jeyaraman, R. *J. Org. Chem.* **1985**, *50*, 284.
6. Lotesta, S. D.; Kiren, S. K.; Sauers, R. R.; Williams, L. J. *Angew. Chem. Int. Ed.* **2007**, *46*, 15.
7. Gilbert, M.; Ferrer, M.; Sanchez-Baeza, F.; Messeguer, A. *Tetrahedron* **1997**, *53*, 8643.
8. Ferrer, M.; Gilbert, M.; Sandez-Baeza, F.; Messeguer, A. *Tetrahedron Lett.*. **1996**, *37*, 3585.
9. Crandall, J. K.; Batal, D. J.; Lin, F.; Reix, T.; Nadol, G. S.; Ng, R. A. *Tetrahedron* **1992**, *48*, 1427.
10. Ye, L.; He, W.; Zhang, L. *J. Am. Chem. Soc.* **2010**, *132*, 8550.
11. Crandall, J. K.; Batal, D. J.; Sebesta, D. P.; Lin, F. *J. Org. Chem.* **1991**, *56*, 1153.
12. Frisch, M. J.; Trucks, G. W.; Schlegel, H. B.; Scuseria, G. E.; Robb, M. A.; Cheeseman, J.R.; Montgomery, J. A. Jr.; Vreven, T.; Kudin, K. N.; Burant, J. C.; Millam, J. M.; Iyengar, S.S.; Tomasi, J.; Barone, V.; Mennucci, B.; Cossi, M.; Scalmani, G.; Rega, N.; Petersson, G.A.; Nakatsuji, H.; Hada, M.; Ehara, M.; Toyota, K.; Fukuda, R.; Hasegawa, J.; Ishida, M.; Nakajima, T.; Honda, Y.; Kitao, O.; Nakai, H.; Klene, M.; Li, X.; Knox, J. E.; Hratchian,H. P.; Cross, J. B.; Adamo, C.;

Jaramillo, J.; Gomperts, R.; Stratmann, R. E.; Yazyev, O.; Austin, A. J.; Cammi, R.; Pomelli, C.; Ochterski, J. W.; Ayala, P. Y.; Morokuma, K.; Voth, G. A.; Salvador, P.; Dannenberg, J. J.; Zakrzewski, V. G.; Dapprich, S.; Daniels, A. D.; Strain, M. C.; Farkas, O.; Malick, D. K.; Rabuck, A. D.; Raghavachari, K.; Foresman, J. B.; Ortiz, J. V.; Cui, Q.; Baboul, A. G.; Clifford, S.; Cioslowski, J.; Stefanov, B. B.; Liu, G.; Liashenko, A.; Piskorz, P.; Komaromi, I.; Martin, R. L.; Fox, D. J.; Keith, T.; Al-Laham, M. A.; Peng, C. Y.; Nanayakkara, A.; Challacombe, M.; Gill, P. M. W.; Johnson B.; Chen,W.; Wong, M. W.; Gonzalez, C.; Pople, J. A.: Gaussian, Inc.: Pittsburgh, 2003.

13. Becke, A. D. J. Chem. Phys. 1993, 98, 5648; Lee, C.; Yang, W.; Parr, R. G. *Phys. Rev.B*. **1988**, *37*, 785.
14. a) Ditchfield, R.; Hehre, W. J.; Pople, J. A. *J. Chem. Phys.* **1971**, *54*, 721; b) Hariharan, P. C.; Pople, J. A. *Mol. Phys.* **1974**, *27*, 209; c) Krishnan, R.; Binkley, J. S.; Seeger, R.; Pople, J. A. *J. Chem. Phys.* **1980**, *72*, 650; d) McLean, A. D.; Chandler, G. S. *J. Chem. Phys.* **1980**, *72*, 5639; e) Clark, T.; Chandrasekhar, J.; Spitznagel, G. W.; Schleyer, P.v.R. *J. Comp. Chem.* **1983**, *4*, 294.
15. Gravestock, M. B.; Knight, D. W.; Lovell, J. S.; Thornton, S. R. *J. Chem. Soc., Perkin Trans. 1* **1999**, *21*, 3143.
16. Nakanishi, A.; Mori, K. *Biosci. Biotechnol. Biochem.* **2005**, *69*, 1007.
17. Covell, D. J.; Vermeulen, N. A.; Labenz, N. A.; White, M. C. *Angew. Chem. Int. Ed.* **2006**, *45*, 8217.
18. Tokunaga, M.; Larrow, J. F.; Kakiuchi, F.; Jacobsen, E. N. *Science* **1997**, *277*, 936.

19. Fürstner, A.; Bouchez, L. C.; Morency, L.; Funel, J. A.; Liepins, V.; Porée, F. H.; Gilmour, R.; Laurich, D.; Beaufils, F.; Tamiya, M *Chem. Eur. J.* **2009**, *15*, 3983.

20. Vicario, J. L.; Job, A.; Wolberg, M.; Mu1ller, M.; Enders, D. *Org. Lett.* **2002**, *4*, 1023.

21. Matsumura, K.; Hashiguchi, S.; Ikariya, T.; Noyori, R. *J. Am. Chem. Soc.* **1997**, *119*, 8738.

22. Cossi, M.; Barone, V. *J. Phys. Chem. A* **1998**, *102*, 1995.

Appendix: Selected ^{1}H and ^{13}C NMR Spectra

^1H NMR (500 MHz, $CDCl_3$)

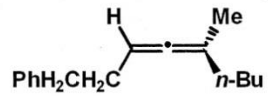

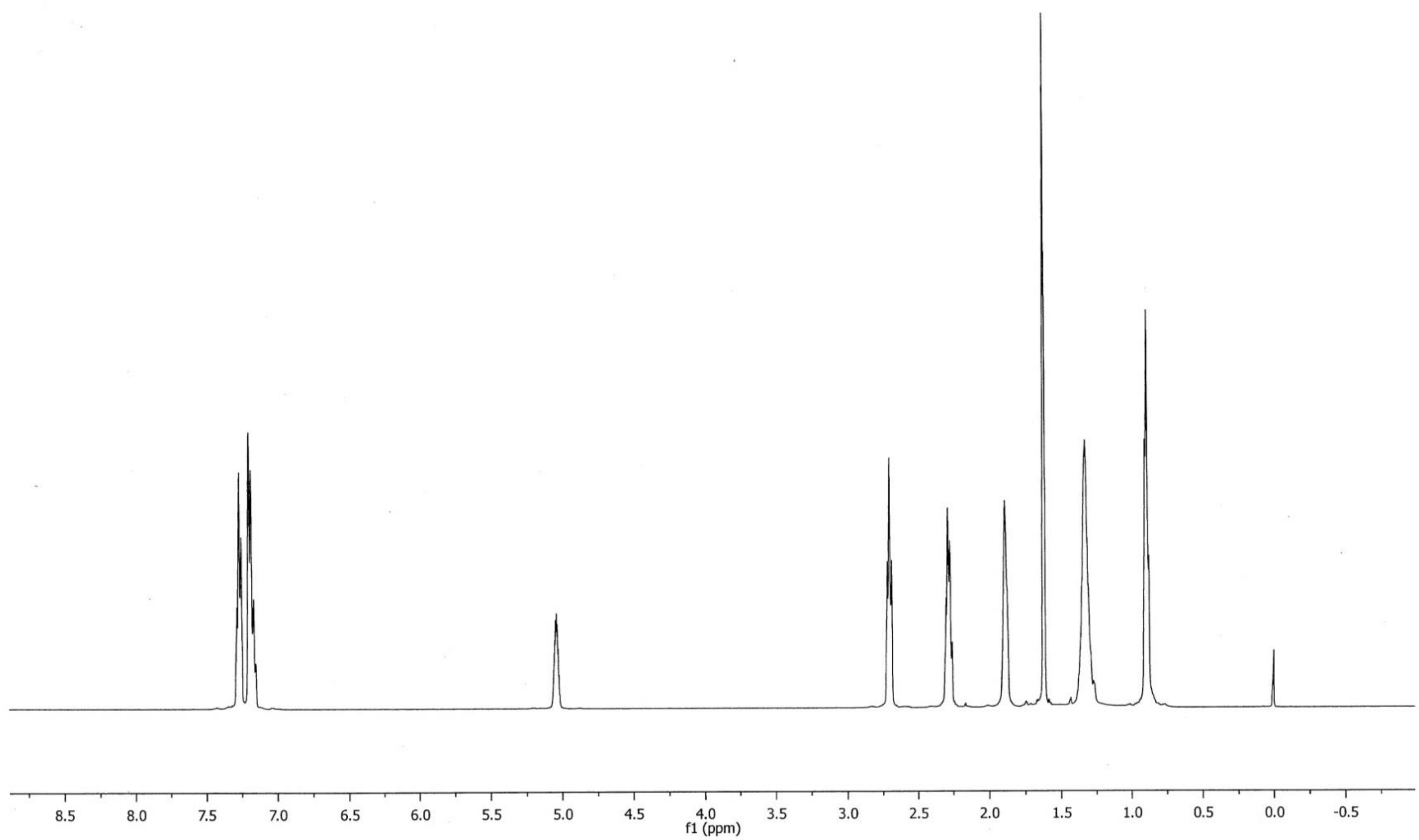

^{13}C NMR (125 MHz, $CDCl_3$)

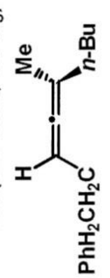

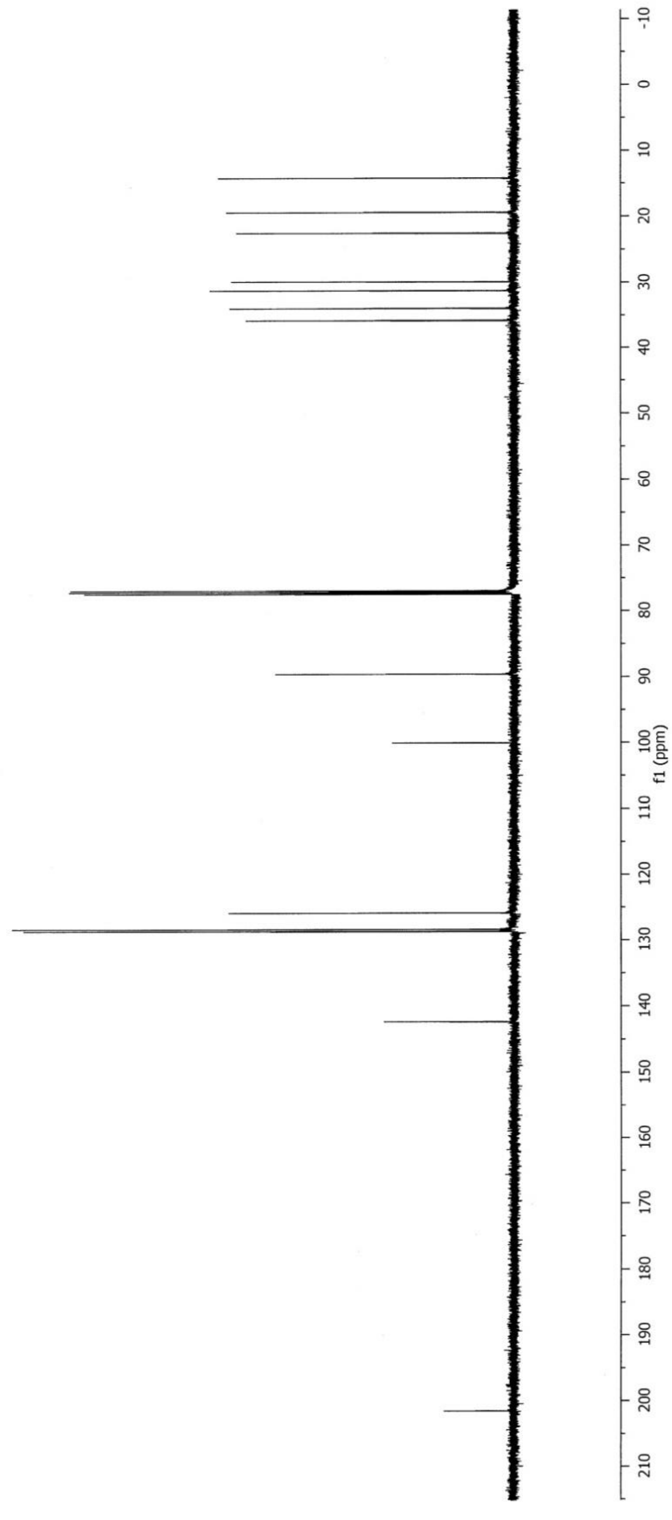

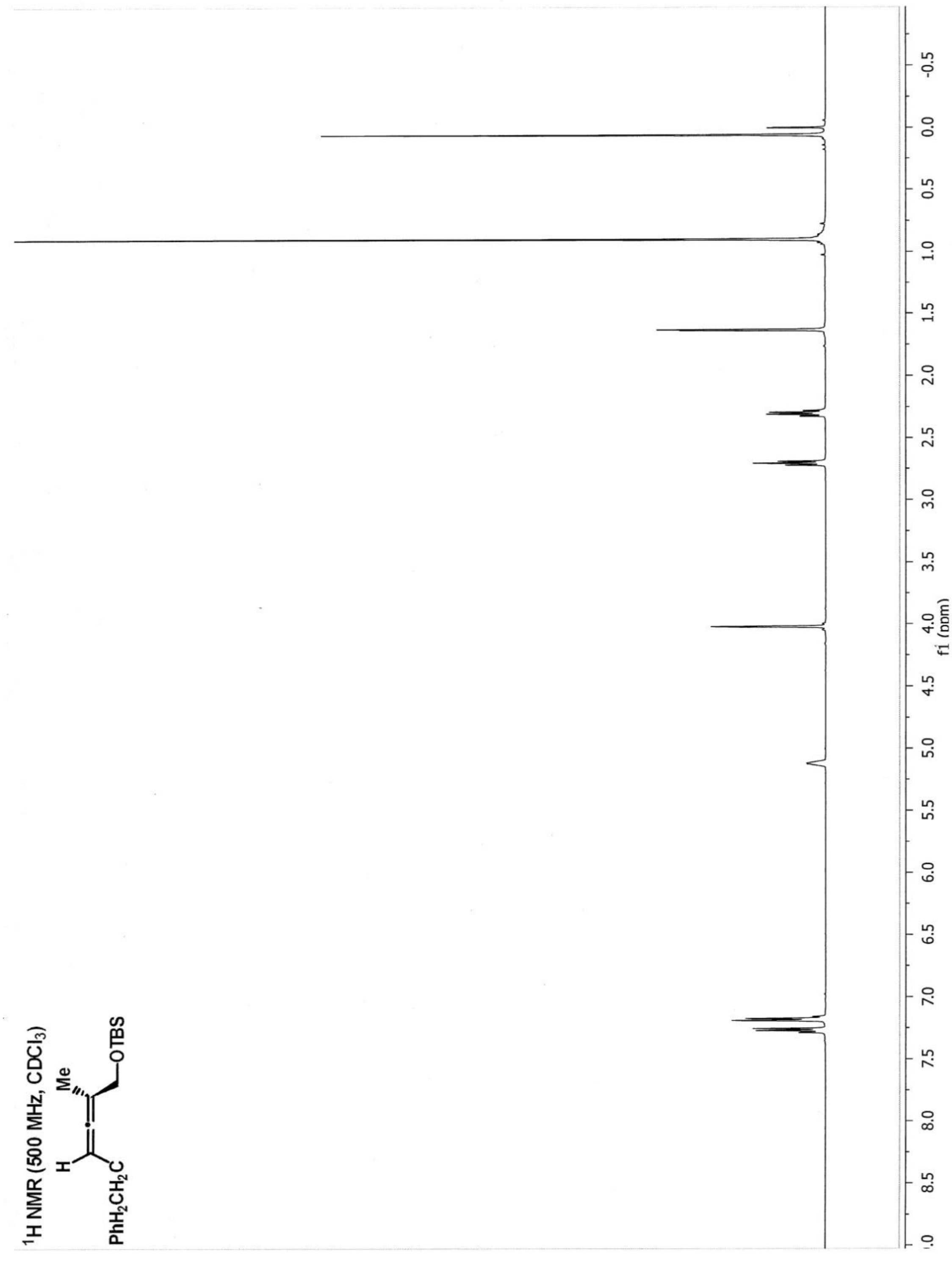

^1H NMR (500 MHz, $CDCl_3$)
H
Me
PhH_2CH_2C
OTBS
-0.5
0.0
0.5
1.0
1.5
2.0
2.5
3.0
3.5
4.0
4.5
5.0
5.5
6.0
6.5
7.0
7.5
8.0
8.5
f1 (ppm)

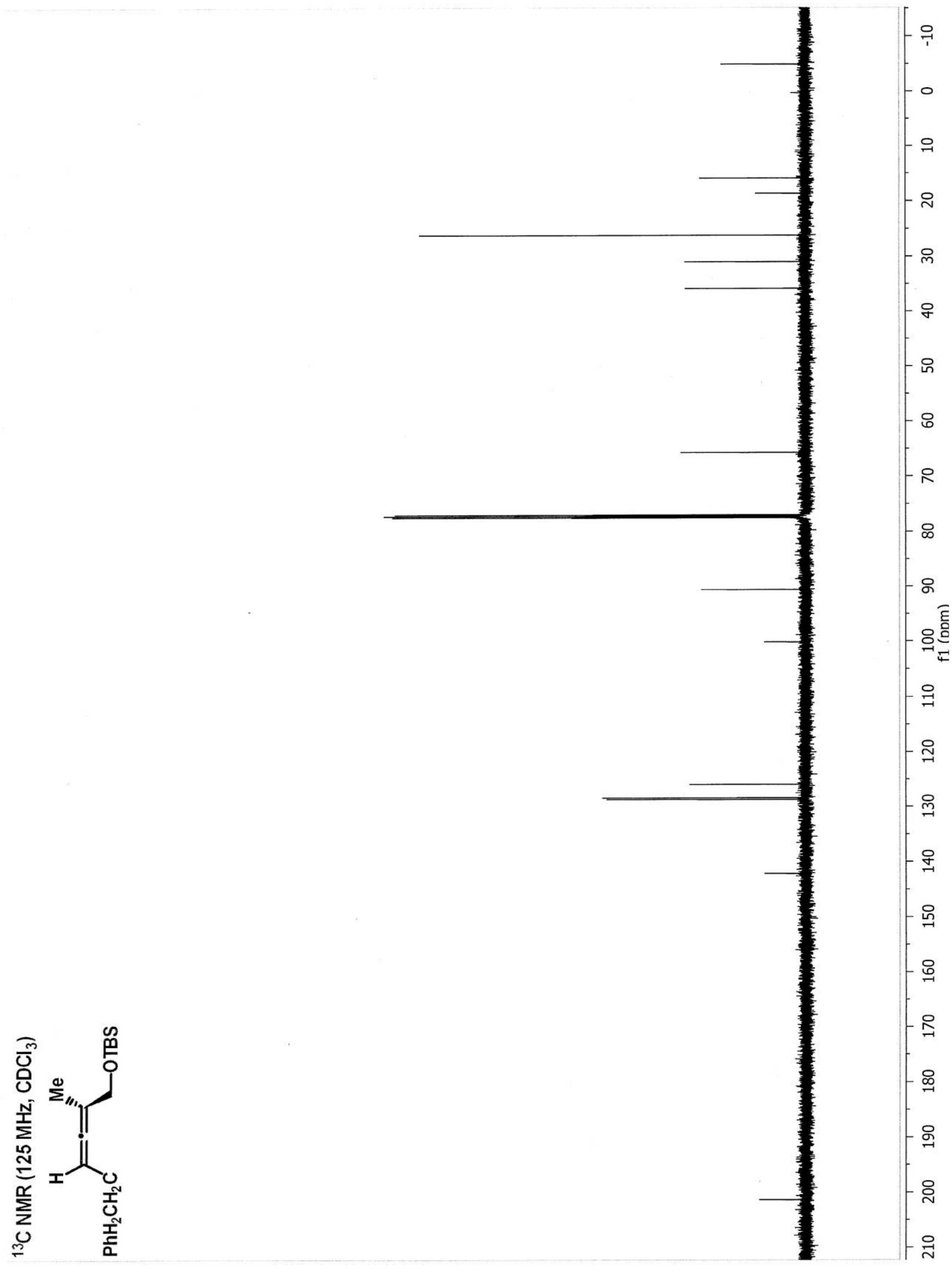

13C NMR (125 MHz, CDCl3)
H
Me
PhH2CH2C
OTBS
f1 (ppm)
210 200 190 180 170 160 150 140 130 120 110 100 90 80 70 60 50 40 30 20 10 0 -10

^1H NMR (500 MHz, $CDCl_3$)

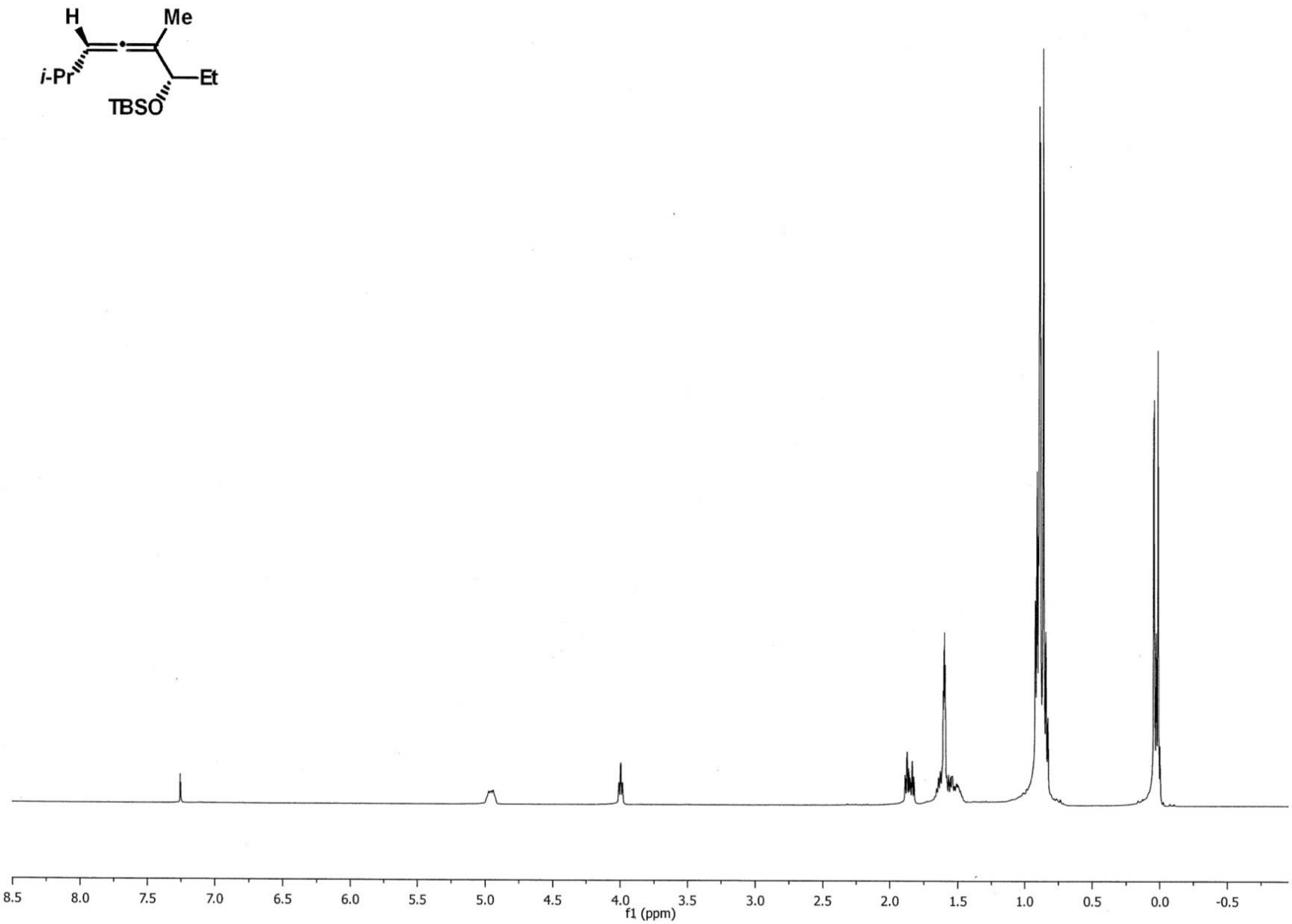

^{13}C NMR (125 MHz, $CDCl_3$)

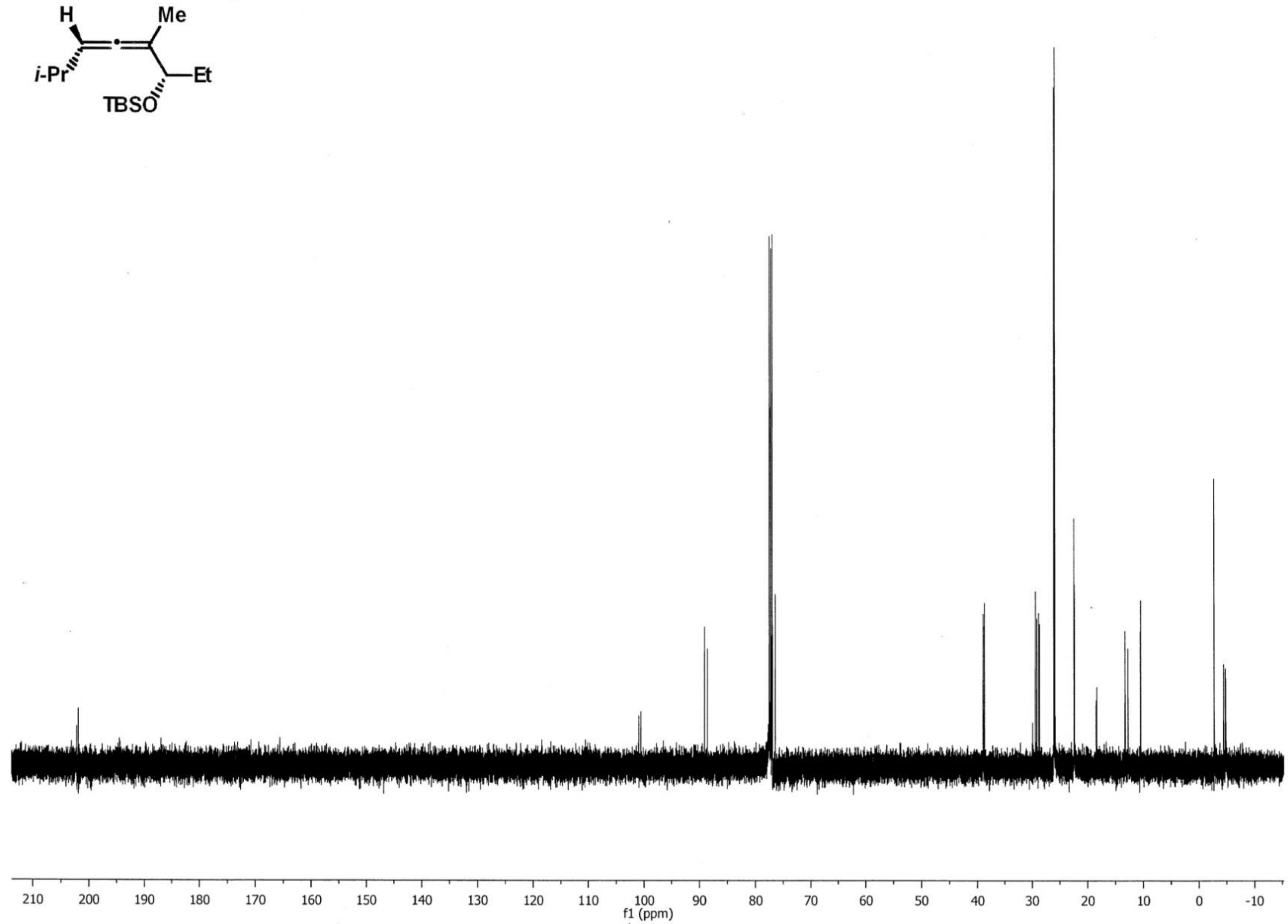

¹H NMR (400 MHz, $CDCl_3$)

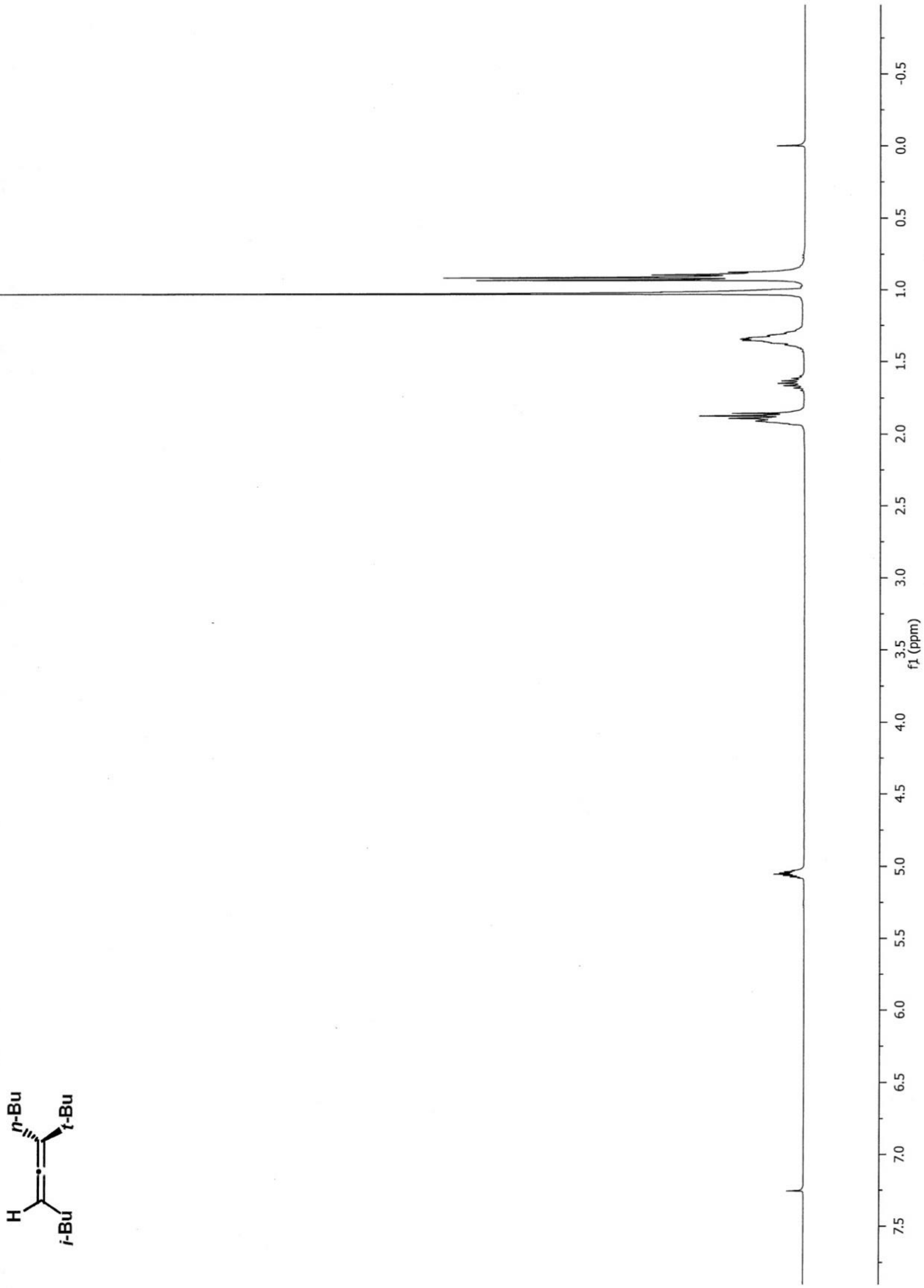

^{13}C NMR (100 MHz, $CDCl_3$)

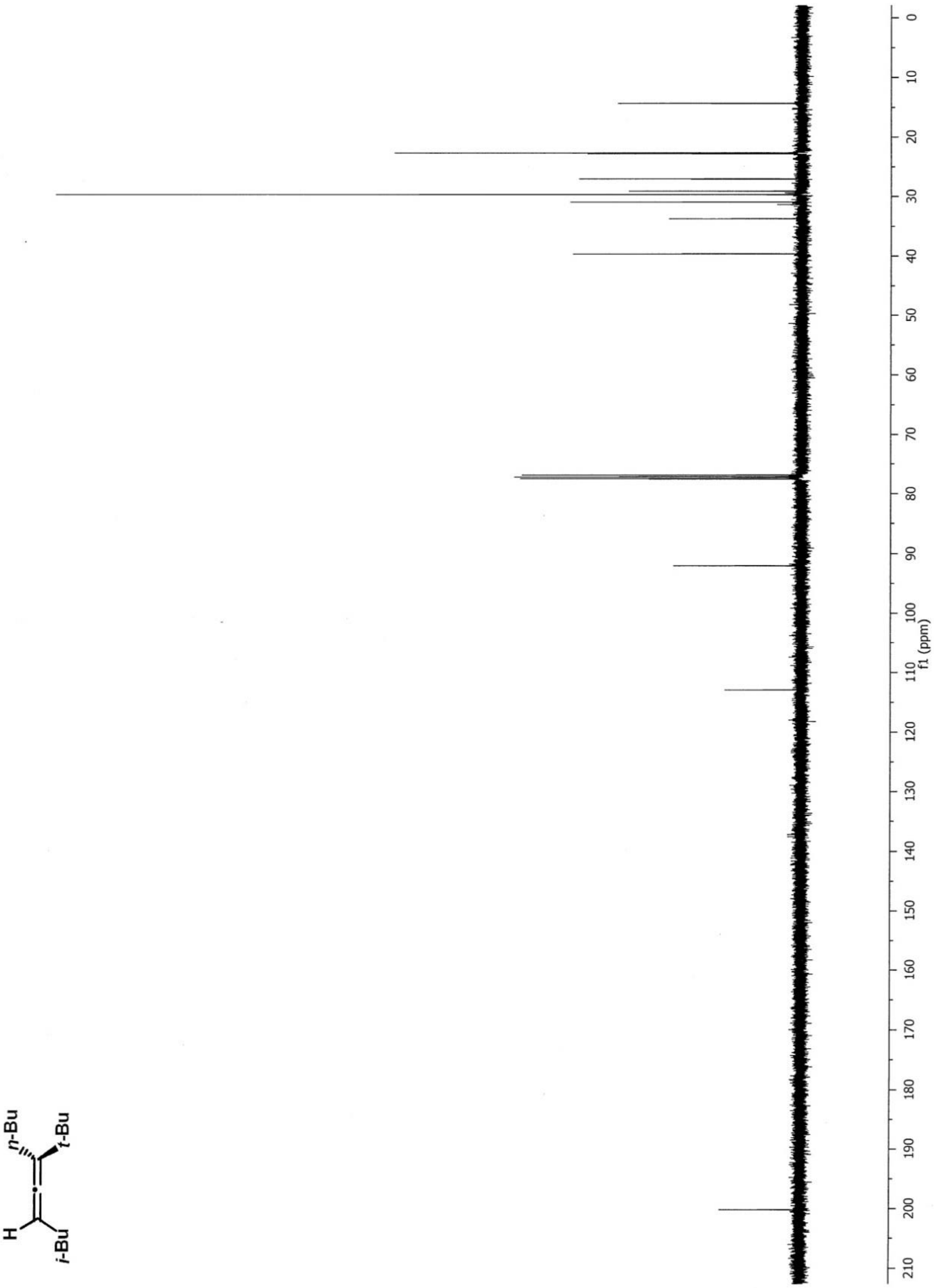

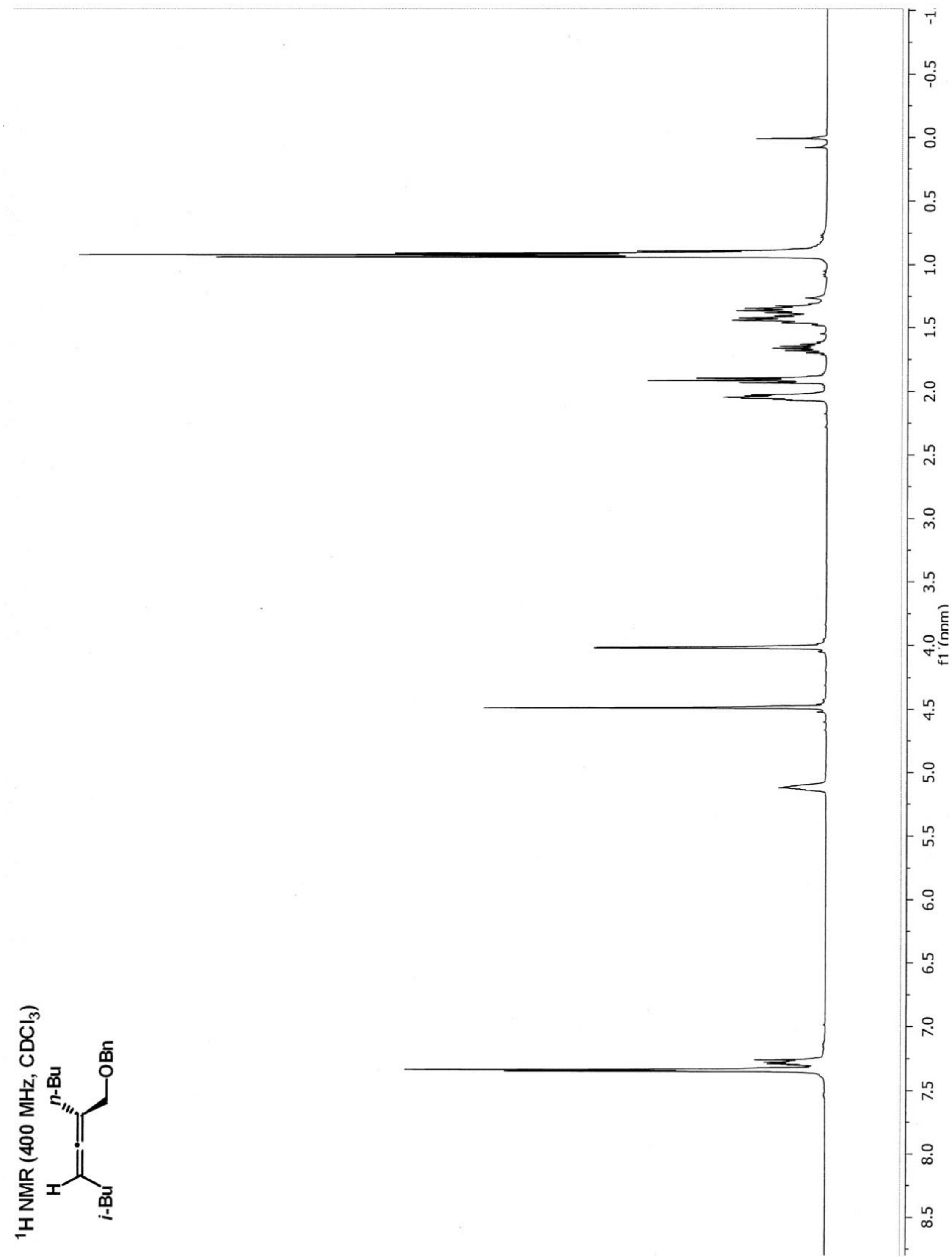

^{1}H NMR (400 MHz, CDCl$_3$)
H
n-Bu
OBn
i-Bu
f1 (ppm)

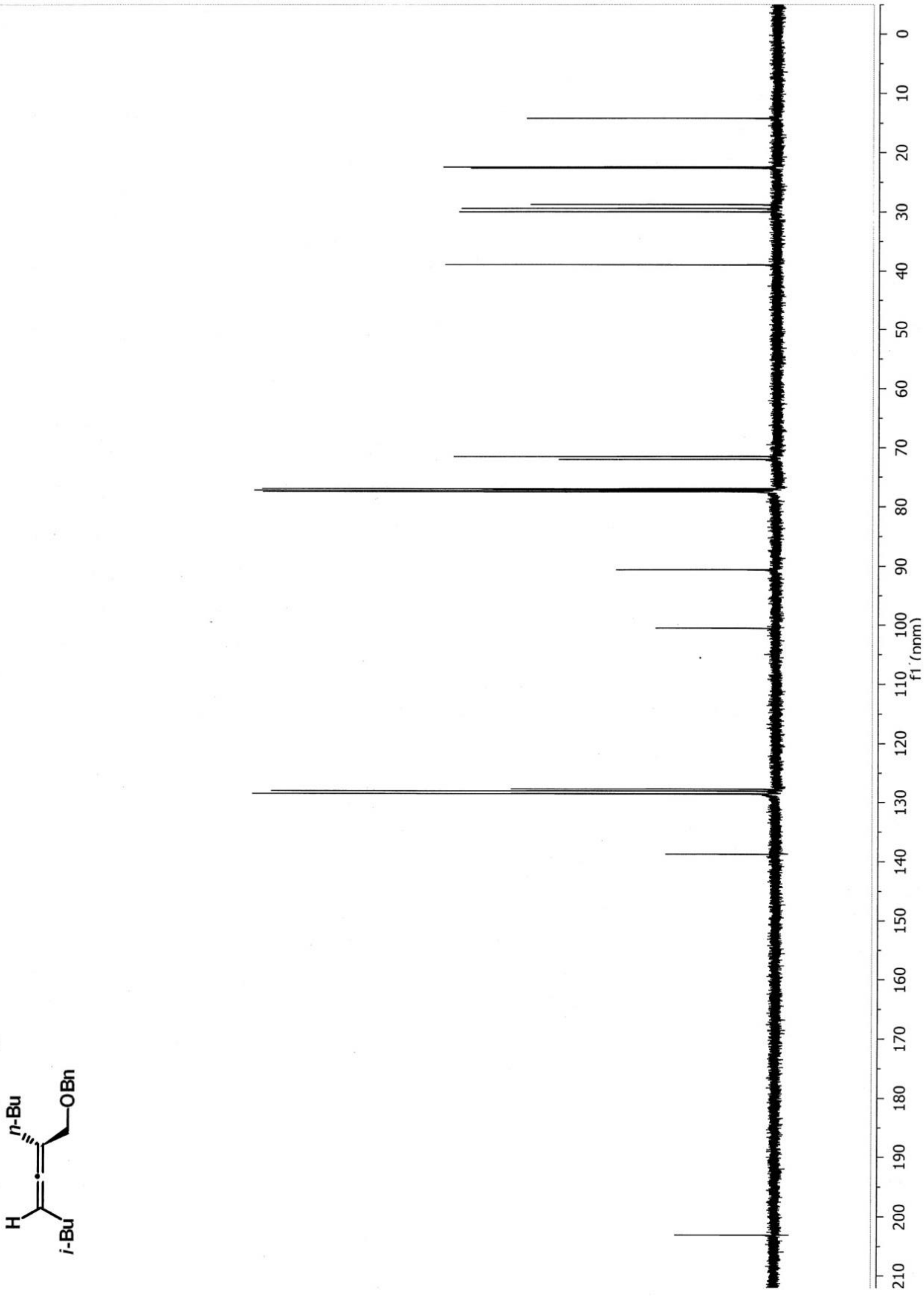

^{13}C NMR (125 MHz, $CDCl_3$)

^1H NMR (500 MHz, $CDCl_3$)

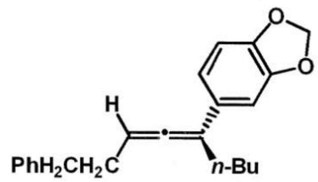

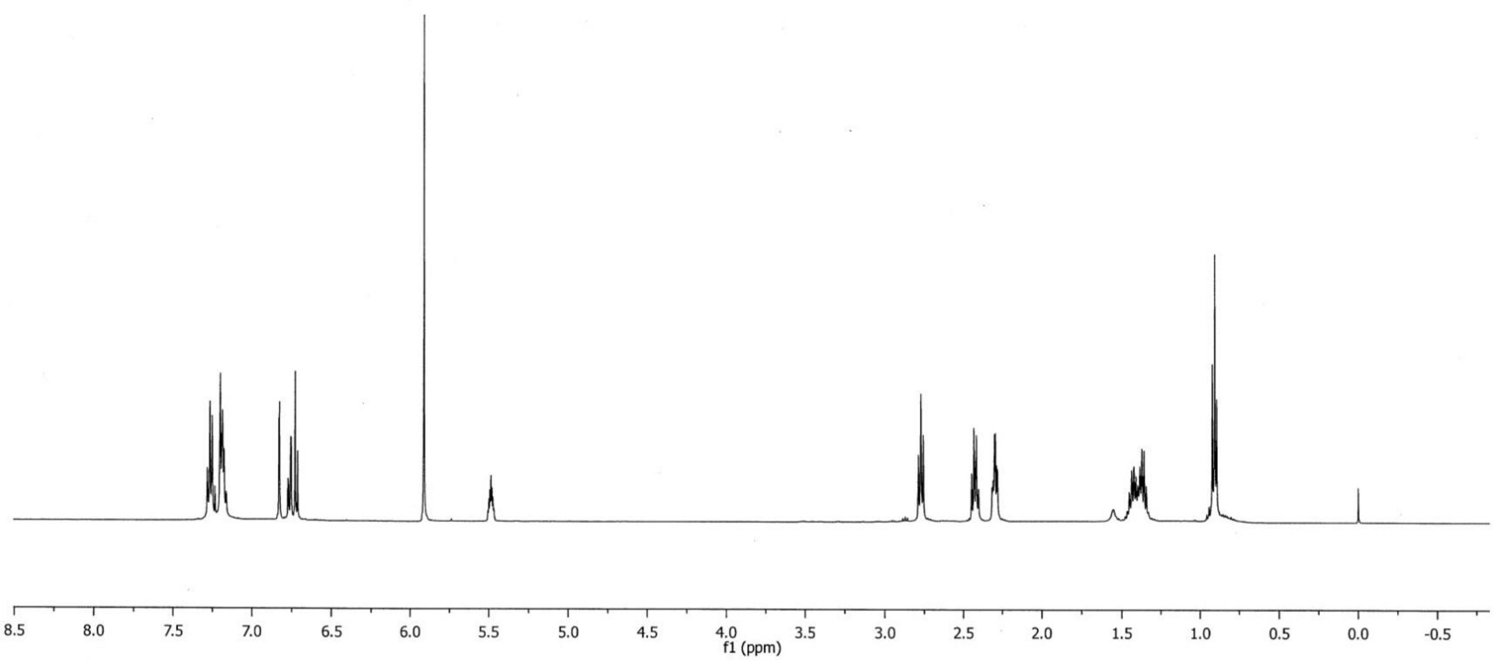

^{13}C NMR (125 MHz, $CDCl_3$)

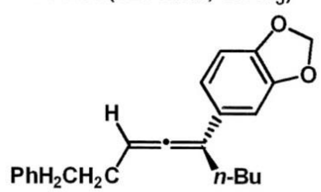

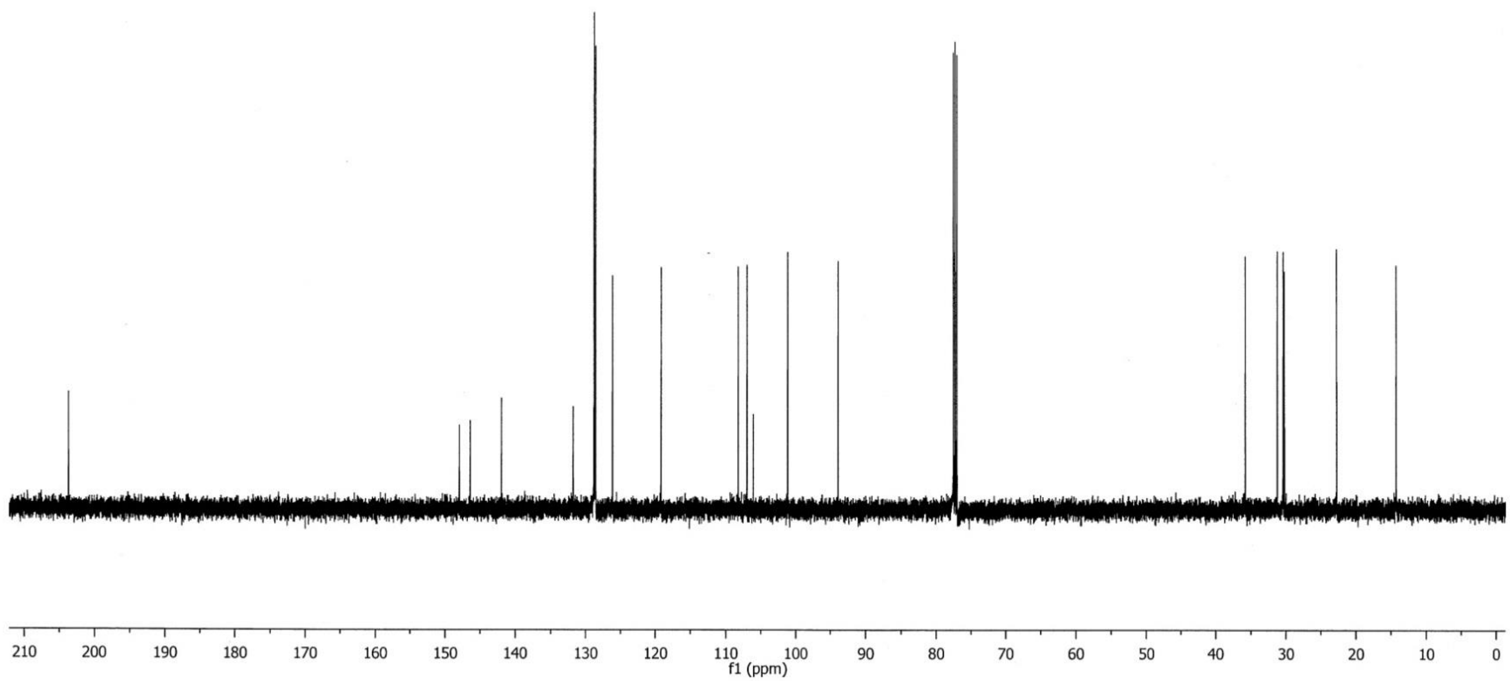

^1H NMR (500 MHz, $CDCl_3$)

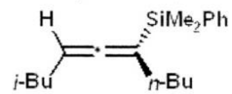

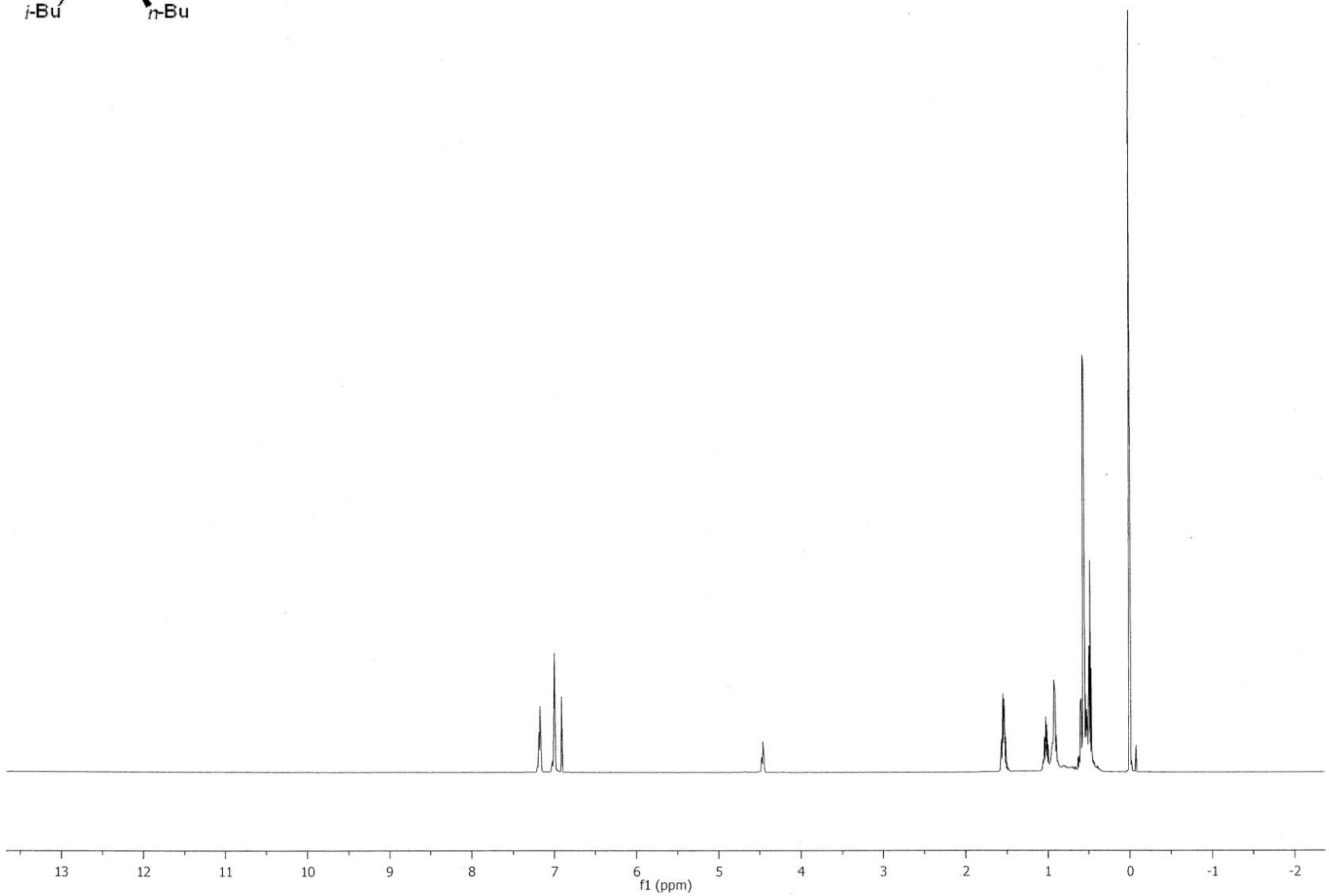

^{13}C NMR (125 MHz, $CDCl_3$)

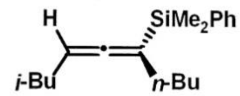

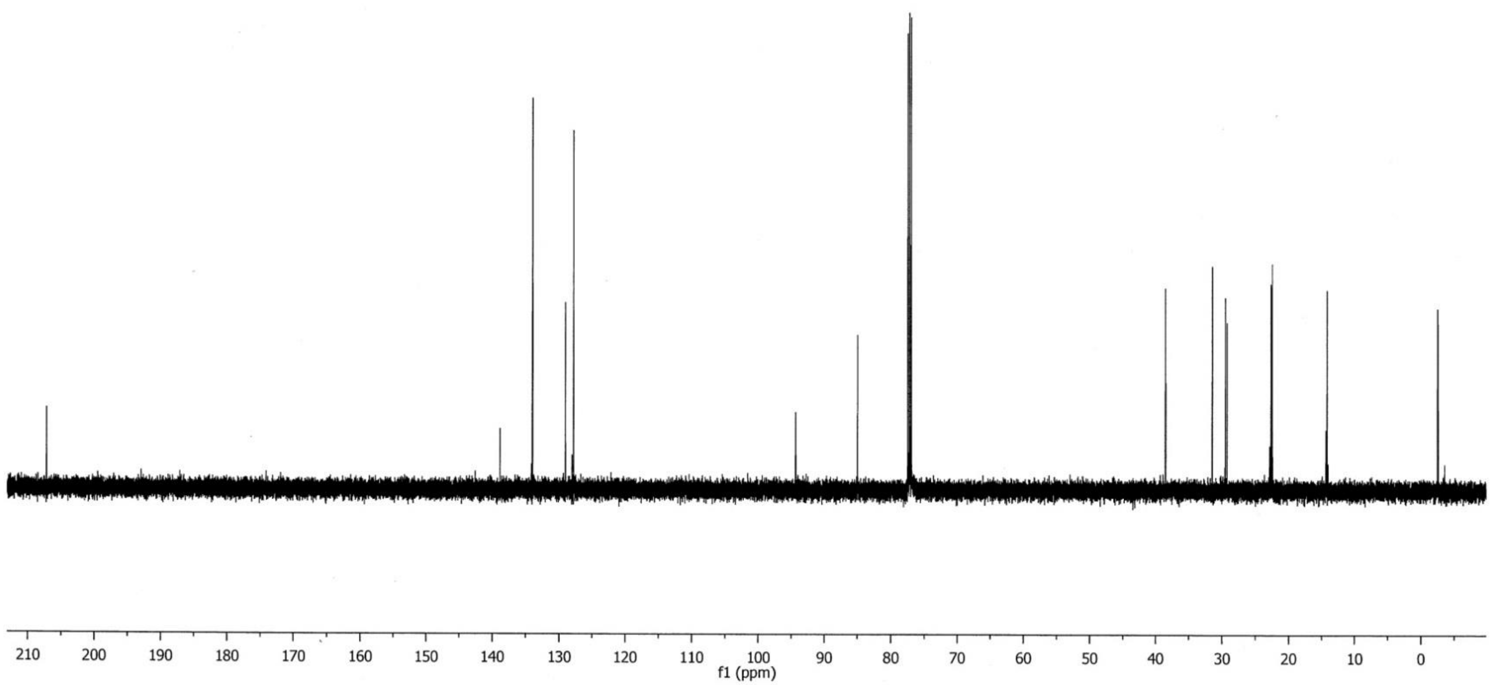

^1H NMR (500 MHz, $CDCl_3$)

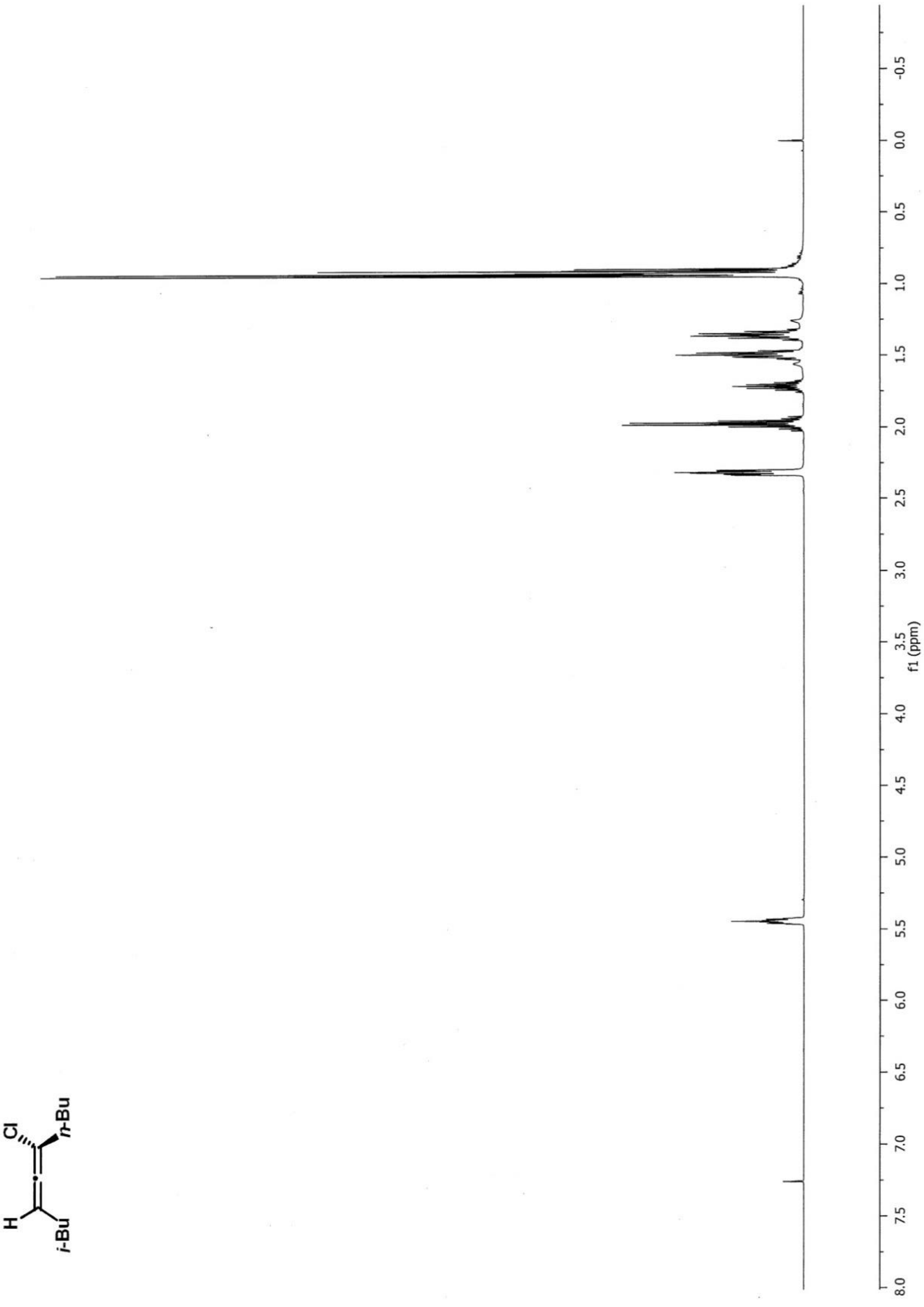

^{13}C NMR (125 MHz, $CDCl_3$)

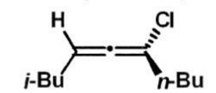

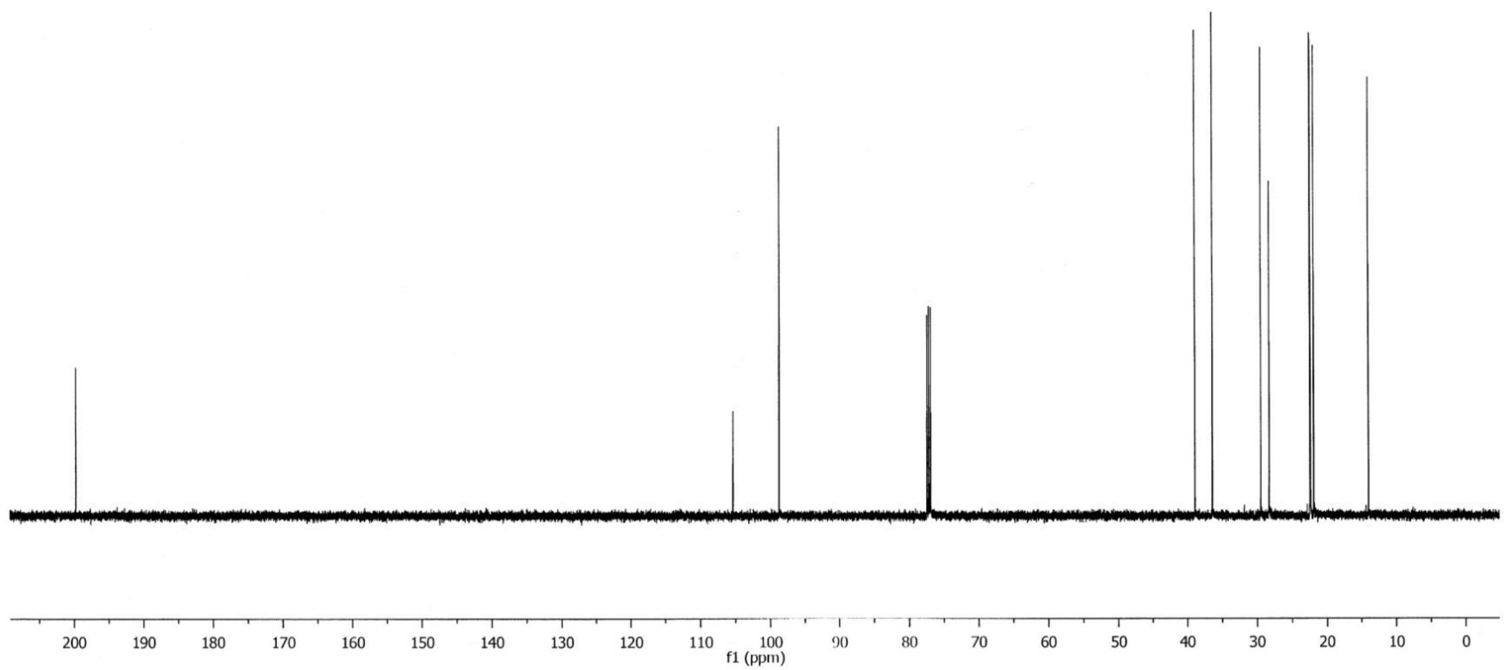

^1H NMR (500 MHz, $CDCl_3$)

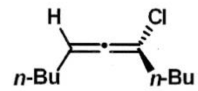

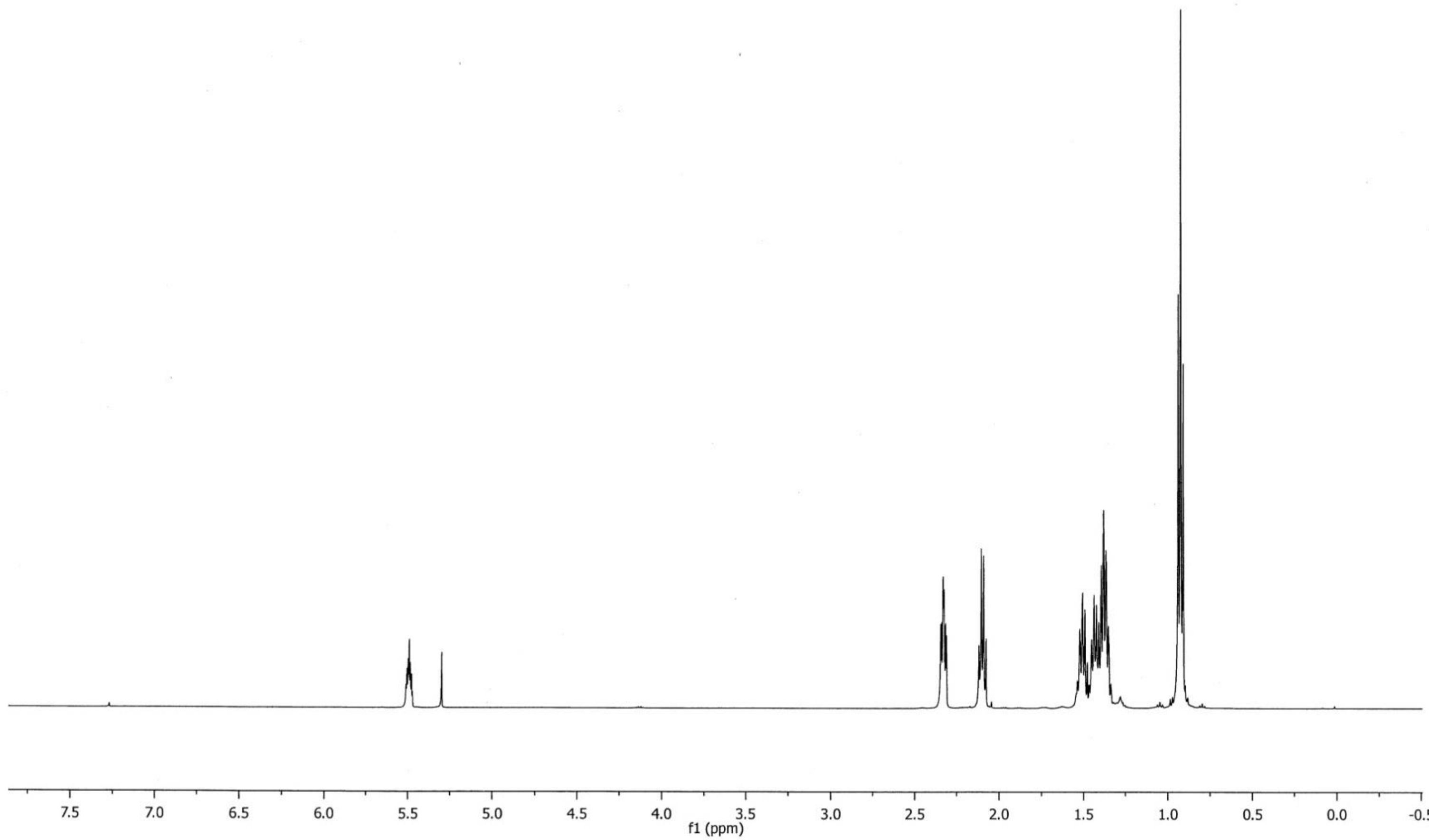

^{13}C NMR (125 MHz, $CDCl_3$)

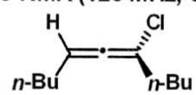

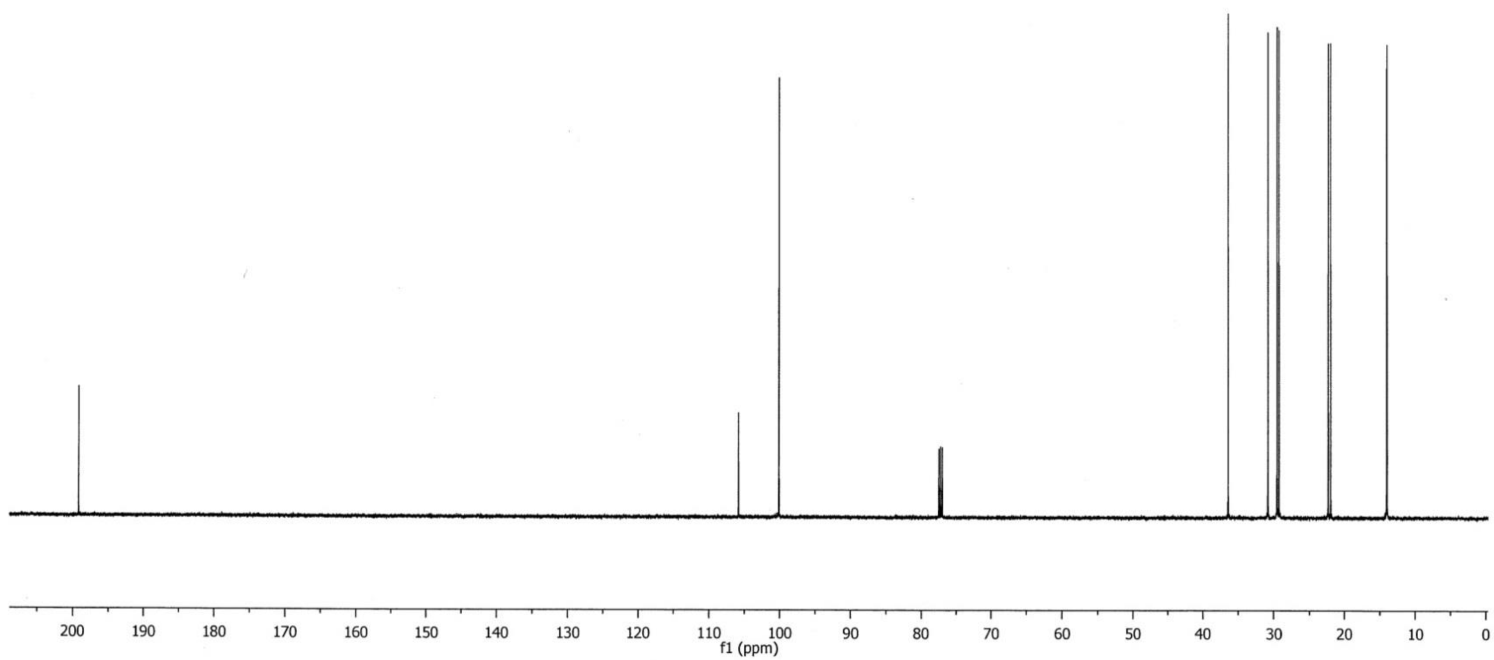

^1H NMR (500 MHz, $CDCl_3$)

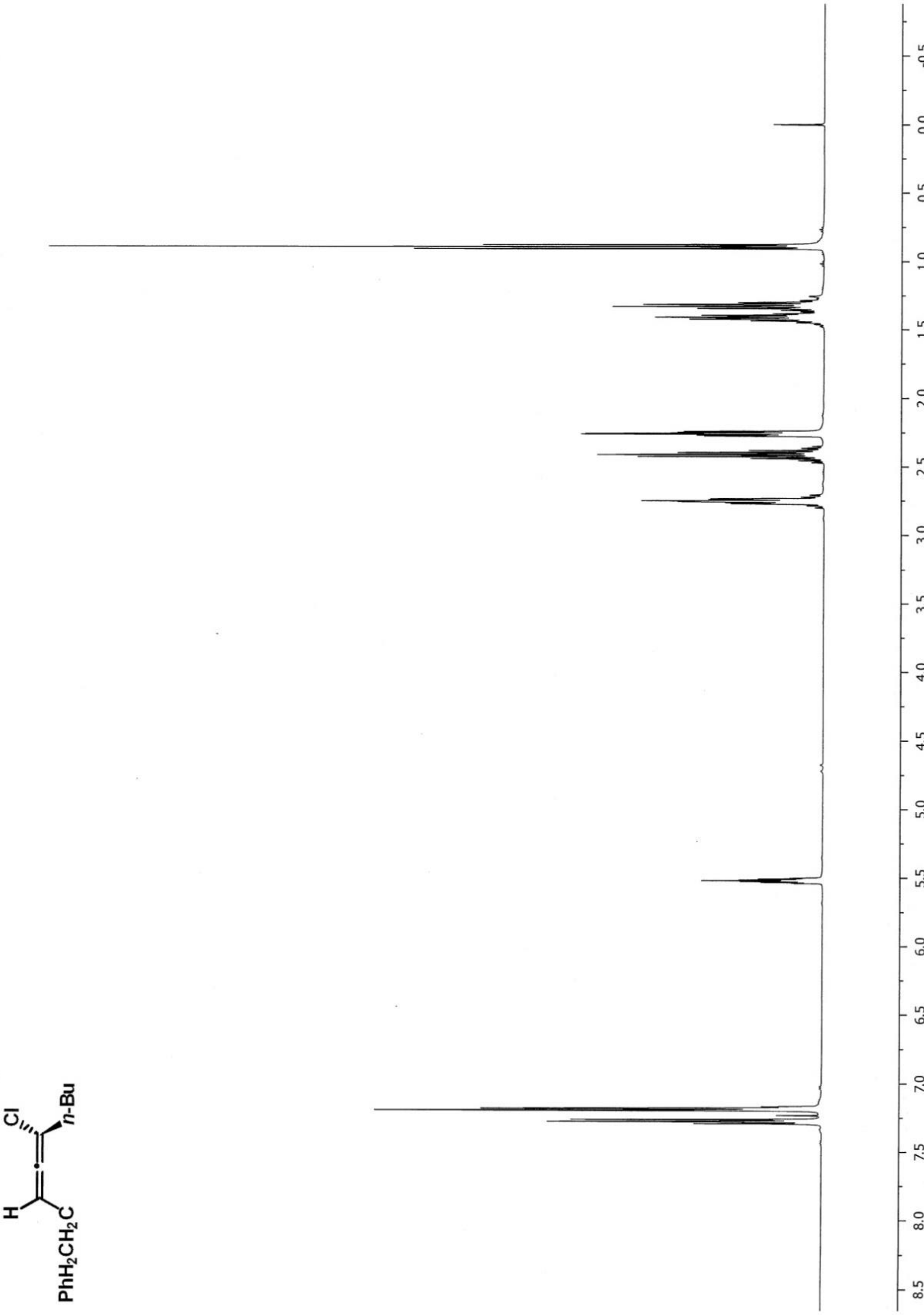

^{13}C NMR (125 MHz, $CDCl_3$)

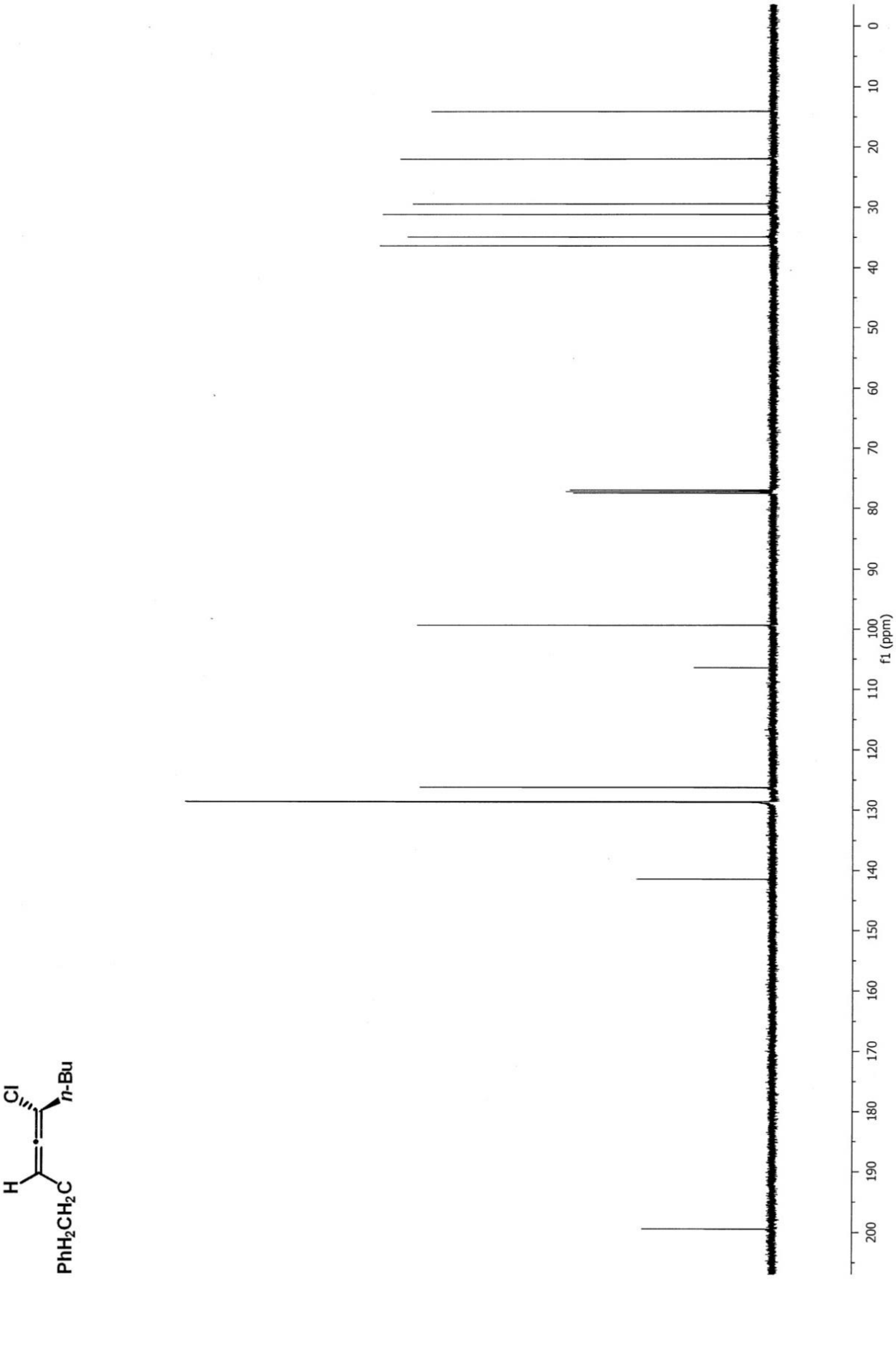

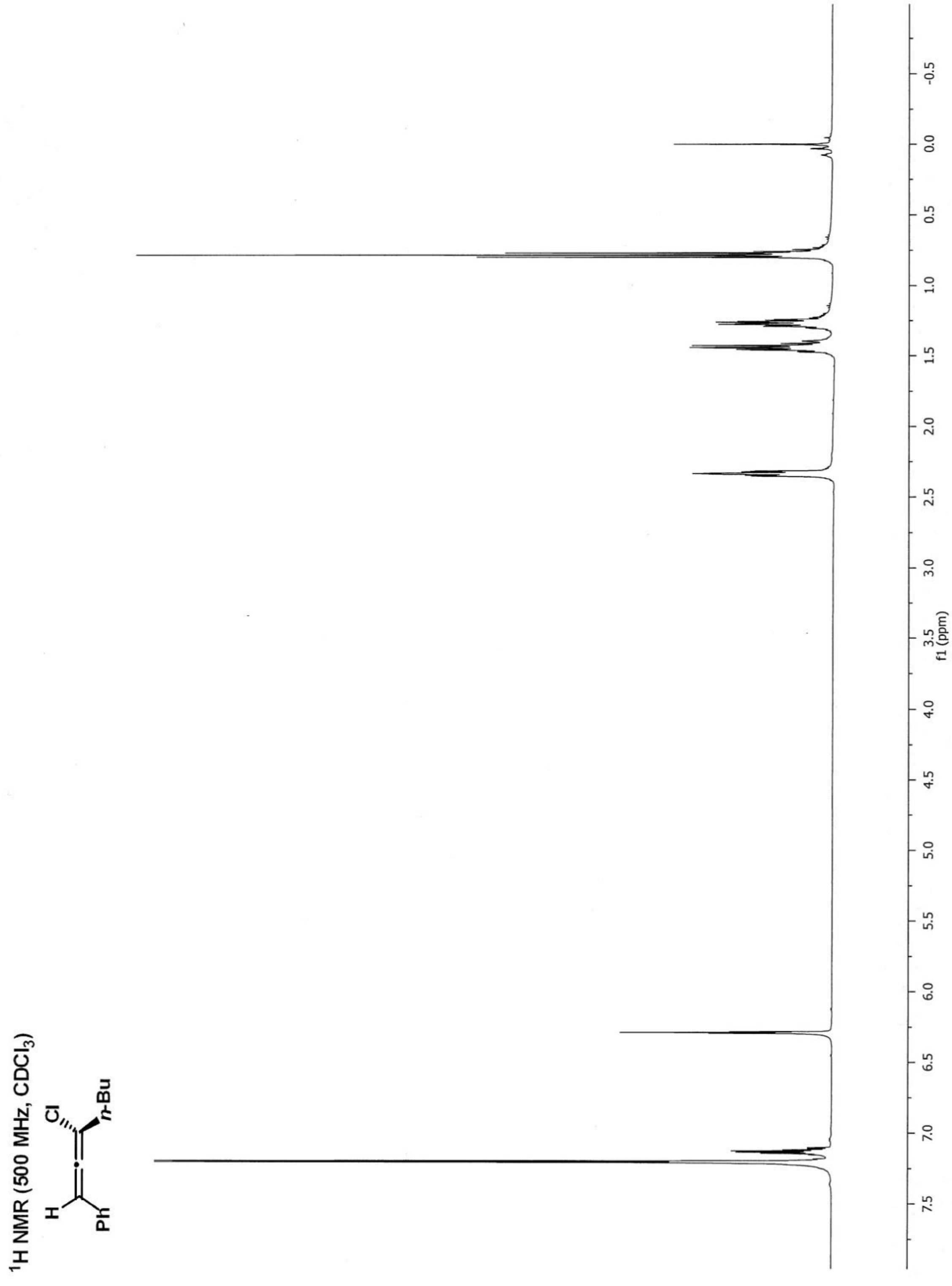

^1H NMR (500 MHz, $CDCl_3$)
H
Ph
Cl
n-Bu
f1 (ppm)
7.5
7.0
6.5
6.0
5.5
5.0
4.5
4.0
3.5
3.0
2.5
2.0
1.5
1.0
0.5
0.0
-0.5

^{13}C NMR (125 MHz, $CDCl_3$)

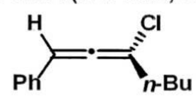

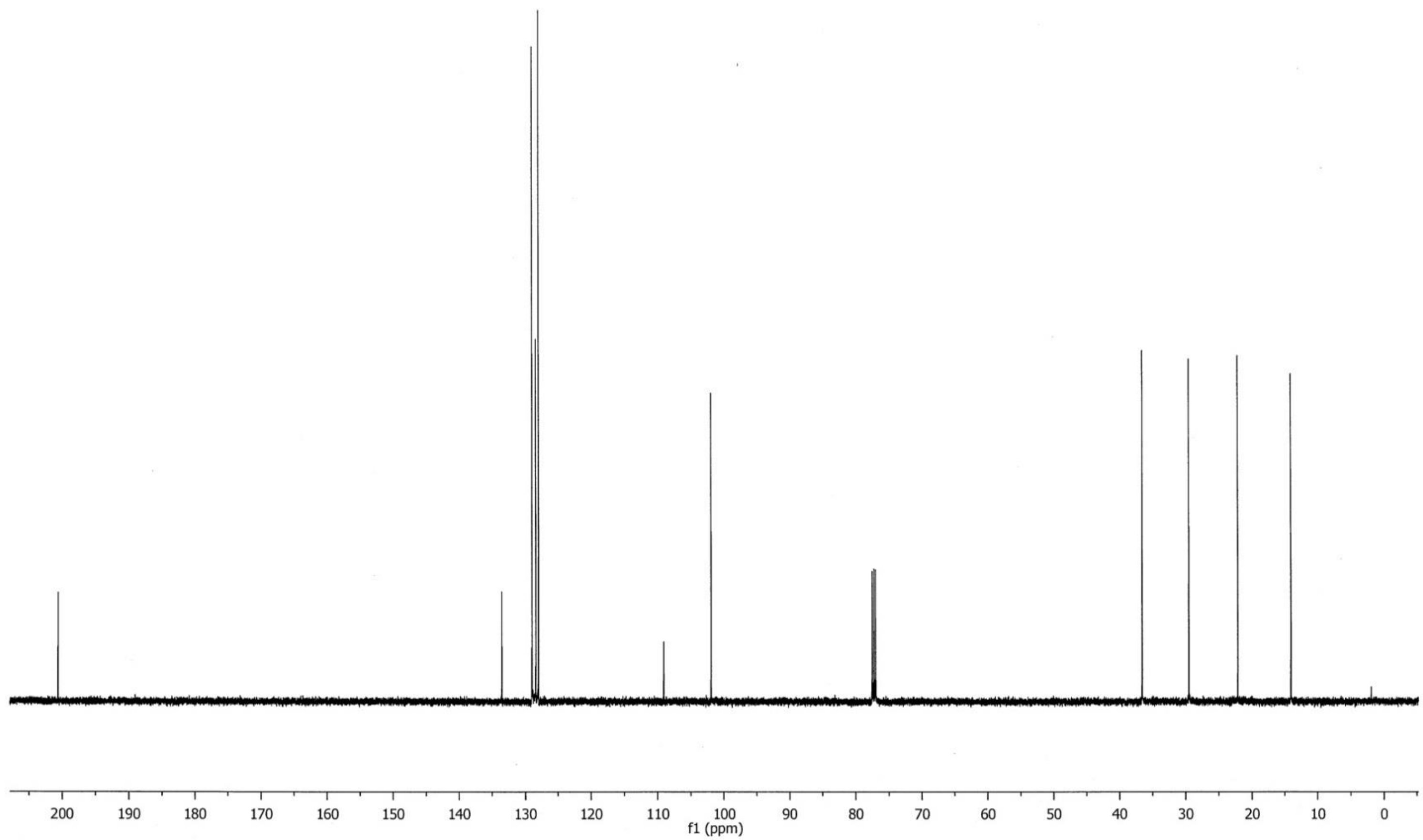

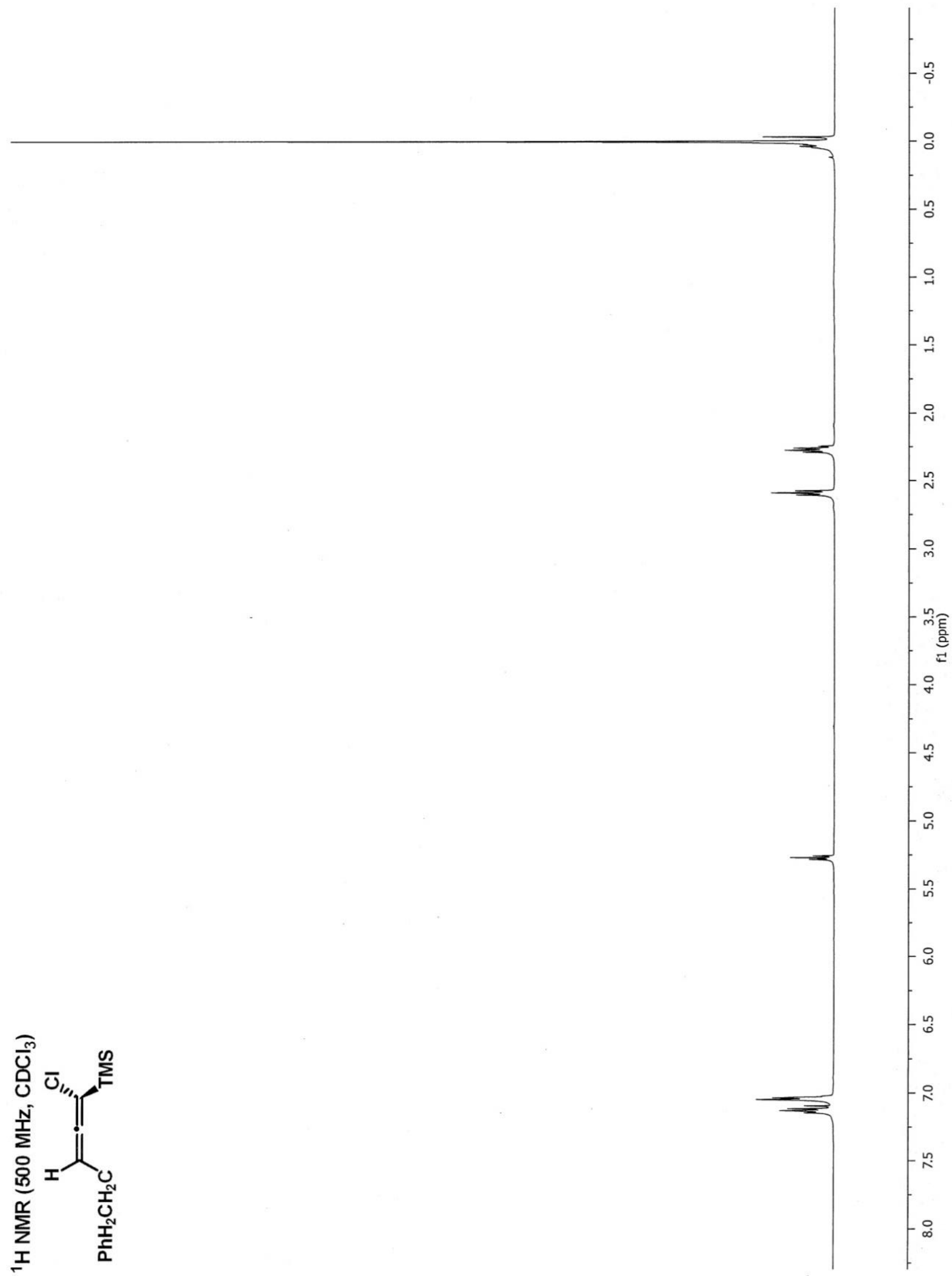

^{1}H NMR (500 MHz, CDCl$_3$)
H
Cl
TMS
PhH$_2$CH$_2$C
f1 (ppm)
-0.5
0.0
0.5
1.0
1.5
2.0
2.5
3.0
3.5
4.0
4.5
5.0
5.5
6.0
6.5
7.0
7.5
8.0

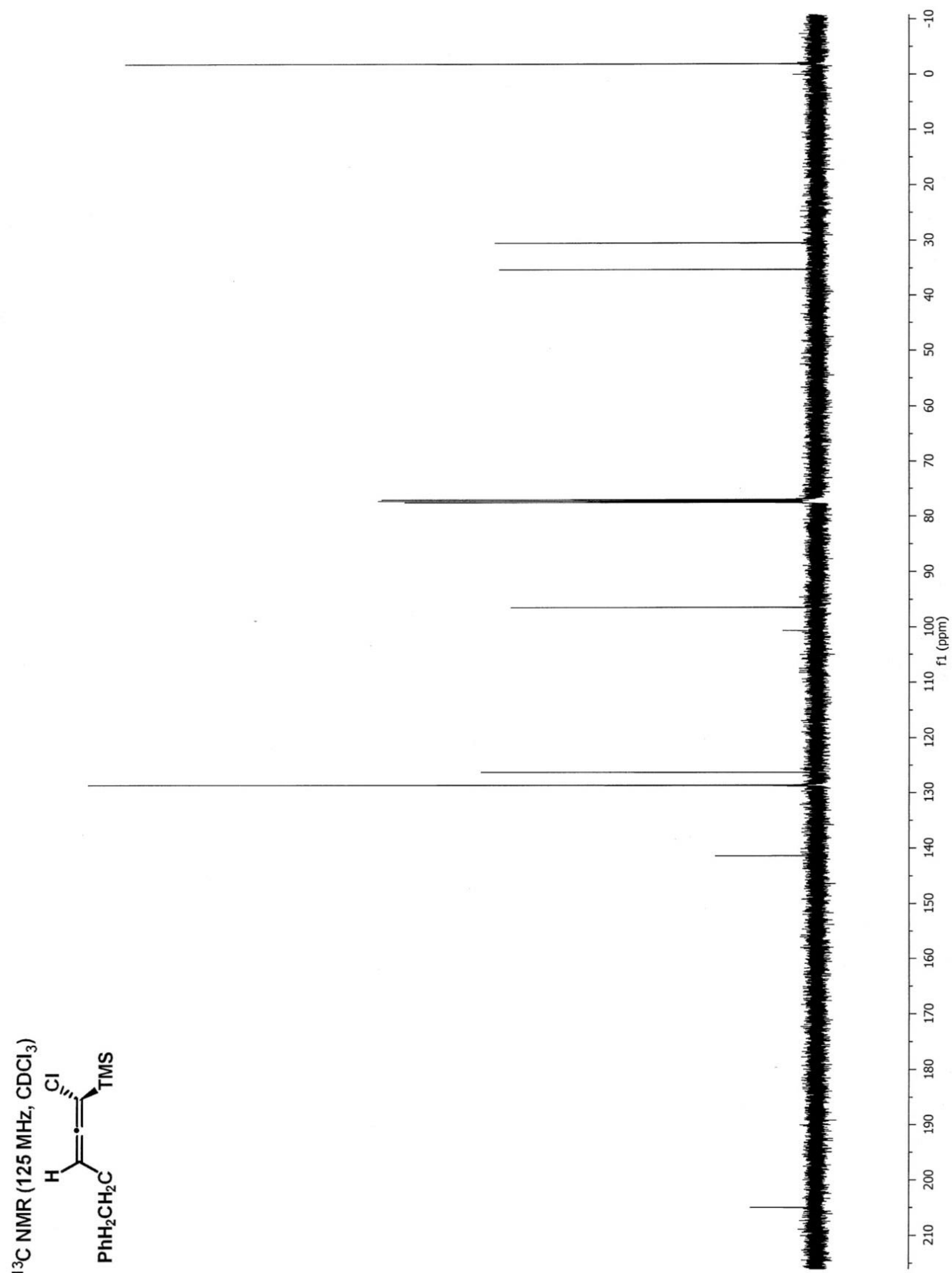

^{13}C NMR (125 MHz, $CDCl_3$)
H
Cl
PhH_2CH_2C
TMS
f1 (ppm)

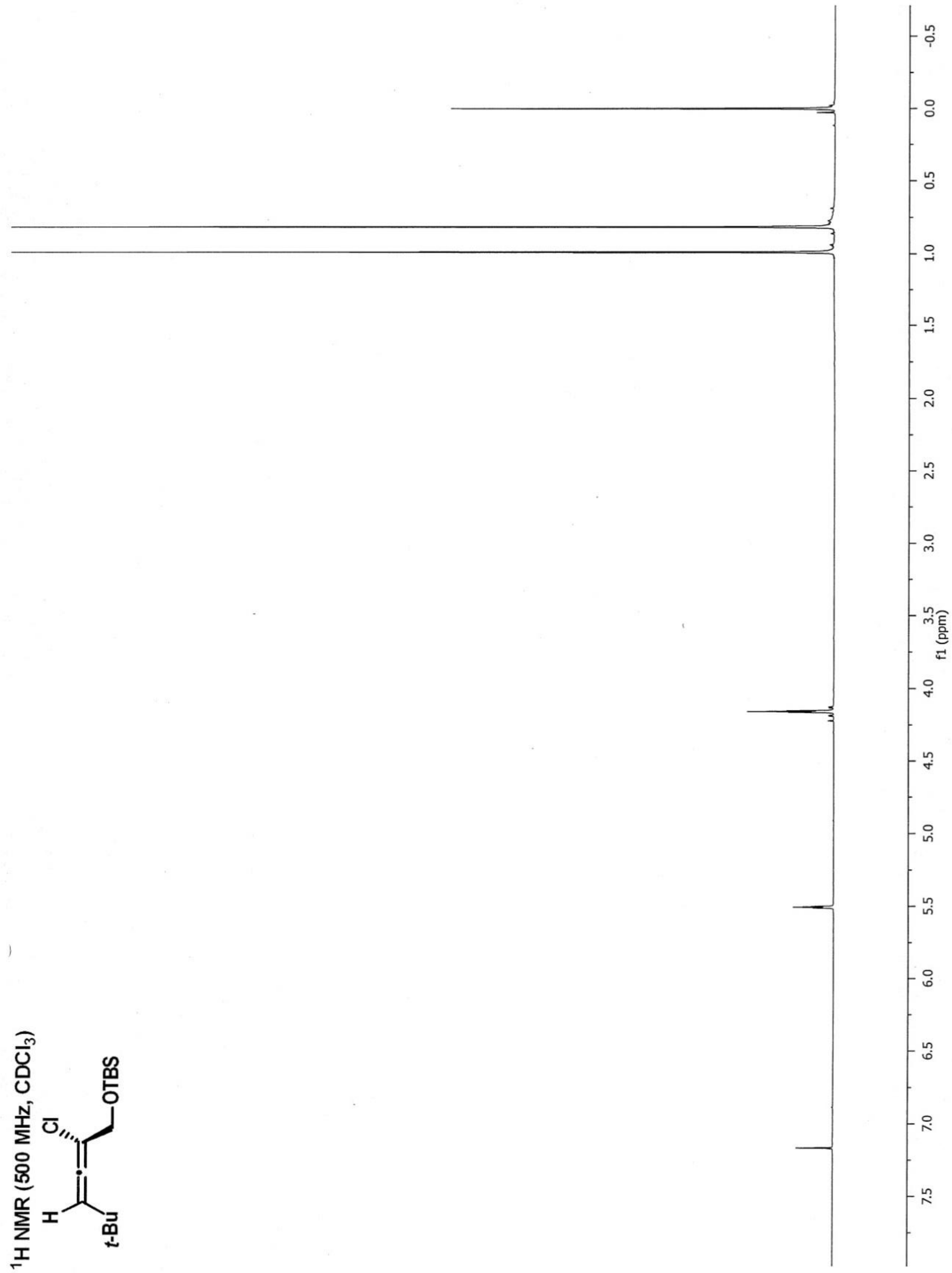

^{1}H NMR (500 MHz, $CDCl_3$)
H
Cl
OTBS
t-Bu
f1 (ppm)
7.5
7.0
6.5
6.0
5.5
5.0
4.5
4.0
3.5
3.0
2.5
2.0
1.5
1.0
0.5
0.0
-0.5

^{13}C NMR (125 MHz, $CDCl_3$)

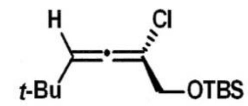

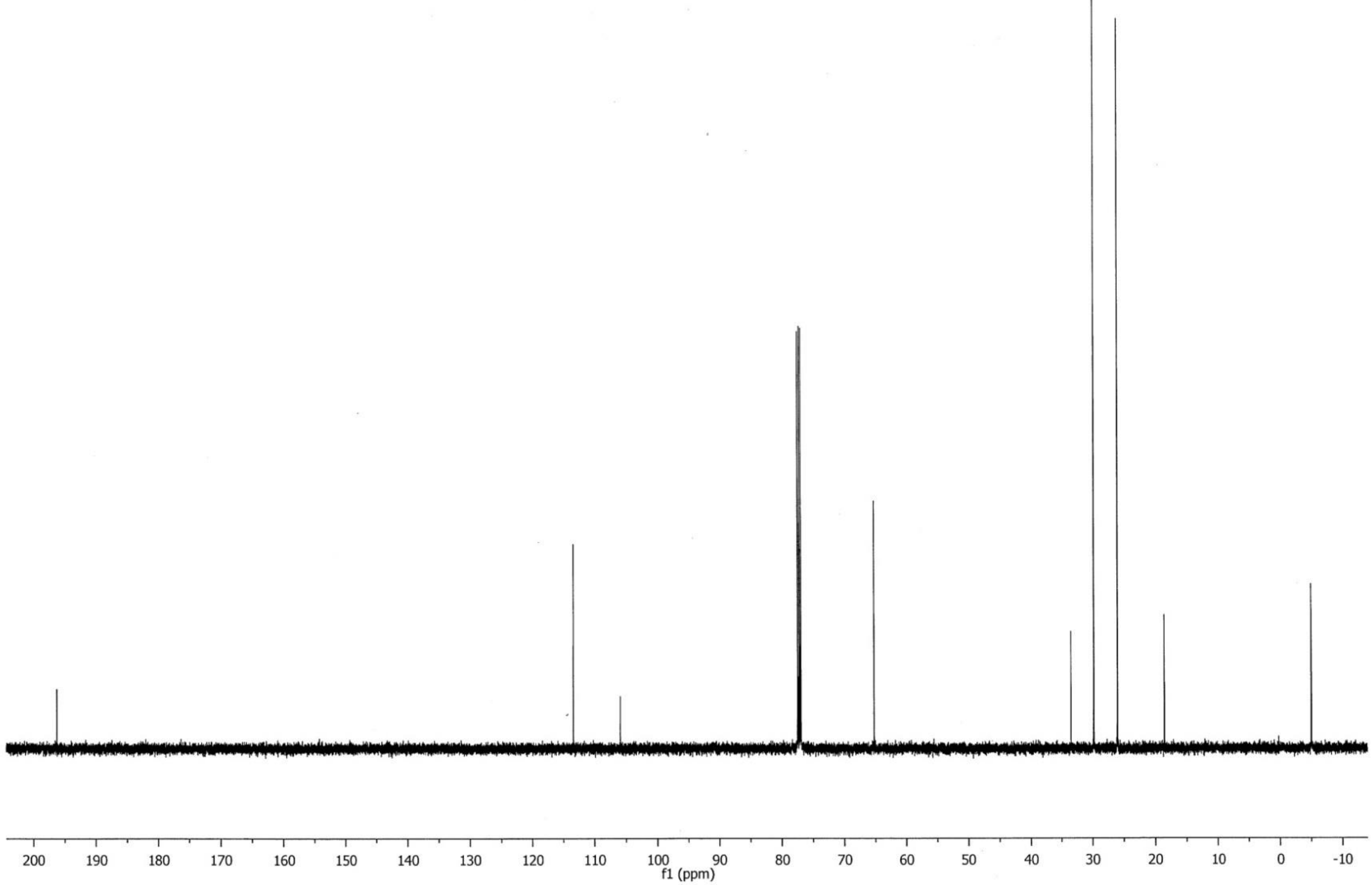

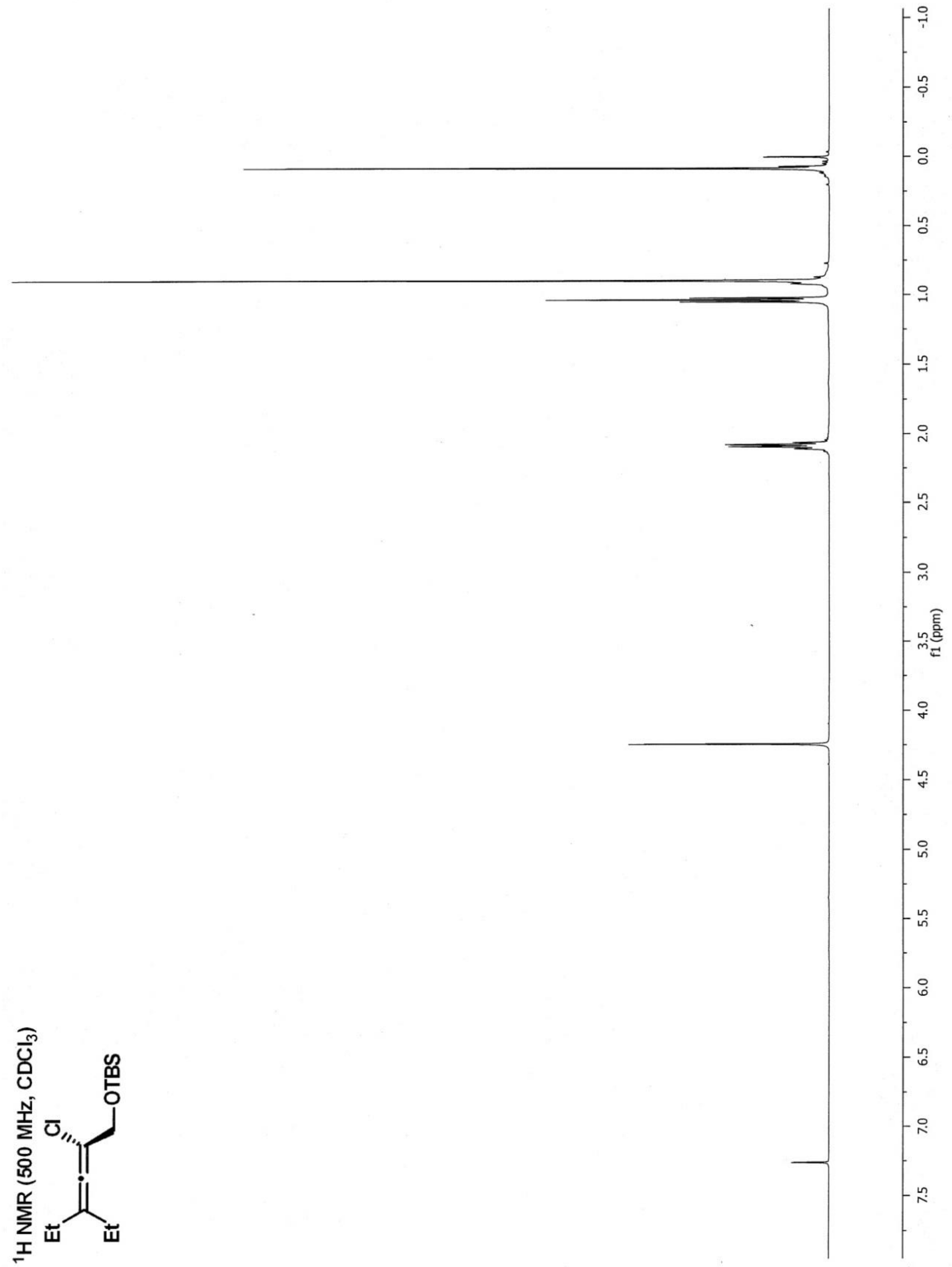

1H NMR (500 MHz, CDCl3)
Et
Et
Cl
OTBS
f1 (ppm)

^{13}C NMR (100 MHz, $CDCl_3$)

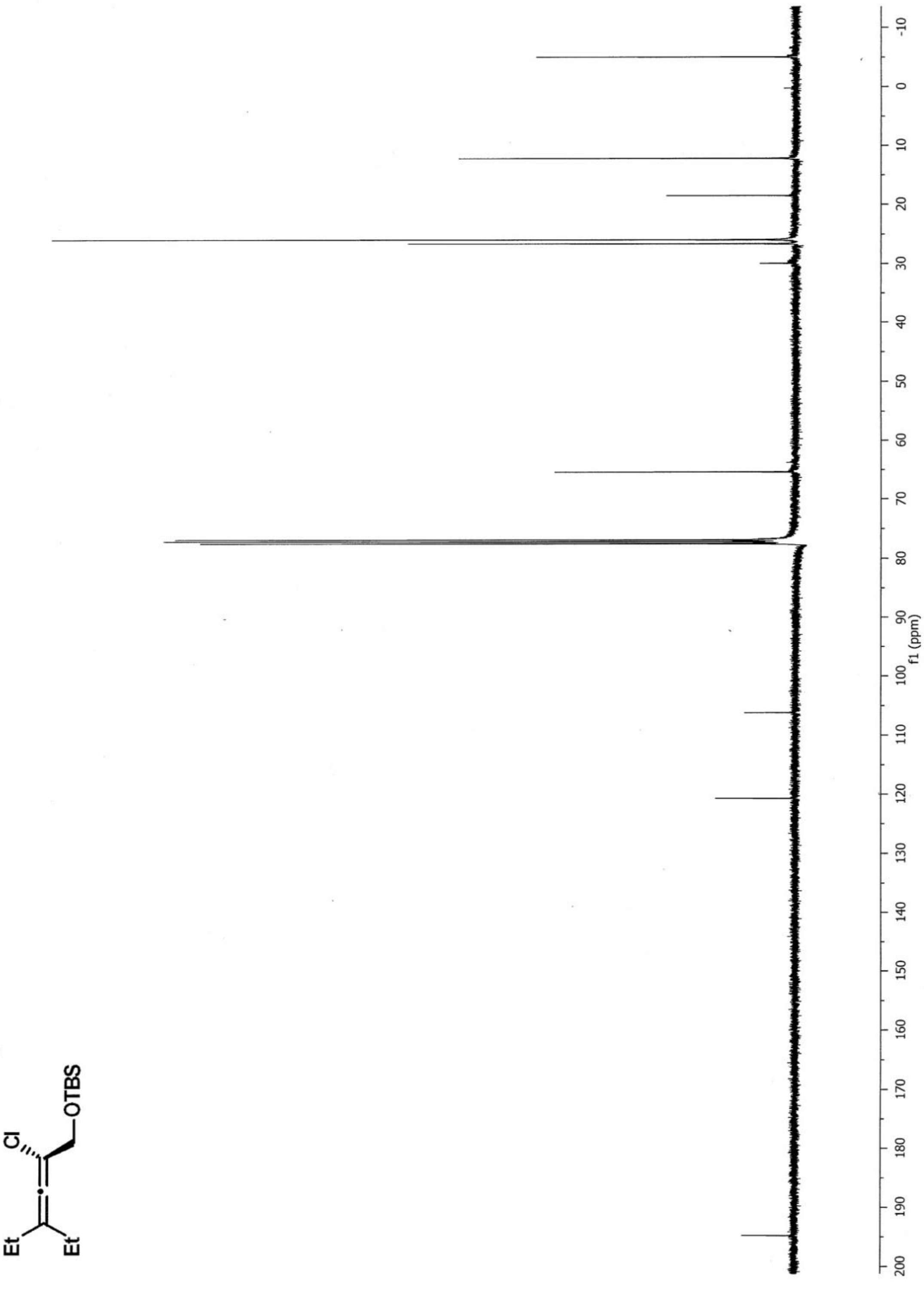

^1H NMR (500 MHz, $CDCl_3$)

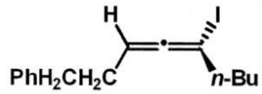

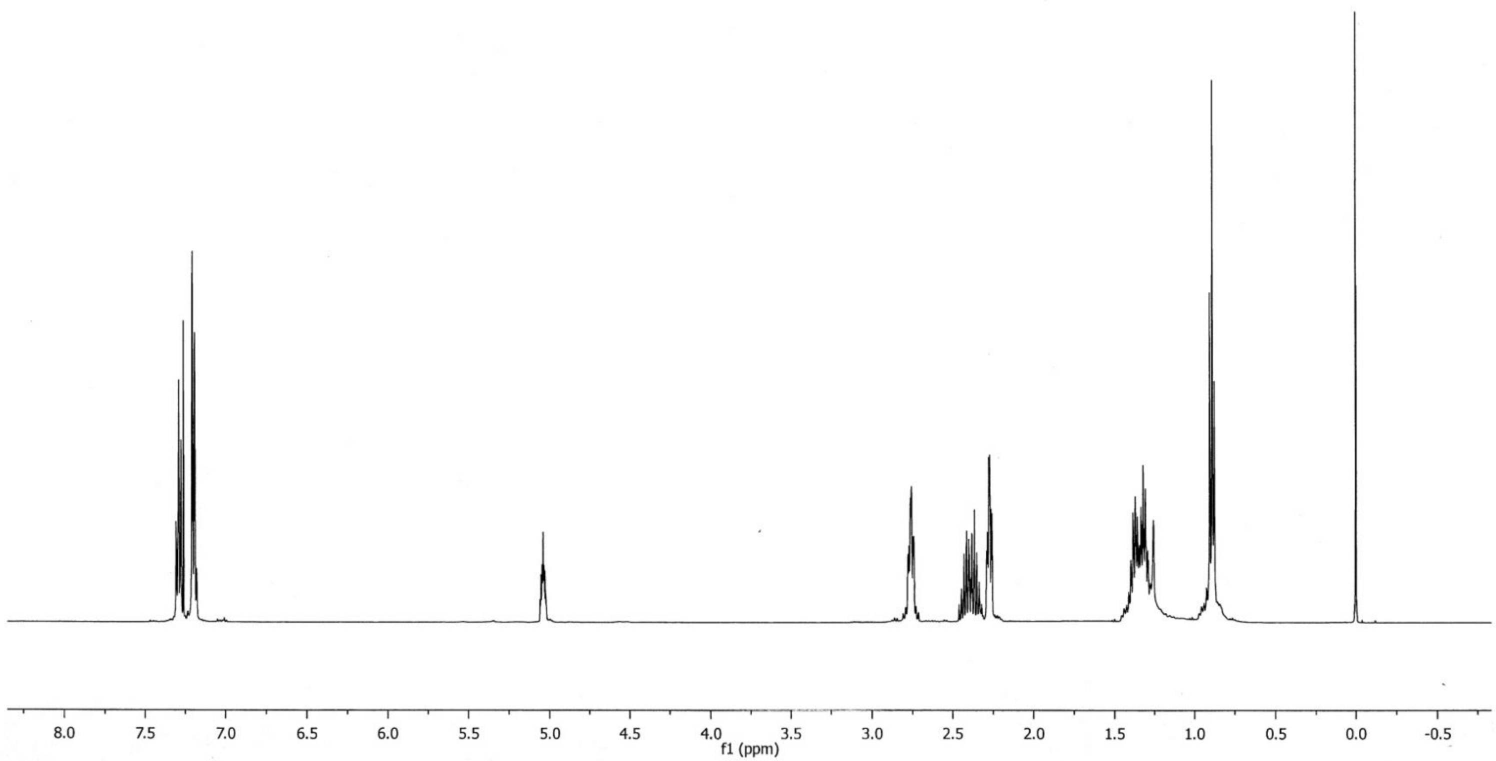

^{13}C NMR (125 MHz, $CDCl_3$)

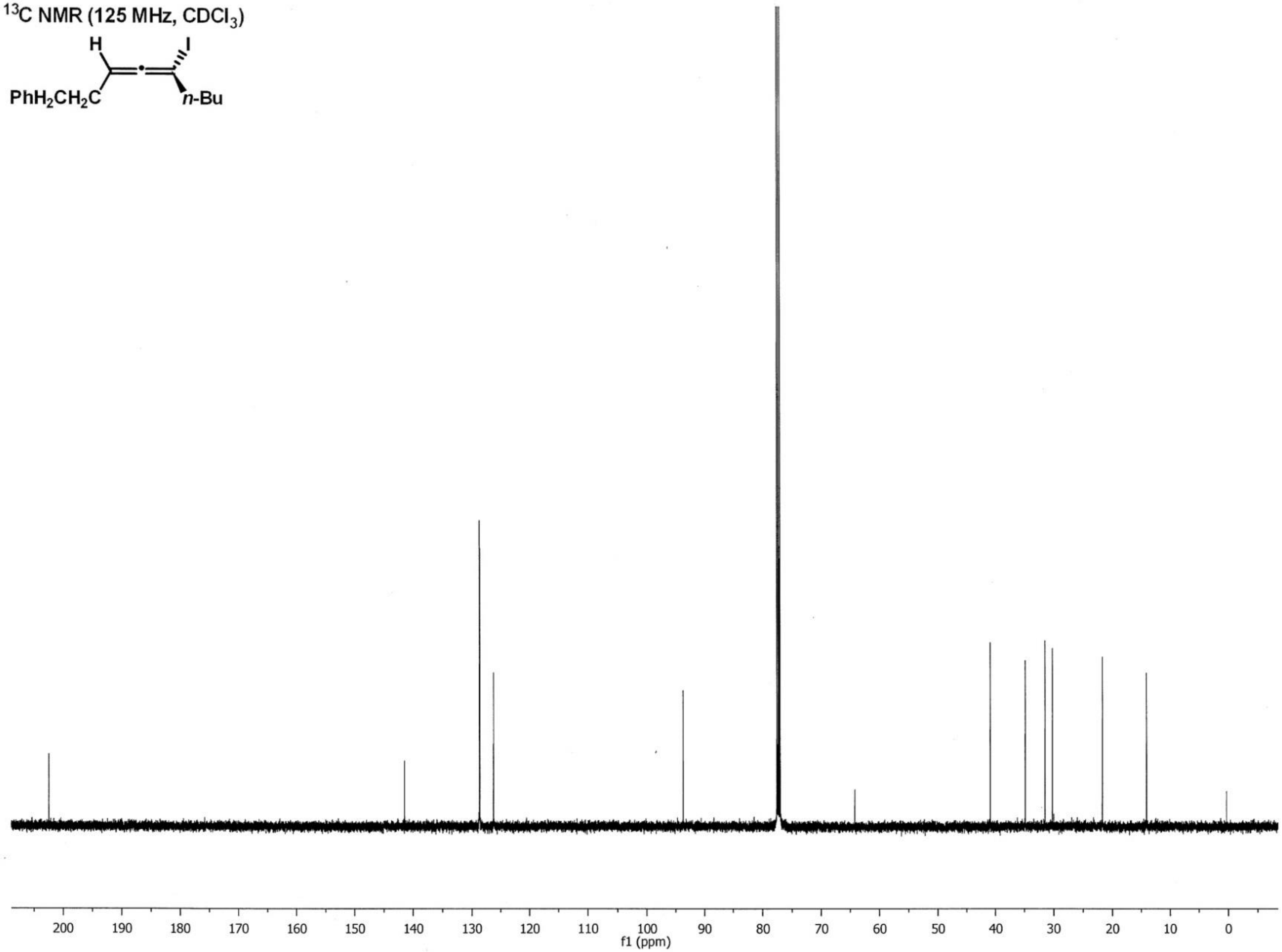

^1H NMR (500 MHz, $CDCl_3$)

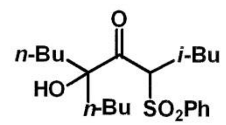

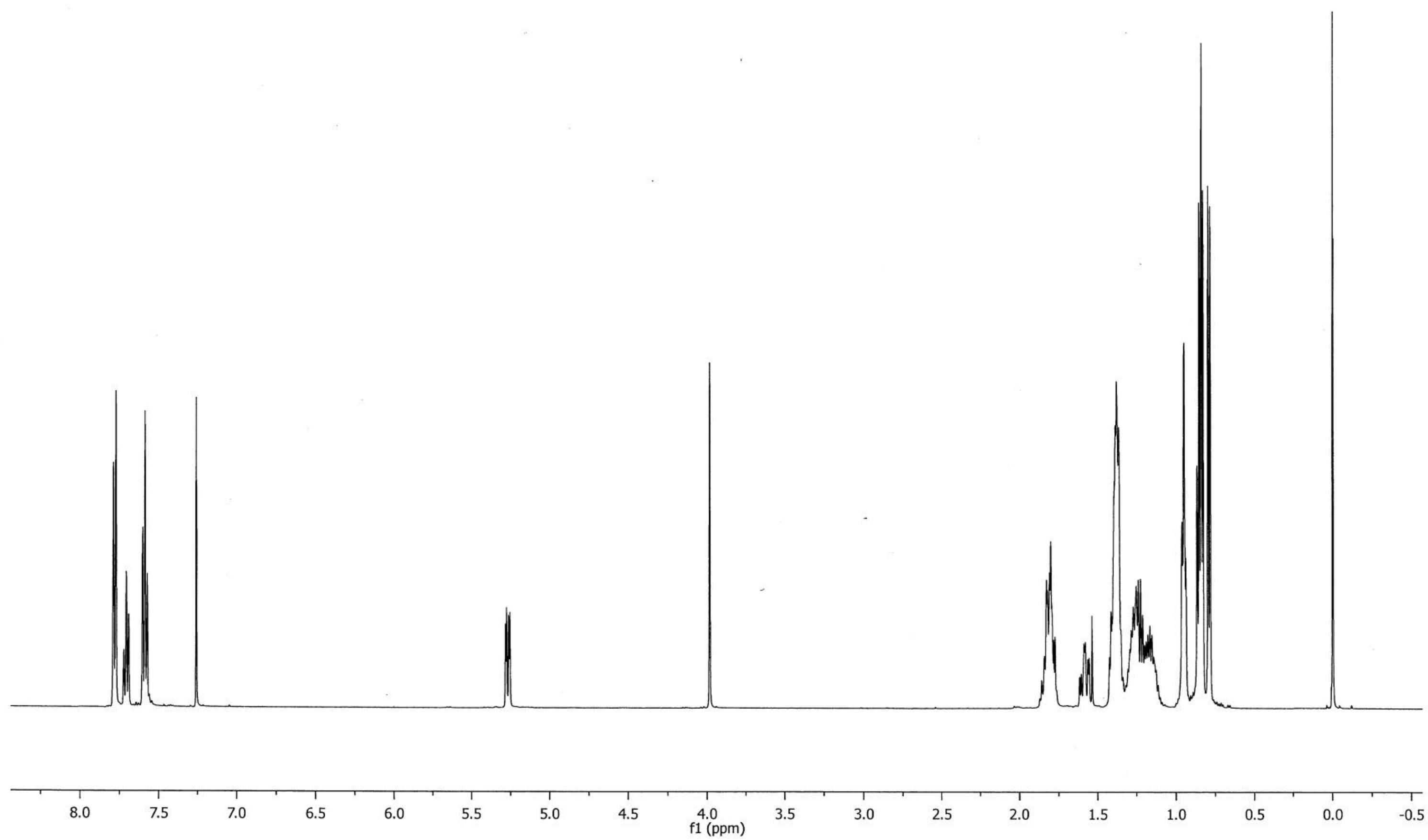

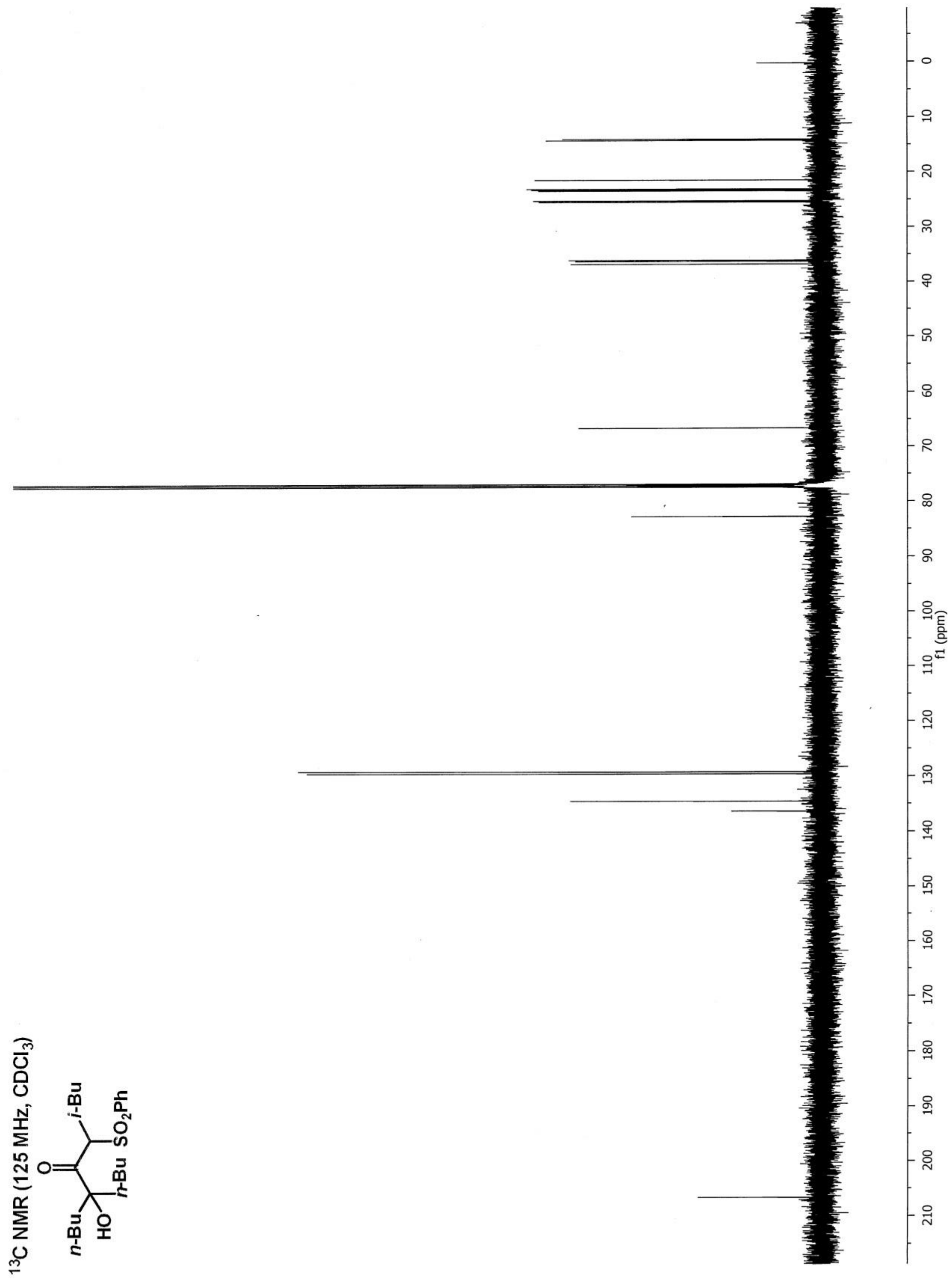

13C NMR (125 MHz, CDCl3)
n-Bu
HO
n-Bu
O
i-Bu
SO2Ph
f1 (ppm)

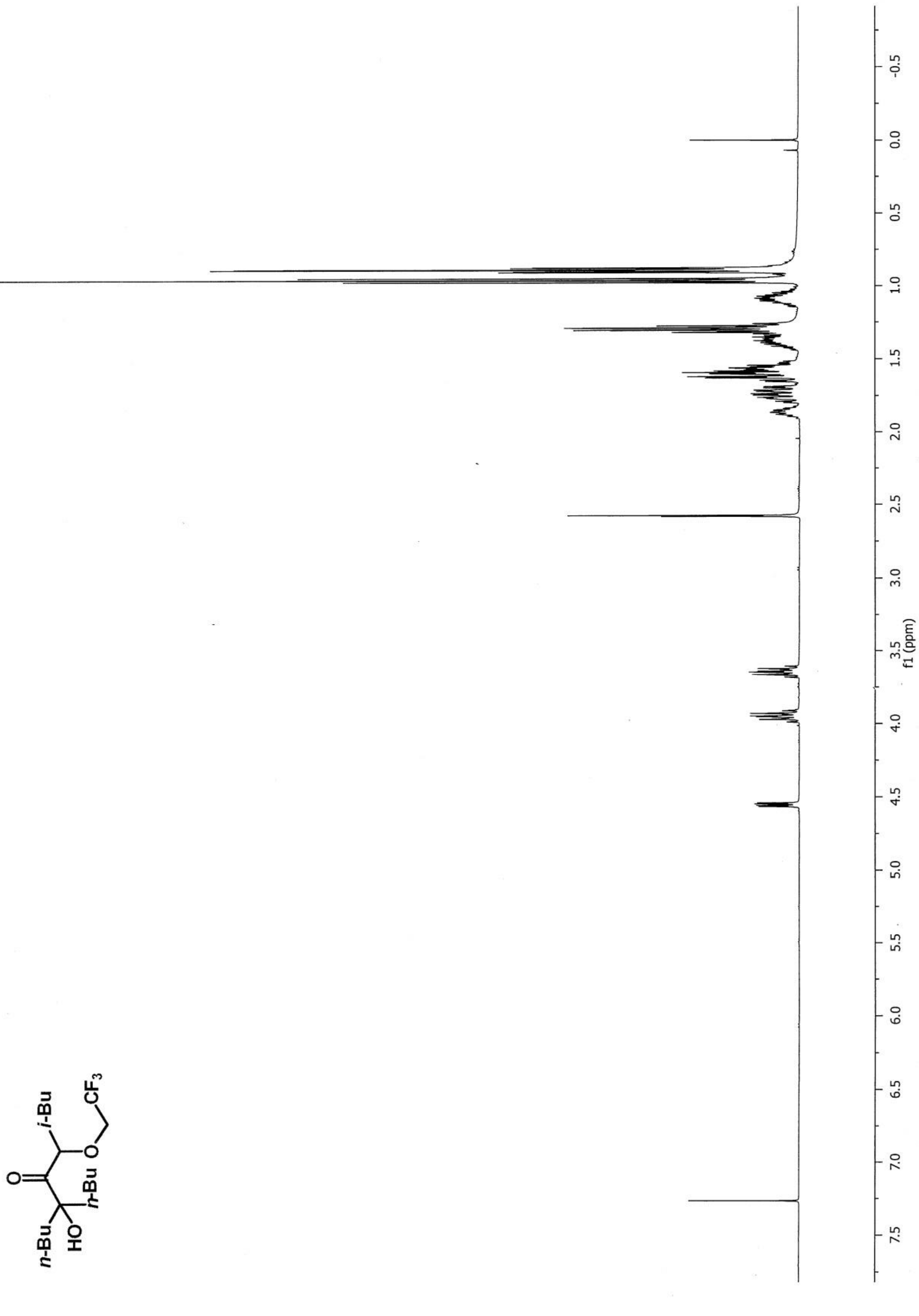

^{1}H NMR (500 MHz, $CDCl_3$)

^{13}C NMR (125 MHz, $CDCl_3$)

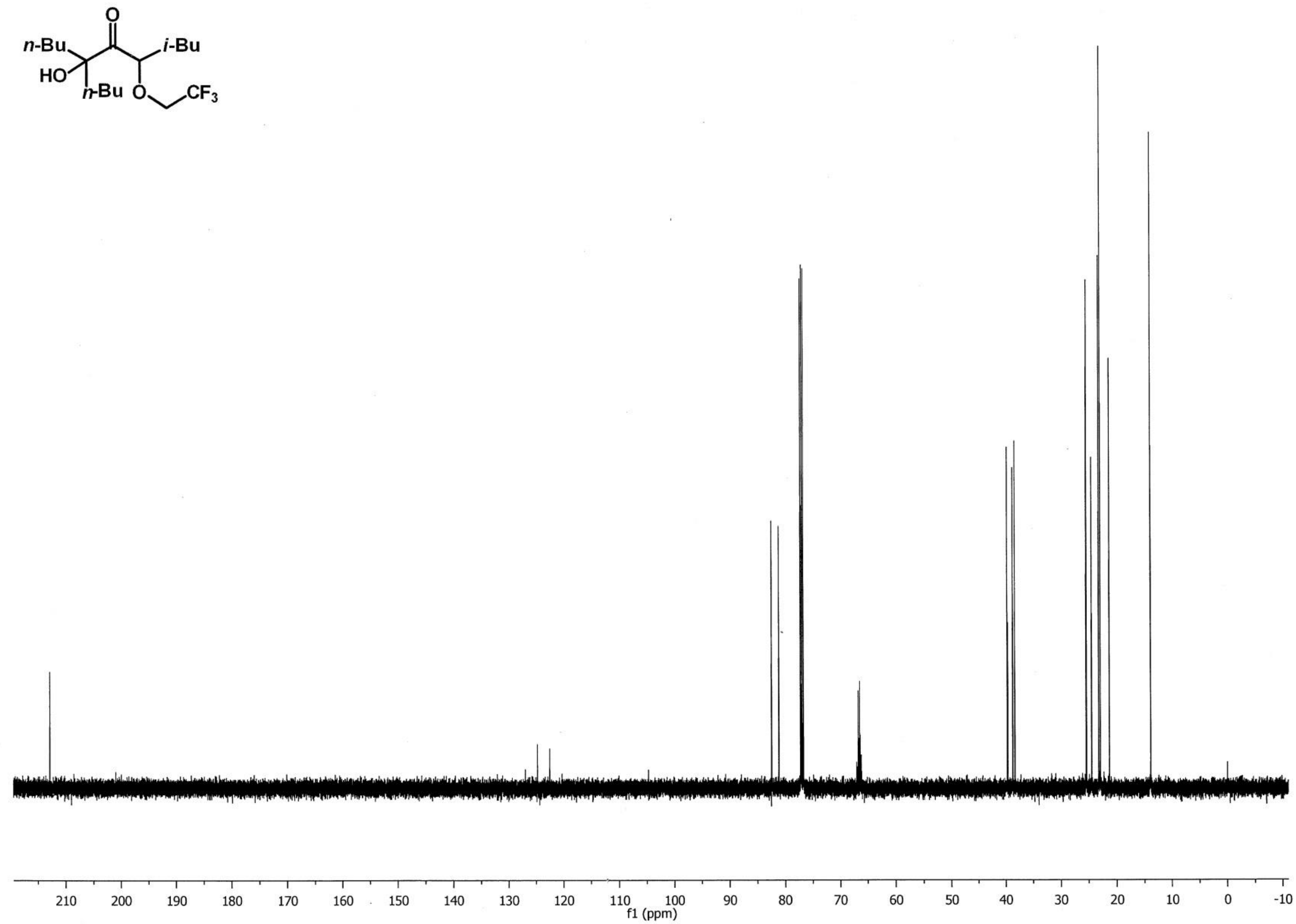

^1H NMR (500 MHz, $CDCl_3$)

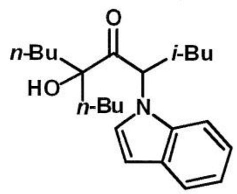

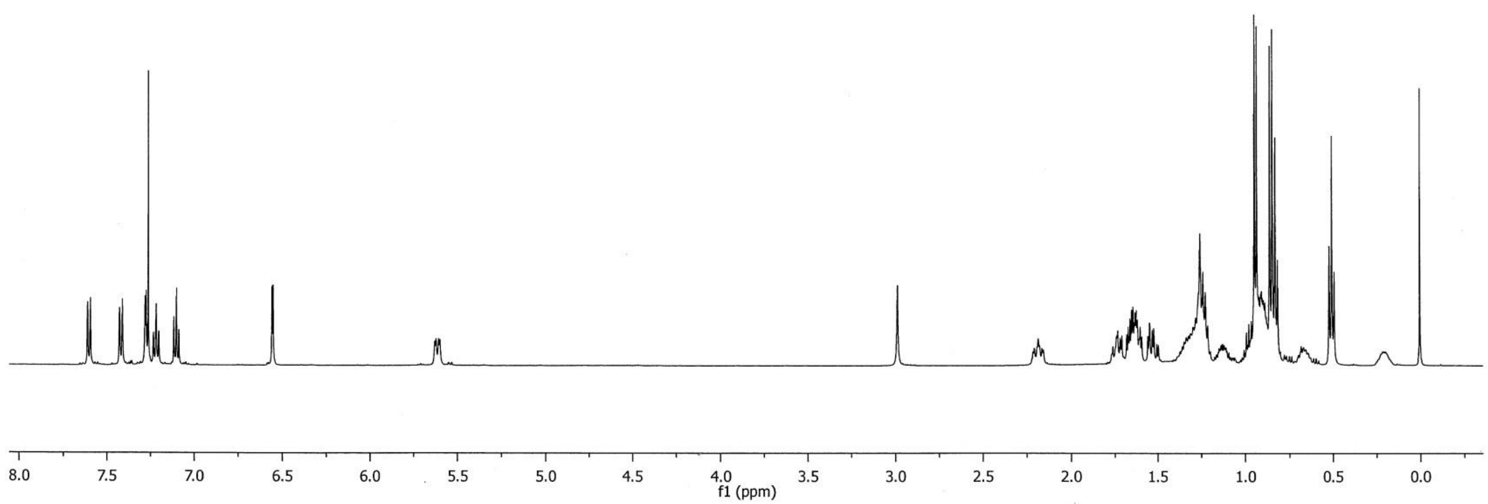

^{13}C NMR (125 MHz, $CDCl_3$)

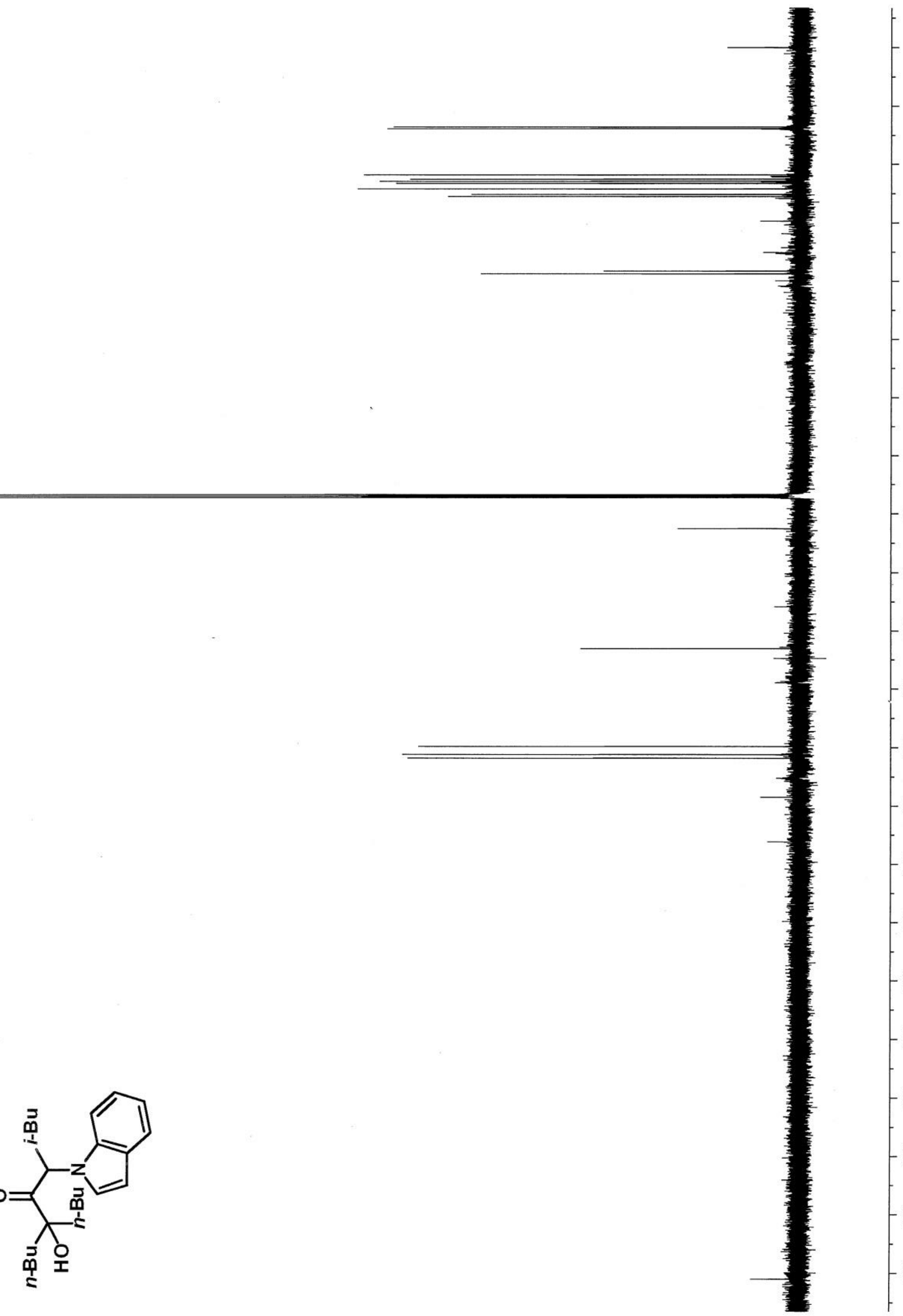

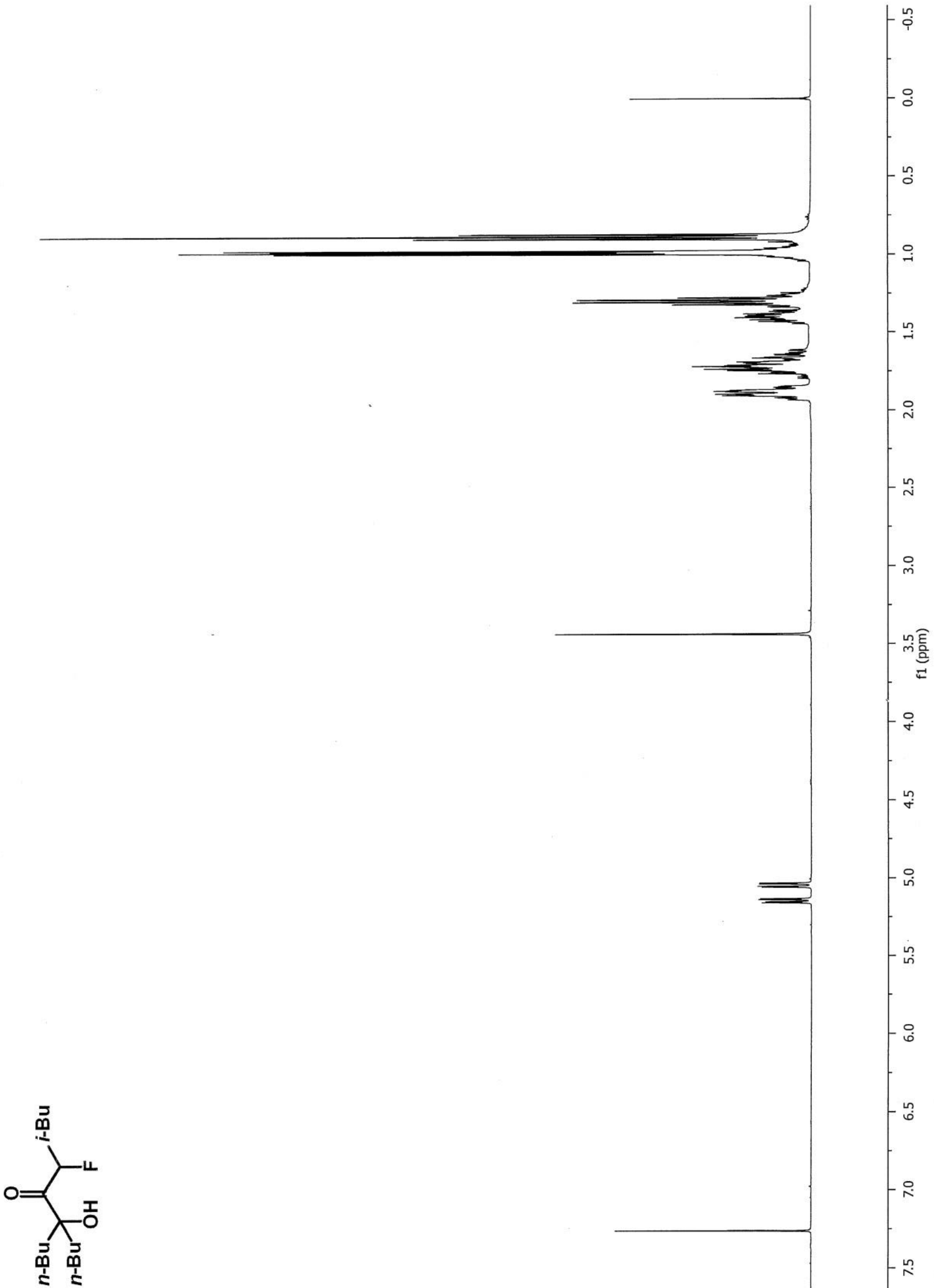

^1H NMR (500 MHz, $CDCl_3$)

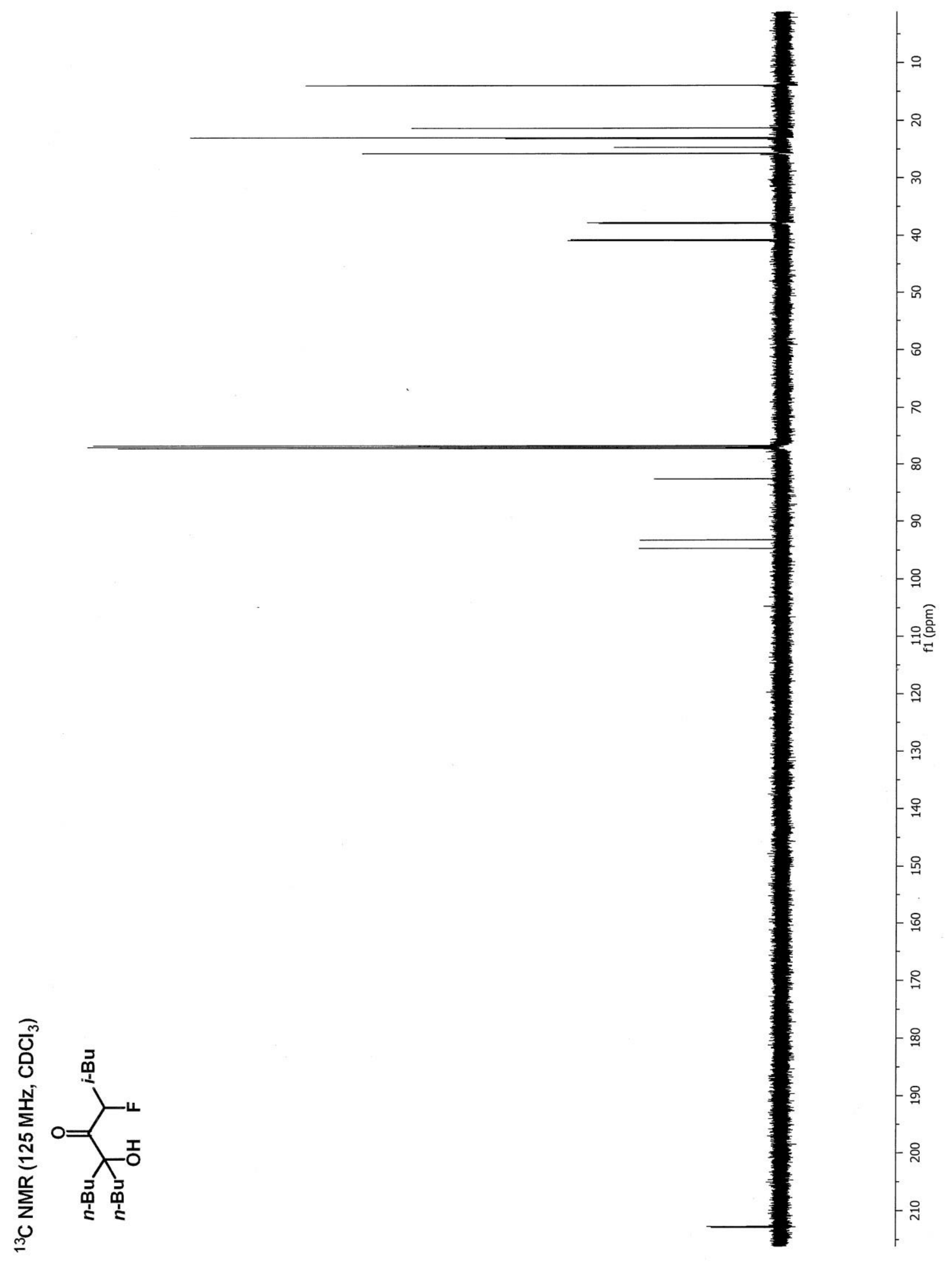
13C NMR (125 MHz, CDCl3)
n-Bu
n-Bu
OH
O
F
i-Bu
f1 (ppm)
10
20
30
40
50
60
70
80
90
100
110
120
130
140
150
160
170
180
190
200
210

^1H NMR (500 MHz, $CDCl_3$)

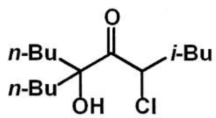

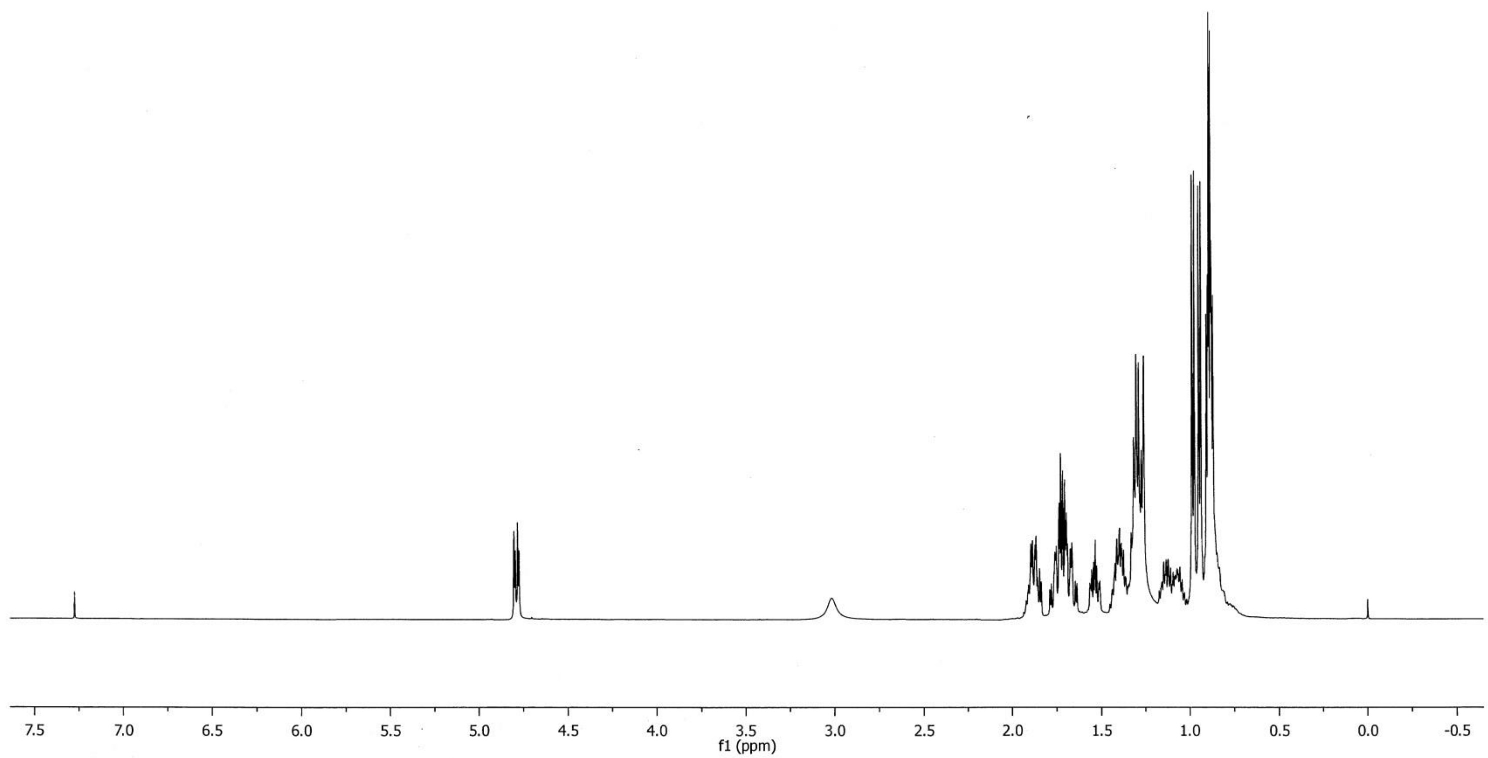

^{13}C NMR (125 MHz, $CDCl_3$)

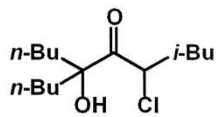

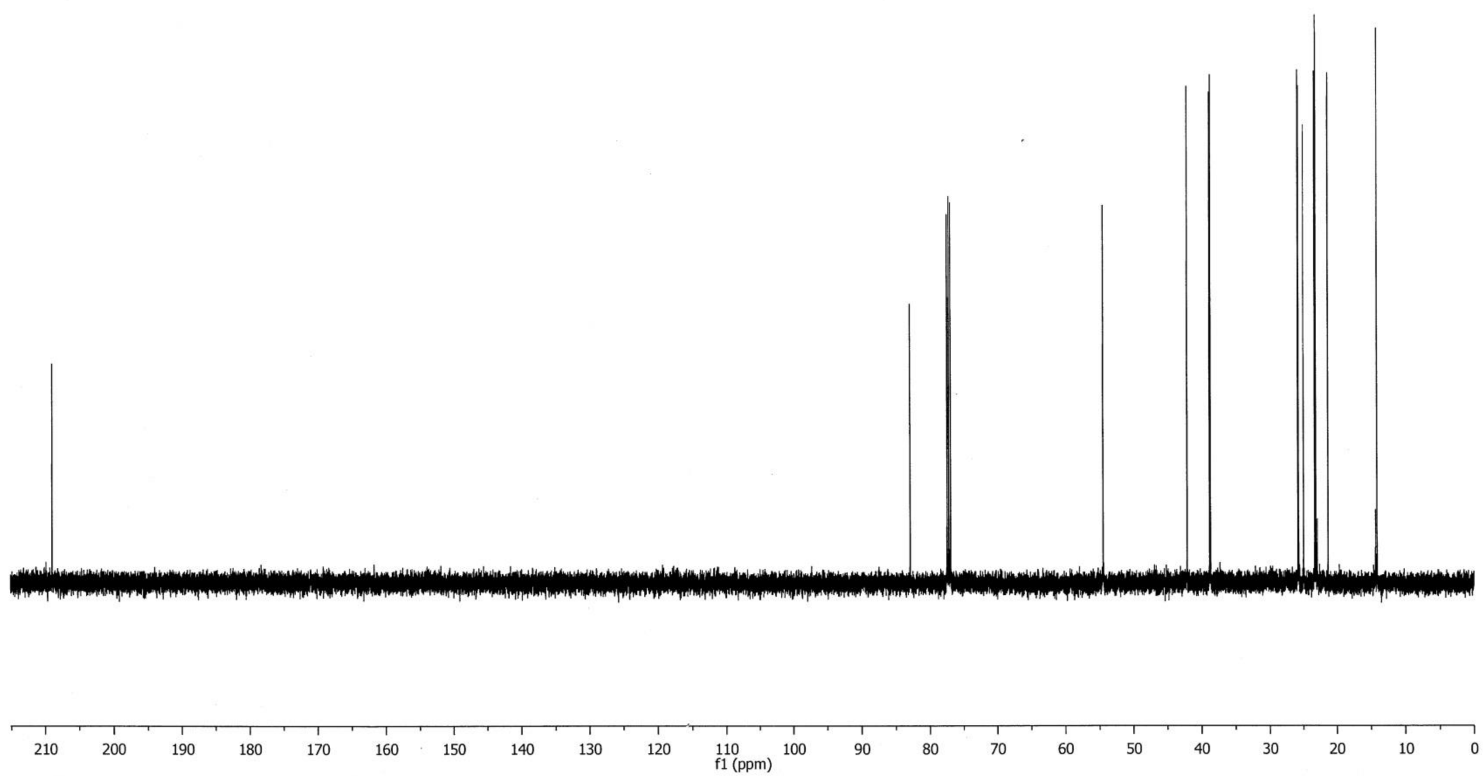

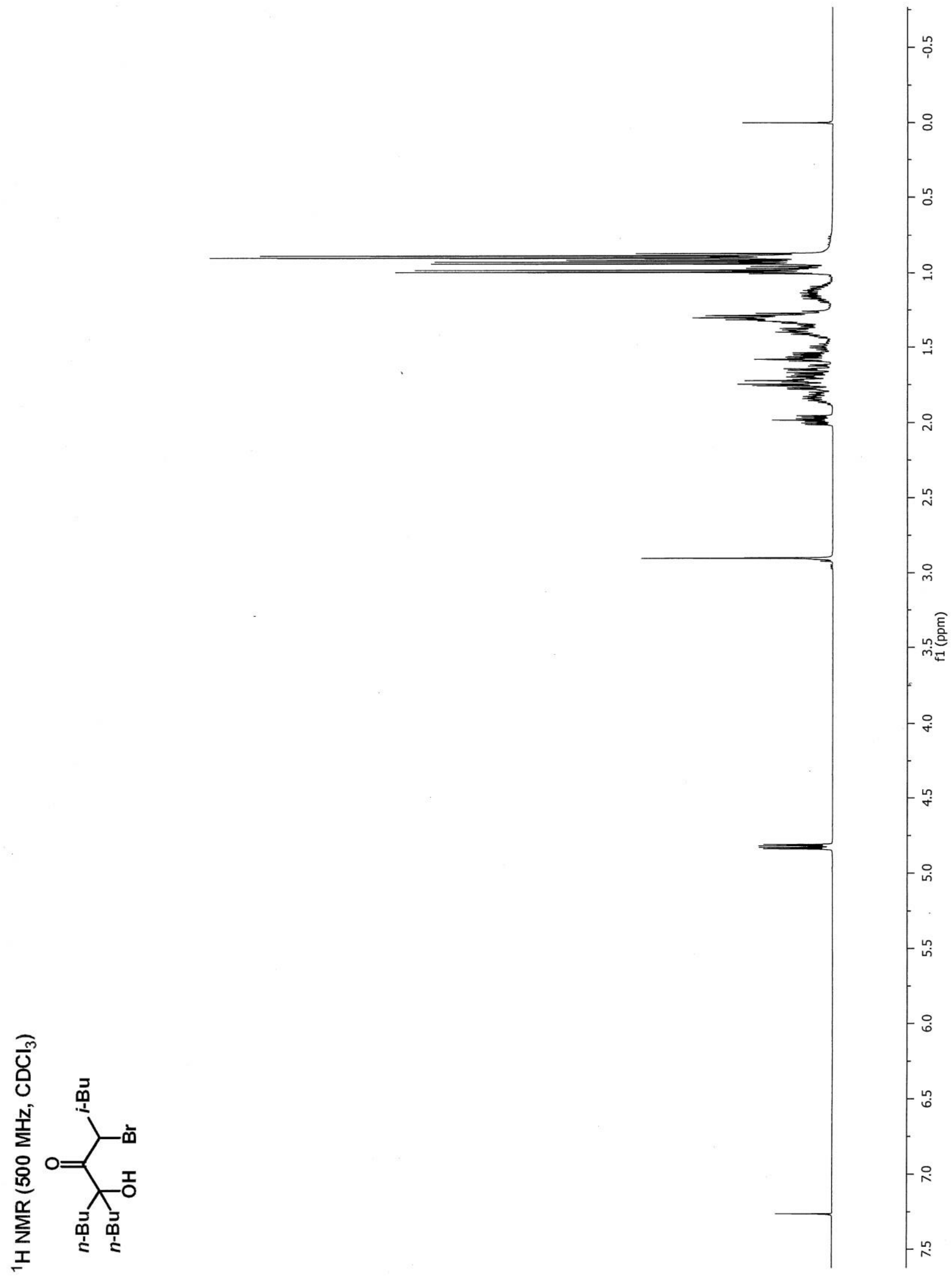

1H NMR (500 MHz, CDCl3)
O
n-Bu
n-Bu
OH
i-Bu
Br
-0.5
0.0
0.5
1.0
1.5
2.0
2.5
3.0
3.5
f1 (ppm)
4.0
4.5
5.0
5.5
6.0
6.5
7.0
7.5

^{13}C NMR (125 MHz, $CDCl_3$)

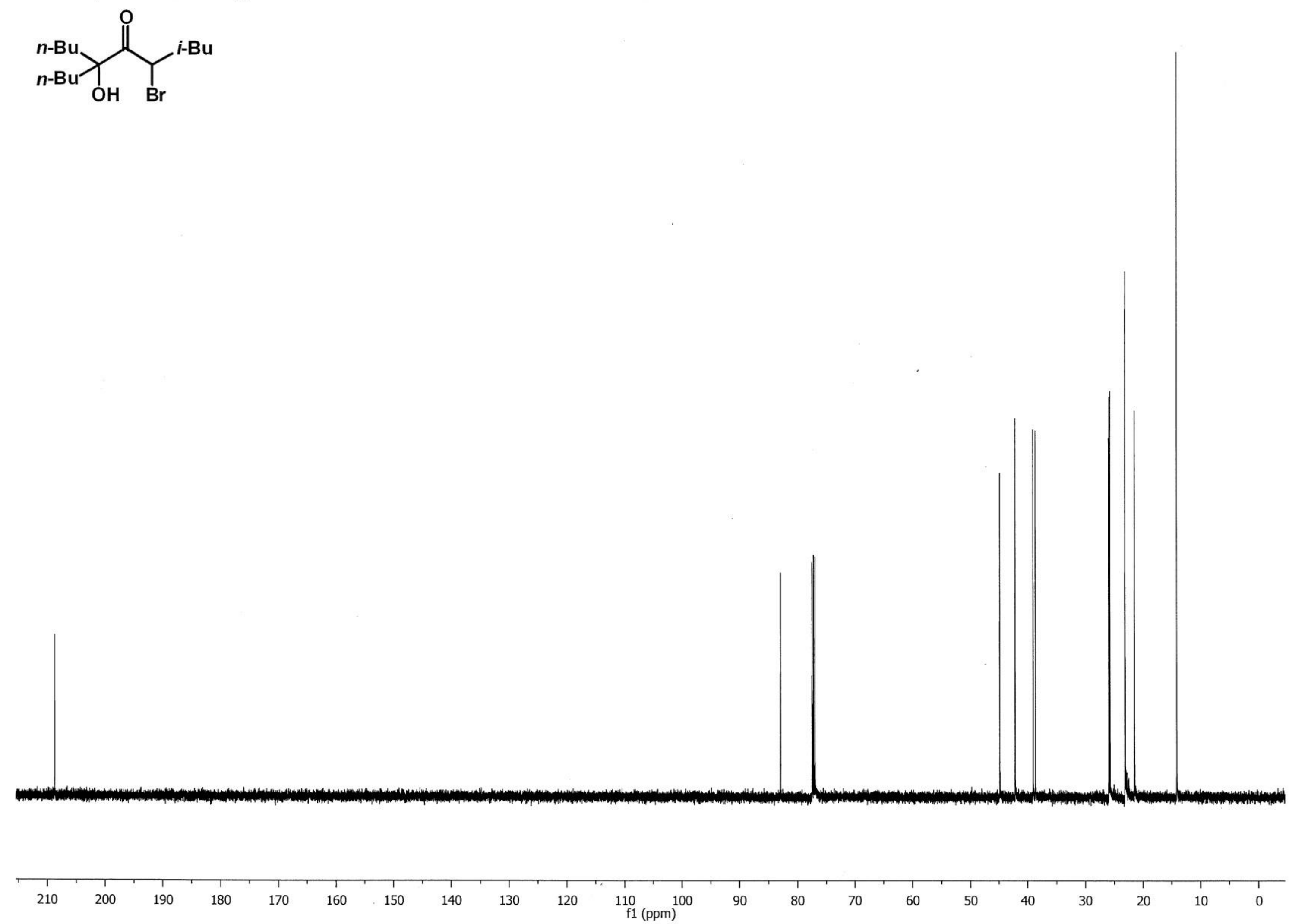

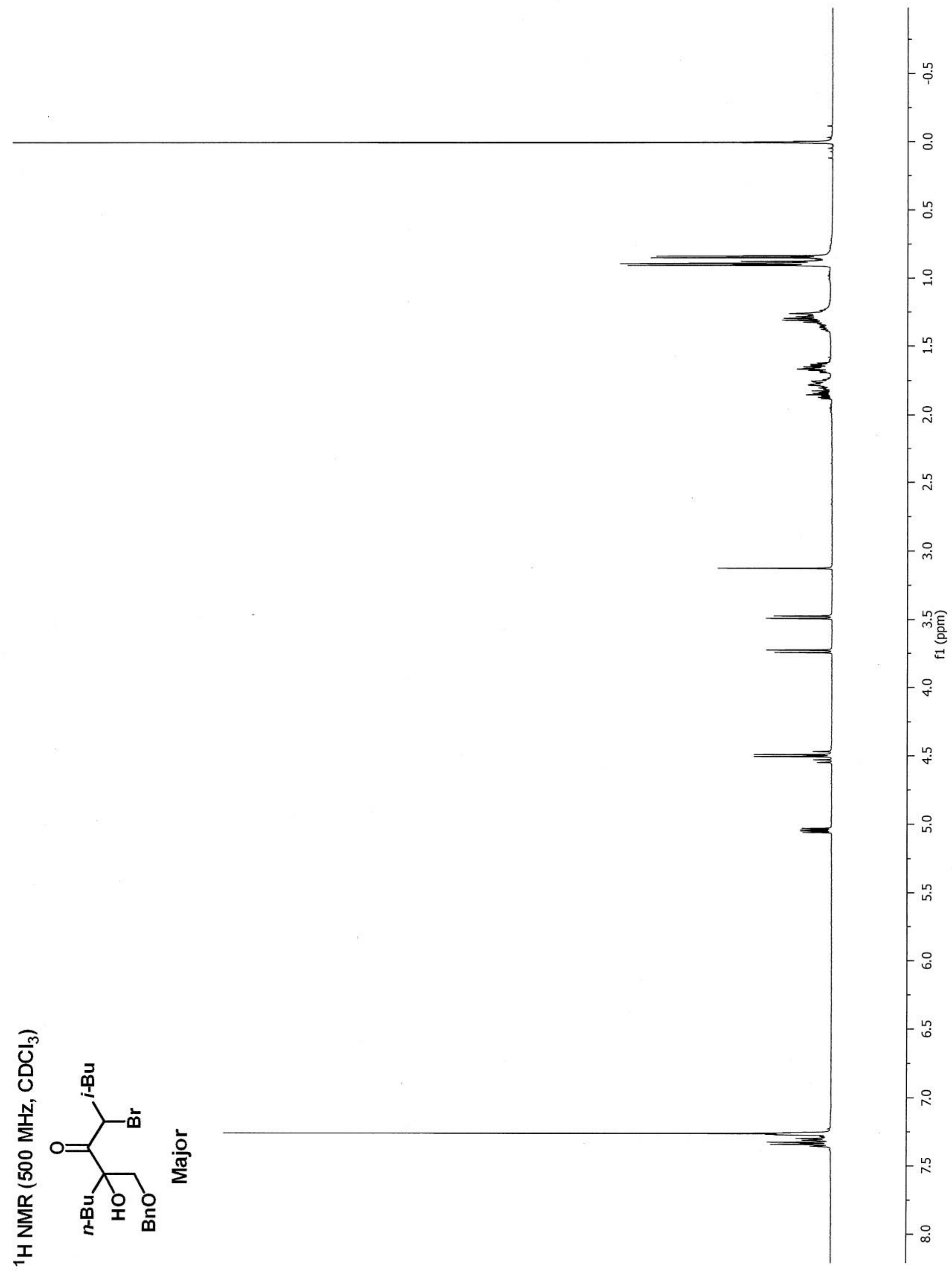

1H NMR (500 MHz, CDCl3)
n-Bu
HO
BnO
O
i-Bu
Br
Major
8.0
7.5
7.0
6.5
6.0
5.5
5.0
4.5
4.0
3.5
3.0
2.5
2.0
1.5
1.0
0.5
0.0
-0.5
f1 (ppm)

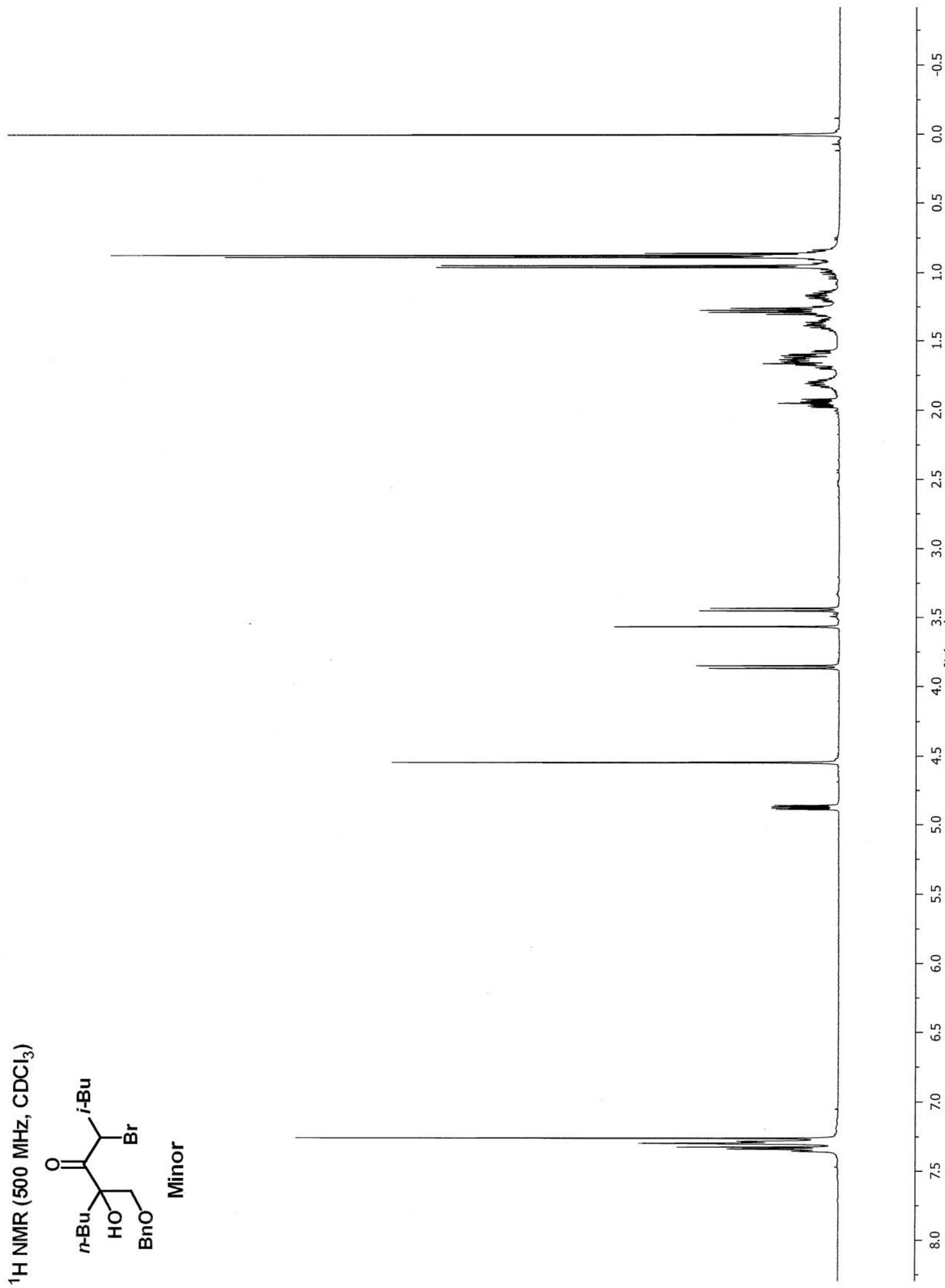

1H NMR (500 MHz, CDCl3)
n-Bu
HO
BnO
O
i-Bu
Br
Minor
f1 (ppm)

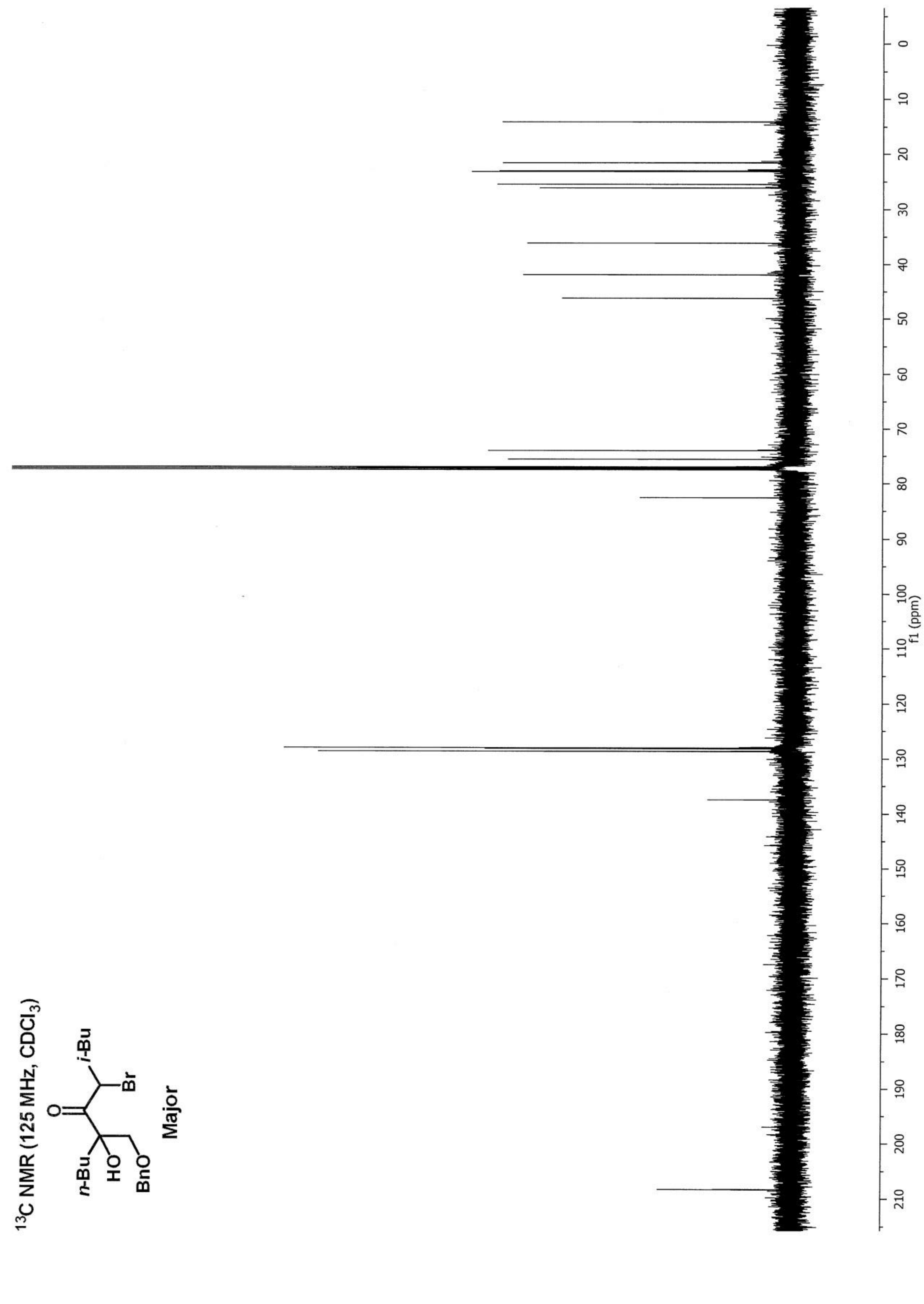
^{13}C NMR (125 MHz, $CDCl_3$)
O
n-Bu
i-Bu
HO
Br
BnO
Major
f1 (ppm)

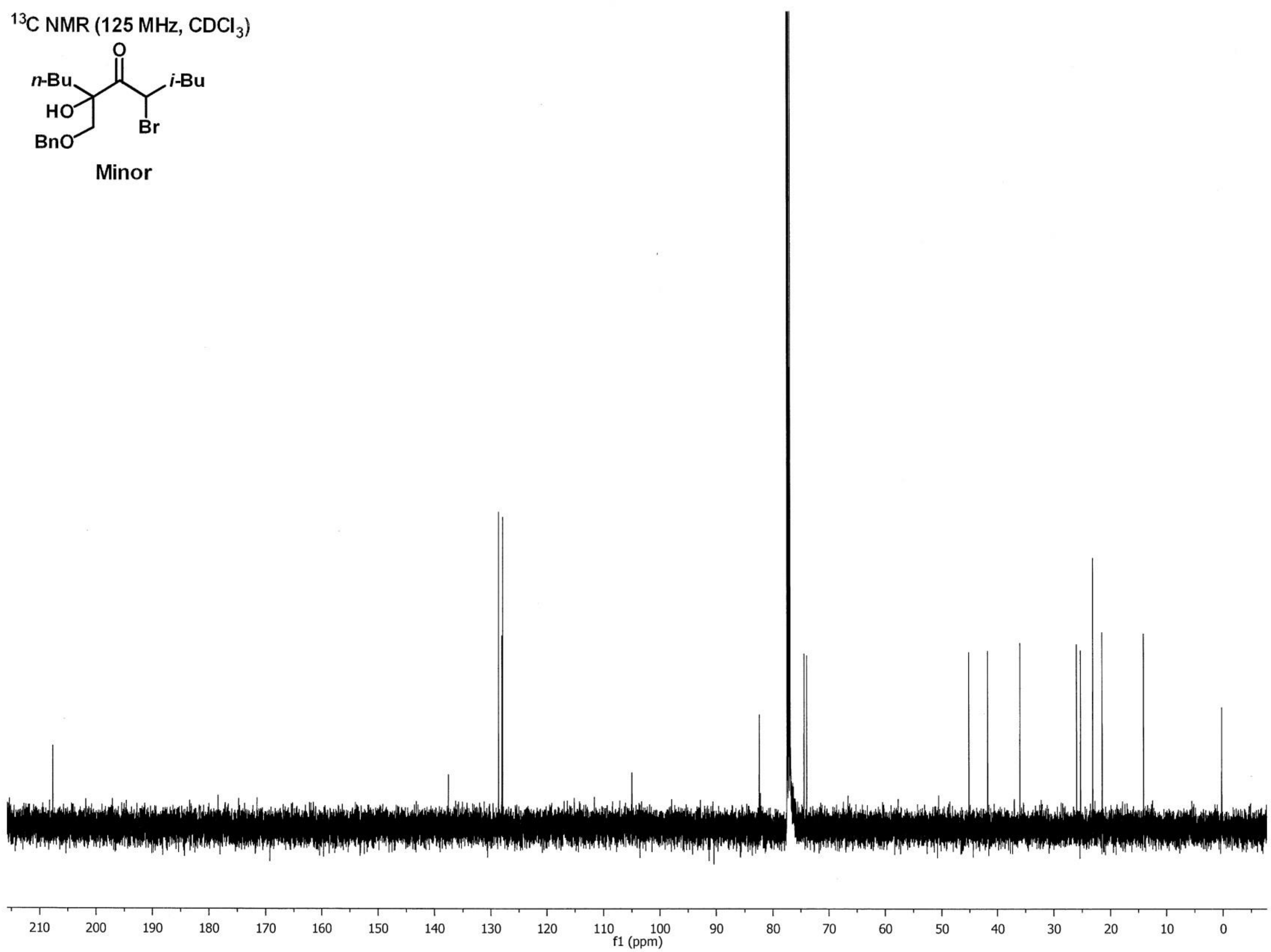

^{13}C NMR (125 MHz, $CDCl_3$)
n-Bu
HO
BnO
O
i-Bu
Br
Minor
210 200 190 180 170 160 150 140 130 120 110 100 90 80 70 60 50 40 30 20 10 0
f1 (ppm)

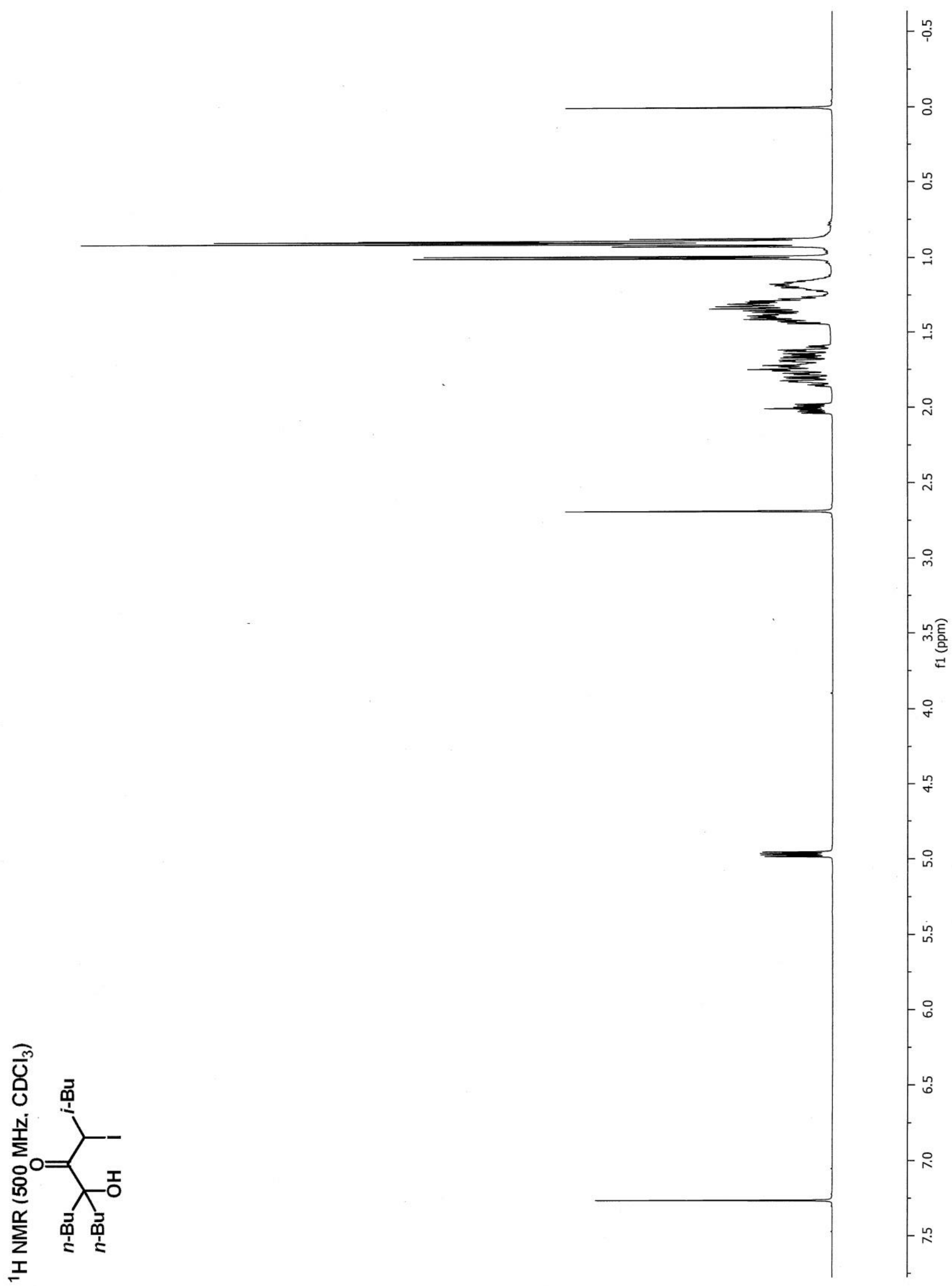

¹H NMR (500 MHz, CDCl3)
n-Bu
n-Bu
OH
O
i-Bu
I
f1 (ppm)
-0.5
0.0
0.5
1.0
1.5
2.0
2.5
3.0
3.5
4.0
4.5
5.0
5.5
6.0
6.5
7.0
7.5

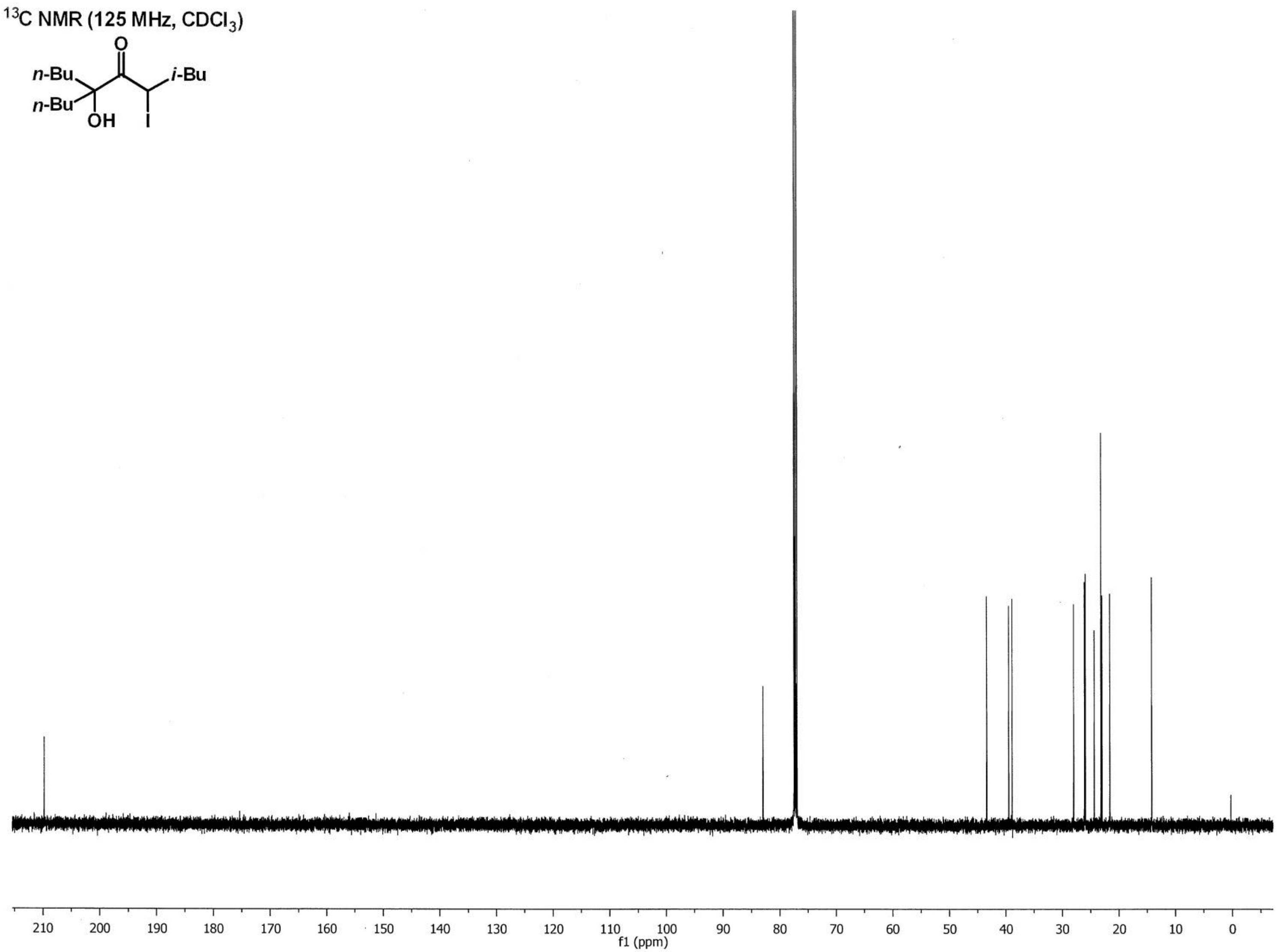

^{13}C NMR (125 MHz, $CDCl_3$)

^1H NMR (500 MHz, $CDCl_3$)

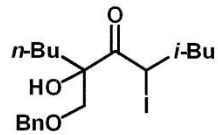

Major

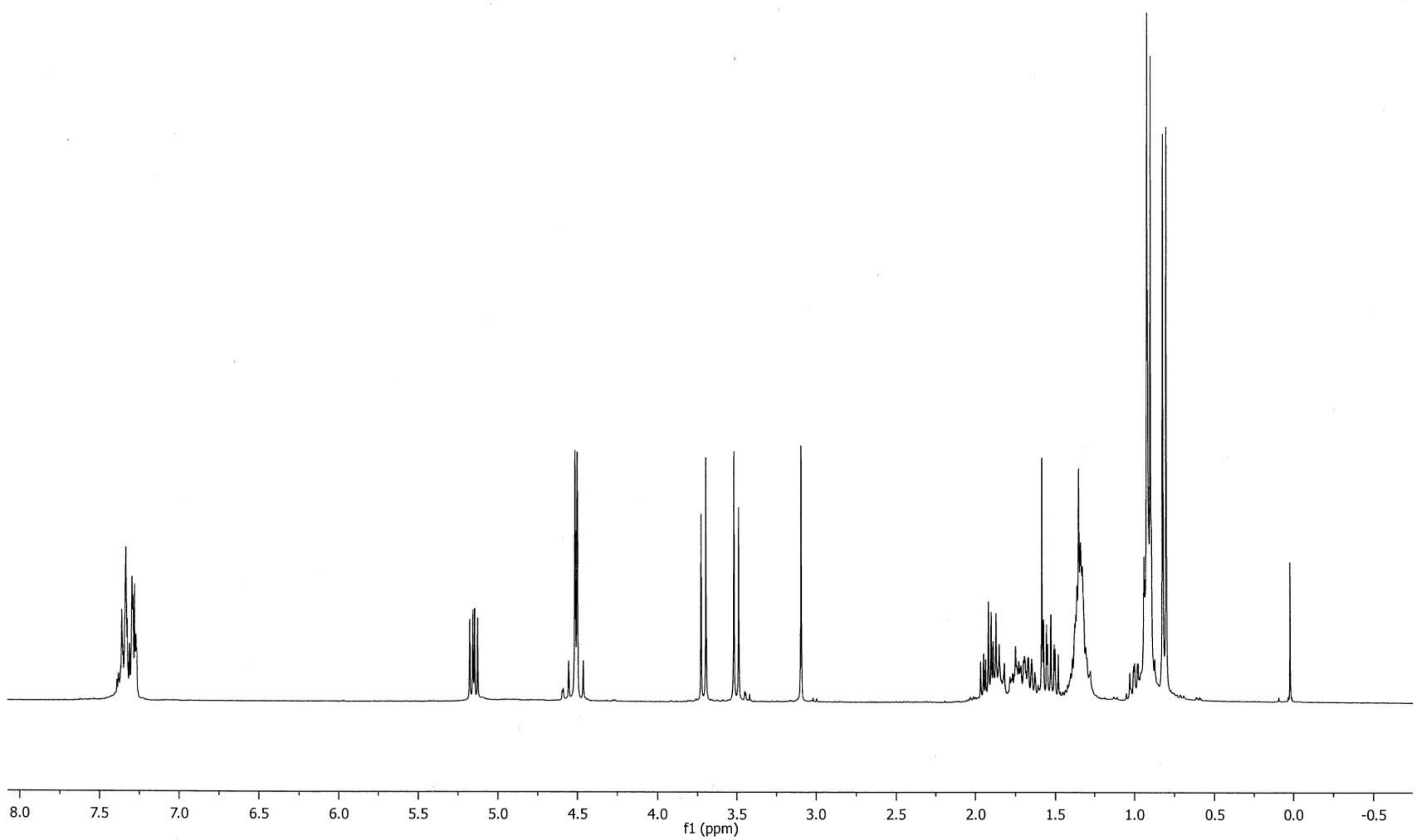

^{1}H NMR (500 MHz, $CDCl_3$)

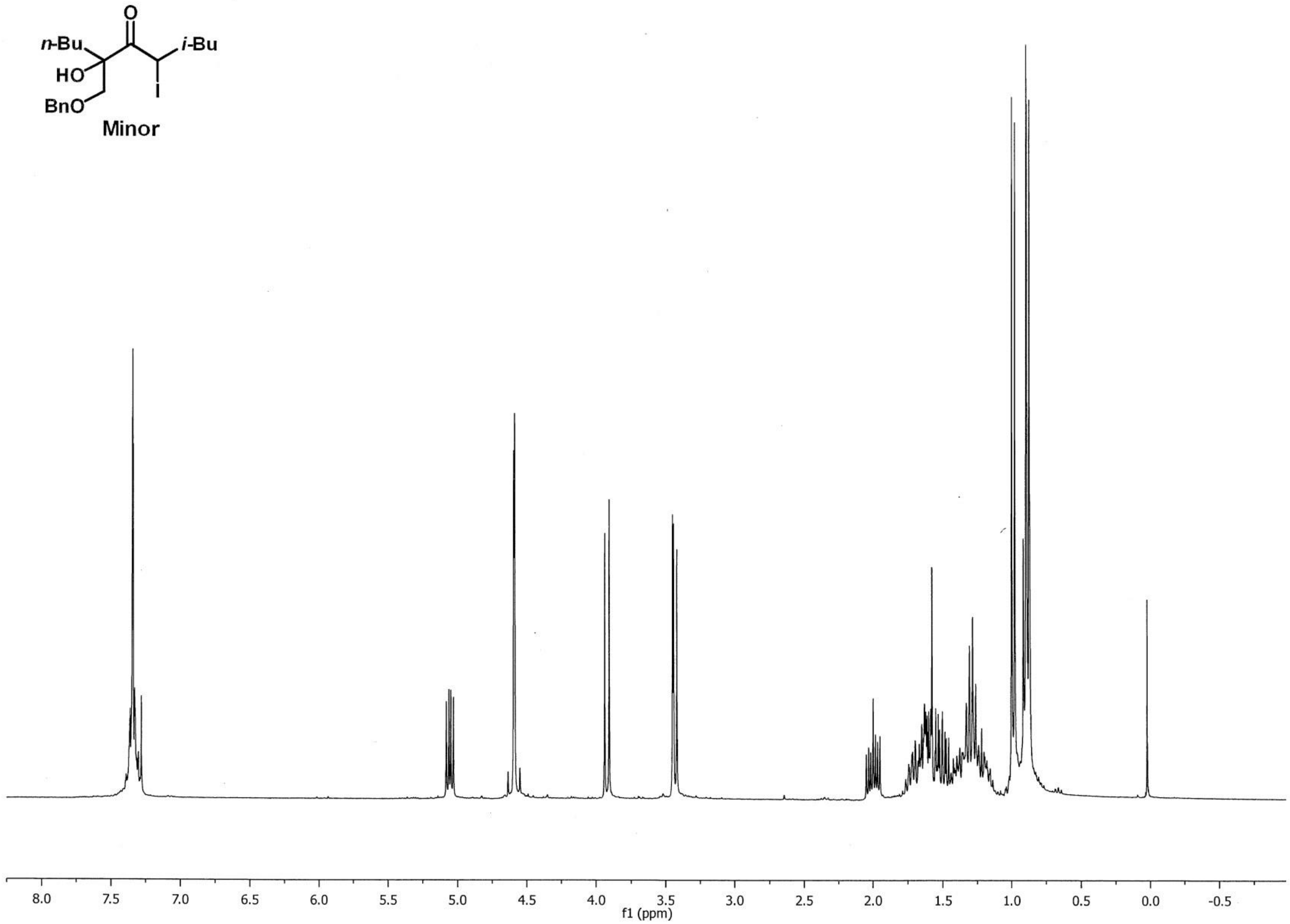

^{13}C NMR (125 MHz, $CDCl_3$)

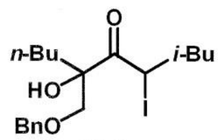

Major

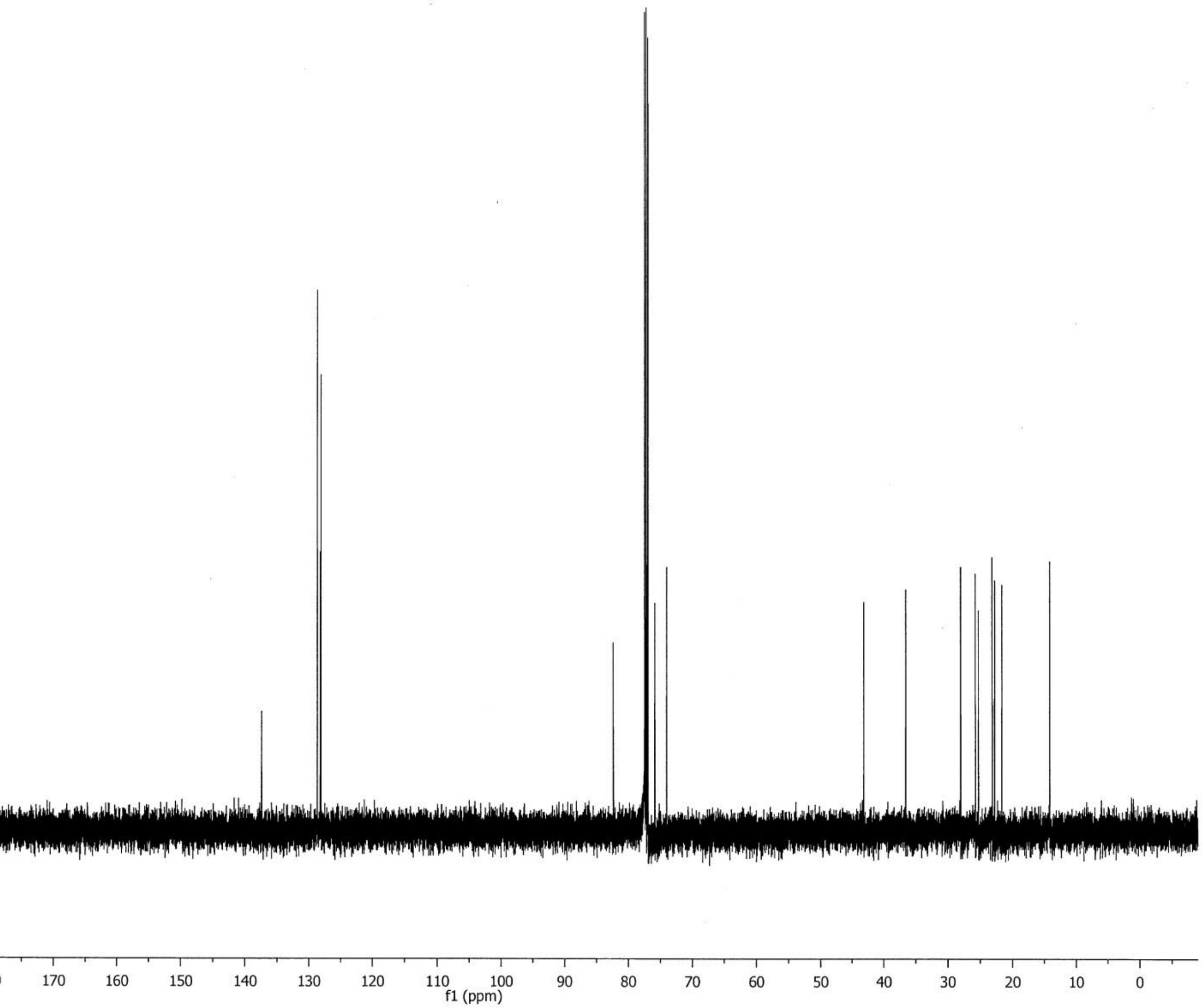

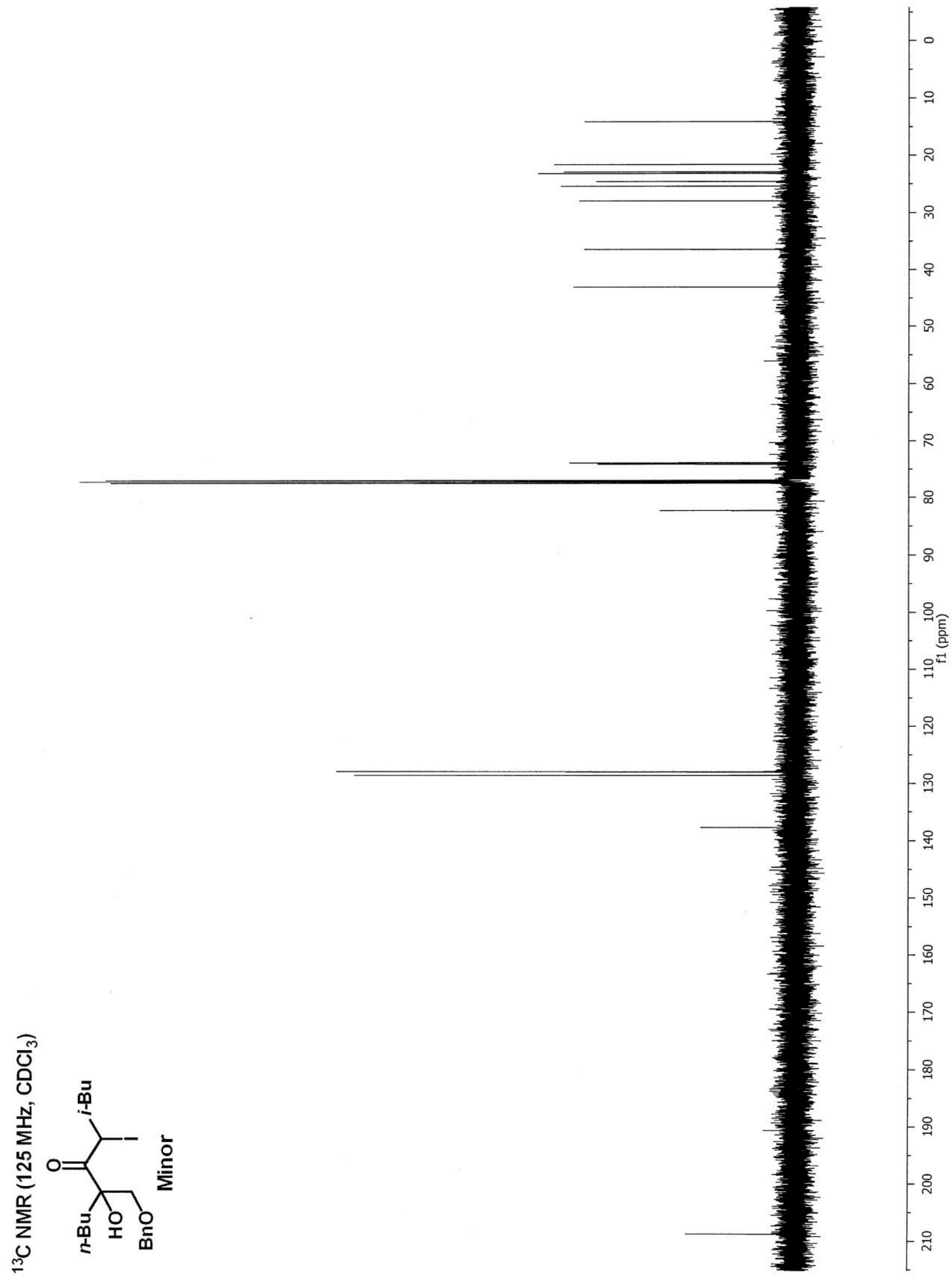

^{13}C NMR (125 MHz, CDCl$_3$)
O
n-Bu
i-Bu
HO
BnO
Minor
f1 (ppm)
0 10 20 30 40 50 60 70 80 90 100 110 120 130 140 150 160 170 180 190 200 210

^1H NMR (500 MHz, $CDCl_3$)

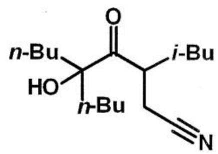

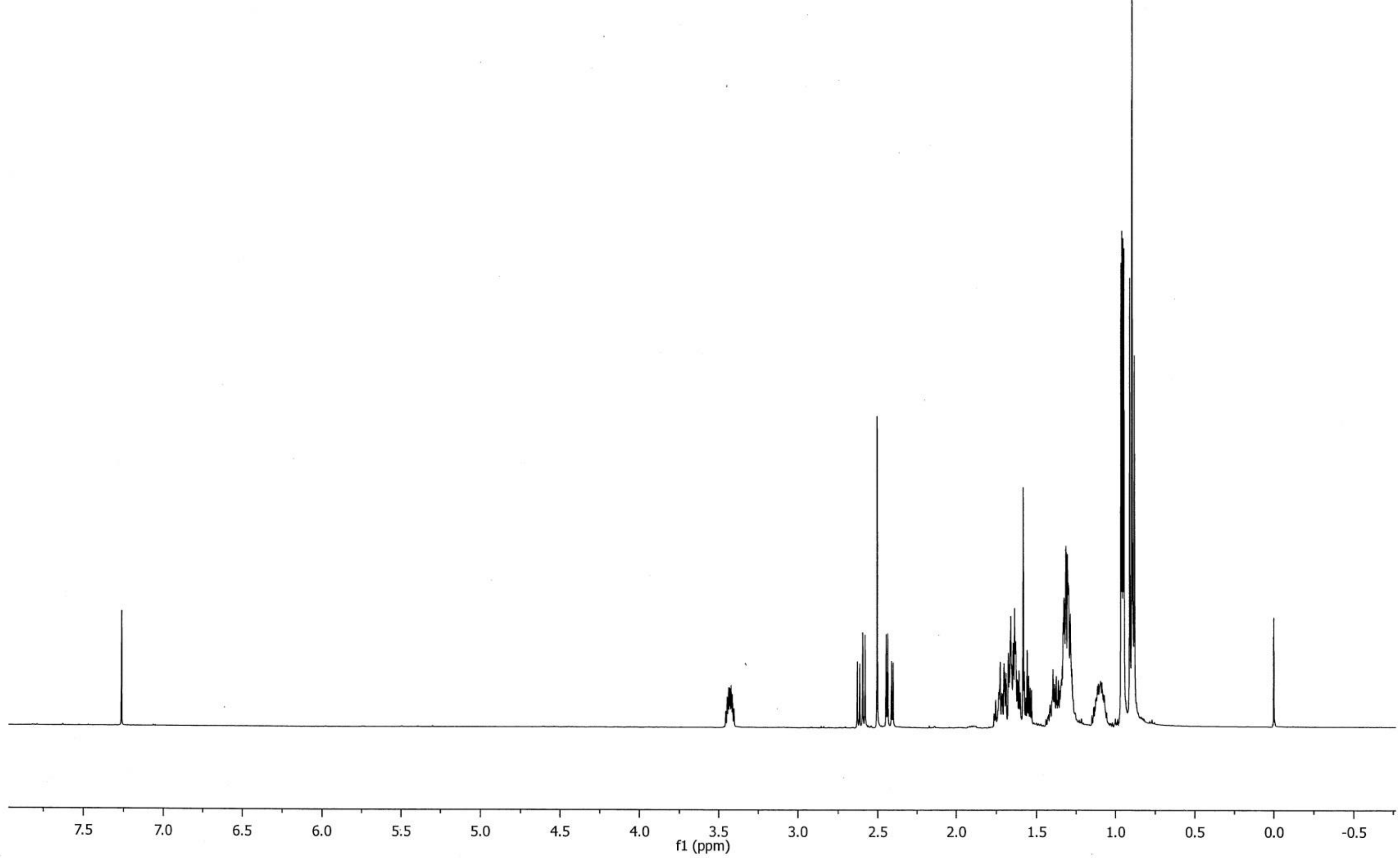

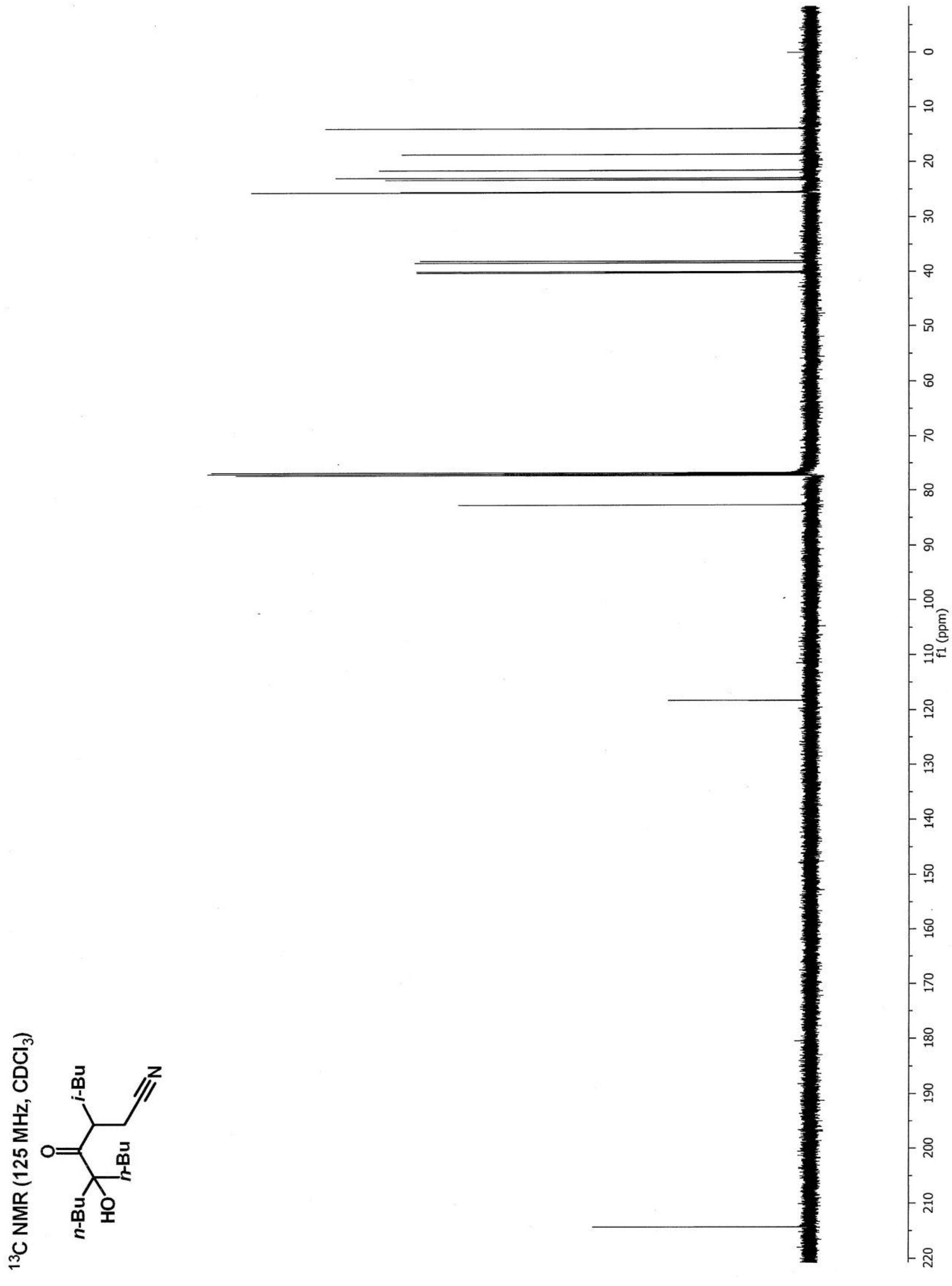
^{13}C NMR (125 MHz, CDCl$_3$)
O
i-Bu
n-Bu
HO
n-Bu
N
f1 (ppm)
0 10 20 30 40 50 60 70 80 90 100 110 120 130 140 150 160 170 180 190 200 210 220

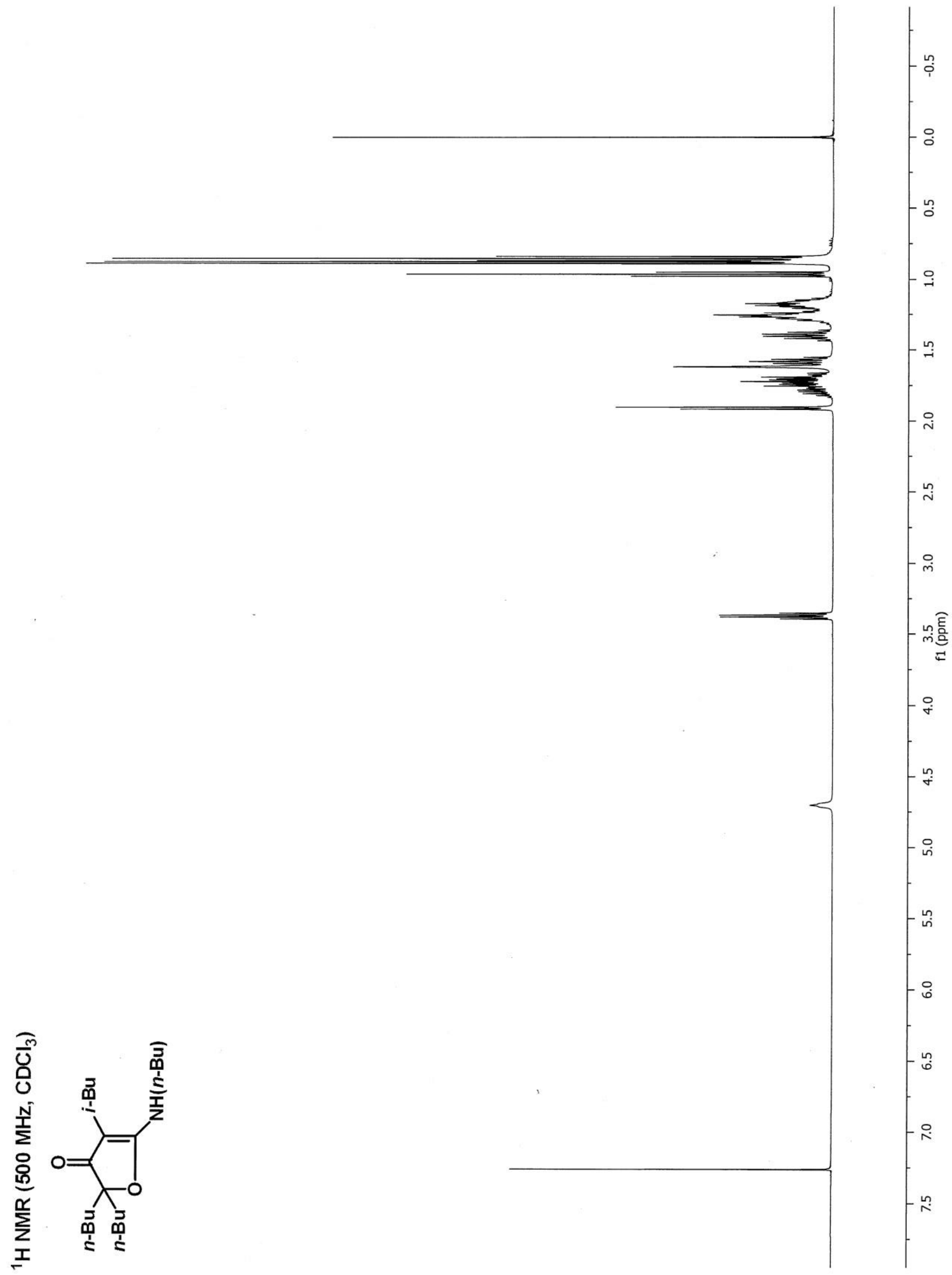
1H NMR (500 MHz, CDCl3)
i-Bu
NH(n-Bu)
n-Bu
n-Bu
O
f1 (ppm)
7.5 7.0 6.5 6.0 5.5 5.0 4.5 4.0 3.5 3.0 2.5 2.0 1.5 1.0 0.5 0.0 -0.5

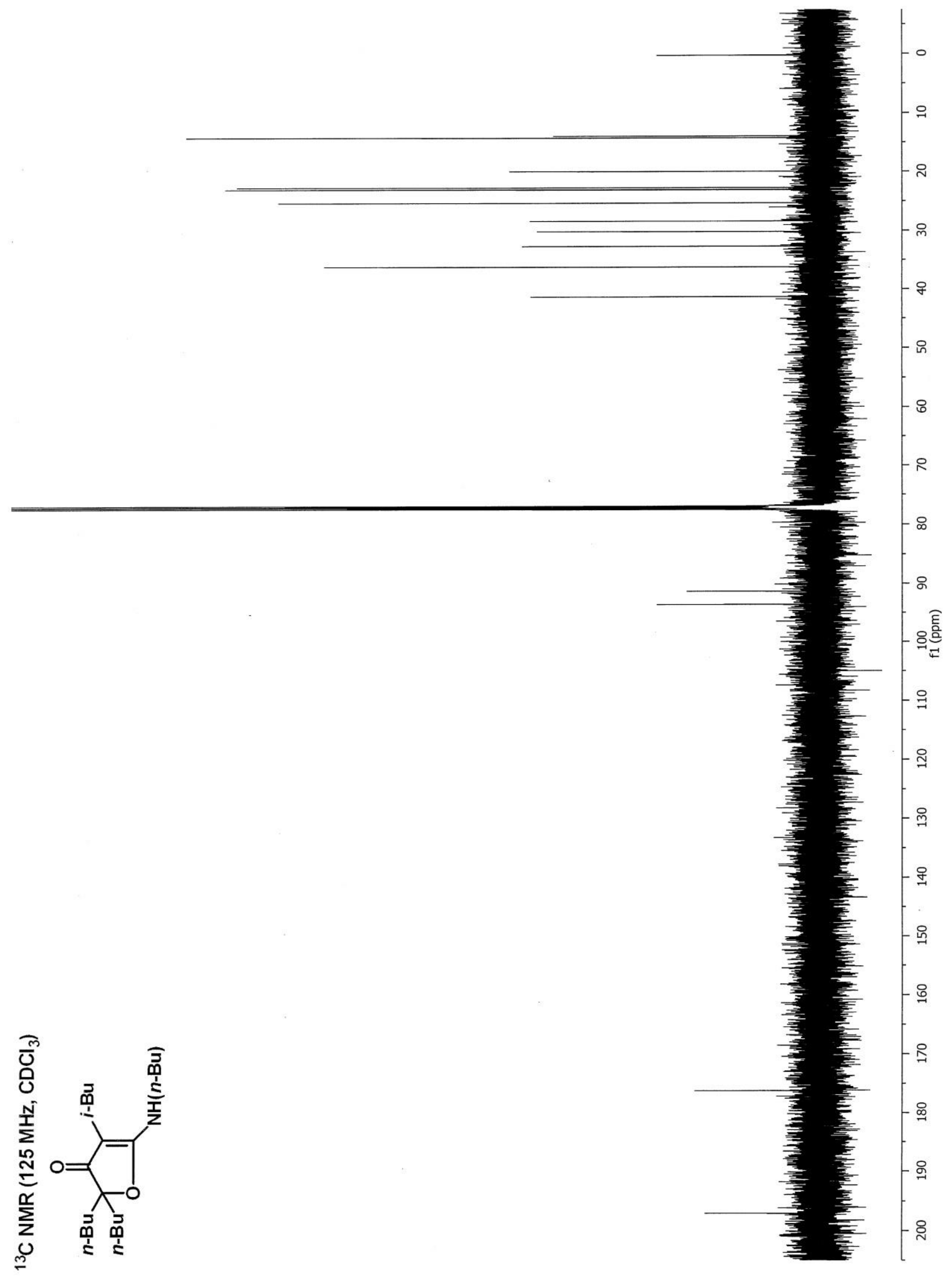

^{13}C NMR (125 MHz, $CDCl_3$)
n-Bu
n-Bu
O
i-Bu
NH(*n*-Bu)
f1 (ppm)

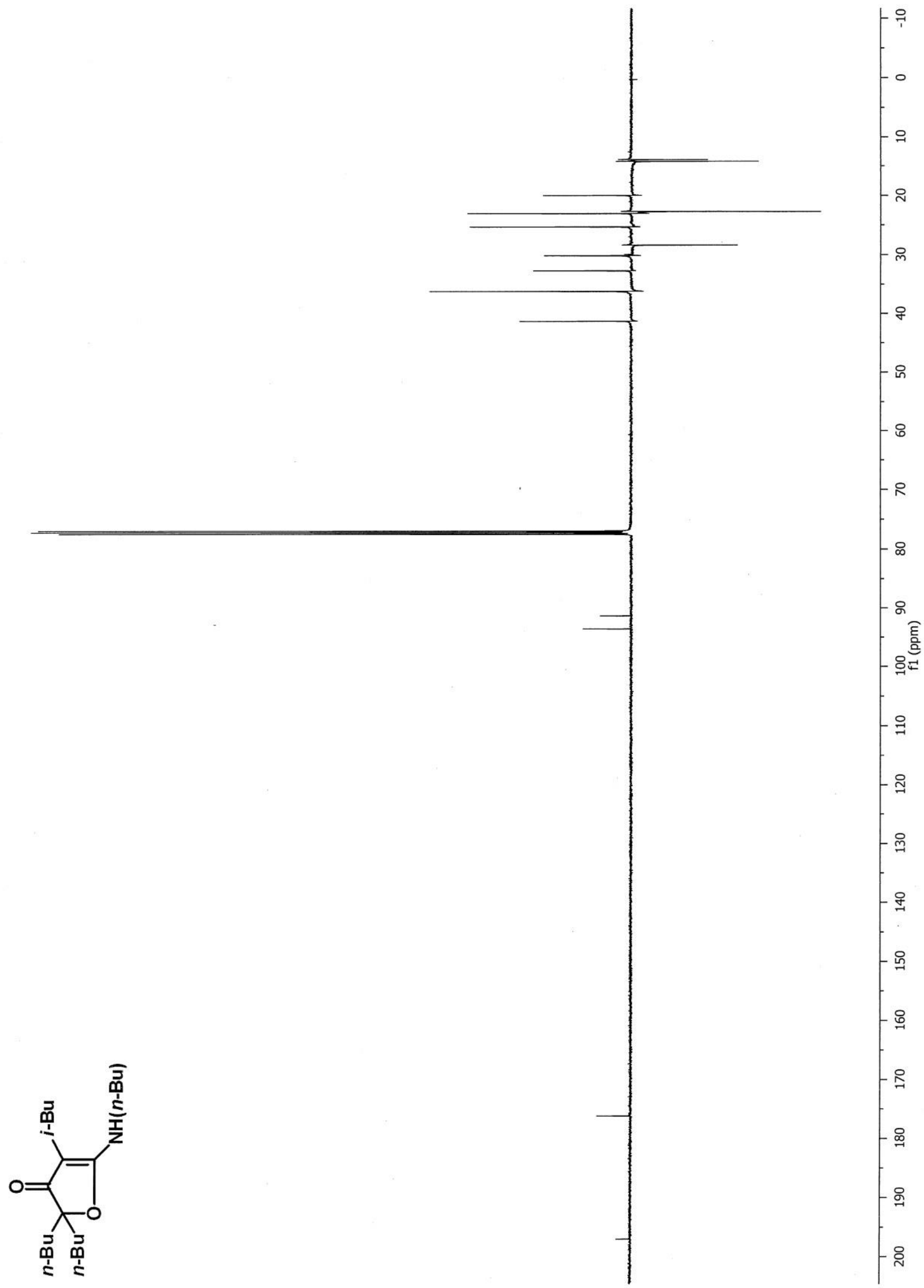

n-Bu
n-Bu
O
O
i-Bu
NH(n-Bu)
f1 (ppm)
-10
0
10
20
30
40
50
60
70
80
90
100
110
120
130
140
150
160
170
180
190
200

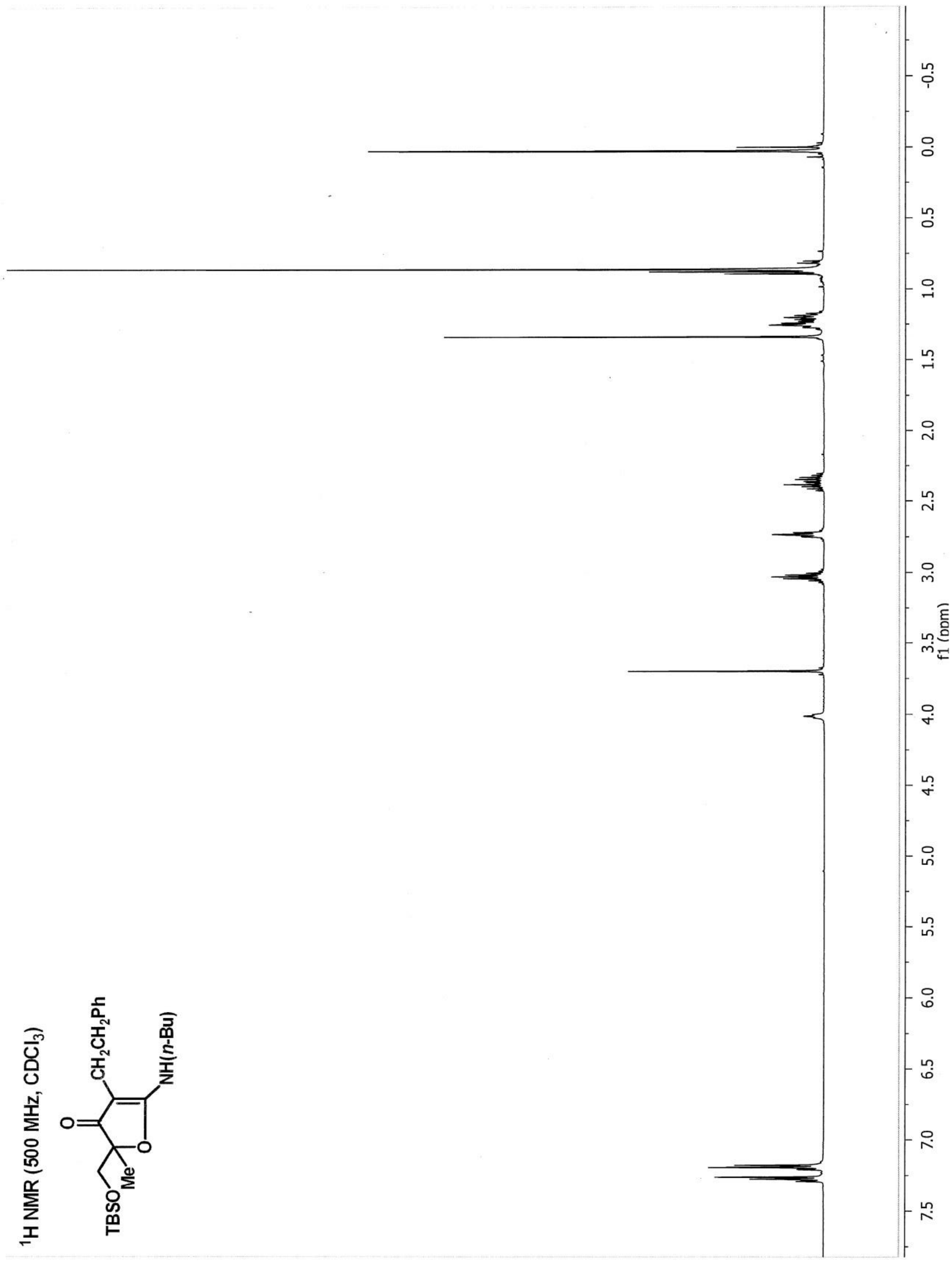

1H NMR (500 MHz, CDCl3)
O
CH2CH2Ph
NH(n-Bu)
TBSO
Me
O
-0.5
0.0
0.5
1.0
1.5
2.0
2.5
3.0
3.5
f1 (ppm)
4.0
4.5
5.0
5.5
6.0
6.5
7.0
7.5

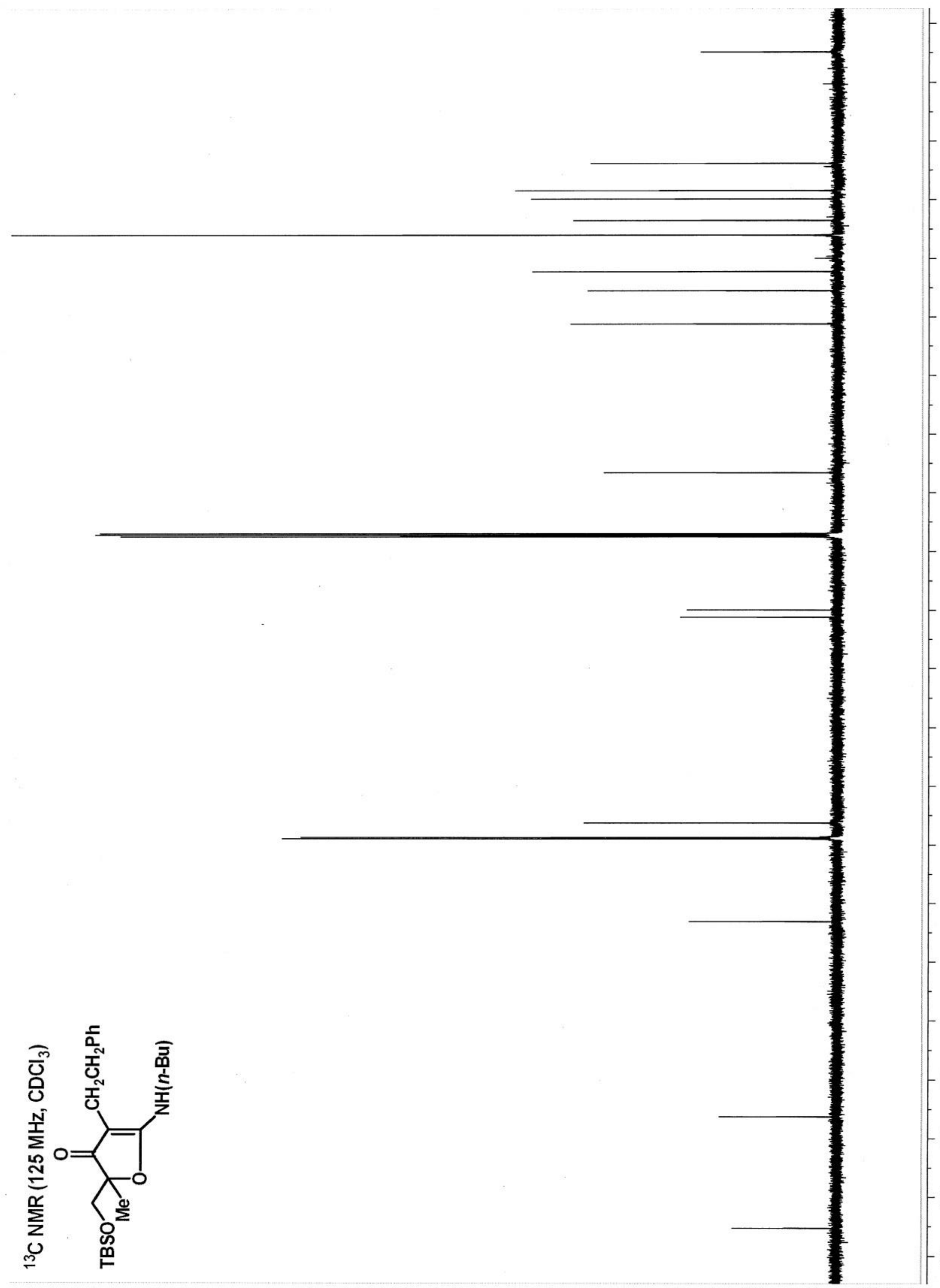
13C NMR (125 MHz, CDCl3)
TBSO
Me
O
O
CH2CH2Ph
NH(n-Bu)
f1 (ppm)
200 190 180 170 160 150 140 130 120 110 100 90 80 70 60 50 40 30 20 10 0 -10

^{1}H NMR (500 MHz, $CDCl_3$)

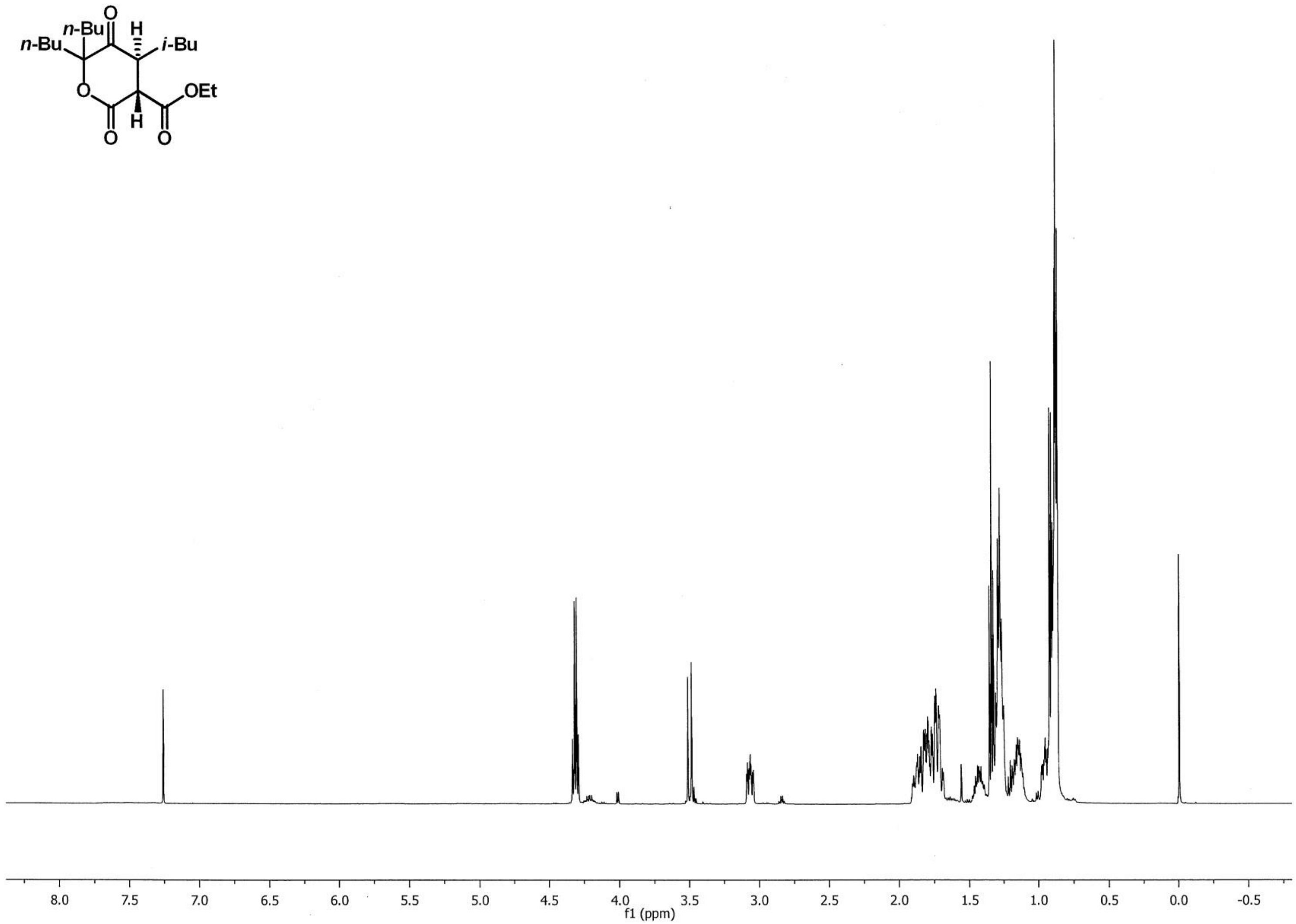

^{13}C NMR (125 MHz, $CDCl_3$)

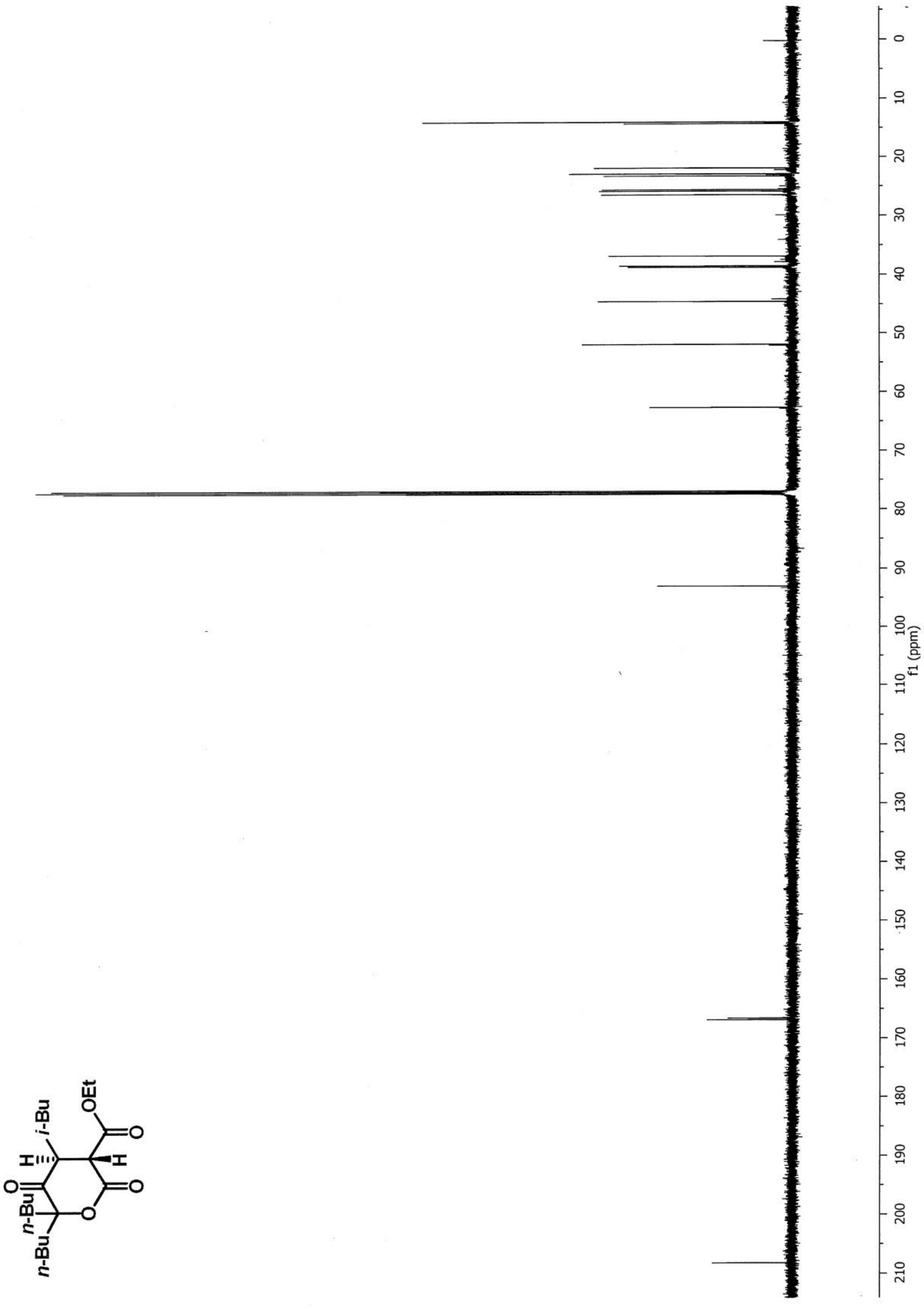

^1H NMR (400 MHz, $CDCl_3$)

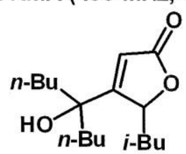

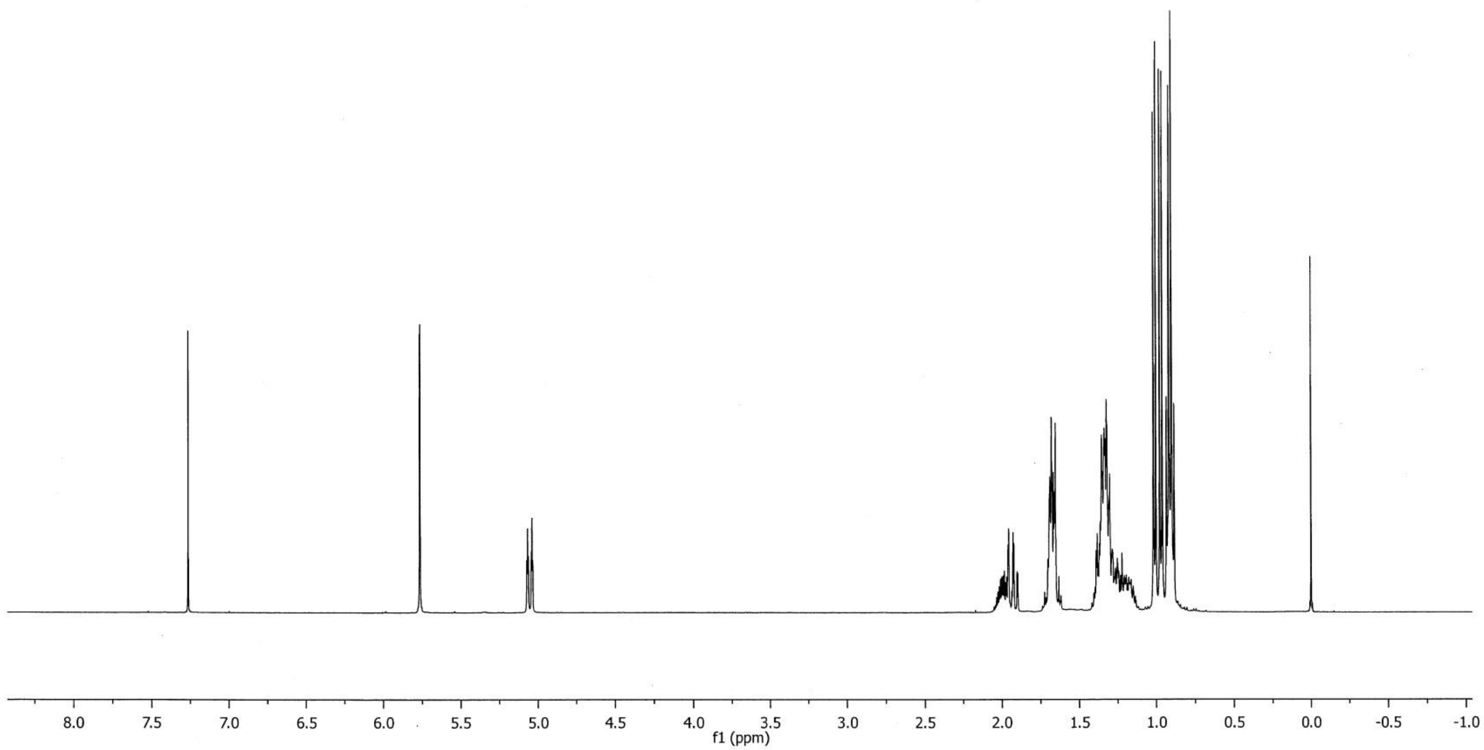

^{13}C NMR (100 MHz, $CDCl_3$)

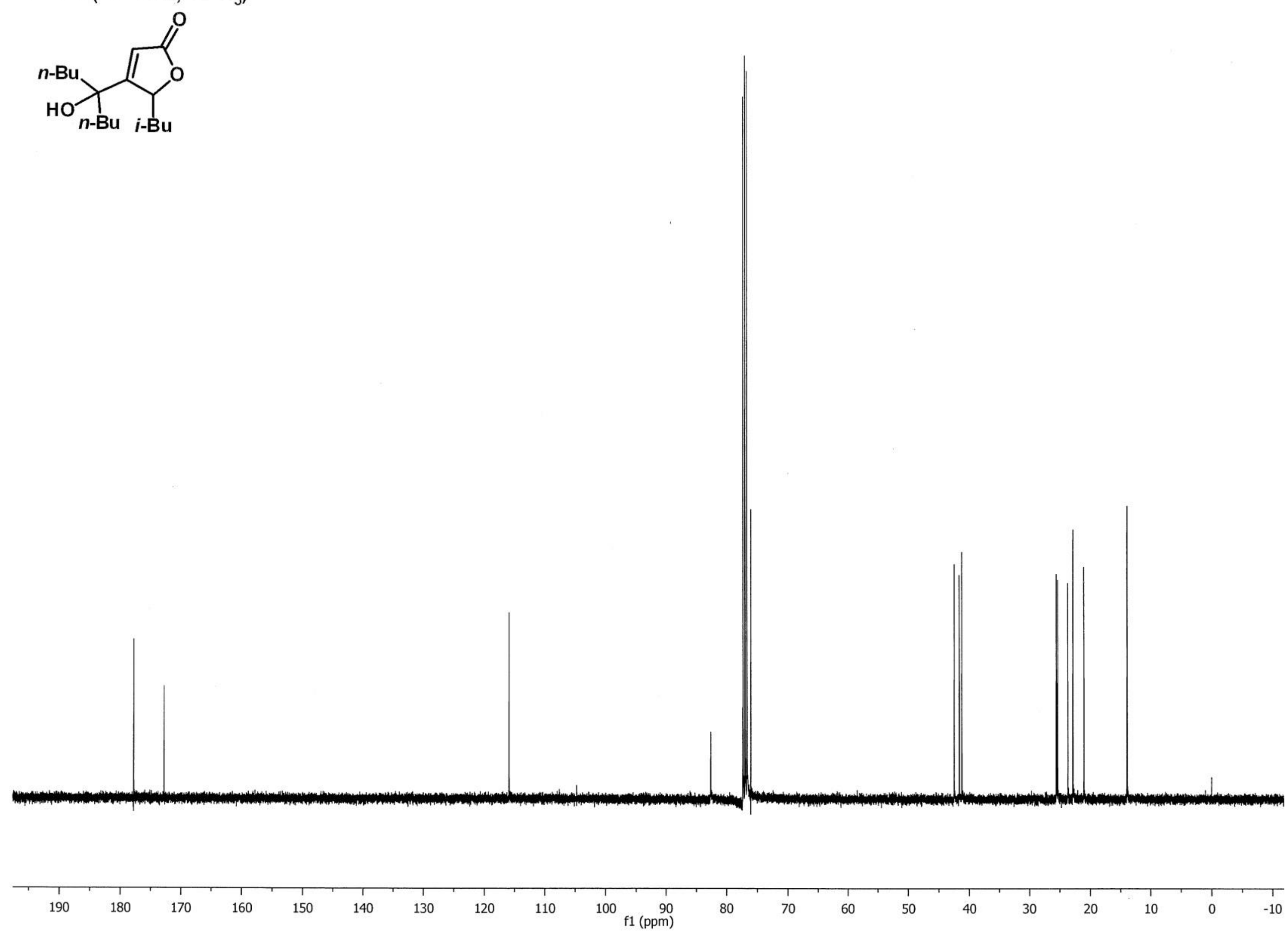

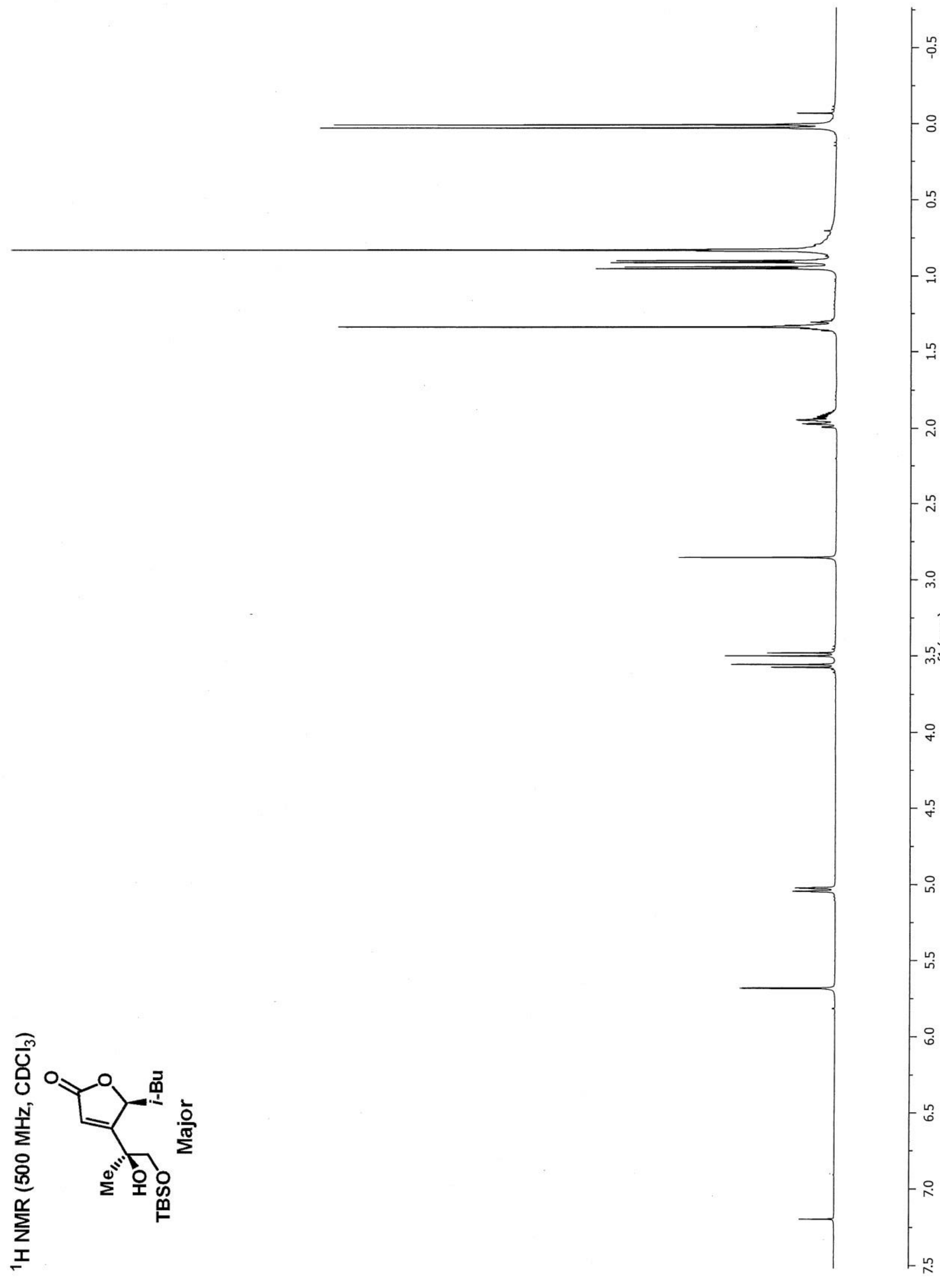

1H NMR (500 MHz, CDCl3)
Me
HO
TBSO
O
O
i-Bu
Major
f1 (ppm)
7.5
7.0
6.5
6.0
5.5
5.0
4.5
4.0
3.5
3.0
2.5
2.0
1.5
1.0
0.5
0.0
-0.5

^1H NMR (500 MHz, $CDCl_3$)

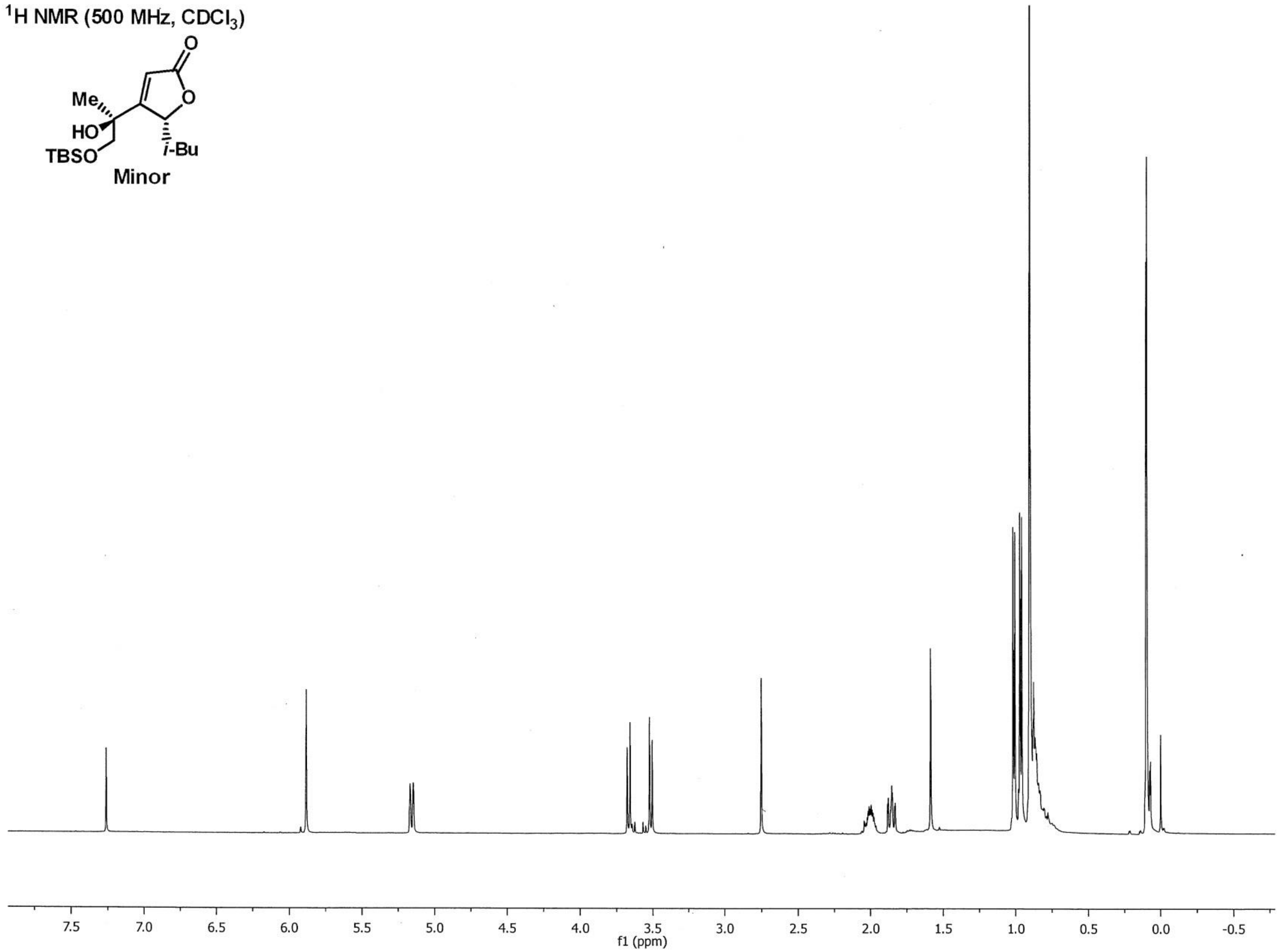

^{13}C NMR (125 MHz, $CDCl_3$)

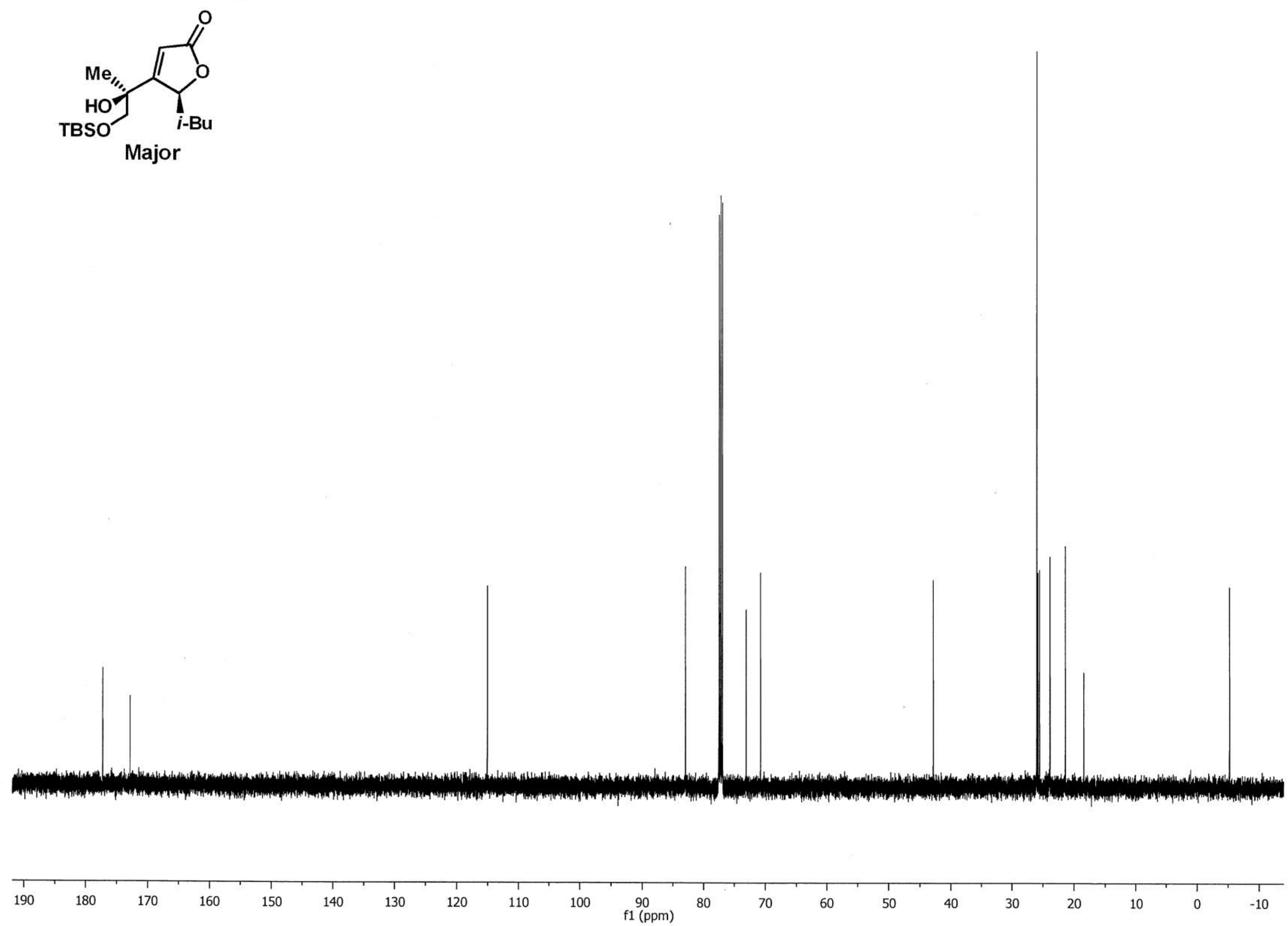

^{13}C NMR (125 MHz, $CDCl_3$)

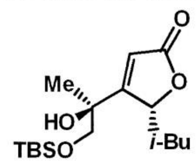

Minor

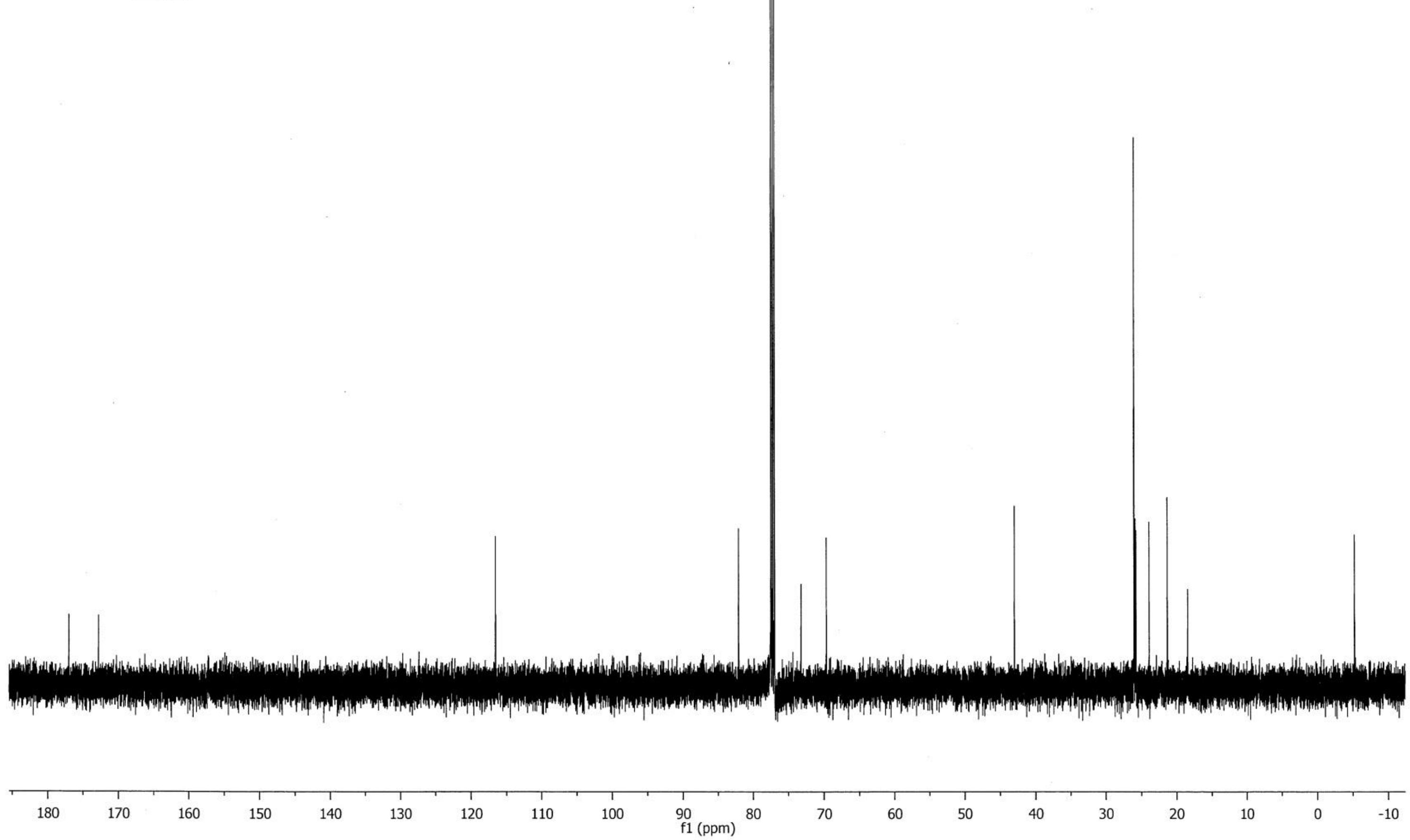

^1H NMR (500 MHz, $CDCl_3$)

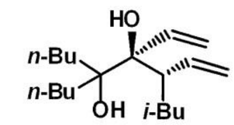

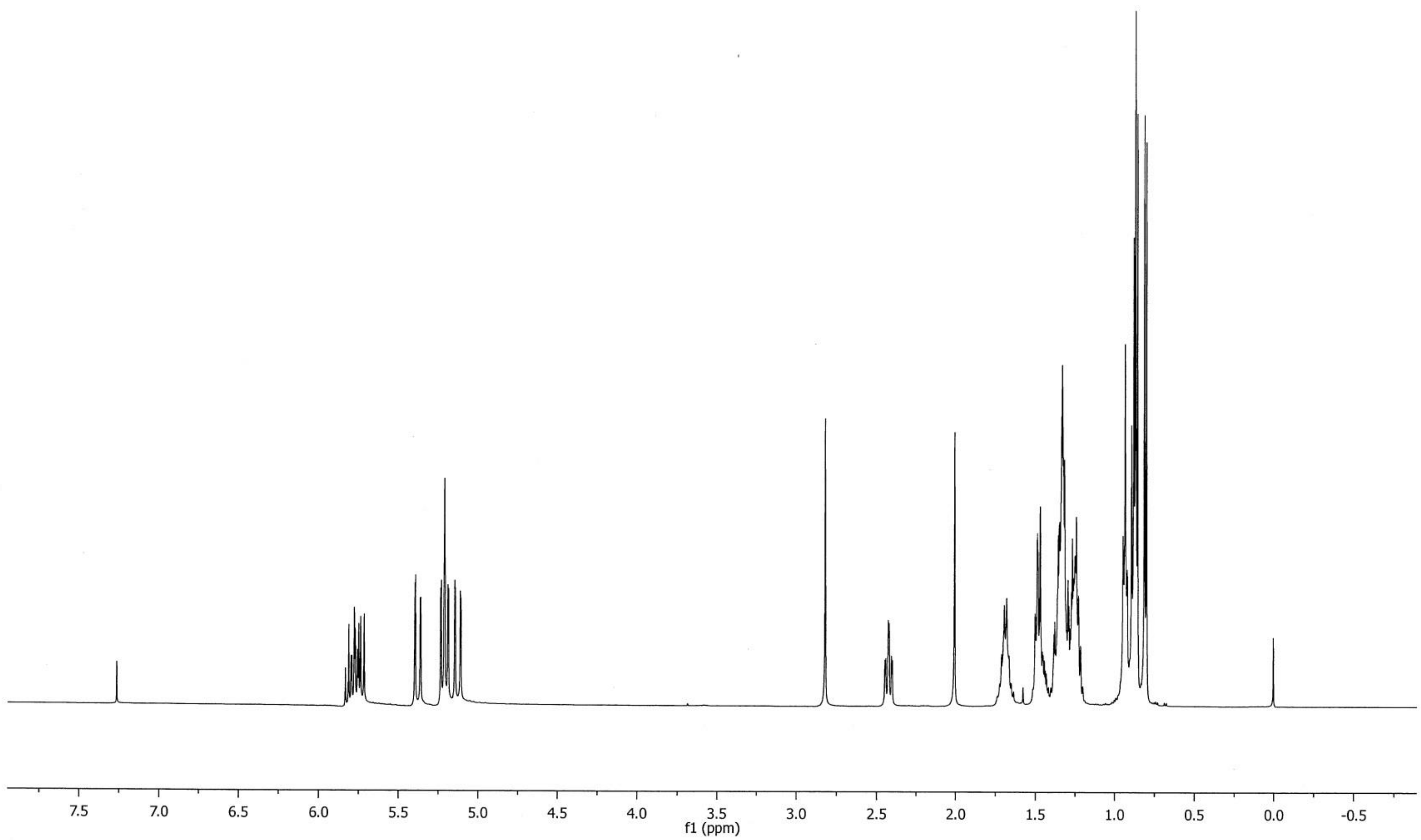

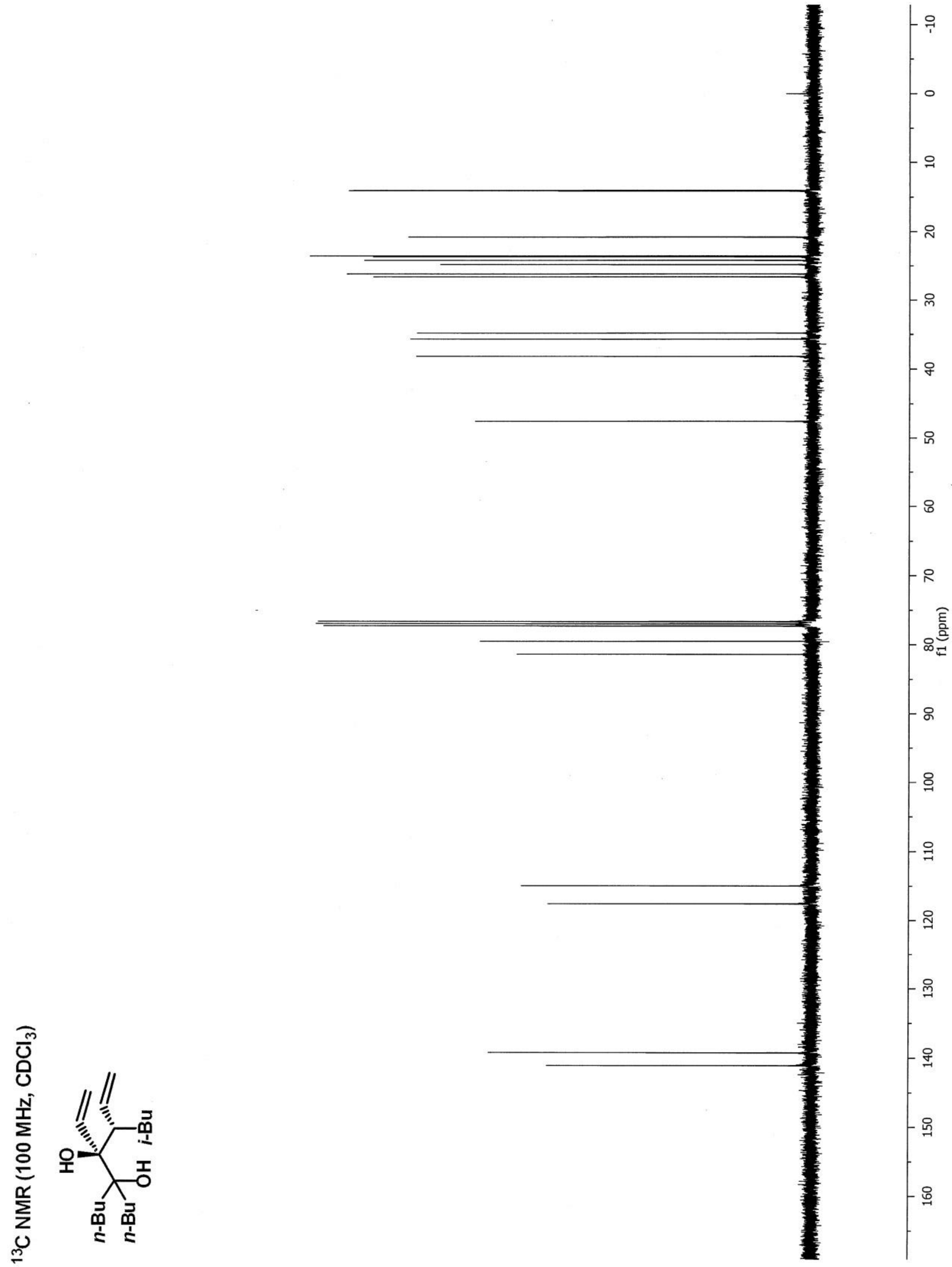
^{13}C NMR (100 MHz, CDCl$_3$)
HO
n-Bu
n-Bu
OH
i-Bu
f1 (ppm)
-10
0
10
20
30
40
50
60
70
80
90
100
110
120
130
140
150
160

^{1}H NMR (400 MHz, $CDCl_3$)

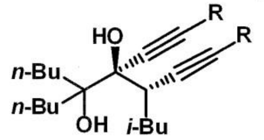

(R= n-Bu)

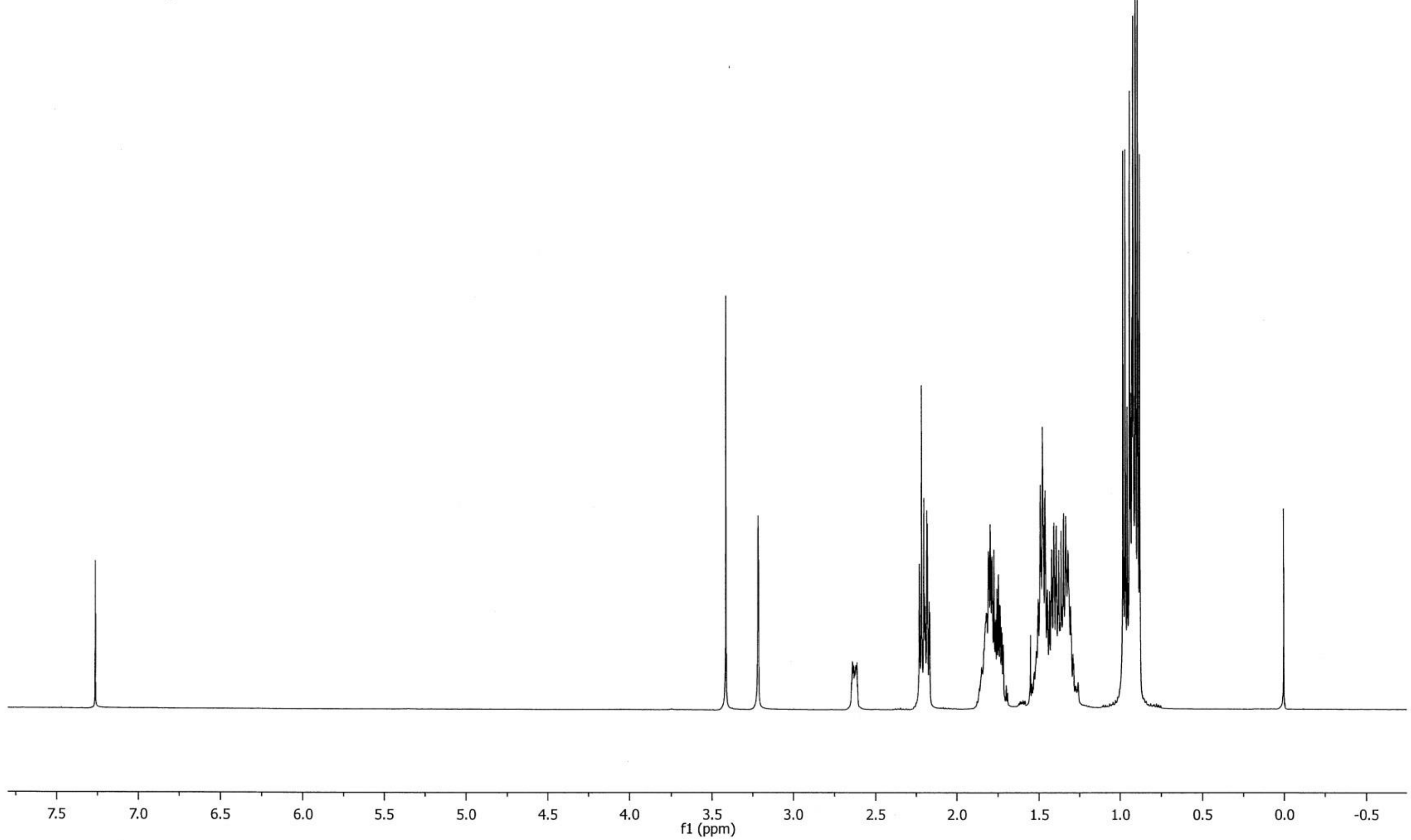

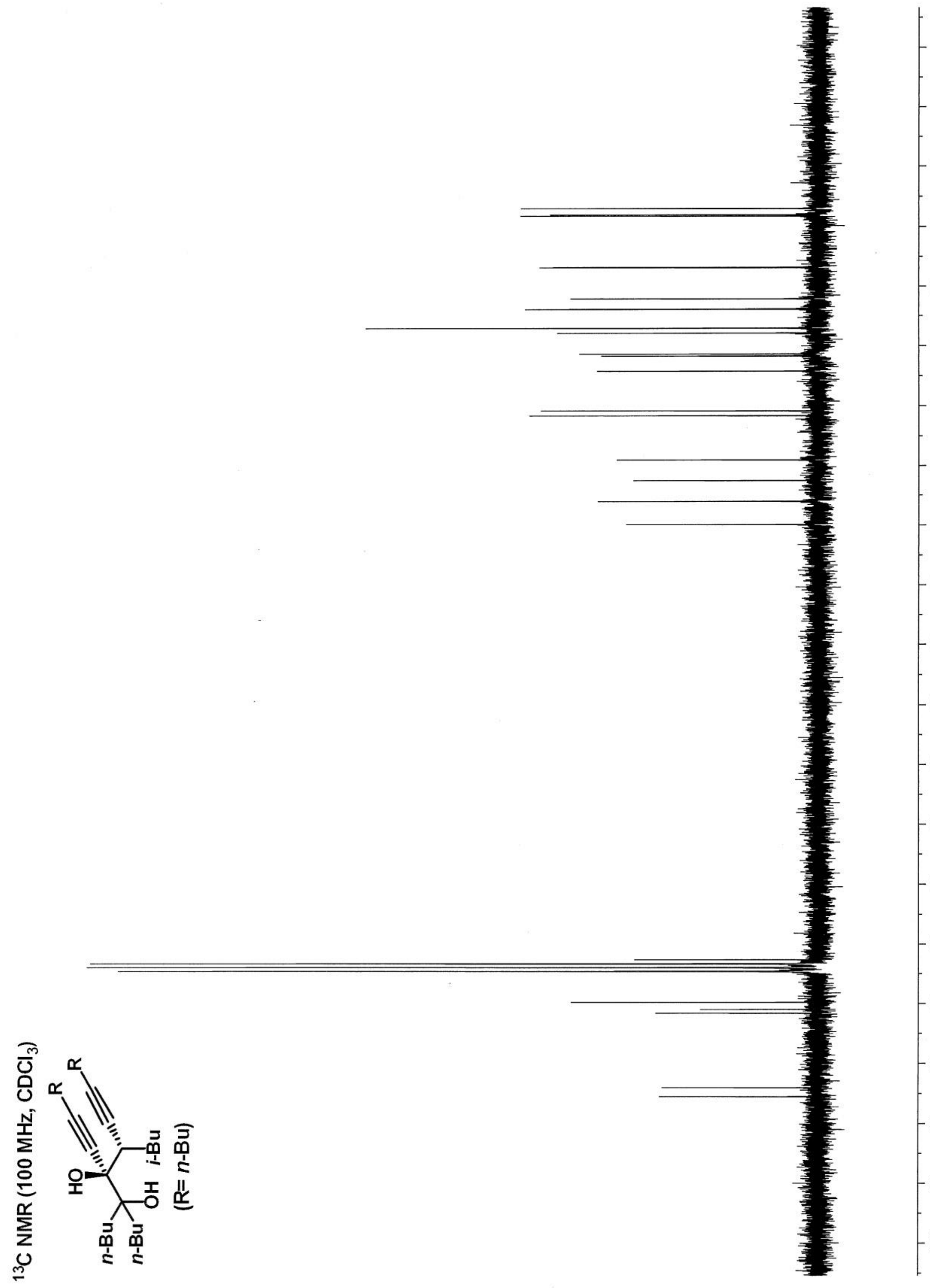

^{13}C NMR (100 MHz, CDCl$_3$)
R
R
HO
n-Bu
n-Bu
OH
i-Bu
(R= n-Bu)
0
5
10
15
20
25
30
35
40
45
50
f1 (ppm)
55
60
65
70
75
80
85
90
95
100

^1H NMR (400 MHz, $CDCl_3$)

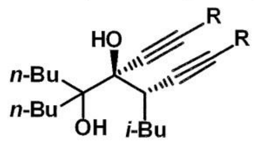

(R= TMS)

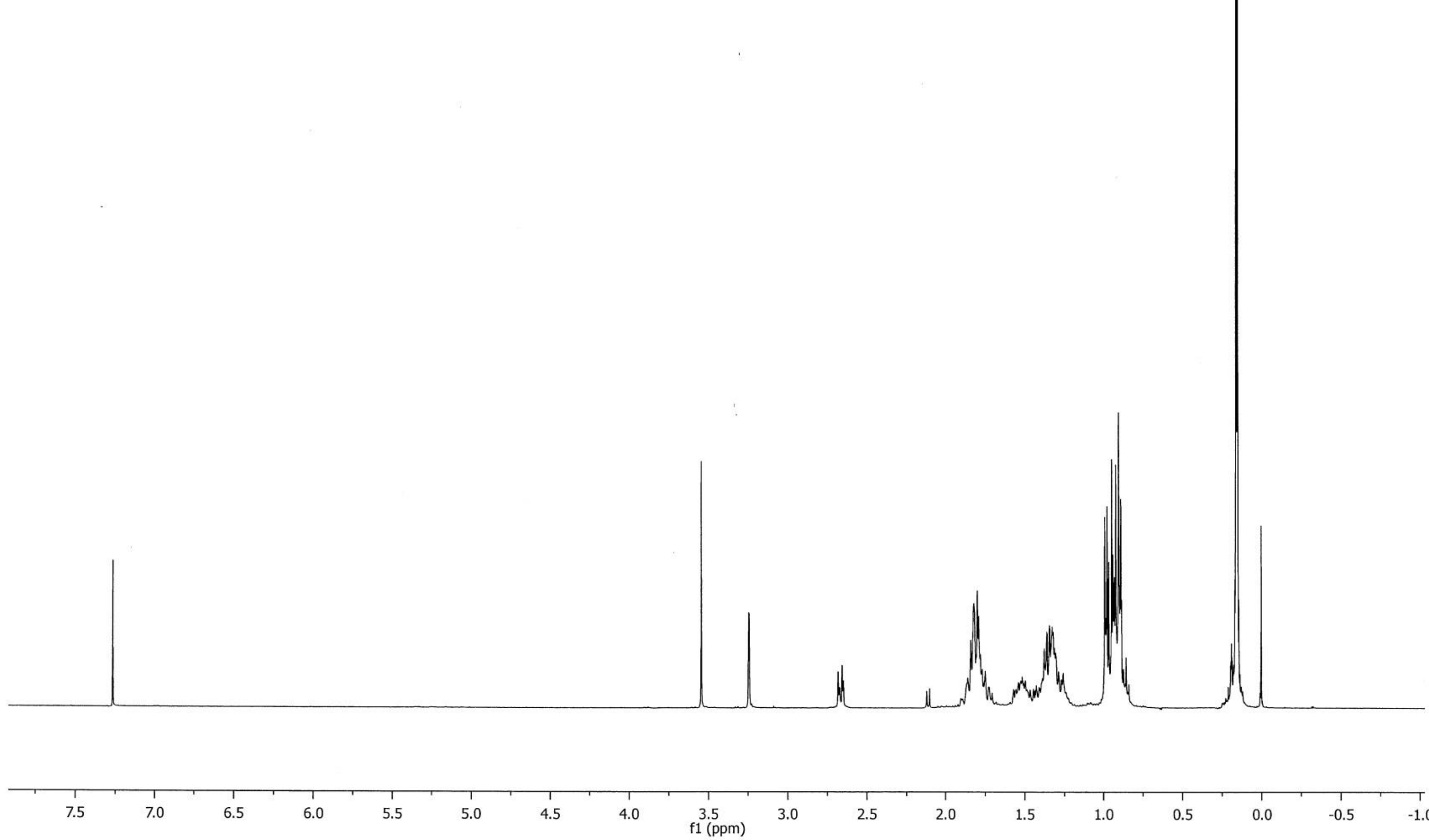

^{13}C NMR (100 MHz, $CDCl_3$)

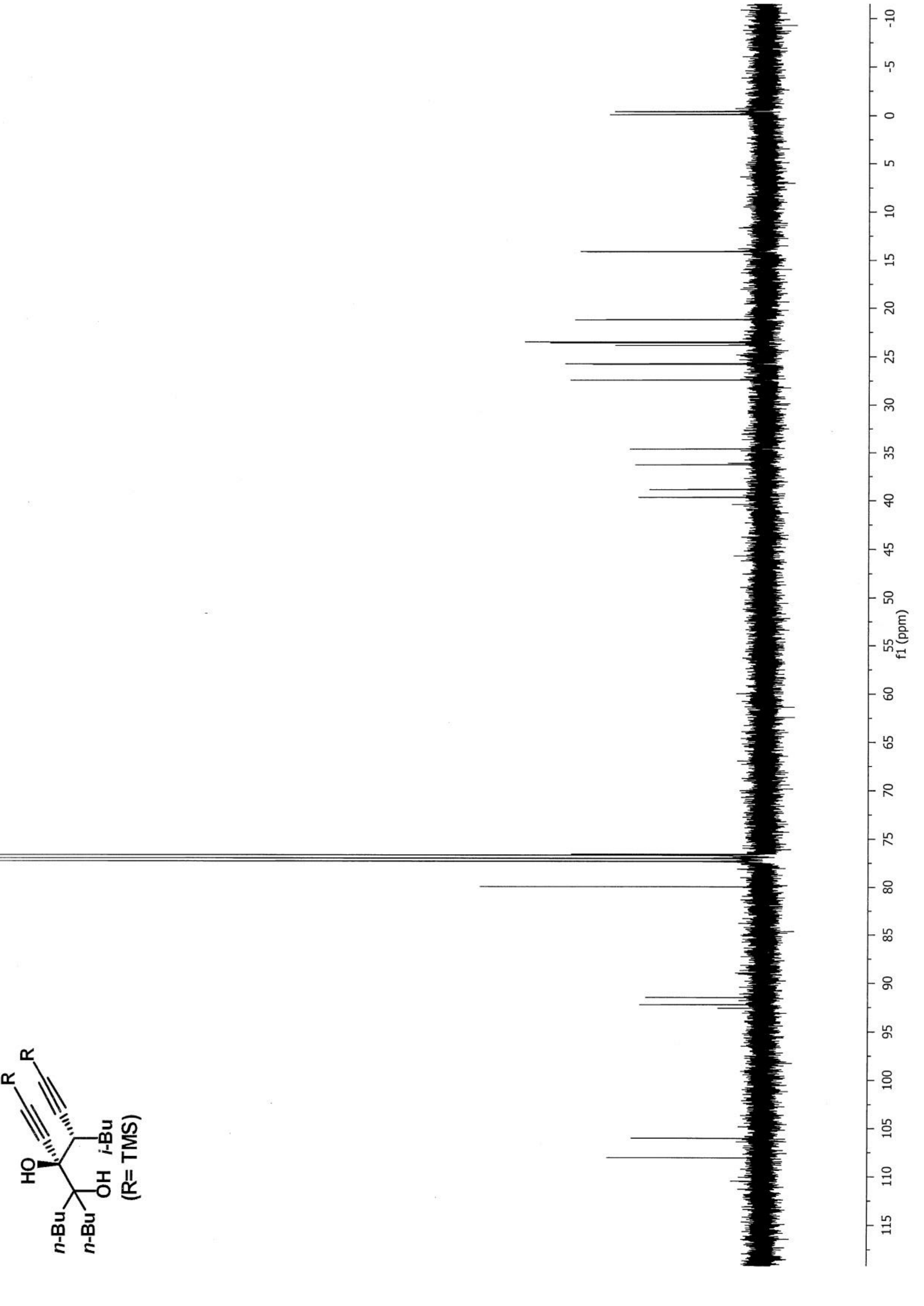

^1H NMR (500 MHz, $CDCl_3$)

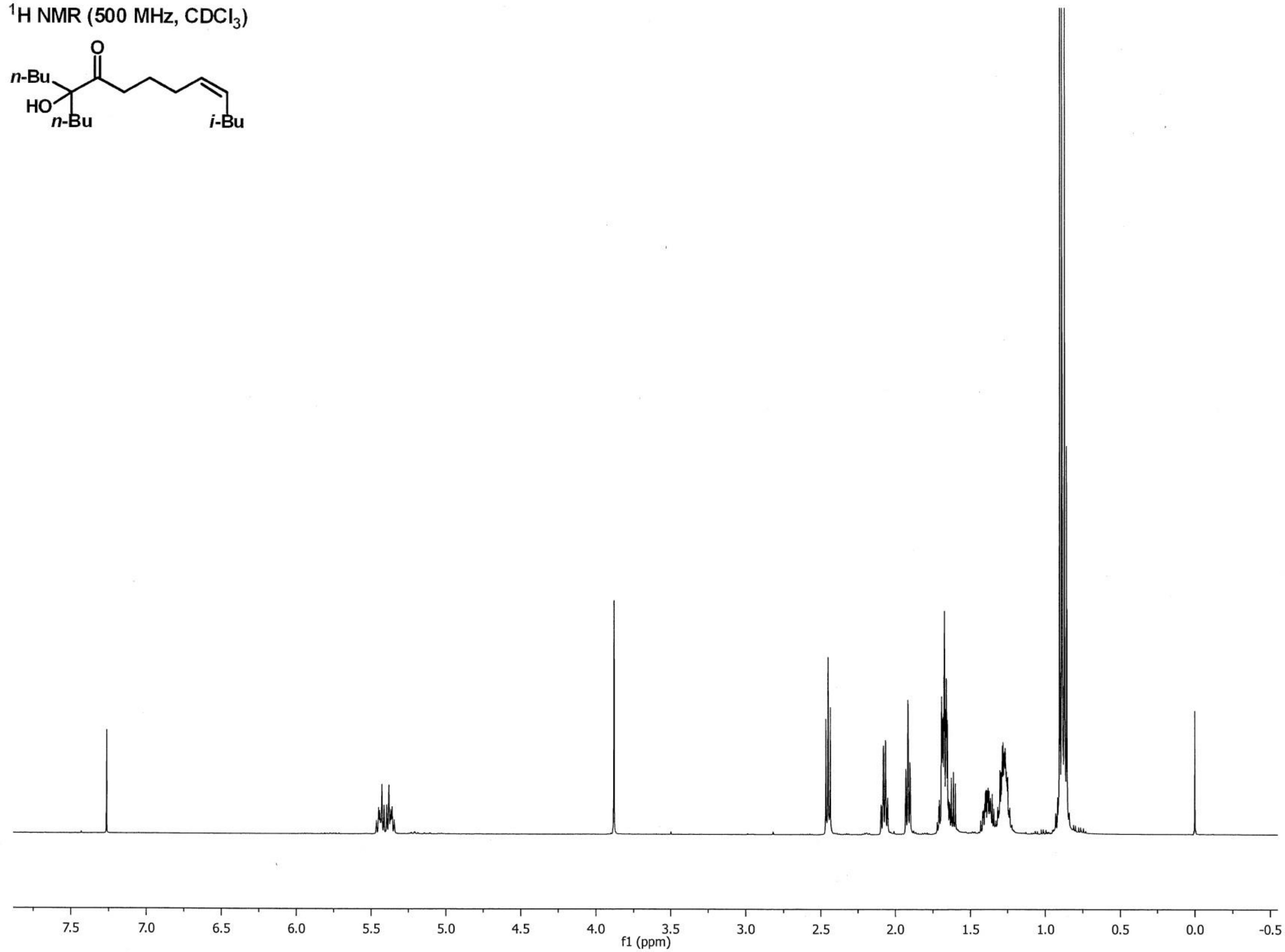

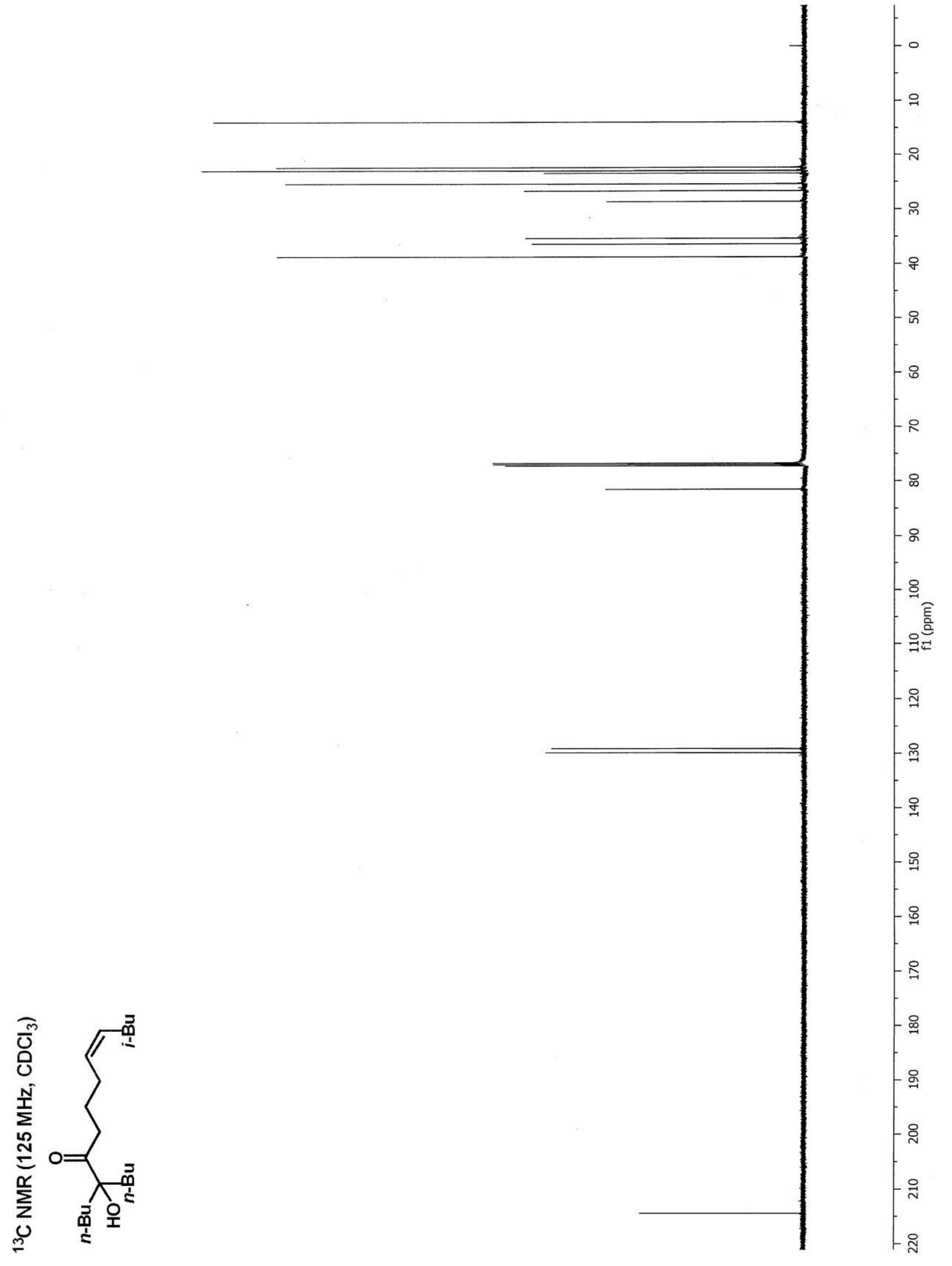

^{13}C NMR (125 MHz, $CDCl_3$)
n-Bu
HO
n-Bu
O
i-Bu
f1 (ppm)
0
10
20
30
40
50
60
70
80
90
100
110
120
130
140
150
160
170
180
190
200
210
220

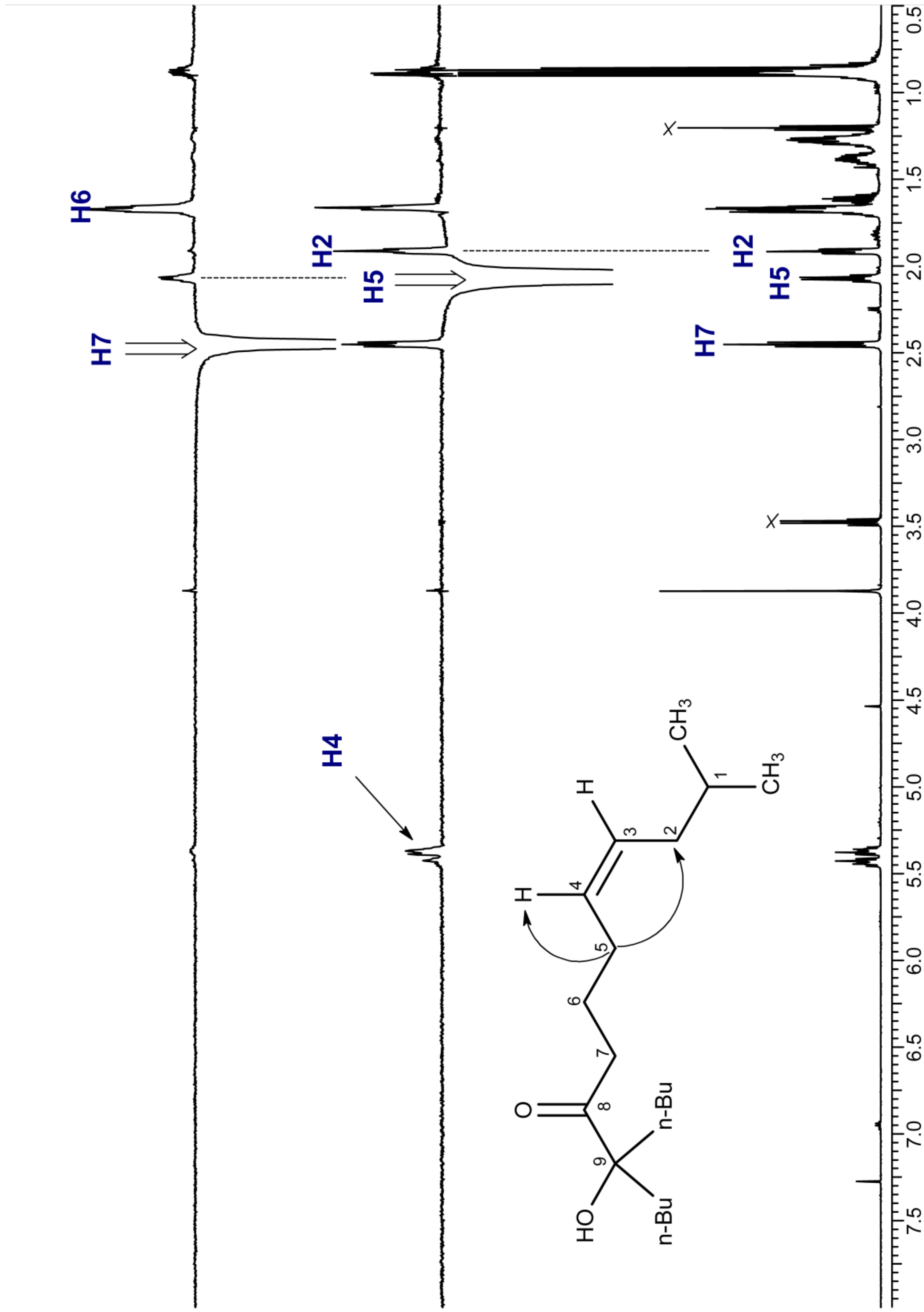

H6
H7
H2
H5
H4
H2
H5
H7
CH3
CH3
H
H
O
HO
n-Bu
n-Bu

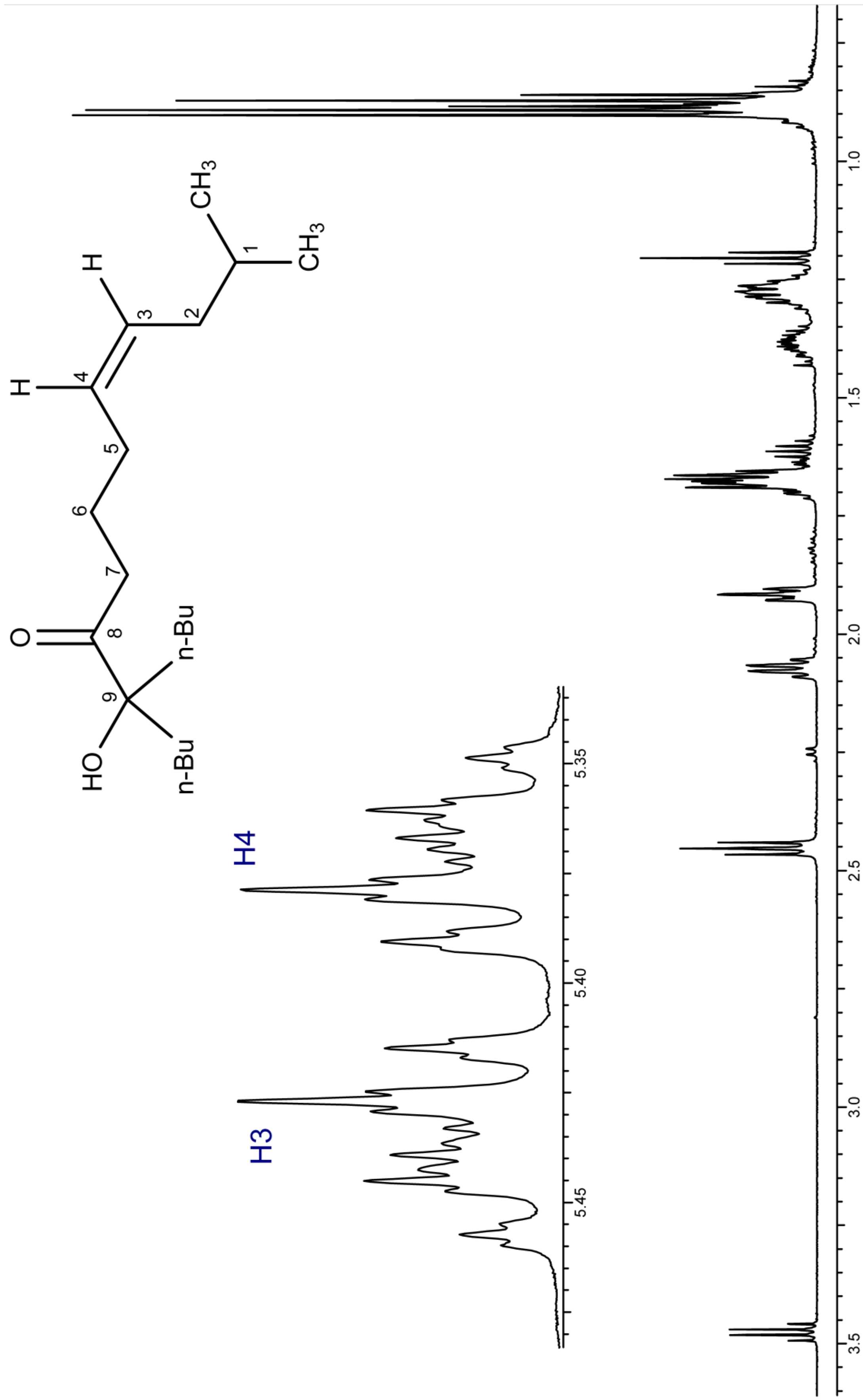

O
HO
n-Bu
n-Bu
H
H
CH_3
CH_3
1
2
3
4
5
6
7
8
9
H4
H3
5.35
5.40
5.45
1.0
1.5
2.0
2.5
3.0
3.5

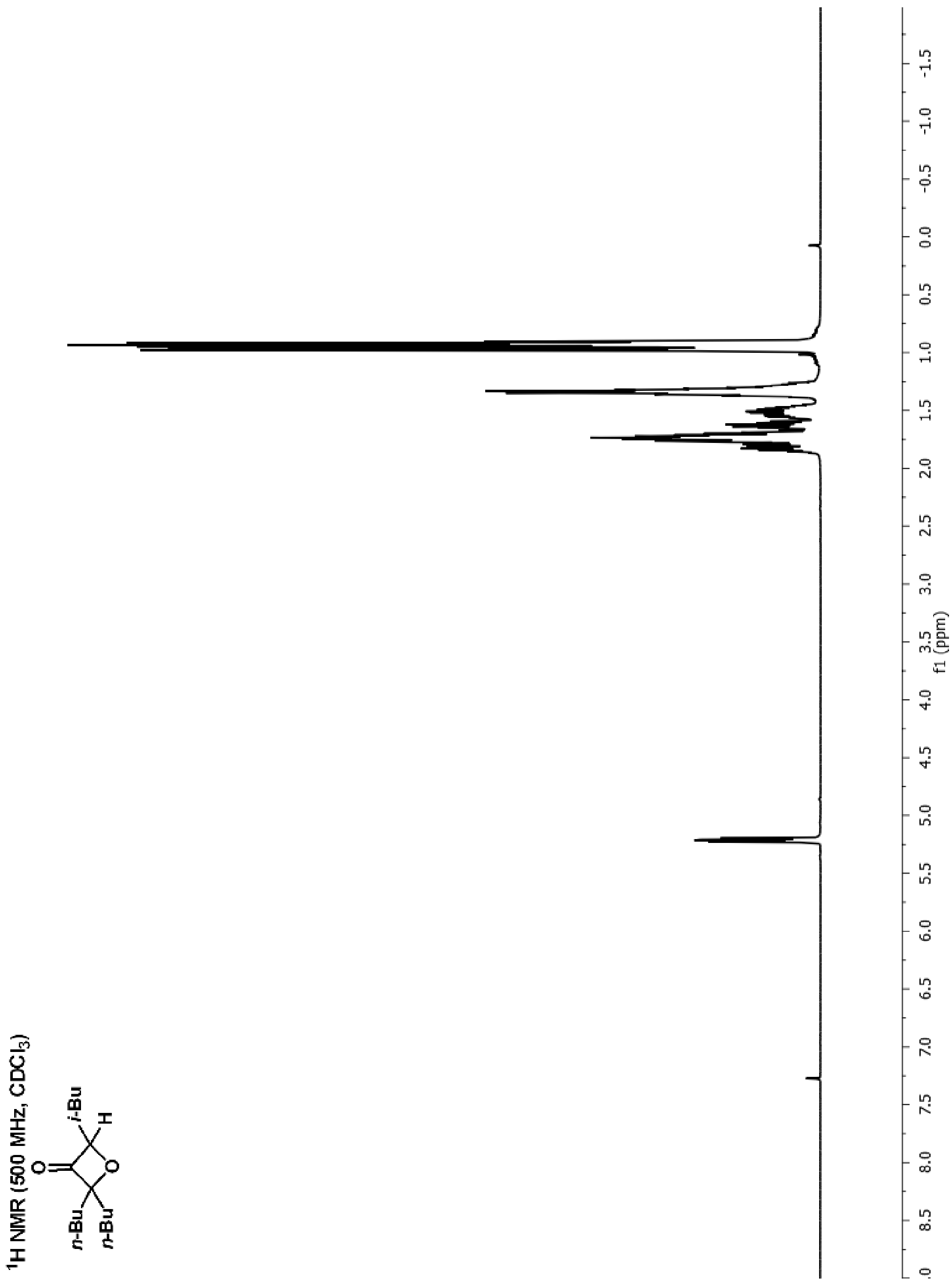

1H NMR (500 MHz, CDCl3)
n-Bu
n-Bu
O
i-Bu
H
O
f1 (ppm)

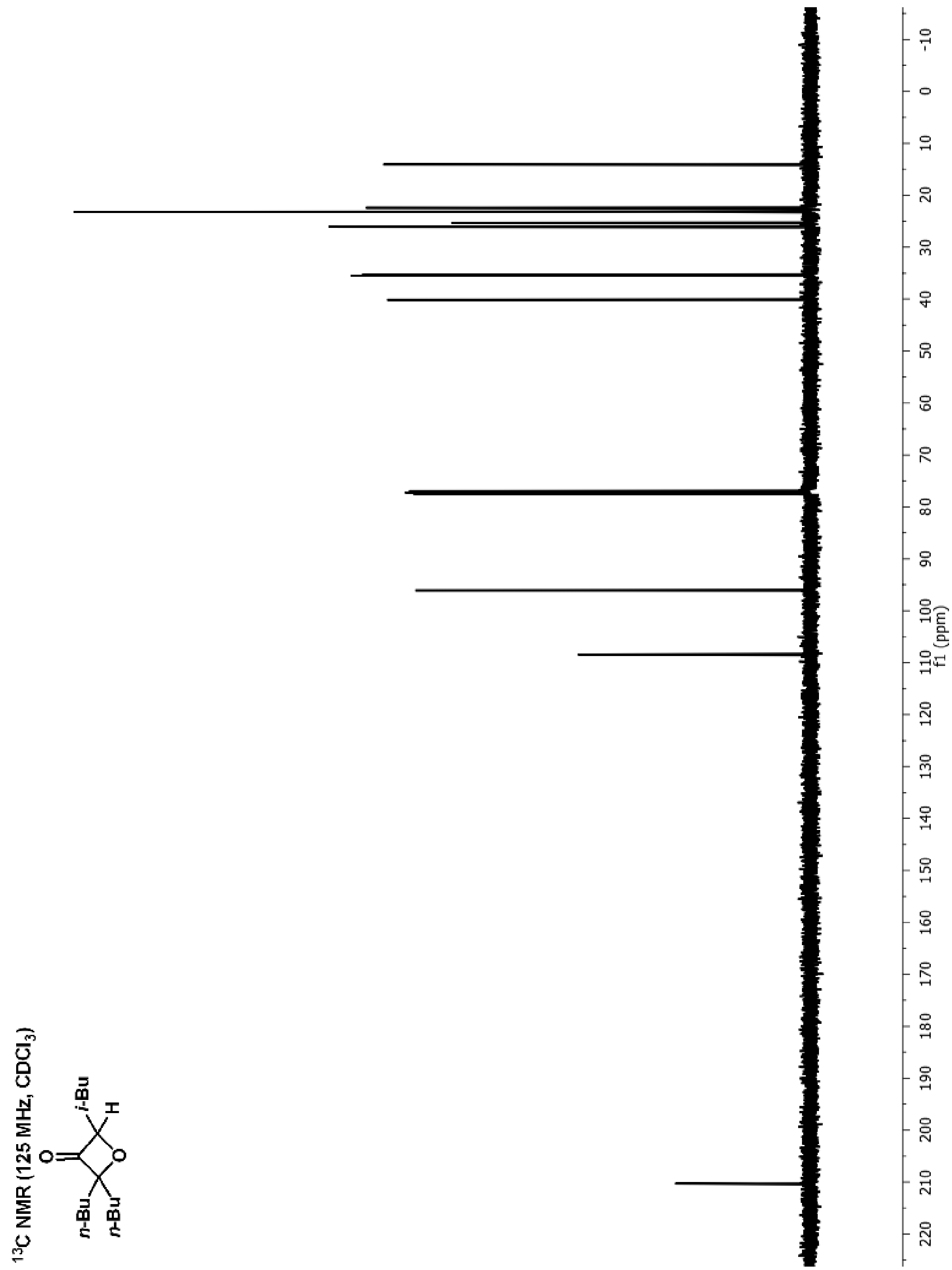

^{13}C NMR (125 MHz, CDCl$_3$)
O
n-Bu
n-Bu
i-Bu
H
O
220
210
200
190
180
170
160
150
140
130
120
110
100
90
80
70
60
50
40
30
20
10
0
-10
f1 (ppm)

^1H NMR (400 MHz, $CDCl_3$)

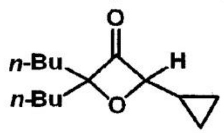

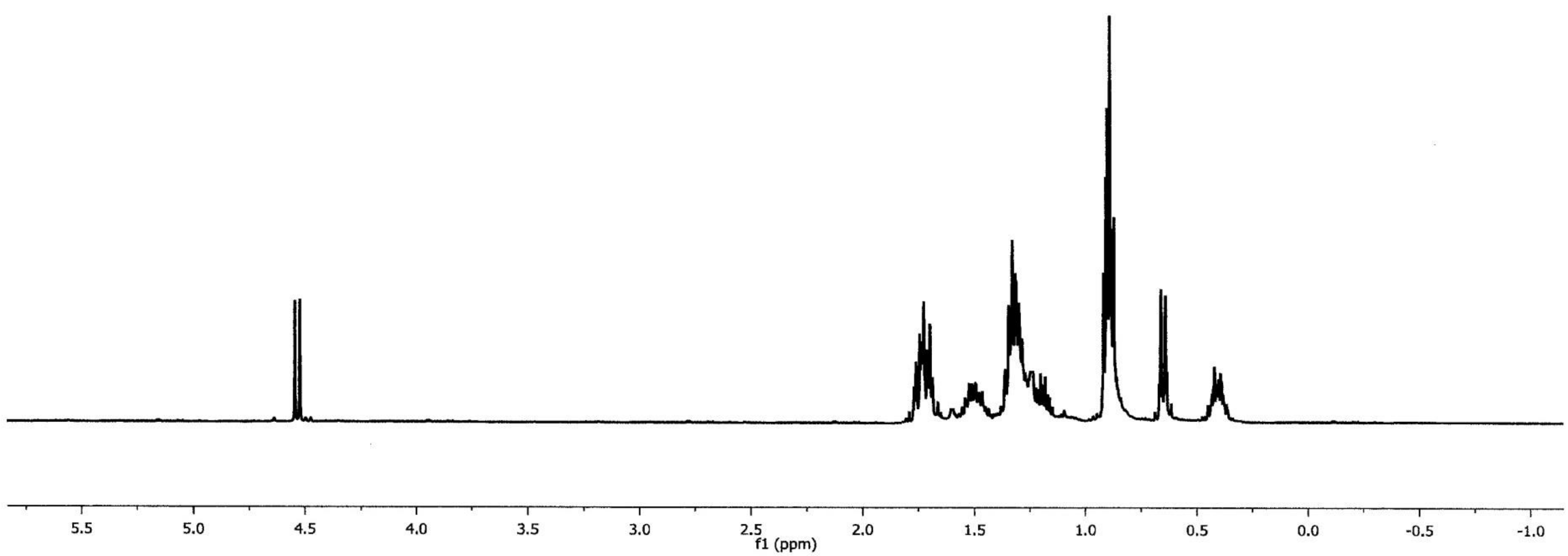

^{13}C NMR (100 MHz, $CDCl_3$)

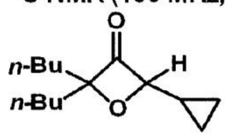

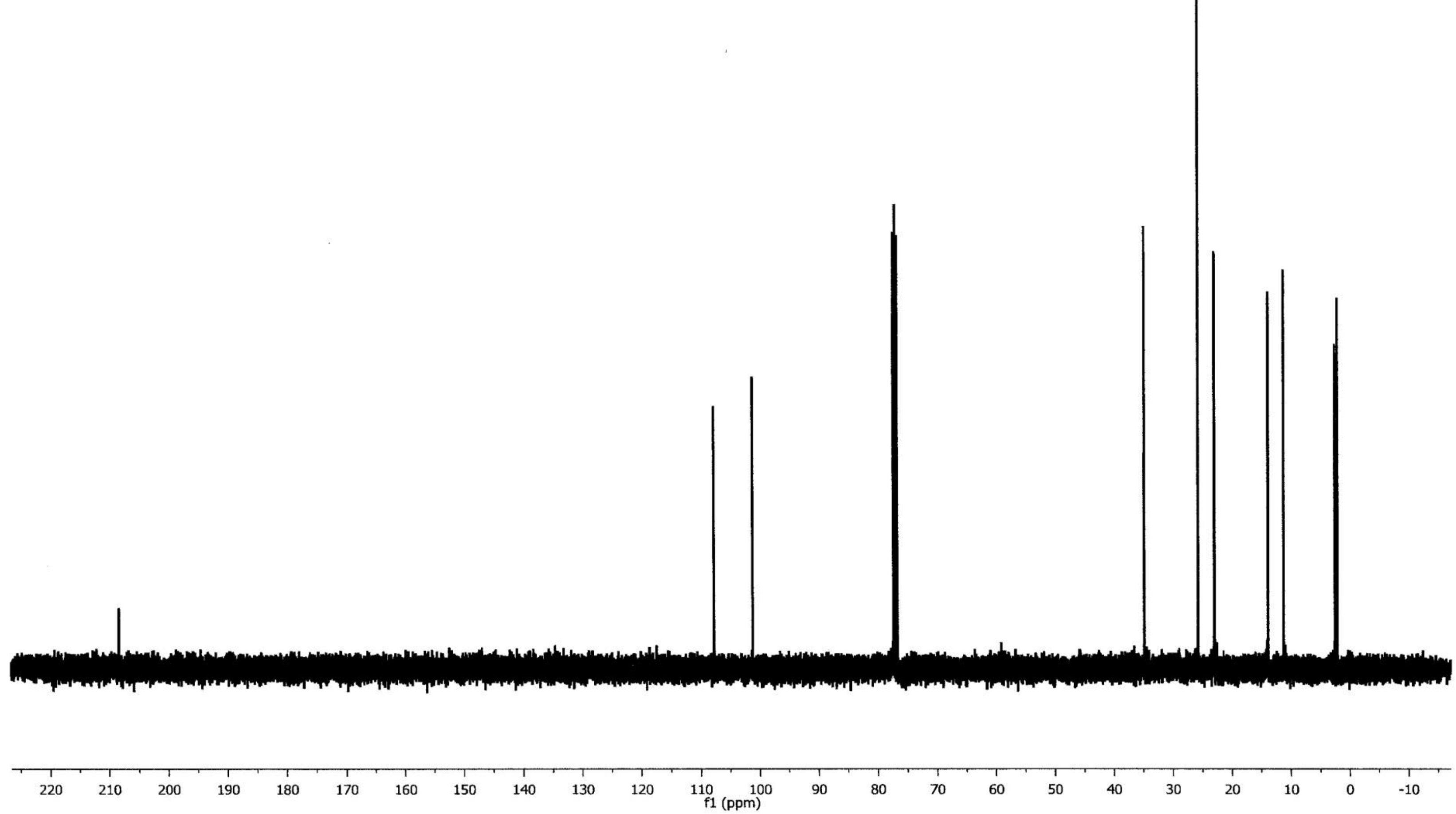

^1H NMR (500 MHz, $CDCl_3$)

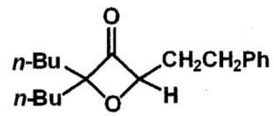

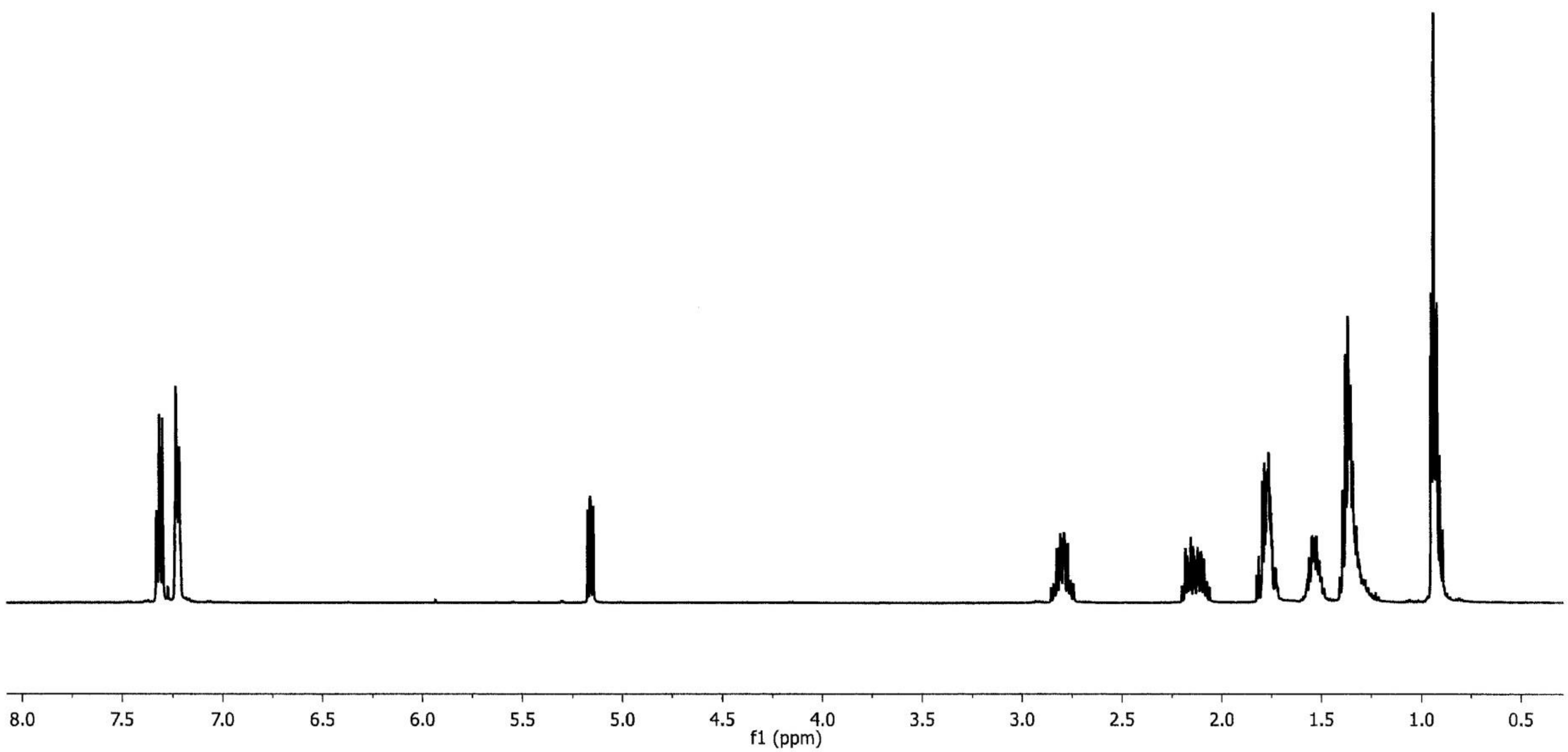

^{13}C NMR (125 MHz, $CDCl_3$)

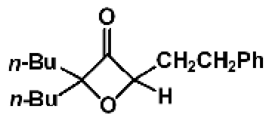

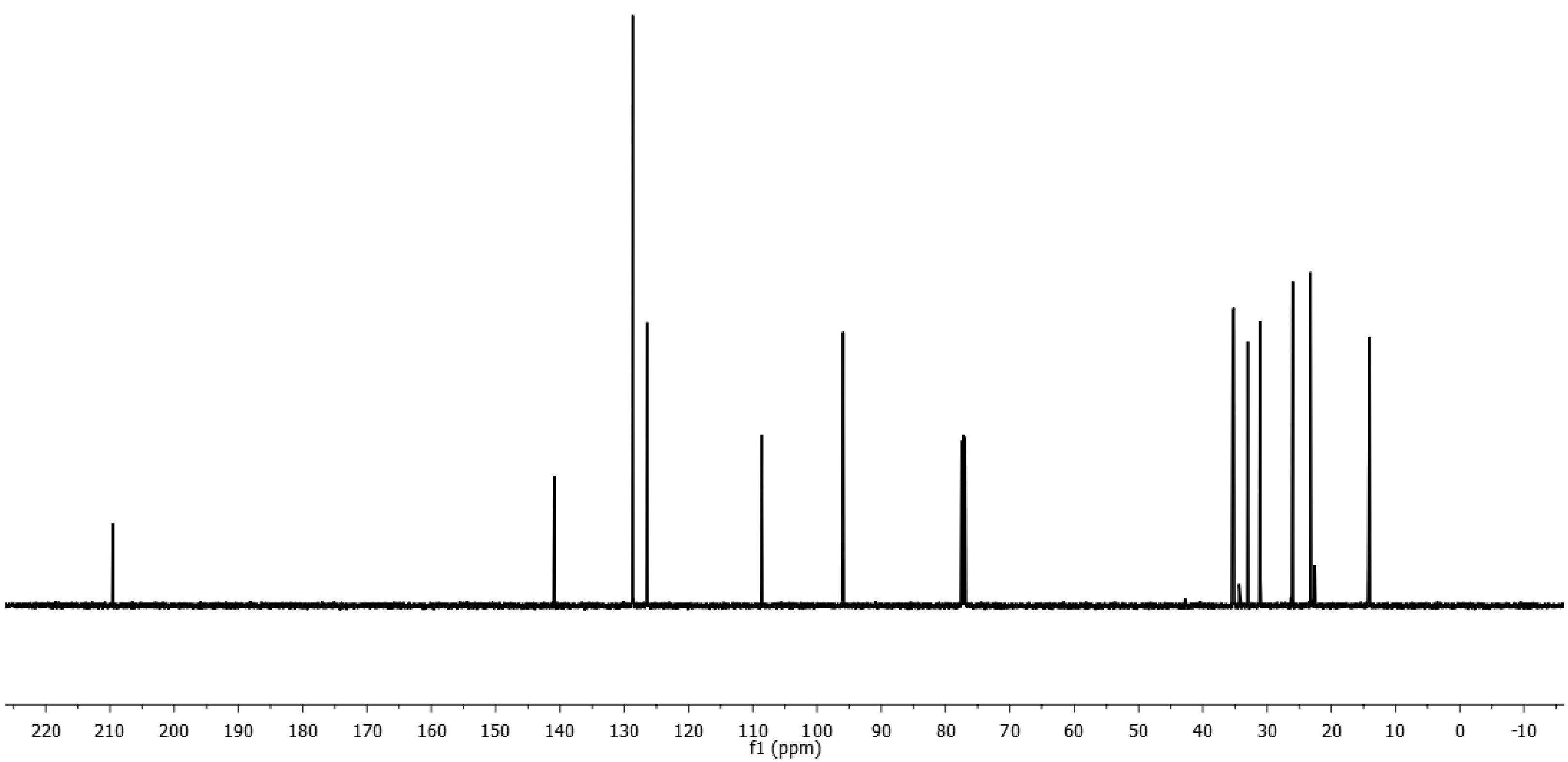

^1H NMR (500 MHz, $CDCl_3$)

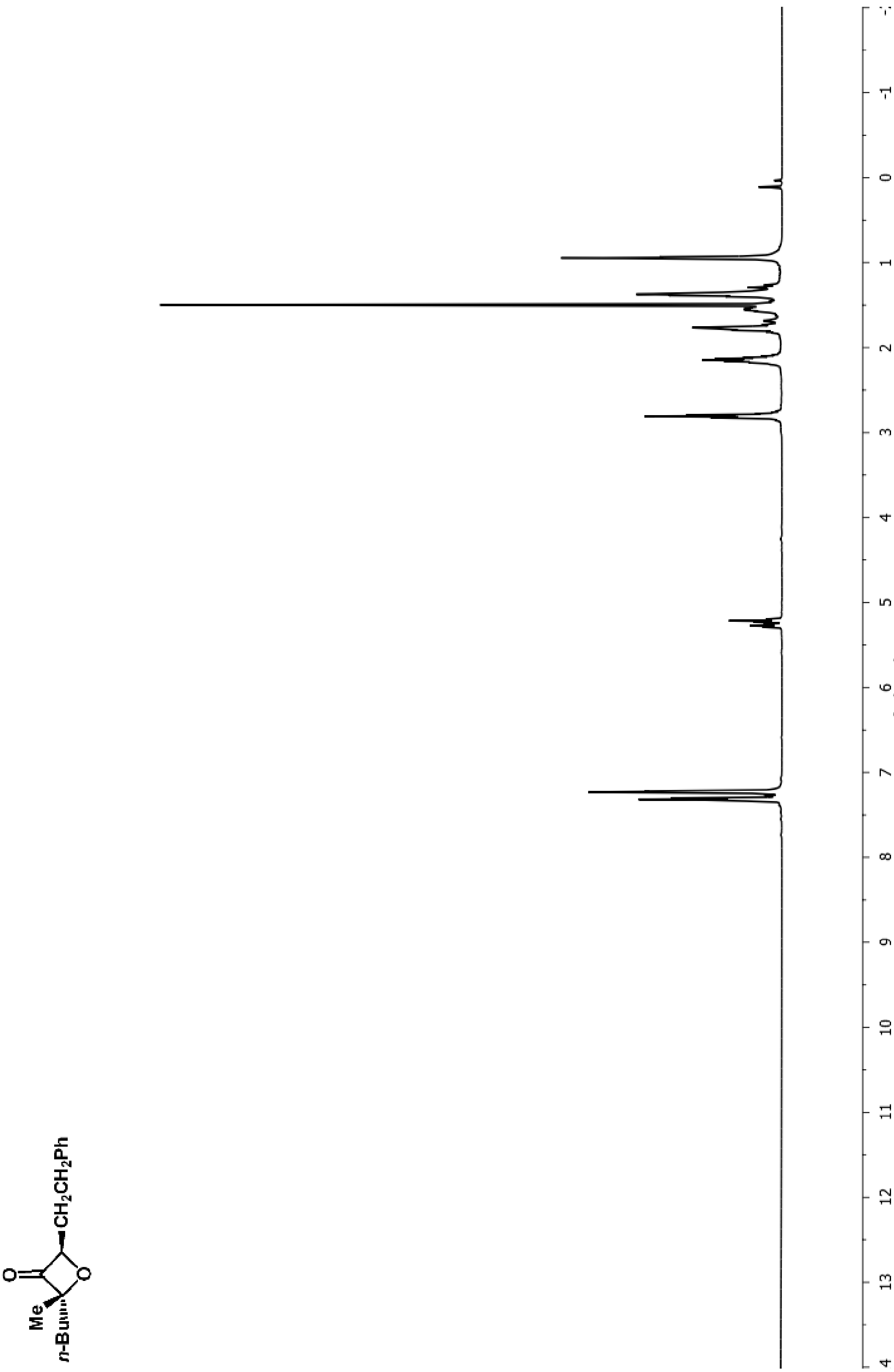

^{13}C NMR (125 MHz, $CDCl_3$)

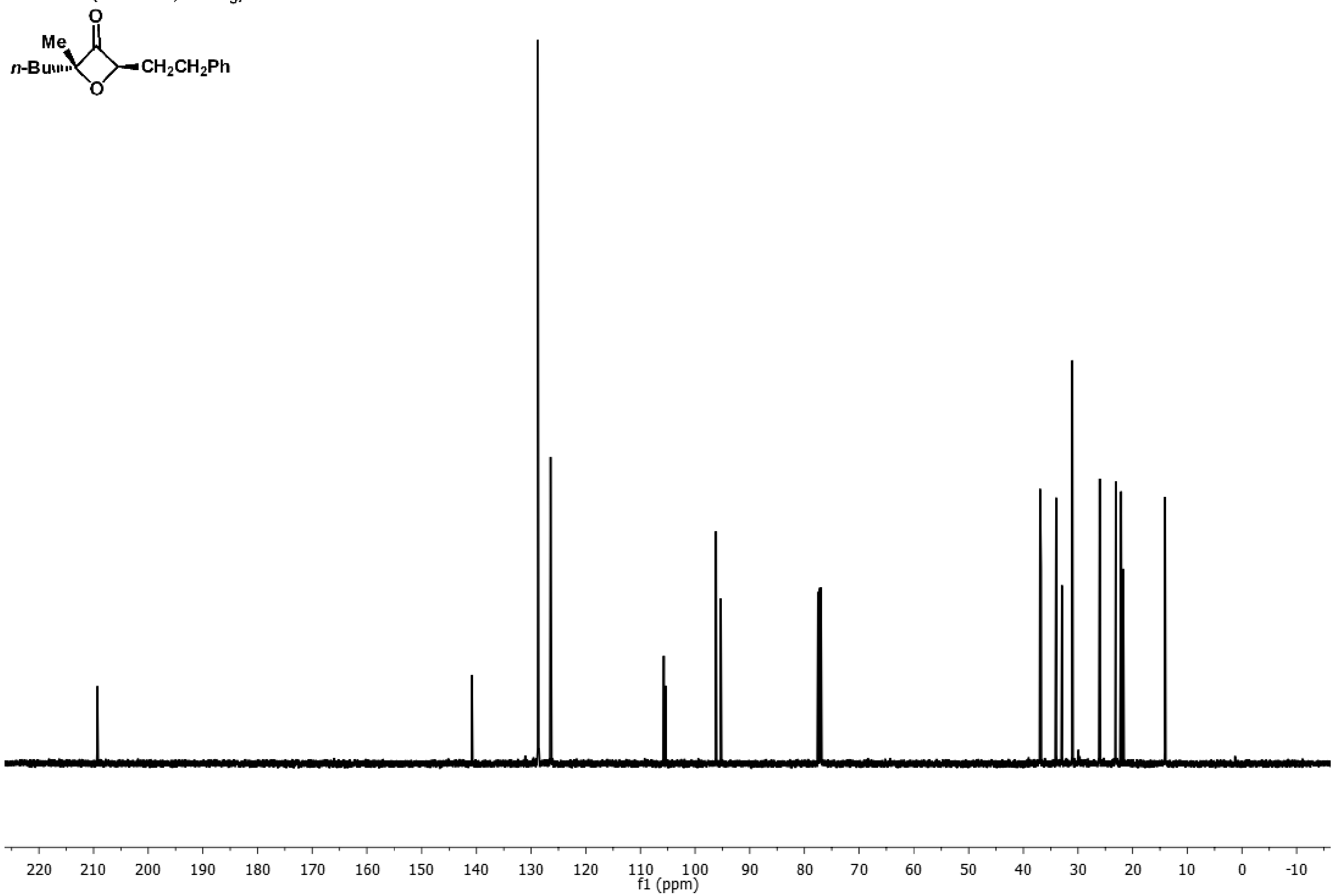

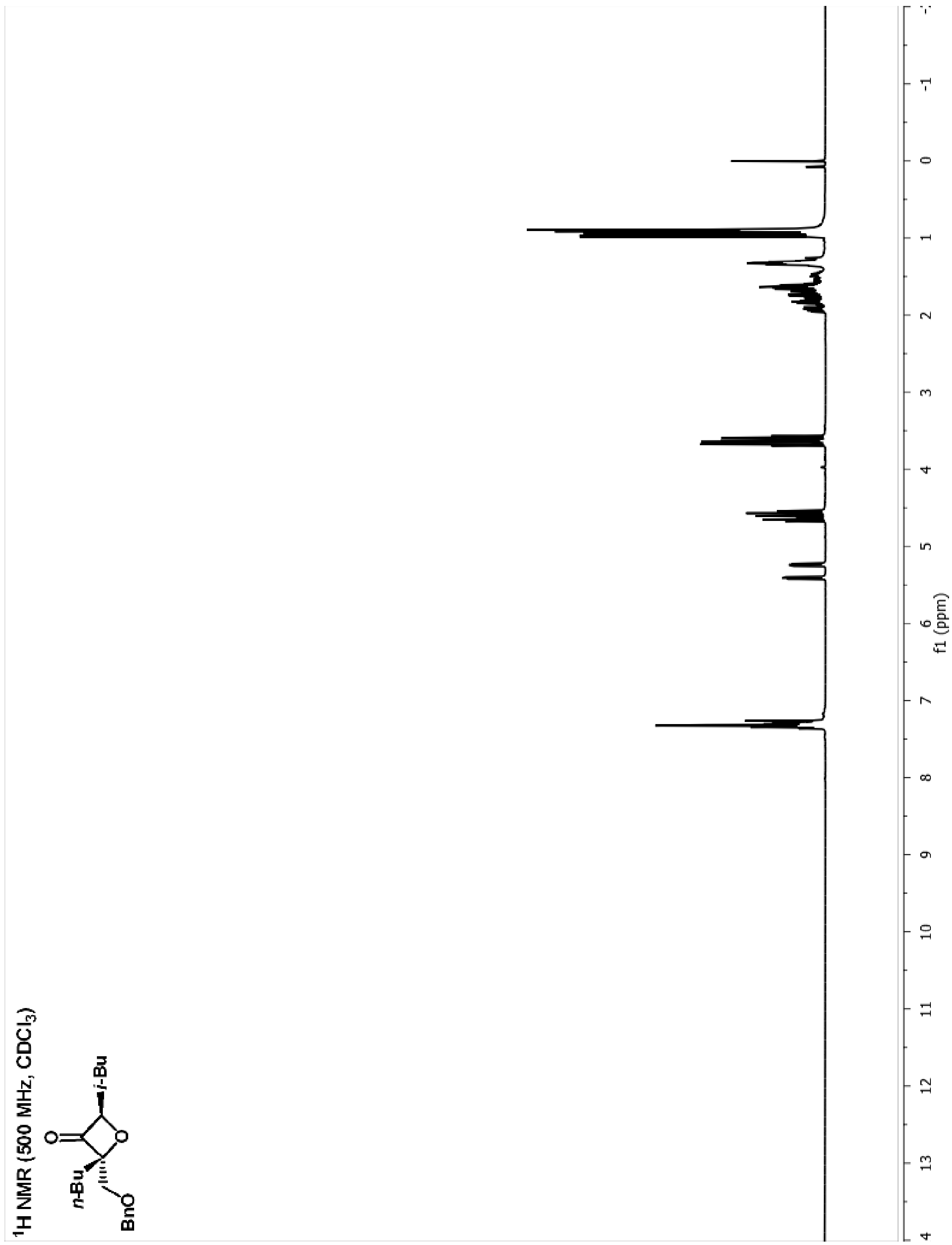

¹H NMR (500 MHz, CDCl3)
n-Bu
i-Bu
BnO
O
f1 (ppm)

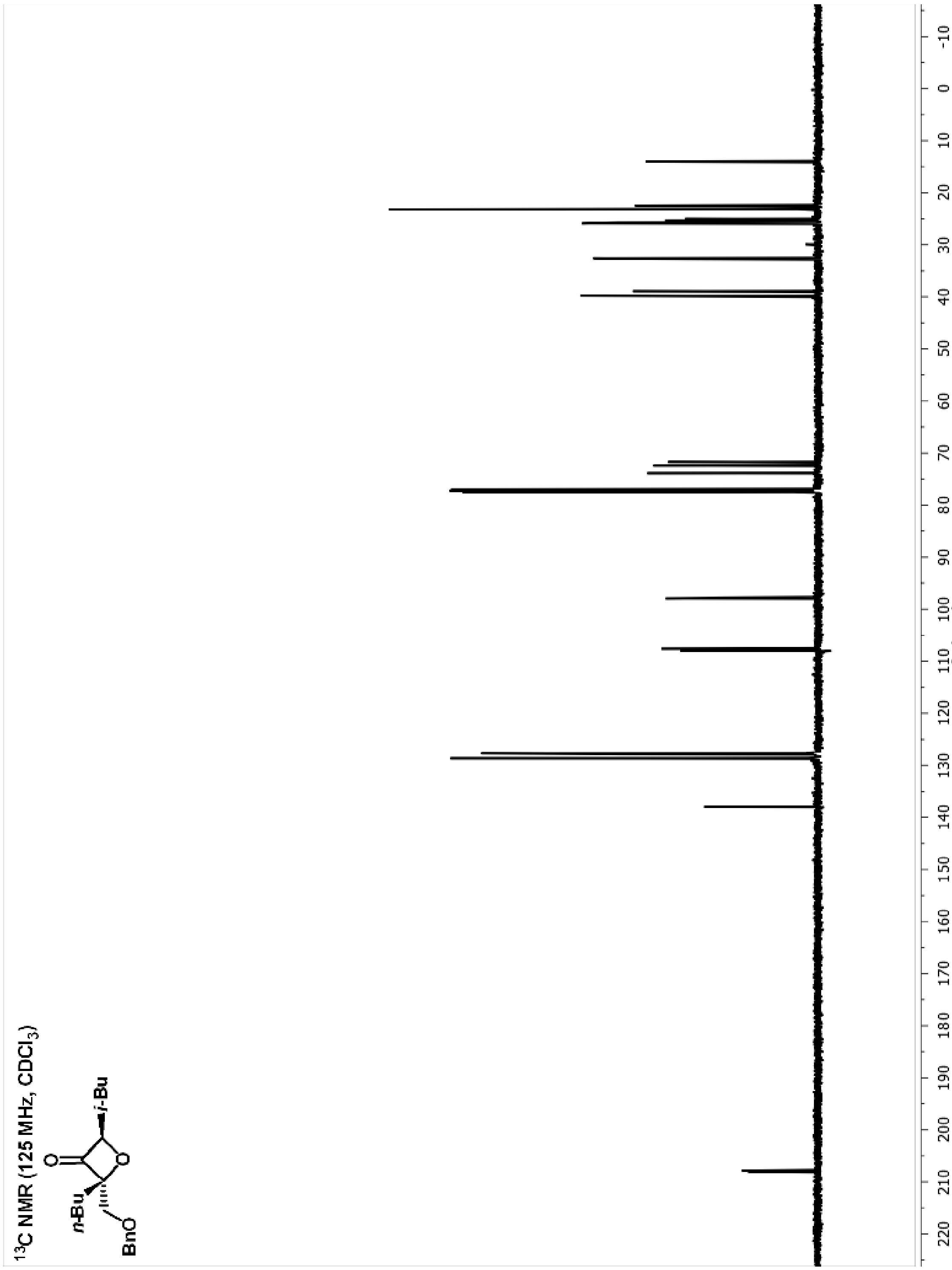
13C NMR (125 MHz, CDCl3)
n-Bu
i-Bu
O
BnO
f1 (ppm)
220 210 200 190 180 170 160 150 140 130 120 110 100 90 80 70 60 50 40 30 20 10 0 -10

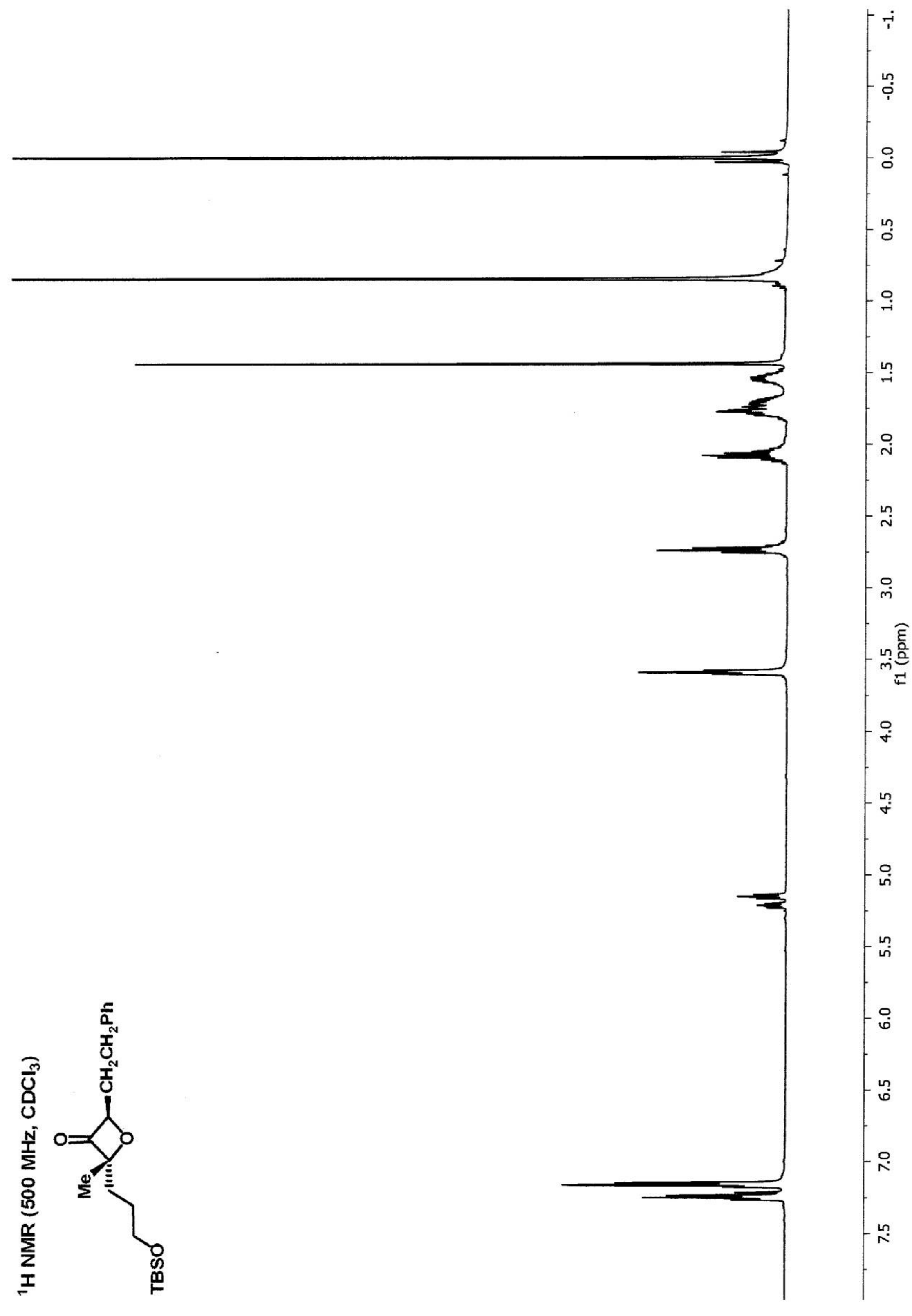

^1H NMR (500 MHz, $CDCl_3$)
TBSO
Me
O
CH_2CH_2Ph
f1 (ppm)
7.5 7.0 6.5 6.0 5.5 5.0 4.5 4.0 3.5 3.0 2.5 2.0 1.5 1.0 0.5 0.0 -0.5 -1.

^{13}C NMR (125 MHz, $CDCl_3$)

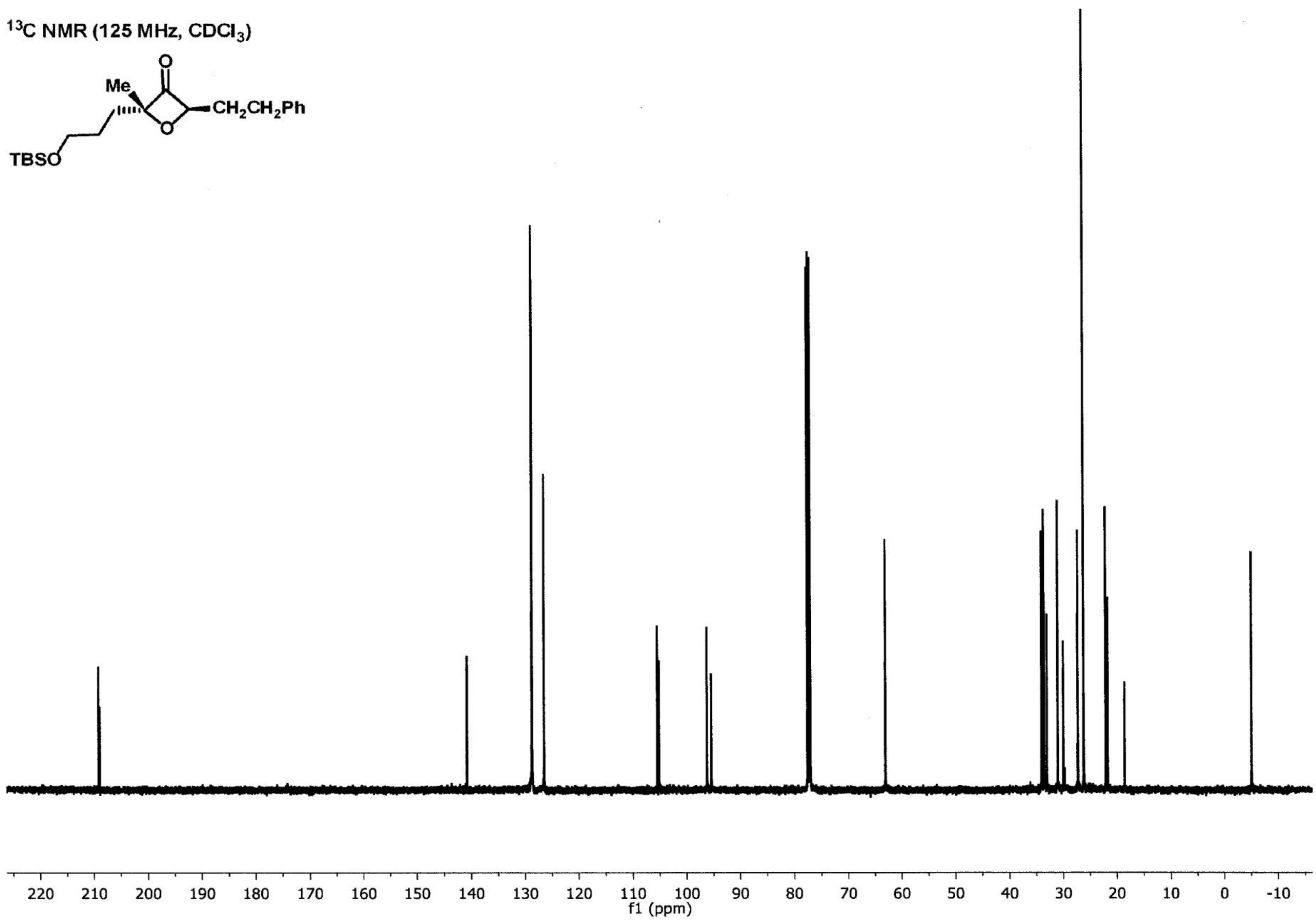

^1H NMR (500 MHz, $CDCl_3$)

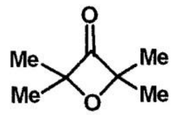

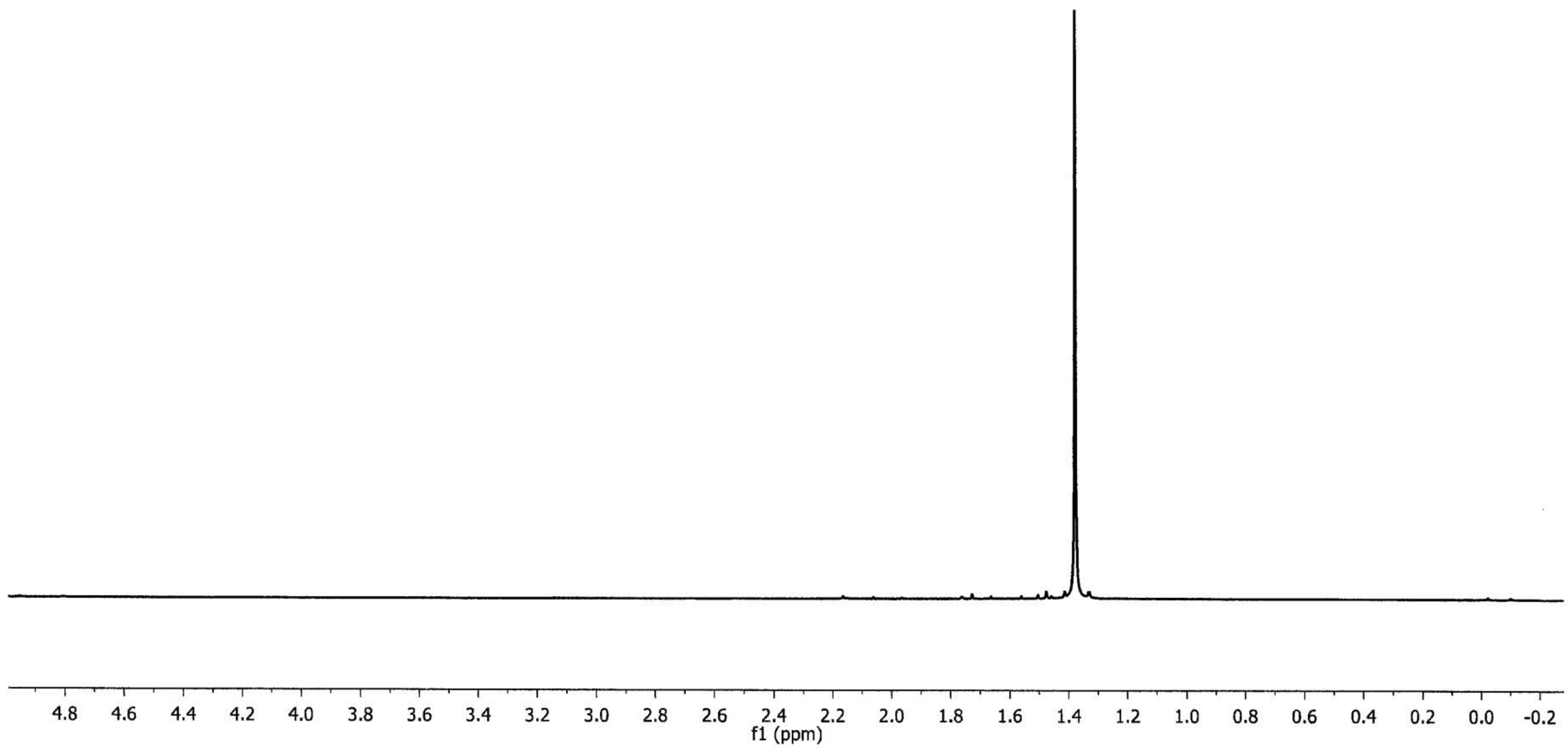

^{13}C NMR (125 MHz, $CDCl_3$)

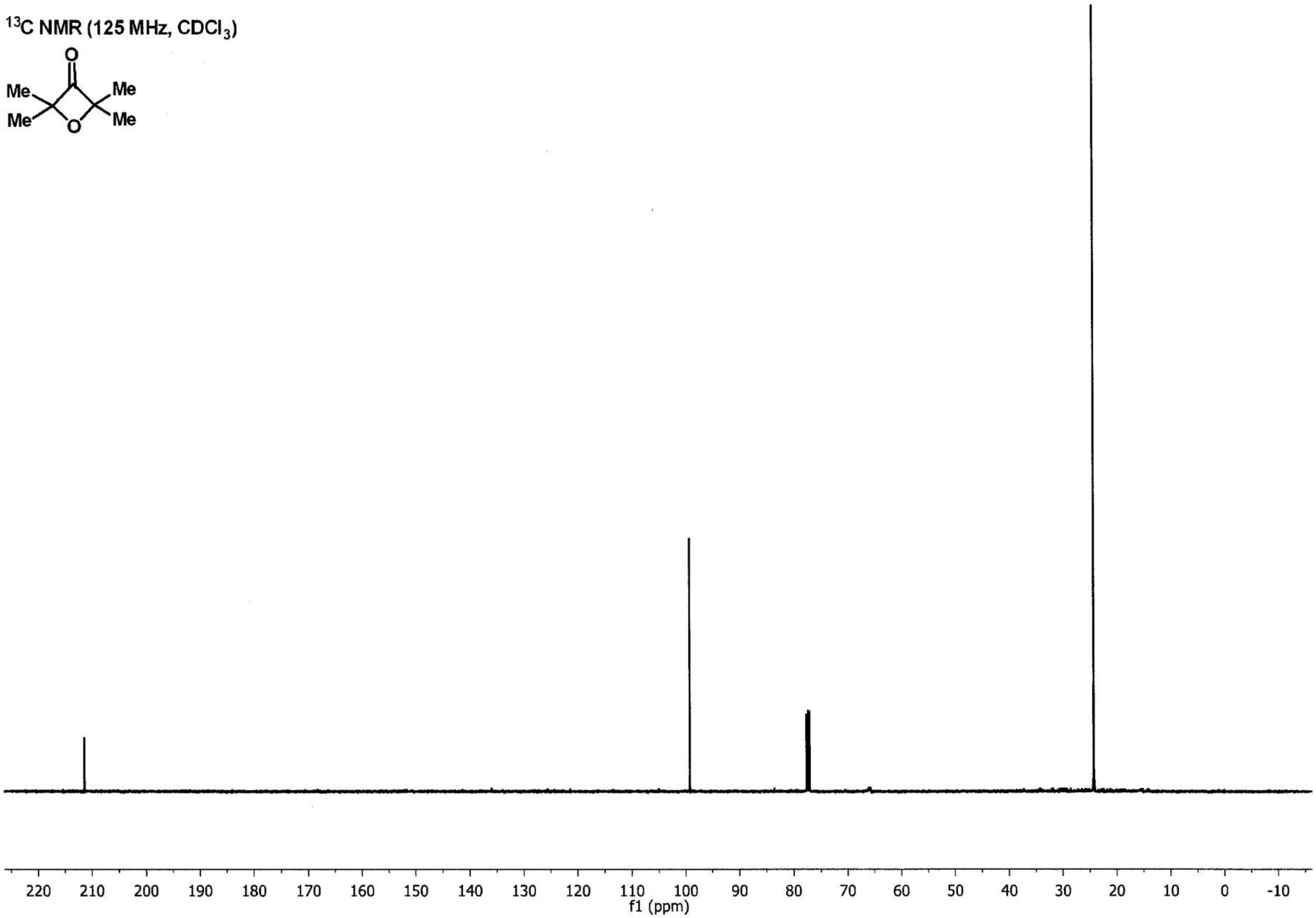

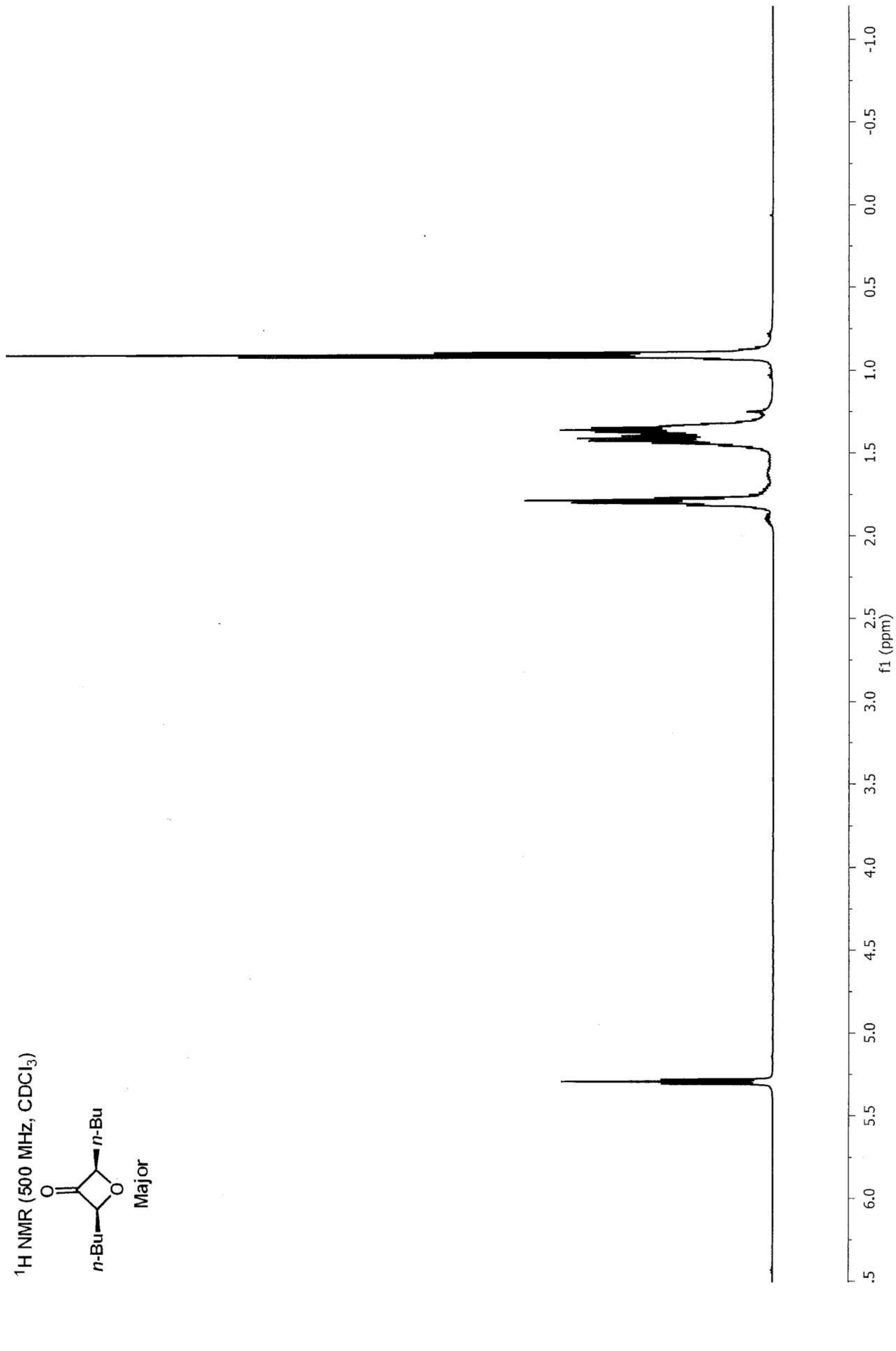

¹H NMR (500 MHz, CDCl₃)
n-Bu
O
n-Bu
O
Major
-1.0
-0.5
0.0
0.5
1.0
1.5
2.0
2.5
f1 (ppm)
3.0
3.5
4.0
4.5
5.0
5.5
6.0
.5

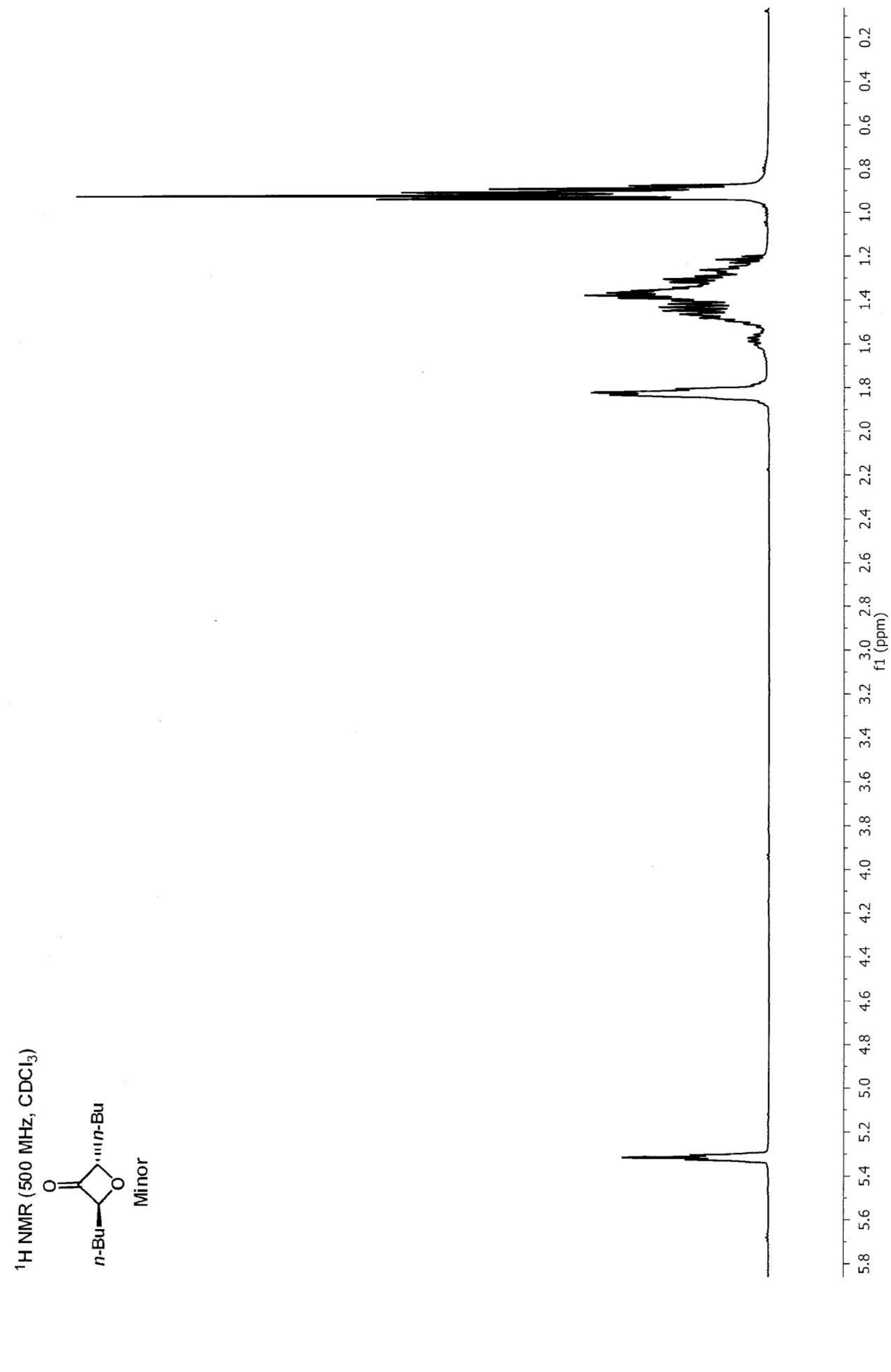

¹H NMR (500 MHz, CDCl3)
n-Bu
n-Bu
O
O
Minor
f1 (ppm)

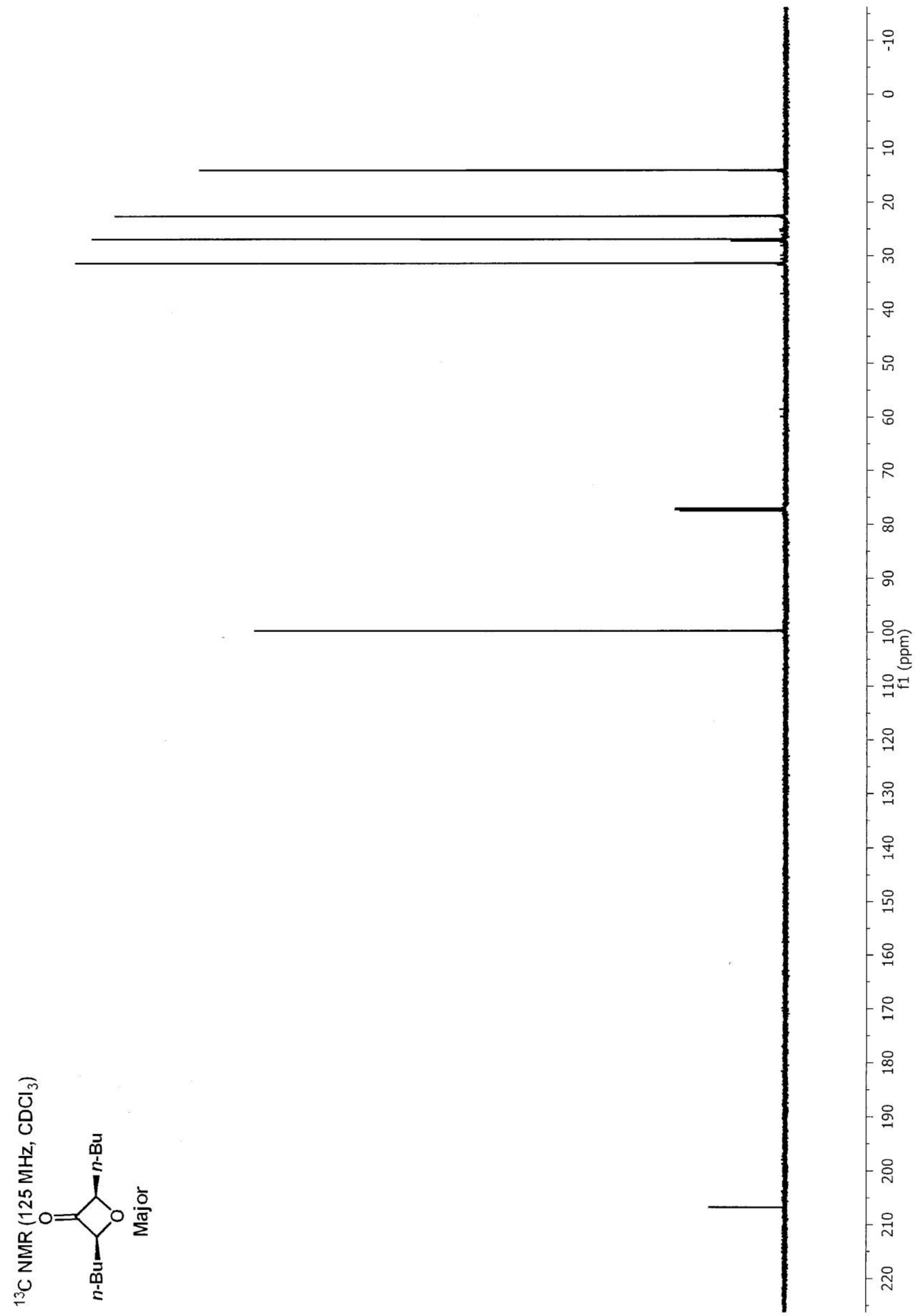
13C NMR (125 MHz, CDCl3)
n-Bu
n-Bu
Major
f1 (ppm)

^{13}C NMR (125 MHz, $CDCl_3$)

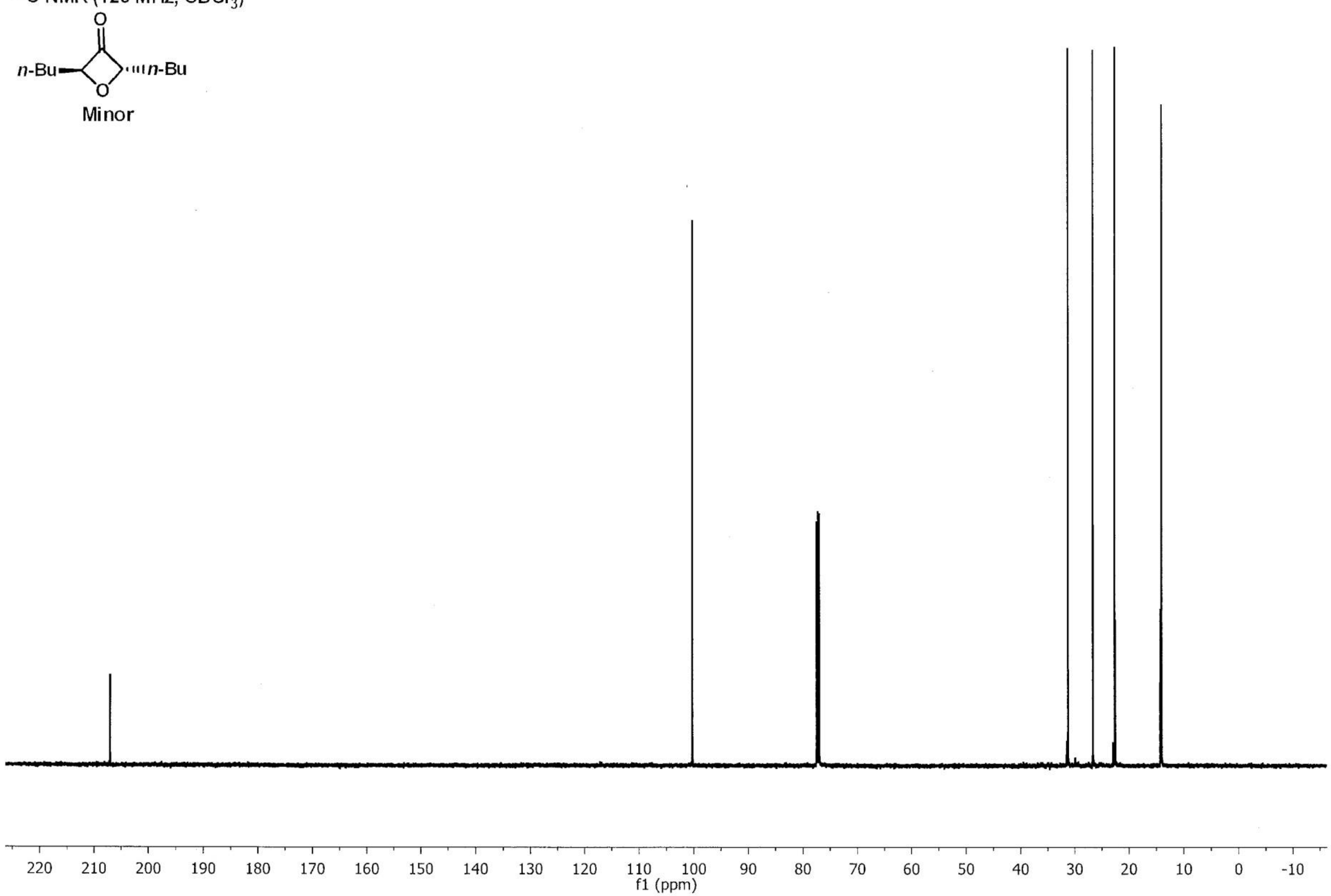

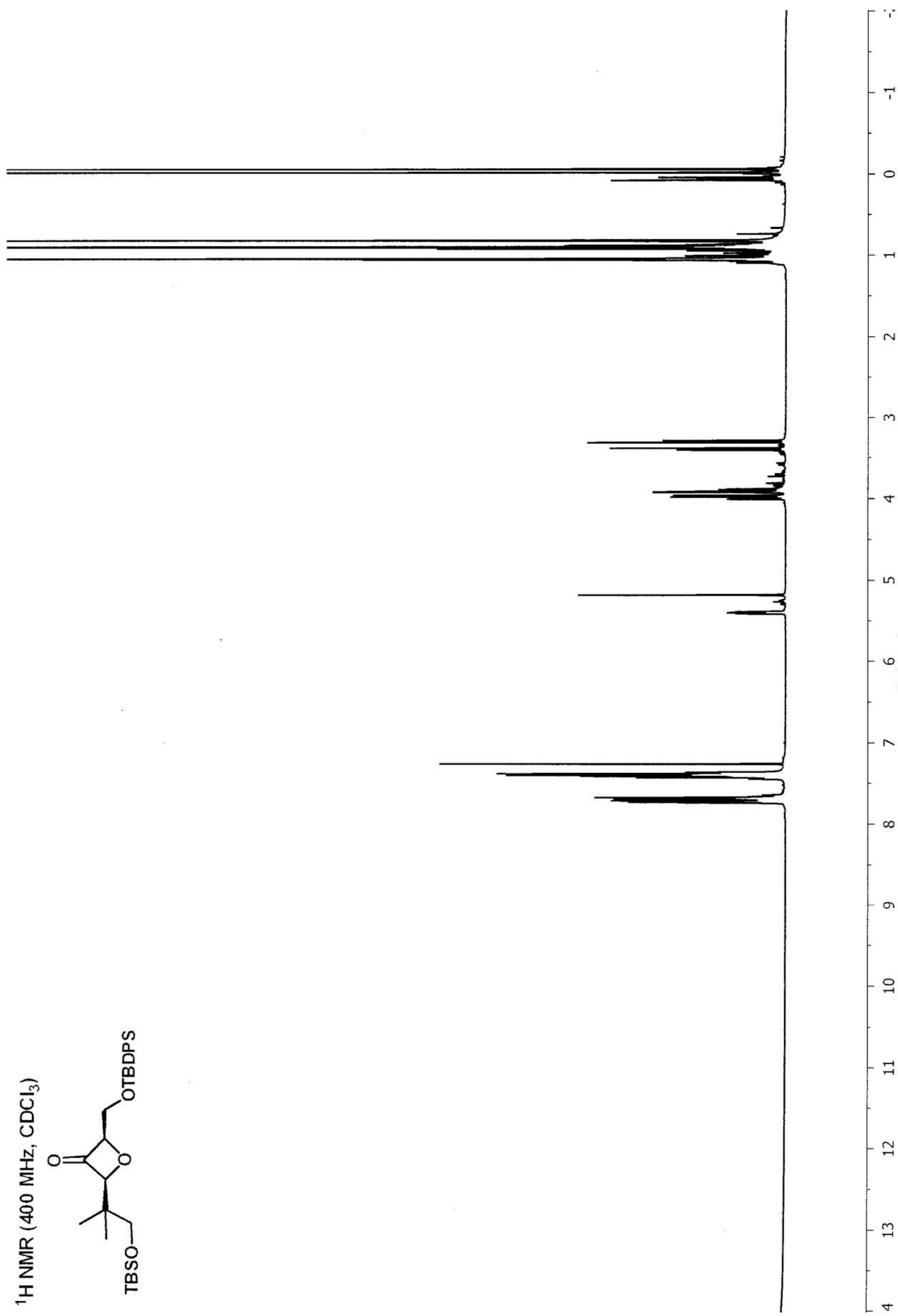

1H NMR (400 MHz, CDCl3)
O
TBSO
OTBDPS
f1 (ppm)
-2
-1
0
1
2
3
4
5
6
7
8
9
10
11
12
13
14

^{13}C NMR (125 MHz, $CDCl_3$)

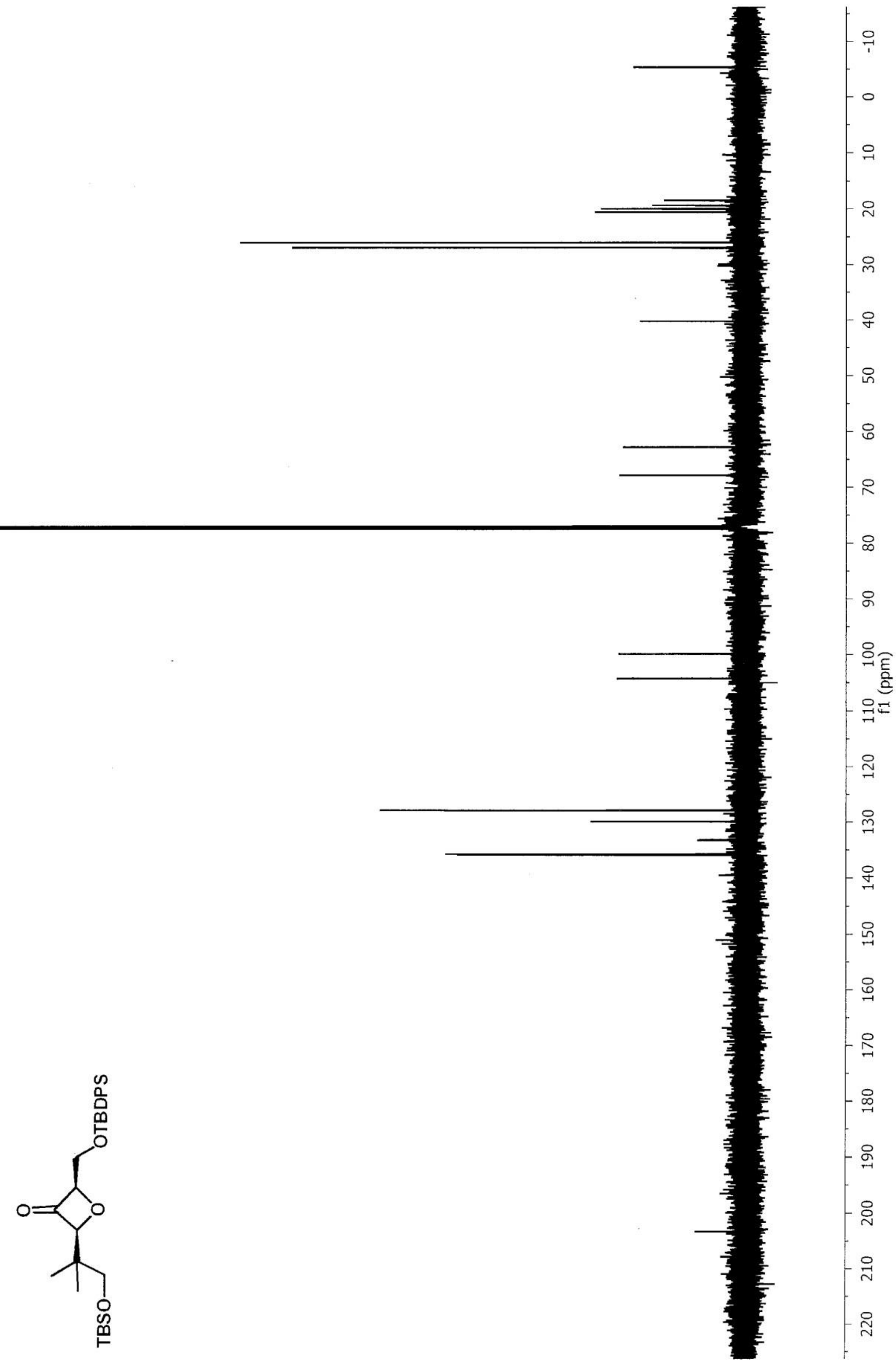

^1H NMR (500 MHz, $CDCl_3$)

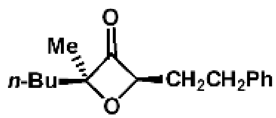

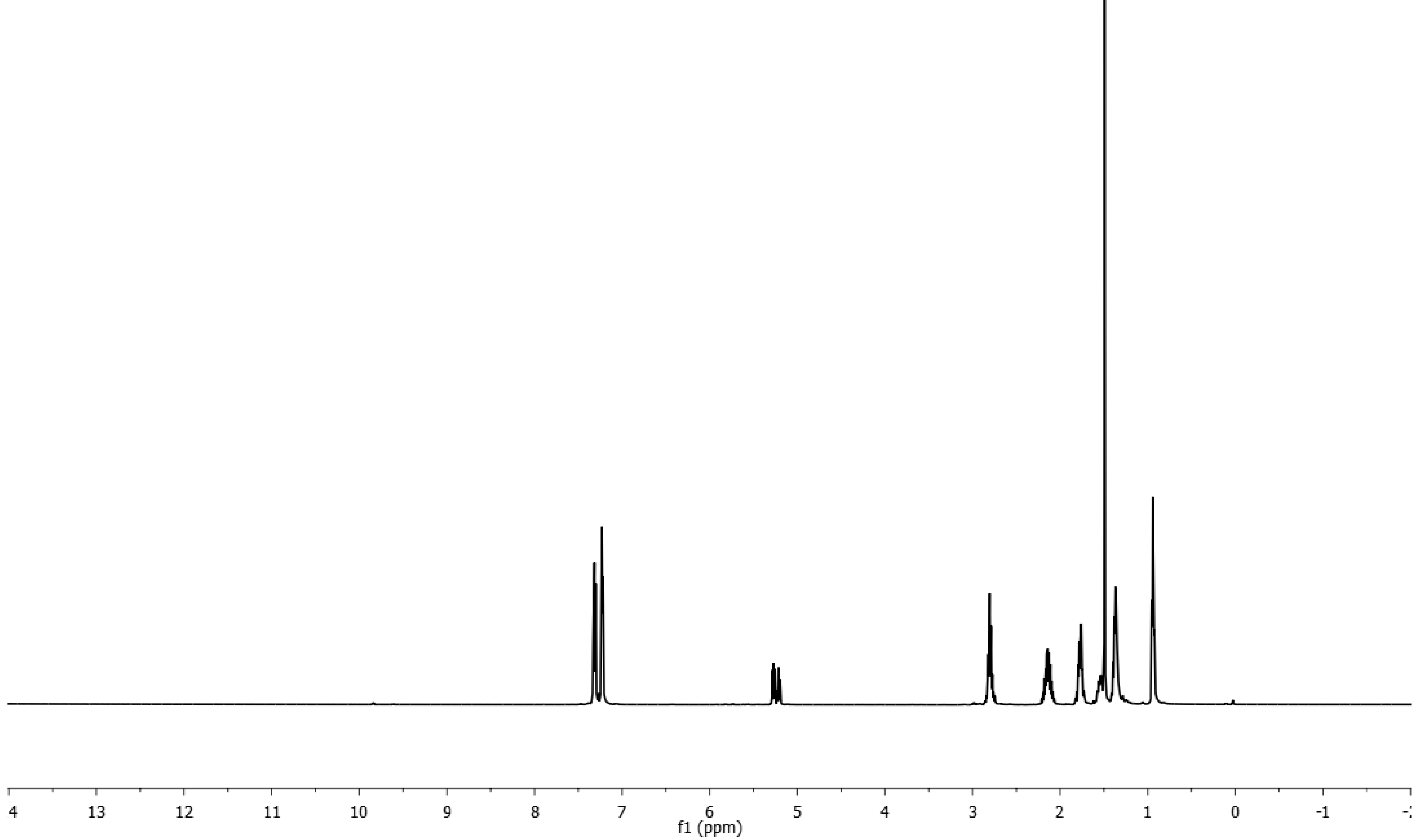

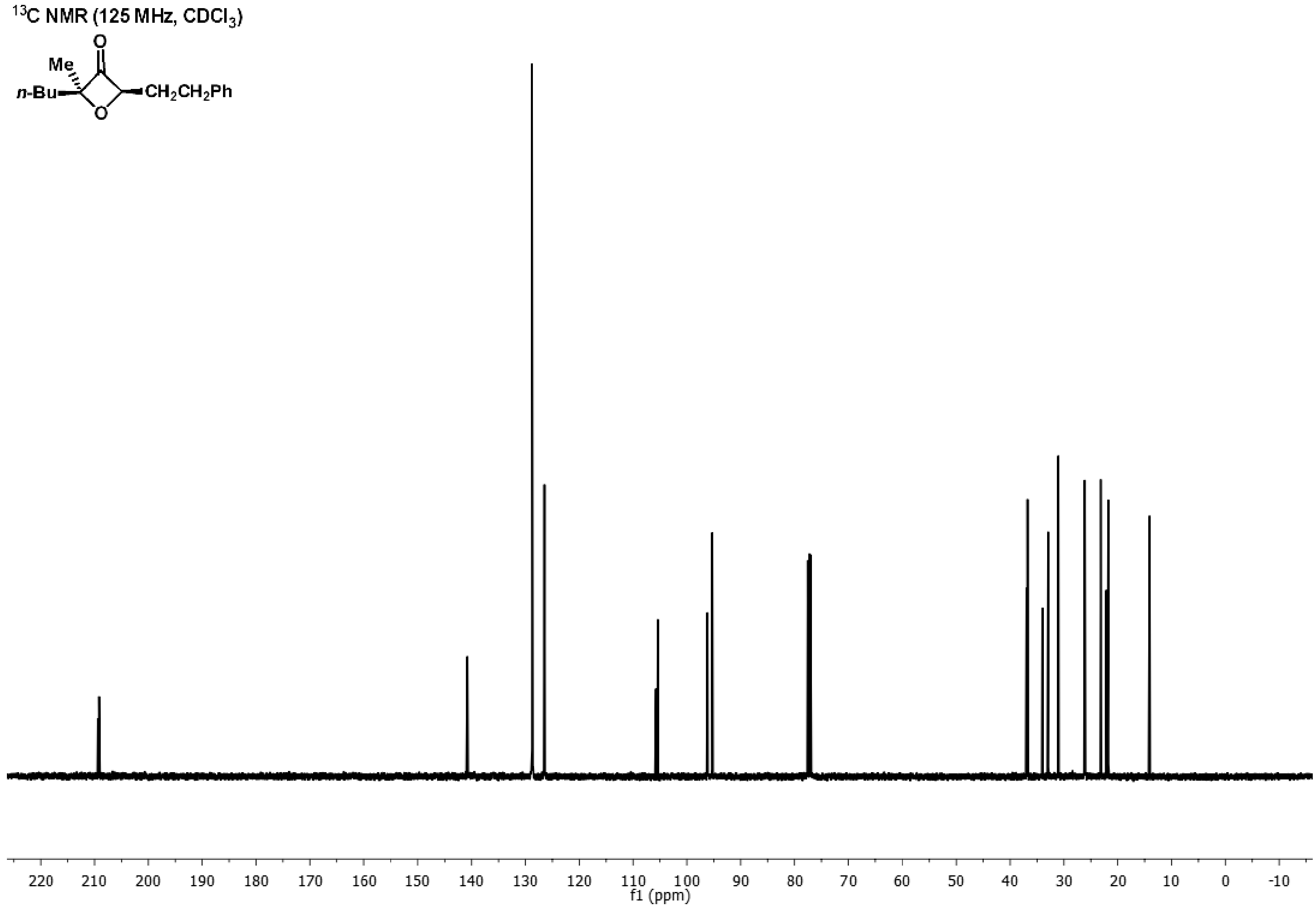

^{13}C NMR (125 MHz, $CDCl_3$)
Me
O
n-Bu
O
CH_2CH_2Ph
220
210
200
190
180
170
160
150
140
130
120
110
100
90
80
70
60
50
40
30
20
10
0
-10
f1 (ppm)

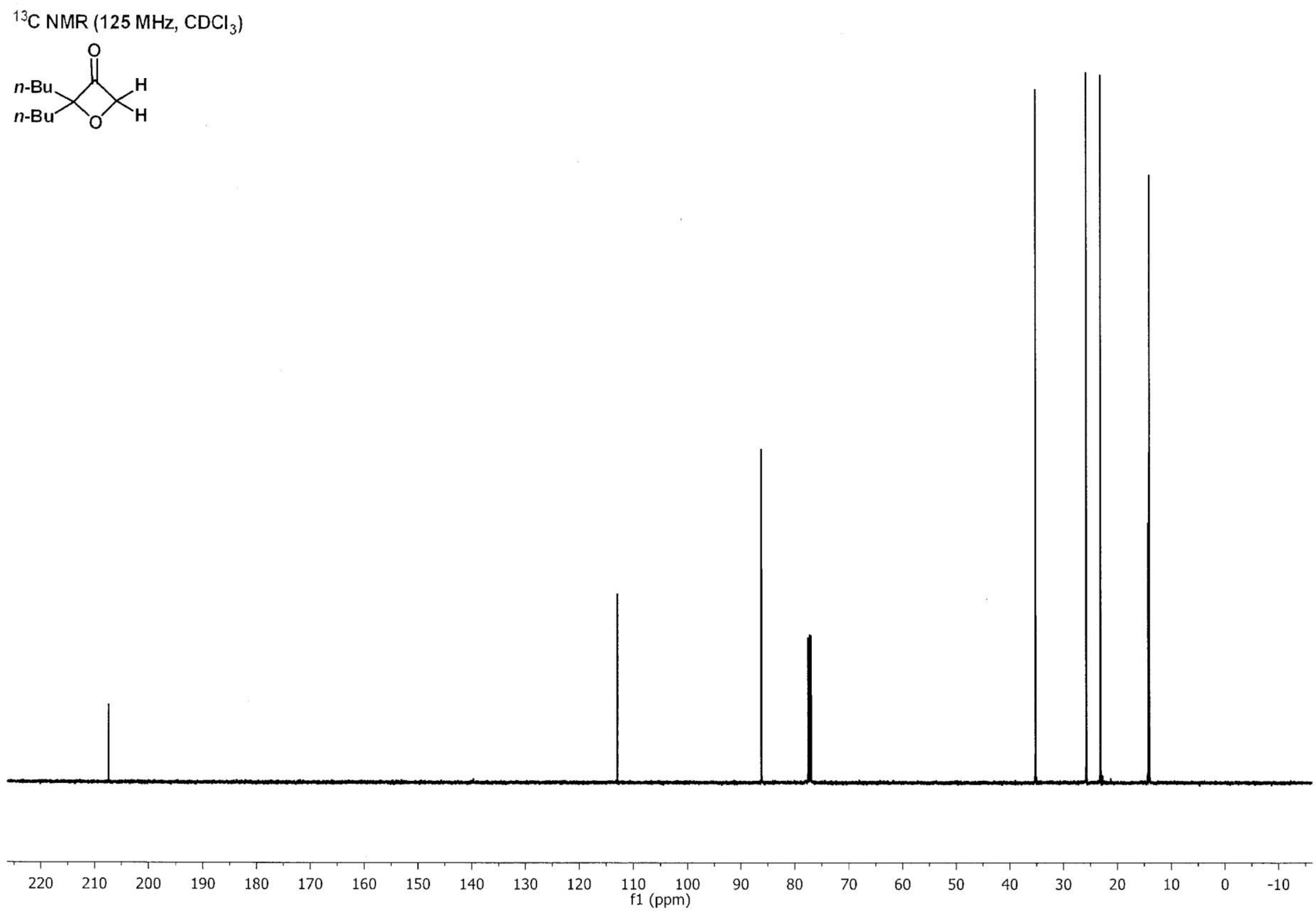

13C NMR (125 MHz, CDCl3)
n-Bu
n-Bu
O
O
H
H
220 210 200 190 180 170 160 150 140 130 120 110 100 90 80 70 60 50 40 30 20 10 0 -10
f1 (ppm)

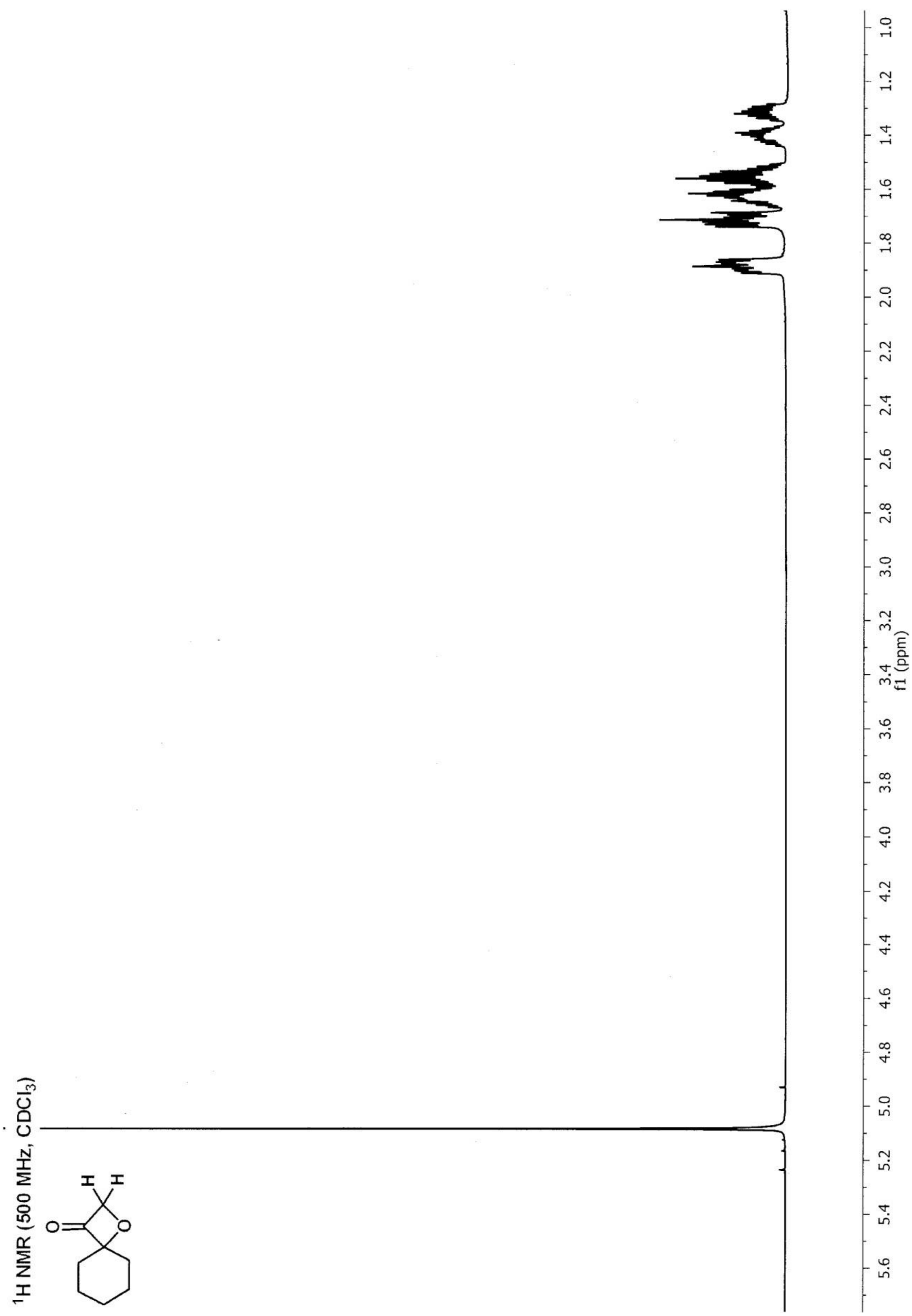

1H NMR (500 MHz, CDCl3)
f1 (ppm)

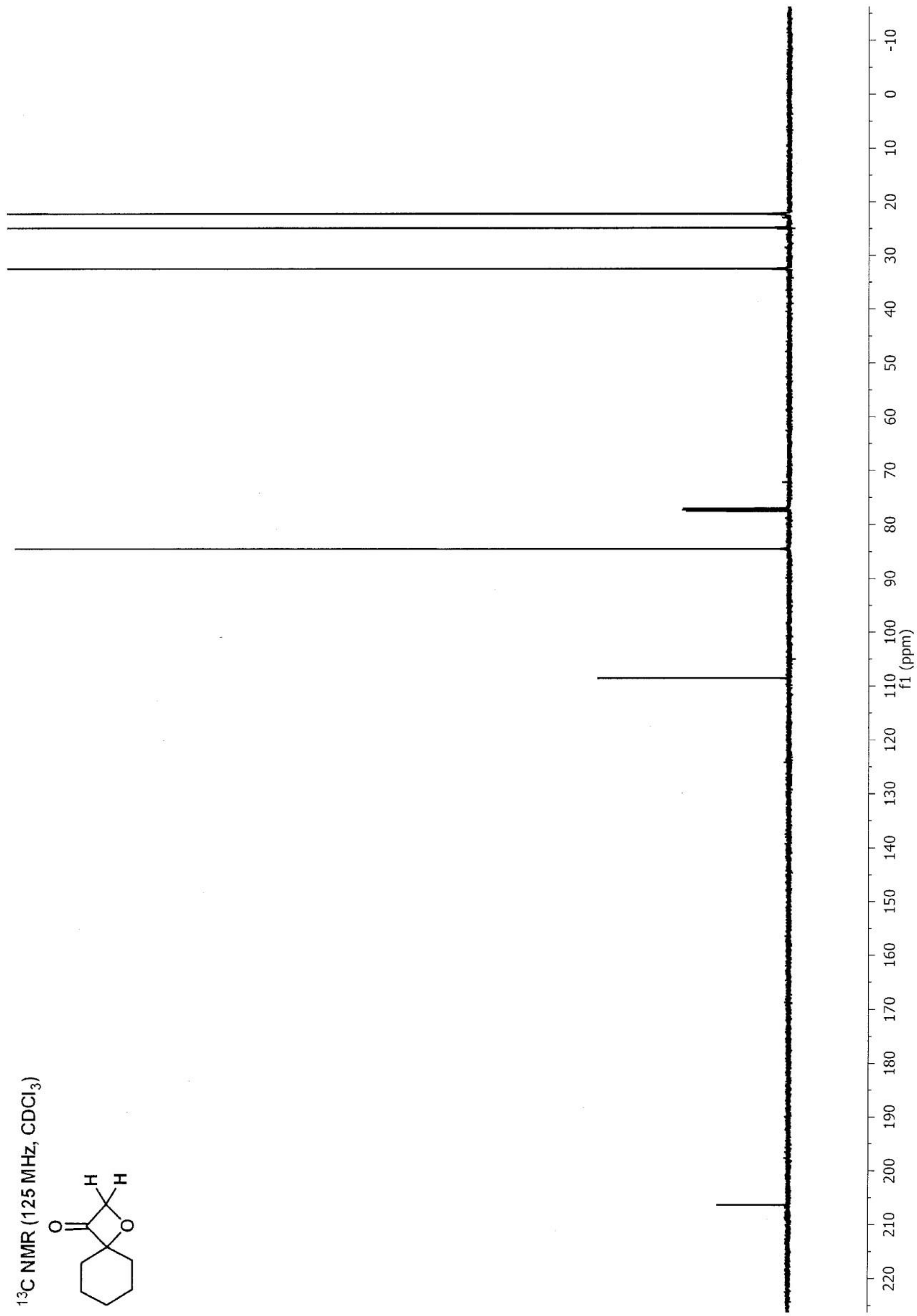

^{13}C NMR (125 MHz, CDCl$_3$)
f1 (ppm)

^1H NMR (500 MHz, $CDCl_3$)

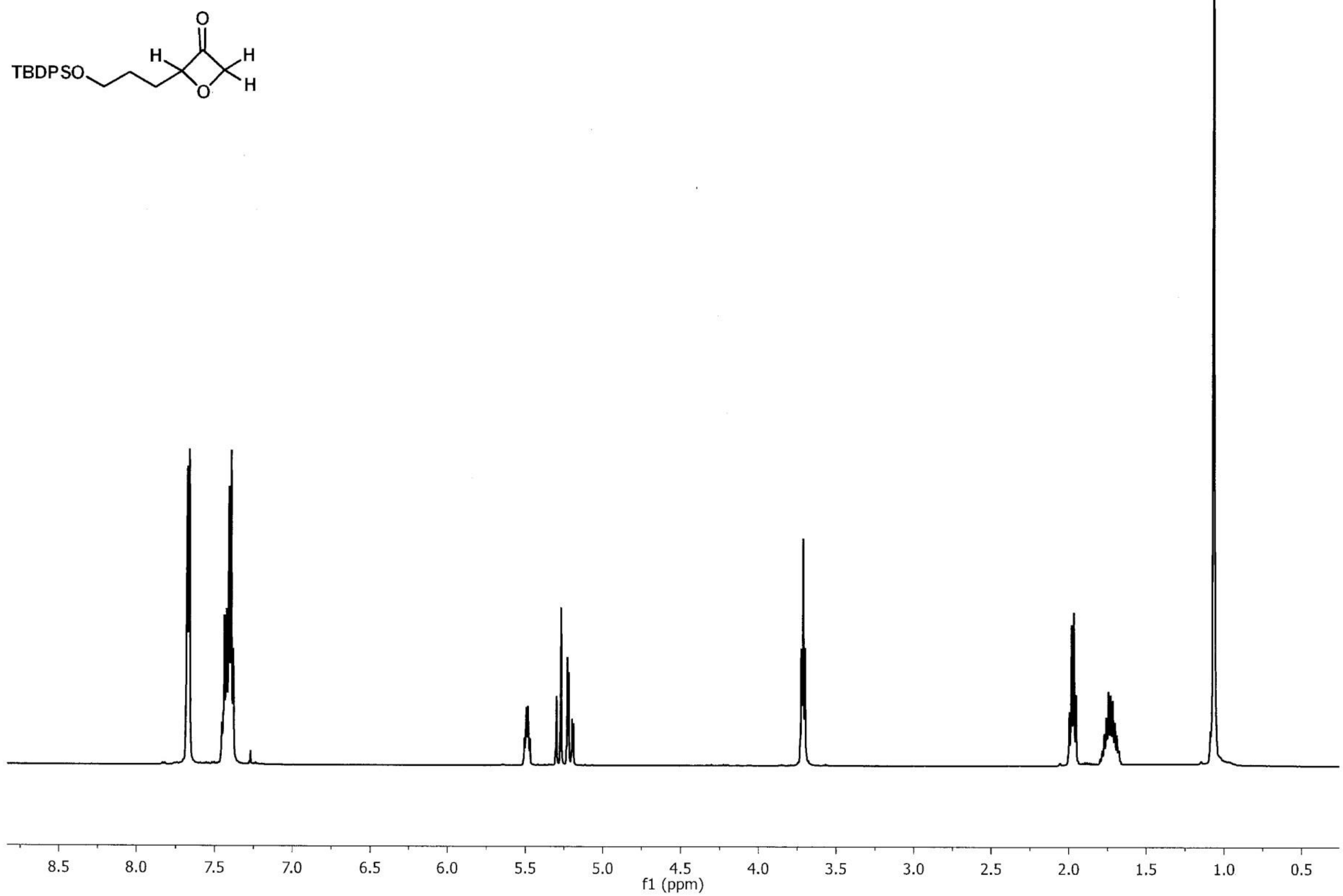

^{13}C NMR (125 MHz, $CDCl_3$)

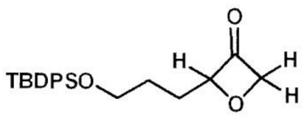

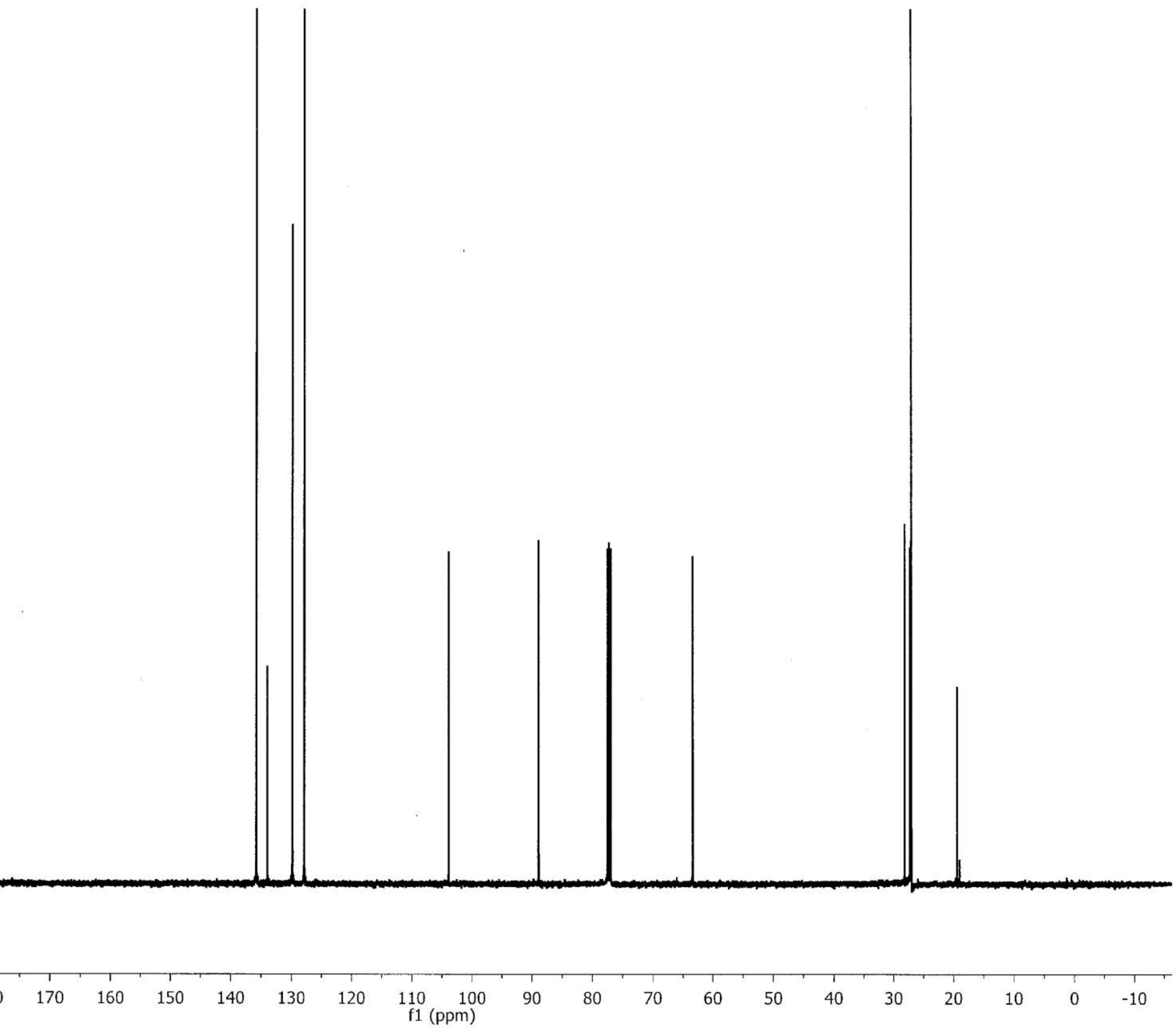

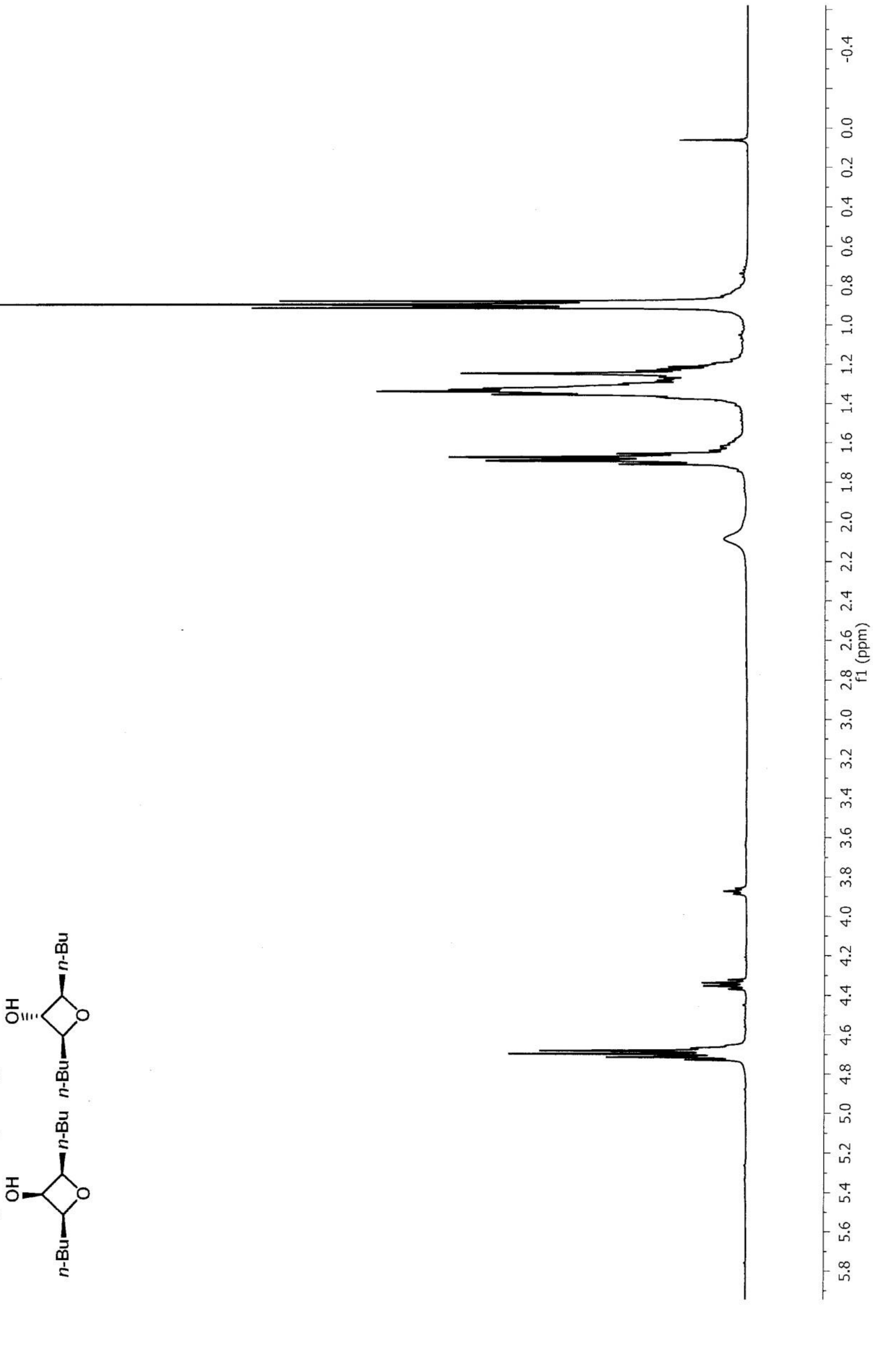

^{1}H NMR (400 MHz, $CDCl_3$)

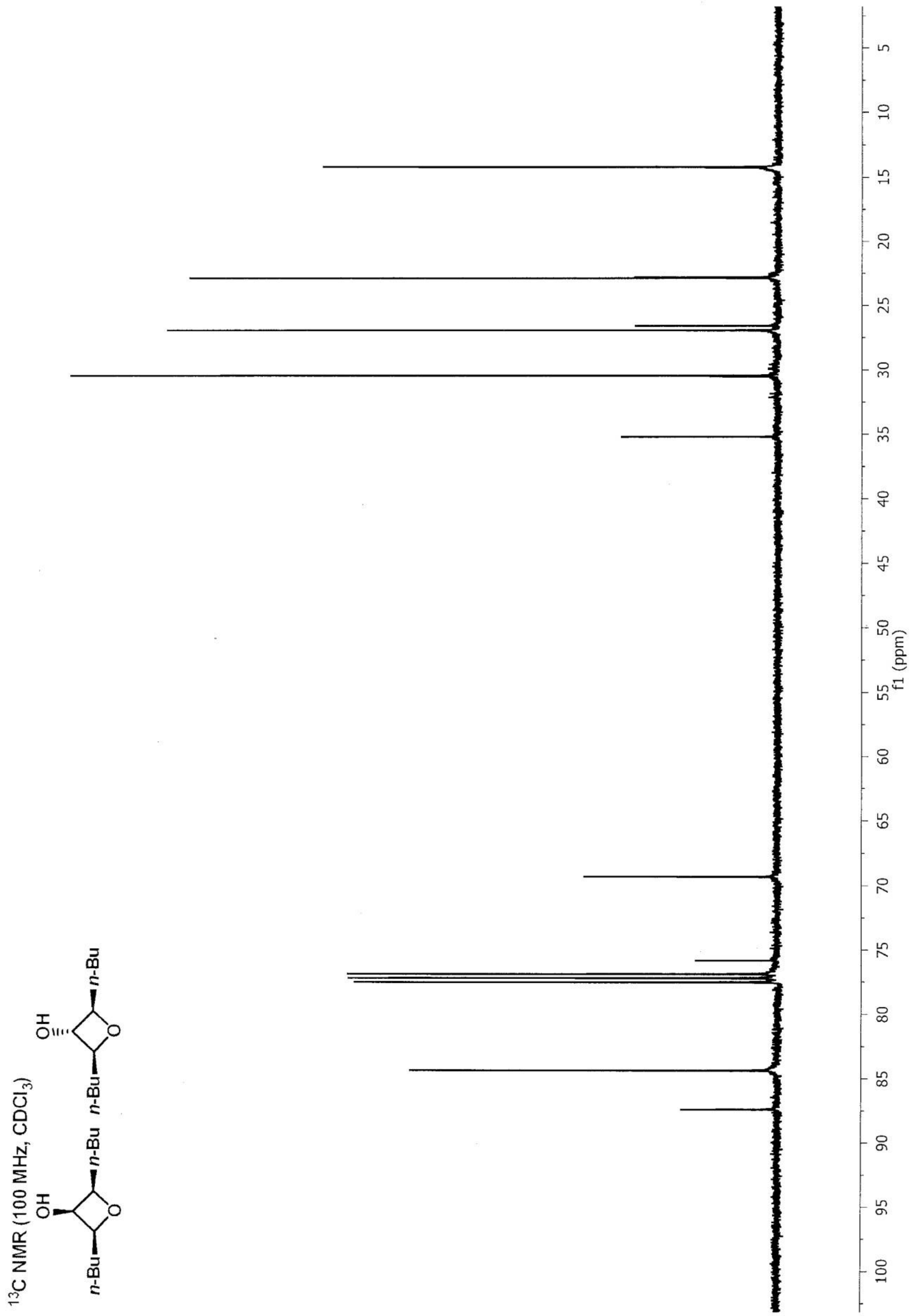

^{13}C NMR (100 MHz, CDCl$_3$)
OH
n-Bu
n-Bu
O
OH
n-Bu
n-Bu
O
5
10
15
20
25
30
35
40
45
50
55
60
65
70
75
80
85
90
95
100
f1 (ppm)

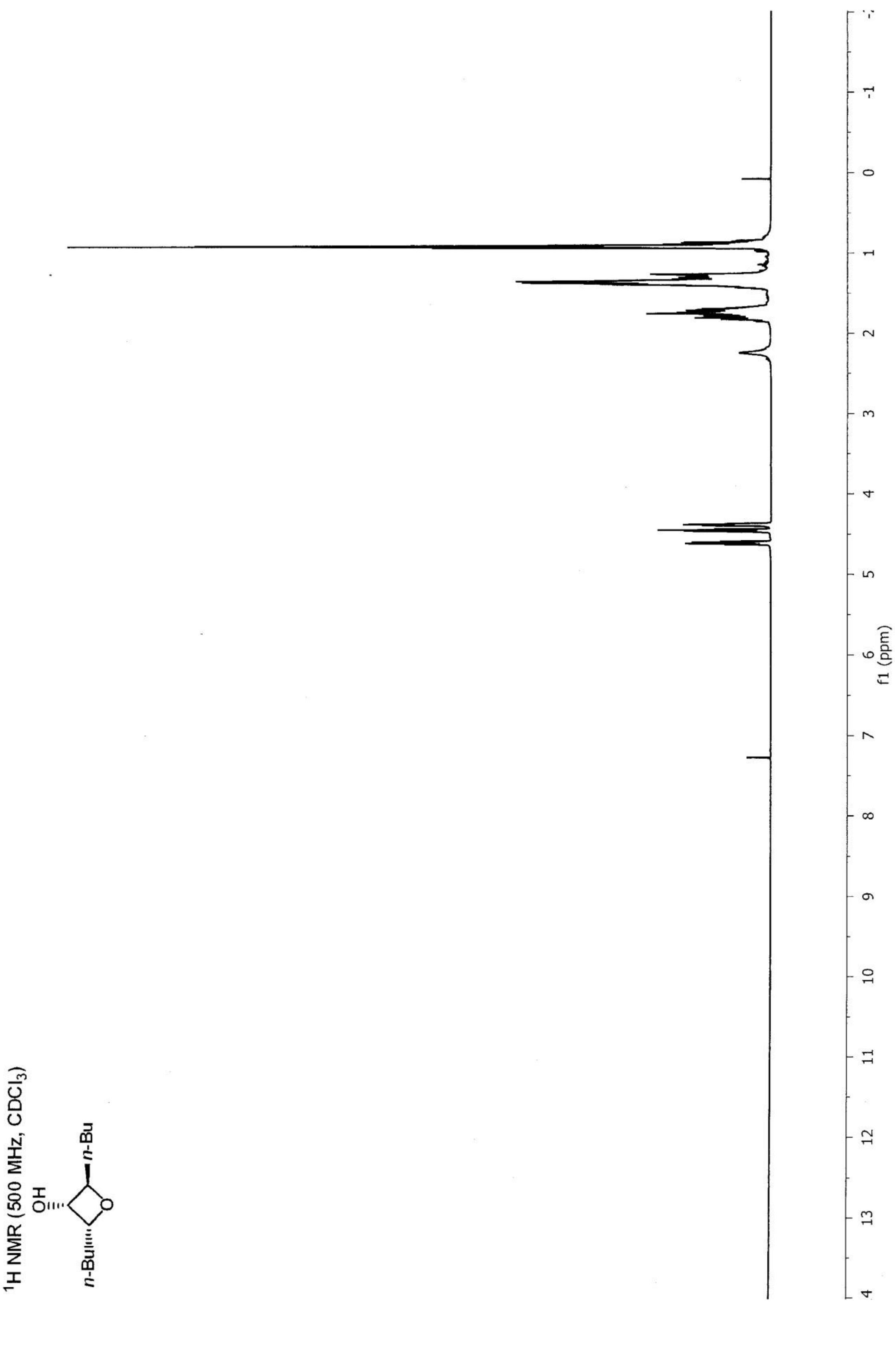

1H NMR (500 MHz, CDCl3)
OH
n-Bu
n-Bu
O
14 13 12 11 10 9 8 7 6 5 4 3 2 1 0 -1 -2
f1 (ppm)

^{13}C NMR (125 MHz, $CDCl_3$)

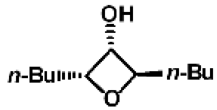

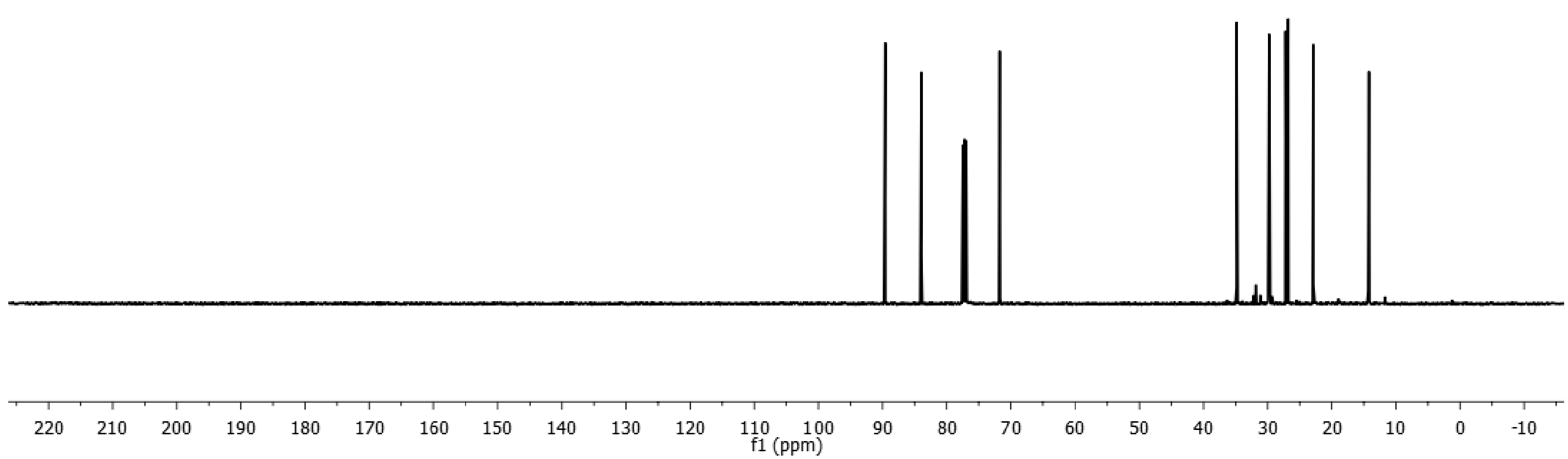

HPLC Profile of S4.17

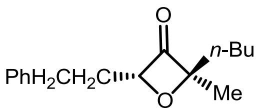 Daicel Chiralpak OD-H, n-hexane/i-PrOH= 99/1, Flow rate = 0.5 ml/min, t_R= 15.1 min (minor) and t_R= 18.0 min (major).

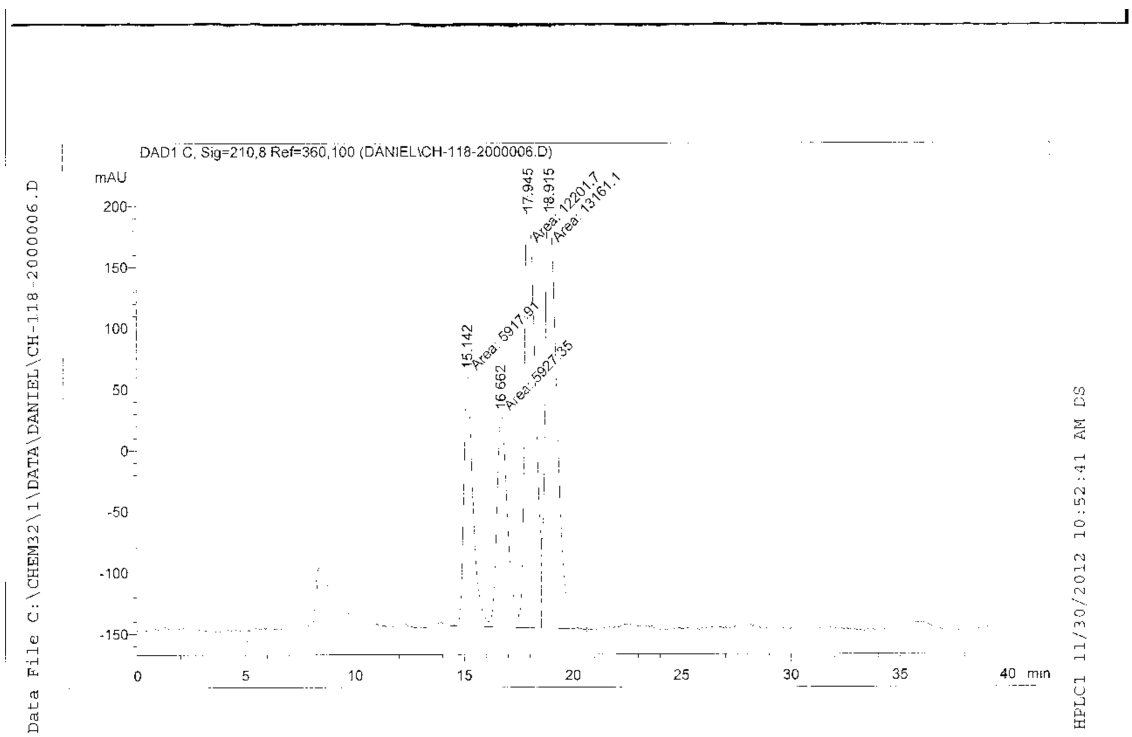

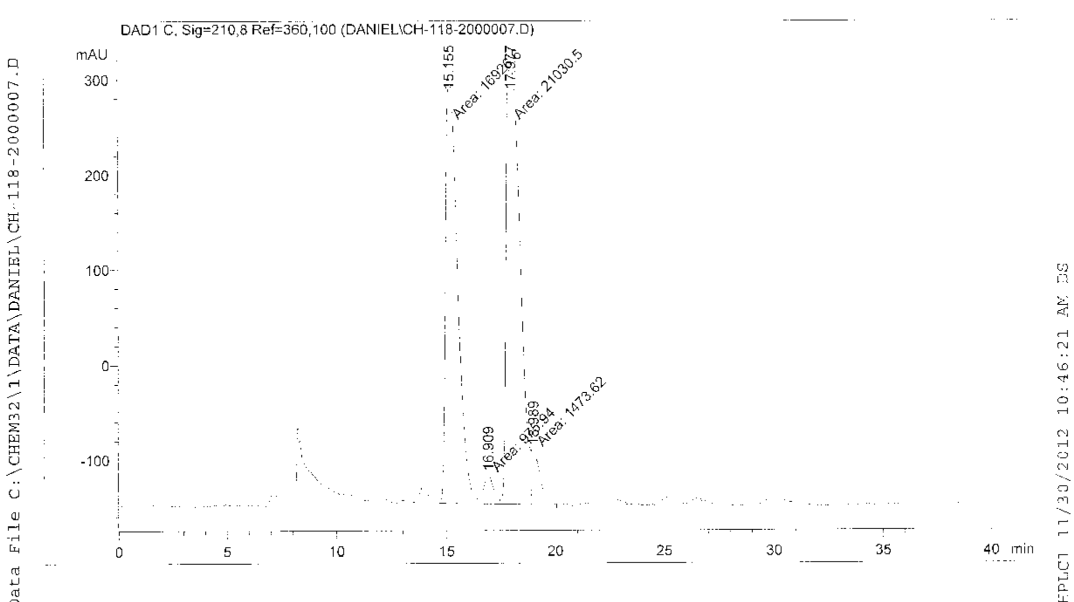

HPLC Profile of S4.25

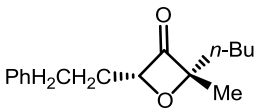

Daicel Chiralpak OD-H, n-hexane/i-PrOH= 99/1, Flow rate = 0.5 ml/min., t_R= 16.6 min (major) and t_R= 19.0 min (minor).

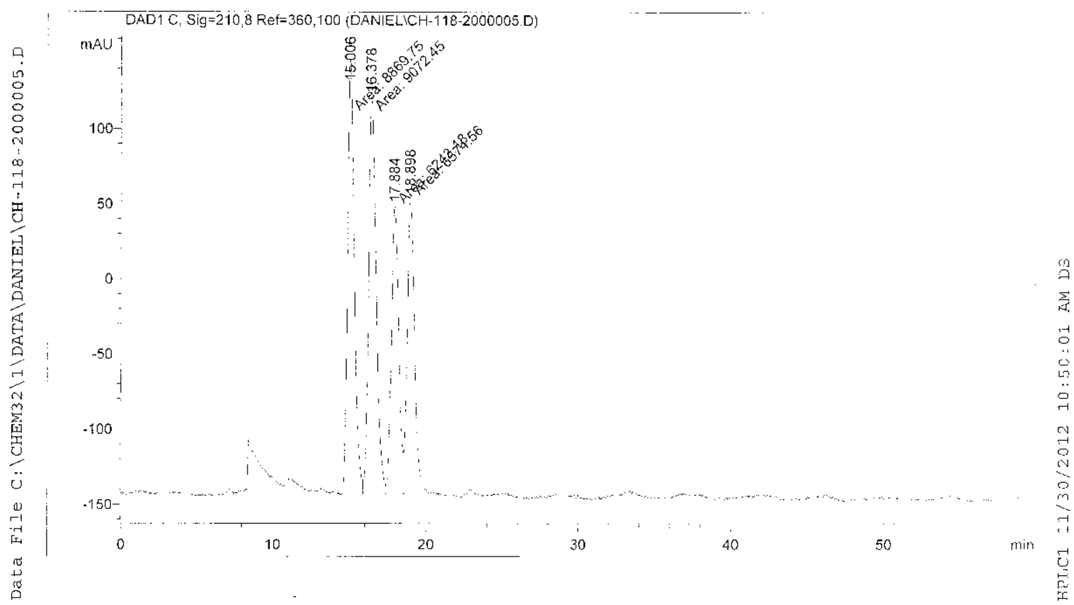

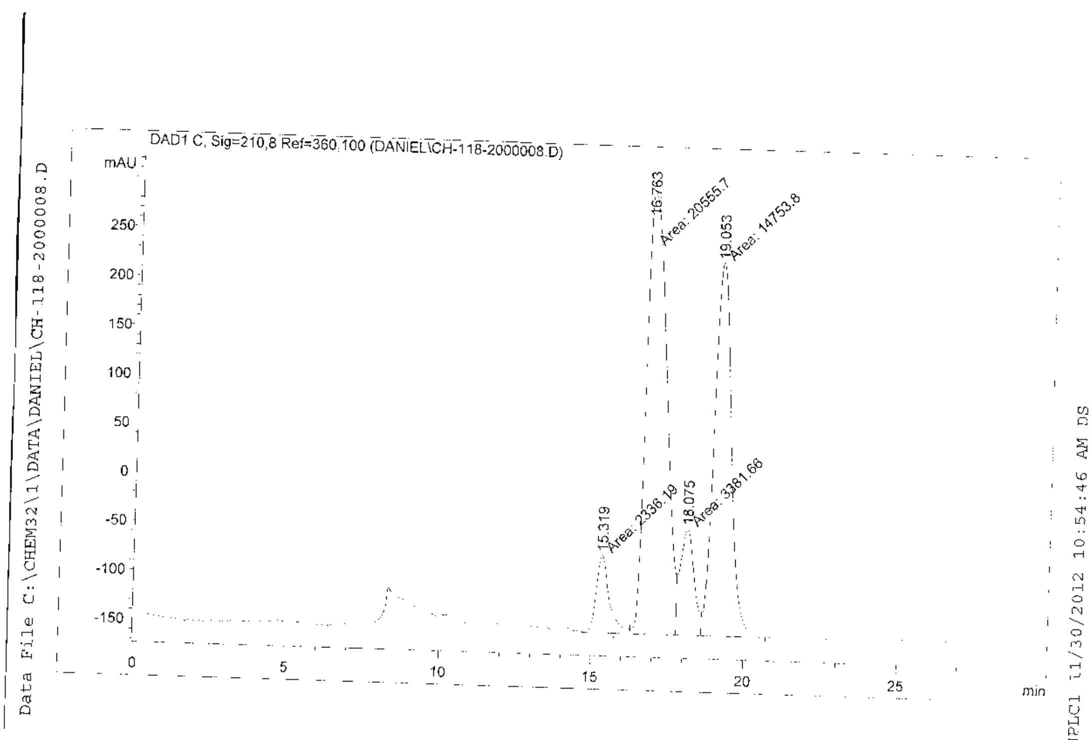

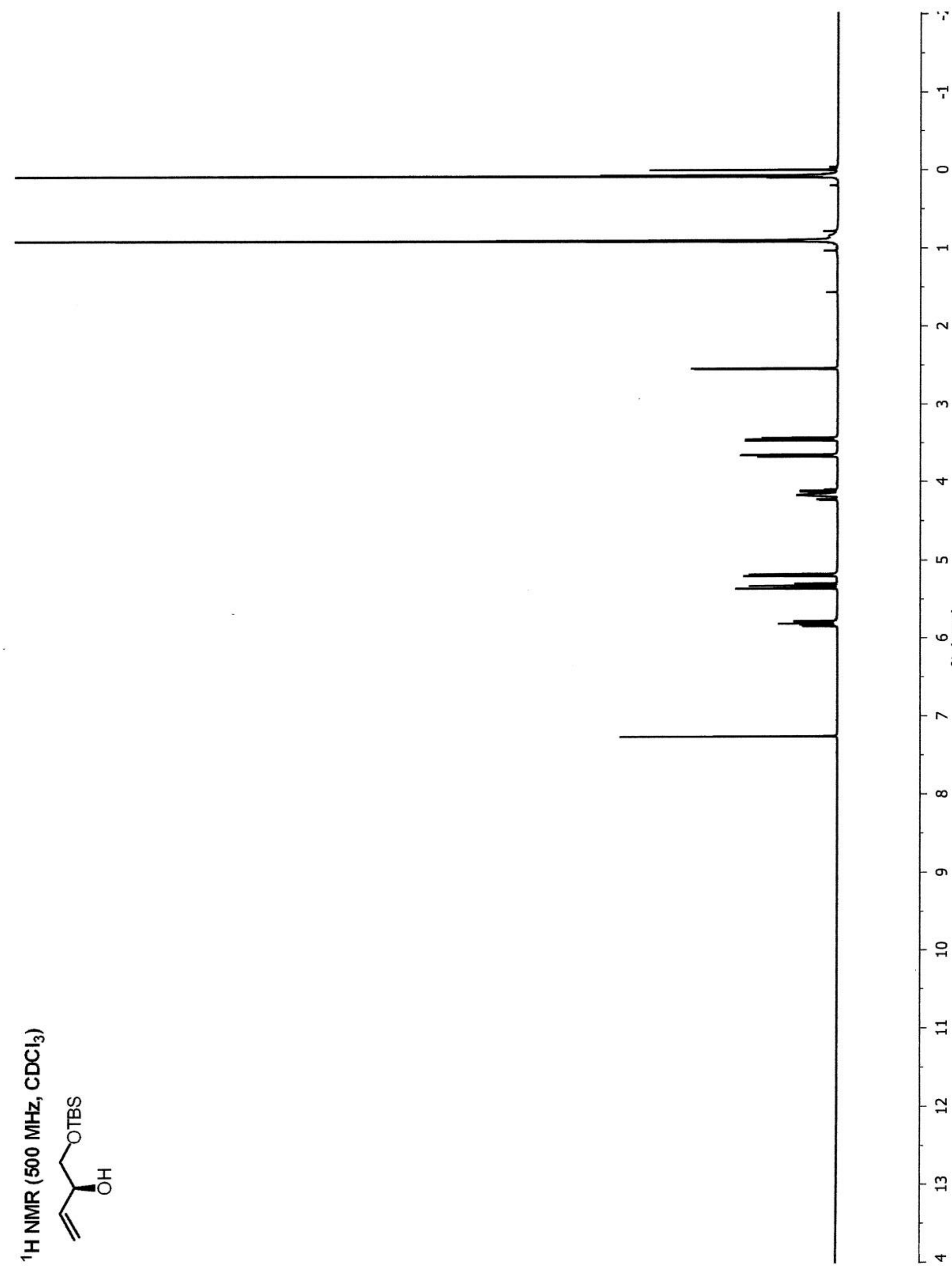

^1H NMR (500 MHz, $CDCl_3$)
OTBS
OH
f1 (ppm)

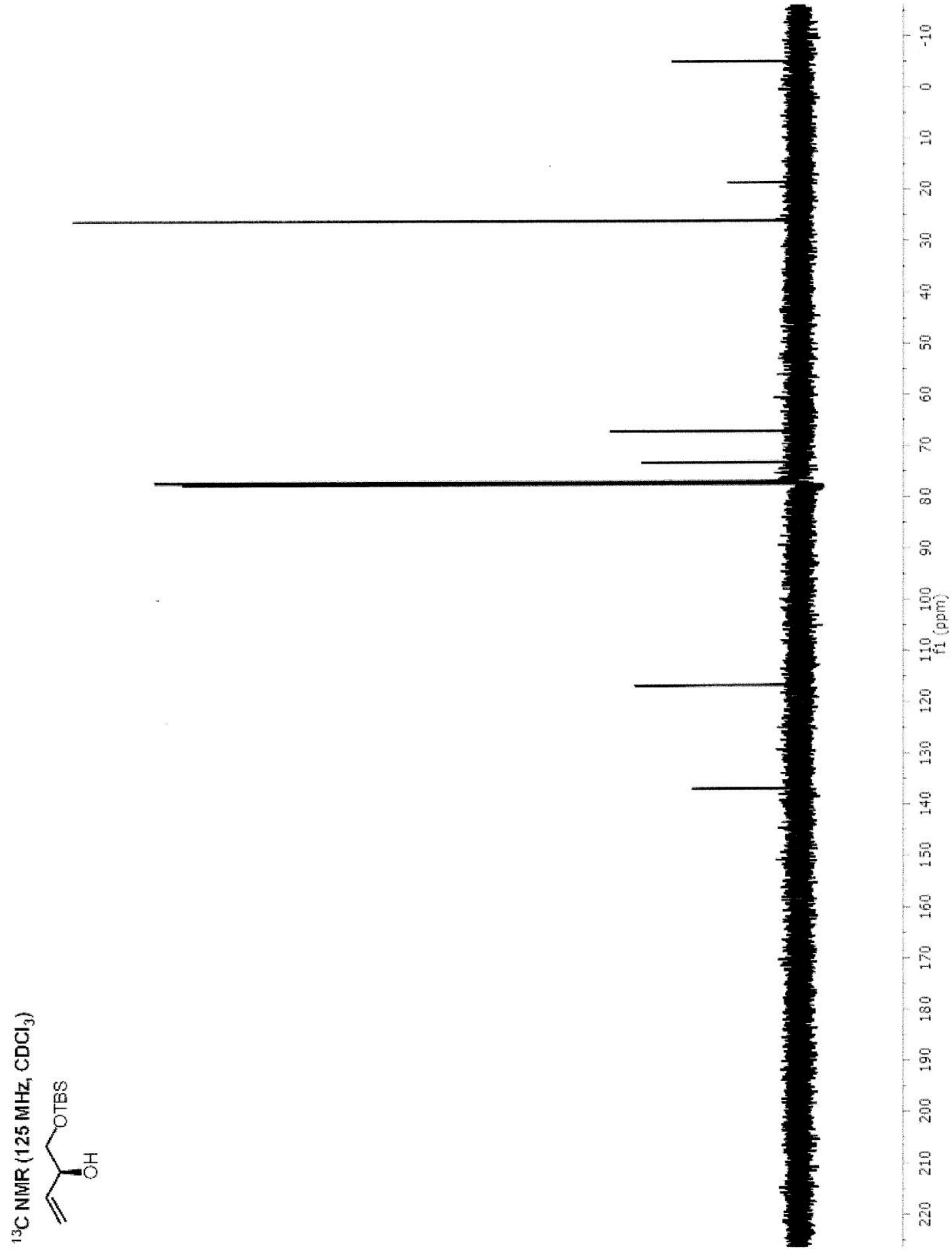
^{13}C NMR (125 MHz, CDCl$_3$)
OTBS
OH
f1 (ppm)
220 210 200 190 180 170 160 150 140 130 120 110 100 90 80 70 60 50 40 30 20 10 0 -10

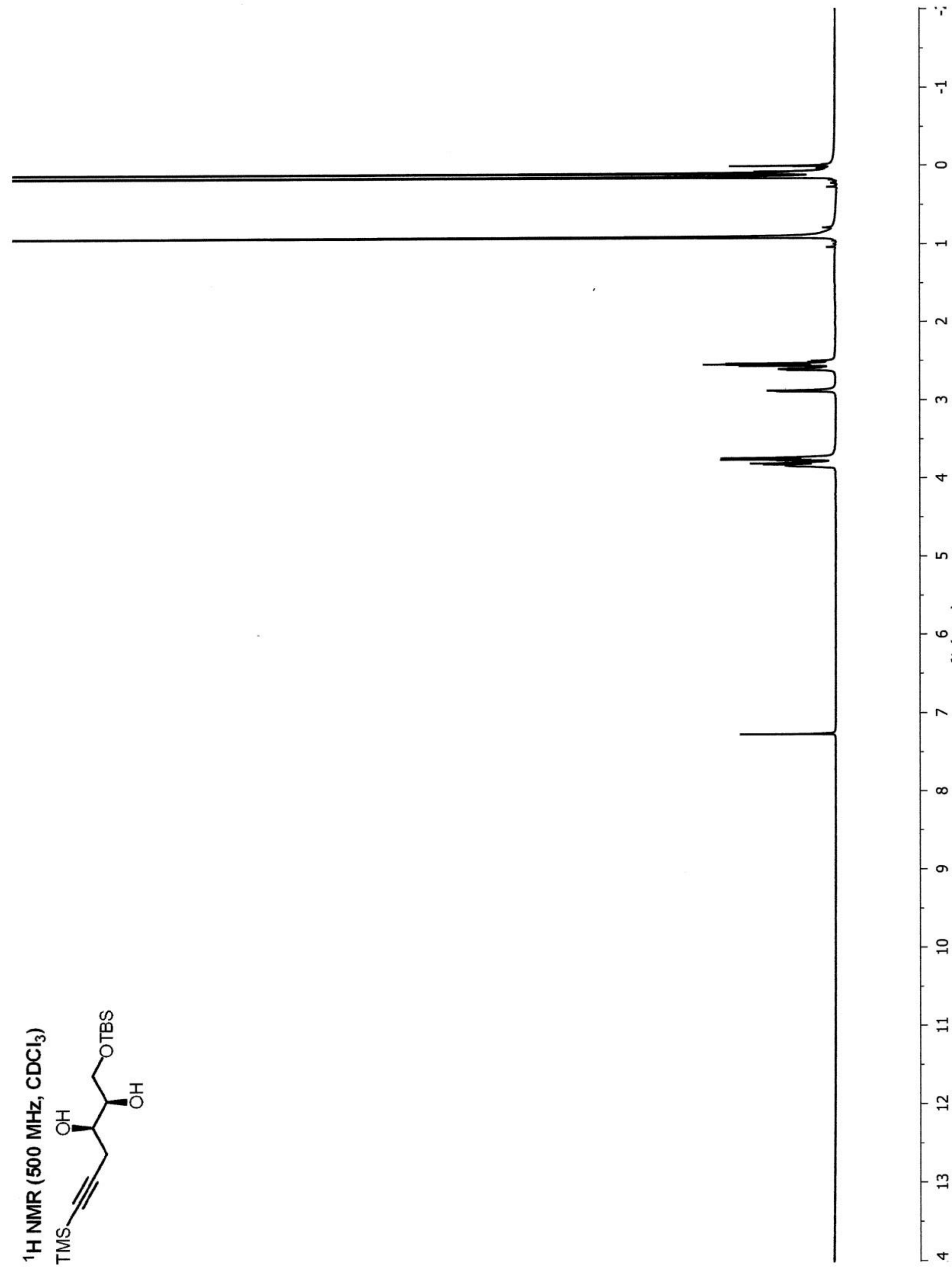

¹H NMR (500 MHz, CDCl₃)
TMS
OH
OTBS
OH
f1 (ppm)

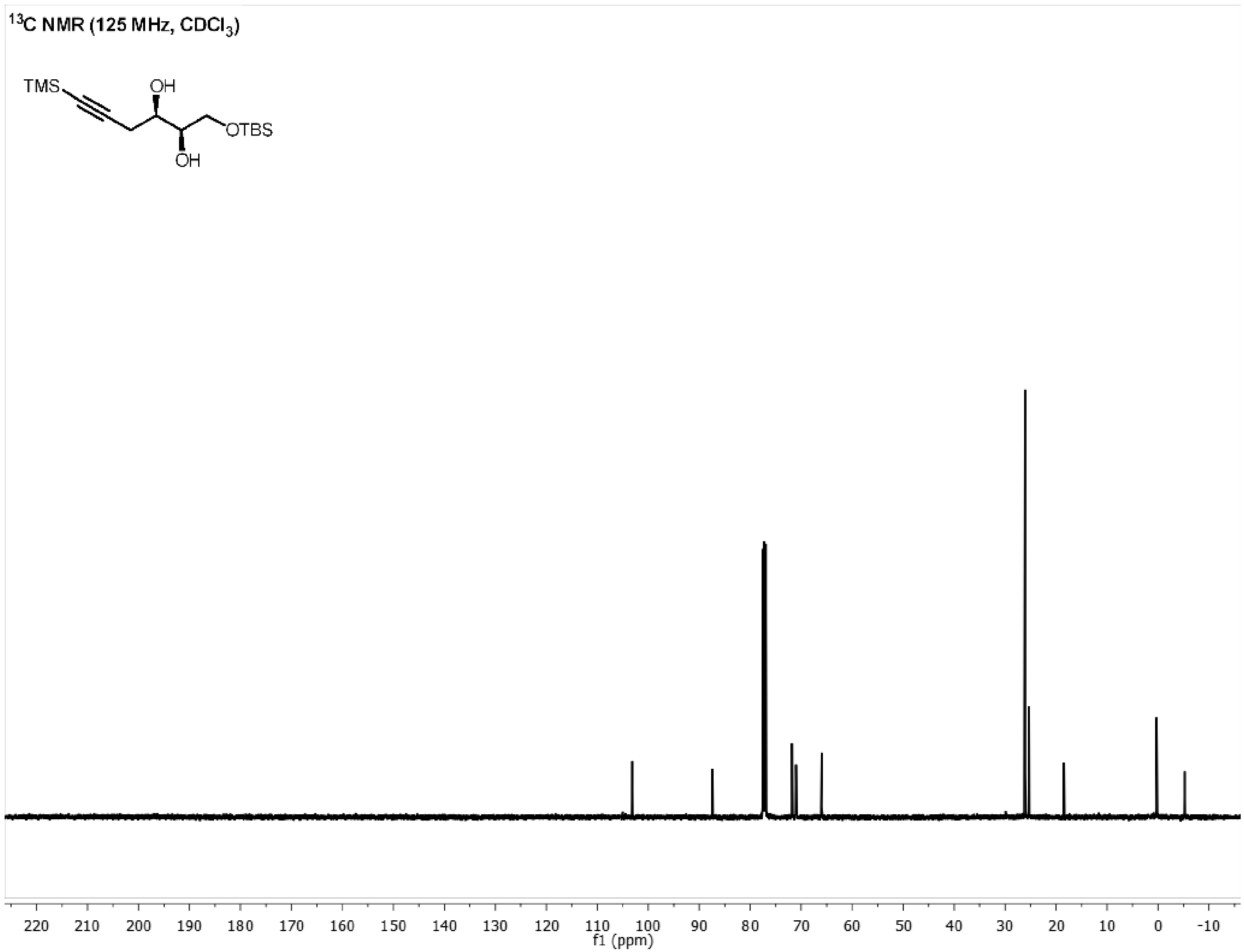
^{13}C NMR (125 MHz, $CDCl_3$)
TMS
OH
OH
OTBS
220 210 200 190 180 170 160 150 140 130 120 110 100 90 80 70 60 50 40 30 20 10 0 -10
f1 (ppm)

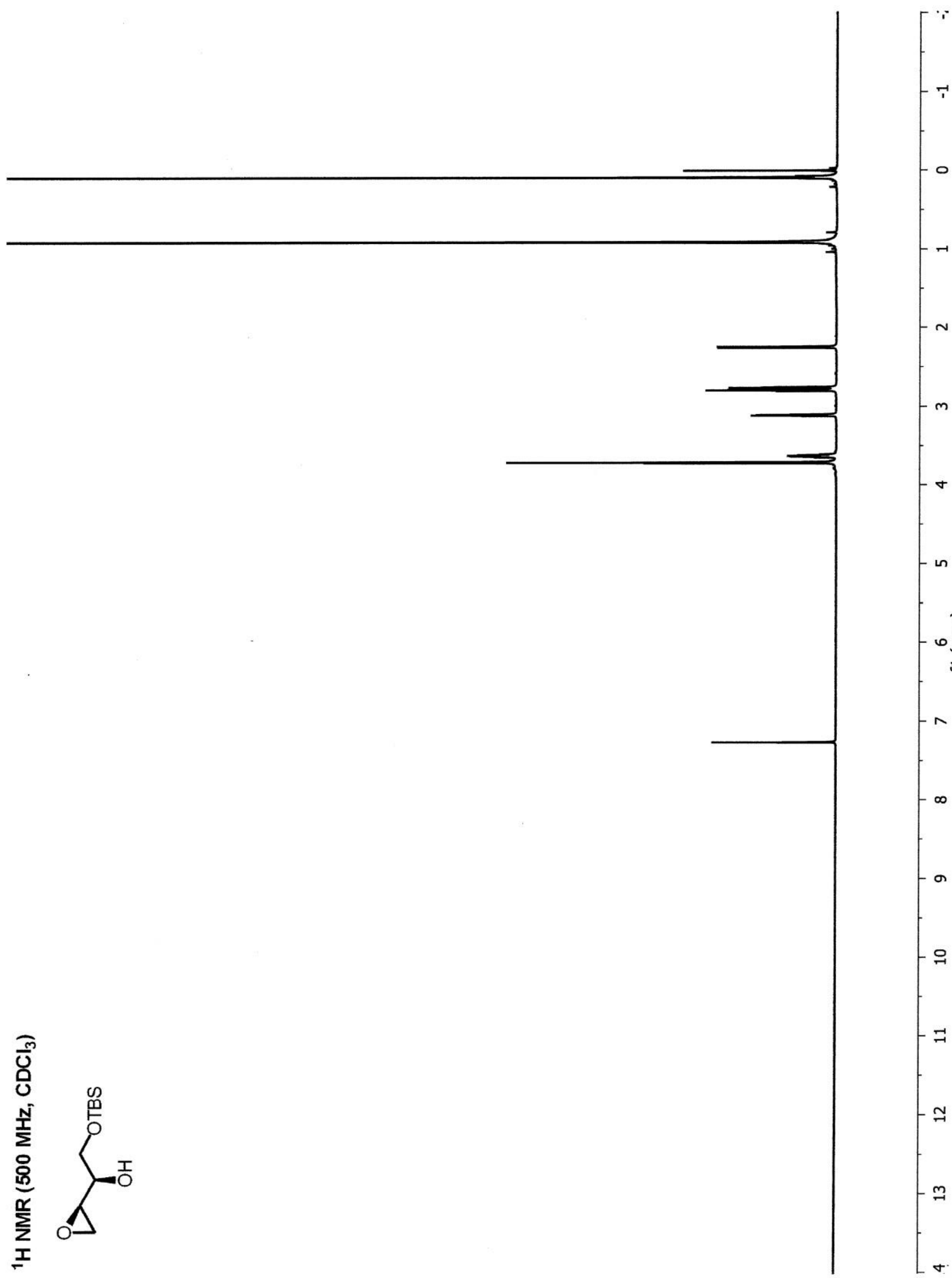
1H NMR (500 MHz, CDCl3)
OTBS
OH
O
f1 (ppm)
14 13 12 11 10 9 8 7 6 5 4 3 2 1 0 -1 -2

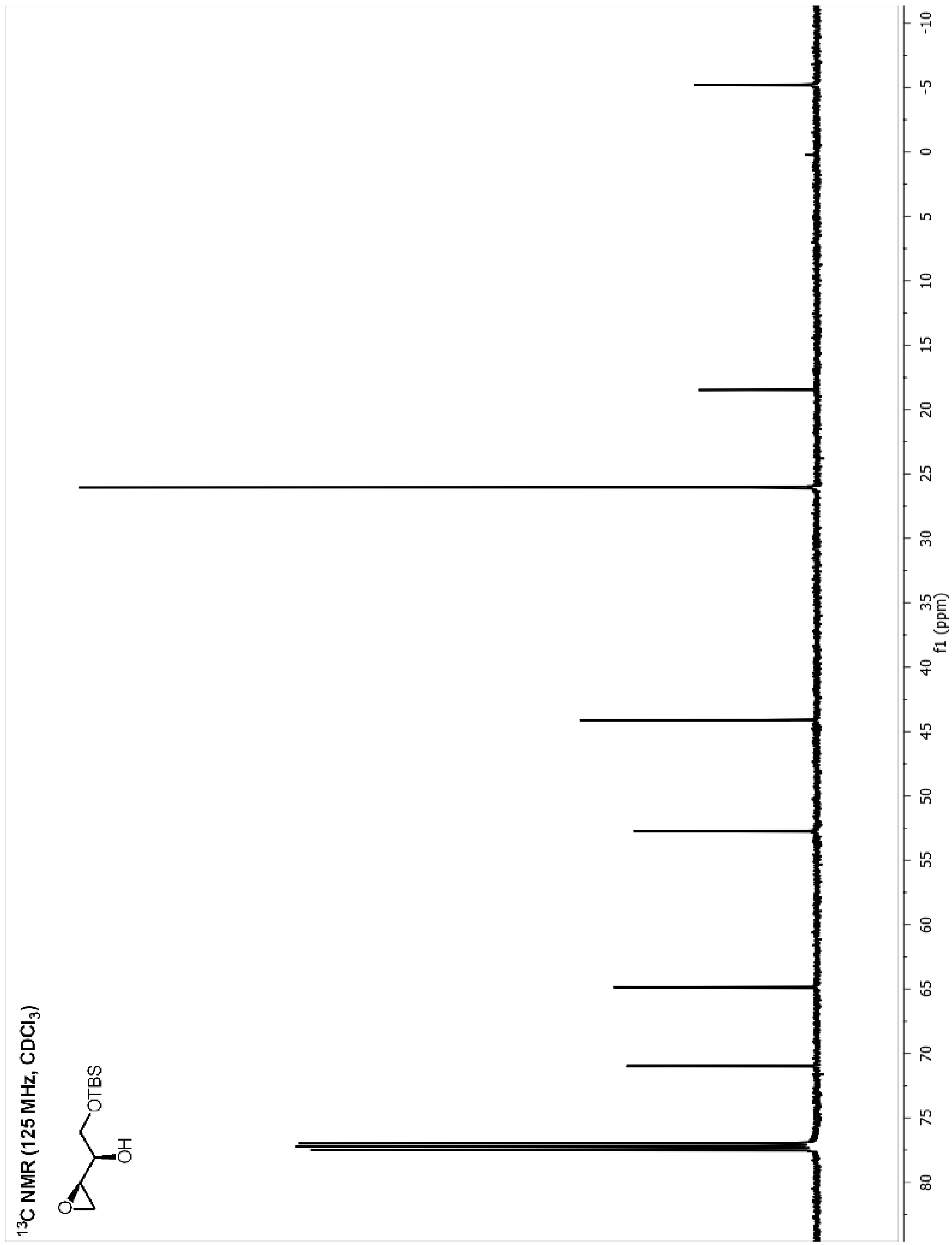

^{13}C NMR (125 MHz, $CDCl_3$)
OTBS
OH
O
f1 (ppm)
80
75
70
65
60
55
50
45
40
35
30
25
20
15
10
5
0
-5
-10

^1H NMR (500 MHz, $CDCl_3$)

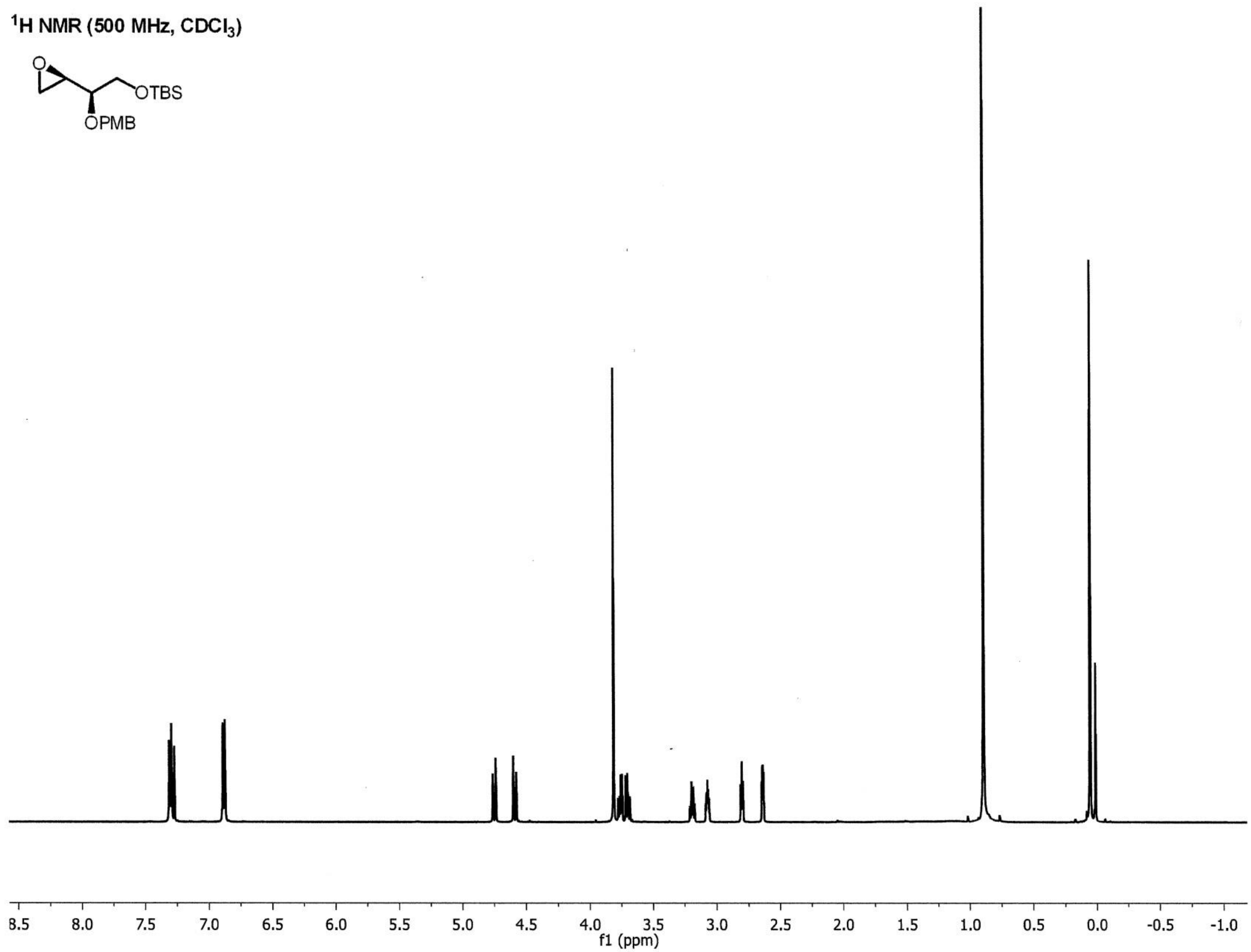

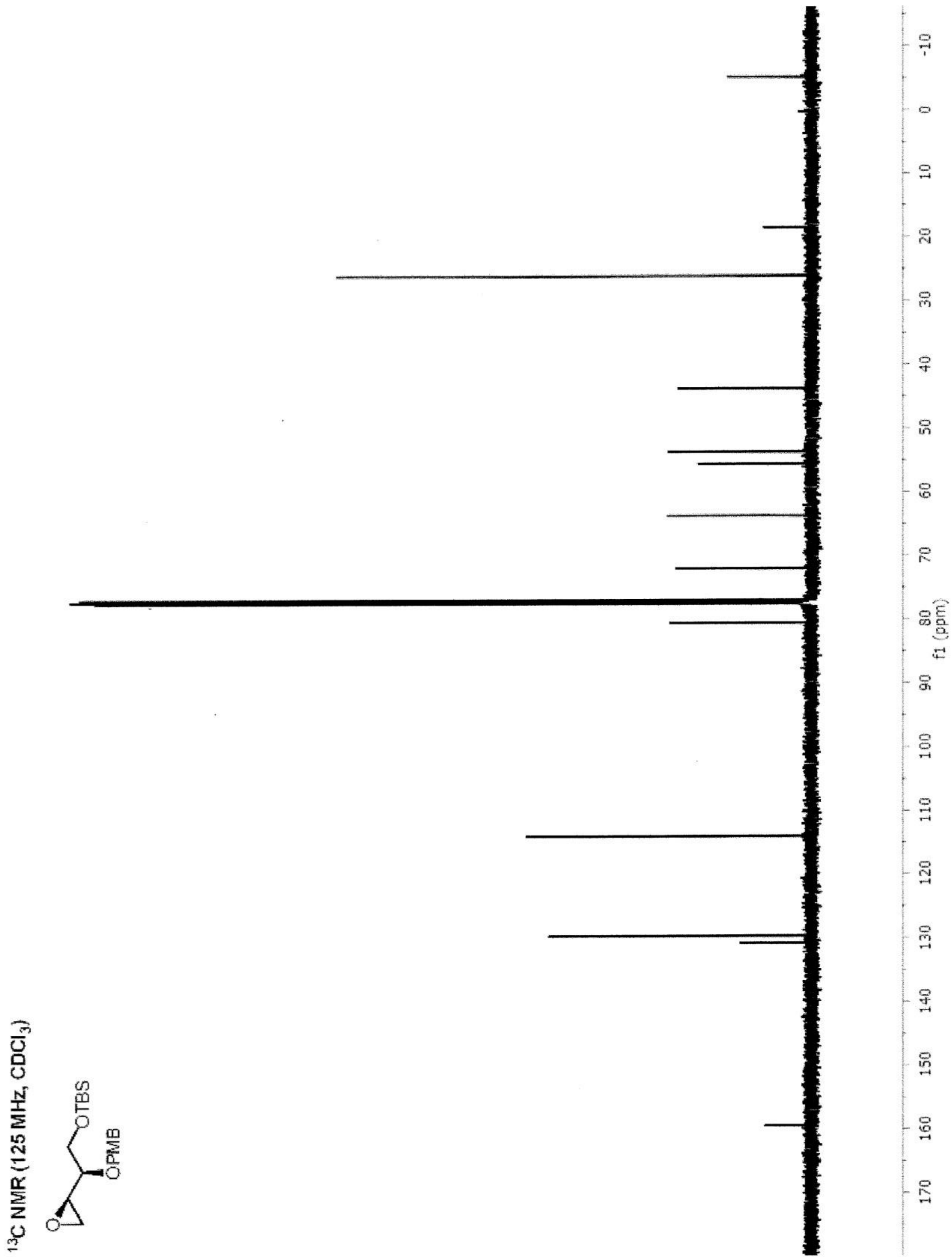
^{13}C NMR (125 MHz, CDCl$_3$)
OTBS
OPMB
O
f1 (ppm)
-10 0 10 20 30 40 50 60 70 80 90 100 110 120 130 140 150 160 170

^{1}H NMR (500 MHz, $CDCl_3$)

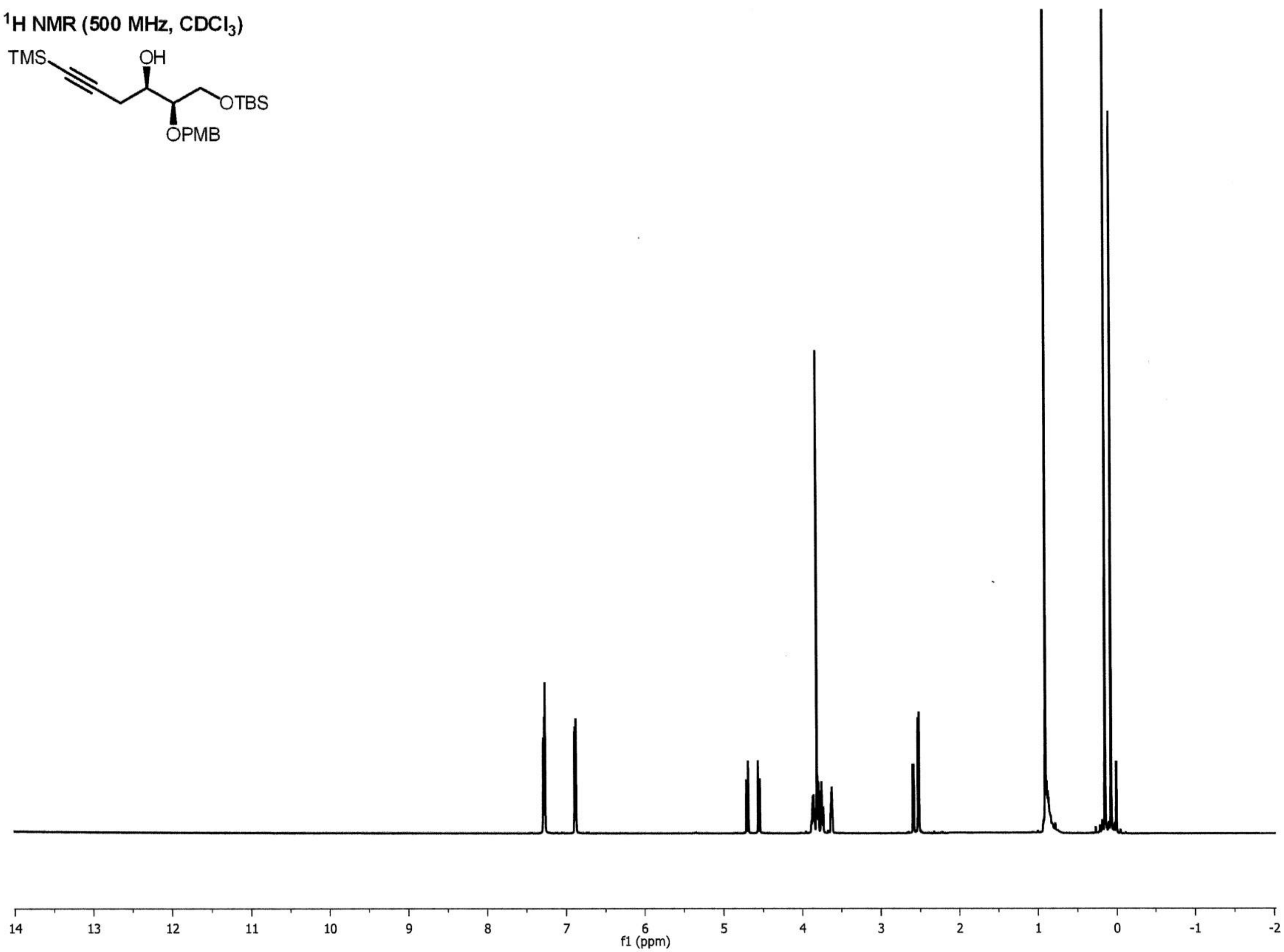

^{13}C NMR (125 MHz, $CDCl_3$)

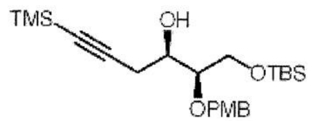

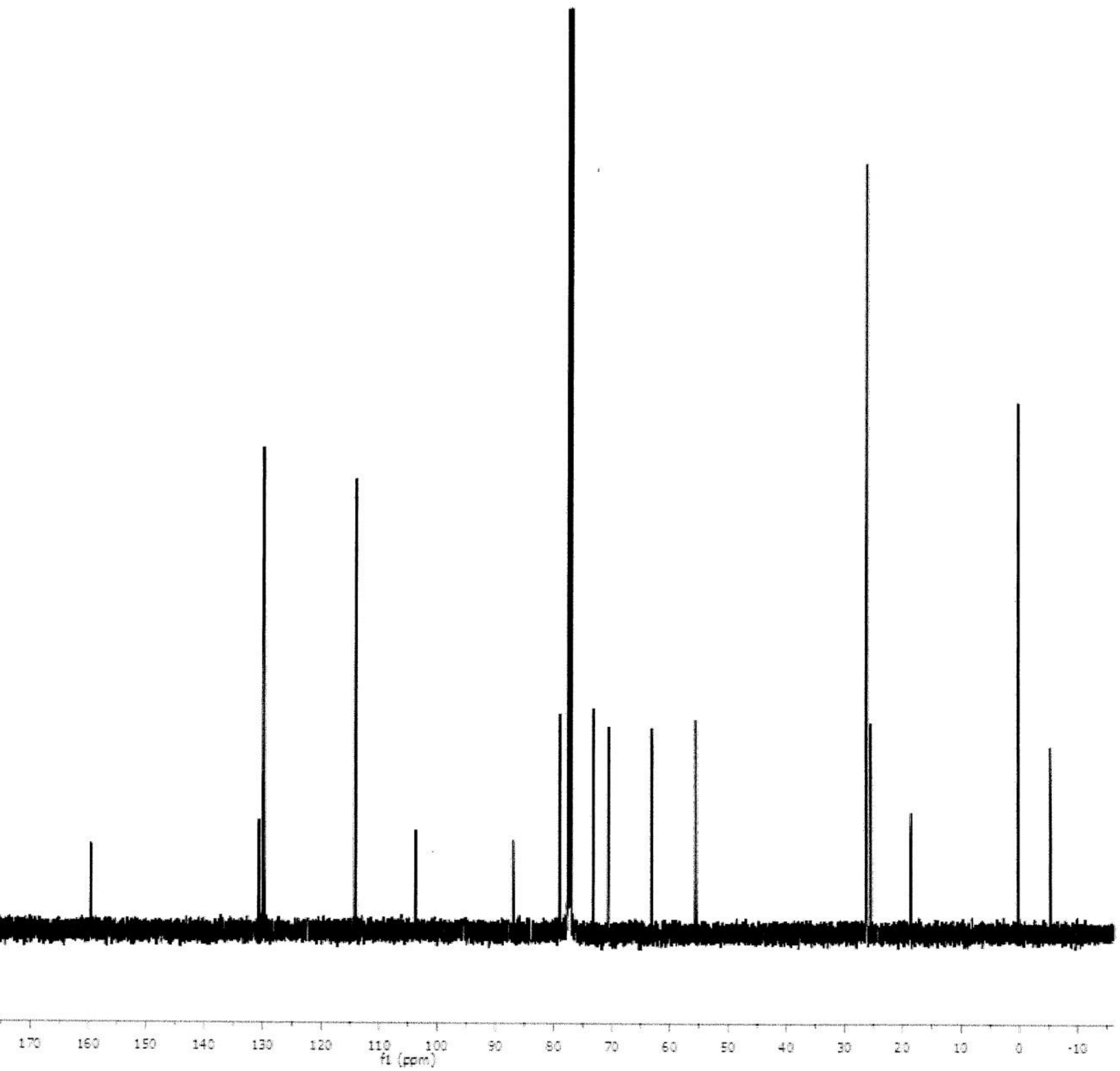

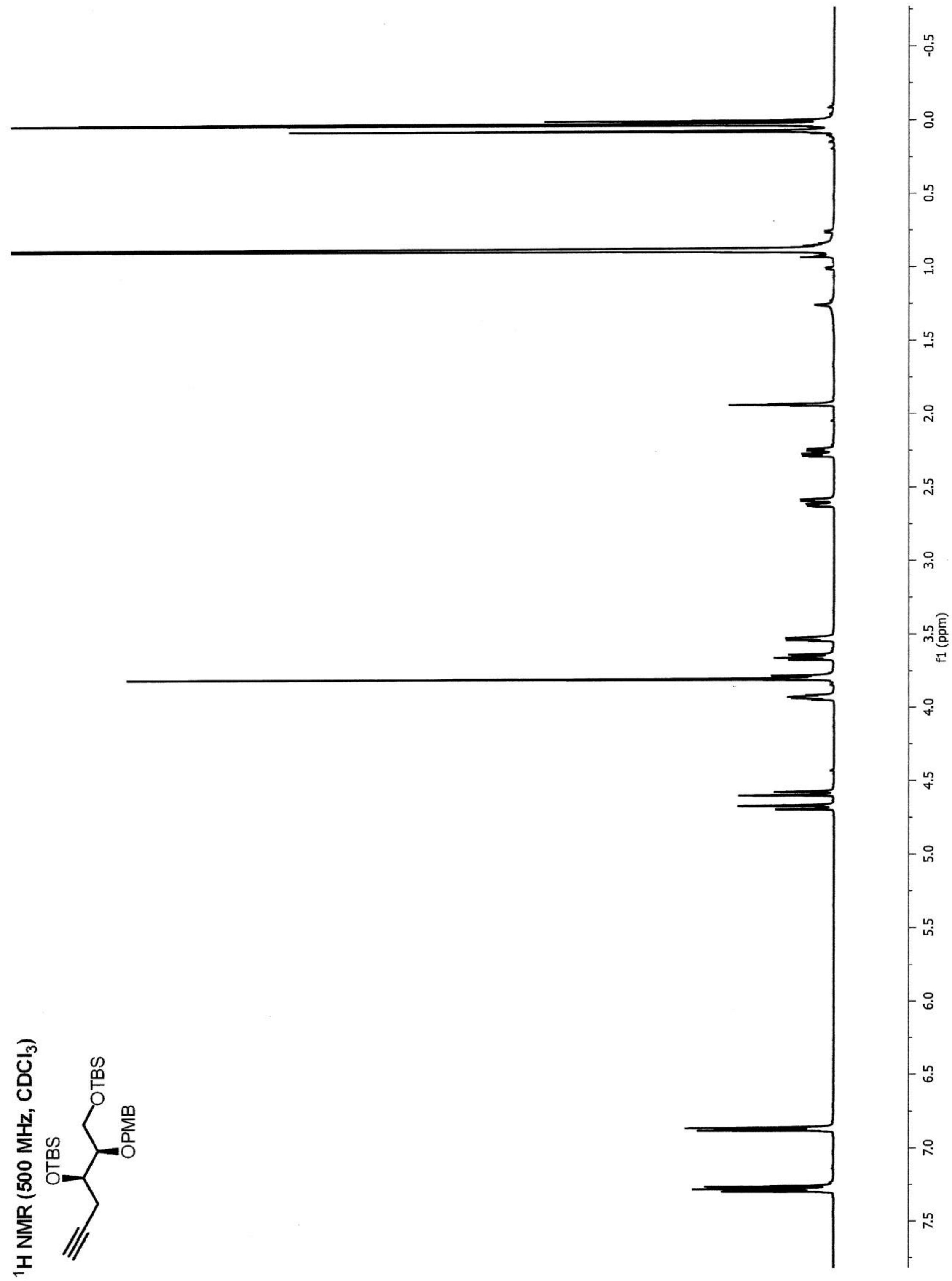

1H NMR (500 MHz, CDCl3)
OTBS
OTBS
OPMB
f1 (ppm)
-0.5
0.0
0.5
1.0
1.5
2.0
2.5
3.0
3.5
4.0
4.5
5.0
5.5
6.0
6.5
7.0
7.5

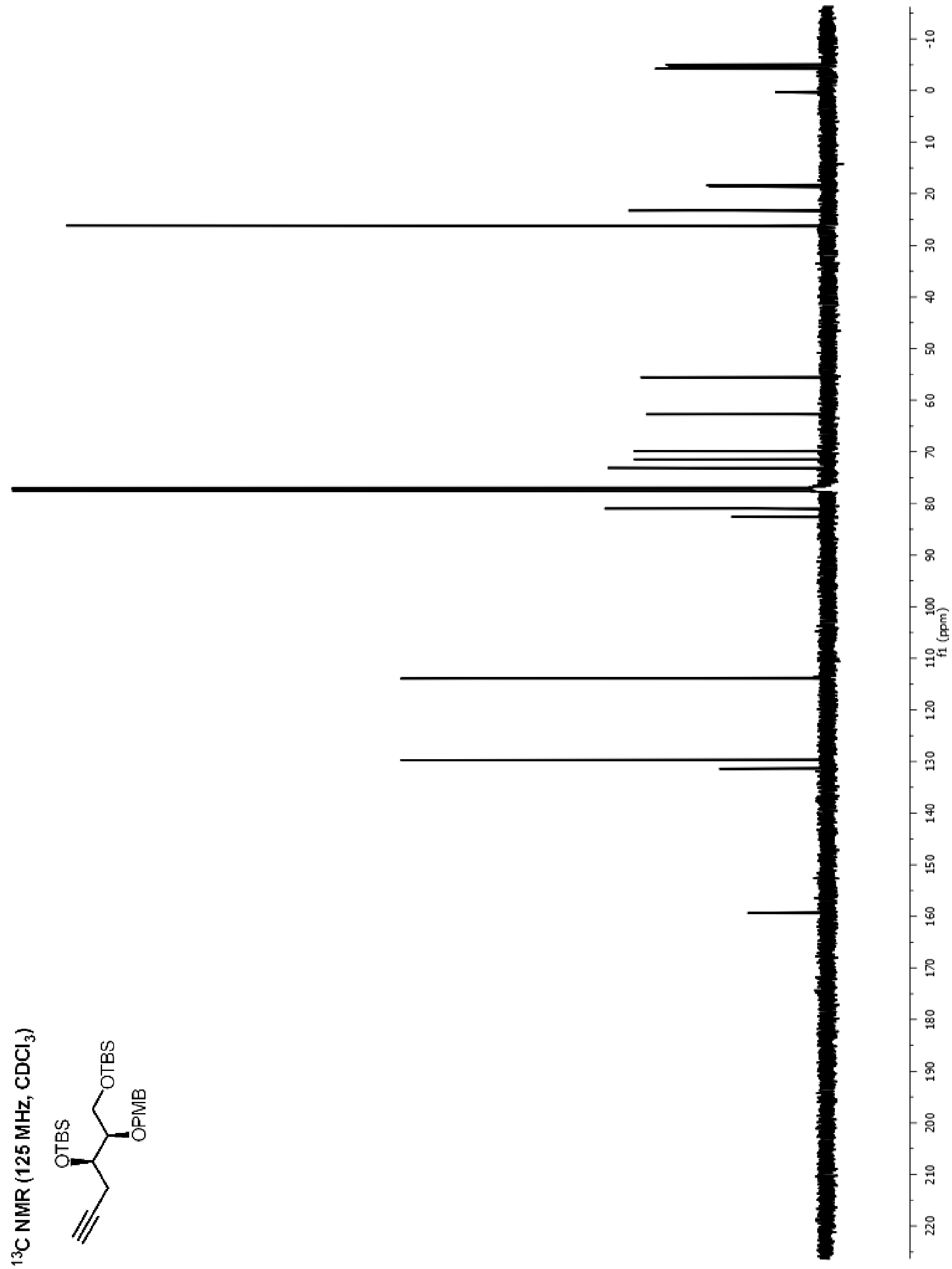
13C NMR (125 MHz, CDCl3)
OTBS
OTBS
OPMB
f1 (ppm)
-10
0
10
20
30
40
50
60
70
80
90
100
110
120
130
140
150
160
170
180
190
200
210
220

^{1}H NMR (500 MHz, $CDCl_3$)

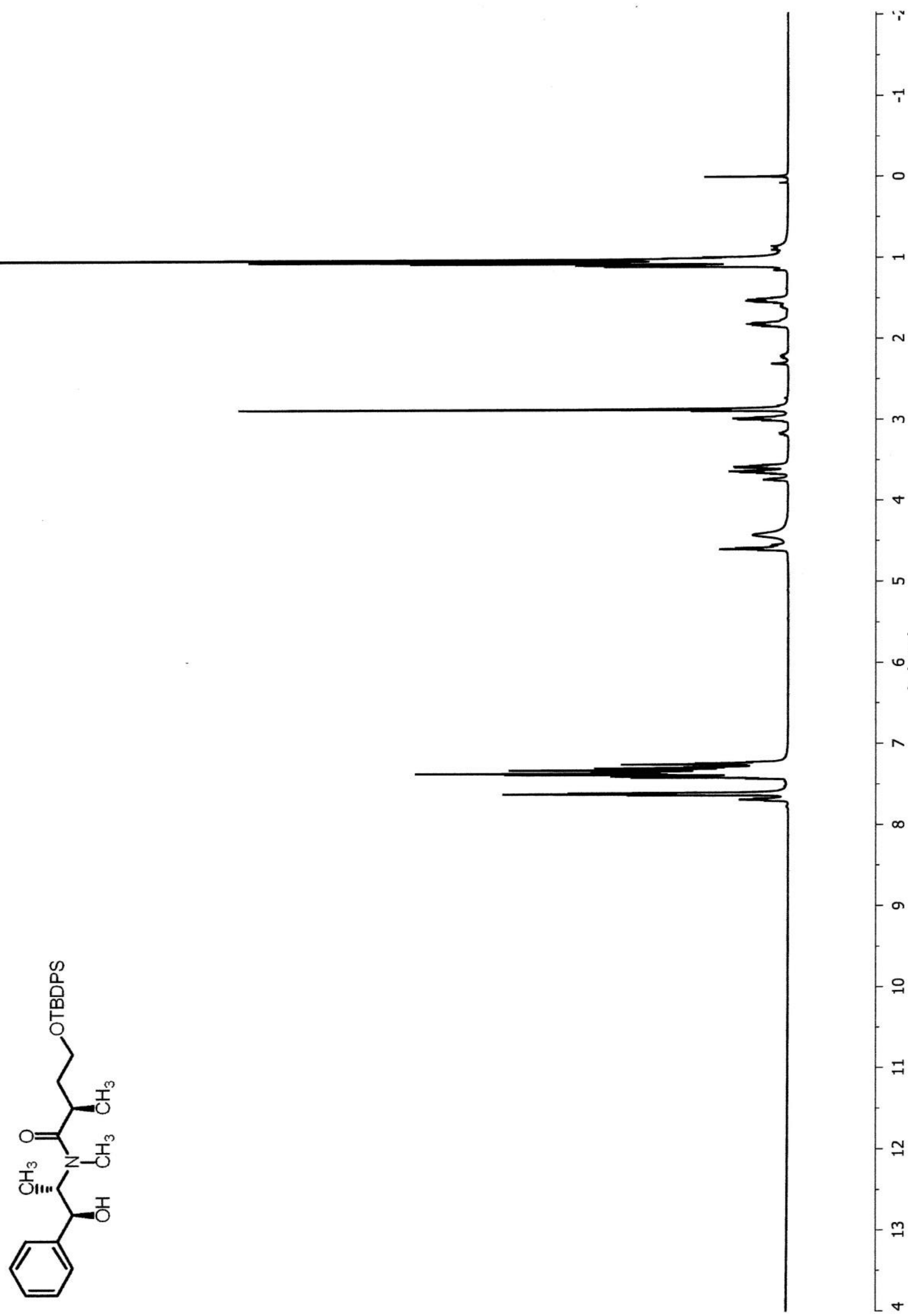

^{13}C NMR (125 MHz, $CDCl_3$)

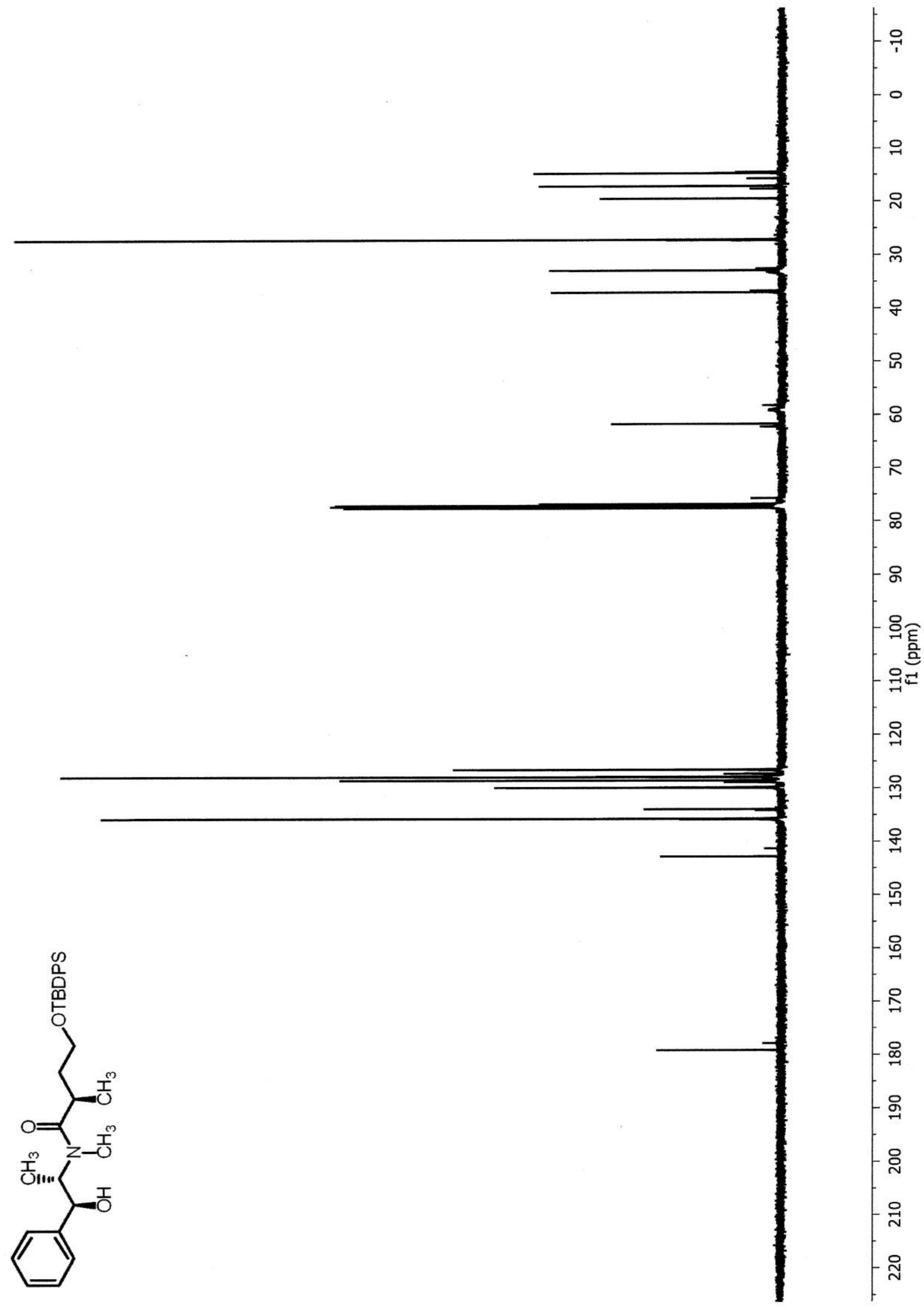

^1H NMR (500 MHz, $CDCl_3$)

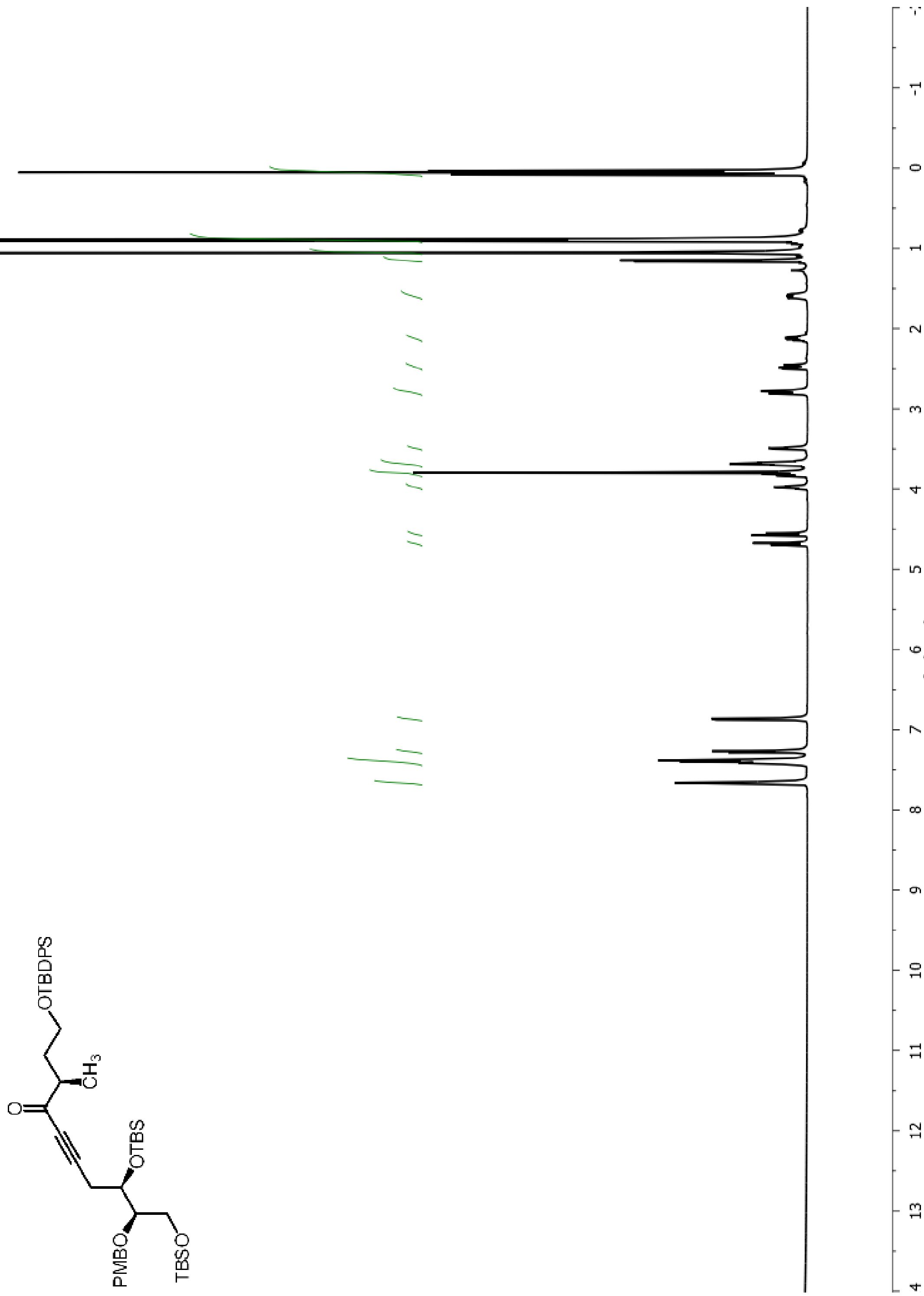

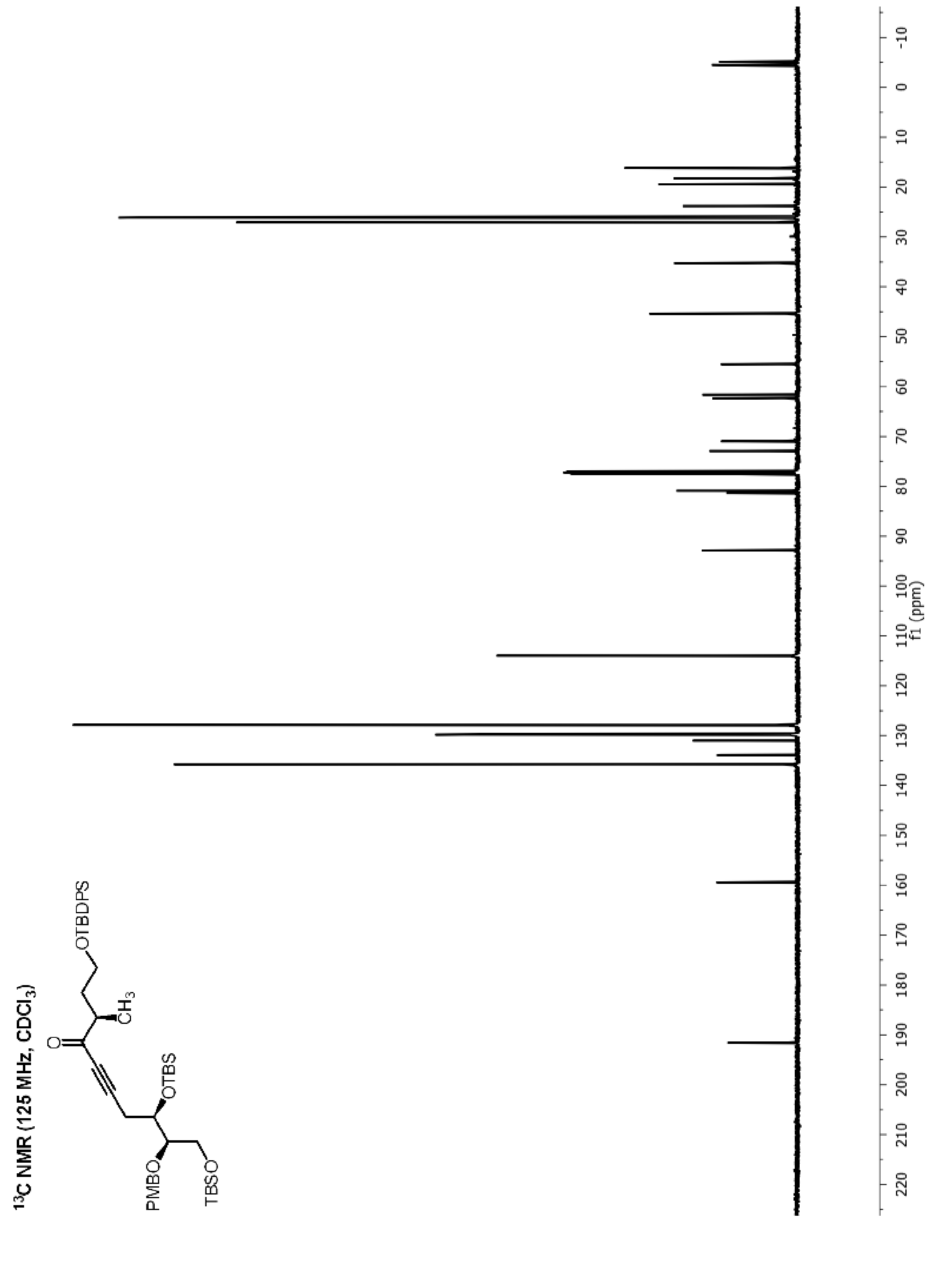

13C NMR (125 MHz, CDCl3)
OTBDPS
O
CH3
OTBS
PMBO
TBSO
f1 (ppm)
220 210 200 190 180 170 160 150 140 130 120 110 100 90 80 70 60 50 40 30 20 10 0 -10

^1H NMR (500 MHz, $CDCl_3$)

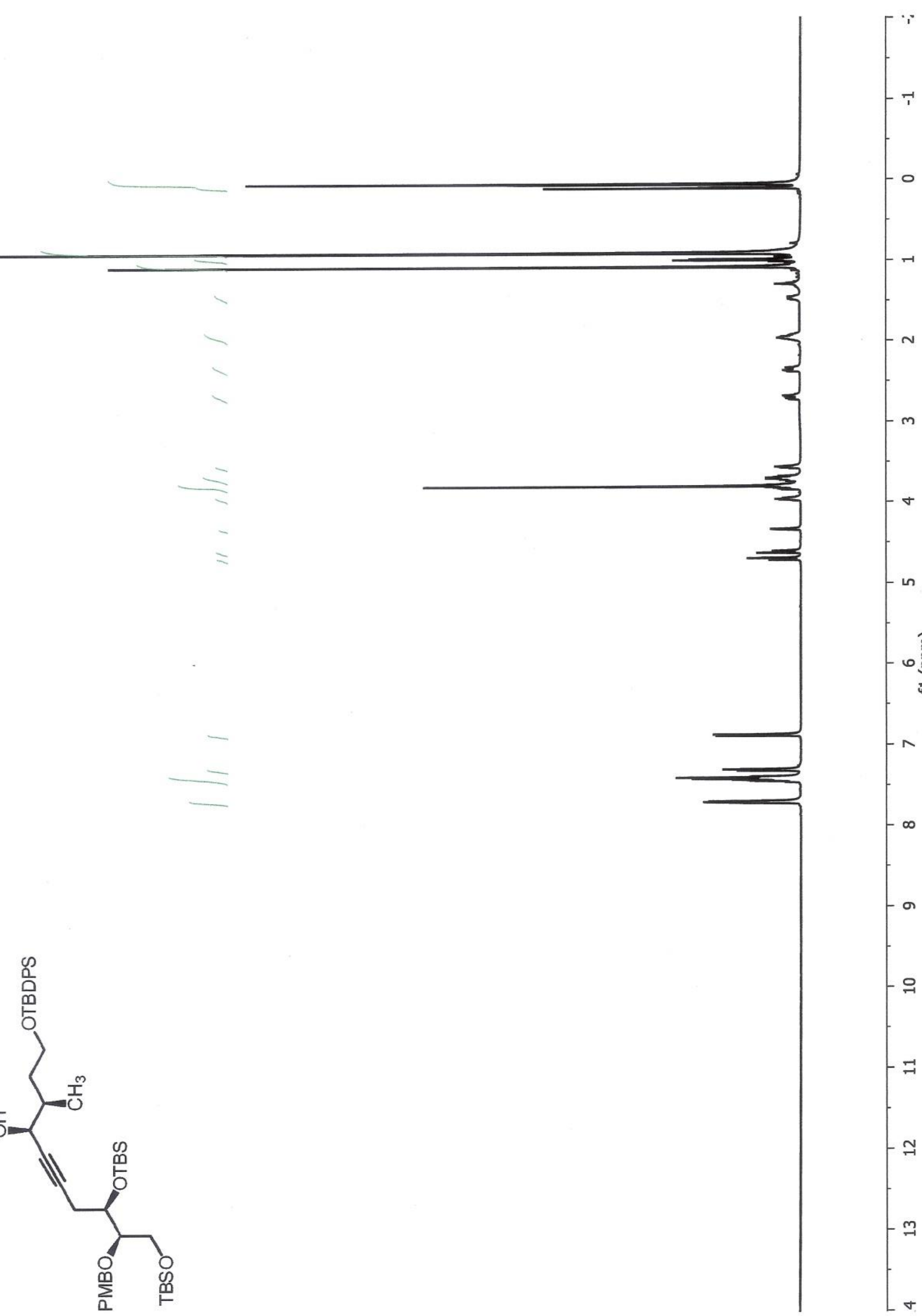

^{13}C NMR (125 MHz, $CDCl_3$)

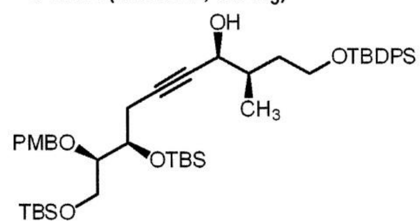

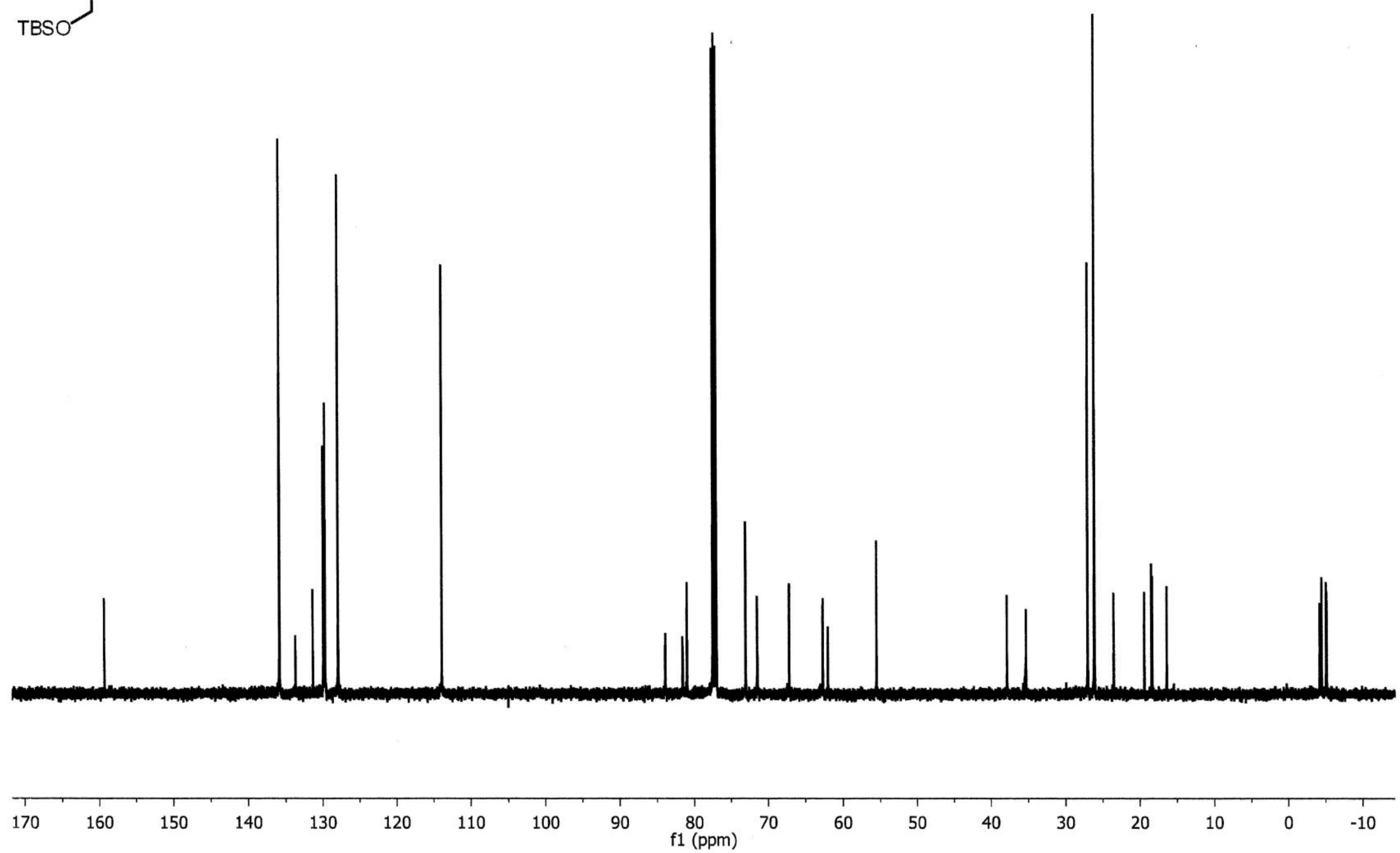

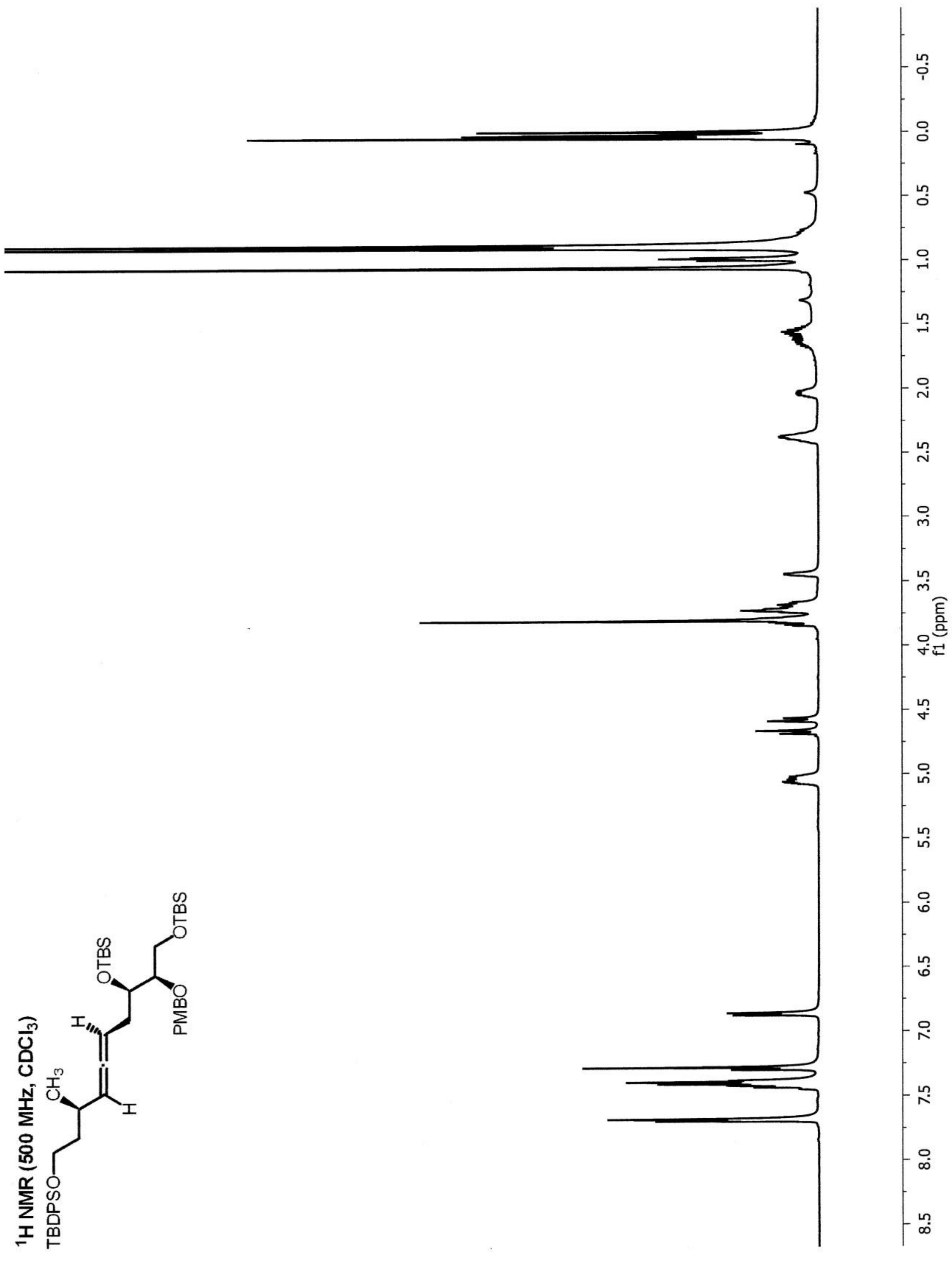

^1H NMR (500 MHz, $CDCl_3$)
TBDPSO
CH_3
H
H
OTBS
PMBO
OTBS
f1 (ppm)

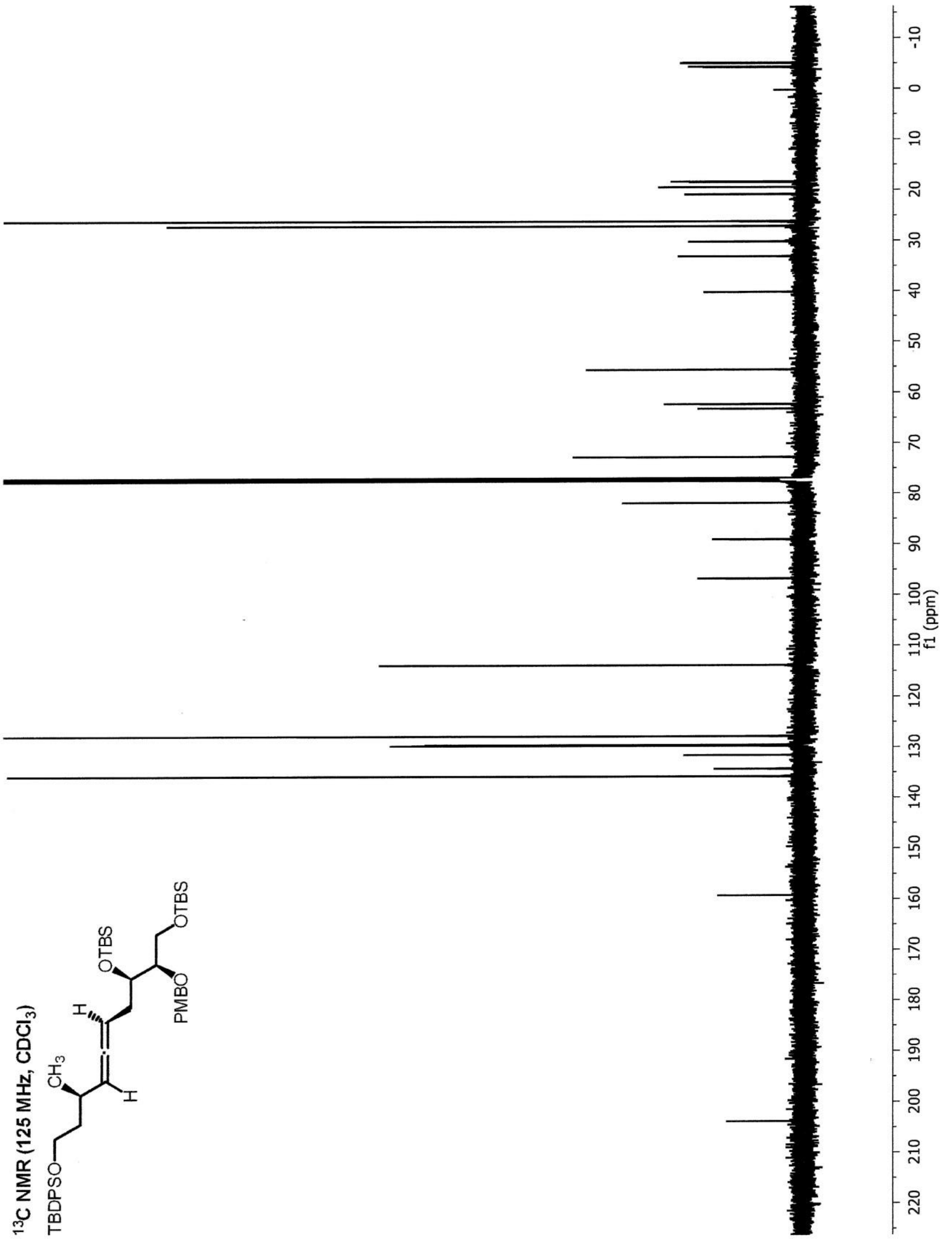
¹³C NMR (125 MHz, CDCl₃)
TBDPSO
CH₃
H
H
OTBS
OTBS
PMBO
220 210 200 190 180 170 160 150 140 130 120 110 100 90 80 70 60 50 40 30 20 10 0 -10
f1 (ppm)

^1H NMR (300 MHz, $CDCl_3$)

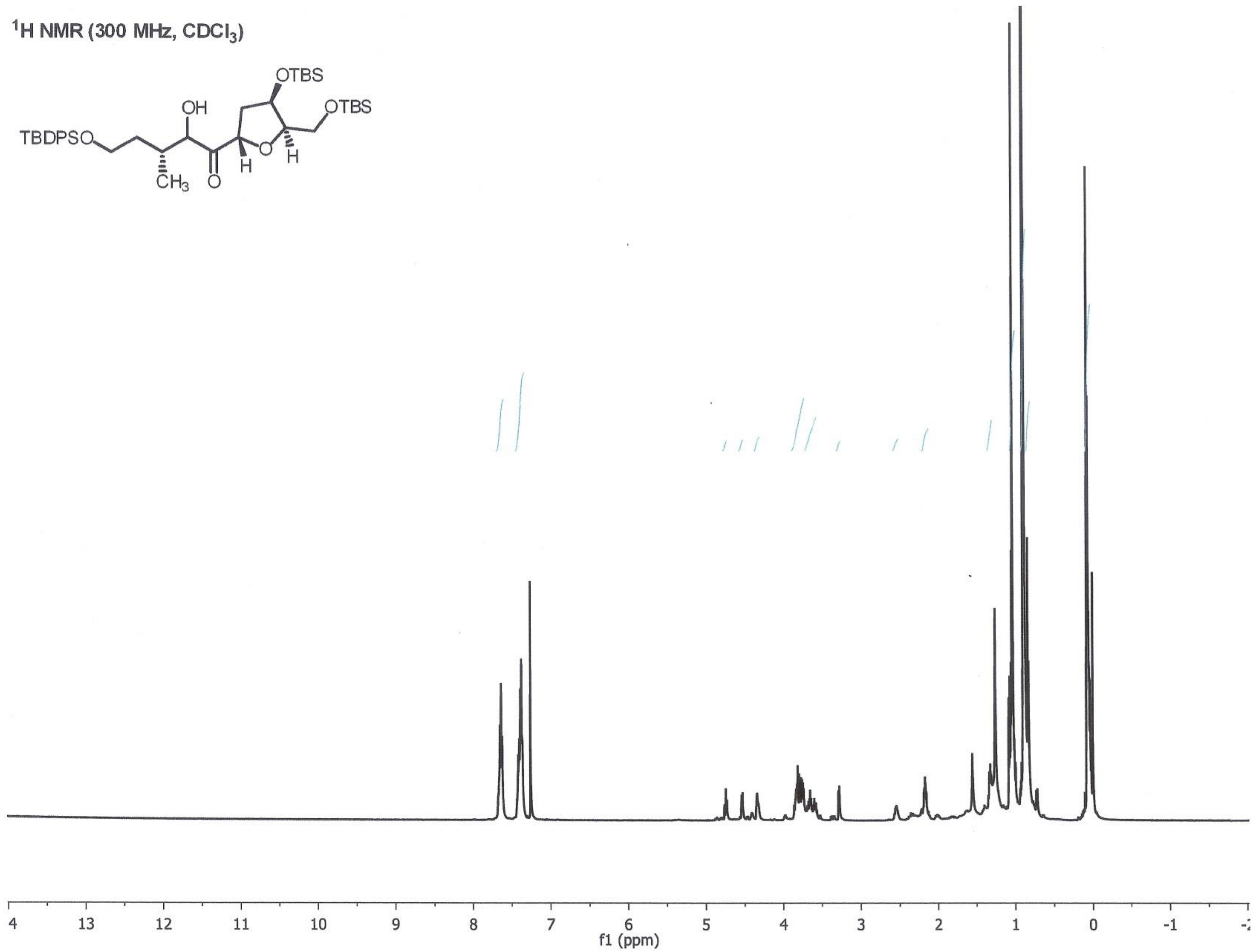

^{13}C NMR (100 MHz, $CDCl_3$)

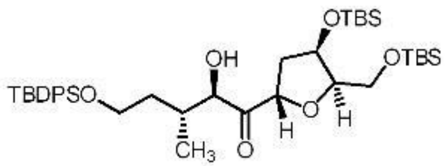

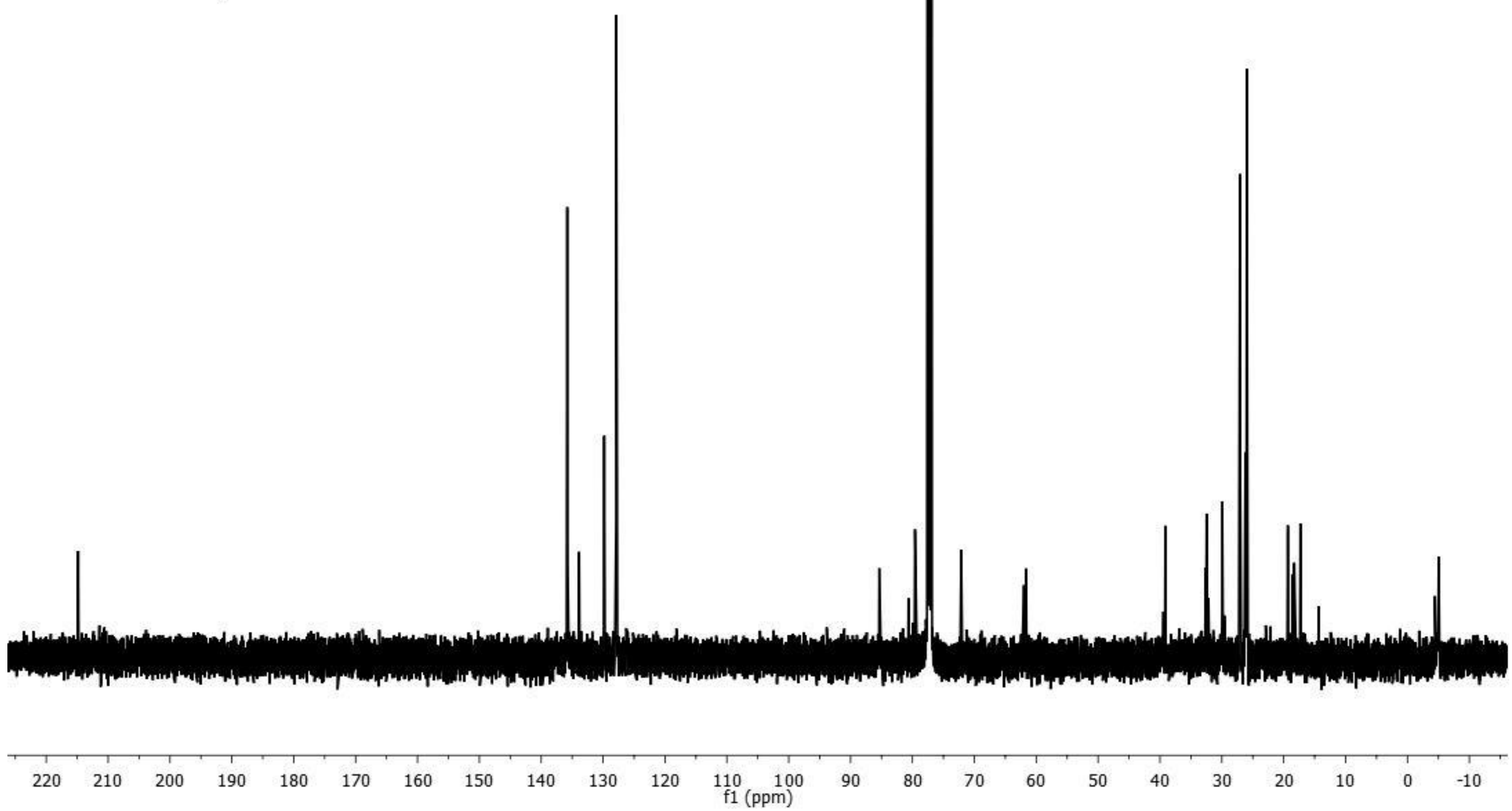

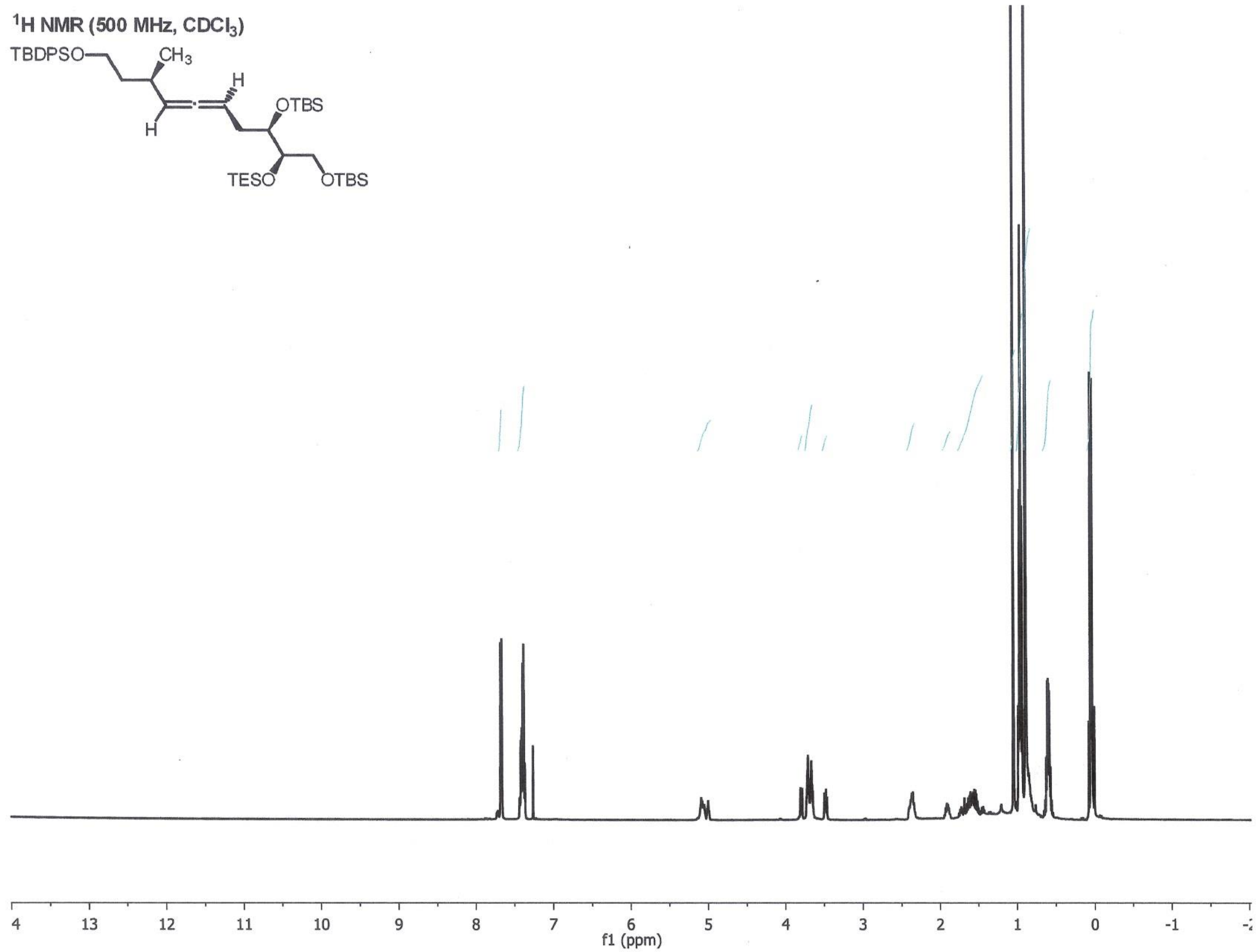

1H NMR (500 MHz, CDCl3)
TBDPSO
CH3
H
H
OTBS
TESO
OTBS
4
13
12
11
10
9
8
7
6
5
4
3
2
1
0
-1
f1 (ppm)

^{13}C NMR (125 MHz, $CDCl_3$)

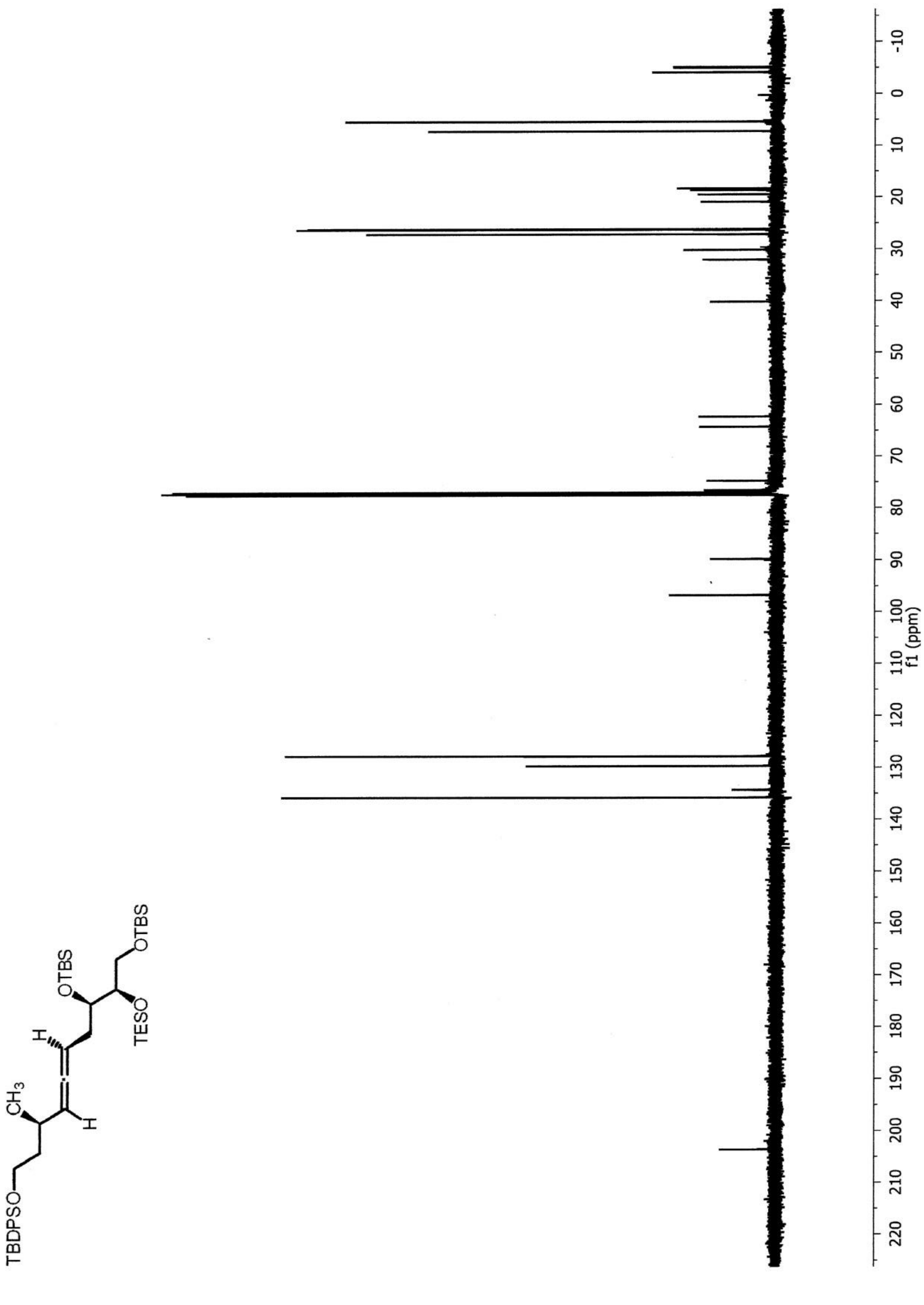

^{1}H NMR (400 MHz, $CDCl_3$)

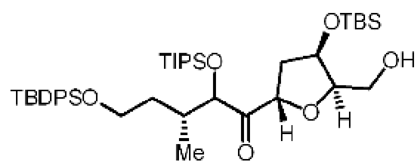

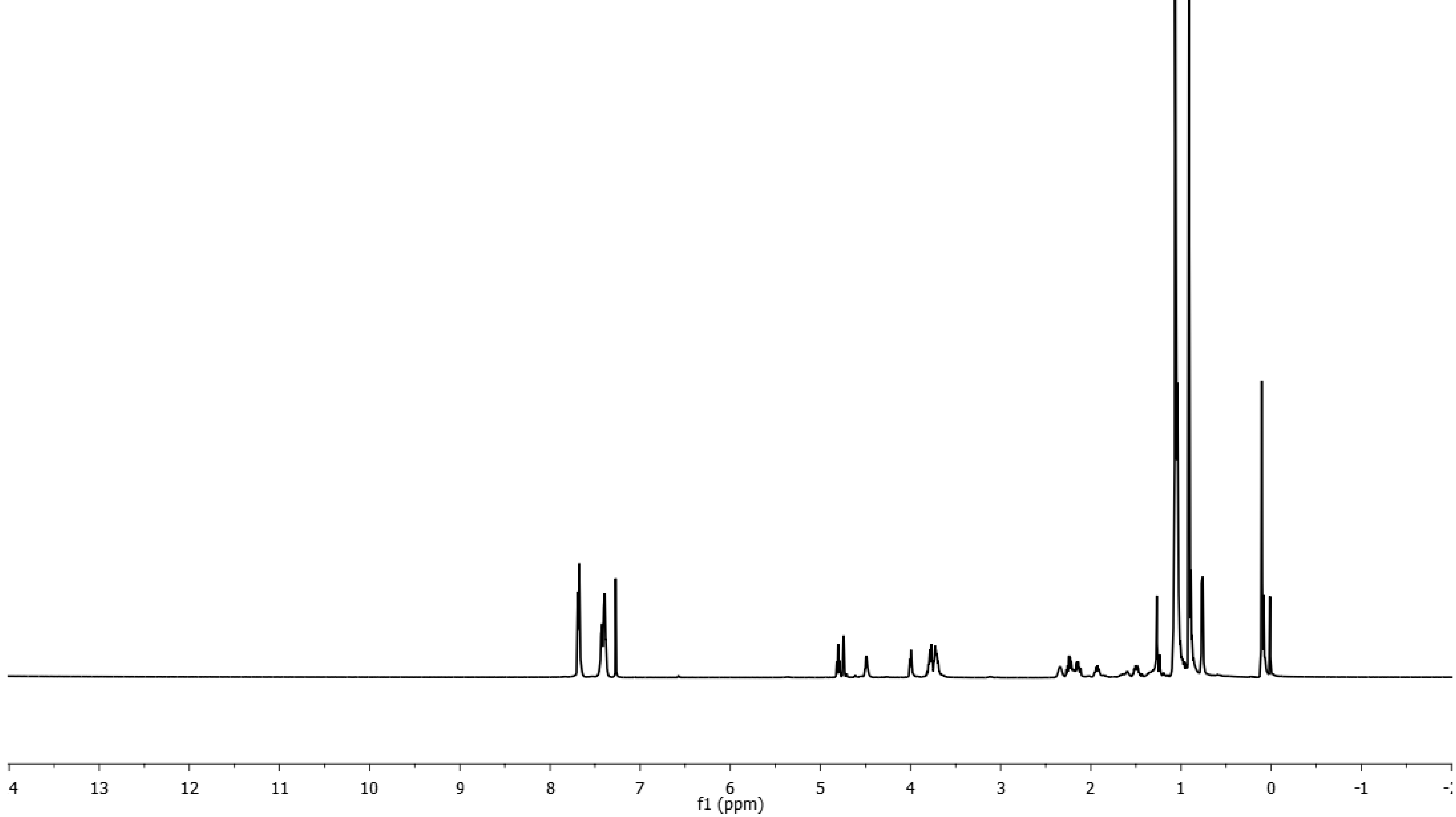

^{13}C NMR (125 MHz, $CDCl_3$)

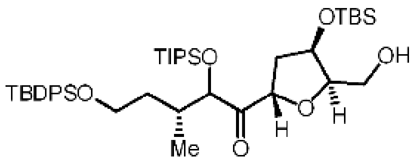

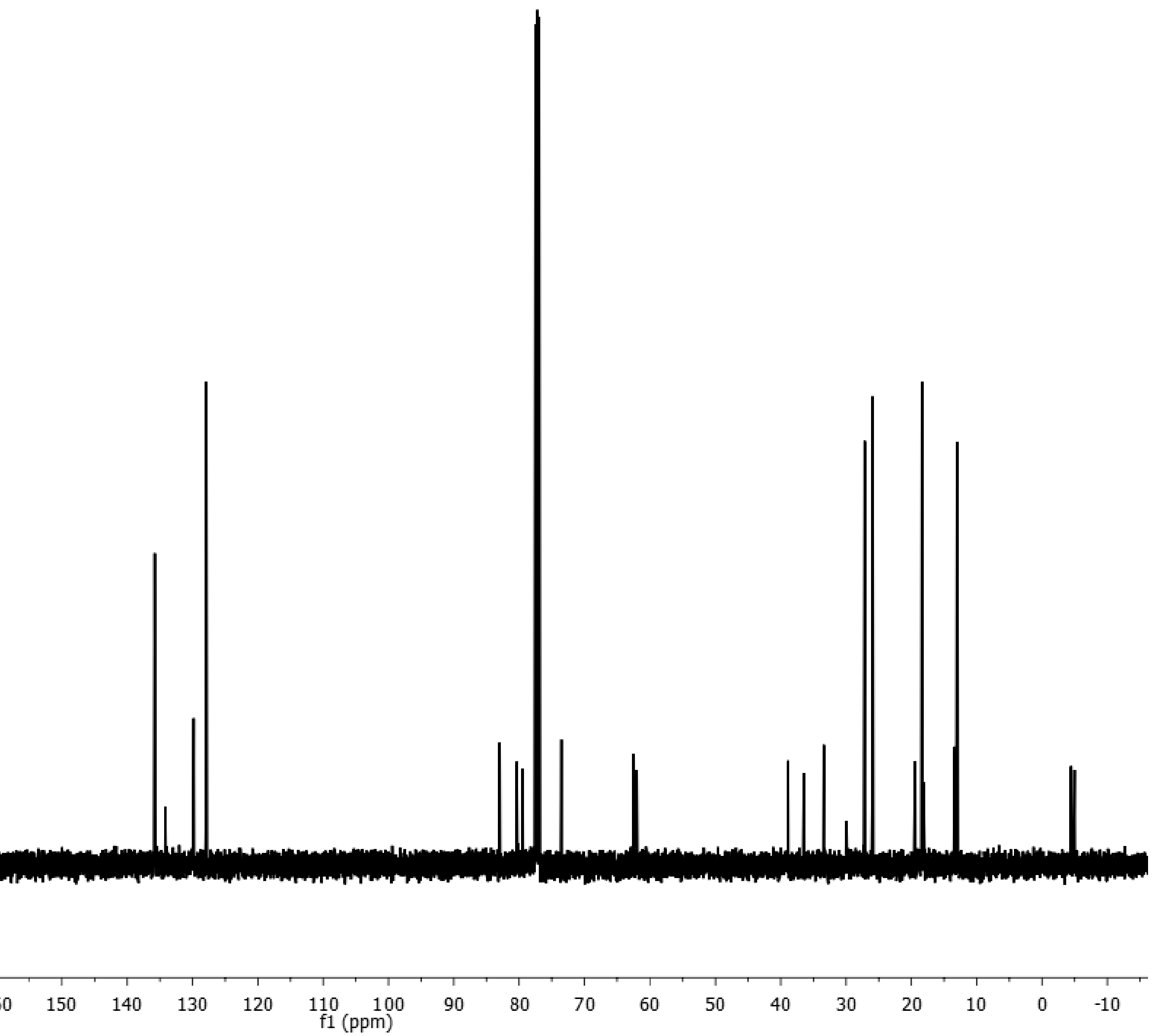

^{13}C NMR (125 MHz, $CDCl_3$)

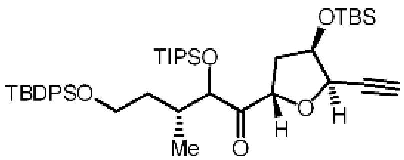

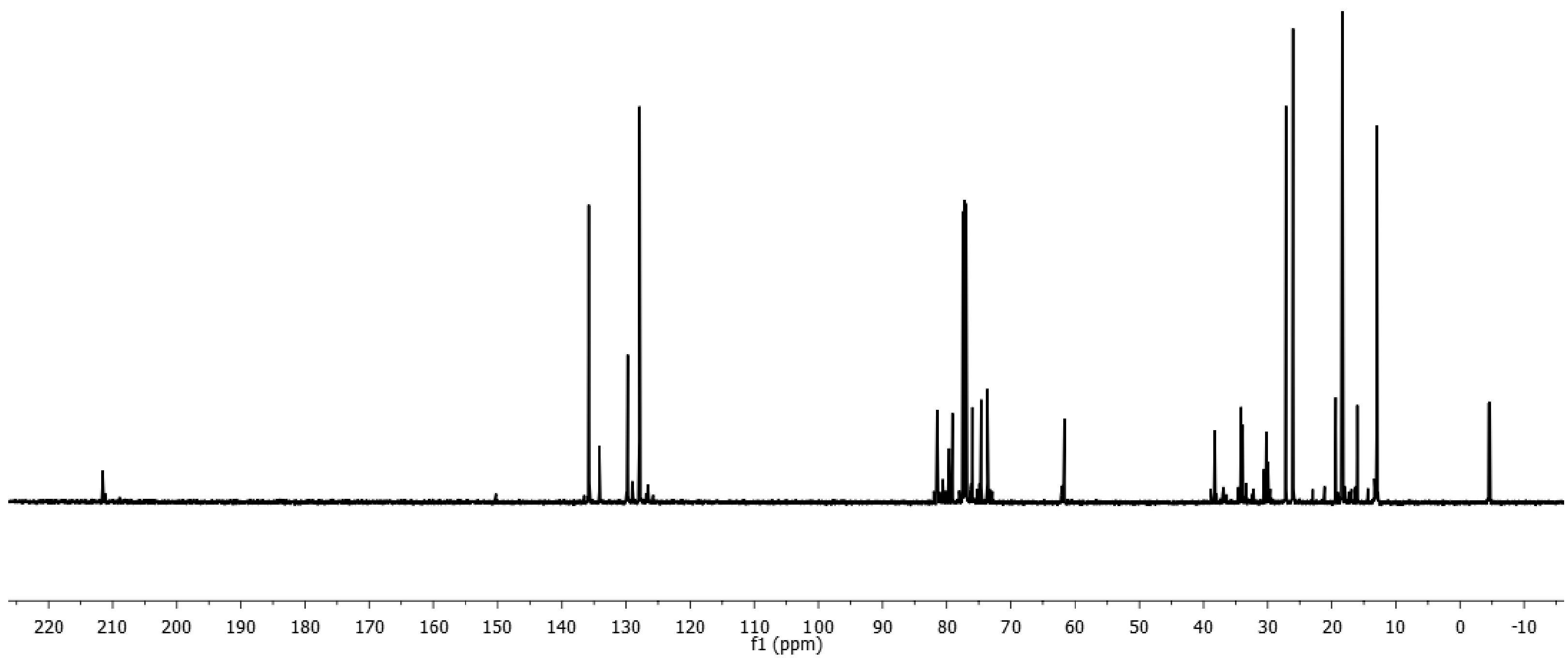

^{1}H NMR (500 MHz, $CDCl_3$)

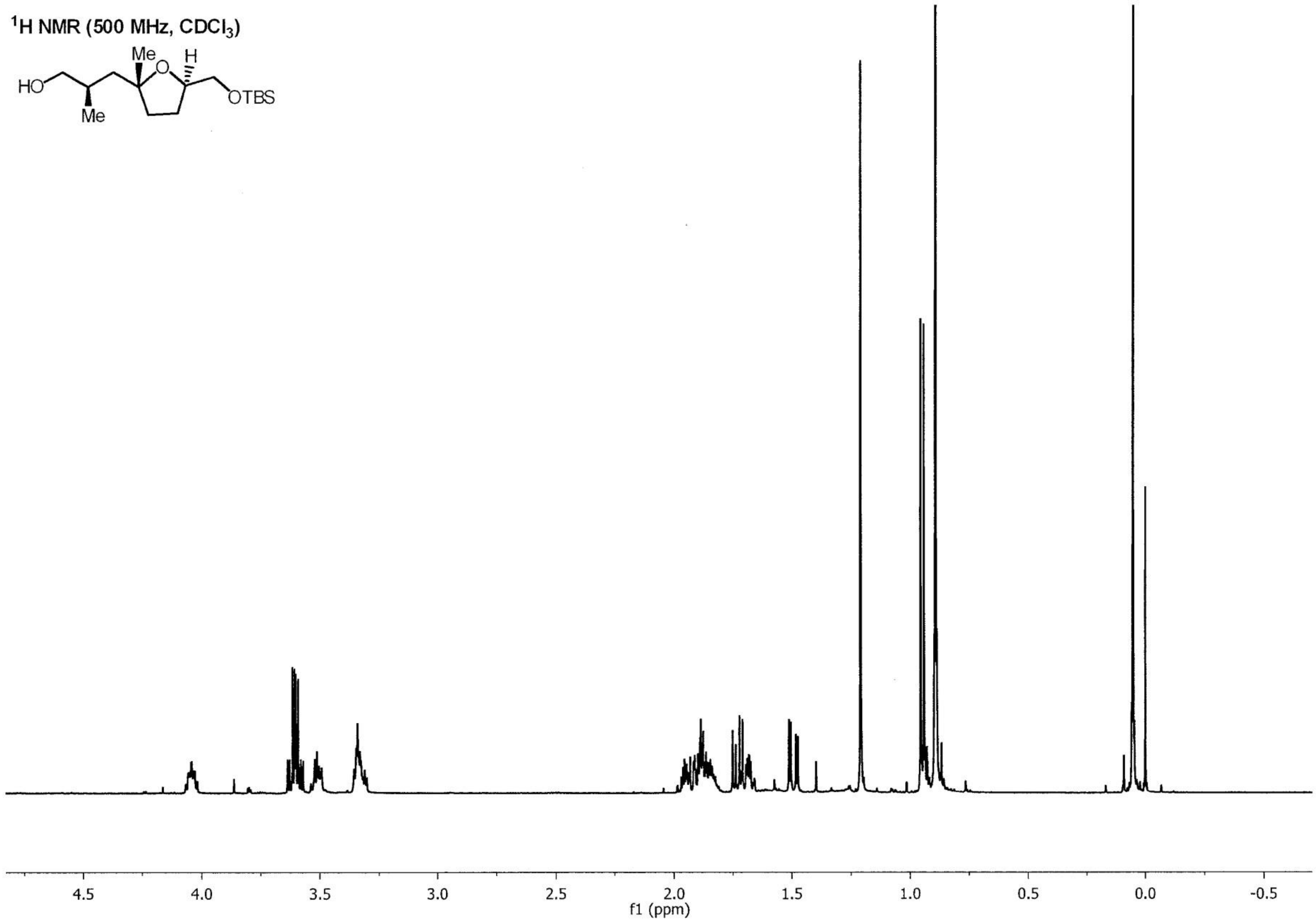

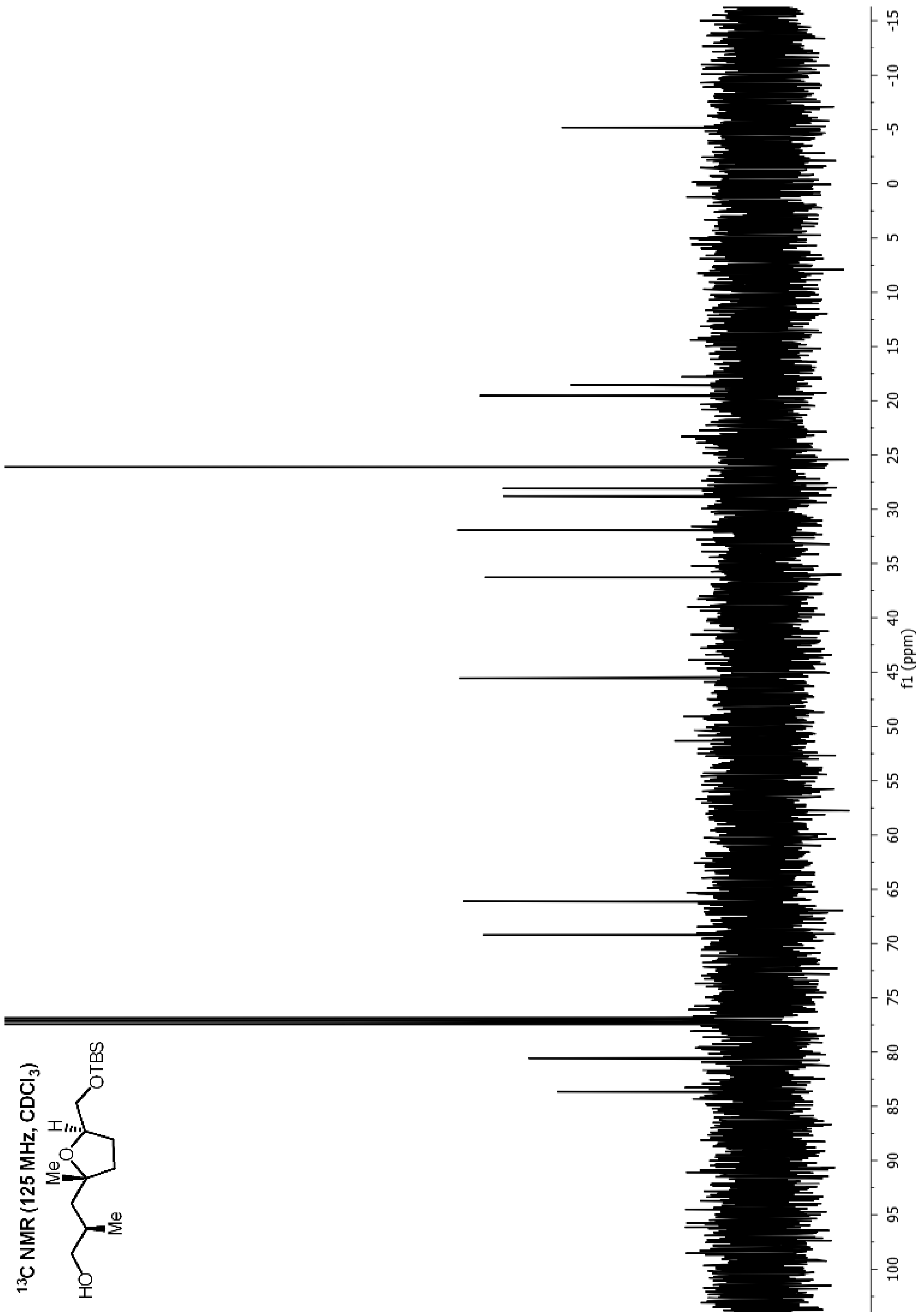

^{13}C NMR (125 MHz, $CDCl_3$)
HO
Me
Me
O
H
OTBS
f1 (ppm)
-15
-10
-5
0
5
10
15
20
25
30
35
40
45
50
55
60
65
70
75
80
85
90
95
100

^{1}H NMR (400 MHz, $CDCl_3$)

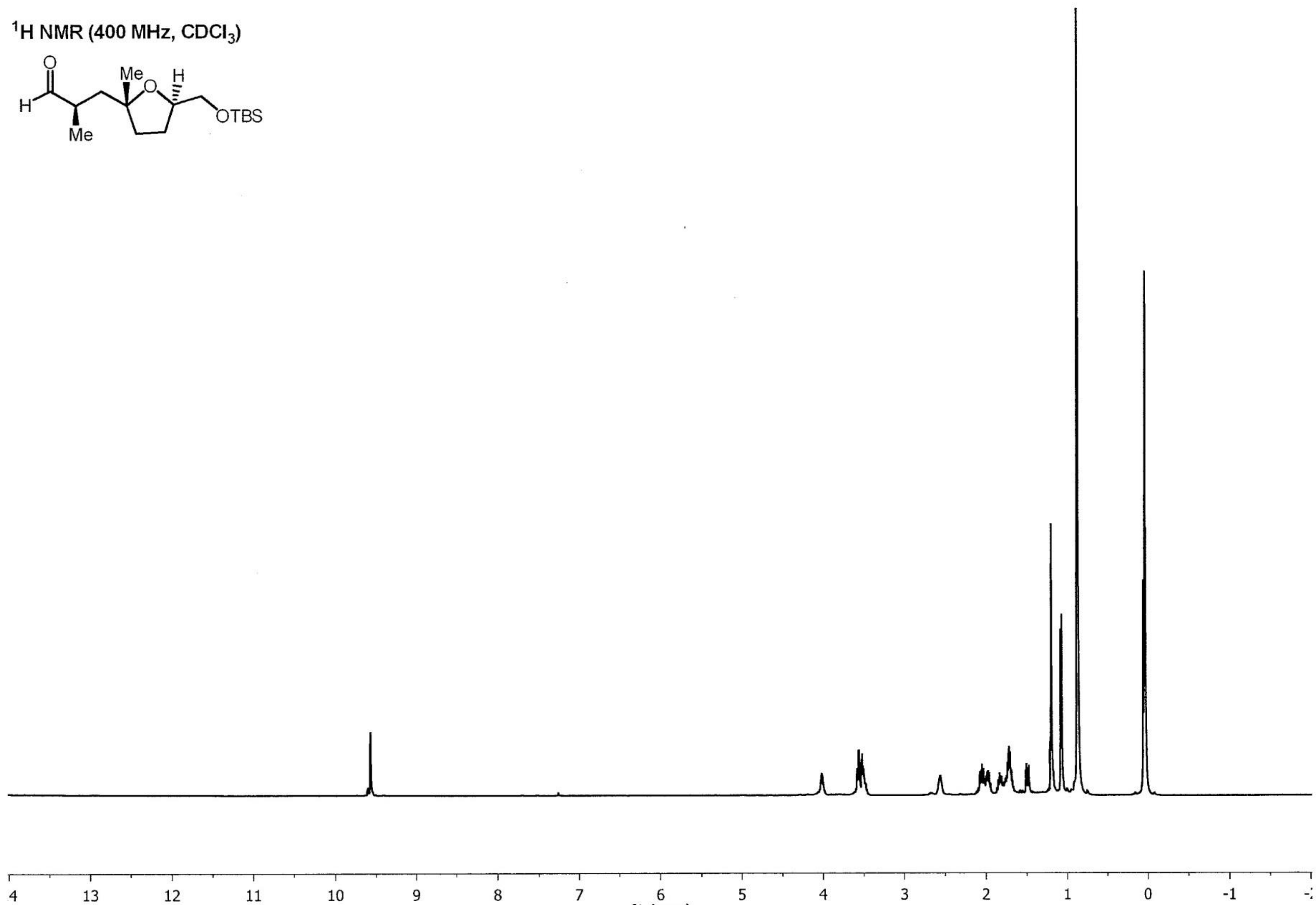

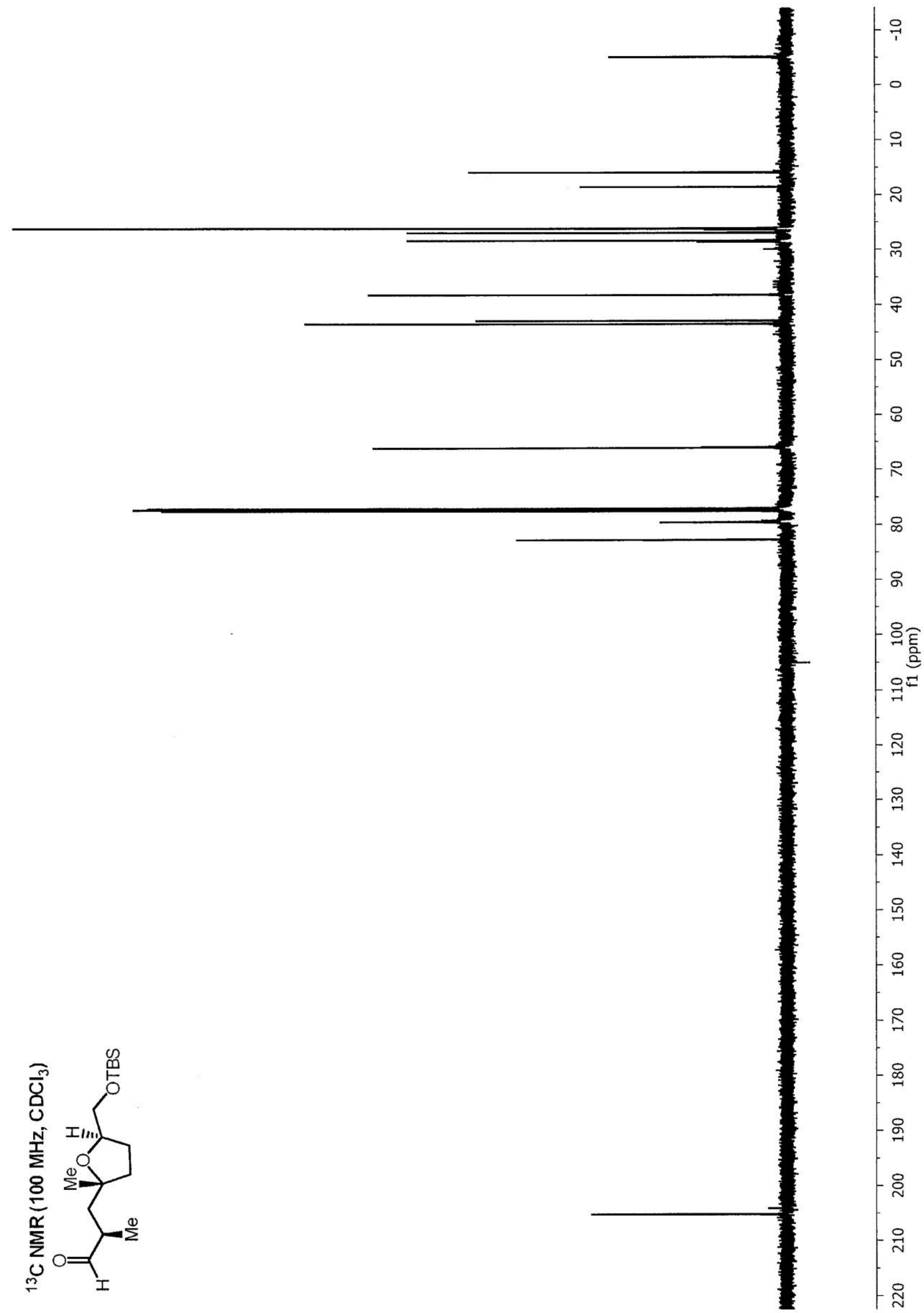

^{13}C NMR (100 MHz, $CDCl_3$)
OTBS
Me
H
O
Me
H
O
f1 (ppm)
-10
0
10
20
30
40
50
60
70
80
90
100
110
120
130
140
150
160
170
180
190
200
210
220

[1]H NMR (400 MHz, $CDCl_3$)

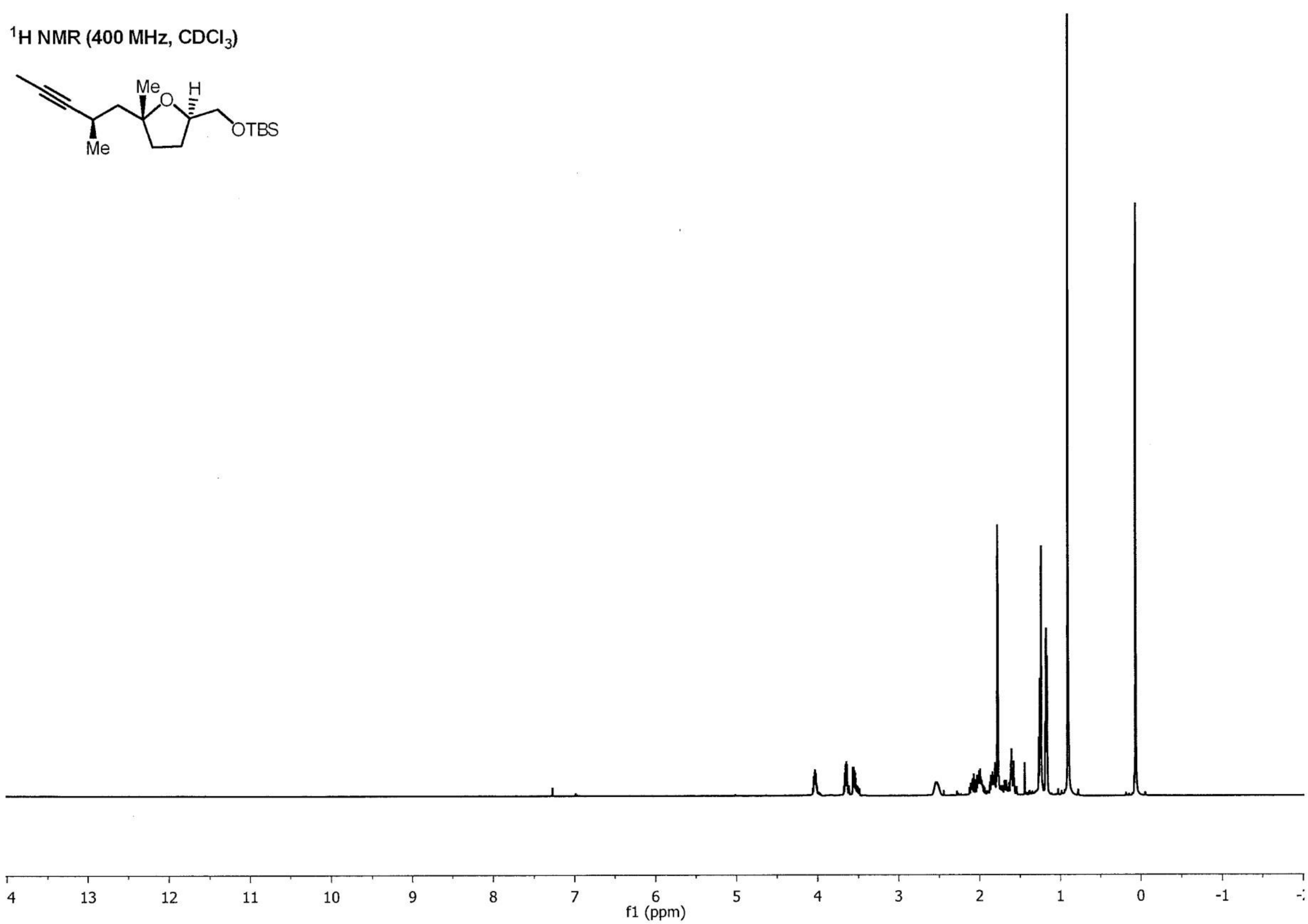

^{13}C NMR (100 MHz, $CDCl_3$)

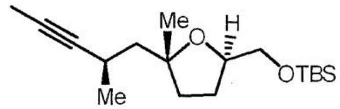

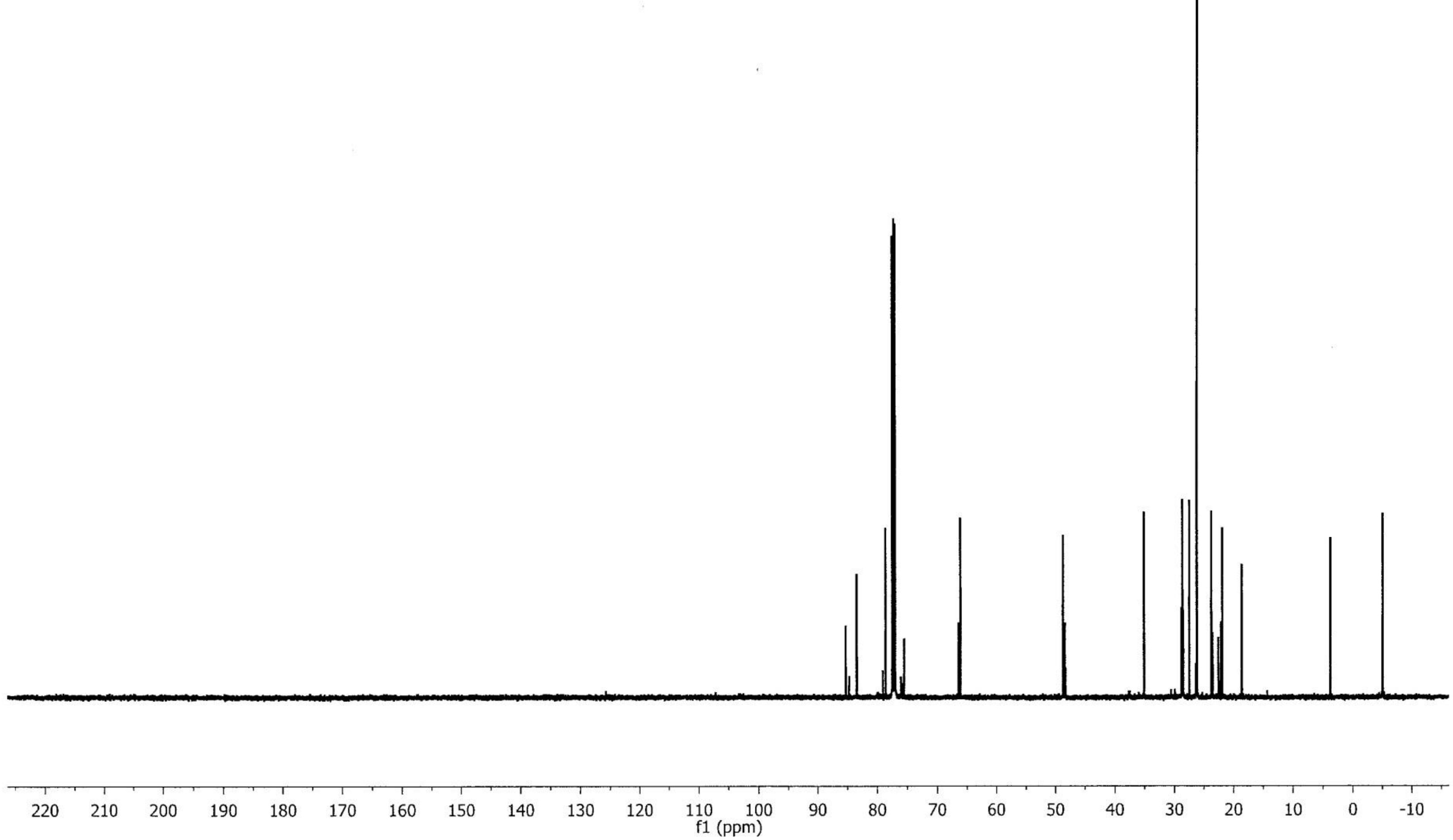

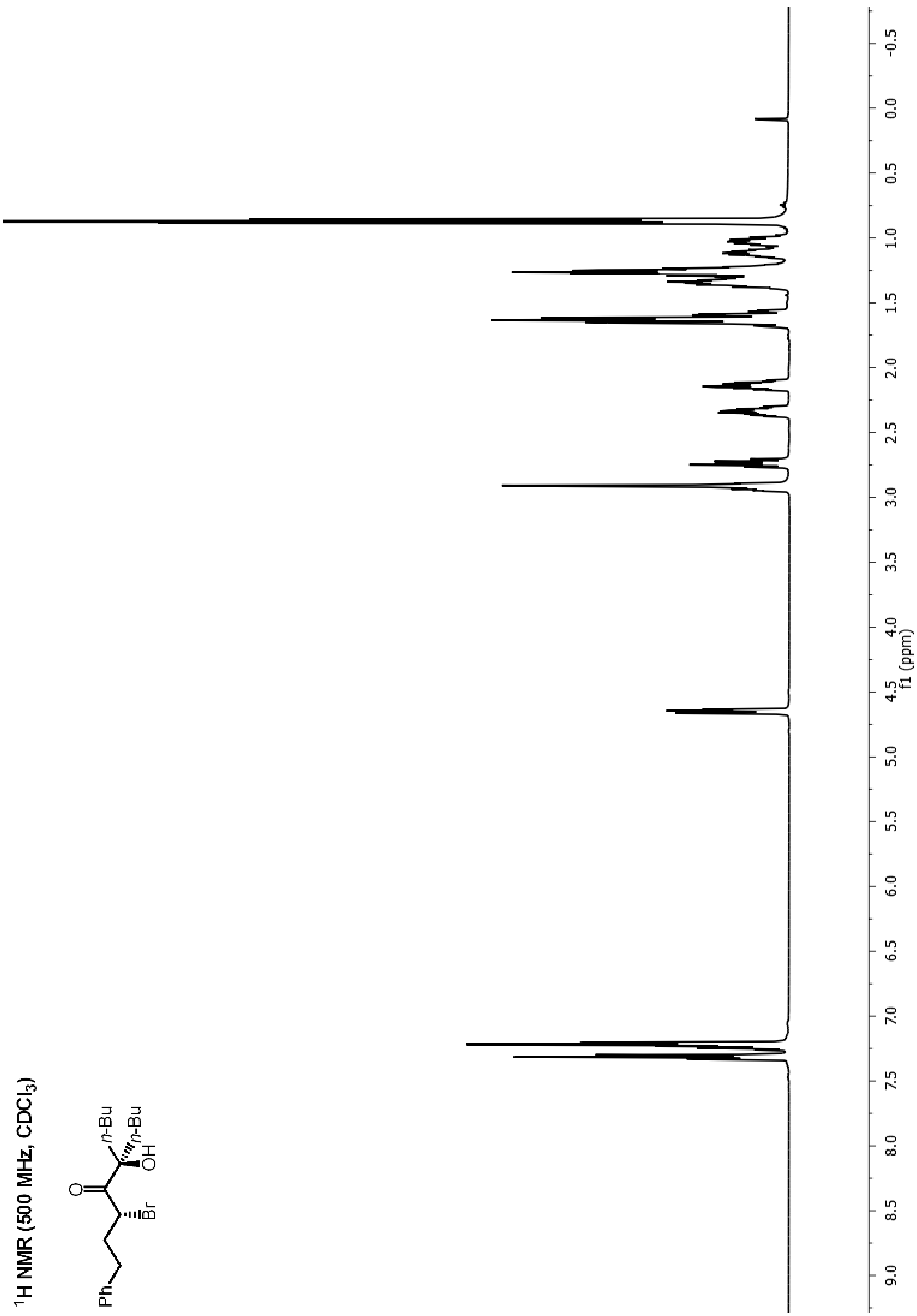

1H NMR (500 MHz, CDCl3)
Ph
Br
O
n-Bu
n-Bu
OH
f1 (ppm)
-0.5
0.0
0.5
1.0
1.5
2.0
2.5
3.0
3.5
4.0
4.5
5.0
5.5
6.0
6.5
7.0
7.5
8.0
8.5
9.0

^{13}C NMR (125 MHz, $CDCl_3$)

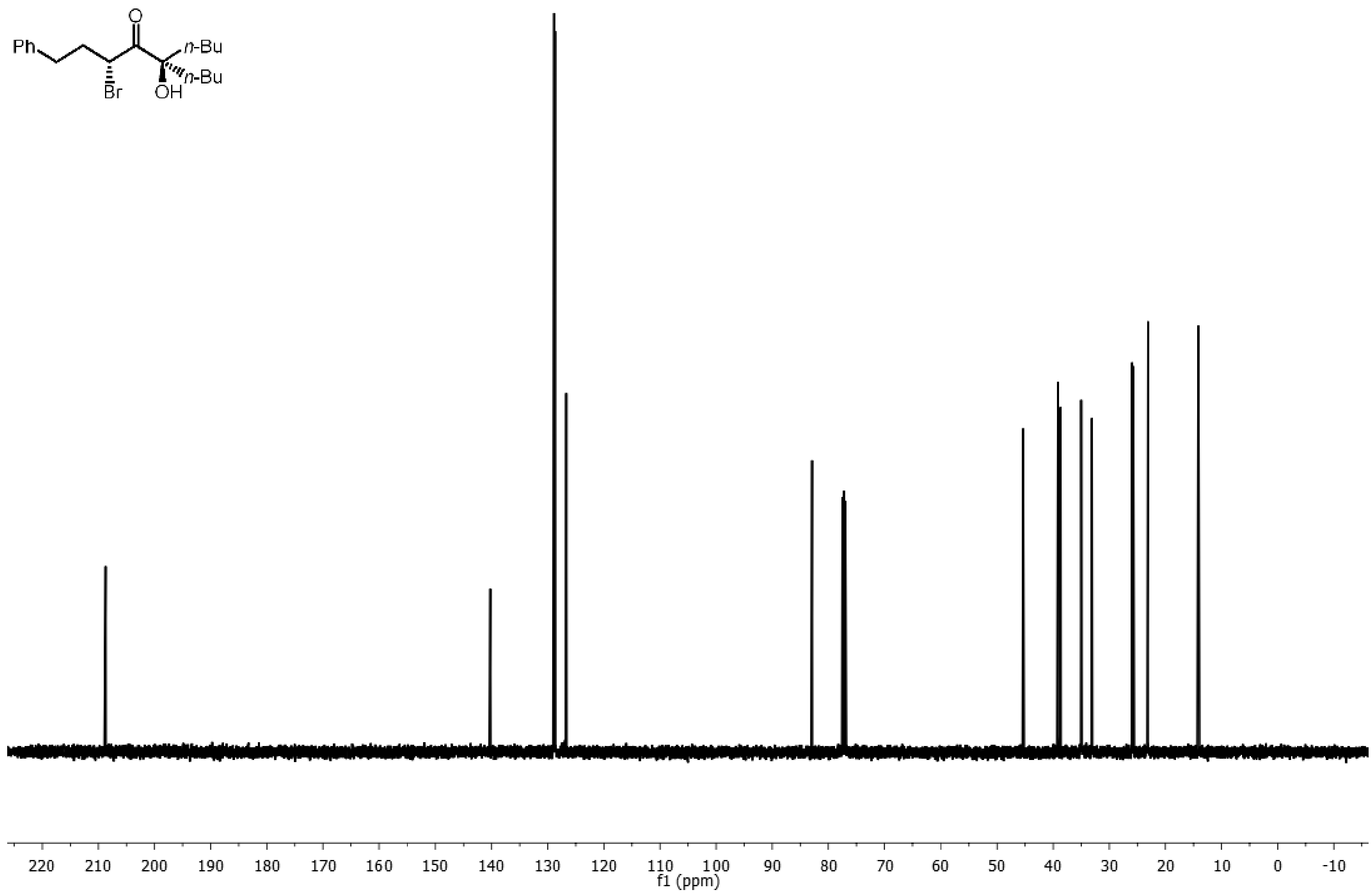

^1H NMR (400 MHz, $CDCl_3$)

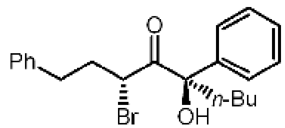

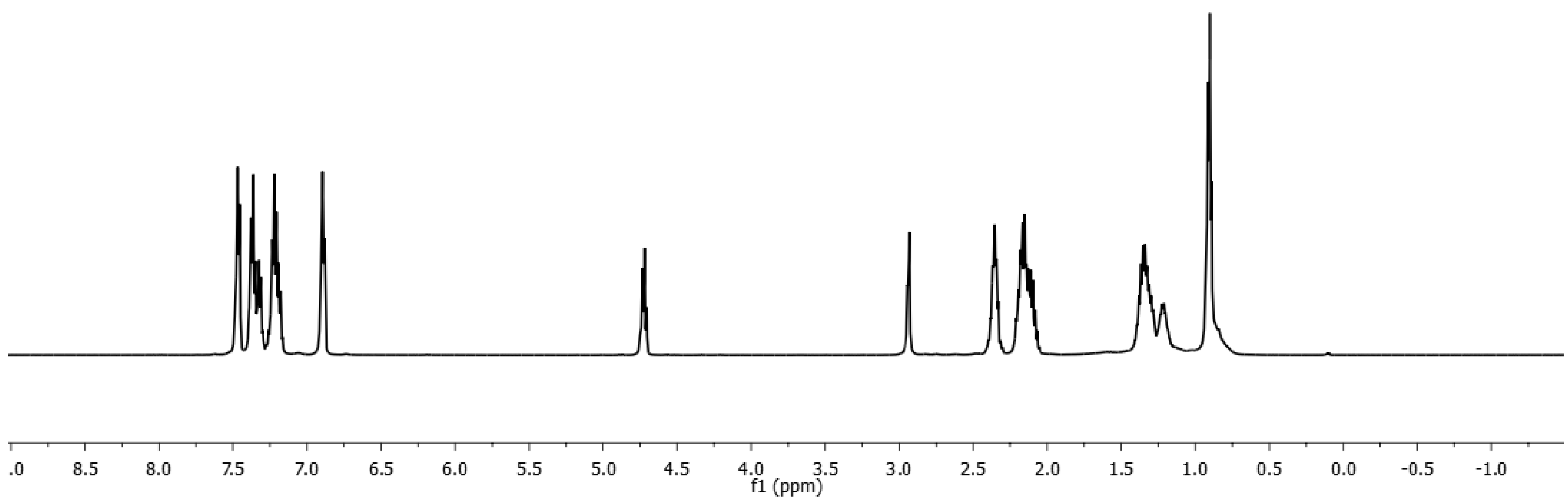

^{13}C NMR (100 MHz, $CDCl_3$)

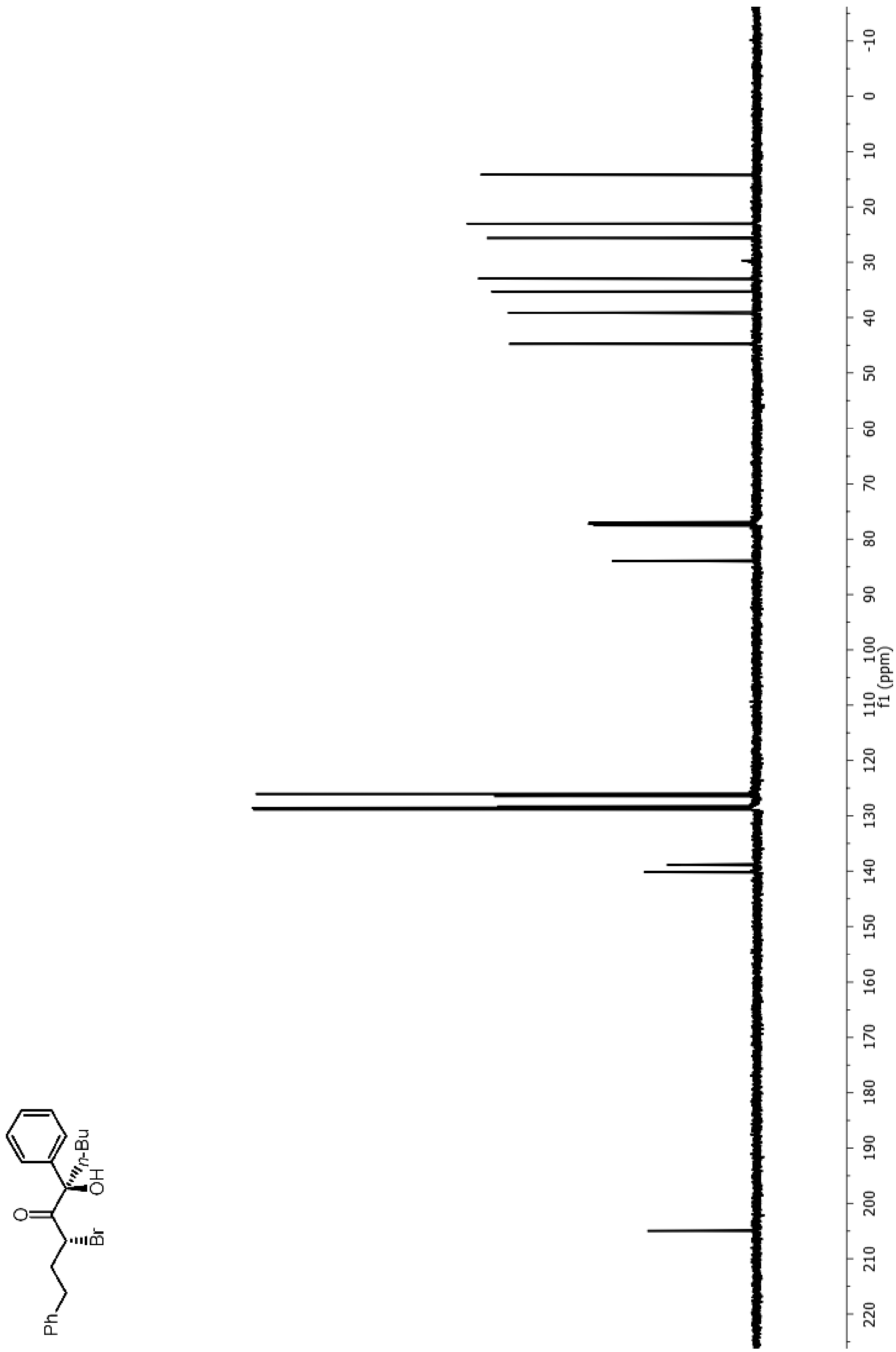

^{1}H NMR (500 MHz, $CDCl_3$)

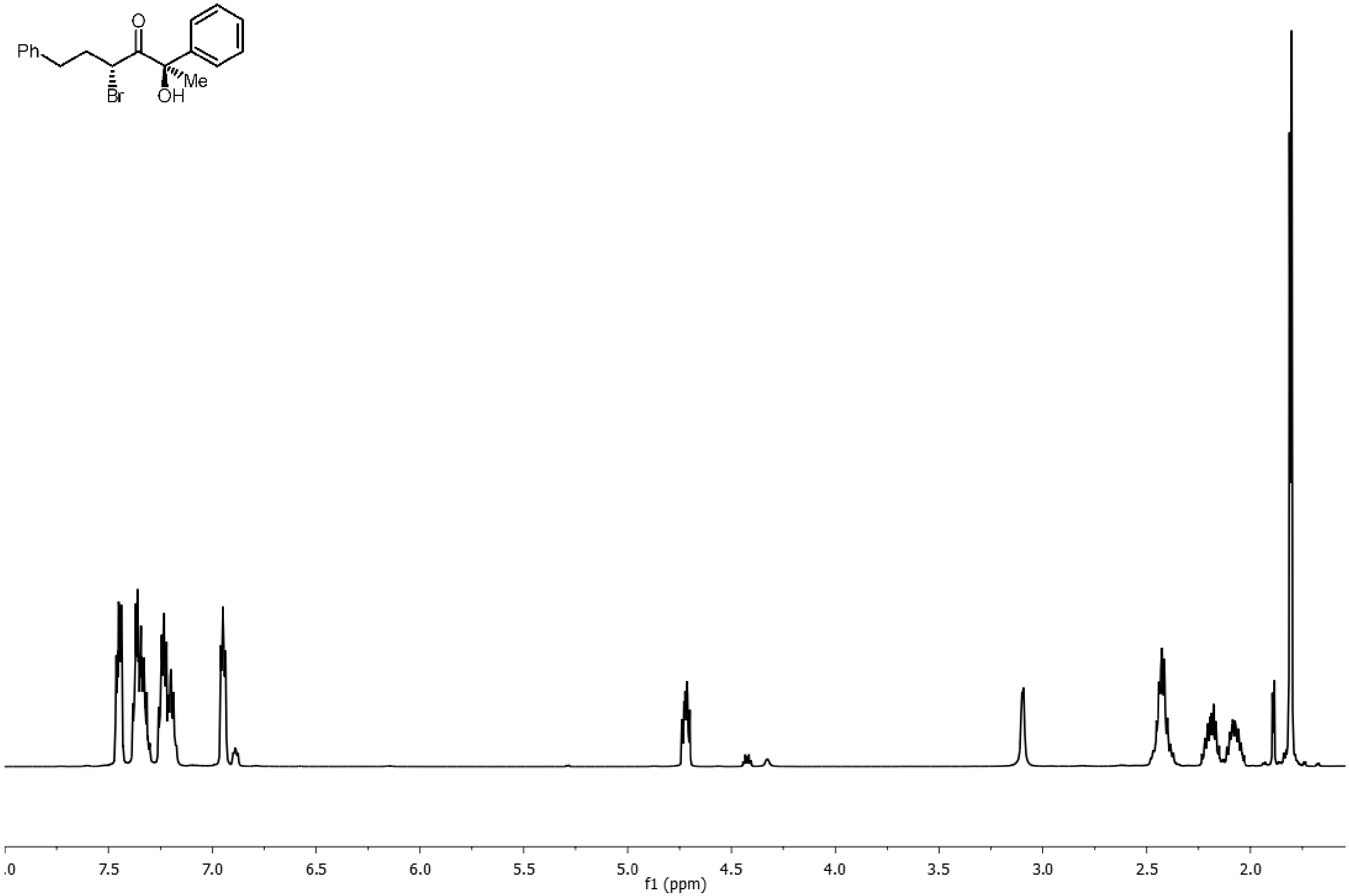

^{13}C NMR (125 MHz, $CDCl_3$)

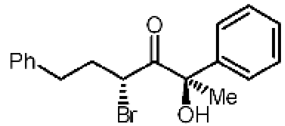

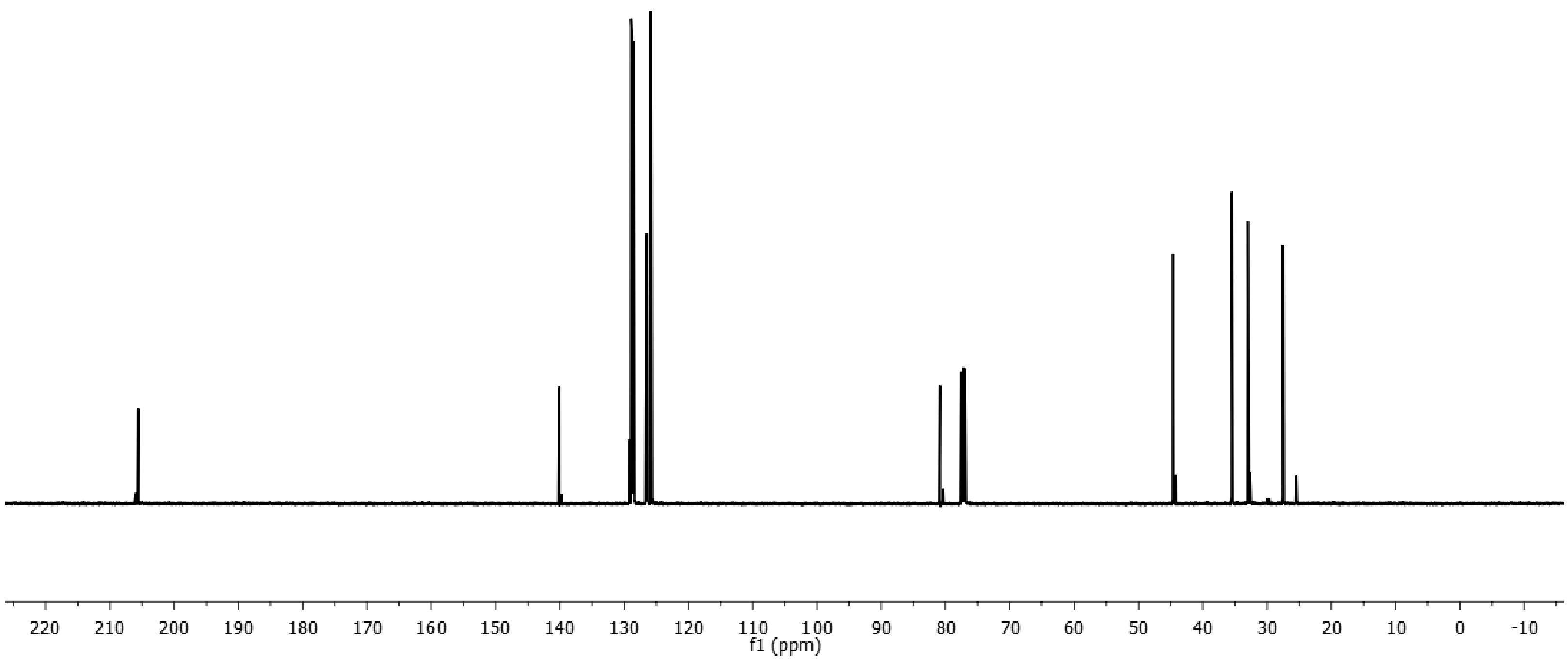

^{1}H NMR (500 MHz, $CDCl_3$)

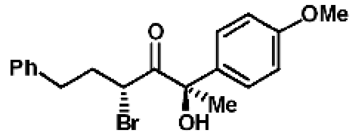

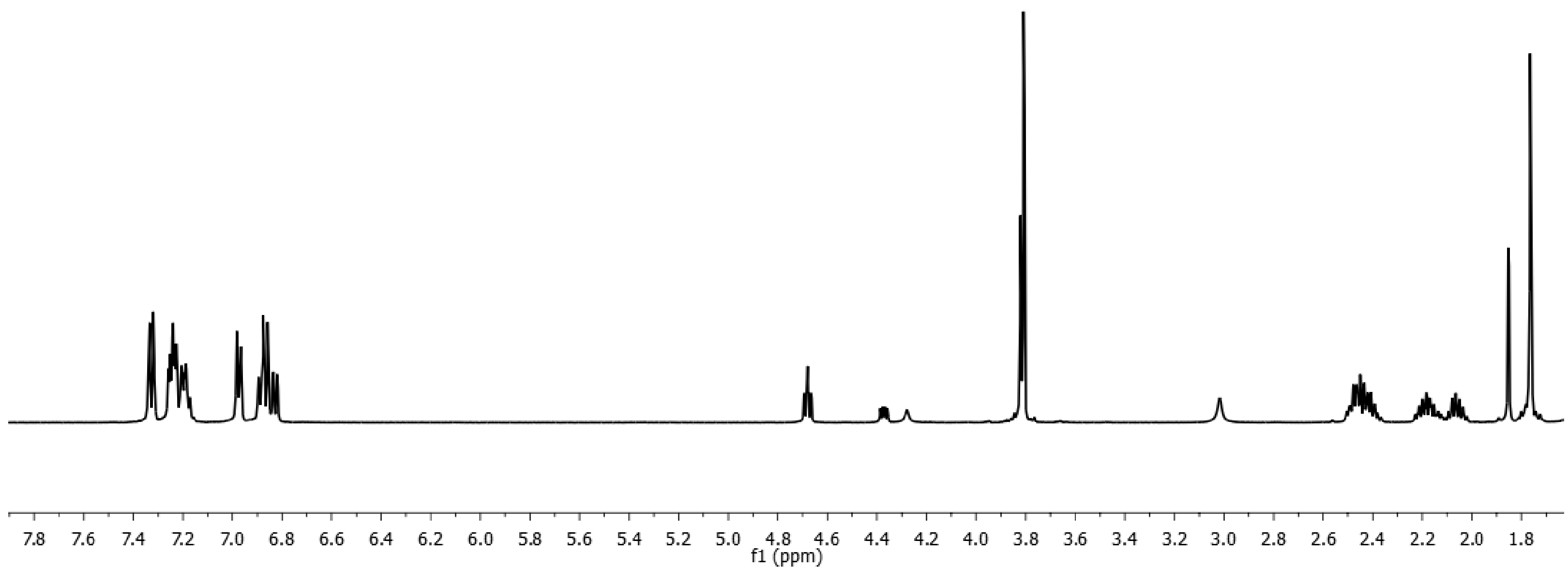

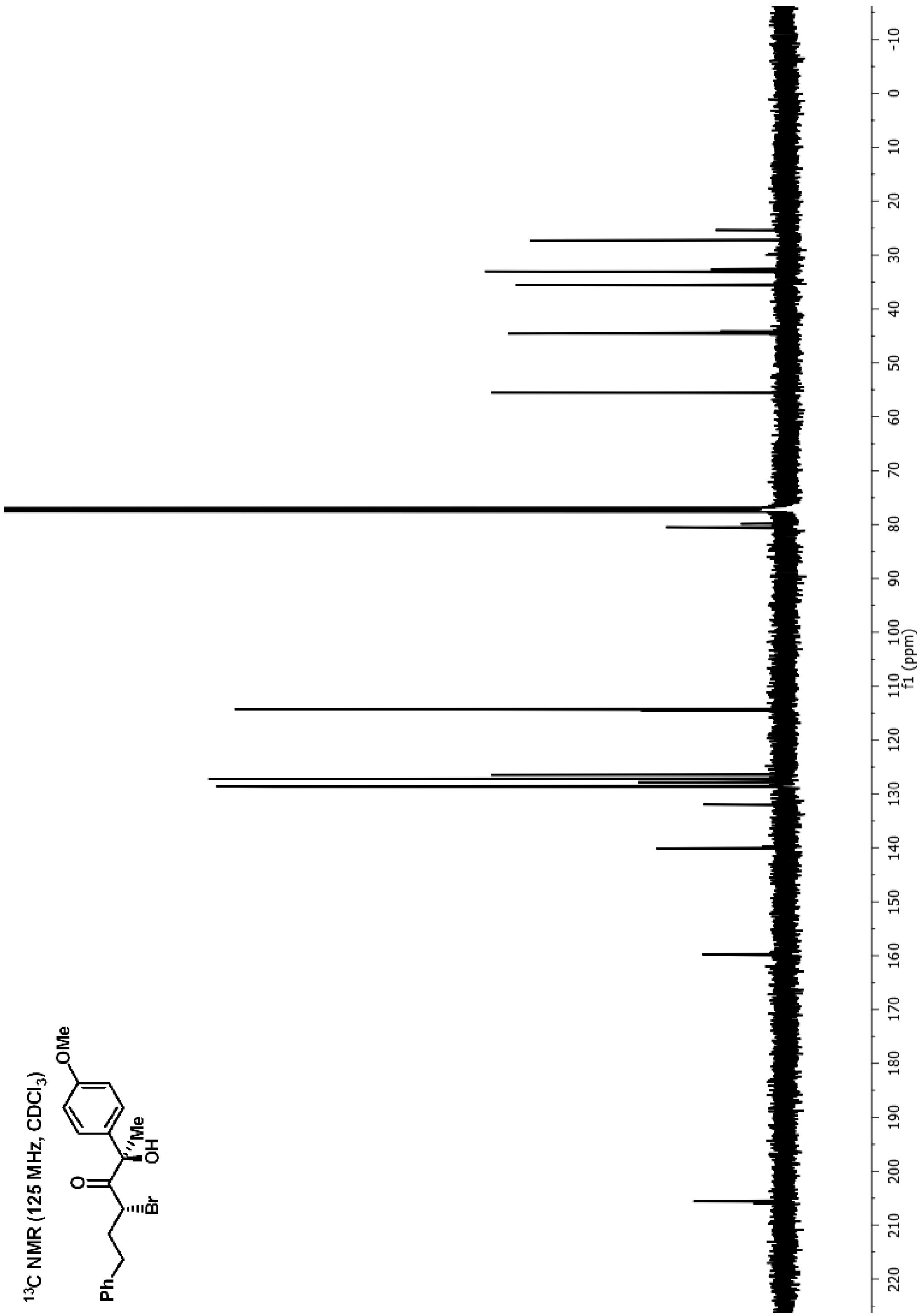

^{13}C NMR (125 MHz, CDCl$_3$)
OMe
O
Me
OH
Br
Ph
f1 (ppm)
220 210 200 190 180 170 160 150 140 130 120 110 100 90 80 70 60 50 40 30 20 10 0 -10

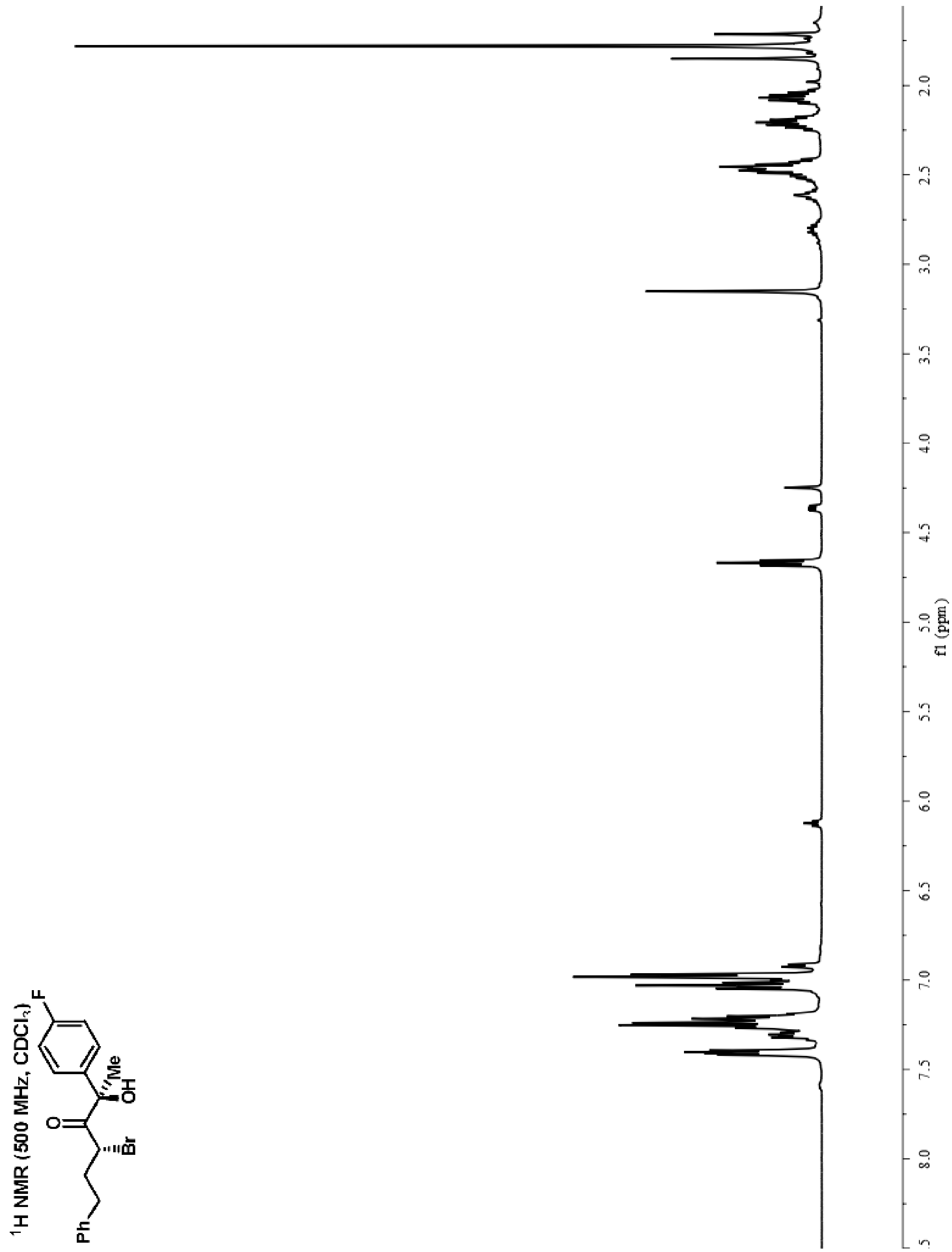

^1H NMR (500 MHz, $CDCl_3$)
Ph
O
Br
Me
OH
F
f1 (ppm)

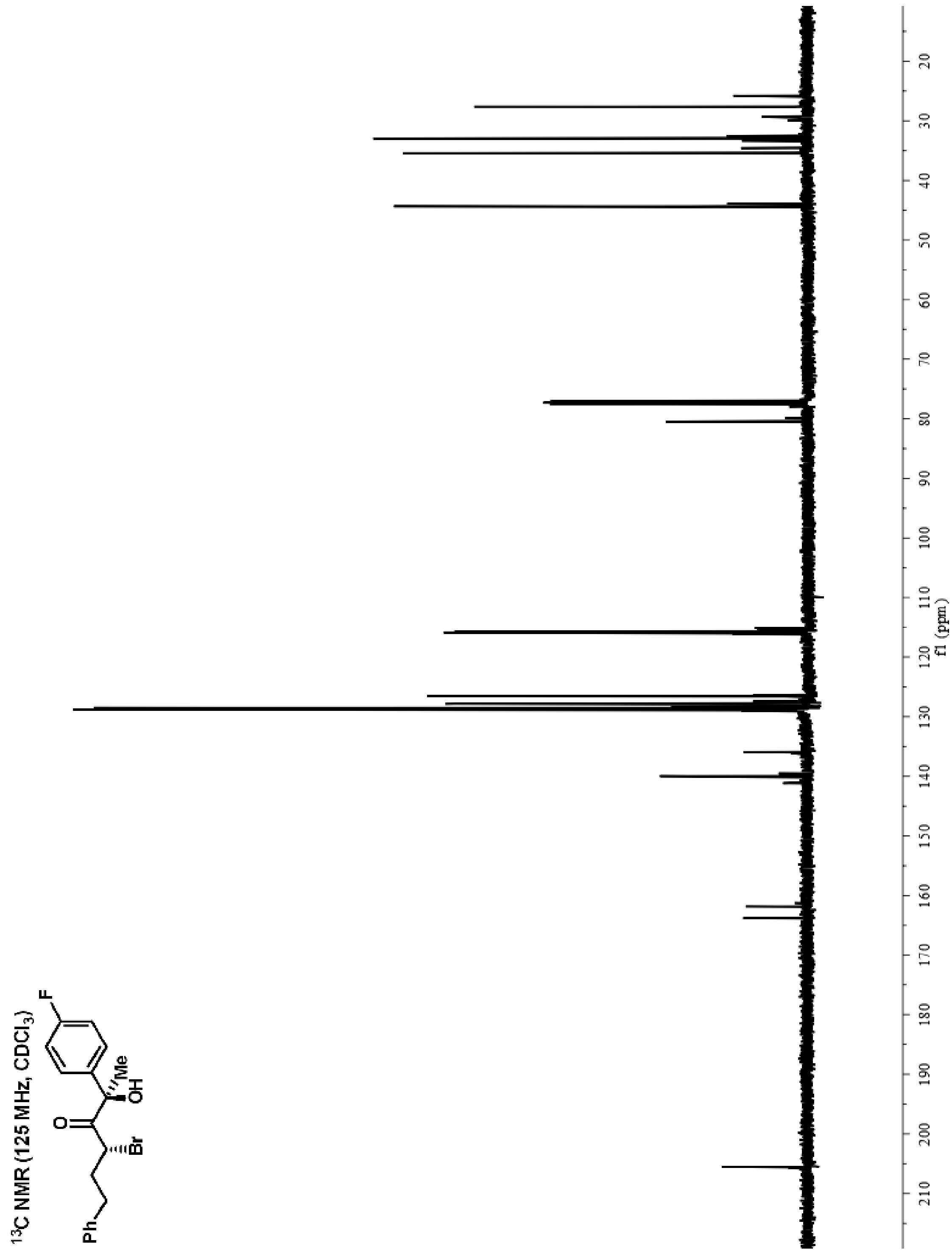

^{13}C NMR (125 MHz, CDCl$_3$)
F
Me
OH
O
Br
Ph
20
30
40
50
60
70
80
90
100
110
120
130
140
150
160
170
180
190
200
210
f1 (ppm)

^1H NMR (500 MHz, $CDCl_3$)

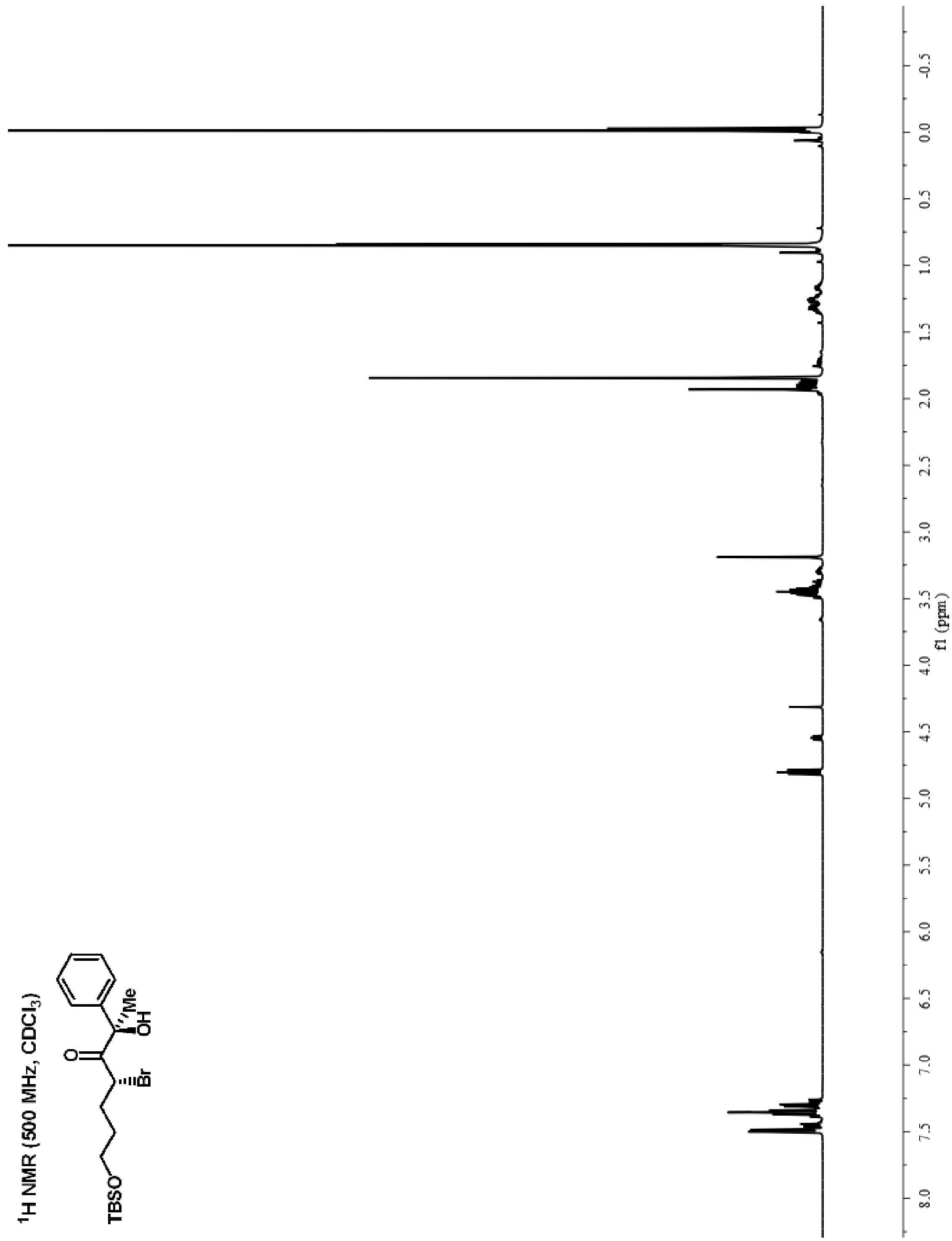

^{13}C NMR (125 MHz, $CDCl_3$)

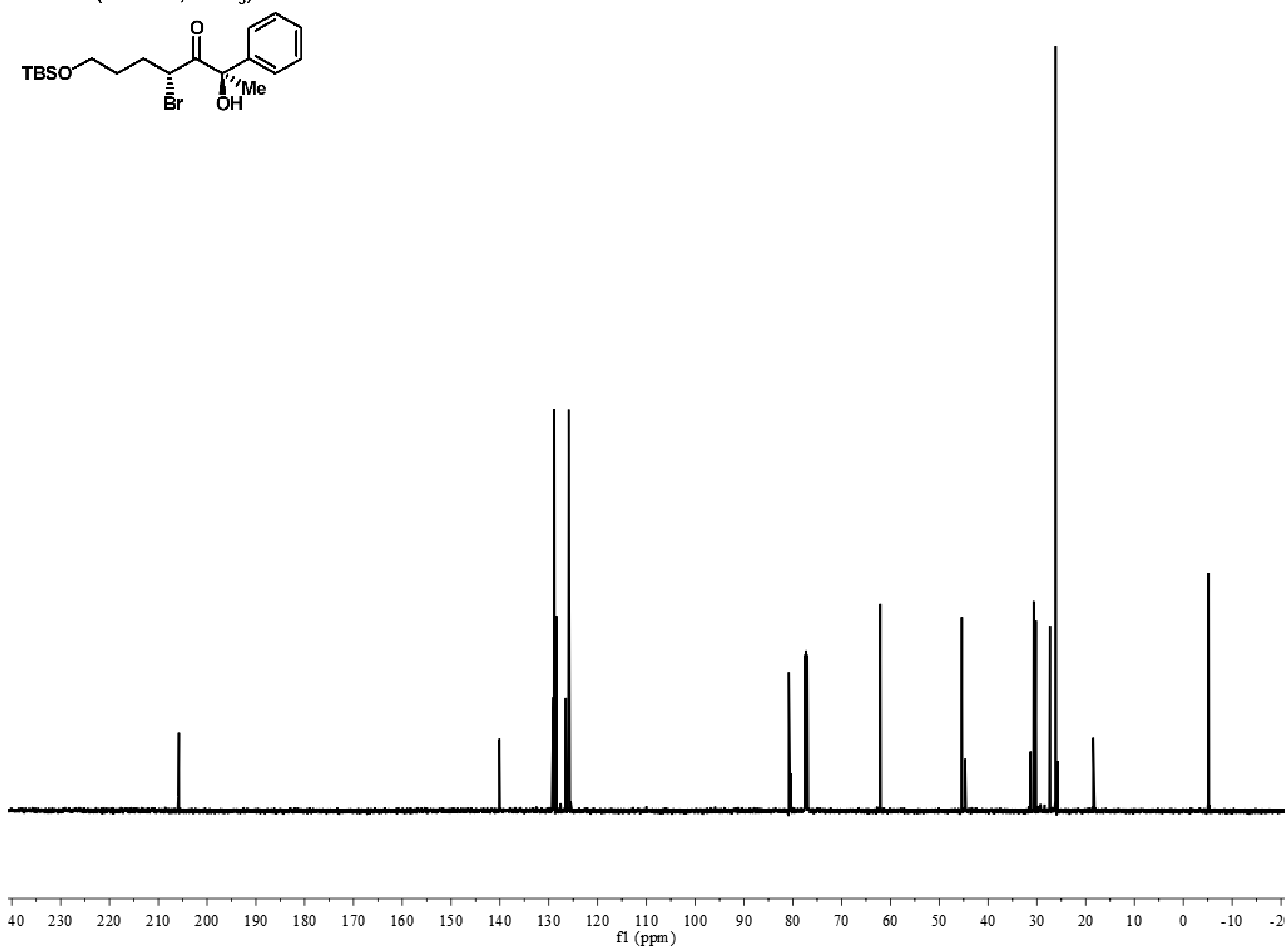

^{1}H NMR (500 MHz, $CDCl_3$)

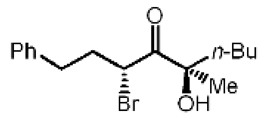

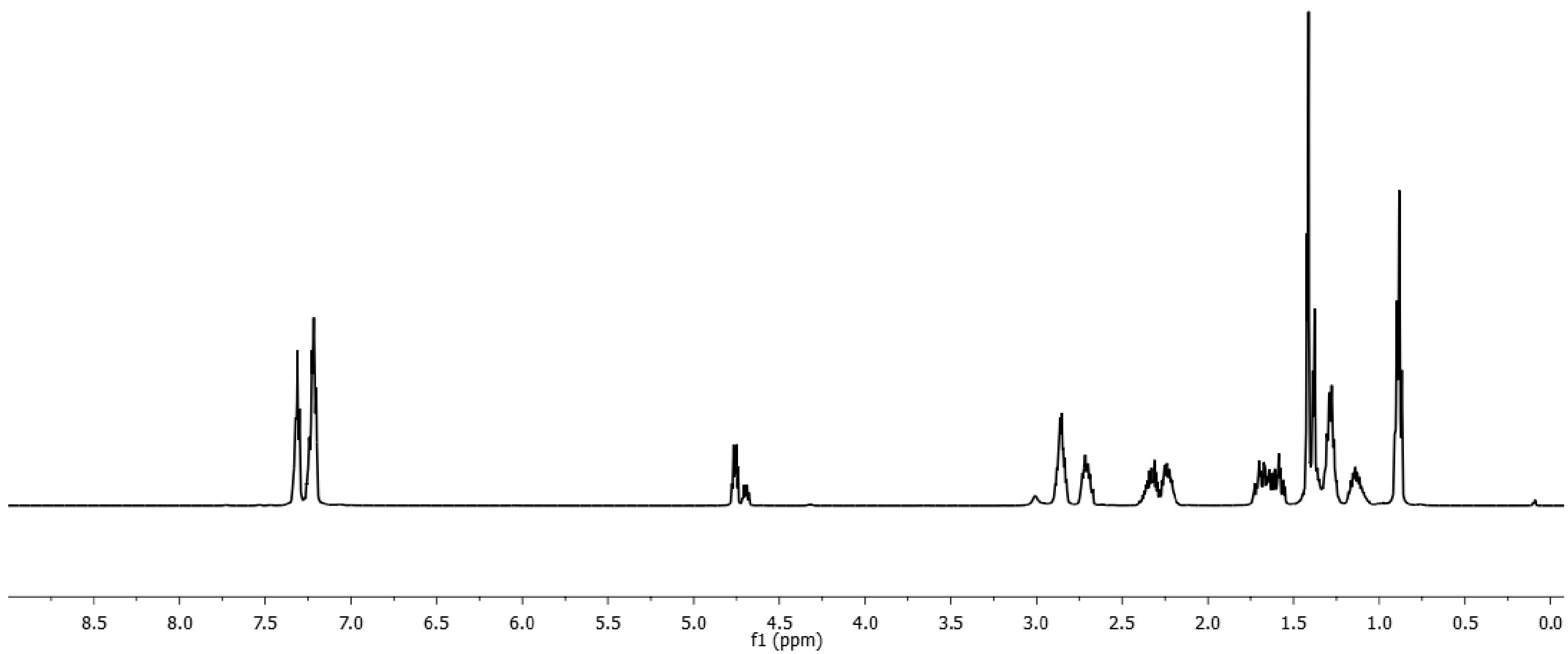

^{13}C NMR (125 MHz, $CDCl_3$)

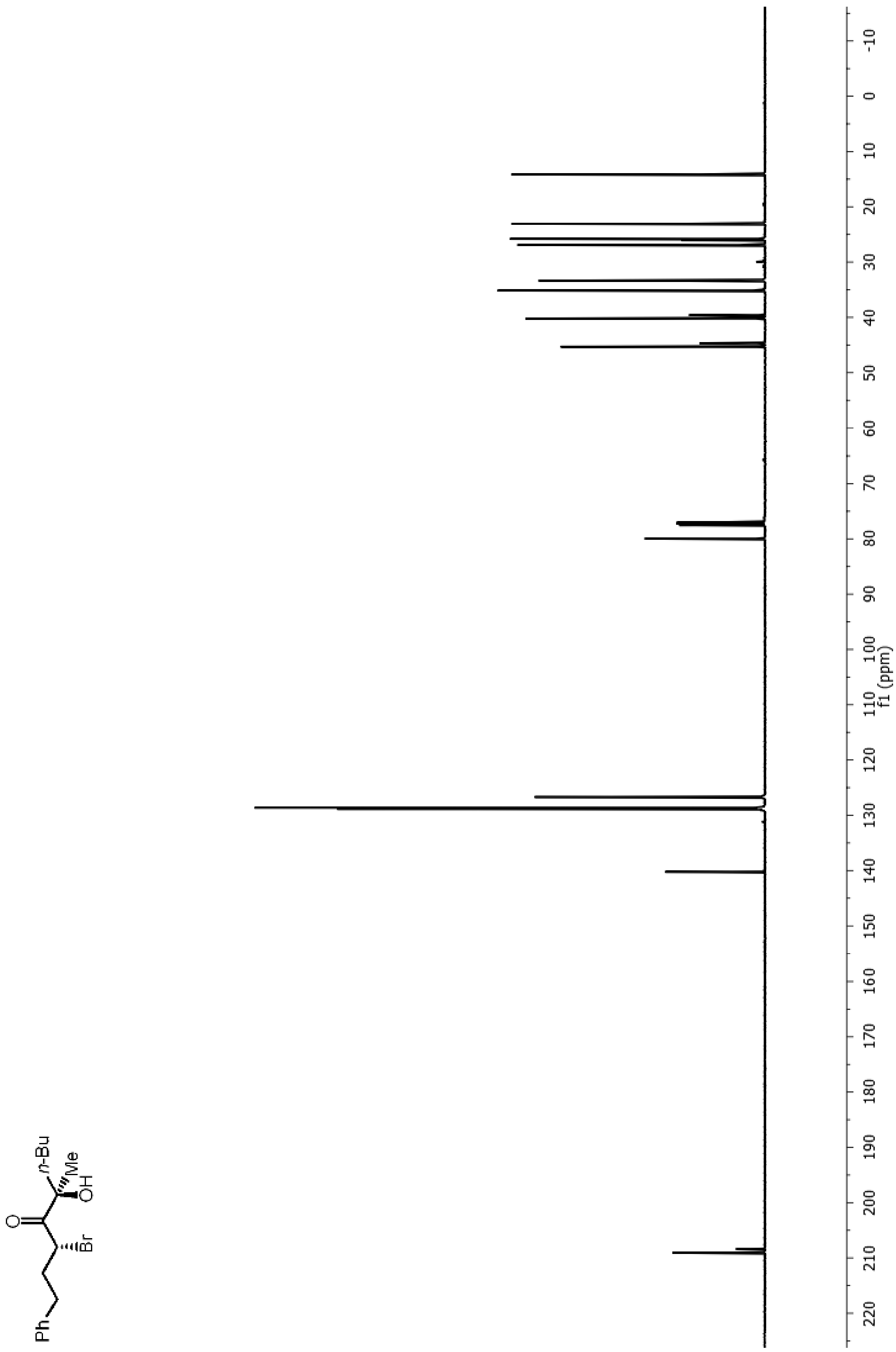

^{1}H NMR (500 MHz, C_6D_6)

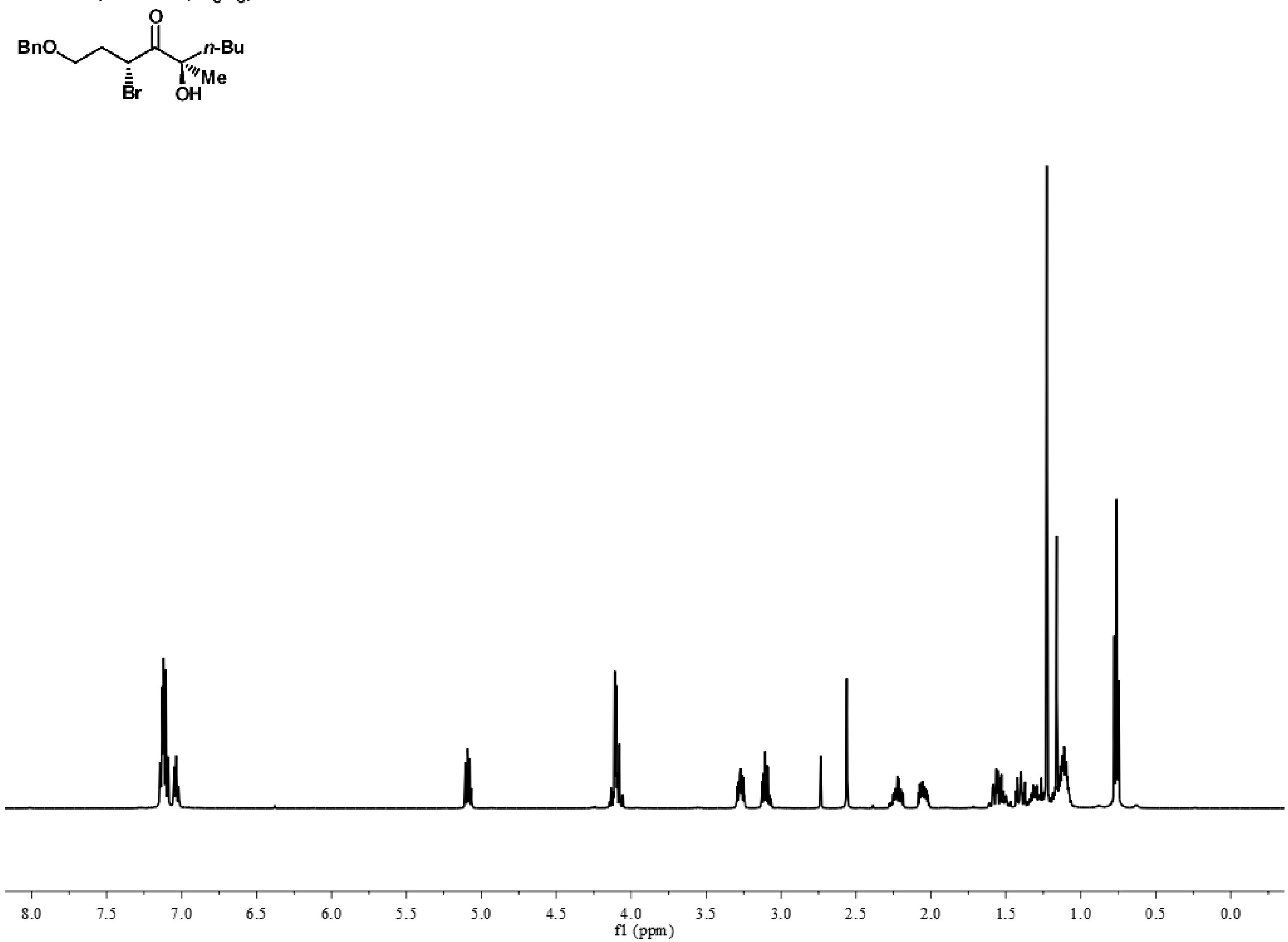

^{13}C NMR (125 MHz, C_6D_6)

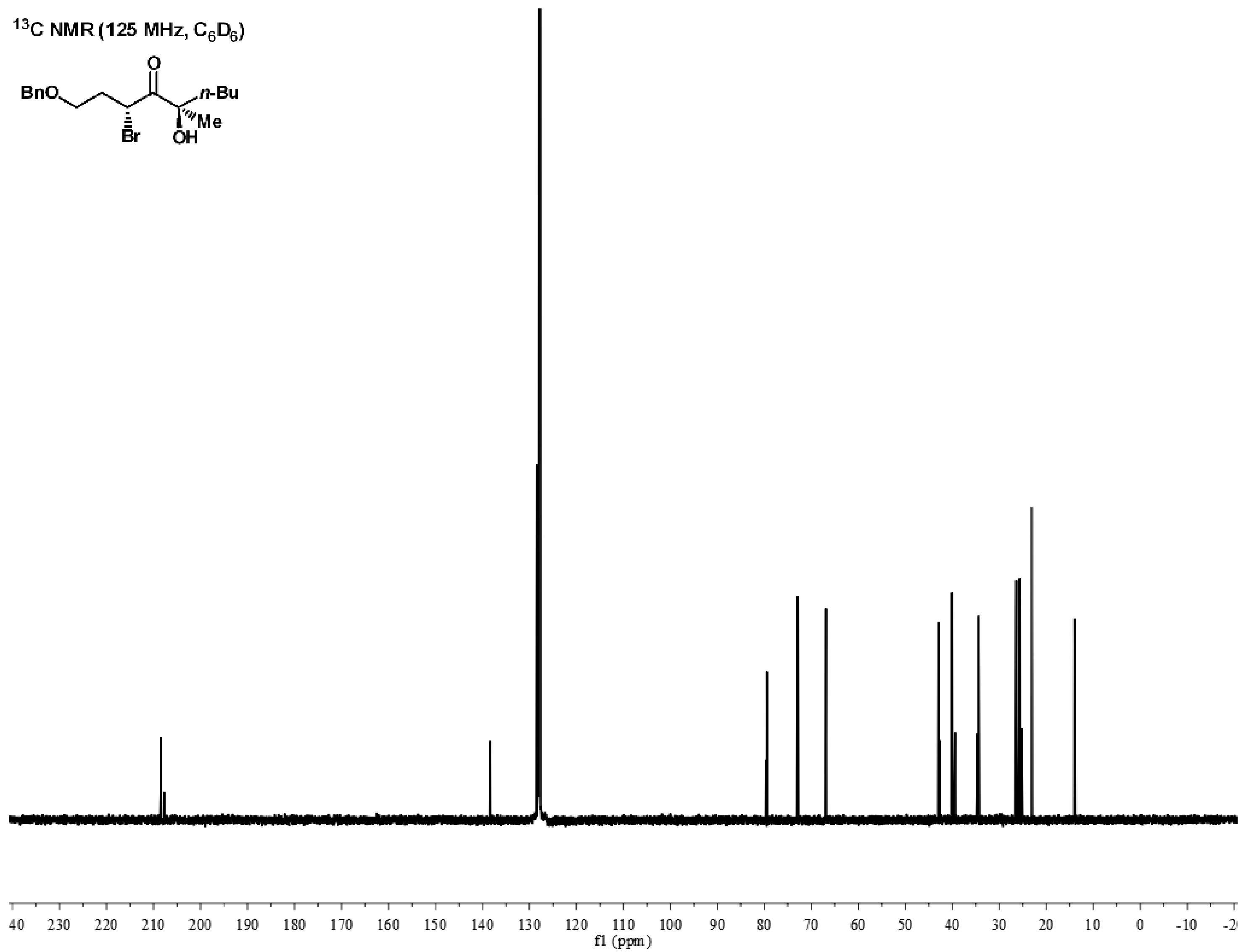

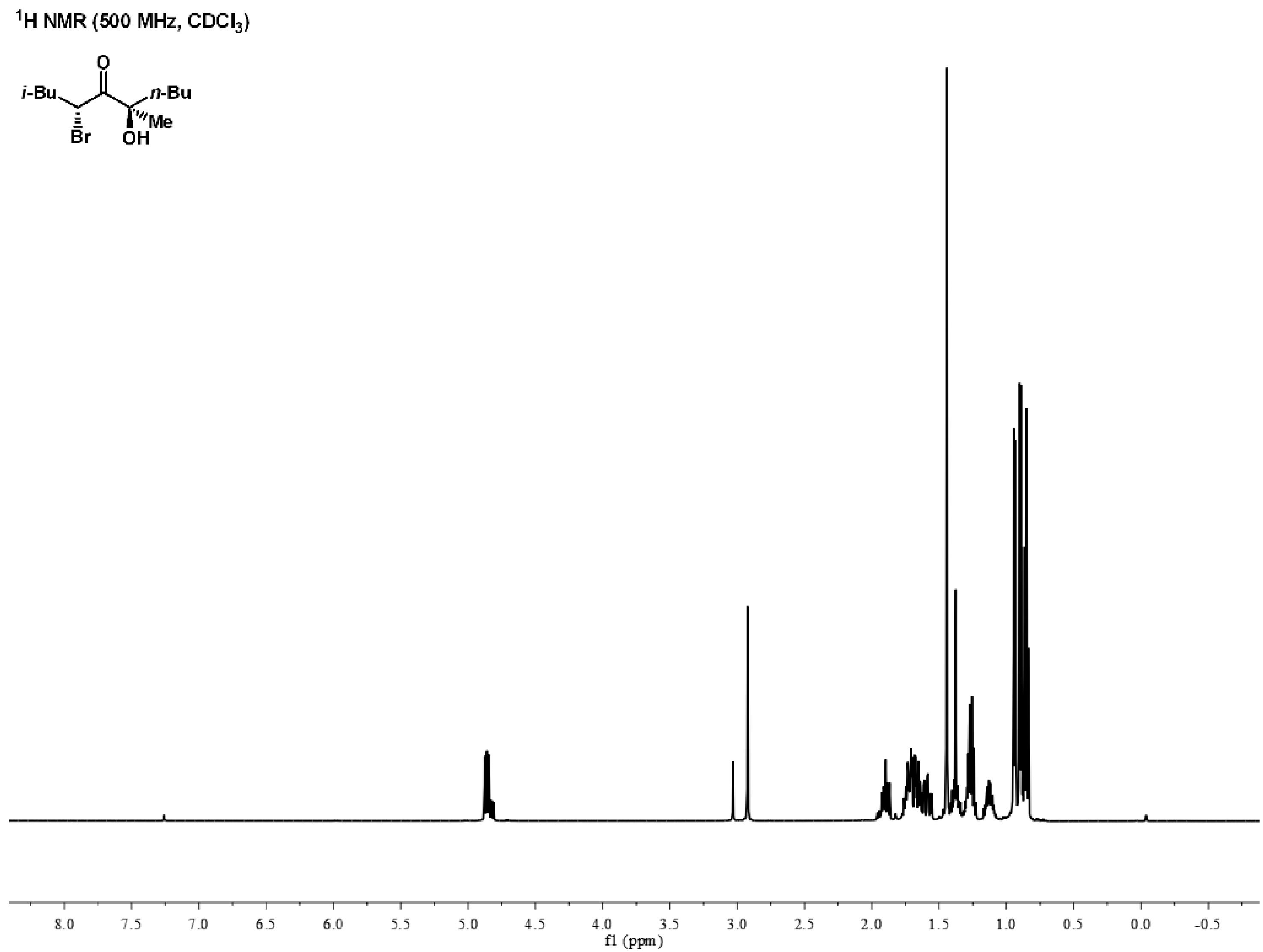

1H NMR (500 MHz, CDCl3)
i-Bu
n-Bu
Me
Br
OH
O
8.0
7.5
7.0
6.5
6.0
5.5
5.0
4.5
4.0
3.5
3.0
2.5
2.0
1.5
1.0
0.5
0.0
-0.5
f1 (ppm)

^{13}C NMR (125 MHz, $CDCl_3$)

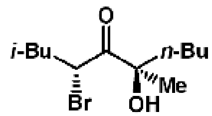

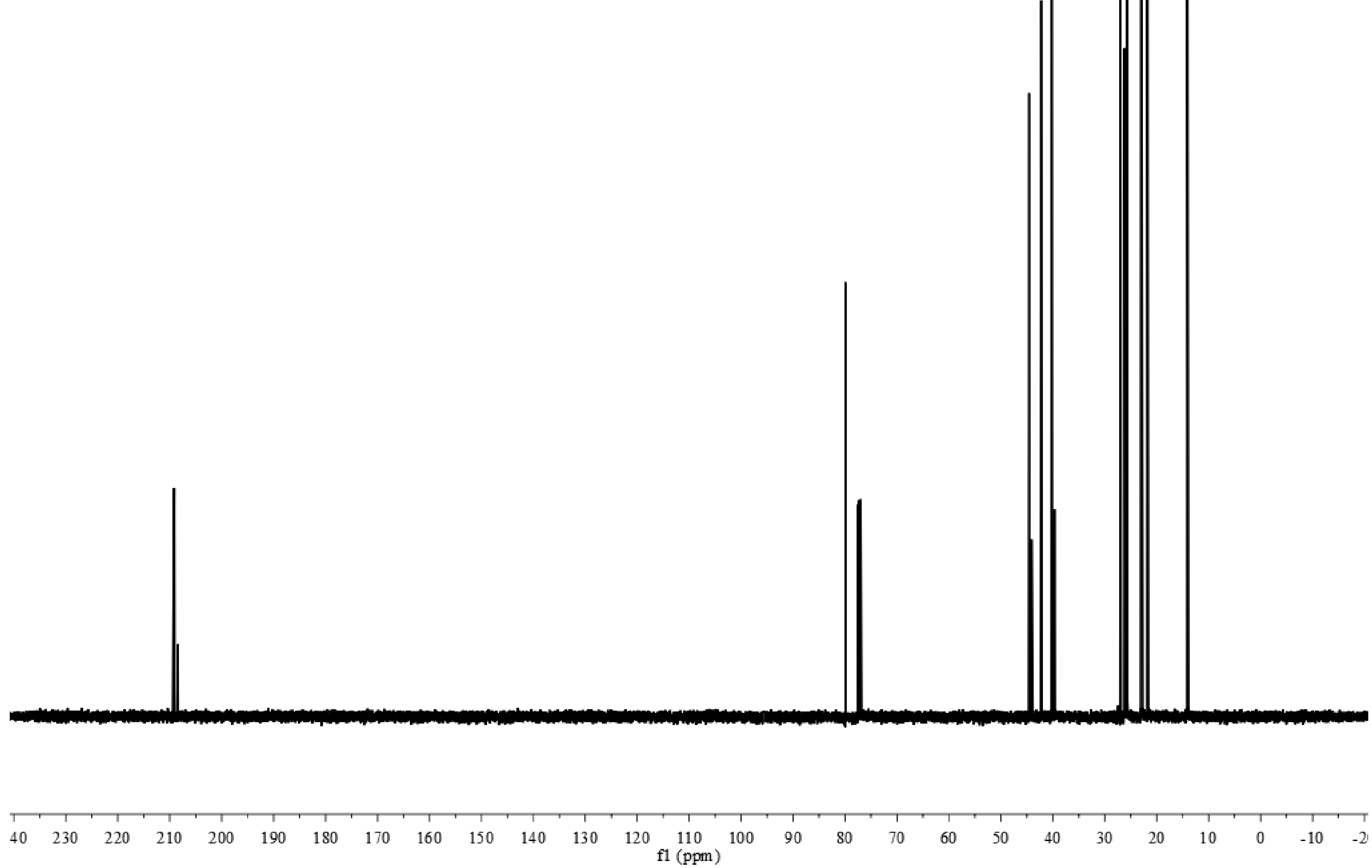

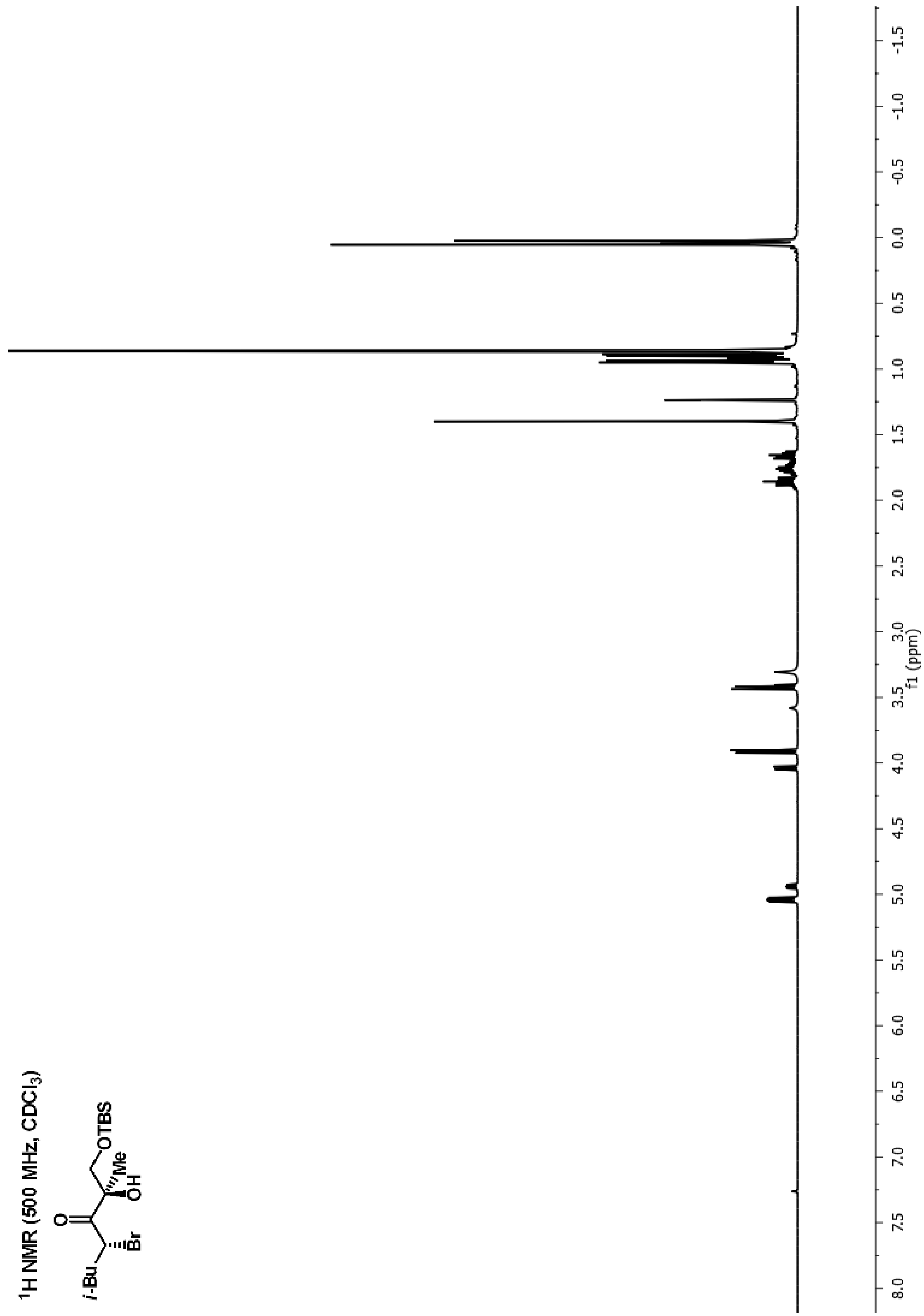

1H NMR (500 MHz, CDCl3)
i-Bu
Br
O
OH
Me
OTBS
f1 (ppm)
8.0 7.5 7.0 6.5 6.0 5.5 5.0 4.5 4.0 3.5 3.0 2.5 2.0 1.5 1.0 0.5 0.0 -0.5 -1.0 -1.5

^{13}C NMR (125 MHz, $CDCl_3$)

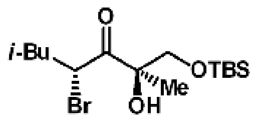

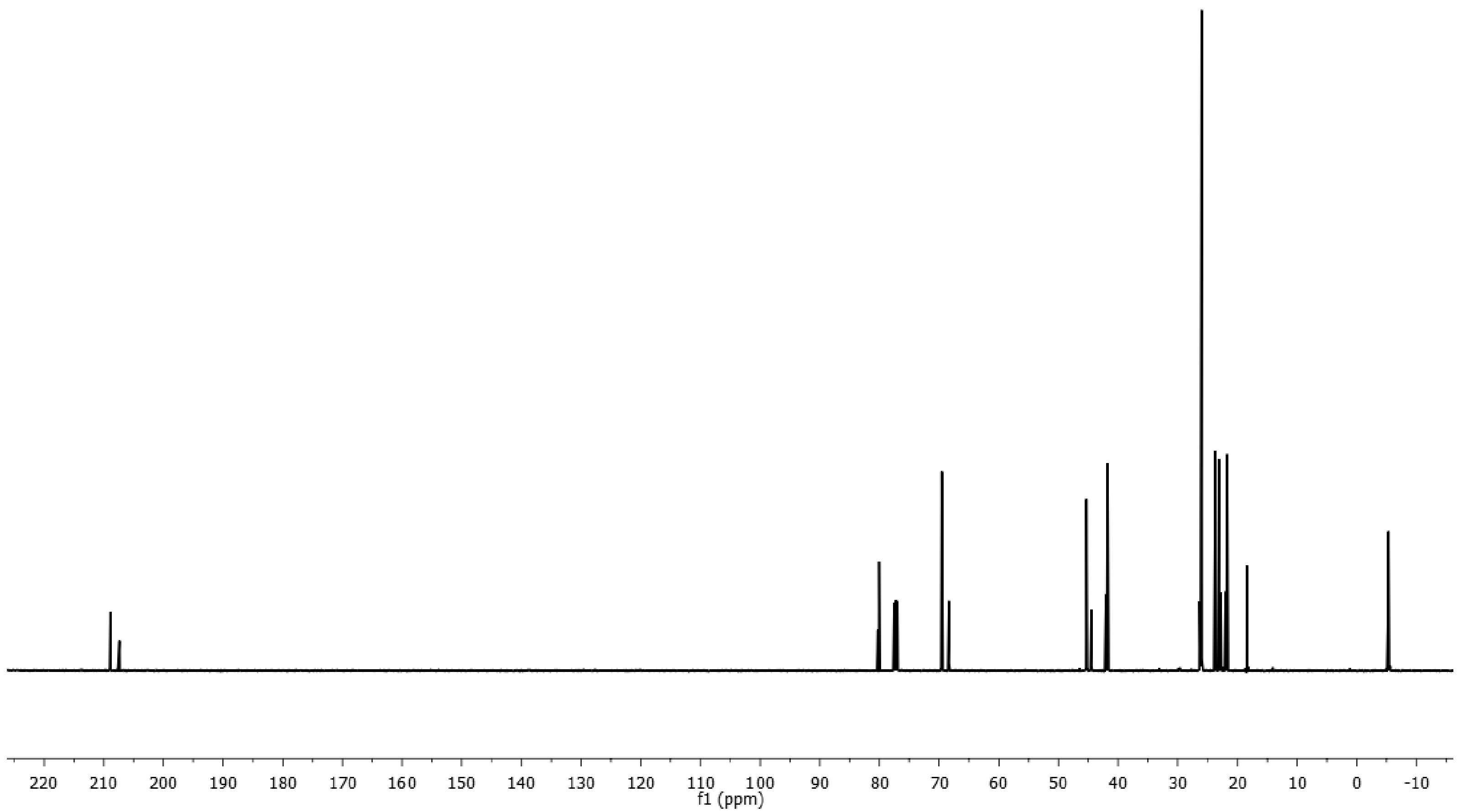

^1H NMR (500 MHz, C_6D_6)

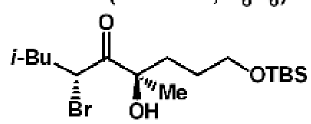

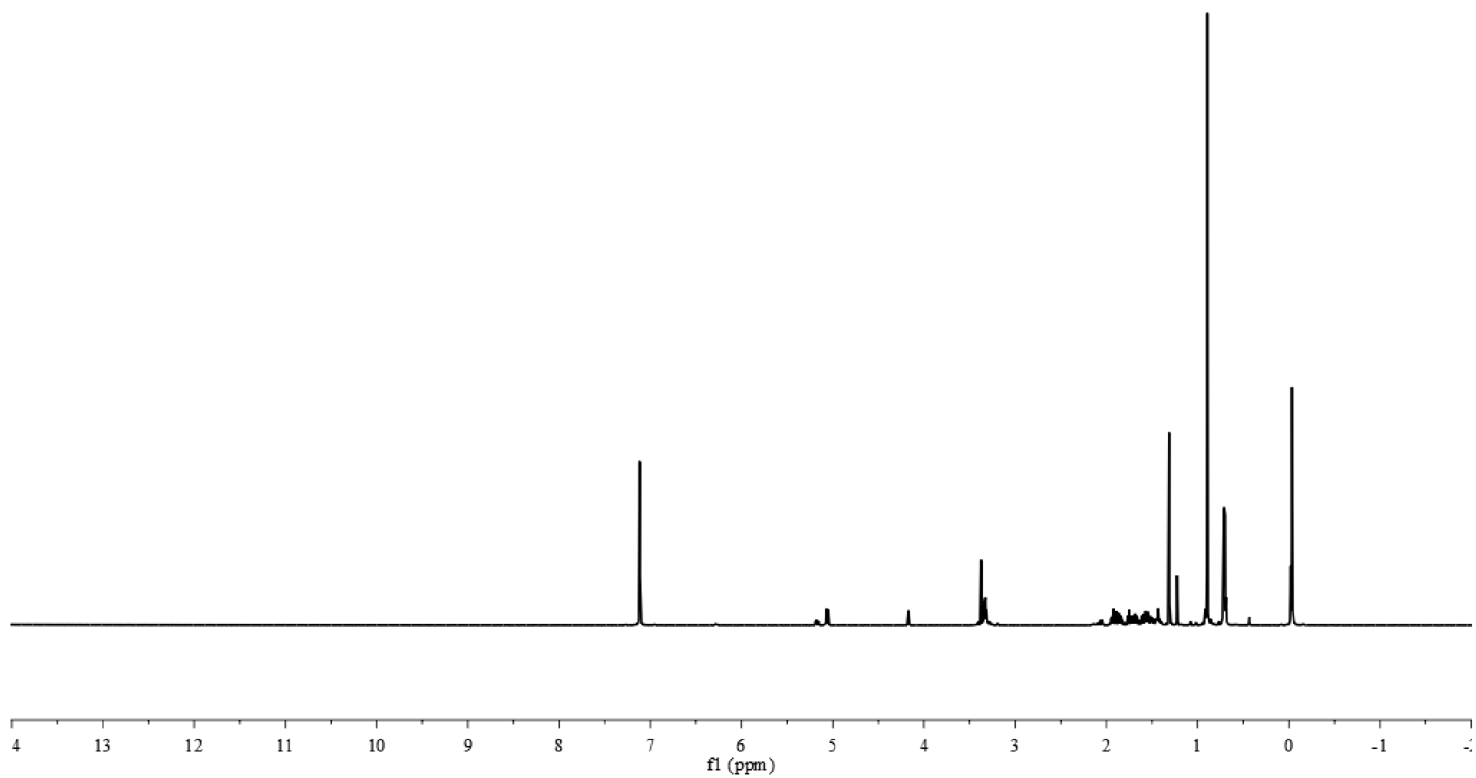

^{13}C NMR (125 MHz, C_6D_6)

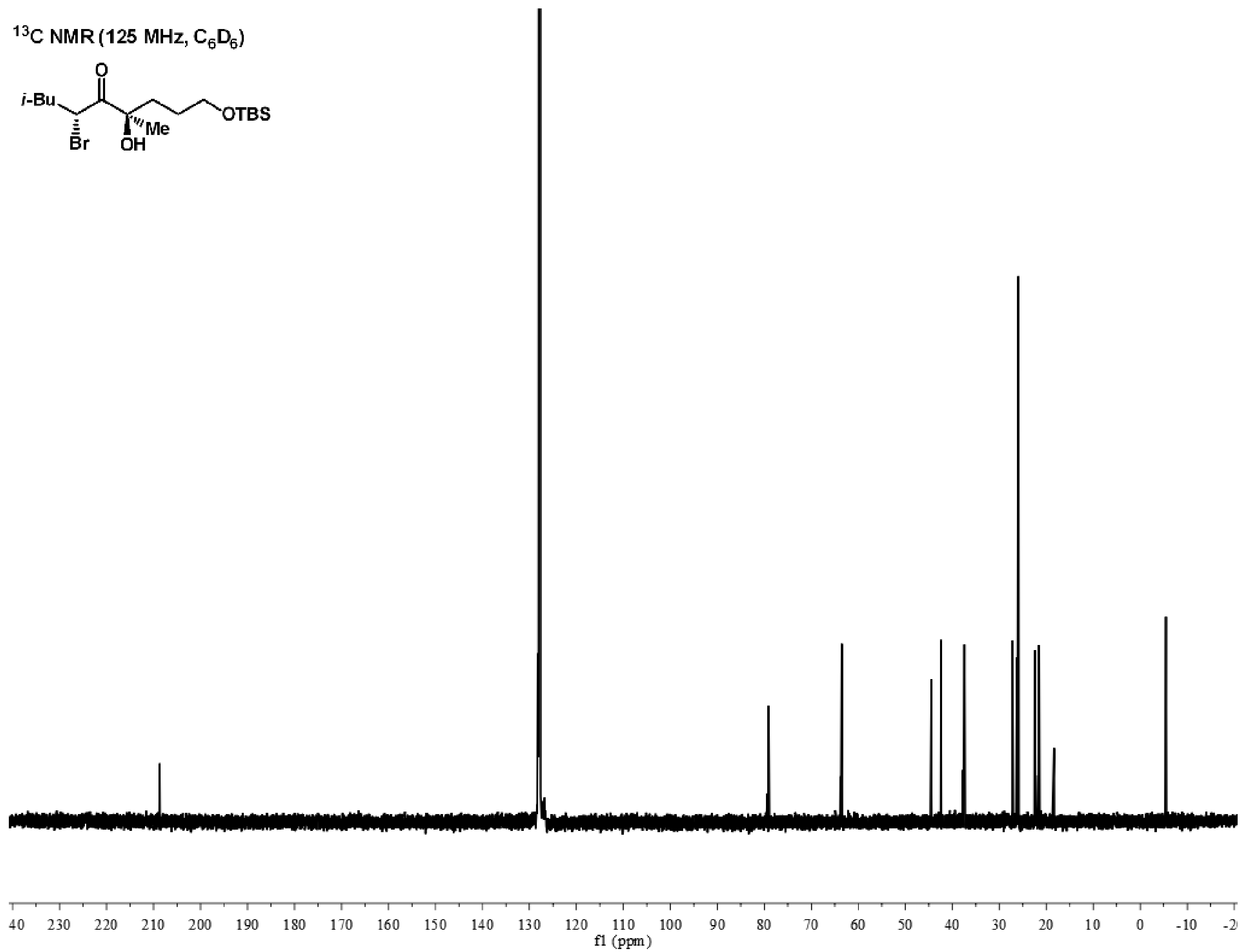

^1H NMR (500 MHz, $CDCl_3$)

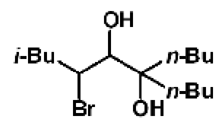

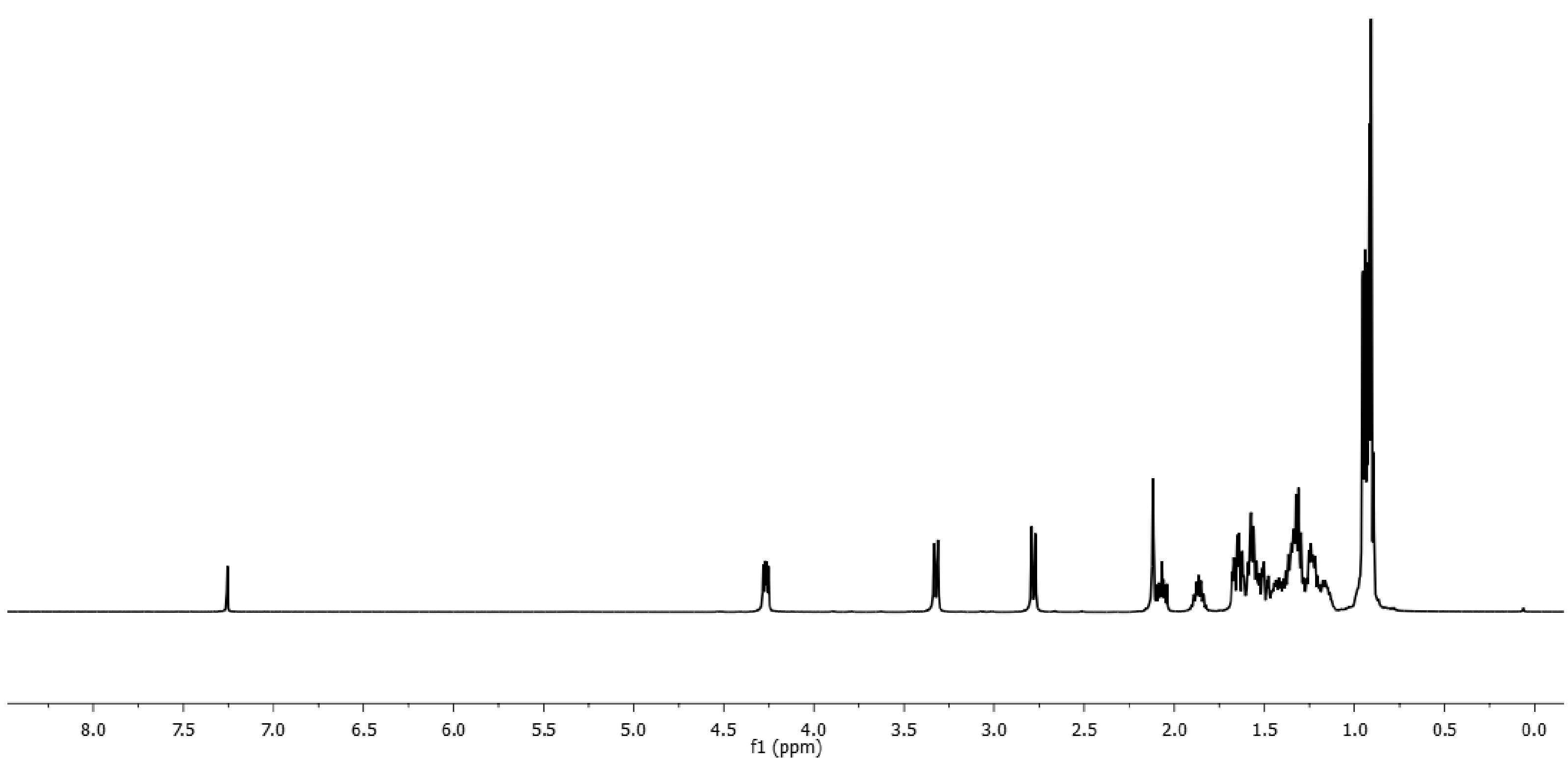

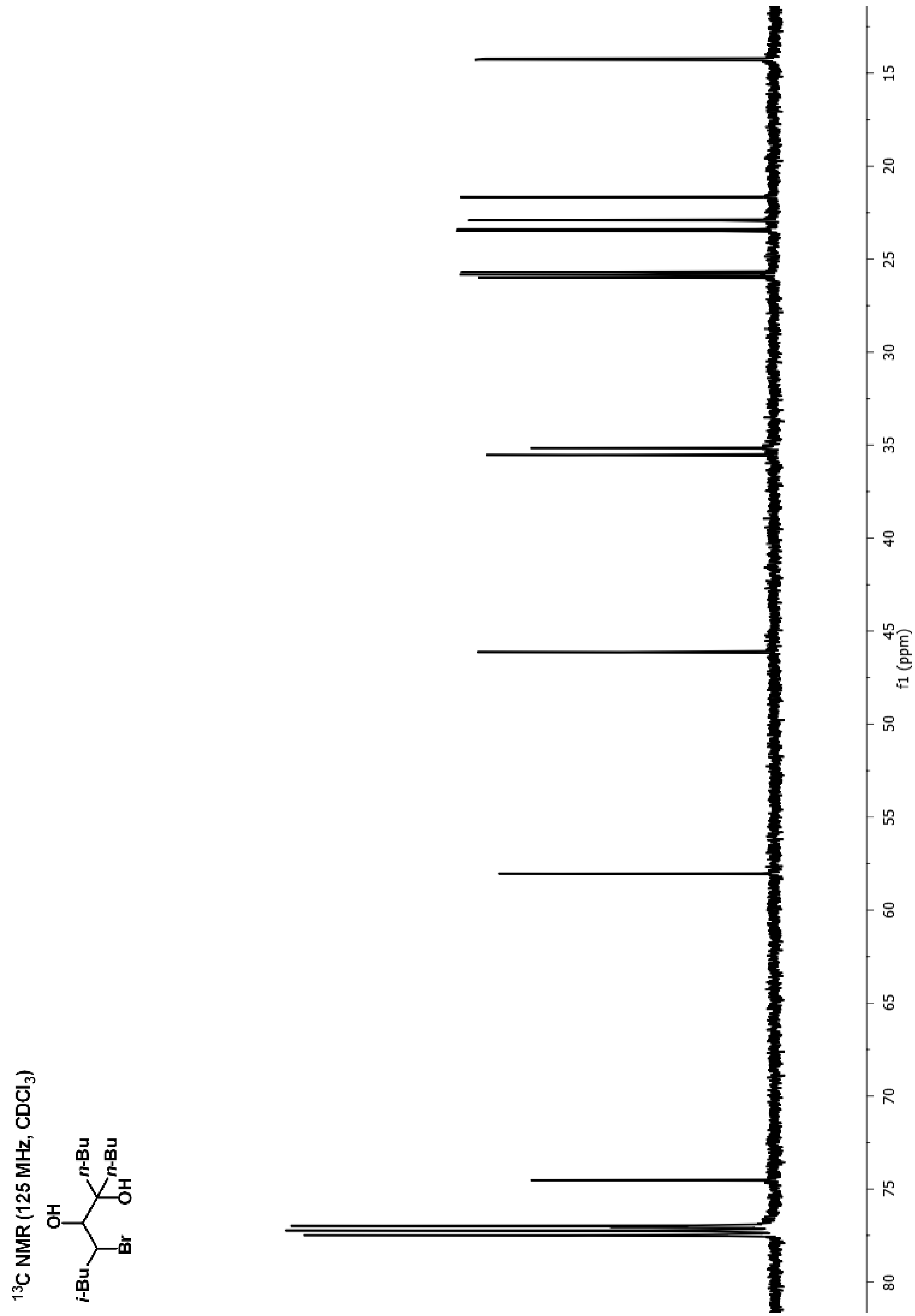

^{13}C NMR (125 MHz, $CDCl_3$)
i-Bu
OH
Br
n-Bu
n-Bu
OH
80
75
70
65
60
55
50
45
40
35
30
25
20
15
f1 (ppm)

^1H NMR (400 MHz, $CDCl_3$)

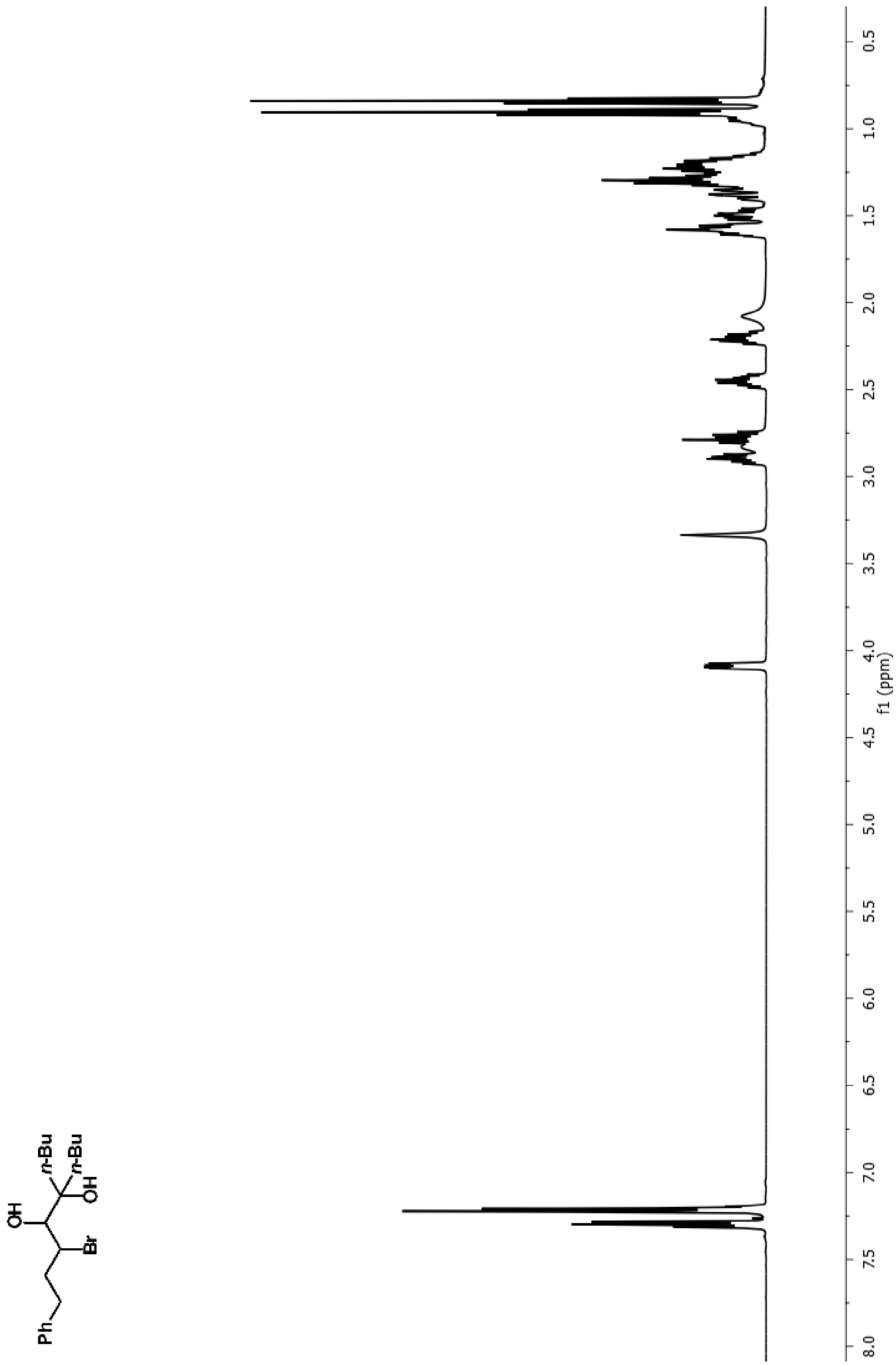

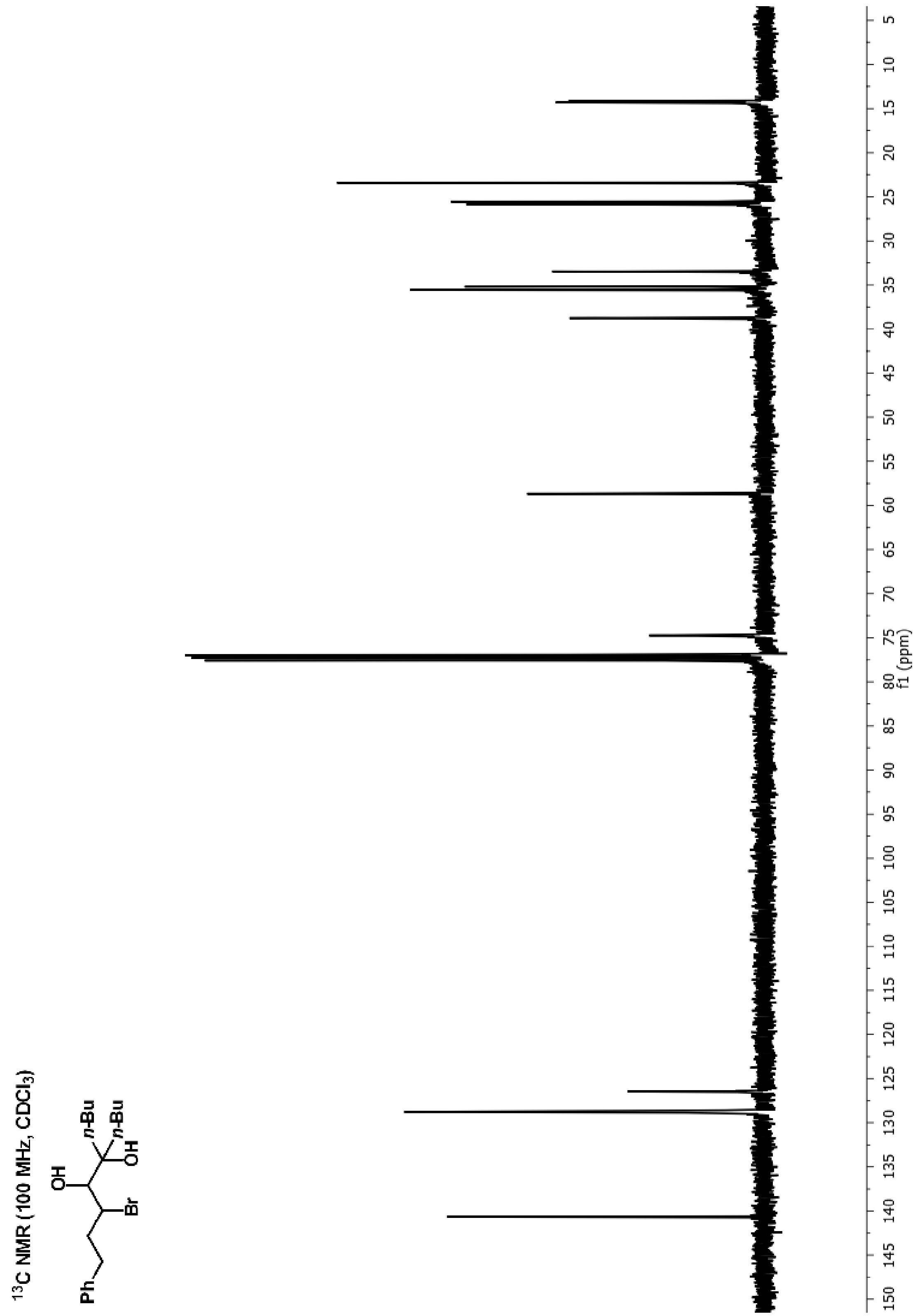

^{13}C NMR (100 MHz, $CDCl_3$)
Ph
OH
Br
n-Bu
n-Bu
OH
f1 (ppm)